Assessment of osteoporotic fractures and risk prediction, volume II

Edited by
Zhi-Feng Sheng, Xiangbing Wang and Xiaoguang Cheng

About Frontiers

Frontiers is more than just an open access publisher of scholarly articles: it is a pioneering approach to the world of academia, radically improving the way scholarly research is managed. The grand vision of Frontiers is a world where all people have an equal opportunity to seek, share and generate knowledge. Frontiers provides immediate and permanent online open access to all its publications, but this alone is not enough to realize our grand goals.

Frontiers journal series

The Frontiers journal series is a multi-tier and interdisciplinary set of open-access, online journals, promising a paradigm shift from the current review, selection and dissemination processes in academic publishing. All Frontiers journals are driven by researchers for researchers; therefore, they constitute a service to the scholarly community. At the same time, the *Frontiers journal series* operates on a revolutionary invention, the tiered publishing system, initially addressing specific communities of scholars, and gradually climbing up to broader public understanding, thus serving the interests of the lay society, too.

Dedication to quality

Each Frontiers article is a landmark of the highest quality, thanks to genuinely collaborative interactions between authors and review editors, who include some of the world's best academicians. Research must be certified by peers before entering a stream of knowledge that may eventually reach the public – and shape society; therefore, Frontiers only applies the most rigorous and unbiased reviews. Frontiers revolutionizes research publishing by freely delivering the most outstanding research, evaluated with no bias from both the academic and social point of view. By applying the most advanced information technologies, Frontiers is catapulting scholarly publishing into a new generation.

What are Frontiers Research Topics?

Frontiers Research Topics are very popular trademarks of the *Frontiers journals series*: they are collections of at least ten articles, all centered on a particular subject. With their unique mix of varied contributions from Original Research to Review Articles, Frontiers Research Topics unify the most influential researchers, the latest key findings and historical advances in a hot research area.

Find out more on how to host your own Frontiers Research Topic or contribute to one as an author by contacting the Frontiers editorial office: frontiersin.org/about/contact

Assessment of osteoporotic fractures and risk prediction, volume II

Topic editors

Zhi-Feng Sheng — Central South University, China
Xiangbing Wang — The State University of New Jersey, United States
Xiaoguang Cheng — Beijing Jishuitan Hospital, China

Table of contents

Editorial: Assessment of osteoporotic fractures and risk prediction, volume II

Dandan Xie[1,2], ZhiFeng Sheng[2]*, Xiangbing Wang[3] and Xiaoguang Cheng[4]

[1]Department of Clinical Nutrition, the First Affiliated Hospital of Hainan Medical University, Haikou, Hainan, China, [2]Health Management Center, National Clinical Research Center for Metabolic Diseases, Hunan Provincial Key Laboratory of Metabolic Bone Diseases, Department of Metabolism and Endocrinology, The Second Xiangya Hospital of Central South University, Changsha, Hunan, China, [3]Divisions of Endocrinology, Metabolism, and Nutrition, The State University of New Jersey, New Brunswick, NJ, United States, [4]Department of Radiology, Beijing Jishuitan Hospital, Beijing, China

KEYWORDS

osteoporosis, fracture, risk factors, prediction, assessment

Editorial on the Research Topic
Assessment of osteoporotic fractures and risk prediction, volume II

With the progressive aging of the population, the prevalence of osteoporosis (OP) and associated fractures continues to rise, posing a significant global public health challenge. Recent reports have indicated that the annual incidence of osteoporotic fractures surpasses that of myocardial infarction, breast cancer, and prostate cancer combined (1). Hence, accurate prediction and early identification of individuals at risk of fractures are of utmost importance in mitigating osteoporotic fracture occurrences, improving patients' quality of life and alleviating the burden on healthcare systems.

In our endeavor to gain deeper insights into the etiology, pathogenesis, diagnosis, treatment, epidemiological characteristics, and risk prediction of osteoporotic fractures, we organized a Research Topic that garnered an overwhelming response. The multitude of submissions received, especially those pertaining to early assessment of osteoporotic fractures, surpassed our initial expectations. Consequently, we have expanded this Research Topic into a two-volume collection to accommodate the significant number of high-quality submissions. In this summary, we present an overview of the contributions enclosed in the second volume.

In a series of contributions, multiple studies have focused on osteoporotic vertebral fractures (OVFs). Guo et al. conducted a study involving 2,874 postmenopausal women in Beijing, assessing four tools for identifying painful new OVF. Their findings revealed that the Fracture Risk Assessment Tool (FRAX) without bone mineral density (BMD) was the preferred option, while the Beijing Friendship Hospital Osteoporosis Screening Tool and Osteoporosis Self-Assessment Tool for Asians showed promise as simpler screening tools (Guo et al.). Another study developed and validated a deep learning model utilizing X-ray imaging data to enable artificial intelligence-based diagnosis and classification of vertebral compression fracture types. This technological advancement is expected to enhance the

diagnostic accuracy of vertebral compression fractures in primary healthcare settings (Xu et al.). For patients with chronic OVF undergoing surgical treatment, Xin et al. reported that a scoring system based on five clinical characteristics—age, BMI, BMD, preoperative pelvic incidence-lumbar lordosis, and posterior ligamentous complex injury—exhibited good sensitivity and specificity in predicting the development of proximal junctional kyphosis after posterior internal fixation. Patients with a score of 6-11 were identified as being at high risk (Du et al.). In an analysis of patients treated with percutaneous vertebroplasty for compressive OVF, the authors identified BMD, bone cement disc leakage, and larger side bone cement volume/vertebral body volume ratio (LSBCV/VBV) as independent risk factors for postoperative adjacent vertebral compression fractures, with a significantly increased incidence observed when LSBCV/VBV reached 13.82% (Zhou et al.).

Regarding potential biomarkers of OP, N6-methyladenosine modulators have been useful as diagnostic biomarkers and for subtype identification in postmenopausal OP (Zhang et al.). Additionally, sclerostin has been identified as a potential biomarker for physical exercise in OP (Oniszczuk et al.). Another study reviewed the application of metabolomics in OP research (Zhao et al.). Regarding the prediction and screening of OP and fractures, Kong et al. identified chronic airway disease as a major risk factor for fractures in osteopenic women and proposed predictive models for major osteoporotic and hip fractures (Kong et al.). Furthermore, a small sample study initially compared the differences in vertebral mechanical properties estimated by finite element analysis with two computed tomography (CT) reconstruction kernels and evaluated their accuracy in the screening and classification of OP (Jiang et al.), which holds importance for the development of CT-based OP opportunistic screening tools. Two additional studies explored the association of hand grip strength and obstructive sleep apnea-hypopnea syndrome with BMD and fracture risk, respectively (Song et al., Wang et al.).

Moreover, within volume II; of this Research Topic, several studies have focused on fracture risk assessment in specific diseases. For type 2 diabetes mellitus (T2DM), one investigation demonstrated the utility of rheumatoid arthritis-adjusted FRAX as a valid clinical tool for evaluating fracture risk in postmenopausal T2DM patients, and a threshold of 4.156 mmol/L for advanced glycation end products was identified as a predictor of fracture risk (Gao et al.). However, the study found no significant association between metformin use and fracture risk in T2DM patients (Wang et al.). In another randomized study, the impact of antiretroviral therapy on bone quality in HIV-infected patients was investigated, switching from tenofovir disoproxil fumarate to tenofovir alafenamide for 24 weeks resulted in improved bone quality, independent of BMD (Soldado- Folgado et al.).

To summarize, this Research Topic provides significant insights into the screening, prediction, diagnosis, prognosis, and risk factors associated with BMD and fractures in OP, as well as disease-specific fracture risk studies. These findings, encompassing both molecular

and clinical investigations, underscore the applicability of predictive tools and biomarkers for osteoporotic fractures while emphasizing the need to enhance the capacity of primary care institutions in identifying and diagnosing osteoporotic fractures. We believe that this Research Topic will contribute to the advancement of fracture prediction and identification in high-risk populations, ultimately reducing fracture incidence in clinical practice.

Author contributions

Funding

Conflict of interest

The authors declare that the research was conducted in the absence of any commercial or financial relationships that could be construed as a potential conflict of interest.

Publisher's note

Reference

1. LeBoff MS, Greenspan SL, Insogna KL, Lewiecki EM, Saag KG, Singer AJ, et al. The clinician's guide to prevention and treatment of osteoporosis. *Osteoporos Int* (2022) 33(10):2049–102. doi: 10.1007/s00198-021-05900-y

Check for updates

*CORRESPONDENCE
Yunsheng Ou
ouyunsheng2001@163.com

A predictive scoring system for proximal junctional kyphosis after posterior internal fixation in elderly patients with chronic osteoporotic vertebral fracture: A single-center diagnostic study

Xing Du[1,2], Guanyin Jiang[1,2], Yong Zhu[1,2], Wei Luo[1,2] and Yunsheng Ou[1,2]*

[1]Department of Orthopedics, The First Affiliated Hospital of Chongqing Medical University, Chongqing, China, [2]Orthopedic Laboratory of Chongqing Medical University, Chongqing, China

Objective: To establish a predictive scoring system for proximal junctional kyphosis (PJK) after posterior internal fixation in elderly patients with chronic osteoporotic vertebral fracture (COVF).

Materials and methods: The medical records of 88 patients who were diagnosed with COVF and underwent posterior internal fixation in our hospital from January 2013 to December 2017 were retrospectively analyzed. The included patients were divided into two groups according to whether they suffered PJK after surgery, namely, the PJK group (25 cases) and non-PJK group (63 cases). The following clinical characteristics were recorded and analyzed: age, gender, body mass index (BMI), bone mineral density (BMD), smoking history, fracture segment, proximal junction angle, sagittal vertebral axis, pelvic incidence (PI)−lumbar lordosis (LL), pelvic tilt (PT), sacral slope (SS), posterior ligamentous complex (PLC) injury, upper instrumented vertebra, lower instrumented vertebra, and the number of fixed segments. The prevalence of these clinical characteristics in the PJK group was evaluated, and the scoring system was established using logistic regression analysis. The performance of the scoring system was also prospectively validated.

Results: The predictive scoring system was established based on five clinical characteristics confirmed as significant predictors of PJK, namely, age > 70 years, BMI > 28 kg/m^2, BMD < −3.5 SD, preoperative PI-LL > 20°, and PLC injury. PJK showed a significantly higher score than non-PJK (7.80 points *vs.* 2.83 points, *t*=9.556, *P*<0.001), and the optimal cutoff value for the scoring system was 5 points. The sensitivity and specificity of the scoring system for predicting postoperative PJK were 80.00% and 88.89%, respectively, in the derivation set and 75.00% and 80.00% in the validation set.

Conclusion: The predictive scoring system was confirmed with satisfactory sensitivity and specificity in predicting PJK after posterior internal fixation in elderly COVF patients. The risk of postoperative PJK in patients with a score of 6−11 is high, while the score of 0−5 is low.

Introduction

Osteoporotic fracture (OF) is a worldwide clinical challenge. Osteoporotic vertebral fractures (OVFs) are the most common form of OF and often occur in the thoracolumbar vertebrae of the elderly (1). OVF with a course of more than 3 months is defined as chronic osteoporotic vertebral fractures (COVFs) (2). The early-stage clinical symptoms of elderly COVF patients are not obvious, but with the increase of age, the degree of osteoporosis and the kyphosis are progressively aggravated, resulting in intractable lumbago pain and even delayed paralysis, which seriously affect the life quality of patients (3). The clinical efficacy of conservative treatment for elderly COVF is rarely satisfactory (4). At present, the main treatment of elderly COVF is posterior long segmental internal fixation, which can effectively maintain the spine stability, correct the kyphosis, and reduce the risk of fracture vertebral collapse and kyphosis progression (5).

However, the risk of proximal junction kyphosis (PJK) after posterior long segment internal fixation is high with the reported incidence of 6%–40% because the thoracolumbar spine is located at the junction of spinal force line transmission (6). Although most PJK patients have mild clinical symptoms, severe PJK patients may develop into proximal borderline failure (PJF), or even neurological impairment, and consequently require a revision operation (7). Furthermore, most PJK patients are elderly people, they have poor bone condition and many medical complications; thus, the risk of PJK revision surgery is really high (8). Therefore, in the treatment of elderly COVF by posterior long segmental internal fixation, it is of great significance to actively detect the risk factors of PJK.

Although two studies have reported the risk factors for PJK (6, 7), they had limited guiding implications for clinical work due to the totally different risk factors reported by them. In addition, the two studies did not focus on elderly patients. Thus, the risk factors for postoperative PJK in elderly COVF are remain controversial, and further studies are still needed.

Therefore, in this research, we hypothesized that the ability of predicting PJK after posterior internal fixation in aged COVF can be enhanced by establishing a scoring system *via* investigating the risk factors of PJK after surgery.

Materials and methods

This study was approved by the Ethics Committee of the First Affiliated Hospital of Chongqing Medical University (2017-97). All of the participants provided their written informed consent to participate in this study. The work has been reported in line with the STARD criteria (9).

Patient selection

We retrospectively reviewed the medical records of hospitalized patients diagnosed with COVF in our department from January 2013 to December 2017 to form the derivation set (Figure 1).

Inclusion criteria: (1) The diagnosis was single-segment COVF; (2) age ≥ 60 years old; (3) preoperative CT showed that the posterior wall of the vertebral collapses and protrudes into the spinal canal but without exceeding 1/3 of the spinal canal; (4) patients who underwent posterior long segments internal fixation (≥5 segments); (5) patients treated with conventional non-operative treatment for more than 3 months but no significant improvement in symptoms; and (6) bone density showed T value ≤ −2.5 standard deviation (SD).

Exclusion criteria: (1) Previous history of spinal surgery or severe spinal cord injury; (2) patients with idiopathic or congenital spinal deformity, spinal tumor, infection, or tuberculosis; (3) pathological vertebral fracture; (4) lower limb surgery history, which may affect imaging data measurement; and (5) less than 12 months follow-up or incomplete medical record data.

Surgical procedure

All surgeries were performed by experienced spinal surgeons in the same medical group. After general anesthesia, the patient was
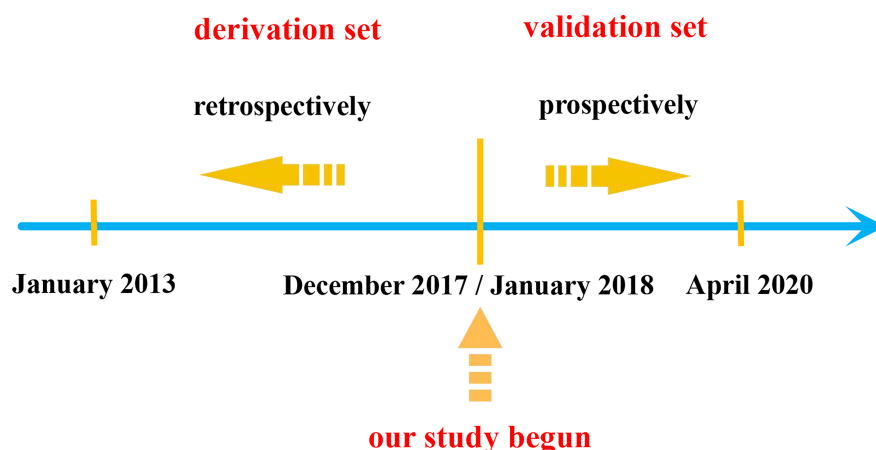
FIGURE 1
Schematic of patient inclusion in derived and validation sets in this study.

placed in a prone position with a sponge pad placed under the chest and pelvis to make the abdomen suspended. After disinfection and towel spreading, a C-arm X-ray machine was used to locate the fractured vertebra, and then, the posterior median incision was made with the kyphosis vertex as the center. Next, the paravertebral muscles were separated, and at least two normal vertebrae were exposed with the injured vertebrae as the center. The vertebral and its upper and lower articular processes of the fixed segments were exposed, and pedicle screws were inserted into two vertebrae above and below the fractured vertebra. For patients with severe osteoporosis, the fixation segment can be appropriately extended and the channel of pedicle screws can be strengthened with bone cement, mainly strengthening one-to-two groups of proximal and distal screws. Then, single-segment pedicle subtraction osteotomy (PSO) was performed to correct the kyphosis. Firstly, the bone rongeur was used to remove the spinous process, lamina, and bilateral pedicle of the osteotomy vertebrae. Next, a short titanium rod was used alternately to temporarily fix the upper and lower adjacent segments of the osteotomy vertebrae. Then, a short titanium rod alternate was used to temporarily fix the adjacent sections of the vertebrae, and then, the vertebral vertebra and lower vertebral vertebra were removed for spinal canal decompression, the nerve root was revealed and protected and finally placed on the connection of both sides, and the screws were tightened one by one. The parietal vertebra and the lamina of the upper and lower vertebrae were then removed for spinal canal decompression, with care taken to expose and protect the nerve roots. Finally, prebent connecting titanium rods were placed on both sides and the nuts were tightened one by one. After C-arm X-ray fluoroscopy verified the satisfactory correction of kyphosis and the examination of no active bleeding, the wound was flushed, the drain was placed, and the surgical incision was closed layer by layer.

Data collection

Based on the results of previous studies and our experience, we included the possible following predictors for posterior PJK, which mainly included the patient- related data, preoperative imaging data, and surgery-related data.

(1) Patient-related data: (a) age ≥ 70 years. (b) The gender was female. (c) Body mass index (BMI) > 28 kg/m^2. (d) The T-value of bone mineral density (BMD) < -3.5 SD. (e) Had a smoking history. (f) The fracture segment was T_{12} or L_1 vertebrae.

(2) Preoperative imaging data (Figure 2): (a) proximal junction angle (PJA) > 5°: PJA was the angle between the lower endplates of the upper instrumented vertebra (UIV) and upper endplates of the second distal vertebrae of the UIV (UIV+2). (b) sagittal vertebral axis (SVA) > 50 mm: SVA was the vertical distance between the C7 plumb line and the posterior upper angle of S1. (c) Pelvic incidence (PI)—lumbar lordosis (LL) > 20°: PI was the angle between the line A and B. Line A is between the midpoint of the S1 endplate and the midpoint of the line that connects the center of two femoral heads. Line B is the perpendicular of the S1 upper endplate passing through the midpoint of the S1 endplate. (d) Pelvic tilt (PT) > 30°: PT was the angle between the plumb line and the straight line between the midpoint of the S1 endplate and the midpoint of the line that connects the center of two femoral heads. (e) Sacral slope (SS) > 25°: SS was the angle between the S1 endplate and the horizontal line. (f) posterior ligamentous complex (PLC) injury: PLC injury was a single or combined injury of the supraspinous ligament, interspinous ligament, and ligamentum flavum, which may be accompanied by facet fracture.

(3) Surgery-related data: (a) the UIV location was T_{10} to T_{12} vertebrae. (b) The lower instrumented vertebra (LIV) was S_1 vertebrae. (c) Number of fixed segments > 7.
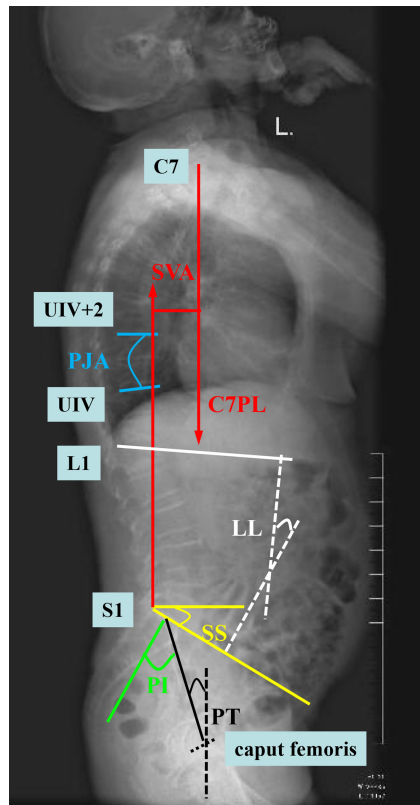
(4) Follow-up outcomes: postoperative PJK was defined as postoperative PJA $\geq$ 10° and increased by more than 10° compared with preoperative. The final follow-up time was 2 years after surgery.

Development of the scoring system

Firstly, all the included patients were divided into two groups, namely, the PJK group and non-PJK group according to the 2-year postoperative follow-up outcomes. Secondly, univariate analysis was conducted on the patient-related data, preoperative imaging data, and surgery-related data of the two groups. Based on the results of univariate analysis, the index with $P<0.05$ was considered a possible predictor for postoperative PJK. Next, multivariate logistic regression analysis was performed for the indexes with $P<0.05$ in univariate analysis. According to the results of multivariate logistic regression analysis, the indexes with $P<0.05$ were considered the final predictors for postoperative PJK and, thus, determined as the items of the scoring system. Then, we established the weighted score of each item based on the relative

size of the odds ratio (OR) according to the method reported by our previous research (10). Finally, we made the appropriate cutoff points for the scoring system using receiver operator characteristic receiver operator characteristic (ROC) curves corresponding to the point on the curve nearest the upper left corner of the ROC graph.

Validation of the scoring system

From January 2018 to April 2020, we prospectively included patients to validate the accuracy of the scoring system (Figure 1).

The following criteria were used to determine whether a patient should be prospectively included in the validation set. The inclusion criteria were as follows: (1) elderly patients (age $\geq$60 years) who were preoperatively diagnosed with single-segment COVF. (2) Preoperative bone density showed that the T-value $\leq$ −2.5 SD. (3) Patients who have the surgical indication. The exclusion criteria were as follows: (1) a previous history of spinal surgery, lower limb surgery, and severe spinal cord injury; (2) patients with idiopathic or congenital spinal deformity, spinal tumor, infection, or tuberculosis; and (3) pathological vertebral fracture.

The patients included in the study signed informed consent and then underwent long posterior segmental fixation surgery. After surgery, the spinal surgeon reviewed the patient's clinical data and calculated the score according to the scoring system and then predicted whether this patient will suffer from PJK (defined as the predictive outcome). At the follow-up of 2 years after surgery, the included patient was assessed whether they actually developed PJK (defined as the final follow-up outcome). The accuracy of the scoring system was evaluated by comparing the consistency between the predictive outcome and the final follow-up outcome.

Statistical analysis

The clinical characteristics were subjected to univariate logistic regression analysis, and the significant factors were evaluated by multivariate logistic regression analysis. The items of the scoring system were determined by multivariate logistic regression, and the weighted score of each item was based on the relative size of the OR. The optimal cutoff point was made by using ROC curves. $P < 0.05$ was the set of statistical significance. The SPSS version 10.0 software was used for statistical analysis.

Results

Derivation of the scoring system

A total of 88 patients were included in the derivation set, including 25 cases in the PJK group and 63 cases in the non-PJK group, and the incidence of postoperative PJK was 28.41%.

Univariate analysis showed that age > 70 years, BMI > 28 kg/m^2, BMD < −3.5 SD, preoperative PJA > 5°, preoperative SVA > 50 mm, preoperative PI-LL > 20°, PLC injury, UIV location = T$_{10}$~T$_{12}$, LIV location = S$_1$, and the number of fixed segments > 7 were the risk factors of postoperative PJK (Table 1).

Multivariate logistic regression analysis was carried out on the significant findings in univariate analysis and showed five clinical characteristics, namely, age > 70 years, BMI > 28 kg/m^2, BMD < −3.5 SD, preoperative PI-LL > 20°, and PLC injury were significant predictors of postoperative PJK (Table 2).

We developed a scoring system based on these five clinical characteristics that were conformed significant predictors of postoperative PJK. The variables with a significant predictive value for postoperative PJK were given the weighted scores according to the relative value of the OR in multivariate logistic regression analysis: age > 70 years, BMI > 28 kg/m^2, BMD < −3.5 SD, preoperative PI-LL > 20°, and PLC injury were weighted as 3 points, 1 point, 3 points, 2 points, and 2 points, respectively. The score was then calculated by determining the total number of points, ranging from 0 to 11 (Table 3).

The histogram distribution of the score values is shown in Figure 3. Remarkably, the PJK group showed a significantly higher score than the non-PJK group (7.80 points vs. 2.83 points, t=9.556, P<0.001). The optimal cutoff value of the predictive scoring system was 5 points, and the area under the curve (AUC) was 0.921 (95% CI: 0.875–0.985, P<0.001) (Figure 4).

Validation of the scoring system

Finally, a total of 42 patients were prospectively included in the validation set, including 12 cases in the PJK group and 30 cases in the non-PJK group according to the 2-year postoperative follow-up outcomes. A comparison of the performance of the score system on the derivation set and validation set is shown in Table 4. Based on the cuoff value of 5 points, the sensitivity and specificity of the scoring system for predicting postoperative PJK were 80.00% and 88.89%, respectively, in the derivation set and 75.00% and 80.00% in the validation set.

TABLE 1 Univariate analysis of related variables of predicting postoperative proximal junctional kyphosis (PJK).

Variables	PJK group (N=25)	Non-PJK group (N=63)	Sensitivity (%)	Specificity (%)	P-value
Gender = Male	10/25	19/63	40.00	69.84	0.376
Age > 70 years	16/25	8/63	64.00	87.30	<0.001
BMI > 28 kg/m^2	17/25	8/63	68.00	87.30	<0.001
BMD < −3.5 SD	19/25	13/63	76.00	79.37	<0.001
Smoking history	9/25	22/63	36.00	65.08	0.924
Fracture segment =T$_{12}$ or L$_1$	18/25	40/63	72.00	36.51	0.448
Preoperative PJA > 5°	12/25	15/63	44.00	76.19	0.026
Preoperative SVA > 50 mm	15/25	22/63	60.00	65.08	0.032
Preoperative PI-LL > 20°	17/25	16/63	68.00	74.60	<0.001
Preoperative PT > 30°	21/25	43/63	84.00	31.75	0.135
Preoperative SS > 25°	11/25	29/63	44.00	53.97	0.863
PLC injury	19/25	14/63	76.00	77.77	<0.001
UIV location = T$_{10}$~T$_{12}$	17/25	22/63	68.00	65.08	0.005
LIV location = S$_1$	16/25	23/63	64.00	63.49	0.019
Number of fixed segments > 7	16/25	25/63	64.00	60.31	0.039

PJK, proximal junctional kyphosis; BMI, body mass index; BMD, bone mineral density; SD, standard deviation; PJA, proximal junction angle; SVA, sagittal vertebral axis; PI, pelvic incidence; LL, lumbar lordosis; PT, pelvic tilt; SS, sacral slope; PLC, posterior ligamentous complex; UIV, upper instrumented vertebra; LIV, lower instrumented vertebra.

TABLE 2 Multivariate analysis of related variables of predicting postoperative PJK.

	Regression coefficient (β)	Odds ratio (OR)	P-value
Age > 70 years	3.16	23.57	<0.001
BMI > 28 kg/m^2	2.03	7.61	0.022
BMD < −3.5 SD	3.08	21.76	<0.001
Preoperative PI-LL > 20°	2.55	12.81	0.019
PLC injury	2.60	13.46	0.014

TABLE 3 The scoring system for predicting postoperative PJK.

Variables	Score
Age > 70 years	
Yes	3
No	0
BMI > 28 kg/m^2	
Yes	1
No	0
BMD < −3.5 SD	
Yes	3
No	0
Preoperative PI-LL > 20°	
Yes	2
No	0
PLC injury	
Yes	2
No	0

Discussion

Risk factors of proximal junctional kyphosis after surgery

In our present study, age >70 years was found a risk factor of postoperative PJK. A previous study reported that PJK was more likely to occur when people are over 55 years old, and the risk of PJK increased with age (11). Kim et al. and Yang et al. also found that PJK had a higher incidence in people whose age was over 60 years (12, 13). The reasons may be as follows: (1) in patients with spinal deformity, degenerative changes may occur in

paravertebral muscle tissue over time; (2) the degeneration of the paravertebral muscles can cause uneven stress in the discs and spinal facet joint, which can also accelerate the degeneration of the spine. Moreover, advanced age was also considered to be an important risk factor for revision surgery for PJK (7).

This study concluded that BMI >28 kg/m^2 predicted a high risk of postoperative PJK, and this conclusion was similar to the previous study. Previous research reported that patients with BMI >25 kg/m^2 were prone to suffer from PJK after surgery (14), which may be due to the following reasons: (1) the obese patient has a heavier load on the spine and implants, and the weight of the body moves forward, resulting in increased stress on adjacent segments of the surgery (15); (2) in obese patients, the strength of the paravertebral muscle was significantly weakened, and the dissection of the lamina and spinous muscles may further affect the muscle function and ultimately accelerate the proximal joint degeneration (16).

In this study, BMD < −3.5 SD was confirmed an independent risk factor for PJK after surgery. O'Leary et al. also showed that osteoporosis patients were more prone to develop PJK because the reduction of bone mass and the destruction of the bone ultrastructure can reduce the screw-holding force and increase the risk of the screw loosening and pulling out (17). Moreover, decreased bone mineral density was associated with decreased paravertebral muscle tissue, which, together, may lead to spinal instability and accelerate the development of PJK (18).

This study found that preoperative PI-LL > 20° was an independent predictor of postoperative PJK, which was similar to the result of the previous study. PI-LL was an important imaging index reflecting whether the lumbar lordosis angle was compatible with the shape of the pelvis, indicating the compensatory state of the sagittal balance of the spine (19).
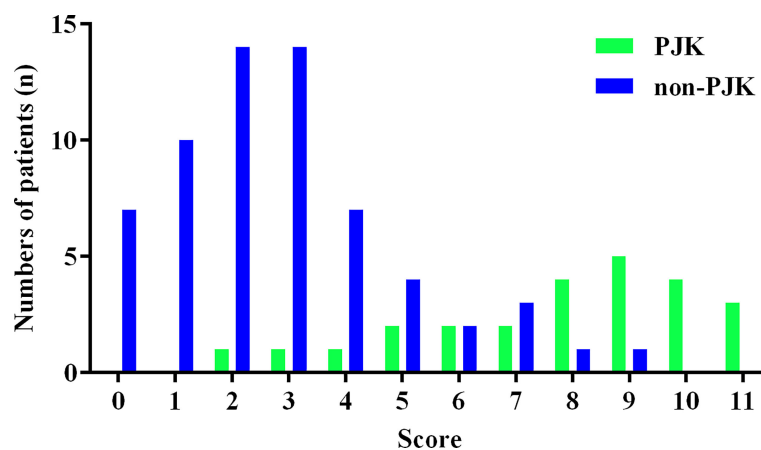
FIGURE 3
Histogram distribution of proximal junctional kyphosis (PJK) and non-PJK for each score of the predictive scoring system.

FIGURE 4
ROC curve analysis of the predictive scoring system. The optimal cutoff point based on the ROC curve analysis of scores was 5 points.
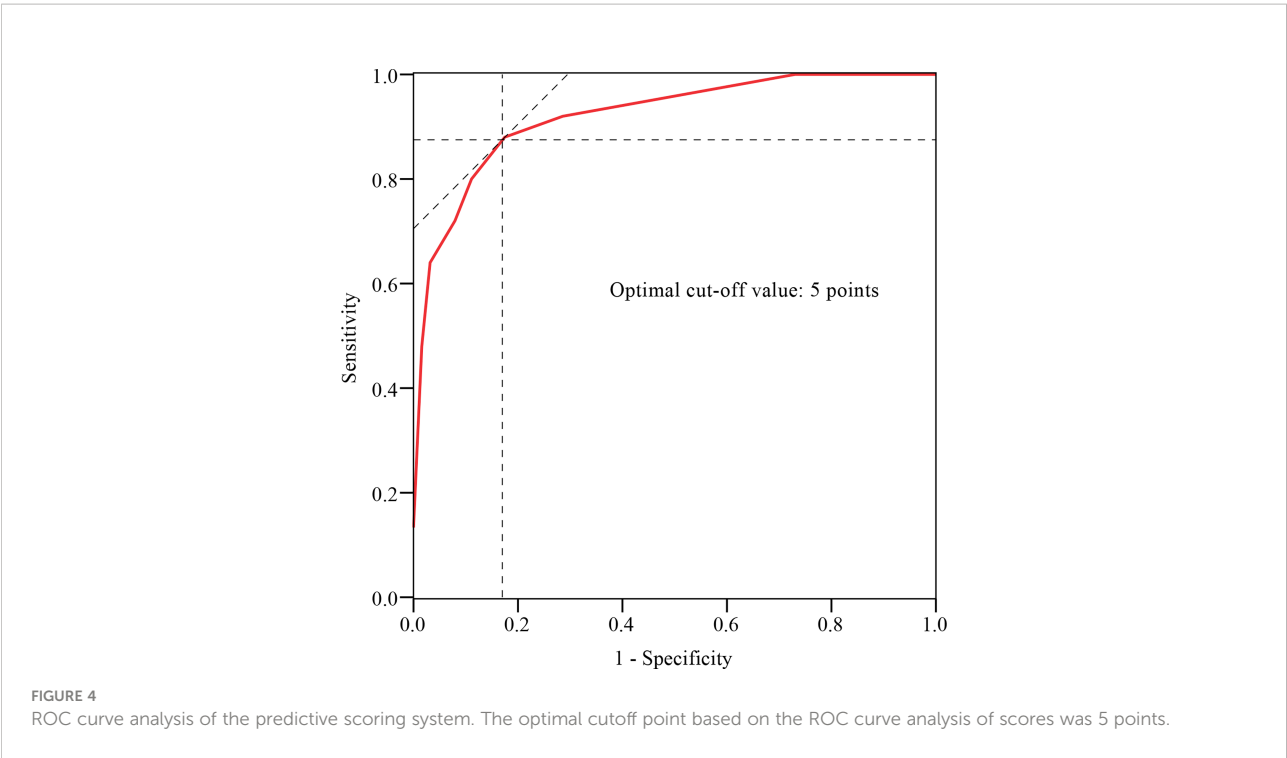
Senteler et al. found that higher PI-LL would increase the compression force and shear force of the $L_3 \sim L_5$-moving segments, leading to the accelerated degeneration of adjacent vertebral segments, thus increasing the risk of PJK (20). Aoki et al. found that when the preoperative PI-LL was between 10° and 20°, patients could obtain better clinical efficacy and the incidence of postoperative PJK was lower (21).

The results of our study suggested that PLC injury was an independent risk factor for postoperative PJK, and this conclusion was similar to a previous study (22). Surgery may change the local anatomy and biomechanics of the spine, leading to the development of PJK (23). For example, posterior spinal surgery may cause damage to proximal soft tissues, including supraspinal and intermuscular ligaments, and spinal facet joint capsule injuries, which may lead to local stability loss and PJK (24).

Managements to reduce the risk of postoperative proximal junctional kyphosis

Protective measures for patients' own factors mainly include: (a) lumbar back muscle function exercise. With the increase of a patients' age, paravertebral muscle atrophy and fat infiltration are serious, leading to the decline of paravertebral muscle strength, which is closely related to the occurrence of postoperative PJK (25). Therefore, appropriate muscle function training can help reduce the risk of PJK. (b) Lose weight. Weight loss can reduce the physical stress in the muscles and bones of the proximal junction, thereby reducing the risk of postoperative PJK (26). (c) Anti-osteoporosis treatment. Standard anti-osteoporosis treatment can improve bone calcium content and bone strength, which is conducive to maintain the stability of the

TABLE 4 Comparison of performance of the scoring system on derivation set and validation set.

		Derivation set			Validation set		
		PJK (score ≥ 6)	Non-PJK (score ≤ 5)	Total	PJK (score ≥ 6)	Non-PJK (score ≤ 5)	Total
Outcomes	PJK	20	5	25	9	3	12
	Non-PJK	7	56	63	6	24	30
	Total	27	61	88	15	27	42
Sensitivity (%)		80.00			75.00		
Specificity (%)		88.89			80.00		

spinal internal fixation system and reduce screw loosening and pulling out (27).

The imaging-related factors affecting postoperative PJK were mainly sagittal sequence reconstruction. Therefore, a preoperative full measurement and analysis of spinal imaging data and the intervention of high-risk groups by identifying high risk factors are of great significance to reduce the risk of PJK after surgery. We suggest that, according to the sagittal evaluation criteria and sagittal spinal sequence score of adult spinal deformity formulated by the Scoliosis Research Society (SRS) (28, 29), a reasonable surgical plan should be formulated to properly correct the deformity and take into account the overall balance of the spine.

Protective measures for surgery-related factors mainly include: (a) soft tissue protection. When exposing the distal vertebral region, attention should be paid to the protection of the muscle–ligament complex to minimize the damage to the supraspinal and interspinous ligaments. The separation of the paraspinal muscles at the junction should be carefully handled to retain the ligament structure and muscle attachment of the midline to the maximum extent (30). (b) The enhancement of ligaments in the junction area. Ligamentous augmentation by tendon transplantation or silk reinforcement can reduce the stress at the junction and increase the strength of PLC (31). (c) Non-rigid fixation (32). The use of lamina hooks in the proximal fixation area provides a relatively non-rigid fixation structure that helps to protect adjacent segmental facet joints and intervertebral discs, prevent excessive stress concentration in the junction area, and reduce the occurrence of PJK or PJF.

Our study also has limitations. First, this study was a retrospective analysis research. Second, the sample size was small and the follow-up time was short. Third, other potential factors that may contribute to PJK, such as disease course and comorbidity, were not analyzed in this study.

Conclusion

The scoring system, which was based on five clinical characteristics, namely, age > 70 years, BMI > 28 kg/m^2, BMD < −3.5 SD, preoperative PI-LL > 20°, and PLC injury, seems to achieve satisfactory sensitivity and specificity in predicting PJK after posterior internal fixation in elderly COVF patients. The risk of postoperative PJK in patients with a score of 6–11 is high, while the score of 0–4 is low.

Data availability statement

The raw data supporting the conclusions of this article will be made available by the authors, without undue reservation.

Ethics statement

The studies involving human participants were reviewed and approved by the Ethics Committee of the First Affiliated Hospital of Chongqing Medical University. The patients/participants provided their written informed consent to participate in this study.

Author contributions

Conception and design: XD and YO. Data analysis and interpretation: XD, GJ, and YZ. Data collection and management: XD, GJ, and WL. Manuscript writing and critical revisions: all authors. Overall responsibility: XD and YO. All authors have read and approved the manuscript.

Conflict of interest

The authors declare that the research was conducted in the absence of any commercial or financial relationships that could be construed as a potential conflict of interest.

Publisher's note

All claims expressed in this article are solely those of the authors and do not necessarily represent those of their affiliated organizations, or those of the publisher, the editors and the reviewers. Any product that may be evaluated in this article, or claim that may be made by its manufacturer, is not guaranteed or endorsed by the publisher.

Supplementary material

The Supplementary Material for this article can be found online at: http://www.frontiersin.org/article/10.3389/fendo.2022.923778/full#supplementary-material.

References

1. Prost S, Pesenti S, Fuentes S, Tropiano P, Blondel B, et al. Treatment of osteoporotic vertebral fractures. *Orthop Traumatol Surg Res* (2021) 107 (1S):102779. doi: 10.1016/j.otsr.2020.102779

2. Hao DJ, Yang JS, Tuo Y, Ge CY, He BR, Liu TJ, et al. Reliability and application of the new morphological classification system for chronic symptomatic osteoporotic thoracolumbar fracture. *J Orthop Surg Res* (2020) 15 (1):348. doi: 10.1186/s13018-020-01882-5

3. Xu Z, Hao D, Dong L, Yan L, He B, et al. Surgical options for symptomatic old osteoporotic vertebral compression fractures: a retrospective study of 238 cases. *BMC Surg* (2021) 21(1):22. doi: 10.1186/s12893-020-01013-1

4. Zuo XH, Zhu XP, Bao HG, Xu CJ, Chen H, Gao XZ, et al. Network meta-analysis of percutaneous vertebroplasty, percutaneous kyphoplasty, nerve block, and conservative treatment for nonsurgery options of acute/subacute and chronic osteoporotic vertebral compression fractures (OVCFs) in short-term and long-

term effects. *Med (Baltimore)* (2018) 97(29):e11544. doi: 10.1097/MD.00000000
00011544

5. Ishikawa Y, Watanabe K, Katsumi K, Ohashi M, Shibuya Y, Izumi T, et al. Short-versus long-segment posterior spinal fusion with vertebroplasty for osteoporotic vertebral collapse with neurological impairment in thoracolumbar spine: a multicenter study. *BMC Musculoskelet Disord* (2020) 21(1):513. doi: 10.1186/s12891-020-03539-0

6. Tamai K, Terai H, Suzuki A, Nakamura H, Watanabe K, Katsumi K, et al. Risk factors for proximal junctional fracture following fusion surgery for osteoporotic vertebral collapse with delayed neurological deficits: A retrospective cohort study of 403 patients. *Spine Surg Relat Res* (2018) 3(2):171–7. doi: 10.22603/ssrr.2018-0068

7. Jang HJ, Park JY, Kuh SU, Chin DK, Kim KS, Cho YE, et al. The fate of proximal junctional vertebral fractures after long-segment spinal fixation : Are there predictable radiologic characteristics for revision surgery? *J Korean Neurosurg Soc* (2021) 64(3):437–46. doi: 10.3340/jkns.2020.0236

8. Goldstein CL, Brodke DS, Choma TJ. Surgical management of spinal conditions in the elderly osteoporotic spine. *Neurosurgery* (2015) 77 Suppl 4: S98–107. doi: 10.1227/NEU.0000000000000948

9. Bossuyt PM, Reitsma JB, Bruns DE, Gatsonis CA, Glasziou PP, Irwig L, et al. STARD 2015: an updated list of essential items for reporting diagnostic accuracy studies. *BMJ* (2015) 351:h5527. doi: 10.1136/bmj.h5527.

10. Du X, She Y, Ou Y, Zhu Y, Luo W, Jiang D., et al. A scoring system for outpatient orthopedist to preliminarily distinguish spinal metastasis from spinal tuberculosis: A retrospective analysis of 141 pa tients. *Dis Markers* (2021) 2021:6640254. doi: 10.1155/2021/6640254

11. Cerpa M, Sardar Z, Lenke L. Revision surgery in proximal junctional kyphosis. *Eur Spine J* (2020) 29(Suppl 1):78–85. doi: 10.1007/s00586-020-06320-y

12. Kim HJ, Bridwell KH, Lenke LG, Park MS, Ahmad A, Song KS, et al. Proximal junctional kyphosis results in inferior SRS pain subscores in adult deformity patients. *Spine (Phila Pa 1976)* (2013) 38(11):896–901. doi: 10.1097/BRS.0b013e3182815b42

13. Yang J, Khalifé M, Lafage R, Kim HJ, Smith J, Shaffrey CI, et al. What factors predict the risk of proximal junctional failure in the long term, demographic, surgical, or radiographic?: results from a time-dependent ROC curve. *Spine (Phila Pa 1976)* (2019) 44(11):777–84. doi: 10.1097/BRS.0000000000002955

14. Agarwal N, Angriman F, Goldschmidt E, Zhou J, Kanter AS, Okonkwo DO, et al. Relationship between body mass index and sagittal vertical axis change as well as health-related quality of life in 564 patients after deformity surgery. *J Neurosurg Spine* (2019) 31(5):1–6. doi: 10.3171/2019.4.SPINE18485

15. Yagi M, Fujita N, Okada E, Tsuji O, Nagoshi N, Asazuma T, et al. Fine-tuning the predictive model for proximal junctional failure in surgically treated patients with adult spinal deformity. *Spine (Phila Pa 1976)* (2018) 43(11):767–73. doi: 10.1097/BRS.0000000000002415

16. Pennington Z, Cottrill E, Ahmed AK, Passias P, Protopsaltis T, Neuman B, et al. Paraspinal muscle size as an independent risk factor for proximal junctional kyphosis in patients undergoing thoracolumbar fusion. *J Neurosurg Spine* (2019) 31 (3):380–8. doi: 10.3171/2019.3.SPINE19108

17. O'Leary PT, Bridwell KH, Lenke LG, Good CR, Pichelmann MA, Buchowski JM, et al. Risk factors and outcomes for catastrophic failures at the top of long pedicle screw constructs: a matched cohort analysis performed at a single center. *Spine (Phila Pa 1976)* (2009) 34(20):2134–9. doi: 10.1097/BRS.0b013e3181b2e17e

18. Kim DK, Kim JY, Kim DY, Rhim SC, Yoon SH. Risk factors of proximal junctional kyphosis after multilevel fusion surgery: More than 2 years follow-up data. *J Korean Neurosurg Soc* (2017) 60(2):174–80. doi: 10.3340/jkns.2016.0707.014

19. Hey HWD, Tan JH, Ong B, Kumar A, Liu G, Wong HK., et al. Pelvic and sacral morphology and their correlation with pelvic incidence, lumbar lordosis, and lumbar alignment changes between standing and sitting postures. *Clin Neurol Neurosurg* (2021) 211:107019. doi: 10.1016/j.clineuro.2021.107019

20. Senteler M, Weisse B, Snedeker JG, Rothenfluh DA. Pelvic incidence-lumbar lordosis mismatch results in increased segmental joint loads in the unfused and fused lumbar spine. *Eur Spine J* (2014) 23(7):1384–93. doi: 10.1007/s00586-013-3132-7

21. Aoki Y, Nakajima A, Takahashi H, Sonobe M, Terajima F, Saito M, et al. Influence of pelvic incidence-lumbar lordosis mismatch on surgical outcomes of short-segment transforaminal lumbar interbody fusion. *BMC Musculoskelet Disord* (2015) 16:213. doi: 10.1186/s12891-015-0676-1

22. Hostin R, McCarthy I, O'Brien M, Bess S, Line B, Boachie-Adjei O, et al. Incidence, mode, and location of acute proximal junctional failures after surgical treatment of adult spinal deformity. *Spine (Phila Pa 1976)* (2013) 38(12):1008–15. doi: 10.1097/BRS.0b013e318271319c

23. Zhu WY, Zang L, Li J, Guan L, Hai Y. A biomechanical study on proximal junctional kyphosis following long-segment posterior spinal fusion. *Braz J Med Biol Res* (2019) 52(5):e7748. doi: 10.1590/1414-431x20197748

24. Yagi M, Nakahira Y, Watanabe K, Nakamura M, Matsumoto M, Iwamoto M. The effect of posterior tethers on the biomechanics of proximal junctional kyphosis: The whole human finite element model analysis. *Sci Rep* (2020) 10 (1):3433. doi: 10.1038/s41598-020-59179-w

25. Gengyu H, Jinyue D, Chunjie G, Bo Z, Yu J, Jiaming L, et al. The predictive value of preoperative paraspinal muscle morphometry on complications after lumbar surgery: a systematic review. *Eur Spine J* (2022) 31(2):364–79. doi: 10.1007/s00586-021-07052-3

26. Soroceanu A, Burton DC, Diebo BG, Smith JS, Hostin R, Shaffrey CI, et al. Impact of obesity on complications, infection, and patient-reported outcomes in adult spinal deformity surgery. *J Neurosurg Spine* (2015) 23(5):656–64. doi: 10.3171/2015.3.SPINE14743

27. Karikari IO, Metz LN. Preventing pseudoarthrosis and proximal junctional kyphosis: How to deal with the osteoporotic spine. *Neurosurg Clin N Am* (2018) 29 (3):365–74. doi: 10.1016/j.nec.2018.03.005

28. Schwab F, Ungar B, Blondel B, Buchowski J, Coe J, Deinlein D, et al. Scoliosis research society-Schwab adult spinal deformity classification: a validation study. *Spine (Phila Pa 1976)* (2012) 37(12):1077–82. doi: 10.1097/BRS.0b013e31823e15e2

29. Yilgor C, Sogunmez N, Boissiere L, Yavuz Y, Obeid I, Kleinstück F, et al. Global alignment and proportion (GAP) score: Development and validation of a new method of analyzing spinopelvic alignment to predict mechanical complications after adult spinal deformity surgery. *J Bone Joint Surg Am* (2017) 99(19):1661–72. doi: 10.2106/JBJS.16.01594

30. Yuan L, Zeng Y, Chen Z, Li W, Zhang X, Mai S.. Degenerative lumbar scoliosis patients with proximal junctional kyphosis have lower muscularity, fatty degeneration at the lumbar area. *Eur Spine J* (2021) 30(5):1133–43. doi: 10.1007/s00586-020-06394-8

31. Bess S, Harris JE, Turner AW, LaFage V, Smith JS, Shaffrey CI, et al. The effect of posterior polyester tethers on the biomechanics of proximal junctional kyphosis: a finite element analysis. *J Neurosurg Spine* (2017) 26(1):125–33. doi: 10.3171/2016.6.SPINE151477

32. Lange T, Schmoelz W, Gosheger G, Eichinger M, Heinrichs CH, Boevingloh AS, et al. Is a gradual reduction of stiffness on top of posterior instrumentation possible with a suitable proximal implant? a biomechanical study. *Spine J* (2017) 17 (8):1148–55. doi: 10.1016/j.spinee.2017.03.021

Effect of Body Surface Area on Severe Osteoporotic Fractures: A Study of Osteoporosis in Changsha China

Xi-Yu Wu[1], Hong-Li Li[2], Yi Shen[3], Li-Hua Tan[4], Ling-Qing Yuan[1], Ru-Chun Dai[1], Hong Zhang[1], Yi-Qun Peng[1], Zhong-Jian Xie[1] and Zhi-Feng Sheng[1]*

[1] Hunan Provincial Key Laboratory of Metabolic Bone Diseases, National Clinical Research Center for Metabolic Diseases, Department of Metabolism and Endocrinology, The Second Xiangya Hospital of Central South University, Changsha, China, [2] Department of Endocrinology, The First Hospital of Lanzhou University, Lanzhou, China, [3] Department of Orthopaedics, The Second Xiangya Hospital, Central South University, Changsha, China, [4] Department of Radiology, The Second Xiangya Hospital, Central South University, Changsha, China

Clinical vertebral fractures and femoral neck fractures are severe osteoporotic fractures that increase morbidity and mortality. Anthropometric variables are associated with an increased risk of osteoporotic fractures, but it is not clear whether body surface area (BSA) has an effect on clinically severe osteoporotic fractures. The study included total of 3,694 cases of clinical vertebral fractures and femoral neck fractures (2,670 females and 1,024 males) and 3,694 controls without fractures who were matched with the cases by sex and age. There was a significant positive correlation between BSA and bone mineral density (BMD) in female and male fracture patients (females: $r = 0.430–0.471$, $P < 0.001$; males: $r = 0.338–0.414$, $P < 0.001$). There was a significant systematic increase in BMD in both genders at various skeletal sites, grouped by BSA quartile. The osteoporosis rates of the lumbar spine (97.9%), femoral neck (92.4%) and total hip (87.1%) in the female Q1 group were significantly higher than those in the Q4 group ($P < 0.001$), which were 80.0%, 57.9% and 36.9%, respectively, in the Q4 group; the osteoporosis rates of the lumbar spine, femoral neck, and total hip were 53.9%, 59.4%, and 36.3% in the male Q1 group, and 15.2%, 21.9%, and 7.03% in the Q4 group, which were significantly lower than those in the Q1 group ($P < 0.001$). In age-adjusted Cox regression models, the risk of fracture in the remaining three groups (Q2, Q3, and Q4) for weight, BMI, and BSA for both genders, compared with the highest quartile (Q1 by descending quartile stratification) were significantly higher. In models adjusted for age and BMD, only men in the BSA Q3 (HR = 1.55, 95% CI = 1.09–2.19) and BSA Q4 groups (HR = 1.41, 95% CI = 1.05–1.87) had significantly higher fracture risks. In models adjusted for age, height, weight, BMI, and BSA, low BMD was the greatest fracture risks for both sexes. Our results showed that BSA was closely related to BMD, prevalence of osteoporosis, and fracture risk, and that a decline in BSA may be a new potential risk factor for osteoporotic fractures in Chinese men.

Keywords: osteoporosis, osteoporotic fracture, body surface area, bone mineral density, fracture risk

BACKGROUND

Osteoporosis is a systemic bone disease that is characterized by a decrease in bone mass, a deterioration of the microstructure of bone tissue, and a decrease in bone strength, leading to an increase in bone fragility and susceptibility to fractures (1). Clinical vertebral and femoral neck fractures are severe osteoporotic fractures that result in increased disability, morbidity, and mortality (2–11) higher healthcare costs (11–15), and affect health-related quality of life (16–21). Although studies have shown a very low incidence of osteoporotic fractures in the Chinese mainland population (22), the incidence of osteoporotic fractures is increasing rapidly with the urbanization and aging of the Chinese population (23). It is estimated that by 2050, half of the world's osteoporotic fractures will occur in Asia, primarily in China (24). As a result, osteoporotic fractures will become an even more serious public health problem in the Chinese mainland.

It is well known that low bone mineral density (BMD) is an important risk factor for osteoporotic fractures (24, 25), but there are many other risk factors for osteoporotic fractures besides BMD (11, 26, 27), such as age, sex, height, weight, body mass index (BMI), past fragility fractures, long-term glucocorticoid, a history of falls, parental hip fractures, long-term smoking, long-term drinking, rheumatoid arthritis, dementia, and various types of secondary osteoporosis. Therefore, most fragility fractures occur in non-osteoporotic individuals (28, 29). Studies have shown that the relationship between anthropometric indicators (height, weight, and BMI) and fracture risk varies by skeletal site, including the risk of hip fractures, clinical vertebral fractures, and wrist fracture in women, which decreases significantly with increasing BMI (30). Moreover, the risk of ankle fractures in women increases with weight gain, the risk of upper arm/shoulder and collarbone fractures decreases with height, and the risk of pelvic and rib fractures have a negative association with being underweight, and a positive association with being obese (30). A higher BMI leads to a significant increase in the risk of ankle, calf, and humerus fractures, but there is a significant decrease in hip and wrist fractures among obese women (31). A US study found that 58% of men with fractures were obese, that 62% of hip fractures and 68% of non-vertebral fractures occurred in overweight and obese men, and that a higher BMI in men was associated with an increased risk of fractures (32). Body surface area (BSA) is an anthropometric parameter that reflects body size, and our previous studies have found that age-related BSA is positively associated with BMD and the prevalence of osteoporosis at different skeletal sites in the reference population (33). However, whether BSA is associated with osteoporotic fractures is not clear. The purpose of this study was to investigate the effect of BSA, which reflects body size, on clinical vertebral fractures and femoral neck fractures, in an attempt to discover new potential risk factors for the prevention of clinically severe osteoporotic fractures. Therefore, we decided to study the relationships of BSA and BMD with the prevalence of osteoporosis in patients with clinically severe osteoporotic fractures, and the effect of BSA on severe osteoporotic fractures.

MATERIALS AND METHODS

Participants

The study was conducted from March 2011 to October 2021 at the Second Xiangya Hospital of Central South University, Changsha, China. Patients diagnosed with osteoporotic fractures by imaging were considered potential subjects for the case group. The inclusion criteria for severe osteoporotic fractures were patients who came to the hospital with symptoms of vertebral fractures or femoral neck fractures, patients who reported low-injury fractures that occurred from falling from a standing height or less, or occurred without falling. A vertebral body fracture was confirmed by a radiologist based on a lateral vertebral radiograph and a femoral neck fracture was confirmed a by radiologist based on a proximal femoral radiograph, using semi-quantitative methods (34). Patients were excluded from the study if their fractures were caused by trauma (such as a car accident or a fall from a chair or higher) or they had local pathological fractures caused by cancer, bilateral hip fractures, non-vertebral fractures, or non-femoral neck fractures. A total of 3,694 patients with severe osteoporotic fractures met the inclusion criteria, including 2,670 women, who were 40–94 years-old and had a mean (± SD) age of 67.5 ± 8.61 years, and 1,024 men, who were 40–100 years-old and had a mean age of 65.8 ± 12.4 years. These patients had 3,181 vertebral fractures (2,296 females and 885 males) and 513 femoral neck fractures (374 females and 139 males).

The data of 3,694 patients assigned to the control group were obtained from a reference population of a BMD database, which was established by us before the study (35, 36). A 1:1 ratio between the control group and the case group was used, according to sex and age. The inclusion criterion for the control group was having no history of a low- or a high-injury fracture, and the exclusion criteria were osteosclerosis, skeletal fluorosis, or abnormally increased BMD. This study was approved by the Ethics Committee of Second Xiangya Hospital affiliated with the Central South University. All the participants were of Han ethnicity.

BMD Measurement

The lumbar spine (L1–L4), femoral neck, and total hip BMDs were measured by fan-beam dual-energy X-ray (DXA) absorptiometry (Hologic Delphi A; Hologic, Bedford, MA, USA). If the lumbar vertebrae of patients with vertebral body fractures were filled with postoperative artificial bone cement or contained installed metal brackets, these lumbar vertebrae were excluded from the analysis. The right hip was measured if the patient had a left femoral neck fracture or had a hip replacement. If patients had bilateral femoral neck or hip fractures, the hip measurements were discarded and these patients were excluded from the study. BMD was measured twice in 33 subjects. The root-mean-square coefficients of precision (root-mean-square CV; RMSCV) were 0.86%, 1.17%, and 0.88% for the lumbar spine, femoral neck, and total hip, respectively. The long-term (> 17 years) CV of routine quality control phantom measured daily by DXA bone densitometer was < 0.45%. Using our own BMD reference database for women and men (35, 36), we calculated the sex-specific BMD T-score of the lumbar spine, femoral neck, and total hip. According to the World Health Organization

(WHO) definition (37), participants with a T-score > −1.0 had normal BMD; those with a −2.5 < T-score ≤ −1.0, whereas those with a T-score ≤ −2.5, when compared with the same sex peak BMD, were classified as having osteopenia and osteoporosis, respectively.

BSA Estimation and BMI Classification

BSA was estimated based on the average height and weight of Chinese adults (38); its estimation formula for males was $BSA = 79.8106 \times H^{0.7271} \times W^{0.3980}$; and its estimation formula for females was $BSA = 84.4673 \times H^{0.6997} \times W^{0.4176}$; where BSA was expressed in cm^2, height (H) in cm, and body weight (W) in kg. According to the BMI classification criteria for overweight and obesity in Chinese adults (39), a BMI < 18.5 kg/m^2 was considered a low body weight, a BMI = 18.5–23.9 kg/m^2 was considered a normal body weight, a BMI = 24.0–27.9 kg/m^2 was considered overweight, and a BMI ≥ 28.0 kg/m^2 was considered obese.

Statistical Analysis

All analyses were performed using SPSS V23.0 for Windows (SPSS Inc., Chicago, IL, USA). Kolmogorov-Smirnov test (K-S test) was used to explore normal distribution of the data. The K-S test results showed that the age, height and weight of the subjects of both genders and the age at menopause (AM) and years since menopause (YSM) of women did not meet the normal distribution criteria (Z = 1.495–2.471, P = 0.023 to < 0.001), the rest of the indicators (BMI, BSA and BMD) basically met the normal distribution standard (Z = 0.466–1.306, P = 0.982–0.066). The indicators that did not meet the standard of normal distribution were expressed by median and range. If there was a significant difference between groups, test for two independent samples was used. Indicators meeting the normal distribution criteria were expressed as mean and standard deviation (SD) and one-way analysis of variance (ANOVA). The relationship between BSA and BMD at various skeletal sites was analyzed using Pearson's correlation. The patients in the case group were divided into quartiles according to their BSA, and the differences in mean BMD, prevalence of osteoporosis, and fracture risks were compared among these four subgroups. The relationships of different variables with the risk of osteoporotic fracture were analyzed by multivariate Cox regression models, which produced multivariate hazard ratios (HRs) for fractures and their 95% confidence intervals (CIs). The multivariate analysis included adjustments for age, height, weight, BMI, and BSA or BMD. The differences in the prevalence of osteoporosis and osteopenia between genders and across different groups of fracture patients were compared using the chi-square test. A P < 0.05 was considered statistically significant.

RESULTS

Characteristics of the Participants

The rates of obesity, overweight, and normal BMI in fracture patients were, respectively, 5.24%, 28.6%, and 56.0% for females, and 4.88%, 23.0%, and 60.7% for males. **Table 1** showed that the median age of each sex in the case group was exactly the same as that of the control group, as the sex and age of the case group were exactly the same as the control group. In both sexes, the median height, weight, BMI, BSA, and BMD at each bone site in the case group were significantly lower than the medians in the control group. The median age at menopause (AM) of females in the case group was significantly younger than the median of females in the control group, and the median years since menopause (YSM) was significantly older in the case group than that in the control group. The median age and YSM of females in the single vertebral fracture (SVF) subgroup were significantly lower than those in the multiple vertebral (2 or more) fracture (MVF) and multiple sites fracture (MSF) subgroups, while their FN-BMD and Hip-BMD were significantly higher than those in the MVF and MSF subgroups (**Table 1**). The median height, weight, and BSA of the females in the SVF group were significantly higher than the medians of the females in the MVF group. The median age, SYM, height, weight, BSA, and LS-BMD of the MVF group were significantly lower than the medians of the MSF group. Among the male cases, the median age of the SVF subgroup was significantly lower than the medians of the MVF and MSF subgroups, and their FN-BMD and Hip-BMD were significantly higher than those of the MVF and MSF subgroups (**Table 1**). The median weight, BMI, and BSA of the males in the SVF subgroup were significantly higher than the medians in the MVF subgroup. The median age, height, BSA, and LS-BMD in the MVF subgroup were significantly lower than the medians in the MSF subgroup.

Among the cases (**Table 2**), the prevalence of osteoporosis in the lumbar spine, femoral neck, and total hip were, respectively, 89.6%, 76.6%, and 61.9% in female cases and 31.2%, 39.6%, and 19.7% in male cases. The rate of osteoporosis was significantly higher in female cases than male cases, with the majority of female cases suffering from osteoporosis. The rate of low bone mass in the lumbar spine, femoral neck and total hip were, respectively, 9.33%, 21.7%, and 34.1% in female cases and 58.5%, 56.9%, and 64.5% in male cases, and the rates of low bone mass and normal BMD were also significantly higher in male cases than female cases.

Association of BSA With the BMD and Prevalence of Osteoporosis

Figure 1 showed the correlation between BSA and BMD in the case group by sex and skeletal site. BSA had a significant positive correlation with BMD in females and males, but the correlations between BSA and BMD (r = 0.430–0.471, P < 0.001) were higher for females than they were for males (r = 0.338–0.414, P < 0.001). The correlation of BSA with Hip-BMD was higher than the correlation of BSA with LS-BMD and FN-BMD. **Figure 2** showed the BSA of the case group stratified into quartiles, and compared the mean BMD of each BSA quartile for three skeletal sites. The analyses of the BMD of males and females found BMD exhibited a significant positive trend across BSA quartiles in both sexes at each site; that was, Q1<Q2<Q3<Q4. **Figure 3** showed the BSA of the case group stratified into quartiles, and compared the prevalence of osteoporosis for each BSA quartile. The analyses

TABLE 1 | Comparison of basic characteristics among cases of fractures and controls.

Parameter	Control	Case	Fracture subgroup		
			SVF	MVF	MSF
Female					
n (%)	2670	2670	855 (32.0)	1201 (45.0)	614 (23.0)
Age (years)[a]	68.0 (40–94)	68.0 (40–94)	67.0 (40–93)[cd]	68.0 (40–94)[f]	70.0 (40–93)[c]
AM (years)[a]	50.0 (40–64)	49.0 (40–60)[b]	48.0 (40–58)[c]	49.0 (40–60)	49.0 (40–59)
YSM (years)[a]	18.0 (1–54)	19.0 (1–47)[b]	18.0 (1–43)[cd]	19.0 (1–44)[f]	21.0 (1–47)[cd]
Height (cm)[a]	152.0 (134–170)	150.0 (112–173)[b]	151.5 (130–172)[ce]	149.0 (121–173)[cf]	152.0 (112–173)[c]
Weight (kg)[a]	55.0 (30–94)	51.0 (26–93)[b]	52.0 (26–82.5)[ce]	50.0 (28–93)[cf]	52.0 (31–75)[c]
BMI (kg/m^2)	23.8 ± 3.46	22.7 ± 3.33[b]	22.7 ± 3.38	22.6 ± 3.42	22.7 ± 3.04
BSA (m^2)	1.51 ± 0.12	1.46 ± 0.13[b]	1.48 ± 0.12[ce]	1.44 ± 0.13[cf]	1.47 ± 0.12[c]
LS-BMD (g/cm^2)	0.760 ± 0.136	0.620 ± 0.110[b]	0.635 ± 0.099[cd]	0.592 ± 0.109[cf]	0.654 ± 0.115[c]
FN-BMD (g/cm^2)	0.612 ± 0.109	0.507 ± 0.093[b]	0.529 ± 0.086[cd]	0.496 ± 0.098[c]	0.498 ± 0.089[c]
Hip-BMD (g/cm^2)	0.688 ± 0.127	0.585 ± 0.114[b]	0.615 ± 0.105[cd]	0.570 ± 0.119[c]	0.573 ± 0.109[c]
Male					
n (%)	1024	1024	381 (37.2)	436 (42.6)	207 (20.2)
Age (years)[a]	66.0 (40–100)	66.0 (40–100)	62.0 (40–100)[cd]	66.0 (40–95)[f]	72.0 (40–96)[c]
Height (cm)[a]	165.0 (142–188)	163.0 (132–180)[b]	163.0 (132–180)[f]	162.0 (142–179)[cf]	165.0 (142–178)[c]
Weight (kg)[a]	67.0 (34–107)	59.0 (30–100)[b]	60.0 (30–100)[e]	56.0 (31–91)[c]	60.0 (36–90)
BMI (kg/m^2)	24.6 ± 3.19	22.4 ± 3.31[b]	22.6 ± 3.18[e]	21.9 ± 3.26	22.3 ± 3.59
BSA (m^2)	1.74 ± 0.13	1.64 ± 0.15[b]	1.65 ± 0.14[e]	1.61 ± 0.15[cf]	1.66 ± 0.15[c]
LS-BMD (g/cm^2)	0.971 ± 0.148	0.720 ± 0.120[b]	0.731 ± 0.088[d]	0.687 ± 0.117[cf]	0.770 ± 0.153[c]
FN-BMD (g/cm^2)	0.741 ± 0.123	0.582 ± 0.102[b]	0.599 ± 0.087[cd]	0.577 ± 0.102	0.561 ± 0.122[c]
Hip-BMD (g/cm^2)	0.875 ± 0.133	0.691 ± 0.124[b]	0.714 ± 0.111[cd]	0.677 ± 0.125[c]	0.678 ± 0.138

[a]Values are median (range). Other values are mean ± SD.

AM, age at menopause; YSM, years since menopause; BMI, body mass index; BSA, body surface area; LS, lumbar spine; BMD, bone mineral density; FN, femoral neck; Hip, total hip; SVF, single vertebral fracture; MVF, multiple vertebral (2 or more) fracture; MSF, multiple sites fracture (vertebral accompany other sites and femoral neck fractures).

[b]P = 0.014 to < 0.001 compared with control.

[c]P = 0.045 to < 0.001 compared with case.

[d]P = 0.008 to < 0.001 compared with MVF and MSF.

[e]P = 0.002 to < 0.001 compared with MVF.

[f]P = 0.005 to < 0.001 compared with MSF.

found that the prevalence of osteoporosis was highest when BSA was lowest (Q1) for both sexes at all three skeletal sites. The lowest BSA quartile (Q1) had the highest prevalence and highest BSA quartile (Q4) had the lowest prevalence for both sexes at all three sites. However, only the female femoral neck and total hip showed significant sequential decreases in the prevalence of osteoporosis across quantiles; that was, prevalence exhibited a trend of Q1>Q2>Q3>Q4.

Fracture Hazard Ratios

Table 3 showed the fracture hazard ratios (HRs) of seven variables with the anthropometric index and BMD for each quartile of each variable (Q1 = highest to Q4 = lowest) based on multivariate Cox regression. In the age-adjusted models, regardless of sex, the fracture hazard ratios (HR1) for weight, BMI, BSA, LS-BMD, FN-BMD, and Hip-BMD were significantly higher in the Q2, Q3, and Q4 groups (P = 0.019 to < 0.001) than the reference group (Q1); only the female Q4 group with the smallest height (height ≤ 147.9 cm) had a significantly higher HR1 (HR1 = 1.38, P < 0.001); HR1 also was significantly higher in the Q3 and Q4 groups of males. In the models adjusted for age and BMI, the increases in HR2 for each quantile of weight, BMI, and BSA of females were no longer statistically significant, but there was a significant increase in HR2 for the height Q4 group of females (HR2 = 1.12, P = 0.017). The HR2 was also significantly higher in the BSA Q3 (HR2 = 1.55, P = 0.015) and BSA Q4 (HR2 = 1.41, P = 0.020) groups of males. In the models adjusted for age, height, weight, BMI, and BSA, the HR2 in the female each quantile (Q2 to Q4) varied from 2.30 to 4.42 as BMD

TABLE 2 | Number and rates of osteoporosis, osteopenia and normal BMD in fractures using gender specific T-scores.

Skeletal site	Female (n = 2670)			Male (n = 1024)		
	Osteoporosis n (%)	Osteopenia n (%)	NBMD n (%)	Osteoporosis n (%)[c]	Osteopenia n (%)[c]	NBMD n (%)[c]
Lumbar spine	2393 (89.6)[a]	249 (9.33)[a]	28 (1.05)[b]	319 (31.2)[a]	599 (58.5)[e]	106 (10.4)[a]
Femoral neck	2044 (76.6)[b]	579 (21.7)[b]	47 (1.76)[b]	406 (39.6)[b]	583 (56.9)[be]	35 (3.42)[b]
Total hip	1652 (61.9)	911 (34.1)	107 (4.01)	202 (19.7)	660 (64.5)[e]	162 (15.8)

NBMD, normal bone mineral density.

[a]P = 0.006 to < 0.001 compared with femoral neck and total hip on same parameter.

[b]P = 0.001 to < 0.001 compared with total hip on same parameter.

[c]P = 0.003 to < 0.001 compared with female on same parameter.

[e]P < 0.001 compared with osteoporosis on same parameter.
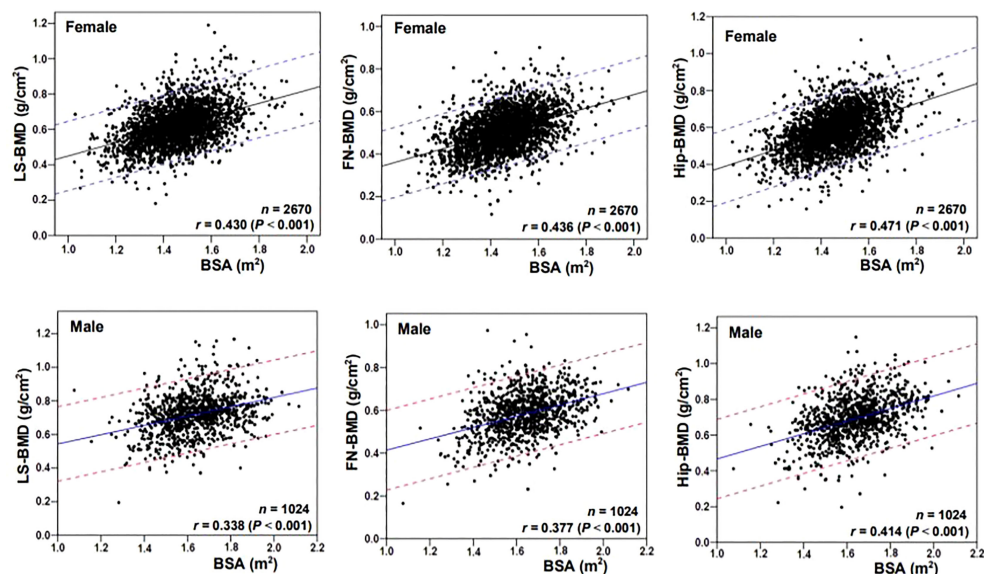
FIGURE 1 | Correlation scatter diagrams of the body surface area (BSA) with BMD at various skeletal sites. LS, lumbar spine; BMD, bone mineral density; FN, femoral neck; Hip, total hip.

decreased; in the male each quantile, the same measures varied from 3.48 to 8.74 (**Table 3**). **Table 4** showed the fracture HRs based on Cox regression, according to the diagnostic criteria for osteoporosis, with normal BMD as the reference. The HRs for low bone mass (LBM) and osteoporosis varied by gender and skeletal site, with the HRs of females with lumbar spine, femoral neck, and total hip osteoporosis being, respectively, about 1.6 (4.09/2.55), 2.5 (10.9/4.29), and 1.2 times (4.03/3.33) higher than those for LBM, and the fracture HRs of females with osteoporosis was greater than that of females with LBM. The HRs of males with LBM for the lumbar spine, femoral neck, and total hip were approximately 3.2 (26.1/8.08), 1.1 (13.1/12.2), and 0.8 times (9.18/11.7) higher, respectively, than those for osteoporosis, and the HRs of the lumbar spine and femoral neck of males with LBM were somewhat greater than those with osteoporosis. However, the fracture HRs of the total hip of

males with LBM were somewhat lower than males with osteoporosis.

DISCUSSION

This paper reported the results of a sex- and age-matched case-control study, in which patients with clinically severe osteoporotic vertebral fractures, and femoral neck fractures served as cases, and the control group was a reference population (35, 36) without any fractures. We found that anthropometric indicators (height, weight, BMI, and BSA) and BMD at various skeletal sites were associated with fracture risks that were significantly lower in both genders in the case group than in the control group, suggesting that the overall decrease in
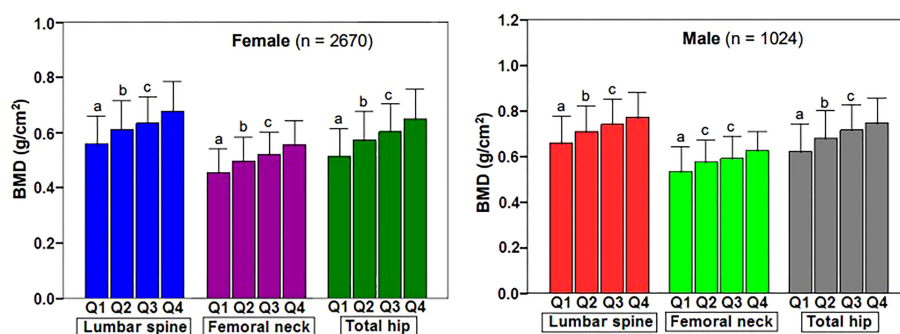
FIGURE 2 | Changes of BMD at various skeletal sites in body surface area of fracture patients stratified by quartile. BMD, bone mineral density; Q1, first quartile; Q2, second quartile; Q3, third quartile; Q4, fourth quartile; LS, lumbar spine (L1–L4); FN, femoral neck; TH, total hip. [a]$P < 0.001$ compared with Q2, Q3 and Q4. [b]$P = 0.001$ to < 0.001 compared with Q3 and Q4. [c]$P = 0.003$ to < 0.001 compared with Q4.
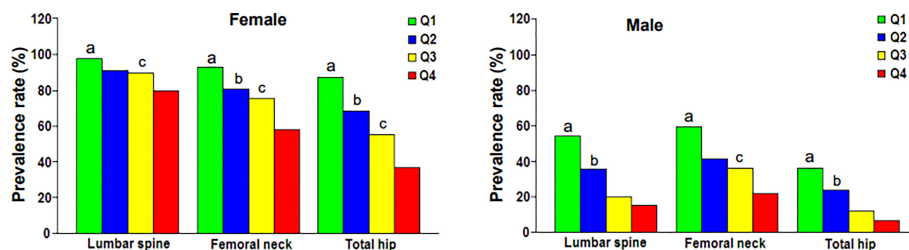
FIGURE 3 | Prevalence rate of osteoporosis at various skeletal regions according to body surface area quartile. Q1, first quartile; Q2, second quartile; Q3, third quartile; Q4, fourth quartile. [a]P = 0.003 to < 0.001 compared with Q2, Q3 and Q4. [b]P = 0.028 to < 0.001 compared with Q3 and Q4. [c]P = 0.001 to < 0.001 compared with Q4.

these parameters may be the direct cause of fractures. Regardless of gender, the MVF subgroup of the case group had the lowest BMD, which may be an important cause of MVFs. Due to multiple vertebral compression fractures, the height of the MVF subgroup was significantly lower in both genders. In the MSF subgroup, the proportion of patients with femoral neck fractures was greater (60.9% in women and 67.1% in men), and

the majority of femoral neck fractures occurred in older adults; as a result, the age of both women and men in the MSF subgroup were significantly higher.

Our study showed that female patients with clinically severe osteoporotic fractures had very high rates of osteoporosis in the lumbar spine (89.6%) and total hip (61.9%), whereas the rates in male patients were very low (only 31.2%% and 19.7%,

TABLE 3 | The effect of anthropometry and BMD stratification on fracture hazard ratio (HR).

Variable	Female (n = 5340)		Male (n = 2048)	
	HR1 (95% CI)[a]	HR2 (95% CI)	HR1 (95% CI)[a]	HR2 (95% CI)
Height Q1	Ref	Ref	Ref	Ref
Q2	0.91 (0.73–1.13)	0.66 (0.49–1.08)[b]	1.13 (0.80–1.60)	0.77 (0.34–1.79)[b]
Q3	1.03 (0.93–1.14)	0.95 (0.83–1.08)[b]	**1.25 (1.04–1.50)**	1.31 (0.87–1.96)[b]
Q4	**1.38 (1.28–1.49)**	**1.12 (1.02–1.23)**[b]	**1.41 (1.21–1.64)**	1.25 (0.94–1.66)[b]
Weight Q1	Ref	Ref	Ref	Ref
Q2	**1.57 (1.28–1.94)**	1.06 (0.81–1.40)[b]	**2.19 (1.48–3.23)**	1.86 (0.81–4.28)[b]
Q3	**1.45 (1.29–1.61)**	0.97 (0.84–1.12)[b]	**1.67 (1.38–2.03)**	1.14 (0.77–1.69)[b]
Q4	**1.43 (1.32–1.55)**	1.06 (0.96–1.17)[b]	**2.34 (1.90–2.87)**	1.32 (0.99–1.75)[b]
BMI Q1	Ref	Ref	Ref	Ref
Q2	**1.58 (1.28–1.96)**	1.20 (0.92–1.58)[b]	**1.57 (1.10–2.23)**	1.36 (0.62–3.02)[b]
Q3	**1.34 (1.20–1.50)**	0.92 (0.80–1.07)[b]	**1.71 (1.41–2.07)**	1.00 (0.73–1.37)[b]
Q4	**1.28 (1.19–1.38)**	0.99 (0.90–1.09)[b]	**1.91 (1.62–2.25)**	1.21 (0.93–1.57)[b]
BSA Q1	Ref	Ref	Ref	Ref
Q2	**1.55 (1.24–1.93)**	1.19 (0.89–1.57)[b]	**1.80 (1.26–2.59)**	0.72 (0.35–1.48)[b]
Q3	**1.39 (1.25–1.55)**	1.04 (0.90–1.20)[b]	**2.02 (1.63–2.50)**	**1.55 (1.09–2.19)**[b]
Q4	**1.49 (1.37–1.62)**	1.08 (0.97–1.20)[b]	**2.10 (1.72–2.56)**	**1.41 (1.05–1.87)**[b]
LS-BMD Q1	Ref	Ref	Ref	Ref
Q2	**4.18 (3.12–5.61)**	**4.17 (3.11–5.60)**[c]	**9.14 (4.19–19.9)**	**8.74 (3.98–19.2)**[c]
Q3	**3.89 (3.17–4.79)**	**3.93 (3.17–4.87)**[c]	**6.26 (4.02–9.76)**	**6.66 (4.08–10.9)**[c]
Q4	**2.98 (2.55–3.49)**	**2.91 (2.48–3.41)**[c]	**4.03 (2.77–5.86)**	**4.65 (3.12–8.67)**[c]
FN-BMD Q1	Ref	Ref	Ref	Ref
Q2	**3.43 (2.62–4.49)**	**3.35 (2.55–4.40)**[c]	**6.69 (3.96–11.3)**	**5.82 (3.41–9.92)**[c]
Q3	**4.23 (3.39–5.26)**	**4.42 (3.51–5.56)**[c]	**5.12 (3.40–7.71)**	**4.43 (2.92–6.73)**[c]
Q4	**2.79 (2.39–3.27)**	**2.72 (2.32–3.19)**[c]	**4.46 (2.80–7.09)**	**3.82 (2.39–6.11)**[c]
Hip-BMD Q1	Ref	Ref	Ref	Ref
Q2	**2.50 (1.96–3.18)**	**2.52 (1.97–3.22)**[c]	**3.87 (2.45–6.12)**	**3.68 (2.27–5.95)**[c]
Q3	**2.36 (2.04–2.74)**	**2.32 (2.00–2.69)**[c]	**4.07 (2.96–5.61)**	**3.71 (2.64–5.21)**[c]
Q4	**2.37 (2.09–2.70)**	**2.30(2.02–2.61)**[c]	**3.94 (2.70–5.77)**	**3.48 (2.35–5.14)**[c]

BMI, body mass index; BSA, body surface area; LS, lumbar spine; BMD, bone mineral density; FN, femoral neck; Hip, total hip; Q1, first quartile; Q2, second quartile; Q3, third quartile; Q4, fourth quartile.
The height, weight, BMI, BSA and BMDs respectively by quartile descending stratification.
[a]Adjusted for age.
[b]Adjusted for age and BMD.
[c]Adjusted for age, height, weight, BMI and BSA.
Significant HRs are shown in bold.

TABLE 4 | Influence of osteoporosis classification on fracture hazard ratio (HR).

Skeletal site	Female OP classification (n = 5340)			Male OP classification (n = 2048)		
	NBMD	LBM-HR (95% CI)	OP-HR (95% CI)	NBMD	LBM-HR (95% CI)	OP-HR (95% CI)
Lumbar spine	Ref	**2.55 (1.27–5.11)**	**4.09 (3.18–5.27)**	Ref	**26.1 (16.5–41.2)**	**8.08 (4.82–13.5)**
Femoral neck	Ref	**4.29 (2.84–6.47)**	**10.9 (6.17–19.2)**	Ref	**13.1 (8.28–20.6)**	**12.2 (4.55–32.5)**
Total hip	Ref	**3.33 (2.46–4.50)**	**4.03 (3.20–5.08)**	Ref	**9.18 (6.86–12.3)**	**11.7 (4.38–31.3)**

NBMD, normal bone mineral density; LBM, low bone mass (osteopenia); OP, osteoporosis.
Significant HRs are shown in bold.

respectively), and about 2.87 times (89.6/31.2) and 3.14 times (61.9/19.7) higher in women than in men, respectively, yielding significant differences between the sexes. This suggested that severe osteoporotic fractures occur in only a small proportion of females and a large proportion of males who did not have osteoporosis. Our results were similar to those of previous research that found the osteoporotic rate of female fracture patients was significantly higher than that of males (28). The research literature also showed that 44% of non-vertebral fractures and 64% of hip fractures occurred in osteoporotic women, compared to roughly 21% and 39% (28) in men, respectively. In contrast, the majority of osteoporotic fractures in postmenopausal women (approximately 60–82%) were found to occur in individuals with low bone mass and normal BMD (29, 40, 41), and this was attributed to the fact that the proportion of individuals with low bone mass and normal BMD was much higher than the proportion of individuals with osteoporosis (40). Based on the Chinese adult obesity standard (BMI ≥ 28.0 kg/m^2 was considered obese) (39), the obesity rates of the female and male fracture patients in this study were 5.2% and 4.9%, respectively, and the obesity rate was significantly lower than that of 37.5% of women and 58% of men with fractures in North America (32, 42), while the obesity rate of Chinese was only 13.9% (5.2/37.5) and 8.4% (4.9/58) of North American women and men, respectively, which suggested there was a significant racial difference.

We found BSA was strongly associated with BMD, prevalence of osteoporosis, and fracture risk in male and female cases. BSA was significantly and positively associated with lumbar spine, femoral neck, and total hip BMD in cases of both genders (**Figure 1**), and when BSA levels were stratified by ascending quartile, the mean BMD increased significantly (**Figure 2**) from group Q1 (lowest BSA levels) to group Q4 (highest BSA level), while the prevalence of osteoporosis decreased significantly (except for the female lumbar spine) (**Figure 3**). This indicated that BMD increased with increased BSA, whereas the prevalence of osteoporosis decreased with increased BSA. The relationship between BSA and BMD in patients with fractures and its effect on the prevalence of osteoporosis in this study were similar to our previous study of a female reference population (33). When BSA levels were stratified by quartiles in descending order (taking the Q1 group with the highest BSA levels as a reference), an age-adjusted model found as BSA levels decreased sequentially, the fracture risk (HR1) of women in the Q2, Q3, and Q4 groups increased non-linearly by 55%, 39%, and 49%, respectively (**Table 3**), and men had a linear increase in fracture risk of 80%, 102%, and 110%, respectively. In models adjusted for age

and BMD, weight, BMI, and BSA in women, and height, weight, and BMI in men were not significantly associated with fracture risk (HR2), suggesting that these anthropometric indicators were not independent factors of BMD for fracture risk. However, in men, even after adjusting for age and BMD, the fracture risk remained significantly higher in Q3 (HR2 = 1.55) and Q4 (HR2 = 1.41) groups, which suggested that BSA may be a risk factor for clinically severe osteoporotic fractures in men, independent of age and BMD. But BSA was not an independent risk factor for fractures in women. The main reason for the gender differences in the relationship between fracture risk and BSA was that there may be a very complex relationship between HR of fractures and BSA, whether female or male. Secondly, the prevalence of osteoporosis in the female fracture group was about 3 times that of the male group, indicating that the female fracture group lost more BMD and the male fracture group had less BMD loss, and the female fracture group was affected by BMD much more than the male group. Therefore, after adjusted for BMD, the effect of BSA on fracture risk in women was decreased or disappeared, and the effect on fracture risk in men was attenuated decreased but still significant. In this study, the BSA stratification of men was BSA = 1.5895–1.6895 m^2 in group Q3 and BSA ≤ 1.5892 m^2 in group Q4 (the results were not shown), so we determined when BSA ≤ 1.6895 m^2, the risk of severe osteoporotic fracture in men was significantly increased by about 41–55%.

Our study also showed when BMD was stratified by descending quartiles (highest in Q1, lowest in Q4, with Q1 as the reference), and two models that adjusted for age (HR1) or adjusted for age, height, weight, BMI, and BSA (HR2) (**Table 3**), the BMD of the lumbar spine in both sexes and the femoral neck in men decreased gradually with increasing quartiles (from Q2 to Q4), but the fracture HR did not increase with BMD, and decreased linearly, such that the HR2 for Q2, Q3, and Q4 (stratified by LS-BMD) for women was 4.17, 3.93, and 2.91, respectively, and for men it was 8.74, 6.66, and 4.65, respectively. Theoretically, fracture risk should increase with decreasing BMD, but here we found the exact opposite, which was an inexplicable bizarre phenomenon. Further research is needed. However, in the osteoporosis classification (**Table 4**), osteoporotic women with a lower BMD of the lumbar spine, femoral neck, and total hip had fracture HRs that were 1.6, 2.5, and 1.2 times higher, respectively, than those for low bone mass. In contrast to women, the HRs of men with low bone mass in the lumbar spine and femoral neck were 3.2 and 1.1 times higher, respectively, than men with osteoporosis. The reason for the higher fracture risk in men with low bone mass than men with

osteoporosis (except for the hip) may be related to the fact that the proportion of patients with low bone mass fractures was higher. In summary, these findings suggested that the risk of clinically severe osteoporotic fractures was associated with sex, skeletal site, and the methods used to stratify various risk factors.

This study has some limitations. First, it was not a multi-center study, and its results may only be representative of the population in and around Changsha City. Because of China's vast territory, differences between the north and the south and between the east and the west are large, so more extensive multi-center studies are needed. Second, this study did not have a follow-up survey, and its results could not necessarily reflect causality. The third limitation is that the measure of height in patients with vertebral fractures, especially those with multiple vertebral compression fractures, may be unduly low, thereby affecting the accuracy of the BSA and BMI calculations. The BSA was not a direct measurement, but was estimated using a correlation formula based on the subject's height and weight (38), and there may also be a risk of introducing bias. Fourth, whether BSA has the same effect on fracture risk as BMI does is skeletal site-specific and needs to be investigated further.

CONCLUSION

Our study suggested that among patients with clinically severe osteoporotic fractures, the prevalence of osteoporosis in women was approximately three times that in men, and there was a significant difference between the two genders. Obesity rates among women and men with fractures were approximately 14% and 8%, respectively, of those in North American countries. In both genders, BSA was significantly positively associated with BMD in fracture patients, and the prevalence of osteoporosis decreased with increasing BSA. In models adjusted for age and anthropometric measures (height, weight, BMI and BSA), decreased BMD or osteoporosis was the greatest risk factor for fracture risk in both genders, and increased fracture risk varied with sex and BMD at different skeletal sites. In age-adjusted models, fracture risk increased non-linearly and linearly in women and men, respectively, with decreasing BSA levels. In models adjusted for age and BMD, decreased BSA remained a

risk factor for increased fracture risk in men. Therefore, it suggested that lower BSA may be a new potential fracture risk factor independent of BMD in men, and its importance should be considered when assessing clinical fracture risk.

DATA AVAILABILITY STATEMENT

The original contributions presented in the study are included in the article/supplementary material. Further inquiries can be directed to the corresponding author.

ETHICS STATEMENT

The studies involving human participants were reviewed and approved by the Ethics Committee of the Second Xiangya Hospital of Central South University. Written informed consent for participation was not required for this study in accordance with the national legislation and the institutional requirements.

AUTHOR CONTRIBUTIONS

Z-FS and X-YW designed the study and wrote the manuscript. X-YW, H-LL, YS, L-HT, and L-QY conducted data collection and data analysis. R-CD, HZ, Y-QP, and Z-JX acquired data from chart review and performed the analysis. Z-FS, X-YW, H-LL, YS, L-HT, L-QY, R-CD, HZ, Y-QP, and Z-JX reviewed and revised the manuscript. All the authors contributed to the article and approved the submitted version of it.

FUNDING

REFERENCES

1. Sambrook P, Cooper C. Osteoporosis. *Lancet* (2006) 367(9527):2010–8. doi: 10.1016/S0140-6736(06)68891-0
2. Roberts SE, Goldacre MJ. Time Trends and Demography of Mortality After Fractured Neck of Femur in an English Population, 1968-98: Database Study. *BMJ* (2003) 327(7418):771–5. doi: 10.1136/bmj.327.7418.771
3. Johnell O, Kanis JA. An Estimate of the Worldwide Prevalence, Mortality and Disability Associated With Hip Fracture. *Osteoporos Int* (2004) 15:897–902. doi: 10.1007/s00198-004-1627-0
4. Parker M, Johansen A. Hip Fracture. *BMJ* (2006) 333(7557):27–30. doi: 10.1136/bmj.333.7557.27
5. Johnell O, Kanis JA, Oden A, Sernbo I, Redlund-Johnell I, Petterson C, et al. Mortality After Osteoporotic Fractures. *Osteoporos Int* (2004) 15(1):38–42. doi: 10.1007/s00198-003-1490-4

6. Abrahamsen B, van Staa T, Ariely R, Olson M, Cooper C. Excess Mortality Following Hip Fracture: A Systematic Epidemiological Review. *Osteoporos Int* (2009) 20(10):1633–50. doi: 10.1007/s00198-009-0920-3
7. Leslie WD, Brennan SL, Prior HJ, Lix LM, Metge C, Elias B. The Contributions of First Nations Ethnicity, Income, and Delays in Surgery on Mortality Post-Fracture: A Population-Based Analysis. *Osteoporos Int* (2013) 24:1247–56. doi: 10.1007/s00198-012-2099-2
8. Dyer SM, Crotty M, Fairhall N, Magaziner J, Beaupre LA, Cameron ID, et al. A Critical Review of the Long-Term Disability Outcomes Following Hip Fracture. *BMC Geriatr* (2016) 16(1):158. doi: 10.1186/s12877-016-0332-0
9. Magaziner J, Chiles N, Orwig D. Recovery After Hip Fracture: Interventions and Their Timing to Address Deficits and Desired Outcomes—Evidence From the Baltimore Hip Studies. *Nestle Nutr Inst Workshop Ser* (2015) 83:71–81. doi: 10.1159/000382064

10. Pisani P, Renna MD, Conversano F, Casciaro E, Di Paola M, Quarta E, et al. Major Osteoporotic Fragility Fractures: Risk Factor Updates and Societal Impact. *World J Orthop* (2016) 7(3):171–81. doi: 10.5312/wjo.v7.i3.171

11. Compston JE, McClung MR, Leslie WD. Osteoporosis. *Lancet* (2019) 393 (10169):364–76. doi: 10.1016/S0140-6736(18)32112-3

12. Weycker D, Li X, Barron R, Bornheimer R, Chandler D. Hospitalizations for Osteoporosis-Related Fractures: Economic Costs and Clinical Outcomes. *Bone Rep* (2016) 5:186–91. doi: 10.1016/j.bonr.2016.07.005

13. Tatangelo G, Watts J, Lim K, Connaughton C, Abimanyi-Ochom J, Borgström F, et al. The Cost of Osteoporosis, Osteopenia, and Associated Fractures in Australia in 2017. *J Bone Miner Res* (2019) 34(4):616–25. doi: 10.1002/jbmr.3640

14. Borgström F, Karlsson L, Ortsäter G, Norton N, Halbout P, Cooper C, et al. Fragility Fractures in Europe: Burden, Management & Opportunities. *Arch Osteoporos* (2020) 15:1–21. doi: 10.1007/s11657-020-0706-y

15. Kim EG, Bae G, Kwon HY, Yang H. Aging and Direct Medical Costs of Osteoporotic Fractures. *J Bone Miner Metab* (2021) 39(4):589–97. doi: 10.1007/s00774-020-01192-0

16. Svedbom A, Borgstöm F, Hernlund E, Ström O, Alekna V, Bianchi ML, et al. Quality of Life for Up to 18 Months After Low-Energy Hip, Vertebral, and Distal Forearm Fractures-Results From the ICUROS. *Osteoporos Int* (2018) 29 (3):557–66. doi: 10.1007/s00198-017-4317-4

17. Guirant L, Carlos F, Curiel D, Kanis JA, Borgström F, Svedbom A, et al. Health-Related Quality of Life During the First Year After a Hip Fracture: Results of the Mexican Arm of the International Cost and Utility Related to Osteoporotic Fractures Study (MexICUROS). *Osteoporos Int* (2018) 29 (5):1147–54. doi: 10.1007/s00198-018-4389-9

18. Alexiou KI, Roushias A, Varitimidis SE, Malizos KN. Quality of Life and Psychological Consequences in Elderly Patients After a Hip Fracture: A Review. *Clin Interv Aging* (2018) 13:143–50. doi: 10.2147/CIA.S150067

19. Talevski J, Sanders KM, Busija L, Beauchamp A, Duque G, Borgström F, et al. Health Service Use and Quality Recovery 12 Months Following Major Osteoporotic Fracture: Latent Class Analyses of the International Costs and Utilities Related to Osteoporotic Fractures Study (ICUROS). *J Bone Miner Res* (2021) 36(2):252–61. doi: 10.1002/jbmr.418

20. Borhan S, Papaioannou A, Gajic-Veljanoski O, Kennedy C, Ioannidis G, Berger C, et al. Incident Fragility Fractures Have a Long-Term Negative Impact on Health-Related Quality of Life of Older People: The Canadian Multicentre Osteoporosis Study. *J Bone Miner Res* (2019) 34(5):838–48. doi: 10.1002/jbmr.3666

21. Lems WF, Paccou J, Zhang J, Fuggle NR, Chandran M, Harvey NC, et al. Vertebral Fracture: Epidemiology, Impact and Use of DXA Vertebral Fracture Assessment in Fracture Liaison Services. *Osteoporos Int* (2021) 32(3):399–411. doi: 10.1007/s00198-020-05804-3

22. Xu L, Lu A, Zhao X, Chen X, Cummings SR. Very Low Rates of Hip Fracture in Beijing, People's Republic of China the Beijing Osteoporosis Project. *Am J Epidemiol* (1996) 144(9):901–7. doi: 10.1093/oxfordjournals.aje.a009024

23. Xia WB, He SL, Xu L, Liu AM, Jiang Y, Li M, et al. Rapidly Increasing Rates of Hip Fracture in Beijing, China. *J Bone Miner Res* (2012) 27(1):125–9. doi: 10.1002/jbmr.519

24. Cooper C, Campion G, Melton LJ3rd. Hip Fractures in the Elderly: A World-Wide Projection. *Osteoporos Int* (1992) 2(6):285–9. doi: 10.1007/BF01623184

25. Cummings SR, Nevitt MC, Browner WS, Stone K, Fox KM, Ensrud KE, et al. Risk Factors for Hip Fracture in White Women. Study of Osteoporotic Fractures Research Group. *N Engl J Med* (1995) 332(12):767–73. doi: 10.1056/NEJM199503233321202

26. Nguyen ND, Frost SA, Center JR, Eisman JA, Nguyen TV. Development of Prognostic Nomograms for Individualizing 5-Year and 10-Year Fracture Risks. *Osteoporos Int* (2008) 19(10):1431–44. doi: 10.1007/s00198-008-0588-0

27. Wang L, Yang M, Liu Y, Ge Y, Zhu S, Su Y, et al. Differences in Hip Geometry Between Female Subjects With and Without Acute Hip Fracture: A Cross-Sectional Case-Control Study. *Front Endocrinol (Lausanne)* (2022) 13:799381. doi: 10.3389/fendo.2022.799381

28. Schuit SC, van der Klift M, Weel AE, de Laet CE, Burger H, Seeman E, et al. Fracture Incidence and Association With Bone Mineral Density in Elderly Men and Women: The Rotterdam Study. *Bone* (2004) 34(1):195–202. doi: 10.1016/j.bone.2003.10.001

29. Siris ES, Chen YT, Abbott TA, Barrett-Connor E, Miller PD, Wehren LE, et al. Bone Mineral Density Thresholds for Pharmacological Intervention to Prevent Fractures. *Arch Intern Med* (2004) 164(10):1108–12. doi: 10.1001/archinte.164.10.1108

30. Compston JE, Flahive J, Hosmer DW, Watts NB, Siris ES, Silverman S, et al. Relationship of Weight, Height, and Body Mass Index With Fracture Risk at Different Sites in Postmenopausal Women: The Global Longitudinal Study of Osteoporosis in Women (GLOW). *J Bone Miner Res* (2014) 29(2):487–93. doi: 10.1002/jbmr.2051

31. Compston J. Obesity and Fractures in Postmenopausal Women. *Curr Opin Rheumatol* (2015) 27(4):414–9. doi: 10.1097/BOR.0000000000000182

32. Nielson CM, Marshall LM, Adams AL, LeBlanc ES, Cawthon PM, Ensrud K, et al. BMI and Fracture Risk in Older Men: The Osteoporotic Fractures in Men Study (MrOS). *J Bone Miner Res* (2011) 26(3):496–502. doi: 10.1002/jbmr.235

33. Wu XP, Liao EY, Liu SP, Zhang H, Shan PF, Cao XZ, et al. Relationship of Body Surface Area With Bone Density and Its Risk of Osteoporosis at Various Skeletal Regions in Women of Mainland China. *Osteoporos Int* (2004) 15 (9):751–9. doi: 10.1007/s00198-004-1608-3

34. Genant HK, Wu CY, van Kuijk C, Nevitt MC. Vertebral Fracture Assessment Using a Semiquantitative Technique. *J Bone Miner Res* (1993) 8(9):1137–48. doi: 10.1002/jbmr.5650080915

35. Wu XP, Liao EY, Zhang H, Shan PF, Cao XZ, Liu SP. Establishment of BMD Reference Plots and Determination of Peak BMD at Multiple Skeletal Regions in Mainland Chinese Women and the Diagnosis of Osteoporosis. *Osteoporos Int* (2004) 15(1):71–9. doi: 10.1007/s00198-003-1517-x

36. Wu XP, Hou YL, Zhang H, Shan PF, Zhao Q, Cao XZ, et al. Establishment of BMD Reference Databases for the Diagnosis and Evaluation of Osteoporosis in Central Southern Chinese Men. *J Bone Miner Metab* (2008) 26(6):586–94. doi: 10.1007/s00774-008-0877-x

37. Kanis JA, McCloskey EV, Johansson H, Oden A, Melton LJ3rd, Khaltaev N. A Reference Standard for the Description of Osteoporosis. *Bone* (2008) 42 (3):467–75. doi: 10.1016/j.bone.2007.11.001

38. Yu CY, Lin CH, Yang YH. Human Body Surface Area Database and Estimation Formula. *Burns* (2010) 36(5):616–29. doi: 10.1016/j.burns.2009.05.013

39. Zhou BF. Cooperative Meta-Analysis Group of the Working Group on Obesity in China. Predictive Values of Body Mass Index and Waist Circumference for Risk Factors of Certain Related Diseases in Chinese Adults——Study on Optimal Cut-Off Points of Body Mass Index and Waist Circumference in Chinese Adults. *BioMed Environ Sci* (2002) 15(1):83–96.

40. Pasco JA, Seeman E, Henry MJ, Merriman EN, Nicholson GC, Kotowicz MA. The Population Burden of Fractures Originates in Women With Osteopenia, Not Osteoporosis. *Osteoporos Int* (2006) 17(9):1404–9. doi: 10.1007/s00198-006-0135-9

41. Cranney A, Jamal SA, Tsang JF, Josse RG, Leslie WD. Low Bone Mineral Density and Fracture Burden in Postmenopausal Women. *CMAJ* (2007) 177 (6):575–80. doi: 10.1503/cmaj.070234

42. Premaor MO, Ensrud K, Lui L, Parker RA, Cauley J, Hillier TA, et al. Risk Factors for Nonvertebral Fracture in Obese Older Women. *J Clin Endocrinol Metab* (2011) 96(8):2414–21. doi: 10.1210/jc.2011-0076

frontiers | Frontiers in Endocrinology

Retrospective analysis of the relationship between bone mineral density and body composition in a health check-up Chinese population

Yuxin Li [1,2†], Zhen Huang [3†], Yan Gong [1], Yansong Zheng [1*] and Qiang Zeng [1]

[1]Second Medical Center and National Clinical Research Center for Geriatric Diseases, Chinese People's Liberation Army General Hospital, Beijing, China, [2]Academy of Medical Engineering and Translational Medicine, Tianjin University, Tianjin, China, [3]Nanning First People's Hospital (The Fifth Affiliated Hospital of Guangxi Medical University), Nanning, China

Purpose: This study was designed to explore the relationship between bone mineral density (BMD) and body composition indicators in Chinese adults (≥50 years) in order to provide a scientific basis for optimal bone health management.

Method: Individuals ≥50 years old who received physical examinations and routine check-ups at the Health Management Research Institute of PLA General Hospital from September 2014 through March 2022 were included as research subjects in this study. Basic clinical and demographic information were recorded for all subjects, along with smoking and drinking status, height and body weight. A panel of routine blood chemistry and metabolite markers were measured, along with lean muscle mass and body fat mass using body composition bioelectrical impedance analysis (BIA). Body mass index (BMI), body fat percentage (BFP), skeletal muscle mass index (SMI), and bone mineral density (BMD) were calculated for all individuals. For comparative analysis, individuals were grouped based on their BMI, BFP, SMI and BMD T-score. Follow-up examinations were performed in a cohort of 1,608 individuals matched for age, sex, smoking and drinking history for ≥5 years,

Results: In this large cross-sectional study, age, smoking, homocysteine (Hcy) and blood glucose levels were established as independent risk factors for osteoporosis. Multi-factor logistic regression analysis showed that age, sex, BMI, intact parathyroid hormone (iPTH), SMI, BFP, smoking, blood levels of inorganic phosphate (P) and K+ were all significantly associated with osteoporosis risk (P<0.05). A subset of these factors- BMI, SMI, BFP and K+, were determined to be protective. In the cohort followed for ≥5 years, SMI and BMD decreased while BFP and BMI increased significantly (P<0.001) over time.

Conclusion: Risk of osteoporosis may be reduced by increasing body weight, particularly lean muscle mass, while simultaneously controlling BFP.

Introduction

Osteoporosis is a common musculoskeletal disorder among the elderly and a chronic condition which, like many other chronic conditions, requires long-term clinical management (1). This disorder frequently leads to fragility, bone fractures, chronic pain and other symptoms, culminating in a reduced quality of life, disability and death. From 2005 to 2013, the disability-adjusted life year (DALY) for the global population as a result of musculoskeletal disorders increased by 17.7% (2). Another study reported that from 2008 to 2018, 45.9% of Chinese women aged ≥ 65 years suffered from osteoporosis of the lumbar vertebra, hip or femur, while the incidence of osteoporosis for men and women individually aged ≥ 60 years was 6.46% and 29.13%, respectively (3). In 2010, the total number of individuals aged ≥ 50, the age group at highest risk of osteoporotic fractures, reached 158 million. That number is expected to double by 2040 (4, 5). Thus, early screening and intervention for osteoporosis have become important clinical tactics for keeping rates of related fractures and morbidities to the lowest levels possible in this population.

Bone mineral density (BMD) is defined as the mass of bone mineral per unit volume. It is considered the gold-standard indicator of skeletal metabolic status, and used for analyzing the change of bone mass over time. The T-score, which refers to the number of standard deviations that an individual's BMD differs from the peak bone mass of a young healthy individual of the same sex, is the most meaningful indicator for osteoporosis in men aged ≥ 50, and in post-menopausal women. BMD is associated with a variety of factors such as age (6), weight (7), nutrition (8), exposure to sunlight, premature menopause (9), smoking, drinking, genetic factors (10), sex (11, 12), and exercise. Among these factors, heredity, sex and age are unmodifiable, while weight, nutrition, exercise, exposure to sunlight, and lifestyle are modifiable. Body composition indicators such as BMI, BFP and skeletal muscle mass index (SMI) (13) are a result of the combined effects of unmodifiable and modifiable factors on the human body. Therefore, the ultimate impact of these factors can be reflected by body composition indicators. SMI, the percentage of skeletal muscle mass out of total body weight, is a widely recognized indicator used to assess skeletal muscle health and even help diagnose sarcopenia (14, 15).

The interrelationship of body composition and osteoporosis is complex and multifactorial. Possibly because of differences in ethnicity, nutrition, lifestyle habits, and body size or even

algorithms, the conclusions of the current available correlation studies are conflicting. At the same time, the American or European guidelines may not applicable to Asians. The related Chinese population has been less studied. A study completed a 3-year follow-up of 208 men from the Foshan community in Guangdong, China, and this prospective study concluded that bone density at sites other than the skull throughout the body was positively correlated with human skeletal muscle mass parameters, especially SMI, however, the sample size was small, and the follow-up period was only 3 years (16).

Body composition is dictated not only by unmodifiable factors such as heredity, sex and aging (17), but also by acquired lifestyle factors which are very modifiable. Indeed, BMI, BFP and SMI can be modified through a variety of weight control tactics, particularly exercise (14, 18). Body composition can thus be viewed as an aggregate outcome of the cumulative effect of unmodifiable and modifiable factors in the human body. Body composition indicators, therefore, may be useful not only as early predictors of BMD risk, but also as indicators of BMD intervention effectiveness.

Health check-up belongs to opportunistic screening. Although this kind of screening has certain limitations, with the popularization of physical examination in China, the practical significance of this kind of screening is very noteworthy. It is not necessary to make an accurate diagnosis. Finding the tendency of osteoporosis in advance and urging people to intervene in advance can produce good results (19). Because osteoporosis often shows no clinical symptoms in early stages, this condition can only be diagnosed through a combination of objective and sometimes subjective clinical tests. However, previous studies have shown that quantifiable data acquired through peripheral dual-energy X-ray absorptiometry can reveal trends of BMD (20, 21).

This study examined the relationship between BMD and body composition markers, especially SMI, in individuals aged ≥ 50, with the objective of providing data to support clinicians tasked with counseling patients on osteoporosis prevention.

Methods

Study population

All individuals (aged ≥ 50) who received physical examinations and completed related checks at the Health Management Research

Institute of PLA General Hospital from September 2014 through March 2022 were included in this study. A total of 56,462 individuals were included in the baseline study- 32,510 males (57.58%) and 23,952 females (42.42%). Average age of this cohort was 55.95 ± 5.40 years. A subset of 1,608 individuals completed a follow-up examination ≥ 5 years after the initial check. Of these, 1,097 were male (68.22%) and 511 female (31.78%). Exclusion criteria included pre-menopausal women, patients with severe cardiac or renal insufficiency, limb differences or mobility impairments, patients with confirmed malignancies, primary hyper-parathyroidism or Cushing's syndrome, post-gastrectomy, and patients with prescriptions for corticosteroids (22). For individuals who received more than one physical examination during the study period, only results of their first physical examination were taken as baseline data for analysis. See Figure 1 for details of the selection process. The retrospective study protocol was approved (S2019-190-02) by the Chinese People's Liberation Army General Hospital ethics committee. All individuals enrolled were informed that their physical examination data would be de-identified, and signed consent documents.

Lifestyle survey

We input the lifestyle questionnaire into the computer in advance, so that the subjects can input lifestyle information by themselves during the physical examination by means of touch-screen input. Data were collected concerning each subject's basic demographic information, smoking and drinking habits. Smoking was defined as smoking ≥ 10 cigarettes per day for ≥ 1 year, according to the standards in the relevant literature (23), and those who fail to meet the standards are defined as non-smoking. Anyone who smokes less than one cigarette a day and can maintain it for more than a year is called quitting smoking, according to the Chinese clinical smoking cessation guidelines (2015 Edition) (24). Drinking included limited drinking (no drinking, or drinking ≤ 25g of alcohol/day for a male adult, and ≤ 15g of alcohol/day for female adult). Excessive drinking refers to drinking ≥ 25g of alcohol/day for males, and ≥ 15g alcohol/day for females) (25).

Physical examination and body composition measurement

Subjects' height, weight, blood pressure and other vital physiological parameters were captured during routine examination. Weight is measured by electronic scale, and height is measured by Infrared height measuring instrument (OMRON, HNH-318, Japan). All these indicators are obtained according to the quality control standards of physical examination. A body composition analyzer (Inbody720, South
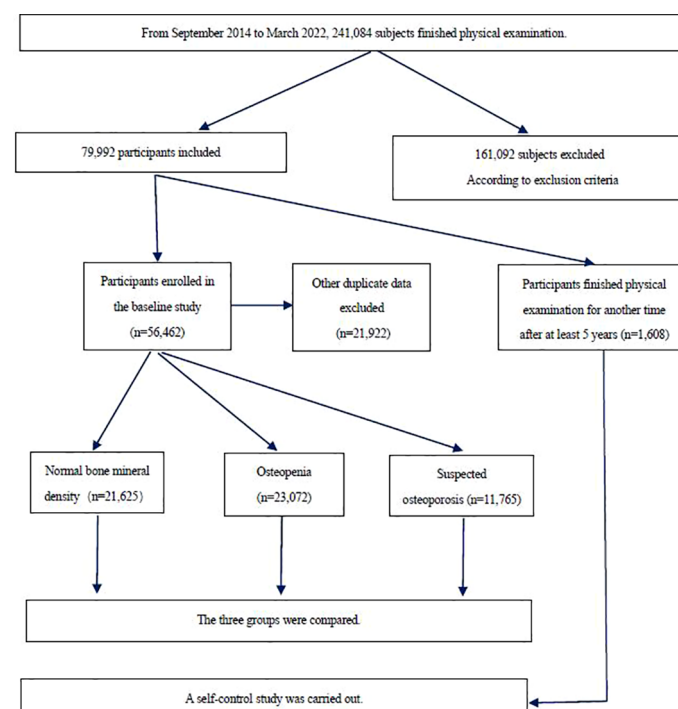
FIGURE 1
Flow chart of the study population.

Korea) was used to measure body composition indicators. For these measurements, an individual in resting state would stand barefoot on the analyzer, arms hanging down in relaxed state, with the front of the soles, heels, thumbs and palms in contact with eight different electrodes. Bioelectrical impedance values would then be measured to obtain body fat and muscle mass, allowing for calculation of other indicators. Height and weight were used to calculate BMI, BFP (body fat mass/weight x 100%) and SMI (muscle mass/weight x 100%). Group classification based on BMI included- underweight (<18.5 kg/m^2), normal weight (18.5-23.9 kg/m^2), overweight (24.0-27.9 kg/m^2), and obese ($\geq$28.0 kg/m^2) [26]. Test results of SMI were arranged into three levels in ascending order- low, moderate and high- divided at 25% and 75%, forming the three groups of low SMI, moderate SMI, and high SMI. Similarly, test results of BFP were arranged, into three levels in ascending order- low, moderate and high- also divided at 25% and 75%, forming the three groups of low BFP, moderate BFP, and high BFP.

Biochemical Parameters

Venous blood was collected from all subjects following an overnight fast, and according to the quality control and testing standards of the Clinical Laboratory of PLA General Hospital [27]. Levels of total cholesterol (TC), triglyceride (TG), high density lipoprotein cholesterol (HDL-C), low density lipoprotein cholesterol (LDL-C), fasting blood glucose (FBG), hemoglobin A1c (HbA1c), Ca^{2+}, K$^+$ and inorganic phosphorus (P), as well as intact parathyroid hormone (iPTH) and total 25-hydroxy-vitamid D (25 (OH)D) were measured in serum samples using electrochemiluminescence method; the enzymatic cycling method was adopted for the measurement of homocysteine (Hcy) [28].

BMD measurement

A dual-energy x-ray bone density device (Osteosys EXA 3000 (GSYJX (J) 2009 No. 3312468), South Korea) was used for the measurement of BMD at one-third distal radius to obtain the mean forearm BMD and T-score. Diagnosis of osteoporosis was determined based on WHO-recommended standards of 1994: Normal BMD = T-score $\geq$ 1.0 SD; osteopenia = -2.5 SD < T-score < -1.0 SD; suspected osteoporosis = T-score $\leq$ -2.5 SD [29].

Follow-up examinations

Individuals included in the baseline study were considered to have completed a follow-up examination if they received an examination $\geq$ 5 years after their initial visit and examination. A longitudinal analysis was then performed over time for each of these subjects.

Statistical analysis

Coded and quantified questionnaire data were analyzed using Stata 11.0. Body composition and blood marker data were expressed as mean ± SD and categorical data were expressed as percentages. For group comparisons, the χ^2 test, t-test, and one-way analysis of variance were carried out. Pairwise comparisons were made using Bonferroni method and multivariate analysis by using logistic regression analysis. For every comparison, $P<0.05$ indicated a statistically significant difference.

Results

Results of baseline BMD screening

A total of 23,072 individuals (40.86%) were determined to have normal BMD, 21,625 (38.30%) had osteopenia, and 11,765 (20.84%) were suspected to have osteoporosis. The mean BMD in the overall cohort was 0.453 ± 0.099g/cm^2. Summaries of blood markers and smoking/drinking in the overall cohort are shown in Table 1.

Compare of blood markers and lifestyle factors associated with BMD

A significant increase was observed in TC, LDL-C, HDL-C, FBG, HbA1c, Hcy, and BFP, in contrast to a decrease in SMI and BMD among the three BMD groups. Compared with the normal group, both the suspected osteoporosis group and the osteopenia group, the latter in particular, had a larger share of individuals who reported limited drinking compared with those who reported excessive drinking. This is contrary to results of most previous studies and can presumably be attributed to a significantly higher percentage of males in the normal group. Despite a higher percentage of males than females in the cohort overall, the percentage of females is lowest in the normal group, higher in the osteopenia group and highest in the suspected osteoporosis group where the percentage of females is almost the same as that of males. See Figure 2A.

Multivariate analysis of osteoporosis screening results

For results of multiple logistics regression in which osteoporosis was used as the dependent variable, and other

TABLE 1   Comparison of three groups of basic data and clinical indexes (n=56,462).

	Normal BMD (n=21,625)	Osteopenia (n=23,072)	Suspected osteoporosis (n=11,765)	Statistics
Gender				χ2 = 357.43, *P*<0.001
Male	13,063 (60.41)	13,559 (58.77)	5,888 (50.05)	
Female	8,562 (39.59)	9,513 (41.23)	5,877 (49.95)	
Smoking status				χ2 = 25.81, *P*<0.001
Non-smoking	14,688 (67.92)	15,303 (66.33)	7,868 (66.88)	
Quit smoking	1,657 (7.66)	1,834 (7.95)	820 (6.97)	
Smoking	5,280 (24.42)	5,935 (25.72)	3,077 (26.15)	
Drinking status				χ2 = 110.17, *P*<0.001
Never drinking or small amount of alcohol	15,190 (70.24)	16,320 (70.74)	8,868 (75.38)	
Excessive drinking	6,435 (29.76)	6,752 (29.26)	2,897 (24.62)	
Age(year)	54.19 ± 4.39	55.87 ± 5.07*	59.33 ± 6.09*#	F=3942.38, *P*<0.001
BFP (%)	26.08 ± 5.70	26.78 ± 5.62*	27.59 ± 5.92*#	F=273.25, *P*<0.001
BMI (kg/m2)	25.18 ± 3.09	25.15 ± 3.24	24.89 ± 3.44*#	F=35.59, *P*<0.001
SMI(%)	68.33 ± 5.64	67.62 ± 5.53*	66.81 ± 5.81*#	F= 282.64, *P*<0.001
BMD(g/cm2)	0.535 ± 0.069	0.437 ± 0.058*	0.332 ± 0.071*#	F=38091.13, *P*<0.001
TC (mmol/L)	4.81 ± 0.92	4.89 ± 0.95*	4.93 ± 0.97*#	F=75.07, *P*<0.001
TG (mmol/L)	1.69 ± 1.25	1.73 ± 1.25*	1.68 ± 1.19#	F=7.04, P=0.0009
LDL-c (mmol/L)	3.10 ± 0.81	3.16 ± 0.84*	3.19 ± 0.86*#	F=46.72, *P*<0.001
HDL-C (mmol/L)	1.29 ± 0.33	1.31 ± 0.34*	1.34 ± 0.35*#	F=65.41, *P*<0.001
FBG (mmol/L)	5.93 ± 1.46	6.00 ± 1.51*	6.09 ± 1.61*#	F=44.54, *P*<0.001
HbA1c (%)	6.01 ± 0.88	6.07 ± 0.89*	6.17 ± 0.97*#	F=122.69, *P*<0.001
Hcy(μmol/L)	12.56 ± 6.31	12.78 ± 6.33*	3.20 ± 6.49*#	F=37.40, *P*<0.001
Ca^{2+} (mmol/L)	2.332 ± 0.086	2.337 ± 0.083*	2.337 ± 0.086*	F=20.18, *P*<0.001
K$^+$ (mmol/L)	4.256 ± 0.307	4.249 ± 0.309*	4.239 ± 0.321*#	F=12.28, *P*<0.001
P (mmol/L)	1.163 ± 0.155	1.176 ± 0.151*	1.188 ± 0.149*#	F=111.74, *P*<0.001
iPTH (pg/ml)	45.35 ± 15.71 (n=2,149)	6.50 ± 16.45 (n=2,526)	48.91 ± 21.05*#(n=1,302)	F=17.25, *P*<0.001
25(OH)D (nmol/L)	17.97 ± 7.64 (n=2,149)	17.91 ± 7.75 (n=2,526)	18.22 ± 7.84(n=1,302)	F=0.72, P=0.4884

BMI, body mass index; BMD, forearm bone mineral density; BFP, body fat percent (body fat/weightx100%); SMI, skeletal muscle mass index (total muscular mass/weight x100%); TC, Total cholesterol; TG, Triglyceride; HDL-C, high density lipoprotein cholesterol; LDL-C, low density lipoprotein cholesterol; FBG, fasting blood glucose; HbA1c, hemoglobin A1c; Hcy, blood homocysteine; P, inorganic phosphorus; iPTH, Intact parathyroid hormone.
*compared with normal bone mineral density, P<0.05.
#compared with osteopenia, P<0.05.

factors as independent variables. The age, sex, BMI, iPTH, SMI, BFP, smoking, P and K+ were all determined to be significantly associated with (*P*<0.001) osteoporosis. Of these, BMI, SMI, BFP and K+ were determined to be protective factors. See in Table 2.

Body composition test results

Based on their BMI, 802 individuals (1.42%) were underweight, 19,889 (25.23%) were normal, 25,802 (45.70%) were overweight, and 9,969 (17.66%) were obese. The division points at 25% and 75% of SMI corresponded to 63.88% and 71.36% of the individuals involved, thereby 14,113 individuals were determined to have low SMI, 28,230 had moderate SMI, and 14,119 had high SMI. The division points at 25% and 75% of BFP corresponded to 23.0% and 30.6% of the individuals,

thereby 14,316 individuals had low BFP, 27,971 had moderate BFP, and 14,175 had high BFP.

There were significant differences among the three groups (normal, osteopenia, suspected osteoporosis) in BMI (*F*=35.59, *P*<0.001). A pairwise comparison found the normal and the Osteopenia group to have no significant differences in BMI, while the suspected osteoporosis group had the lowest BMI. There was a significant positive correlation (*β*=0.1446, *P*<0.001) between BMD and BMI (Figure 2B). The underweight group had the highest share of suspected osteoporosis cases (χ2 = 231.57, *P*<0.001).

BFP showed an upward trend (*F*=273.25, *P*<0.001) from the normal group to the suspected osteoporosis group which was determined to be significant with pairwise comparison. There also was a significant negative correlation (*β*=-0.3839, *P*<0.001) between BMD and BFP (Figure 2C). The group with a high BFP
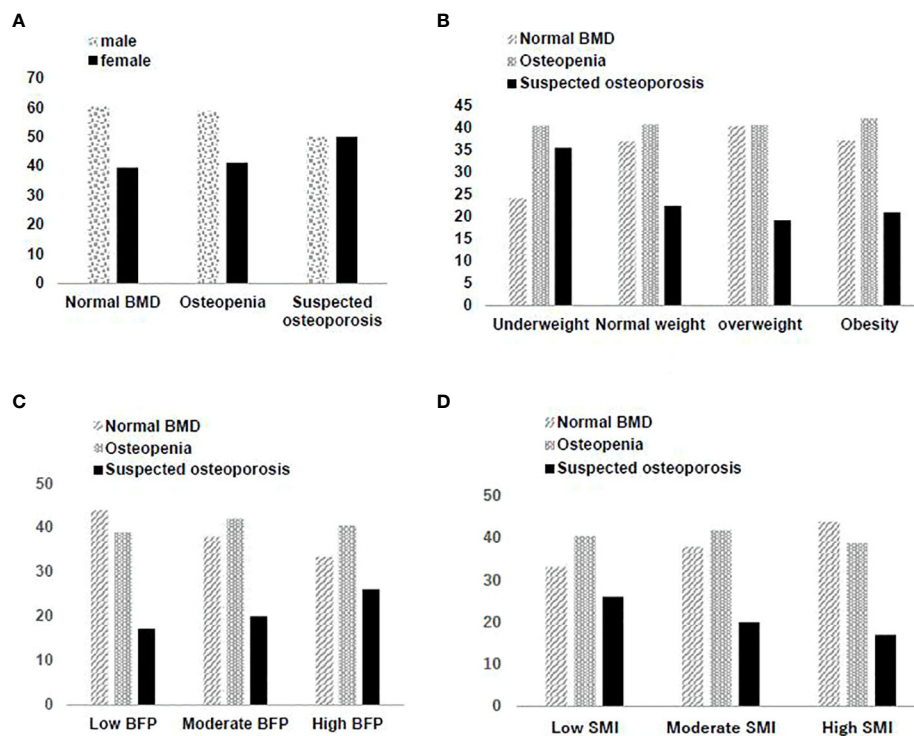
FIGURE 2
(A) Gender distribution in different bone mineral density screening results. **(B)** Distribution of bone mineral density screening results in different BMI groups. **(C)** Distribution of bone mineral density screening results in different BFP groups. **(D)** Distribution of bone mineral density screening results in different SMI groups.

had the highest rate of suspected osteoporosis ($\chi 2 = 524.72$, $P<0.001$).

SMI showed a downward trend ($F=282.64$, $P<0.001$) from the normal group to the suspected osteoporosis group which was determined to be significant with pairwise comparison. There was a significant positive correlation ($\beta=0.3855$, $P<0.001$) between BMD and SMI (Figure 2D). The group with low SMI had the highest rate of suspected osteoporosis, and the group with high SMI had the lowest rate of suspected osteoporosis ($\chi 2 = 538.85$, $P<0.001$).

Longitudinal analysis

To explore the change of body composition and bone mass over time, follow-up examinations were conducted ≥ 5 years later on 1,608 individuals matched for age, sex, and histories of smoking and drinking. Longitudinal analysis of the endpoints recorded at both examinations were performed. Table 3 shows summary analysis of differences between baseline data and re-examination in this cohort after ≥ 5 years. Age, BFP, BMI, FBG, HbA1c, Ca^{2+}, K^+ and 25-(OH)D increased from baseline levels, while SMI, BMD, TC and LDL-C decreased.

Compared with the baseline examination, rates of suspected osteoporosis significantly increased ($\chi 2 = 36.8862$, $P<0.001$) after ≥ 5 years. A comparison of the association between BMD and BMI, BFP and SMI at baseline and follow-up is shown in Table 4. The high SMI group was determined to have the highest BMD at both time points. BMD typically decreases over time, but individuals with a higher SMI have greater bone mass and thus have a lower rate of osteoporosis. Similarly, individuals with a low BFP have the highest BMD.

Discussion

This was a retrospective study which examined the relationship between body composition and BMD from 56,462 individuals. Major findings from this study are that age, sex, BMI, iPTH, SMI, BFP, smoking, P and K+ were all significantly associated with osteoporosis, and that BMI, SMI, BFP and K+ were determined to be protective. Another notable finding is that blood levels of 25-(OH)D showed no statistically significant association with osteopenia or suspected osteoporosis. Of course, this may be related to the fact that we cannot rule out whether the elderly have taken vitamin D supplementation intervention.

TABLE 2   Results of multiple logistic regression analysis (n=56,462).

	Odds Ratio	z	P>|z|	[95% Confidence Interval]
Age (year)	1.158	22.49	0.000	1.143, 1.174
Gender	1.972	4.53	0.000	1.470, 2.644
BMI (kg/m2)	0.885	-6.12	0.000	0.851, 0.920
iPTH	1.009	4.47	0.000	1.004, 1.013
SMI(%)	0.728	-4.11	0.000	0.625, 0.847
BFP (%)	0.766	-3.65	0.000	0.664, 0.884
Smoking status	1.182	3.42	0.001	1.074, 1.301
P (mmol/L)	1.908	2.62	0.009	1.176, 3.096
K^+ (mmol/L)	0.750	-2.57	0.010	0.602, 0.934
Drinking status	1.071	1.50	0.134	0.979, 1.170
Hcy(μmol/L)	1.001	1.27	0.205	0.996, 1.019
Ca^{2+} (mmol/L)	0.686	-0.87	0.384	0.293, 1.603
FBG (mmol/L)	1.031	0.79	0.427	0.956, 1.111
TG (mmol/L)	0.944	-0.80	0.427	0.819, 1.088
HDL-C (mmol/L)	0.881	-0.58	0.562	0.574, 1.351
HbA1c (%)	1.027	0.39	0.699	0.898, 1.172
TC (mmol/L)	1.045	0.23	0.818	0.718, 1.521
LDL-c (mmol/L)	1.026	0.13	0.894	0.703, 1.498
25(OH)D (nmol/L)	1.000	0.07	0.943	0.992, 1.009

BMI, body mass index; BFP, body fat percent (body fat/weightx100%); SMI, skeletal muscle mass index (total muscular mass/weight x100%); TC, Total cholesterol; TG, Triglyceride; HDL-C, high density lipoprotein cholesterol; LDL-C, low density lipoprotein cholesterol; FBG, fasting blood glucose; HbA1c, hemoglobin A1c; Hcy, blood homocysteine; P, inorganic phosphorus; iPTH, Intact parathyroid hormone.

TABLE 3   Comparison of clinical data before and after completion of follow-up (n=1,608).

	Baseline (n=1,608)	Follow-up (n=1,608)	Mean change	Statistics
Age (year)	53.89 ± 3.87	59.42 ± 3.98	5.53	t=-39.915, P<0.001
BFP (%)	24.94 ± 5.44	27.61 ± 5.53	2.68	t =-13.831, P<0.001
BMI (kg/m^2)	24.68 ± 2.93	25.21 ± 2.99	0.52	t =-4.963, P<0.001
SMI (%)	69.68 ± 5.34	66.97 ± 5.52	-2.71	t =14.156, P<0.001
BMD (g/cm^2)	0.478 ± 0.089	0.457 ± 0.097	-0.021	t =6.316, P<0.001
TC (mmol/L)	4.86 ± 0.89	4.69 ± 0.94	-0.17	t = 5.287, P<0.001
TG (mmol/L)	1.68 ± 1.10	1.66 ± 1.10	-0.02	t =0.487, P= 0.626
LDL-c (mmol/L)	3.14 ± 0.79	3.03 ± 0.84	-0.11	t =3.824, P=0.001
HDL-C (mmol/L)	1.30 ± 0.34	1.29 ± 0.34	-0.008	t =0.739, P=0.460
FBG (mmol/L)	5.79 ± 1.18	5.95 ± 1.30	0.15	t =3.378, P=0.001
HbA1c (%)	5.90 ± 0.74	6.06 ± 0.79	0.16	t = -5.845, P<0.001
Hcy (μmol/L)	12.32 ± 5.99	12.41 ± 5.33	0.09	t =0.419, P=0.675
Ca^{2+} (mmol/L)	2.325 ± 0.085	2.335 ± 0.086	0.010	t =3.279, P=0.001
K^+ (mmol/L)	4.226 ± 0.292	4.331 ± 0.318	0.105	t = 9.541, P<0.001
P (mmol/L)	1.156 ± 0.152	1.153 ± 0.154	0.003	t =0.506, P=0.613
iPTH (pg/ml)	46.68 ± 14.31	46.49 ± 16.96	0.191	t =0.089, P=0.929
25 (OH)D (nmol/L)	15.38 ± 6.67	19.11 ± 8.42	3.73	t =3.5547, P=0.0004

BMI, body mass index; BMD, forearm bone mineral density; BFP, body fat percent (body fat/weightx100%); SMI, skeletal muscle mass index (total muscular mass/weight x100%); TC, Total cholesterol; TG, Triglyceride; HDL-C, high density lipoprotein cholesterol; LDL-C, low density lipoprotein cholesterol; FBG, fasting blood glucose; HbA1c, hemoglobin A1c; Hcy, blood homocysteine; P, inorganic phosphorus; iPTH, Intact parathyroid hormone.

Unsurprisingly, age and smoking were determined to be risk factors for osteopenia and osteoporosis, consistent with numerous previous studies (30, 31). Women were determined to be more at risk for osteoporosis, as expected based on a large body of clinical and experimental studies (14, 32). In this study, protective factors seemed to show a greater effect in women, likely due in part because the overall cohort included more men (57.58%) than women (42.42%). It is also notable that the

TABLE 4 The self-control study of BMD grouped by BMI, BFP and SMI. .

	Baseline (n=1,608)					Follow-up (n=1,608)				
	Normal BMD	Osteopenia	Suspected osteoporosis	Total	BMD	Normal BMD	Osteopenia	Suspected osteoporosis	Total	BMD
BMI grouping										
Low weight	2 (9.09)	16 (72.73)	4 (18.18)	22	0.447 ±0.114	0 (0.00)	10 (76.92)	3 (23.08)	13	0.404 ±0.136
Normal weight	25 (3.96)	504 (79.87)	102 (16.17)	631	0.463 ±0.093	15 (2.84)	375 (70.89)	139 (26.28)	529	0.434 ±0.104
Overweight	24 (3.15)	643 (84.49)	94 (12.35)	761	0.489 ±0.084Δ	26 (3.19)	629 (77.08)	161 (19.73)	816	0.470 ±0.090 Δ
Obesity	6 (30.9)	161 (82.99)	27 (13.92)	194	0.487 ±0.089	12 (4.80)	181 (72.40)	57 (22.80)	250	0.467 ±0.089
Statistics		χ2=7.63, P= 0.267			F=11.97, P<0.001		χ2=10.49, P= 0.105			F=18.34, P<0.001
SMI grouping										
Low SMI	4 (1.83)	176 (80.73)	38 (17.43)	218	0.409 ±0.081	12 (2.76)	297 (68.43)	125 (28.80)	434	0.402 ±0.088
Moderate SMI	18 (2.25)	663 (82.88)	119 (14.88)	800	0.471 ±0.086*	30 (3.54)	634 (74.85)	183 (21.61)	847	0.471 ±0.093*
High SMI	35 (5.93)	485 (82.20)	70 (11.86)	590	0.513 ±0.081*#Δ	11 (3.36)	264 (80.73)	52 (15.90)	327	0.496 ±0.086*#Δ
		χ2=19.31, P= 0.001			F=127.98, P<0.001		χ2=18.75, P= 0.001			F=120.36, P<0.001
BFP grouping										
Low BFP	34 (5.81)	482 (82.39)	69 (11.79)	585	0.512 ±0.081†‡Δ	11 (3.51)	253 (80.83)	49 (15.65)	313	0.498 ±0.086†‡Δ
Moderate BFP	18 (2.30)	650 (83.12)	114 (14.58)	782	0.474 ±0.085†	29 (3.54)	615 (75.00)	176 (21.46)	820	0.472 ±0.092†
High BFP	5 (2.07)	192 (79.67)	44 (18.26)	241	0.409 ±0.084	13 (2.74)	327 68.84)	135 (28.42)	475	0.406 ±0.089
		χ2=18.91, P= 0.001			F=132.28, P<0.001		χ2=18.77, P= 0.001			F=120.28, P<0.001

BMI, body mass index; BMD, forearm bone mineral density; BFP, body fat percent (body fat/weight x100%); SMI, skeletal muscle mass index (total muscular mass/weight x100%).
*Compared with low SMI, P<0.05.
#Compared with moderate SMI, P<0.05.
†Compared with high BFP, P<0.05.
‡Compared with moderate BFP, P<0.05.
ΔHighest performance.

percentage of women who shifted from normal BMD to suspected osteoporosis increased ($\chi2$ = 357.43, $P<0.001$) in the baseline study.

The suspected osteoporosis group had the lowest BMI in the three groups, and multivariate analysis determined BMI to be a protective factor. At first glance, these findings would suggest that the higher the BMI, the lower the chance of developing osteoporosis. A deeper dive into these findings suggest a more complex interpretation of these results, however. Specifically, there was a significant positive association between BMD and BMI (β=0.1446, $P<0.001$). Furthermore, it is clear from longitudinal analysis of the 1,608 individuals who completed the ≥ 5-year follow-up that individuals who have an excessively low (i.e. underweight) or high BMI (i.e., obesity) are both more likely to develop osteoporosis. A large number of studies have confirmed that: first, people with an excessively low BMI tend to have

malnutrition, whereas an updated America endocrine guideline in 2020 concluded that adequate protein intake helps to reduce bone loss (31) and that patients after bariatric surgery with major gastric resection have prevalent osteoporosis, also laterally reflecting the Association of malnutrition with osteoporosis or not just calcium and vitamin D supplementation (32). Second, groups with an excessively low BMI are often accompanied by a low SMI, and the mechanisms of osteoporosis with a low SMI are discussed later. And the association between obesity and osteoporosis, which is often explained by the fact that high BMI is positively associated with high BFP, and higher body fat rate and lower BMD, will be discussed later.

As further support of the association between low BMD and obesity, our findings showed a significant positive association between BFP the rate of suspected osteoporosis ($\chi2$ = 524.72, $P<0.001$). Indeed, BMD and BFP had a significant negative

association (β= -0.3839, P<0.001). This was not the case for SMI, however, as it was determined that the higher the SMI level, the lower the rate of suspected osteoporosis ($\chi2$ = 538.85, P<0.001). There was also a significant positive association (β=0.3855, P<0.001) between BMD and SMI, suggesting a lower rate of osteoporosis among individuals with higher SMI or lower BFP. This result is consistent with most prior studies (16, 33, 34).

Our longitudinal analysis of the 1,608 individuals who received baseline and ≥ 5-year follow-up examinations showed that sex, smoking and drinking were not significant factors influencing new rates of suspected osteoporosis. All individuals experienced a similar increase in age across this sample, while simultaneously their BFP, BMI, FBG, HbA1c, Ca^{2+}, K$^+$ and 25-(OH)D levels also significantly increased from baseline. SMI, BMD, TC and LDL-C significantly decreased. These observed changes in FBG and HbA1c might be associated with aging. Since this study did not exclude individuals receiving lipid-lowering medication, the influence of such medication on the changes in TC and LDL-C which were observed cannot be ruled out. This study also did not exclude individuals receiving osteoporosis medications to which the increase of Ca^{2+}, K$^+$ and 25 (OH)D may have been connected. BFP, BMI and SMI are all modifiable factors and the change of SMI and BFP over the ≥ 5-year span may have affected BMI.

The longitudinal analysis further determined that at baseline, the group with a high SMI also had the highest BMD. BMD typically decreases with age, but individuals with a higher SMI have a greater bone mass and thus have a lower rate of osteoporosis. Similarly, individuals with a low BFP have the highest level of BMD. Taken together these data fully support the notion that lowering BFP and increasing SMI can help prevent osteoporosis (35, 36).

Theoretically, the positive association between SMI and BMD and the negative association between SMI and BFP can be attributed to three factors. The first and likely most important, according to some studies, is the mechanical forces between adjacent muscle and bone tissues. Given these forces, resistance exercise is a good way to increase SMI and BMD because this exercise causes these tissues to adapt in response to repetitive actions. The second important factor is the interaction and mutual promotion between the endocrine and paracrine actions of muscle and bone tissues. Skeletal muscle, particularly when contracting, can function as an endocrine organ and secrete myokines such as IGF-1 and irisin (37). Irisin secreted during exercise may play a role as a messenger in the muscle-fat-skeleton-brain axis, promoting energy consumption by fat cells, the differentiation of bone cells and suppressing the maturation of osteoclasts, thus influencing bone metabolism and enhancing bone density (38). The third factor is that increased BFP and enlarged fat cells cause sarcopenic obesity and promote chronic inflammation and insulin resistance. One study showed that apelin secreted by fat cells also regulates bone turnover and lowers BMD, increasing catabolism and leading to sarcopenia (39). Regardless of the underlying mechanisms, from a clinical perspective the most effective and appropriate strategy to prevent osteoporosis-related fractures is lifestyle modification (e.g., exercise and nutrition).

Since 2019, COVID-19 prevention measures such as travel bans, quarantines, and lockdowns, have had a seriously adverse effect on people's lifestyle by reducing exercise, especially among the older adult population. Prolonged sedentary time is likely to increase BFP, lower SMI and reduce muscle force, which manifests as increased risk of falls and a possible surge in osteoporotic fractures. Thus, a greater attention to health management with respect to BMD is required in these times (40).

This study has several limitations, foremost of which are that it was a single-center study which used peripheral dual-energy X-ray absorptiometry for BMD measurement. These limitations were offset by the numerous merits of the study, including the large sample size which included a subset cohort with ≥ 5-year follow-up, use of consistent instrumentation and data harmonization due to the fact that the same medical staff performed every measurement in the entire cohort. Bioelectrical impedance is not a gold standard for evaluating body composition and have some disadvantages, and it is difficult to establish cause-and-effect relationships with cross-sectional design studies. Thus, our findings need further studies to confirm.

In conclusion, this study provides clear evidence that modifiable body composition indicators, including BMI, BFP and SMI, are all factors that significantly influence BMD. From a clinical perspective, these findings suggest that encouraging patients to adopt lifestyle measures to control BFP and increase SMI will help prevent osteoporosis.

Data availability statement

The raw data supporting the conclusions of this article will be made available by the authors, without undue reservation.

Ethics statement

The study protocol was approved by the Chinese People's Liberation Army General hospital ethics committee and complied with the principles of the Declaration of Helsinki and its contemporary amendments. The patients/participants provided their written informed consent to participate in this study.

Author contributions

YZ designed this study, acquired and analyzed the data. YL and ZH wrote the original drafts. YG wrote the review and prepared the tables. QZ reviewed and edited the manuscript. All authors read and approved the final manuscript. YL and ZH

contributed equally as co-first authors. All authors contributed to the article and approved the submitted version.

Conflict of interest

The authors declare that the research was conducted in the absence of any commercial or financial relationships that could be construed as a potential conflict of interest.

Publisher's note

All claims expressed in this article are solely those of the authors and do not necessarily represent those of their affiliated organizations, or those of the publisher, the editors and the reviewers. Any product that may be evaluated in this article, or claim that may be made by its manufacturer, is not guaranteed or endorsed by the publisher.

References

1. Elbers LPB, Raterman HG, Lems WF. Bone mineral density loss and fracture risk after discontinuation of anti-osteoporotic drug treatment: A narrative review. *Drugs* (2021) 81(14):1645–55. doi: 10.1007/s40265-021-01587-x

2. GBD 2016 DALYs and HALE Collaborators. Global, regional, and national disability-adjusted life-years (DALYs) for 333 diseases and injuries and healthy life expectancy (HALE) for 195 countries and territories, 1990-2016: A systematic analysis for the global burden of disease study 2016. *Lancet* (2017) 390 (10100):1260–344. doi: 10.1016/S0140-6736(17)32130-X

3. Zeng Q, Li N, Wang Q, Feng J, Sun D, Zhang Q, et al. The prevalence of osteoporosis in China, a nationwide, multicenter DXA survey. *J Bone Miner Res* (2019) 34(10):1789–97. doi: 10.1002/jbmr.3757

4. Curtis EM, Moon RJ, Harvey NC, Cooper C. The impact of fragility fracture and approaches to osteoporosis risk assessment worldwide. *Bone* (2017) 104:29–38. doi: 10.1016/j.bone.2017.01.024

5. Odén A, McCloskey EV, Kanis JA. Burden of high fracture probability worldwide: secular increases 2010-2040. *Osteoporos Int* (2015) 26(9):2243–8. doi: 10.1007/s00198-015-3154-6

6. Nwogu UB, Agwu KK, Anakwue AC, Idigo FU, Okeji MC, Abonyi EO, et al. Bone mineral density in an urban and a rural children population-a comparative, population-based study in enugu state, Nigeria. *Bone.* (2019) 127:44–8. doi: 10.1016/j.bone.2019.05.028

7. Jiang BC, Villareal DT. Weight loss-induced reduction of bone mineral density in older adults with obesity. *J Nutr Gerontol Geriatr* (2019) 38(1):100–14. doi: 10.1080/21551197.2018.1564721

8. Fabiani R, Naldini G, Chiavarini M. Dietary patterns in relation to low bone mineral density and fracture risk: A systematic review and meta-analysis. *Adv Nutr* (2019) 10(2):219–36. doi: 10.1093/advances/nmy073

9. Taha IM, Allah AMA, Tarhouny SEl. Association of vitamin d gene polymorphisms and bone mineral density in healthy young Saudi females. *Curr Mol Med* (2019) 19(3):196–205. doi: 10.2174/1566524019666190409122155

10. Krela-Kazmierczak I, Wawrzyniak A, Szymczak A, Eder P, Lykowska-Szuber L, Michalak M, et al. Bone mineral density and the 570A>T polymorphism of the bone morphogenetic protein 2 (BMP2) gene in patients with inflammatory bowel disease: A cross-sectional study. *J Physiol Pharmacol* (2017) 68(5):757–64.

11. Dobrolińska M, van der Tuuk K, Vink P, van den Berg M, Schuringa A, Monroy-Gonzalez AG, et al. Bone mineral density in transgender individuals after gonadectomy and long-term gender-affirming hormonal treatment. *J Sex Med* (2019) 16(9):1469–77. doi: 10.1016/j.jsxm.2019.06.006

12. Berry SD, Dufour AB, Travison TG, Zhu H, Yehoshua A, Barron R, et al. Changes in bone mineral density (BMD): A longitudinal study of osteoporosis patients in the real-world setting. *Arch Osteoporos* (2018) 13(1):124. doi: 10.1007/s11657-018-0528-3

13. Hashimoto Y, Osaka T, Fukuda T, Tanaka M, Yamazaki M, Fukui M. The relationship between hepatic steatosis and skeletal muscle mass index in men with type 2 diabetes. *Endocr J* (2016) 63(10):877–84. doi: 10.1507/endocrj.EJ16-0124

14. Kwon HJ, Ha YC, Park HM. The reference value of skeletal muscle mass index for defining the sarcopenia of women in Korea. *J Bone Metab* (2015) 22 (2):71–5. doi: 10.11005/jbm.2015.22.2.71

15. Cruz-Jentoft AJ, Bahat G, Bauer J, Boirie Y, Bruyère O, Cederholm T, et al. Sarcopenia: revised European consensus on definition and diagnosis. *Age Ageing* (2019) 48(1):16–31. doi: 10.1093/ageing/afy169

16. Xu X, Xu N, Wang Y, Chen J, Chen L, Zhang S, et al. The longitudinal associations between bone mineral density and appendicular skeletal muscle mass in Chinese community-dwelling middle aged and elderly men. *PeerJ* (2021) 9: e10753. doi: 10.7717/peerj.10753

17. Al-Sofiani ME, Ganji SS, Kalyani RR. Body composition changes in diabetes and aging. *J Diabetes Complications* (2019) 33(6):451–9. doi: 10.1016/j.jdiacomp.2019.03.007

18. Cruz-Jentoft AJ, Bahat G, Bauer J, Boirie Y, Bruyère O, Cederholm T, et al. Sarcopenia: revised European consensus on definition and diagnosis. *Age Ageing* (2019) 48(4):601. doi: 10.1093/ageing/afz046

19. Mytton OT, Jackson C, Steinacher A, Goodman A, Langenberg C, Griffin S, et al. The current and potential health benefits of the national health service health check cardiovascular disease prevention programme in England: A microsimulation study. *PLoS Med* (2018) 15(3):e1002517. doi: 10.1371/journal.pmed.1002517

20. Shivaprasad C, Marwaha RK, Tandon N, Kanwar R, Mani K, Narang A, et al. Correlation between bone mineral density measured by peripheral and central dual energy X-ray absorptiometry in healthy Indian children and adolescents aged 10-18 years. *J Pediatr Endocrinol Metab* (2013) 26(7-8):695–702. doi: 10.1515/jpem-2012-0359

21. Yue C, Ding N, Xu LL, Fu YQ, Guo YW, Yang YY, et al. Prescreening for osteoporosis with forearm bone densitometry in health examination population. *BMC Musculoskelet Disord* (2022) 23(1):377. doi: 10.1186/s12891-022-05325-6

22. Anam AK, Insogna K. Update on osteoporosis screening and management. *Med Clin North Am* (2021) 105(6):1117–34. doi: 10.1016/j.mcna.2021.05.016

23. Wang Z, McMonagle C, Yoshimitsu S, Budhathoki S, Morita M, Toyomura K, et al. No effect modification of serum bilirubin or coffee consumption on the association of gamma-glutamyltransferase with glycated hemoglobin in a cross-sectional study of Japanese men and women. *BMC Endocr Disord* (2012) 12:24. doi: 10.1186/1472-6823-12-24

24. National Health and Family Planning Commission of China. *China Clinical smoking cessation guideline*. Beijing: People's Medical Publishing House (2015).

25. Wang SS, Lay S, Yu HN, Shen SR. Dietary guidelines for Chinese residents (2016): comments and comparisons. *J Zhejiang Univ Sci B* (2016) 17(9):649–56. doi: 10.1631/jzus.B1600341

26. Chen C, Lu FC. Department of disease control ministry of health, PR china. the guidelines for prevention and control of overweight and obesity in Chinese adults. *BioMed Environ Sci* (2004) 17 Suppl:1–36.

27. Chen Z, Wang F, Zheng Y, Zeng Q, Liu H. H-type hypertension is an important risk factor of carotid atherosclerotic plaques. *Clin Exp Hypertens* (2016) 38(5):424–8. doi: 10.3109/10641963.2015.1116547

28. Roberts RF, Roberts WL. Performance characteristics of a recombinant enzymatic cycling assay for quantification of total homocysteine in serum or plasma. *Clin Chim Acta* (2004) 344(1-2):95–9. doi: 10.1016/j.cccn.2004.02.013

29. Kanis JA. Assessment of fracture risk and its application to screening for postmenopausal osteoporosis. Report of a WHO study group. *World Health Organ Tech Rep Ser* (1994) 843:1–129.

30. Lo SS. Prevalence of osteoporosis in elderly women in Hong Kong. *Osteoporos Sarcopenia* (2021) 7(3):92–7. doi: 10.1016/j.afos.2021.09.001

31. Camacho PM, Petak SM, Binkley N, Diab DL, Eldeiry LS, Farooki A, et al. American Association of clinical endocrinologists/American college of endocrinology clinical practice guidelines for the diagnosis and treatment of postmenopausal osteoporosis-2020 update. *Endocr Pract* (2020) 26(Suppl 1):1–46. doi: 10.4158/GL-2020-0524SUPPL

32. Ieong K, Ardila-Gatas J, Yang J, Zhang X, Tsui ST, Spaniolas K, et al. Bone mineral density changes after bariatric surgery. *Surg Endosc* (2021) 35(8):4763–70. doi: 10.1007/s00464-020-07953-2

33. Delagrange M, Rousseau V, Cessans C, Pienkowski C, Oliver I, Jouret B, et al. Low bone mass in noonan syndrome children correlates with decreased

muscle mass and low IGF-1 levels. *Bone* (2021) 153:116170. doi: 10.1016/j.bone.2021.116170

34. Parulekar AD, Wang T, Li GW, Hoang V, Kao CC. Pectoralis muscle area is associated with bone mineral density and lung function in lung transplant candidates. *Osteoporos Int* (2020) 31(7):1361–7. doi: 10.1007/s00198-020-05373-5

35. Kopiczko A, Adamczyk JG, Gryko K, Popowczak M. Bone mineral density in elite masters athletes: the effect of body composition and long-term exercise. *Eur Rev Aging Phys Act* (2021) 18(1):7. doi: 10.1186/s11556-021-00262-0

36. Marin-Mio RV, Moreira LDF, Camargo M, Périgo NAS, Cerondoglo MS, Lazaretti-Castro M. Lean mass as a determinant of bone mineral density of proximal femur in postmenopausal women. *Arch Endocrinol Metab* (2018) 62 (4):431–7. doi: 10.20945/2359-3997000000059

37. Kirk B, Feehan J, Lombardi G, Duque G. Muscle, bone, and fat crosstalk: the biological role of myokines, osteokines, and adipokines. *Curr Osteoporos Rep* (2020) 18(4):388–400. doi: 10.1007/s11914-020-00599-y

38. Grygiel-Górniak B, Puszczewicz M. A review on irisin, a new protagonist that mediates muscle-adipose-bone-neuron connectivity. *Eur Rev Med Pharmacol Sci* (2017) 21(20):4687–93.

39. Giardullo L, Corrado A, Maruotti N, Cici D, Mansueto N, Cantatore FP. Adipokine role in physiopathology of inflammatory and degenerative musculoskeletal diseases. *Int J Immunopathol Pharmacol* (2021) 35:20587384211015034. doi: 10.1177/20587384211015034

40. Hampson G, Stone M, Lindsay JR, Crowley RK, Ralston SH. Diagnosis and management of osteoporosis during COVID-19: systematic review and practical guidance. *Calcif Tissue Int* (2021) 109(4):351–62. doi: 10.1007/s00223-021-00858-9

Check for updates

Menopause-related cortical loss of the humeral head region mainly occurred in the greater tuberosity

Yeming Wang[1]*, Jian Li[2], Yutao Men[3,4] and Wanfu Wei[1]*

[1]Department of Orthopedics, Tianjin Hospital, Tianjin University, Tianjin, China, [2]Department of Radiology, Tianjin Hospital, Tianjin University, Tianjin, China, [3]Tianjin Key Laboratory for Advanced Mechatronic System Design and Intelligent Control, School of Mechanical Engineering, Tianjin University of Technology, Tianjin, China, [4]National Demonstration Center for Experimental Mechanical and Electrical Engineering Education, Tianjin University of Technology, Tianjin, China

Aims: Proximal humerus fractures are commonly observed in postmenopausal women. The goal of this study was to investigate menopause-related changes in cortical structure of the humeral head.

Materials and methods: Clinical computed tomography (CT) scans of 75 healthy women spanning a wide range of ages (20−72 years) were analyzed. For each subject, cortical bone mapping (CBM) was applied to create a color three-dimensional (3D) thickness map for the proximal humerus. Nine regions of interest (ROIs) were defined in three walls of the humeral head. Cortical parameters, including the cortical thickness (CTh), cortical mass surface density (CM), and the endocortical trabecular density (ECTD), were measured.

Results: Compared to premenopausal women, postmenopausal women were characterized by a significantly lower CTh and CM value in the lateral part of the greater tuberosity. Similar changes were only found in ROI 4, but not in ROIs 5−6 in the lesser tuberosity. Linear regression analysis revealed that the CTh and CM value of ROIs 1, 3, and 4 were negatively associated with age. These results showed that menopause-related loss in CTh and CM was mainly in the greater tuberosity besides the proximal part of the lesser tuberosity. Trabecular bone variable measured as ECTD showed a notably lower value in ROIs 1−9 in postmenopausal vs. premenopausal group. Inverse linear associations for ECTD and age were found in ROIs 2, 3, 5, 6, 7, and 9, indicating no site-specific differences of endocortical trabecular bone loss between the greater and lesser tuberosity.

Conclusions: Menopause-related cortical loss of the humeral head mainly occurred in the lateral part of the greater tuberosity. The increased rate of humeral bone loss in the greater tuberosity may contribute materially to complex proximal humerus fractures.

KEYWORDS

cortical bone, humeral head, menopause, age, greater tuberosity

Introduction

Proximal humerus fractures (PHFs) are common fragility fractures in elderly patients, second only to vertebral and hip fractures in terms of incidence (1). These fractures are associated with low bone mineral density (BMD) and increase in incidence after the age of 50 (1–3). Most PHFs are observed in postmenopausal women (3). Estrogen deficiency after menopause resulted in an unbalanced coupling between resorption and formation in favor of bone resorption, gradually producing microstructural deterioration and reduction of the mineral content of the bone material. Previous studies have concentrated on age-related changes of trabecular microstructure for its distinct remodeling (4, 5). However, cortical bone constitutes 80% of skeletal mineralized bone volume in adults, particularly at appendicular sites where the cortex accounts for the majority of axial load transfer (6, 7). Recent studies on the radius, femur, and humerus had found that bone loss during aging is predominantly cortical in origin and reaches a maximum around the age of 65 years (8, 9). Cortical bone accounted for over 80% of all the bone loss during and after menopause. Porosity increased in the compact-appearing, outer, and inner transitional zones of the cortex (10). In a 3-year prospective study using high-resolution peripheral QCT (HR-pQCT), an increase in endosteal perimeter and cortical porosity at the radius was detected in postmenopausal women, which partly led to an annual decline in the estimated failure load (11). Therefore, cortical loss has a more negative effect on mechanical stability than trabecular bone loss and contributes to skeletal fragility (8–12).

Bone strength is determined not only by bone mass but also by bone morphology as size, shape, and three-dimensional (3D) architecture and microarchitecture. The most important risk factor for bone loss in midlife women is menopause. The increases in the outer diameter of the femoral neck were found to parallel the reduction in BMD and section modulus during the menopause transition (13). These suggest that changes in bone size could contribute to an increased fracture risk, although they may partially compensate for bone loss resulting from endosteal resorption. Several cohort studies demonstrated that deficits in cortical and trabecular bone density and microstructure predict incident fracture independently of femoral neck BMD and FRAX (Fracture Risk Assessment Tool) score (14–16). Cortical BMD, thickness, and area at the tibia were considered as part of the best set of fracture predictors in these studies that can be expected, as the structural properties of cortical bone are proposed to be the major contributors to bone strength (14, 16, 17).

The proximal humerus is relatively under investigation as one of the most common sites of osteoporotic fracture. Few studies have explored age-related changes in trabecular bone properties at the proximal humerus (4, 6, 18). Little data are available for menopause-related changes of the cortical structure in the proximal humerus.

The purpose of the present study was to evaluate the cortical bone characteristics of the proximal humerus in quantitative CT data obtained in healthy women before and after menopause.

Materials and methods

Subjects and study design

Individuals were participants in the aging and osteoporotic PHF study, a single-center prospective ongoing population study of Chinese men and women. Our analytical sample included 75 healthy women, aiming to evaluate menopause-related changes in cortical bone of the humeral head region in the dominant upper extremity. All subjects were Han Chinese. Menopause was defined as the date of the last menses followed by 12 months without menses. Thirty-five (46.7%) women were premenopausal, with a regular cycle in the last 3 months, and 40 (53.3%) were postmenopausal. Subjects with a history of or evidence of metabolic bone disease and those receiving chronic treatment that may affect bone metabolism were excluded from the study. Arm dominance was determined as the arm with which subjects would throw a ball. For this study, no dual-energy X-ray absorptiometry screening was performed prior to enrollment; therefore, no BMD inclusion/exclusion criteria were used. Written informed consent was obtained from all participants, and the study was approved by the institutional review board of Tianjin Hospital.

Cortical bone mapping

CT scanning (Mx 8000 IDT; Philips Medical Systems, Best, Netherlands) was performed at 120 kV (peak) and 168 milliampere-seconds. CT images were created in slice increments of 2.00 mm at a resolution of 0.566 mm × 0.566 mm/pixel with a field of view of 29 cm × 29 cm. Subjects were positioned supine with their arms in neutral position and centered within the gantry of the machine. Each image was analyzed from the slice that included the top of the acromion to the slice that included the inferior angle of the scapula. All CT scanning was performed by JL. CT values of pixels were recorded in Hounsfield units (HUs).

The cortical parameter measurement and mapping technique have been previously described (19, 20). Cortical thickness (CTh) measurement was performed using cortical bone mapping (CBM), implemented by a freely available in-house program called Stradwin (http://mi.eng.cam.ac.uk/~rwp/stradwin/). First, an approximate segmentation of each proximal humerus from the CT data was performed using Stradwin and results in a triangulated surface mesh with ~10 (4) vertices distributed uniformly over the proximal humerus surface. Second, the CT data were sampled at each vertex of the mesh

using 18-mm lines perpendicular to and passing through the humeral cortex and trabeculae. Finally, a model that accounts for the imaging blur was fitted to the data samples. This validated model-based deconvolution process allows the measurement of much smaller features than would normally be visible in the CT data. This process was repeated at all vertices. As a result, color maps on the proximal humerus were created for accurately estimating the CTh (in mm) and cortical mass surface density (CM, the cortical mass per unit surface area), as well as the endocortical trabecular density (ECTD), which is the trabecular density directly adjacent to the cortex.

Definition of the regions of interest for cortical bone distribution assessment

For the evaluation of the bone morphometric analysis, specific regions of interest (ROIs) were defined within the proximal end of the humerus. The specific methodology has been described in detail previously and will be briefly outlined here (18). The cortical bone in the humeral head region was defined as anterior, lateral, and posterior walls. In an anatomical perspective, the anterior wall is equivalent to the lesser tuberosity. The lateral and posterior parts of the greater tuberosity correspond to the lateral and posterior walls. Following the creation of a single 3D thickness map, the humeral head height (H) was determined by measuring the distance between the highest point of the humeral head and

the most distal margin of the articular surface (Figure 1). The height of the humeral head was then quartered by axial planes 1–3 that were equidistant to each other. In each slice, to obtain more details of cortical bone tissue, the longest line (Line 1) between the joint surface and greater tuberosity was drawn; this line was divided into a medial and a lateral segment by line 2, which intersected it at right angles (Figure 2). ROIs 1–9 were established as cortical bone measurement points (Figure 3).

Statistical analysis

The cortical difference between premenopausal vs. postmenopausal group was compared using t tests for

FIGURE 2
Locations of the measuring points in the humeral head region. Line 1, longest diameter between the articular surface and the greater tuberosity. Line 2, vertical bisection of line 1. GT, greater tuberosity; LT, lesser tuberosity.

FIGURE 1
Region of investigation. The humeral head height (H) was the distance between the highest point of the humeral head and the most distal margin of the articular surface. In the humeral head region (HHR), cortical parameters were determined within different trisections of humeral head height. GT, greater tuberosity; LT, lesser tuberosity.
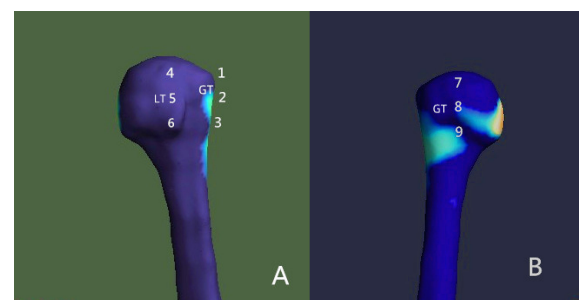
FIGURE 3
Placement of the regions of interest (ROIs) Nine ROIs were defined in the humeral head region. **(A)** Anterior view; **(B)** posterior view. GT, greater tuberosity; LT, lesser tuberosity.

normally distributed values and Kruskal–Wallis test for non-normally distributed values. The correlation between cortical indices and age in ROIs 1–9 was studied by linear regression analysis. All statistical analyses were performed using IBM SPSS Statistics for Windows version 20.0 (IBM SPSS Inc., Chicago, IL, USA). Significance level was set at P < 0.05 for all statistical tests.

Results

Changes in morphology prior to and after menopause

The median age of the premenopausal and postmenopausal groups was 35 years (interquartile range, 27–43 years) and 65 years (interquartile range, 61–67 years), respectively. When compared to the premenopausal women, postmenopausal women were characterized by a significantly lower CTh and CM value of ROIs 1–3 in the lateral part of the greater tuberosity (all P < 0.05). Similar changes were only found in ROI 4 (all P < 0.05) but not in ROIs 5–6 in the anterior wall. In the posterior wall, no difference was detected between the two groups for either CTh or CM. These results indicated that menopause-related loss in CTh and CM was mainly in the greater tuberosity, but also the proximal part of the lesser tuberosity. Trabecular bone parameter measured as ECTD showed a notably lower value in ROIs 1–9 in the postmenopausal group, showing that endocortical trabecular loss occurred in both the greater and lesser tuberosity (all P < 0.05, Table 1).

Age-related differences in cortical bone quality

When pooled across all decades, linear regression analysis revealed that the CTh and CM values of ROIs 1, 3, and 4 were negatively associated with age (all P < 0.05) (Figure 4). Similarly, inverse linear associations for ECTD and age were found in ROIs 2, 3, 5, 6, 7, and 9 (all P < 0.05). It can be seen that the decline of CTh and CM with age occurred in the proximal part of the greater and lesser tuberosity, whereas there was no site-specific difference in endocortical trabecular bone loss between the greater and lesser tuberosity.

Discussion

This study investigated the menopause-related changes in CTh, CM, and ECTD in specific regions of the humeral head region measured in a Chinese cohort by CBM technique. Our principal findings are as follows: 1) The predominant cortical loss occurred in the lateral part of the greater tuberosity after menopause; 2) Obvious cortical loss in the proximal parts of the

TABLE 1 Menopause-related difference in variables of ROIs of the subjects.

Variables	Premenopausal (n=35)	Postmenopausal (n=40)	p value
Age	34.83±9.13	64.80±6.77	
CTh(mm)			
ROI1	5.24±1.28	3.37±1.74	0.00
ROI2	3.31±1.36	2.57±1.51	0.03
ROI3	3.23±1.28	2.34±1.06	0.02
ROI4	4.49±1.44	3.67±1.58	0.02
ROI5	4.10±1.49	3.52±1.71	0.12
ROI6	4.21±1.50	3.56±1.80	0.09
ROI7	2.77±0.99	2.18±0.90	0.84
ROI8	2.34±0.74	2.18±0.91	0.41
ROI9	2.97±1.28	2.79±1.71	0.53
CM(HUmm)			
ROI1	56401.68±17832.52	38621.11±22082.35	0.00
ROI2	45311.95±44759.36	29414.84±17783.92	0.04
ROI3	37257.85±17071.22	26409.81±11929.56	0.03
ROI4	49615.49±18884.85	40749.49±18470.29	0.04
ROI5	46744.91±18571.47	38875.54±19476.03	0.08
ROI6	48107.64±18513.44	40049.46±20818.40	0.08
ROI7	32088.01±13076.91	31503.35±15719.24	0.86
ROI8	26173.71±9264.46	24712.46±10513.65	0.53
ROI9	34894.03±16476.05	32391.99±14546.94	0.49
ECTD(HU)			
ROI1	10112.27±52.88	10015.68±228.10	0.01
ROI2	10085.80±46.49	9975.02±220.37	0.00
ROI3	10066.51±55.49	9953.70±222.96	0.01
ROI4	10140.62±198.61	10025.55±222.67	0.02
ROI5	10110.30±59.89	9995.32±216.77	0.00
ROI6	10122.42±72.51	9996.68±220.12	0.00
ROI7	10129.84±68.45	10020.52±210.33	0.00
ROI8	10097.12±65.95	10000.30±225.45	0.02
ROI9	10092.00±63.28	9972.49±227.40	0.00

The values are given as the mean and the standard deviation. CTh, cortical thickness, CM, cortical mass surface density, ECTD, the endocortical trabecular density.

greater and lesser tuberosity was detected in postmenopausal women; 3) The greater and lesser tuberosity had similar patterns of endocortical trabecular bone loss with aging.

Cortical bone bears the bulk of axial loads in the proximal humerus, and the distribution of the cortex is an important factor in bone strength and fracture prediction (18, 21). Our data demonstrated a main accentuation of cortical bone in the lateral part of the greater tuberosity after menopause. Meanwhile, ECTD decreased obviously in each ROI in the greater and lesser tuberosity, suggesting that excess endocortical resorption in postmenopausal women agreed with earlier histomorphometric analysis (4). The marked decrease of cortical bone thickness and mass surface density in the greater tuberosity indicated a structural weakness, which was closely connected with fracture for stress concentration effects. Focal cortical thinning in the greater tuberosity may play a vital role in
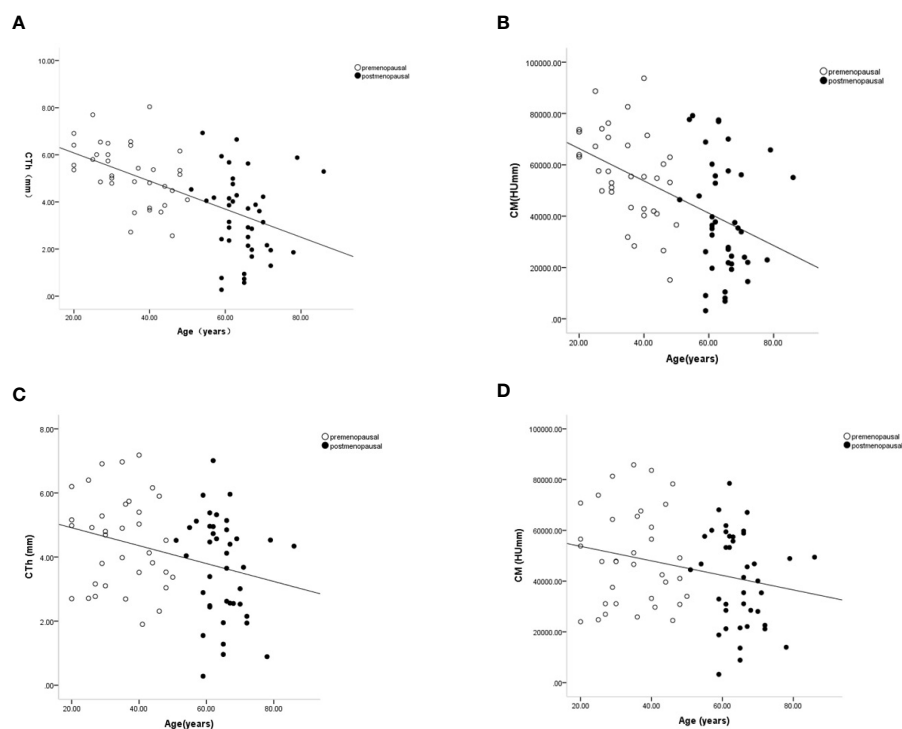
FIGURE 4
Age-related changes in cortical thickness and cortical mass surface density in the proximal part of the lateral wall (ROI 1) **(A, B)** and anterior wall (ROI 4) **(C, D)**. Premenopausal outcomes are indicated by open symbols, postmenopausal outcomes by full symbols. Solid lines represent the fitted mean from the regression models.

proximal humerus fractures associated with falls. Previous studies had focused on spatial differences in proximal humeral CTh and discovered that proximal humerus fractures occur along lines of cortical thinning (22, 23). Furthermore, the isolated greater tuberosity fractures are believed to represent the commencement of a cascade of events that ultimately culminate in a shield-type proximal humerus fracture (23). Our finding might illuminate why complex proximal humerus fractures tend to initiate in a particular zone.

The gross properties of cortical bone change substantially after menopause. However, the pattern and magnitude of bone loss differ at various skeletal sites and may be related to local biomechanical load or to various degrees of response to decreased estrogen (11, 24). In normal gait, the greatest stresses occur in the subcapital and medial midfemoral neck regions, where maximum compressive stresses occur inferiorly (14). Superiorly, smaller-magnitude tensile stresses occur during walking. Accordingly, bone decrement occurs preferentially in the superior region than in the inferior region of the femoral neck during aging (14, 24). In this study, we found that the CTh of the proximal parts of the lateral and anterior walls of the humerus was lower significantly in postmenopausal women and negatively associated with age. Anatomically, the rotator cuff is

attached to both the greater tuberosity and lesser tuberosity (Figure 5). The intrinsic properties of the proximal humerus cortex depend on mechanical loading from the rotator cuff activity, unlike the weight-bearing bones as proximal femur or tibia (21). We speculated that normal daily loading from the rotator cuff cannot prevent menopause and/or age-related cortical loss from the proximal part of the anterior and lateral walls of the humeral head. Consistent with our findings, Shanbhogue et al. (11) observed trabecular separation at the radius but not the tibia with advancing age and during the menopause transition. Taken together, we believed that it is possible that the humerus, as a non–weight-bearing bone, may have a higher sensitivity to decline in bioavailable estrogen levels leading to the observed bone loss.

Our study has several limitations. The most obvious limitation is the cross-sectional nature of the study that limits the ability to reflect age-related changes in bone geometry. Direct comparison of each cortical bone index in the premenopausal and postmenopausal groups could not distinguish between age-related and menopause-related effects. A longitudinal cohort study of women is needed to examine changes in proximal humeral bone health across the menopausal transition. Second, we have evaluated menopause-related cortical bone effects in a
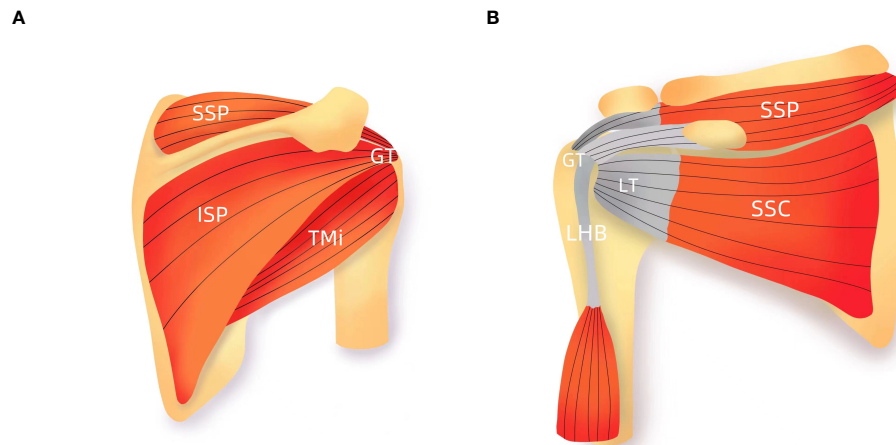
FIGURE 5

Schematic presentation of rotator cuff **(A)** Anterior view; **(B)** posterior view. GT, greater tuberosity; LT, lesser tuberosity; SSC, subscapularis; SSP, supraspinatus; ISP, infraspinatus; TMi, teres minor; LHB, the long head biceps tendon.

Chinese cohort. The current data are not directly translatable to individuals of other racial or ethnic backgrounds since previous work suggests structural differences of the proximal femur between Asians and other ethnicities (11, 24). Finally, microarchitectural changes of the cortical bone in the humeral head region were not analyzed in the study. Some authors recently reported that cortical porosity and thickness have a significant impact on bone loss and mechanical stability (8, 9, 11). Despite this limitation, we identified menopause-related changes in cortical bone of the humeral head region, which are definitely relevant to risk prediction for PHFs.

In summary, we have shown that menopause-related cortical loss of the humeral head mainly occurred in the lateral part of the greater tuberosity. Since fractures initiate from focal cortical thinning, the increased cortical bone loss in the greater tuberosity may contribute materially to complex PHFs. CTh in the proximal part of the lateral and anterior walls exhibited significant age- and menopause-related decline in women. Collectively, cortical loss in the greater tuberosity and the lesser tuberosity showed marked regional heterogeneity under the impact of estrogen deficiency and/or aging. Better understanding of the mechanisms determining local bone loss in elderly proximal humerus is an important topic for future research.

Data availability statement

The raw data supporting the conclusions of this article will be made available by the authors, without undue reservation.

Ethics statement

This study was reviewed and approved by The ethics committee of Tianjin Hospital. The patients/participants provided their written informed consent to participate in this study. Written informed consent was obtained from the individual(s) for the publication of any potentially identifiable images or data included in this article.

Author contributions

YW designed the study and prepared the first draft of the paper. JL and YM contributed to the experimental work. WW was responsible for project Administration. All authors revised the paper critically for intellectual content and approved the final version. All authors agree to be accountable for the work and to ensure that any questions relating to the accuracy and integrity of the paper are investigated and properly resolved.

Funding

This study was supported by Tianjin National Science Foundation of China (18JCYBJC95200).

Conflict of interest

The authors declare that the research was conducted in the absence of any commercial or financial relationships that could be construed as a potential conflict of interest.

Publisher's note

All claims expressed in this article are solely those of the authors and do not necessarily represent those of their affiliated organizations, or those of the publisher, the editors and the reviewers. Any product that may be evaluated in this article, or claim that may be made by its manufacturer, is not guaranteed or endorsed by the publisher.

References

1. Rosas S, Law TY, Kurowicki J, Formaini N, Kalandiak SP, Levy JC. Trends in surgical management of proximal humeral fractures in the Medicare population: A nationwide study of records from 2009 to 2012. *J Shoulder Elbow Surg* (2016) 25 (4):608–13. doi: 10.1016/j.jse.2015.08.011

2. Sumrein BO, Huttunen TT, Launonen AP, Berg HE, Felländer-Tsai L, Mattila VM. Proximal humeral fractures in Sweden-a registry-based study. *Osteoporos Int* (2017) 28(3):901–7. doi: 10.1007/s00198-016-3808-z

3. Park C, Jang S, Lee A, Kim HY, Lee YB, Kim TY, et al. Incidence and mortality after proximal humerus fractures over 50 years of age in South Korea: National claim data from 2008 to 2012. *J Bone Metab* (2015) 22(1):17–21. doi: 10.11005/jbm.2015.22.1.17

4. Barvencik F, Gebauer M, Beil FT, Vettorazzi E, Mumme M, Rupprecht M, et al. Age- and sex-related changes of humeral head microarchitecture: Histomorphometric analysis of 60 human specimens. *J Orthop Res* (2010) 28 (1):18–26. doi: 10.1002/jor.20957

5. Kirchhoff C, Braunstein V, Milz S, Sprecher CM, Fischer F, Tami A, et al. Assessment of bone quality within the tuberosities of the osteoporotic humeral head: Relevance for anchor positioning in rotator cuff repair. *Am J Sports Med* (2010) 38(3):564–9. doi: 10.1177/0363546509354989

6. Mantila Roosa SM, Hurd AL, Xu H, Fuchs RK, Warden SJ. Age-related changes in proximal humerus bone health in healthy, white males. *Osteoporos Int* (2012) 23(12):2775–83. doi: 10.1007/s00198-012-1893-1

7. Holzer G, von Skrbensky G, Holzer LA, Pichl W. Hip fractures and the contribution of cortical versus trabecular bone to femoral neck strength. *J Bone Miner Res* (2009) 24(3):468–74. doi: 10.1359/jbmr.081108

8. Zebaze RM, Ghasem-Zadeh A, Bohte A, Iuliano-Burns S, Mirams M, Price RI, et al. Intracortical remodelling and porosity in the distal radius and post-mortem femurs of women: A cross-sectional study. *Lancet* (2010) 375(9727):1729–36. doi: 10.1016/S0140-6736(10)60320-0

9. Helfen T, Sprecher CM, Eberli U, Gueorguiev B, Müller PE, Richards RG, et al. High-resolution tomography-based quantification of cortical porosity and cortical thickness at the surgical neck of the humerus during aging. *Calcif Tissue Int* (2017) 101(3):271–9. doi: 10.1007/s00223-017-0279-y

10. Bjørnerem Å, Wang X, Bui M, Ghasem-Zadeh A, Hopper JL, Zebaze R, et al. Menopause-related appendicular bone loss is mainly cortical and results in increased cortical porosity. *J Bone Miner Res* (2018) 33(4):598–605. doi: 10.1002/jbmr.3333

11. Shanbhogue VV, Brixen K, Hansen S. Age- and sex-related changes in bone microarchitecture and estimated strength: A three-year prospective study using HRpQCT. *J Bone Miner Res* (2016) 31(8):1541–9. doi: 10.1002/jbmr.2817

12. Marques EA, Carballido-Gamio J, Gudnason V, Sigurdsson G, Sigurdsson S, Aspelund T, et al. Sex differences in the spatial distribution of bone in relation to incident hip fracture: Findings from the AGES-Reykjavik study. *Bone* (2018) 114:72–80. doi: 10.1016/j.bone.2018.05.016

13. Nagaraj N, Boudreau RM, Danielson ME, Greendale GA, Karlamangla AS, Beck TJ, et al. Longitudinal changes in hip geometry in relation to the final menstrual period: Study of women's health across the nation (SWAN). *Bone* (2019) 122:237–45. doi: 10.1016/j.bone.2019.02.016

14. Samelson EJ, Broe KE, Xu H, Yang L, Boyd S, Biver E, et al. Cortical and trabecular bone microarchitecture as an independent predictor of incident fracture risk in older women and men in the bone microarchitecture international consortium (BoMIC): A prospective study. *Lancet Diabetes Endocrinol* (2019) 7 (1):34–43. doi: 10.1016/S2213-8587(18)30308-5

15. Langsetmo L, Peters KW, Burghardt AJ, Ensrud KE, Fink HA, Cawthon PM, et al. Volumetric bone mineral density and failure load of distal limbs predict incident clinical fracture independent HR-pQCT BMD and failure load predicts incident clinical fracture of FRAX and clinical risk factors among older men. *J Bone Miner Res* (2018) 33(7):1302–11. doi: 10.1002/jbmr.3433

16. Biver E, Durosier-Izart C, Chevalley T, van Rietbergen B, Rizzoli R, Ferrari S. Evaluation of radius microstructure and areal bone mineral density improves fracture prediction in postmenopausal women. *J Bone Miner Res* (2018) 33(2):328–37. doi: 10.1002/jbmr.3299

17. Ohlsson C, Sundh D, Wallerek A, Nilsson M, Karlsson M, Johansson H, et al. Cortical bone area predicts incident fractures independently of areal bone mineral density in older men. *J Clin Endocrinol Metab* (2017) 102(2):516–24. doi: 10.1210/jc.2016-3177

18. Wang Y, Li J, Yang J, Dong J. Regional variations of cortical bone in the humeral head region: A preliminary study. *Bone* (2018) 110:194–8. doi: 10.1016/j.bone.2018.02.010

19. Poole KES, Skingle L, Gee AH, Turmezei TD, Johannesdottir F, Blesic K, et al. Focal osteoporosis defects play a key role in hip fracture. *Bone* (2017) 94:124–34. doi: 10.1016/j.bone.2016.10.020

20. Poole KE, Treece GM, Mayhew PM, Vaculík J, Dungl P, Horák M, et al. Cortical thickness mapping to identify focal osteoporosis in patients with hip fracture. *PloS One* (2012) 7(6):e38466. doi: 10.1371/journal.pone.0038466

21. Warden SJ, Carballido-Gamio J, Avin KG, Kersh ME, Fuchs RK, Krug R, et al. Adaptation of the proximal humerus to physical activity: A within-subject controlled study in baseball players. *Bone* (2019) 121:107–15. doi: 10.1016/j.bone.2019.01.008

22. Majed A, Thangarajah T, Southgate D, Reilly P, Bull A, Emery R. Cortical thickness analysis of the proximal humerus. *Shoulder Elbow* (2019) 11(2):87–93. doi: 10.1177/1758573217736744

23. Majed A, Thangarajah T, Southgate DF, Reilly P, Bull A, Emery R. The biomechanics of proximal humeral fractures: Injury mechanism and cortical morphology. *Shoulder Elbow* (2019) 11(4):247–55. doi: 10.1177/1758573218768535

24. Johannesdottir F, Poole KE, Reeve J, Siggeirsdottir K, Aspelund T, Mogensen B, et al. Distribution of cortical bone in the femoral neck and hip fracture: a prospective case-control analysis of 143 incident hip fractures; the AGES-REYKJAVIK study. *Bone* (2011) 48(6):1268–76. doi: 10.1016/j.bone.2011.03.776

Deep learning for screening primary osteopenia and osteoporosis using spine radiographs and patient clinical covariates in a Chinese population

Liting Mao[1], Ziqiang Xia[1], Liang Pan[2], Jun Chen[3], Xian Liu[1], Zhiqiang Li[1], Zhaoxian Yan[1], Gengbin Lin[1], Huisen Wen[1] and Bo Liu[1*]

[1]Department of Radiology, The Second Affiliated Hospital of Guangzhou University of Chinese Medicine, Guangzhou, China, [2]Department of AI Research Lab, Guangzhou YLZ Ruitu Information Technology Co, Ltd, Guangzhou, China, [3]Department of Radiology, ZHUHAI Branch of Guangdong Hospital of Chinese Medicine, Zhuhai, China

Purpose: Many high-risk osteopenia and osteoporosis patients remain undiagnosed. We proposed to construct a convolutional neural network model for screening primary osteopenia and osteoporosis based on the lumbar radiographs, and to compare the diagnostic performance of the CNN model adding the clinical covariates with the image model alone.

Methods: A total of 6,908 participants were collected for analysis, including postmenopausal women and men aged 50−95 years, who performed conventional lumbar x-ray examinations and dual-energy x-ray absorptiometry (DXA) examinations within 3 months. All participants were divided into a training set, a validation set, test set 1, and test set 2 at a ratio of 8:1:1:1. The bone mineral density (BMD) values derived from DXA were applied as the reference standard. A three-class CNN model was developed to classify the patients into normal BMD, osteopenia, and osteoporosis. Moreover, we developed the models integrating the images with clinical covariates (age, gender, and BMI), and explored whether adding clinical data improves diagnostic performance over the image mode alone. The receiver operating characteristic curve analysis was performed for assessing the model performance.

Results: As for classifying osteoporosis, the model based on the anteroposterior+lateral channel performed best, with the area under the curve (AUC) range from 0.909 to 0.937 in three test cohorts. The models with images alone achieved moderate sensitivity in classifying osteopenia, in which the highest AUC achieved 0.785. The performance of models integrating images with clinical data shows a slight improvement over models with anteroposterior or lateral images input alone for diagnosing osteoporosis, in

which the AUC increased about 2%−4%. Regarding categorizing osteopenia and the normal BMD, the proposed models integrating images with clinical data also outperformed the models with images solely.

Conclusion: The deep learning-based approach could screen osteoporosis and osteopenia based on lumbar radiographs.

Introduction

Osteoporosis is a popular metabolic skeletal disorder with characteristics of low bone mineral density (BMD) and thinning of bone trabecula, leading to enhancement of bone fragility and increased risk of fracture (1). Primary osteoporosis is quite common in the elderly. According to a recent nationwide and multicenter investigation in China, among people over 50 years, the rates of osteoporosis were 29.13% and 6.46% for women and men, respectively (2), which are estimated to increase to 39.2% and 7.5%, respectively, by 2050 (3). At present, it has been estimated that a total of 10.9 million men and 49.3 million women suffer from osteoporosis in China (3). Osteopenia, as a precursor of osteoporosis, is also an important risk factor for fragility fractures. Previous studies have indicated that most women who suffer from fragility fractures have been diagnosed with osteopenia (4, 5). However, the majority of osteoporosis and osteopenia cases are undiagnosed until they experience a fracture, which would lead to a high probability of complications and mortality (6, 7). Hence, early detection of osteoporosis and osteopenia is significant to disease prevention and control, which may prevent osteoporotic fractures and lower the burden of this disease.

BMD value is a credible means for the early detection of osteoporosis and osteopenia. Currently, DXA is recognized as the gold standard for diagnosing osteoporosis and osteopenia globally (8). However, due to inaccessibility, knowledge deficits for screening, and high-cost factors of DXA, the application of DXA is limited. As a result, only a few developing countries are using DXA (9). In China, only 2.8% of people aged ≥20 years have undergone testing, while the rate is 3.7% among those aged ≥50 years (10). DXA-based measures of BMD are the sum of cortical bone and cancellous bone, considering two-dimensional structures, which cannot fully explain the geometry, size, and microstructure of

bone (11, 12). It is necessary to explore effective, safe, and cost-balanced substitutes to improve the above situations. Routine lumbar spine x-ray examinations are widely attainable at most hospitals globally. The lumbar spine (LS) radiographs that are ordered for other indications potentially contain useful information about BMD. Utilizing these LS x-ray images to assess BMD synchronously requires no added scanning time, radiation, or additional cost. Thus, this method would be more acceptable to people. However, there were many challenges to evaluating BMD by LS x-ray images, and only a few multicenter studies have been reported presently, which just takes into consideration postmenopausal women aged ≥50 years (13).

In recent years, the deep learning technique represented by the convolutional neural network (CNN) has achieved great success in radiological imaging diagnosis (14, 15). It has been reported that the deep learning technique has been successfully applied to the evaluation of radiological images, such as the differential diagnosis of diseases (16, 17), skeletal maturity assessed by pediatric hand radiographs (18), and the detection of fractures (19–21). This technique has also been applied to aid osteoporosis diagnosis. Numerous modalities have been used: dental radiographs (22), spine radiographs (13, 23), hand and wrist radiographs (24), DXA imaging (25), and spine CT (26, 27). Though some reports are available on osteoporosis diagnosis from spine radiographs using CNN (13, 23), these studies not only have a small number of cases but also did not consider men and clinical covariates. We hypothesized that combining clinical risk factors with image features would improve the models' capability for diagnosing osteoporosis and osteopenia.

The purpose of this study was to screen osteoporosis and osteopenia with LS x-ray images using CNN in postmenopausal women and men ≥50 years, and to explore whether adding clinical covariates improves the diagnostic performance over the image model alone.

Materials and methods

Patient cohort

This retrospective, multicenter study was conducted in a hospital with four independent sub-districts and another large tertiary center in China. The study had been approved by the institutional review board and the ethics committee of the host hospital (Ethics Committee of Guangdong Provincial Hospital of Chinese Medicine ZE2020-299-01), and the informed consent was waived. All images were de-identified before using to protect the privacy of the patients. The clinical and image data of all participants were retrospectively collected from July 2011 to March 2021. Inclusion criteria were as follows: (1) postmenopausal women over 50 years (the menopausal age was identified by medical records or patients' statement) and men aged over 50 years; (2) all patients had performed both LS x-rays and DXA examinations within 3 months, and had not accepted therapies influenced by BMD; and (3) plain radiographs of LS including anteroposterior (AP) and lateral (LAT) images that must clearly show the first to the fourth lumbar vertebrae. Exclusion criteria were as follows: (1) patients with postoperative metal or bone cement implant of the LS (L1–L4); (2) patients who experienced secondary osteoporosis (such as osteoporosis in renal failure, diabetes, and hyperparathyroidism) or lesions, including tumors and inflammatory diseases; (3) patients with serious scoliosis or deformity; (4) patients with vertebral compression fracture (any vertebrae of L1–L4); and (5) images that show low signal-to-noise ratio affecting to outline the region of lumbar vertebrae.

In total, 6,908 patients who satisfied all criteria were included in the study. A total of 5,652 patients from the three sub-districts between July 2011 and September 2020 were randomly divided into a training cohort and a validation cohort at a ratio of 8:1, and another 628 patients obtained from another independent

sub-district between July 2011 and September 2020 were used as test cohort 1; for test cohort 2, 628 patients from another participating center were collected between March 2019 and March 2021. All cases used the same inclusion and exclusion criteria. Figure 1 shows the flowchart of case selection in different participating centers.

Study design

The purpose of this study is to develop artificial intelligence models to classify primary osteoporosis and osteopenia from LS radiographs, and the T-scores of LS obtained from DXA examination were used as a reference standard. According to the WHO criteria, all subjects were classified into three categories: osteoporosis defined as T-score $\leq$ -2.5; osteopenia: $-1 >$ T-score > -2.5; and normal: T-score $\geq$ -1 (28). T-scores were computed referring to the BMD dataset of young Chinese female or male patients aged 20–40 years. We attempted to develop artificial intelligence models based on CNN through a single channel (AP or LAT images were input respectively) and two channels (AP and LAT images are input simultaneously). Furthermore, we add the clinical data (including sex, age, and BMI) to explore whether it can improve the diagnostic performance of the model.

Lumbar vertebra radiographs and BMD measurement

In the training and validation cohorts, the lumbar x-ray examinations were performed by the AXIOM Aristos MX/VX Digital Radiographic (DR) apparatus (Siemens, Germany), with

FIGURE 1

Flowchart of patient selection. BMD, bone mineral density; DXA, dual-energy x-ray absorptiometry; CNN, convolutional neural network.
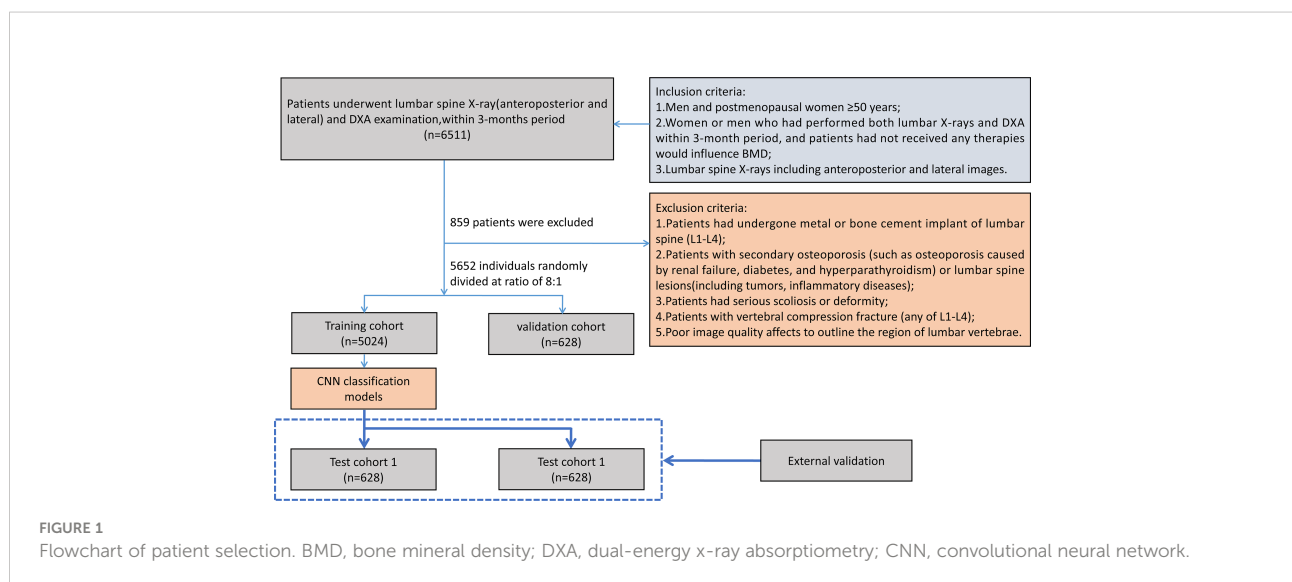
parameters set at 70 kVp for AP imaging and 77 kVp for LAT imaging. In test cohort 1, the images were conducted by the Yiso DR apparatus (Siemens, Germany), and 75 kVp was set for AP and 80 kVp for LAT imaging. In test cohort 2, the lumbar x-ray scans were operated by Revolution XR/d DR apparatus (General Electrical, America), with settings at 75 kVp for AP imaging and 90 kVp for LAT imaging. The mAs were automatically adjusted according to body size for all images.

For all participants, the BMD values of lumbar spine were measured using the dual-energy x-ray absorptiometry (Discovery A, HOLOGIC, USA). The patients' weight and height were measured by the electronic weigher, and the BMI was calculated. The age, weight, and height of patients were acquired from DXA examination records.

Image preprocessing

The pre-processing of images included three steps. Firstly, all the regions of interest (ROIs) were delineated on lumbar vertebrae (L1–L4) from AP and LAT images, and the specific method was as follows: we used the smallest rectangular frame to include the vertebral body, with lateral margin within 2 mm of the edge of the vertebral body, while the upper and lower edges are in the middle of the intervertebral space. All images were delineated by six radiologists with 4–8 years of experience. Secondly, all ROIs were cropped and then each ROI was resized to 512×512 pixels. The filling scale that using gray filling for the blank area is adopted to avoid the lumbar vertebrae being deformed and features destroyed. Finally, in consideration of the differences in x-ray scanning parameters, grayscale normalization was performed in all images to enhance their robustness; Gaussian filtering, histogram equalization, and pixel value normalization were also performed.

Development of the CNN models in the training cohort

The Dense Convolutional Network (DenseNet) [29] was applied in the backbone network, comprising four dense blocks and three transition layers (Figure 2). Each dense block consists of three consecutive operations: batch normalization, followed by a rectified linear unit (ReLU) and a 3×3 convolution (Conv). To reduce the number of input feature maps, a 1×1 convolution was introduced as a bottleneck layer before each 3×3 convolution to improve computational efficiency. The layers between blocks were called transition layers, which were used for convolution and pooling. To further enhance the compactness of the model, we reduced the amount of feature maps at transition layers. Following the last dense block, a full connection (FC) is implemented and then a softmax classifier is attached.

The developed CNN classification model is composed of two channels to carry out auto-analysis of the AP and LAT lumbar vertebra (L1–L4) images. Both channels presented the same structure as mentioned above. The features were extracted through DenseNet, which connected each layer to every other layer in a feed-forward pattern. Through skip connection, each layer in the network was directly connected to the previous layer, which strengthened the transmission of features and thus realized the integration of information flow. For each layer, the feature maps of all preceding layers served as a single input, and the features generated from the current layer were input to the subsequent layers. Thus, it could control the vanishing-gradient problem, enhance feature propagation, emphasize feature reuse, and considerably decrease the quantity of parameters.

Since this was a three-category mission, we developed a three-classification CNN model to perform classification from AP, LAT, and AP+LAT views. The results of each case were output from a single channel and from two channels.

FIGURE 2
Overview of our proposed framework.
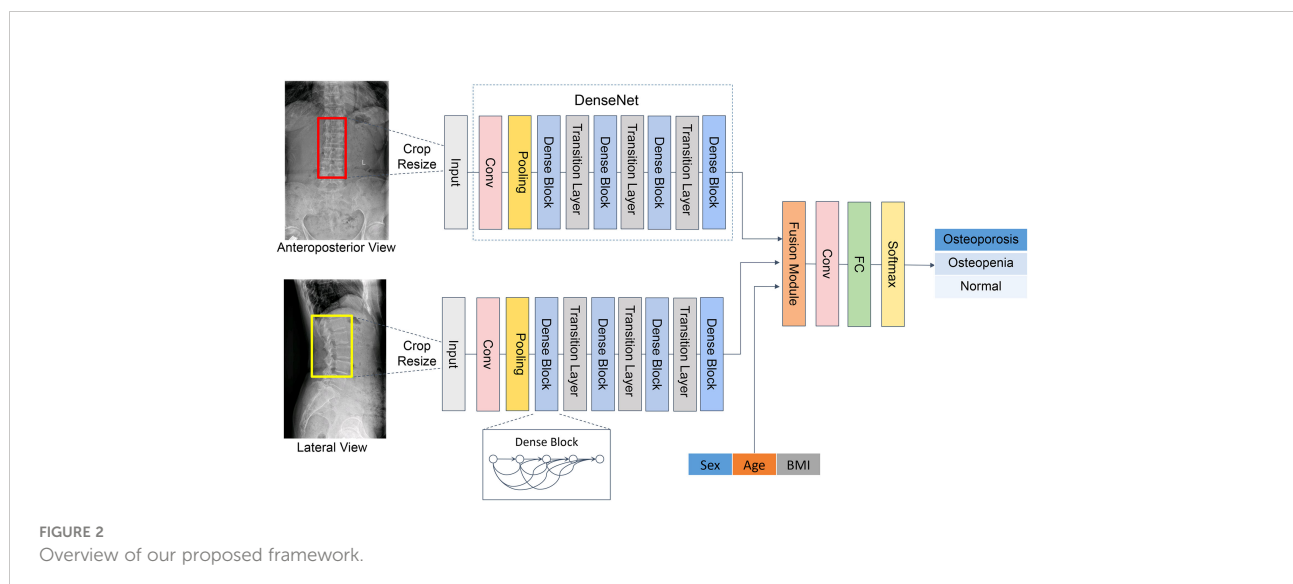
Evaluating the performance of the classification models

A total of 5,652 participants were randomly allocated to training data and validation data at a ratio of 8:1. Independent patients (628 patients) from another sub-district of the same hospital and the other participating center (628 patients) were used as test cohorts that were not included in the training cohorts. The training cohort was used for model development, the validation cohort was employed to filter hyper-parameters and select the best model, and the test cohorts were applied to evaluate the predictive performance of the trained models. The constructed model ultimately classified the patients into osteoporosis, osteopenia, and normal bone mass. Besides image features, we also added clinical covariates (gender, age, and BMI) to the CNN model to explore whether these covariates could improve the performance of the model.

Statistical analysis

Descriptive statistics were expressed as numbers, and continuous variables were expressed as means ± standard deviations (SDs). Categorical variables were compared by using the chi-square test. $p < 0.05$ was considered a statistically significant difference. The receiver operating characteristic (ROC) curve was used to access the diagnostic effectiveness of the CNN models; meanwhile, the area under the curve (AUC) values and 95% confidence intervals (CIs) for sensitivity and specificity were calculated. We used DeLong's method for assessing the statistical difference of AUC between different models. In addition, the positive predictive value (PPV) and

negative predictive value (NPV) were counted. Moreover, the amount of true positives, false positives, false negatives, and true negatives were demonstrated with the confusion matrix.

All the deep convolutional models were complemented by PYTHON (3.6.6, Guido van Rossum, Netherlands). All statistical analyses were carried out by R software (3.0.2, R Core Team, 2013) and MedCalc software (15.6.1, Microsoft Partner, 2015). All experiments were performed under Windows on a machine with an Intel (R) Core (TM) Processor i7-8700 @ 3.20 GHz central processing unit (CPU), an NVIDIA GeForce GTX graphics processing unit (GPU), and a RAM of 64 GB.

Results

Patient demographics

A total of 6,908 patients [mean age, 65.4 years ± 9.3 (SD); range, 50–95 years] including 13,816 lumbar vertebra x-ray images were available for the final analysis. Table 1 lists the clinical and demographic parameters for the training, validation, and two test cohorts. Gender, age, and BMI among the training, validation, and test cohorts demonstrated no statistically significant differences.

According to the DXA-based BMD screening reference standard, all patients were classified into three categories: osteoporosis (n = 2,302, 33.3%), osteopenia (n = 2,601, 37.7%), and normal (n = 2,004, 29.0%). In the training cohort, validation cohort, test cohort 1, and test cohort 2, 38.3%, 35.7%, 36.0%, and 36.0% of patients are osteopenic, and 33.0%, 35.7%, 33.6%, and 33.6% patients are osteoporotic, respectively.

TABLE 1 Demographic characteristics of 6,908 participants.

Characteristics	Training cohort	Validation cohort	Test cohort 1	Test cohort 2	Total
Patients (n)	5024	628	628	628	6,908
Age, years, mean (SD)	65.3 (9.2)	65.6 (9.4)	65.3 (9.3)	65.6 (10.0)	65.4 (9.3)
Sex					
Male	1,594	196	190	169	2,149
Female	3,430	432	438	459	4,759
BMI, kg/m^2, mean (SD)	23.97 (3.48)	24.04 (3.73)	23.93 (3.63)	23.96 (3.38)	23.97 (3.51)
Lumbar spine images					
Anteroposterior	5,024	628	628	628	6,908
Lateral	5,024	628	628	628	6,908
T-score, mean L1–L4	−1.80	−1.86	−1.80	−1.92	−1.82
BMD categories, n (%)					
Normal	1,442 (28.7)	180 (28.6)	191 (30.4)	191 (30.4)	2,004 (29.0)
Osteopenia	1,925 (38.3)	224 (35.7)	226 (36.0)	226 (36.0)	2,601 (37.7)
Osteoporosis	1,657 (33.0)	224 (35.7)	211 (33.6)	211 (33.6)	2,302 (33.3)

Categorical and continuous data were expressed as n (%) and mean (standard deviation, SD), respectively. BMI, body mass index.

The consistency analysis of the delineated ROIs

One hundred cases were randomly selected and assigned to six radiologists with 4–8 years' experience for delineating the ROI synchronously. As to the same case, the area of overlap between ROIs drawn by every two radiologists was calculated respectively. Then, the overlapping ratio was calculated. The specific calculation method of the overlap rate is that the area of overlap is divided by the combined area of the two regions. Results showed that in these 100 cases, the overlapping ratios between each two radiologists were greater than 90%.

Performance of the CNN models with images input alone

Table 2 shows the results of the CNN model in diagnosing osteoporosis on the basis of LS x-ray images. Among the validation cohort and two test cohorts, the models based on the AP+LAT channel for diagnosing osteoporosis achieve the best performance, with an AUC range from 0.909 to 0.937, a sensitivity range from 81.90% to 84.82%, a specificity range from 82.54% to 86.63%, and a negative predictive value range from 90.08% to 91.15%. Comparison of ROC curves was performed between the CNN models constructed with single and combined

image programs (Figure 3). The classification confusion matrices of models based on the AP+LAT channel, which report the number of true-positive, false-positive, true-negative, and false-negative results, are shown in Table 3.

The models with images input alone achieved moderate sensitivity in classifying osteopenia in the validation cohort, in which the highest AUC achieved was 0.785 (95% CI: 0.750–0.816), with a sensitivity of 71.43% and a specificity of 74.01% (Supplementary Table 1). In test cohort 1 and test cohort 2, the highest AUC values were 0.778 and 0.731, respectively (Supplementary Figure 1).

For diagnosing the normal bone mass, the diagnostic efficiency was consistently high among the validation and two test cohorts, in which the highest AUC values were 0.929, 0.926, and 0.911, respectively (Supplementary Table 2).

Performance of the CNN models integrating images with clinical parameters

Before and after the addition of clinical parameters, in test cohort 1, the AUC values of AP images were statistically different only in diagnosing osteoporosis ($p < 0.001$), while those of LAT images were statistically different in diagnosing osteoporosis ($p = 0.047$) and normal BMD ($p = 0.009$). However, the AUC values

TABLE 2 Performance of the CNN model with images inputting for classifying osteoporosis, assessed on the training, validation, and test cohorts.

Datasets	Image projection	AUC (95% CI)	Sensitivity (%)	Specificity (%)	PPV (%)	NPV (%)
Training	AP	0.996 (0.994–0.998)	99.94 (99.61–100)	99.94 (99.76–99.99)	99.88 (99.52–99.98)	99.97 (99.81–100)
	LAT	0.996 (0.994–0.998)	99.94 (99.61–100)	99.97 (99.81–100)	99.94 (99.61–100)	99.97 (99.81–100)
	AP and LAT	0.965 (0.960–0.970)	89.99 (88.42–91.37)	90.01 (88.94–91.00)	81.63 (79.76–83.36)	94.80 (93.96–95.54)
Validation	AP	0.904 (0.877–0.925)	82.14 (76.36–86.80)	85.64 (81.75–88.84)	76.03 (70.06–81.17)	89.64 (86.05–92.41)
	LAT	0.889 (0.861–0.912)	75.45 (69.18–80.83)	85.64 (81.75–88.84)	74.45 (68.17–79.88)	86.28 (82.44–89.42)
	AP and LAT	0.937 (0.914–0.954)	84.82 (79.29–89.12)	86.63 (82.83–89.72)	77.87 (72.03–82.81)	91.15 (87.73–93.71)
Test cohort 1	AP	0.889 (0.861–0.912)	81.52 (75.47–86.38)	81.77 (77.66–85.29)	69.35 (63.15–74.95)	89.74 (86.13–92.51)
	LAT	0.911 (0.885–0.932)	80.09 (73.93–85.13)	86.09 (82.31–89.19)	74.45 (68.17–79.88)	89.53 (86.01–92.27)
	AP and LAT	0.933 (0.909–0.950)	82.94 (77.03–87.62)	85.85 (82.05–88.98)	74.79 (68.63–80.11)	90.86 (87.47–93.44)
Test cohort 2	AP	0.892 (0.864–0.915)	80.48 (74.33–85.48)	81.10 (76.94–84.67)	68.15 (61.90–73.82)	89.21 (85.54–92.06)
	LAT	0.874 (0.845–0.898)	73.81 (67.22–79.51)	81.34 (77.20–84.89)	66.52 (60.02–72.47)	86.08 (82.18–89.26)
	AP and LAT	0.909 (0.883–0.930)	81.90 (75.88–86.73)	82.54 (78.48–85.98)	70.20 (63.99–75.77)	90.08 (86.53–92.80)

AP, anteroposterior; LAT, lateral; AUC, area under the curve; PPV, positive predictive value; NPV, negative predictive value.
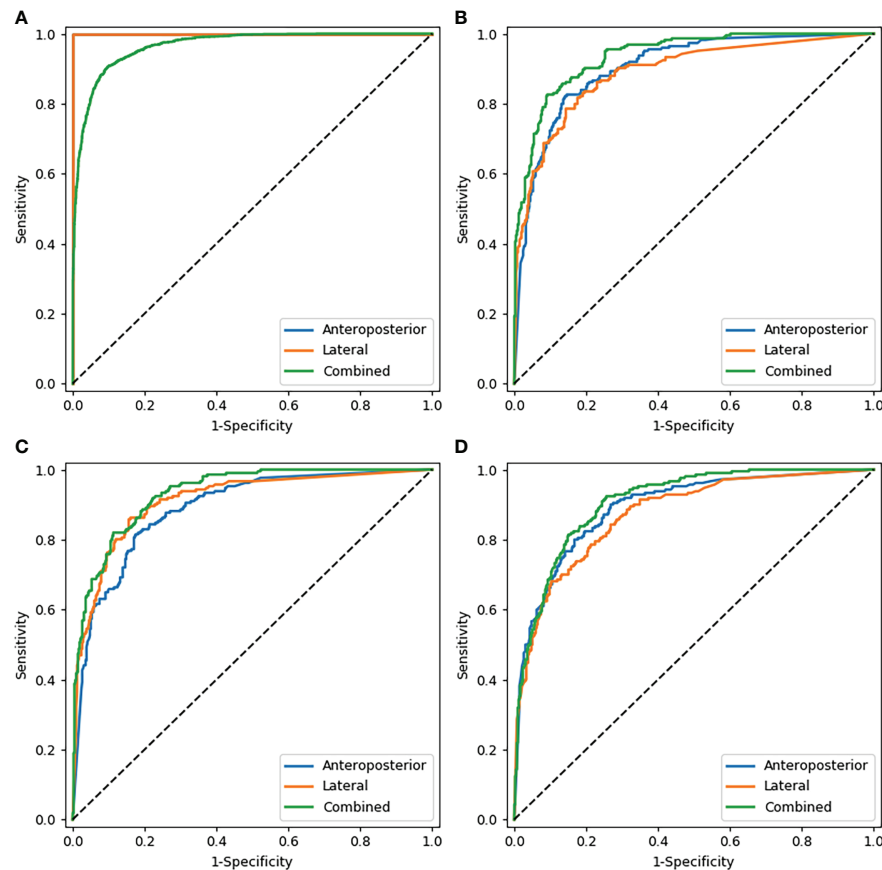
FIGURE 3

Comparison of ROC curves of the CNN models with images alone. **(A–D)** show the models that diagnosed osteoporosis in the training cohort, validation cohort, test cohort 1, and test cohort 2 respectively. Note: In the training cohort **(A)**, since AP and LAT have the same AUC values, the blue line overlaps with the orange line.

of AP+LAT images have no statistical differences in three classifications ($p > 0.05$). In test cohort 2, only the AUC values predicted by LAT images for osteoporosis and osteopenia were statistically different ($p = 0.017$ and $p < 0.001$, respectively), and the other AUC values have no statistical difference ($p > 0.05$).

The performance of the proposed models that integrate images with clinical parameters has shown a slight improvement over models with AP or LAT images alone for diagnosing osteoporosis, in which the AUC increased about 2%–4%. Meanwhile, the specificity and positive predictive

values improved as well (Table 4). In the model diagnosing osteoporosis based on the LAT channel, the AUC value and sensitivity increased in the validation cohort and test cohort 1, while in test cohort 2, the AUC and specificity have improved, but sensitivity slightly declined (from 73.81% to 70.00%). Figure 4 demonstrates the comparison of the efficacy of the CNN models based on LAT image with and without integrating clinical parameters in diagnosing osteoporosis, accessed on the test cohort, validation cohort, and two test cohorts.

TABLE 3 Confusion matrices of predictions and reference standards in validation and two testing datasets based on the AP+LAT channel.

		Validation (prediction)			Test cohort 1 (prediction)			Test cohort 2 (prediction)		
		Osteoporosis	Osteopenia	Normal	Osteoporosis	Osteopenia	Normal	Osteoporosis	Osteopenia	Normal
Truth	Osteoporosis	190	34	0	175	36	0	172	36	2
	Osteopenia	50	160	14	57	144	25	61	129	19
	Normal	4	71	105	2	79	110	12	76	121

TABLE 4 Performance of the CNN model integrating images with clinical parameters inputting for classifying osteoporosis, assessed on the training, validation, and test cohorts.

Datasets	Image projection	AUC (95% CI)	Sensitivity (%)	Specificity (%)	PPV (%)	NPV (%)
Training	AP	0.981 (0.976–0.984)	86.20 (84.42–87.80)	95.75 (95.00–96.40)	90.91 (89.35–92.26)	93.36 (92.47–94.16)
	LAT	0.963 (0.957–0.968)	88.67 (87.02–90.13)	90.37 (89.31–91.34)	81.95 (80.07–83.69)	94.18 (93.30–94.95)
	AP and LAT	0.996 (0.993–0.998)	99.94 (99.61–100)	99.97 (99.81–100)	99.94 (99.61–100)	99.97 (99.81–100)
Validation	AP	0.922 (0.897–0.941)	73.21 (66.83–78.79)	92.57 (89.46–94.85)	84.54 (78.50–89.17)	86.18 (82.48–89.21)
	LAT	0.926 (0.901–0.944)	81.70 (75.87–86.41)	86.88 (83.10–89.94)	77.54 (71.58–82.59)	89.54 (85.98–92.31)
	AP and LAT	0.928 (0.904–0.947)	75.00 (68.70–80.42)	92.08 (88.89–94.44)	84.00 (78.01–88.65)	86.92 (83.26–89.89)
Test cohort 1	AP	0.928 (0.904–0.946)	73.93 (67.37–79.61)	90.17 (86.80–92.77)	79.19 (72.71–84.50)	87.24 (83.63–90.17)
	LAT	0.930 (0.907–0.949)	81.52 (75.47–86.38)	88.73 (85.20–91.52)	78.54 (72.39–83.66)	90.46 (87.09–93.05)
	AP and LAT	0.943 (0.921–0.960)	75.36 (68.87–80.90)	91.61 (88.42–94.01)	81.96 (75.66–86.96)	88.02 (84.50–90.85)
Test cohort 2	AP	0.912 (0.887–0.933)	68.57 (61.76–74.69)	92.34 (89.26–94.63)	81.82 (75.15–87.06)	85.40 (81.72–88.45)
	LAT	0.905 (0.878–0.926)	70.00 (63.24–76.01)	88.76 (85.24–91.54)	75.77 (69.01–81.50)	85.48 (81.73–88.59)
	AP and LAT	0.915 (0.889–0.935)	69.05 (62.25–75.13)	92.58 (89.53–94.83)	82.39 (75.77–87.55)	85.62 (81.96–88.65)

AP, anteroposterior; LAT, lateral; AUC, area under the curve; PPV, positive predictive value; NPV, negative predictive value.

Regarding categorizing osteopenia and normal bone mass, the proposed deep learning model integrating images with clinical parameters also outperformed the models with images inputting alone in test cohorts (Supplementary Tables 3, 4), in which the sensitivity increased particularly.

Discussion

In this multicenter study, we developed a deep learning method based on conventional lumbar spine DR examinations performed for other clinical symptoms, intended to diagnose osteoporosis and osteopenia in postmenopausal women and men over 50 years. Our results revealed that the deep learning method has the prospect of automatic BMD categorization in clinical practice. Moreover, another finding was obtained: the model combining lumbar images with clinical information could improve the performance, particularly based on the LAT channel.

Deep learning uses neural networks as framework, and is performed *via* multiple abstraction layers (30–32). CNN is one of the most common deep learning algorithms; the processing of information is performed by the brain's neurons, which is specialized in handling a large amount of inputs. In this study, we employed DenseNet that connected each layer to every other layer in a feed-forward pattern, requiring less computation to achieve high performance (29). Based on it, we trained a CNN model to evaluate the bone mass in postmenopausal women and men over 50 years old. Our classification models were built on the triple classification of the L1–L4 LS x-ray images divided into normal, osteopenia, and osteoporosis, which differed from general deep learning models on the basis of binary classification. As a screening method for a disease, the high sensitivity of models reduces false-negative categories; therefore, the osteoporotic individuals will be recognized probably and treated accordingly. In our research, sensitivity of the models diagnosing osteoporosis was high among validation and two testing datasets (≥81.90% based on the AP+LAT channel). However, the AUC and sensitivity of the models classifying osteopenia were slightly low, which may be attributed to data imbalance, and the ROI of the LS images (including partial vertebral osteophyte and spinous process in LAT image) input to models distinct from DXA (excluding vertebral osteophyte). The inputting images of models including partial vertebral osteophyte will lead to overestimating bone mass, but somewhat reducing the sensitivity of osteopenia and normal. Moreover, the models have a triple classification, and the T-score of osteopenia was between osteoporosis and normal; thus, part of osteopenia
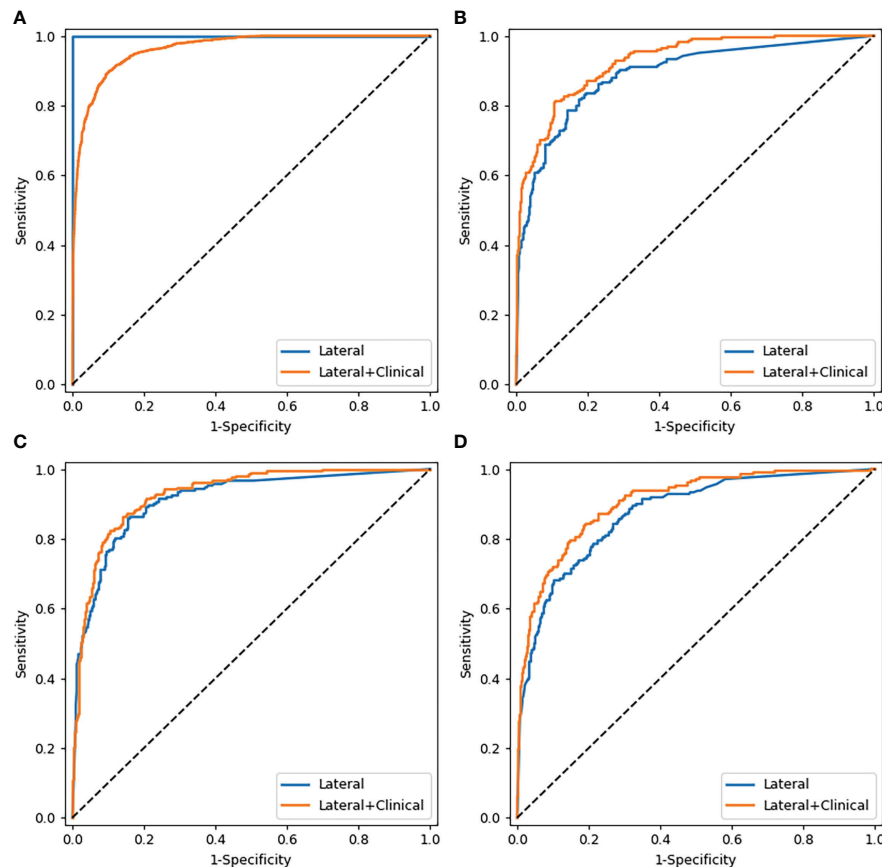
FIGURE 4

Comparison of ROC curves of the CNN models based on lateral images with and without combining clinical parameters. **(A–D)** were the curves of the training cohort, validation cohort, test cohort 1, and test cohort 2, respectively.

may be classified as osteoporosis and normal. Thus, the diagnostic efficiency of the model for classifying osteopenia was lower than the normal. Above all, we analyzed that a considerable percentage of patients enrolled in our research was at the critical point of osteopenia and normal bone mass. Thus, further study is aimed to improve the models' sensitivity in the diagnosis of osteopenia.

Osteoporosis is a major health disease with the increase in the aging population, affecting post-menopausal women most frequently, and is gradually considered as a clinical problem among elderly men. In their life, about 50% of women and 20% of men will suffer from osteoporotic fracture (33). The risk of subsequent fractures following an initial fracture is increased and the adjusted hazard ratios were higher in men than in women (34). However, few studies have analyzed osteoporosis in men. On account of this, men aged ≥50 years were also included in our study. Furthermore, majority of the studies demonstrated that advancing age, gender, and low body weight were the additional risk factors of fracture for both men and women (35, 36). Thus, we obtained the models

combined LS radiographs with age, gender, and BMI, to evaluate whether the clinical variables would affect the effectiveness of the CNN models in categorizing osteoporosis and osteopenia. The results revealed that it was helpful to improve the sensitivity of models classifying osteopenia, but it did not have much significance in classifying osteoporosis or the BMD. The main reason may be that the sensitivity of models in categorizing osteoporosis was comparatively high, and the deep learning is mainly about automatically acquiring the internal features of images.

Summarily, our study has several strengths. First, this research is a multicenter study with a large data volume, including internal and external validation; hence, the results are relatively stable. Zhang et al. (13) constructed a deep CNN model to classify osteoporosis and osteopenia that is based on the AP and LAT LS radiographs of 808 postmenopausal women. Their model diagnosing osteoporosis achieved an AUC of 0.767 with a sensitivity of 73.7%. In contrast to the previous study (13), the AUC (0.93 vs. 0.77) and sensitivity (82.9% vs. 73.7%) of our models in the diagnosis of

osteoporosis improved significantly. Second, the groups of study included not only postmenopausal women but also men over 50 years old. The AI model is more applicable to clinical practice due to the completeness of subjects. Third, our model could diagnose osteoporosis and osteopenia through image features extracted from conventional lumbar radiographs. Thus, this method has the potential to be applied in detecting osteoporosis and osteopenia for many "opportunistic screening" without additional costs.

There are also some potential limitations to this study. Firstly, the retrospective inclusion of subjects who underwent paired LS radiographs and DXA examinations may have led to selection bias. Secondly, DXA examinations could not eliminate the effect of cortex, hyperosteogeny, and arteriosclerosis sclerosis on BMD measurement (11), which might underestimate the actual loss of bone mass. Similarly, the proposed method may also be influenced by aortic sclerosis, bowel gas, and osteophytic spurs, which may cause overestimating BMD values. Moreover, individuals who suffered from lumbar vertebra tumor, inflammatory diseases, serious scoliosis, or deformity were not appropriate for the CNN models as well. Thirdly, all the ROIs were delineated manually, which was time-consuming though it was relatively accurate. Fourthly, women or men under 50 years old were not included in this study. Therefore, the application of our results to these populations is limited. Lastly, the developed deep learning models could not predict the exact fracture risk of individuals, and it needs further study.

Conclusions

In conclusion, our research showed that the proposed deep learning models based on routine lumbar spine radiographs obtained for other reasons attained favorable performance on BMD classification in men and postmenopausal women aged ≥50, which would be an available tool for clinicians in opportunistic osteoporosis screening without additional radiation exposure or cost. It could be applied in the circumstance that lumbar spine radiograph is available but DXA examination is lacking, and it is especially suitable for patients with physical examination. Early detection of osteoporosis and osteopenia is beneficial to identify those at risk of fracture and provide treatment to prevent further losses.

Data availability statement

The original contributions presented in the study are included in the article/Supplementary Material. Further inquiries can be directed to the corresponding author.

Ethics statement

This study was reviewed and approved by the institutional review board and the ethics committee of the host hospital (Ethics Committee of Guangdong Provincial Hospital of Chinese Medicine ZE2020-299-01). The requirement for written informed consent was waived due to the retrospective nature of the study.

Author contributions

All authors contributed to the article and approved the submitted version. Study concept and design: BL and LM. Acquisition of data: LM, ZX, and XL. Analysis of data: ZL, GL, HW and ZY. Drafting of the manuscript: LM, LP and BL. Critical revision: JC and XL. Statistical analysis: LP and LM.

Funding

Conflict of interest

LP was employed by Guangzhou YLZ Ruitu Information Technology Co, Ltd.

The remaining authors declare that the research was conducted in the absence of any commercial or financial relationships that could be construed as a potential conflict of interest.

Publisher's note

All claims expressed in this article are solely those of the authors and do not necessarily represent those of their affiliated organizations, or those of the publisher, the editors and the reviewers. Any product that may be evaluated in this article, or claim that may be made by its manufacturer, is not guaranteed or endorsed by the publisher.

Supplementary material

The Supplementary Material for this article can be found online at: https://www.frontiersin.org/articles/10.3389/fendo.2022.971877/full#supplementary-material

References

1. Lee JJ, Aghdassi E, Cheung AM, Morrison S, Cymet A, Peeva V, et al. Ten-year absolute fracture risk and hip bone strength in Canadian women with systemic lupus erythematosus. *J Rheumatol* (2012) 39(7):1378–84. doi: 10.3899/jrheum.111589

2. Cui Z, Meng X, Feng H, Zhuang S, Liu Z, Zhu T, et al. Estimation and projection about the standardized prevalence of osteoporosis in mainland China. *Arch Osteoporos* (2019) 15(1):2. doi: 10.1007/s11657-019-0670-6

3. Zeng Q, Li N, Wang Q, Feng J, Sun D, Zhang Q, et al. The prevalence of osteoporosis in China, a nationwide, multicenter DXA survey. *J Bone Miner Res* (2019) 34(10):1789–97. doi: 10.1002/jbmr.3757

4. Schuit SCE, van der Klift M, Weel AEAM, de Laet CEDH, Burger H, Seeman E, et al. Fracture incidence and association with bone mineral density in elderly men and women: the Rotterdam study. *Bone* (2004) 34(1):195–202. doi: 10.1016/j.bone.2003.10.001

5. Wainwright SA, Marshall LM, Ensrud KE, Cauley JA, Black DM, Hillier TA, et al. Hip fracture in women without osteoporosis. *J Clin Endocrinol Metab* (2005) 90(5):2787–93. doi: 10.1210/jc.2004-1568

6. Brown C. Osteoporosis: Staying strong. *Nature* (2017) 550(7674):S15–7. doi: 10.1038/550S15a

7. Liow MHL, Ganesan G, Chen JDY, Koh JSB, Howe TS, Yong EL, et al. Excess mortality after hip fracture: fracture or pre-fall comorbidity? *Osteoporosis Int* (2021) 32(12):2485–92. doi: 10.1007/s00198-021-06023-0

8. Dimai HP. Use of dual-energy X-ray absorptiometry (DXA) for diagnosis and fracture risk assessment; WHO-criteria, T- and z-score, and reference databases. *Bone* (2017) 104:39–43. doi: 10.1016/j.bone.2016.12.016

9. Choi YJ. Dual-energy X-ray absorptiometry: Beyond bone mineral density determination. *Endocrinol Metab (Seoul Korea)* (2016) 31(1):25–30. doi: 10.3803/EnM.2016.31.1.25

10. China NHCO. *Epidemiological investigation of osteoporosis in China* (2021). Available at: http://www.phsciencedata.cn/Share/jsp/PublishManager/foregroundView/1/9eaadbb3-bd64-4531-9d9f-753ec183f26d.

11. Ito M, Hayashi K, Yamada M, Uetani M, Nakamura T. Relationship of osteophytes to bone mineral density and spinal fracture in men. *Radiology* (1993) 189(2):497–502. doi: 10.1148/radiology.189.2.8210380

12. Chang G, Honig S, Brown R, Deniz CM, Egol KA, Babb JS, et al. Finite element analysis applied to 3-T MR imaging of proximal femur microarchitecture: lower bone strength in patients with fragility fractures compared with control subjects. *Radiology* (2014) 272(2):464–74. doi: 10.1148/radiol.14131926

13. Zhang B, Yu K, Ning Z, Wang K, Dong Y, Liu X, et al. Deep learning of lumbar spine X-ray for osteopenia and osteoporosis screening: A multicenter retrospective cohort study. *Bone* (2020) 140:115561. doi: 10.1016/j.bone.2020.115561

14. Chartrand G, Cheng PM, Vorontsov E, Drozdzal M, Turcotte S, Pal CJ, et al. Deep learning: A primer for radiologists. *Radiographics* (2017) 37(7):2113–31. doi: 10.1148/rg.2017170077

15. Yasaka K, Akai H, Kunimatsu A, Kiryu S, Abe O. Deep learning with convolutional neural network in radiology. *Jpn J Radiol* (2018) 36(4):257–72. doi: 10.1007/s11604-018-0726-3

16. Yasaka K, Akai H, Abe O, Kiryu S. Deep learning with convolutional neural network for differentiation of liver masses at dynamic contrast-enhanced CT: A preliminary study. *Radiology* (2018) 286(3):887–96. doi: 10.1148/radiol.2017170706

17. Kiryu S, Yasaka K, Akai H, Nakata Y, Sugomori Y, Hara S, et al. Deep learning to differentiate parkinsonian disorders separately using single midsagittal MR imaging: a proof of concept study. *Eur Radiol* (2019) 29(12):6891–9. doi: 10.1007/s00330-019-06327-0

18. Larson DB, Chen MC, Lungren MP, Halabi SS, Stence NV, Langlotz CP. Performance of a deep-learning neural network model in assessing skeletal maturity on pediatric hand radiographs. *Radiology* (2018) 287(1):313–22. doi: 10.1148/radiol.2017170236

19. Urakawa T, Tanaka Y, Goto S, Matsuzawa H, Watanabe K, Endo N. Detecting intertrochanteric hip fractures with orthopedist-level accuracy using a deep convolutional neural network. *Skeletal Radiol* (2019) 48(2):239–44. doi: 10.1007/s00256-018-3016-3

20. Derkatch S, Kirby C, Kimelman D, Jozani MJ, Davidson JM, Leslie WD. Identification of vertebral fractures by convolutional neural networks to predict nonvertebral and hip fractures: A registry-based cohort study of dual X-ray absorptiometry. *Radiology* (2019) 293(2):405–11. doi: 10.1148/radiol.2019190201

21. Cheng CT, Ho TY, Lee TY, Chang CC, Chou CC, Chen CC, et al. Application of a deep learning algorithm for detection and visualization of hip fractures on plain pelvic radiographs. *Eur Radiol* (2019) 29(10):5469–77. doi: 10.1007/s00330-019-06167-y

22. dLee KS, Jung SK, Ryu JJ, Shin SW, Choi J. Evaluation of transfer learning with deep convolutional neural networks for screening osteoporosis in dental panoramic radiographs. *J Clin Med* (2020) 9(2):392–405. doi: 10.3390/jcm9020392

23. Lee S, Choe EK, Kang HY, Yoon JW, Kim HS. The exploration of feature extraction and machine learning for predicting bone density from simple spine X-ray images in a Korean population. *Skeletal Radiol* (2020) 49(4):613–8. doi: 10.1007/s00256-019-03342-6

24. Tecle N, Teitel J, Morris MR, Sani N, Mitten D, Hammert WC. Convolutional neural network for second metacarpal radiographic osteoporosis screening. *J Handb Surg Am* (2020) 45(3):175–81. doi: 10.1016/j.jhsa.2019.11.019

25. Hussain D, Han SM. Computer-aided osteoporosis detection from DXA imaging. *Comput Methods Programs BioMed* (2019) 173:87–107. doi: 10.1016/j.cmpb.2019.03.011

26. Valentinitsch A, Trebeschi S, Kaesmacher J, Lorenz C, Loffler MT, Zimmer C, et al. Opportunistic osteoporosis screening in multi-detector CT images *via* local classification of textures. *Osteoporos Int* (2019) 30(6):1275–85. doi: 10.1007/s00198-019-04910-1

27. Fang Y, Li W, Chen X, Chen K, Kang H, Yu P, et al. Opportunistic osteoporosis screening in multi-detector CT images using deep convolutional neural networks. *Eur Radiol* (2021) 31(4):1831–42. doi: 10.1007/s00330-020-07312-8

28. Camacho PM, Petak SM, Binkley N, Diab DL, Eldeiry LS, Farooki A, et al. American Association of clinical endocrinologists/American colloege of endocrinology clinical practice guidelines for the diagnosis and treatment and of postmenopausal osteoporosis-2020 update executive summary. *Endocr Pract* (2020) 26(5):564–70. doi: 10.4158/GL-2020-0524

29. Huang G, Liu Z, Van Der Maaten L, Weinberger KQ. Densely connected convolutional networks, *IEEE Computer Society* (2017) 24(5):2261–9. doi: 10.1109/CVPR.2017.243

30. Le QV. *A tutorial on deep learning part 1: Nonlinear classifiers and the back propagation algorithm*. Mountain View, CA: Google Inc (2015).

31. Le QV. *A tutorial on deep learning part 2: autoencoders, convolutional neural networks and recurrent neural networks*. Mountain View, CA: Google Inc (2015).

32. Lecun Y, Bengio Y, Hinton G. Deep learning. *Nature* (2015) 521(7553):436–44. doi: 10.1038/nature14539

33. Force USPS. Screening for osteoporosis in postmenopausal women: Recommendations and rationale. *Am Fam Med* (2002) 137(6):526–8. doi: 10.7326/0003-4819-137-6-200209170-00014

34. Morin SN, Yan L, Lix LM, Leslie WD. Long-term risk of subsequent major osteoporotic fracture and hip fracture in men and women: a population-based observational study with a 25-year follow-up. *Osteoporos Int* (2021) 32(12):2525–32. doi: 10.1007/s00198-021-06028-9

35. Anpalahan M, Morrison SG, Gibson SJ. Hip fracture risk factors and the discriminability of hip fracture risk vary by age: a case-control study. *Geriatr Gerontol Int* (2014) 14(2):413–9. doi: 10.1111/ggi.12117

36. Curry SJ, Krist AH, Owens DK, Barry MJ, Caughey AB, Davidson KW, et al. Screening for osteoporosis to prevent fractures US preventive services task force recommendation statement. *JAMA-J Am Med Assoc* (2018) 319(24):2521–31. doi: 10.1001/jama.2018.7498

Check for updates

*CORRESPONDENCE
Xiaoguang Cheng
Xiao65@263.net

Differences in spine volumetric bone mineral density between grade 1 vertebral fracture and non-fractured participants in the China action on spine and hip status study

Yandong Liu[1], Aihong Yu[2], Kai Li[1], Ling Wang[1], Pengju Huang[1], Jian Geng[1], Yong Zhang[3], Yang-yang Duanmu[4], Glen M. Blake[5] and Xiaoguang Cheng[1]* on behalf of CASH study team

[1]Radiology Department, Peking University Fourth School of Clinical Medicine, Beijing, China, [2]Radiology Department, Beijing Anding Hospital Capital Medical University, Beijing, China, [3]Intervention Department, Beijing Chao-Yang Hospital, Capital Medical University, Beijing, China, [4]South Medical Image Center, The First Affiliated Hospital of University of Science and Technology of China (USTC), Anhui, China, [5]School of Biomedical Engineering and Imaging Sciences, King's College London, St Thomas' Hospital, London, United Kingdom

Purpose: This study evaluated the prevalence of vertebral fractures (VF) in middle-aged and elderly Chinese men and women and explored the differences in lumbar spine volumetric bone mineral density (vBMD) derived from quantitative CT (QCT) between those with a grade 1 vertebral fracture and non-fractured individuals.

Materials and methods: 3,457 participants were enrolled in the China Action on Spine and Hip Status (CASH) study and had upper abdominal CT examinations. Vertebral fractures were identified by Genant's semi-quantitative method from lateral CT scout views or CT sagittal views. L1-3 vBMD was measured by Mindways QCT Pro v5.0 software. The characteristics of different fracture severity groups were compared using one-way ANOVA, independent-samples t-tests, and Kruskal-Wallis H-tests.

Results: 1267 males (aged 62.77 ± 9.20 years) and 2170 females (aged 61.41 ± 9.01 years) were included in the analysis. In men, the prevalence of VF increased from 14.7% at age<50 years to 23.2% at age $\geq$70 years, and in women from 5.1% at age<50 years to 33.0% at age $\geq$70 years. Differences in mean age and vBMD were found between the different fracture grade groups. After age stratification, vBMD differences in men aged < 50 years old disappeared ($p = 0.162$) but remained in the older age bands. There was no significant difference in mean vBMD between those with multiple mild fractures and those with a single mild fracture.

Conclusion: In women, the prevalence of VF increased rapidly after age 50, while it grew more slowly in men. In general, with the exception of men <50 years old, participants with a grade 1 VF had lower vBMD than non-fractured individuals. The majority of women younger than 50 with a grade 1 VF had normal bone mass. We recommend that a vertebral height reduction ratio of <25% be diagnosed as a deformity rather than a fracture in people under the age of 50. The presence of multiple mild fractured vertebrae does not imply lower BMD.

Introduction

Vertebral fracture (VF) is the most common osteoporotic fracture (1) but is easily missed in clinical practice because it is often asymptomatic (2). Not only can VF itself result in a poor prognosis (3), but it can also predict subsequent incident fractures (4, 5), so identification of VF, especially asymptomatic VF, is critical to prompting medical attention and preventing bad outcomes (2). Evaluation of the prevalence of VF in the population is an important aspect of public health. Cui et al. reported the prevalence of VF in postmenopausal Chinese women (6). However, the cohort of Cui's study was limited to a single city and only included postmenopausal women over 50 years old. Until now, there has been no national data on the prevalence of VF in middle-aged Chinese women or middle-aged and elderly men. In this study, VF status in China was evaluated based on a nation-wide multi-center study (7).

The Genant semiquantitative (GSQ) method, in which vertebrae are categorized as grade 0 (non-fractured), 1 (mild), 2 (moderate) or 3 (severe) according to their reduction in height, is the most widely used criterion in epidemiological and clinical studies for evaluating osteoporotic vertebral fractures from radiographs (8–11) and was employed in the present study (8). However, the validity of Grade 1 VFs has been challenged over the years, and some researchers disregard Grade 1 deformities as a feature of VF (2, 12–15). In contrast, other research teams have presented evidence to support the relationship between Grade 1 VFs or minor vertebral deformities, bone mineral density

---

Abbreviations: VF, vertebral fracture; GSQ, Genant semiquantitative; BMD, bone mineral density; DXA, dual-energy X-ray absorptiometry; aBMD, areal bone mineral density; vBMD, volumetric bone mineral density; VFA, vertebral fracture assessment; QCT, quantitative computed tomography; CASH, China Action on Spine and Hip Status; WC, waist circumference; HC, hip circumference; BMI, body mass index; ESP, European spine phantom; ISCD, International Society for Clinical Densitometry; FV, fractured vertebra; SD, standard deviation.

(BMD), and further incident fractures (16–22). These studies were all based on conventional radiography or DXA-assisted vertebral fracture assessment (VFA), and bone mineral density (BMD) was evaluated by dual-energy X-ray absorptiometry (DXA) and represented by T-scores or areal BMD (aBMD, g/cm^2). There is little literature in this field based on volumetric BMD (vBMD mg/cm^3) derived from quantitative computed tomography (QCT), another recognized technique for diagnosing osteoporosis. Compared with DXA, a 2-dimensional method, QCT measures vBMD from a 3-dimensional image (23) and can avoid the influence caused by scoliosis, osteoarthritis of spine and calcification of vessel and/or ligament. Some studies illustrated that vBMD may be a more accurate predictor of fracture risk than aBMD (24, 25). The current study explored the differences in vBMD between participants with Grade 1 VF and those without any evidence of a vertebral radiographic deformity. Furthermore, vBMD was also compared between those with a single Grade 1 VF and those with multiple Grade 1 VFs, an aspect that, to the best of our knowledge, has not previously been discussed.

Materials and methods

China action on spine and hip status study

The cohort for this study was a subgroup of the China Action on Spine and Hip Status (CASH) study (NCT 01758770) (7). A total of 12 centers from 6 provinces (3 from Sichuan, 3 from Jiangsu, 1 from Shanxi, 1 from Shaanxi, 1 from Liaoning, and 1 from Jiangxi) and 1 municipality (2 from Beijing) participated in this study. The protocol and informed consent documents for the CASH study were reviewed and approved by the institutional review board of the Beijing Jishuitan Hospital (approval numbers No. 201210-01; No. 201512-02). The inclusion criteria are that participants should be aged over 40

years old and able to give informed consent. Exclusion criteria are pregnant women, individuals with metal implants in the lumbar spine, use of medications or the existence of any disease or condition known to have a major influence on BMD, and inability to give informed consent.

Participants and data collection

The CASH study CT scans were performed between March 2013 and August 2017. All participants lived near one of the 12 centers and were willing to undergo a spine CT scan. A total of 3457 participants between 40 and 82 years old were enrolled in the study.

For most participants, social-demographic data, height, weight, waist circumference (WC), and hip circumference (HC) were recorded by a trained health physician before or after their CT scan. For the others, the information was supplemented by the baseline data based on the assumption that those data did not change in the follow-up period. Body mass index (BMI) and waist-hip ratio (WHR) were calculated by weight (kg)/height squared (m2) and WC (cm)/HC (cm) respectively.

Quantitative computed tomography volumetric bone mineral density measurement

Mindways (Austin, TX, USA) QCT phantom and software were used at all centers. The phantom was scanned with each participant to ensure the accuracy and precision of the vBMD measurements. Participants lay on the phantom and had upper abdominal CT examinations with a fixed table height and scan parameters. At the same time, the CT scout views including the T4-S1 vertebrae were obtained. The detailed scan protocol was reported in a previous paper (7). To eliminate any discrepancy between different CT scanners, ten scans of a European spine phantom (ESP, No.145) were performed on each CT scanner. All QCT data were transferred to the Beijing Jishuitan Hospital for analysis and quality control.

The L1 to L3 vertebrae vBMD values were measured by Mindways QCT Pro v5.0 software according to the manufacturer's protocol. For each participant, the average value of L1 to L3 vBMD was calculated and obtained through cross-calibration. The final value was regarded as the lumbar spine vBMD value. Following the criteria of the International Society for Clinical Densitometry (ISCD) 2007 (26) and the Chinese Expert Consensus on the Diagnosis of Osteoporosis (27), a vBMD value ≥120 mg/cm^3 was defined as normal, a value between 80 and 119 mg/cm^3 as osteopenia, and a value < 80mg/cm^3 as osteoporosis.

Identification of vertebral fracture

The lateral CT scout view images of 3340 participants were evaluated by an expert MSK radiologist (XGC) with many years of experience in vertebral fracture assessment. The digital images were displayed and viewed with a professional DICOM view workstation. The capability and reliability of lateral CT scout views in assessing vertebral fractures has been verified (28, 29). Under ideal conditions, CT scout view images can assess the T4-L4 vertebrae. However, due to limitations in actual scanned area or overlapping of ribs, all T4-L4 vertebrae could be assessed in only 683 images and all T5-L4 vertebrae in 864 images. In most cases, the assessable range was from T6 to L4. The fracture status of another 117 participants was diagnosed based on the CT sagittal views of the T10-L4 vertebrae because of the lack of CT scout views.

Genant's semi-quantitative (GSQ) method (8) was used as the criterion of vertebral fracture: vertebral height reductions of>20% to 25%,>25% to 40%, and>40% were defined as grade 1 (mild), grade 2 (moderate), and grade 3 (severe), respectively (Figure 1). Vertebrae with a grade ≥1 were identified as fractured, and the fracture severity of each individual was decided by the highest grade in that person. Grade 2 and grade 3 were merged into a single group for further analysis. Finally, all cases were divided into three groups: a non-fractured group; a grade 1 group; and a grade 2 and 3 group. The grade 1 group was further divided into two sub-groups according to the number of fractured vertebra (FV): FV=1 and FV≥2.

Statistical analyses

vBMD was the observed variable in this study, while age, BMI, and WHR were the potential covariates. All the results were gender-specific. A comparison of vBMD, age, BMI, and WHR between the non-fracture group, the grade 1 group, and the grade 2 and 3 group was performed first. Then, the non-fracture group was compared with the grade 1 group after age stratification. Characteristics of sub-groups by the number of fractured vertebrae in the grade 1 group in different age bands were also compared. Continuous variables were shown as the mean ± standard deviation (SD), and ordinal categorical variables as numbers (n) and percentages (%). For the comparison of multiple sets of continuous variables, one-way ANOVA followed by a Bonferroni *post hoc* test was used if the variances were equal. Otherwise, Tamhane's T2 test was chosen. Two groups of continuous variables were tested by an independent-samples t-test. Ordinal and categorical variables were tested with a Kruskal-Wallis H-test. Covariance analysis was used to eliminate the influence of covariates. Statistical analyses were performed by IBM SPSS Statistical 26.0 software. P<0.05 was considered statistically significant.
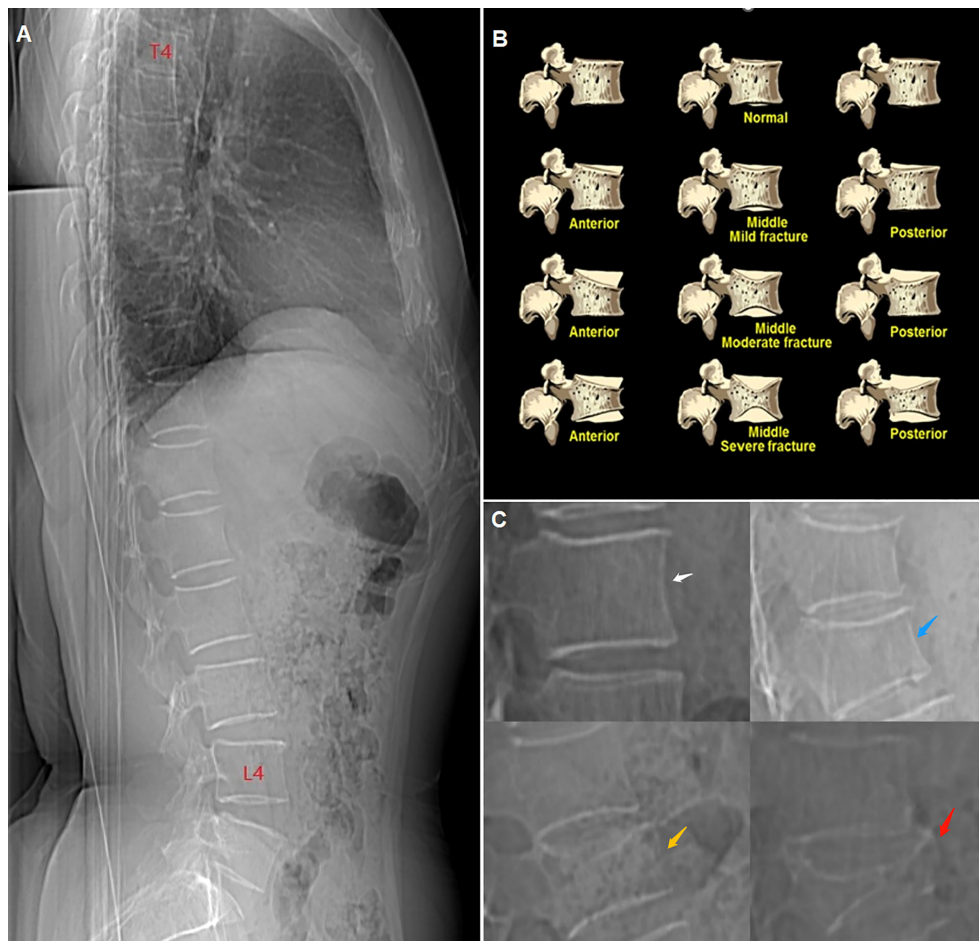
FIGURE 1
(A) CT lateral scout view of the vertebrae from T4 to L4. **(B)** schematic diagram of Genant's semiquantitative (GSQ) method. **(C)** compression degree of vertebrae showed in CT lateral scout view, white arrow: non-fractured (grade 0), blue arrow: mild (grade 1), yellow arrow: moderate (grade 2), red arrow: severe (grade 3).

Results

Twenty of 3457 participants were excluded. For six participants, their age or sex did not match the CASH database. Another 14 participants were missing their vBMD results. The statistical analysis included a total of 3437 participants, among whom there were 1267 males aged 62.77 ± 9.20 years and 2170 females aged 61.41 ± 9.01 years.

Prevalence

All participants were grouped into four age bands for men and the same number for women; those aged<50 years, 50-59 years, 60-69 years, and ≥70 years, respectively. The prevalence of VF and osteoporosis in men and women, respectively, is shown in Table 1, together with the corresponding average vBMD results. In men,

the prevalence of VF increased from 14.7% at age<50 years to 23.2% at age ≥70 years, with the percentage of osteoporotic men increasing from 3.1% to 36.5%, while the average vBMD decreased from 139.90 ± 31.61mg/cm^3 to 92.63 ± 33.61 mg/cm^3. In women, the prevalence of VF increased from 5.1% at age<50 years to 33.0% at age ≥70 years, with the percentage of osteoporotic women increasing from 1.6% to 69.3%, while the average vBMD decreased from 151.04 ± 34.06 mg/cm3 to 68.47 ± 31.47 mg/cm3.

Figure 2 shows plots of the prevalence of VF and osteoporosis and the variation of vBMD with age. The male prevalence of VF was much higher than the female prevalence in the group less than 50 years old, while it was lower in the group ≥70 years old. The prevalence crossed over for the group aged 60 to 69 years (women 15.9%, men 18.0%). Compared with VF, the osteoporosis prevalence cross-over point is earlier: between 50 and 59 years. In those aged<50 years, the percentage of osteoporotic women was lower than in men, and the average vBMD was higher accordingly.

TABLE 1   The prevalence of vertebral fractures (VFs), osteoporosis (OP) and the mean ± standard deviation of vBMD by gender and age bands.

Age		<50y	50-59y	60-69y	≥70y	Total
Sex						
Male	Total Number (n)	129	293	522	323	1267
	VF Number(n) and Prevalence (%)	19 (14.7)	48 (16.4)	94 (18.0)	75 (23.2)	236 (18.6)
	OP Number(n) and Prevalence (%)	4 (3.1)	22 (7.5)	80 (15.3)	118 (36.5)	224 (17.7)
	vBMD (mg/cm^3)	139.90 ± 31.61	120.89 ± 29.07	110.22 ± 32.87	92.63 ± 33.61	111.23 ± 34.96
Female	Total Number (n)	254	604	882	430	2170
	VF Number(n) and Prevalence (%)	13 (5.1)	41 (6.8)	140 (15.9)	142 (33.0)	336 (15.5)
	OP Number(n) and Prevalence (%)	4 (1.6)	77 (12.7)	373 (42.3)	298 (69.3)	752 (34.7)
	vBMD (mg/cm^3)	151.04 ± 34.06	117.78 ± 34.63	87.24 ± 29.51	68.47 ± 31.47	99.49 ± 40.91

VF, vertebral fracture; OP, osteoporosis; vBMD, QCT volumetric bone mineral density; y, years.

At 50-59 years, female vBMD (117.78 ± 34.63 mg/cm^3) was slightly lower than male (120.89 ± 29.07 mg/cm^3) and the prevalence of osteoporosis was slightly higher (women 12.7%, men 7.5%). The difference increased with increasing age. At age ≥70, the prevalence of osteoporosis in women (69.3%) was nearly twice that in men (36.5%). The prevalence of VF in the group ≥50 years old among the different geographic regions of China is shown in Figure 3.

Characteristics

The characteristics of participants by gender and vertebral fracture grades identified by Genant's semi-quantitative criteria are shown in Table 2. Male age did not differ significantly between the grade 1 group (63.57 ± 9.3 years) and the other two groups, but the age of the non-fracture group (62.47 ± 9.16 years) differed significantly from the grade 2 and 3 group (67.03 ± 9.04 years) with p = 0.010. The non-fracture, grade 1, and grade 2 and 3 groups had vBMD values of 114.47 ± 34.88 mg/cm^3, 99.24 ± 30.71 mg/cm^3, and 84.99 ± 34.74 mg/cm^3 respectively. The differences between the non-fractured and the two fracture groups were statistically significant, while the difference between the two fracture groups was non-significant. In the non-fracture group, the proportion of people with normal bone density is the largest (43.9%), while the proportion with osteoporosis is the smallest (15.4%). Most men in the grade 1 group (47.0%) and grade 2 and 3 group (47.2%) had osteopenia, while the latter group had the highest proportion with osteoporosis (36.1%). There were no significant differences among the three groups in BMI (p=0.649) or WHR (p=0.824).

In women, the average age of grade 2 and 3 vertebral fracture cases (69.77 ± 6.67 years) was significantly older than that of grade 1 cases (65.98 ± 8.06 years), and the latter was significantly older than the non-fracture participants (60.37 ± 8.82 years). Grade2 and 3 cases showed the lowest vBMD value (50.25 ±

23.82 mg/cm^3) and the highest percentage with osteoporosis (92.0%), while the non-fracture participants had the highest vBMD (105.31 ± 39.63 mg/cm^3) and the lowest percentage with osteoporosis (28.3%). The grade 1 group was located between the other two. After controlling for age, the differences between groups remained significant (p<0.001). There was no significant difference among the three groups in BMI (p=0.441). The WHR of the non-fracture group (0.83 ± 0.07) was significantly different from the grade 1 (0.85 ± 0.07) and grade 2 and 3 groups (0.86 ± 0.07), while the latter two were the same (p=1.000). However, the difference between the non-fracture group and fracture groups became non-significant after stratification by age.

Comparison of volumetric bone mineral density after age-stratification

In this part of the study, male and female participants were divided into three age bands; those aged<50 years, 50-65 years, and ≥ 65 years, respectively. A comparison of age and vBMD between the non-fracture group and the grade 1 vertebral fracture group is shown in Table 3. There was no significant difference between the two groups in mean male age after stratifying by age. In men, the mean BMD of the grade 1 vertebral fracture group was lower than the non-fracture group in all three age bands, but there was no statistical difference for those<50 years old (p=0.162). In contrast, the differences were statistically significant in the other two age bands. Participants with normal bone density in the age band<50 years accounted for 70.6% of the grade 1 group compared with 80.0% of the non-fracture group, a difference that was not statistically significant. The percentage of participants with normal bone density in the grade 1 group decreased to 29.3% and 16.8% in the 50-65 year and ≥65 year age bands respectively. Meanwhile, the prevalence of osteoporosis increased to 15.8%
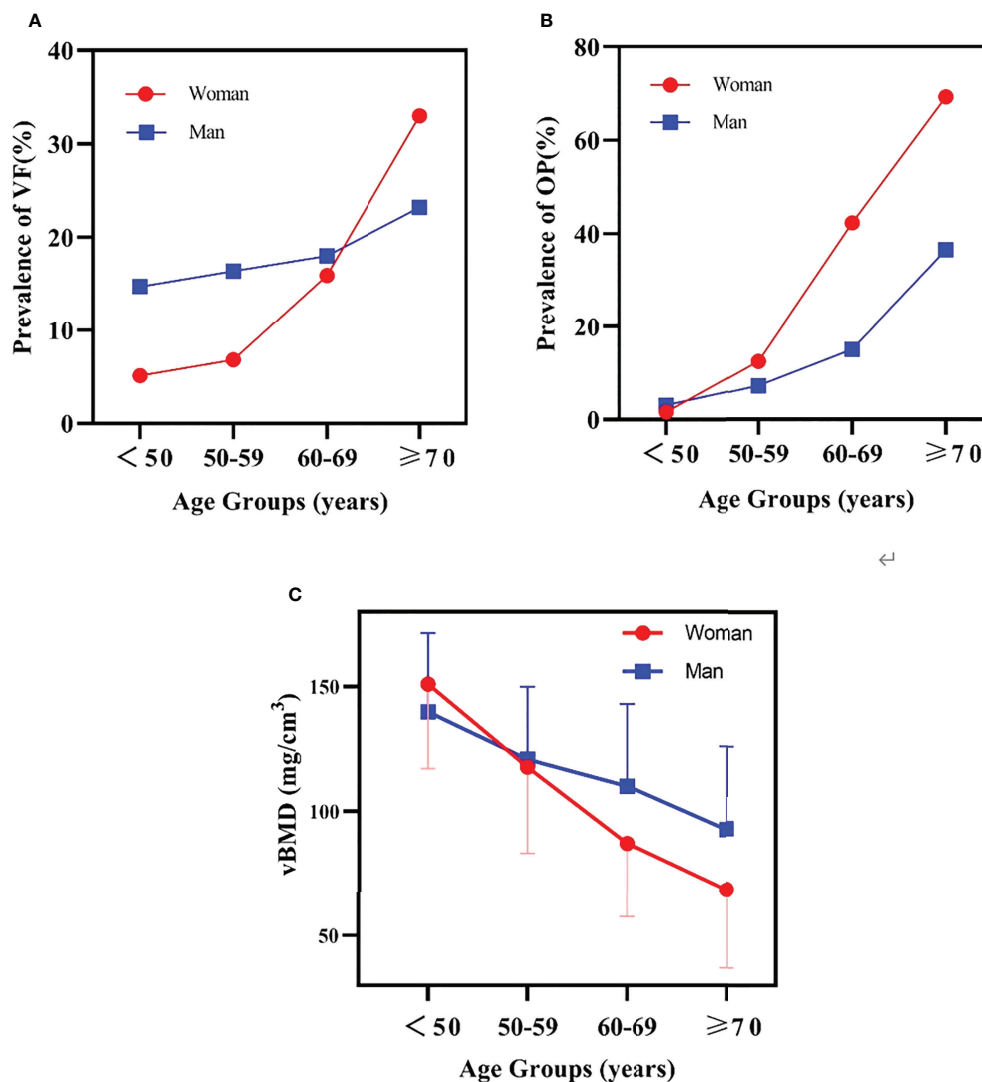
FIGURE 2
(A) the prevalence of vertebral fracture (VF) variation with age. **(B)** the prevalence of osteoporosis (OP) variation with age. **(C)** the mean and SD of bone mineral density (BMD) variation with age.

and 39.6% respectively. These proportions were significantly different from the non-fracture group.

For women, age was significantly different between the non-fracture and grade 1 vertebral fracture groups in the 50-65 year and ≥65 year age bands (p<0.001), but not at age<50 years (p = 0.050). In the non-fracture group, vBMD in females was always significantly higher than in the grade 1 vertebral fracture group. These differences remained after adjustment for age. In the grade 1 group, 58.3% of participants in the<50 year age band had normal bone density. For ages between 50-65 years, most female participants had osteopenia (54.2%), and the percentage with osteoporosis (33.7%) was higher than those with normal bone density (12.1%). Of the women aged ≥65 years in the grade 1 group, 78.9% were osteoporotic. The proportion was statistically

significantly higher than the non-fracture group for all age bands.

The grade 1 vertebral fracture group was divided into two sub-groups according to the number of fractured vertebrae (FV): single fracture (FV=1) and multiple fractures (FV≥2) (Table 4). There were no significant differences between any pairs of results in Table 4.

Discussion

In this nation-wide multi-center study of 3457 Chinese middle-aged and elderly adults, we evaluated the prevalence of
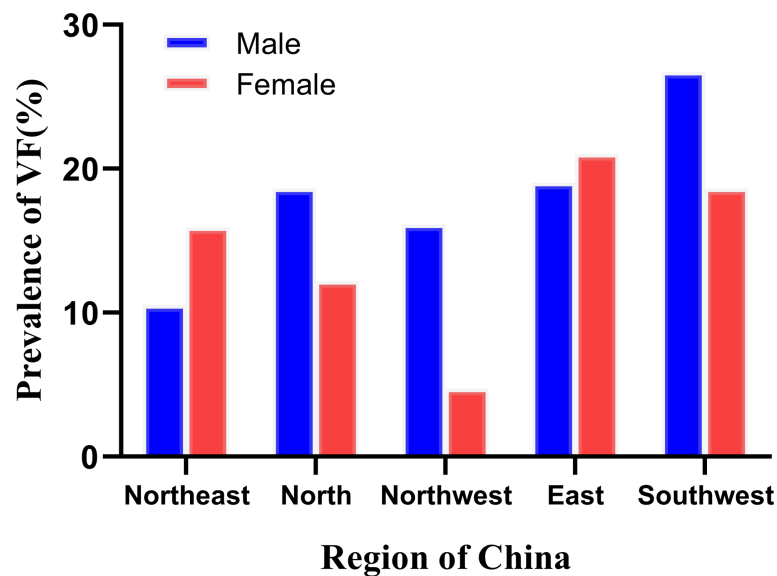
FIGURE 3

The prevalence of vertebral fracture (VF) in the ≥50 years group across different regions of China.

TABLE 2   Characteristics of eligible participants by gender and vertebra fracture grades identified by Genant's semi-quantitative criteria.

Characteristics	Male				Female			
	Non-fracture (n=1031)	Grade 1 (n=200)	Grade 2and3 (n=36)	p	Non-fracture (n=1834)	Grade 1 (n=237)	Grade 2and3 (n=99)	p
Age(y)	62.47 ± 9.16	63.57 ± 9.3	67.03 ± 9.04	0.006▲	60.37 ± 8.82	65.98 ± 8.06	69.77 ± 6.67	<0.001△
vBMD (mg/cm³), n (%)	114.47 ± 34.88	99.24 ± 30.71	84.99 ± 34.74	<0.001*▲▲	105.31 ± 39.63	75.00 ± 32.62	50.25 ± 23.82	<0.001*△
Normal	453 (43.9)	53 (26.5)	6 (16.7)	<0.001	601 (32.8)	21 (8.9)	1 (1.0)	<0.001
Osteopenia	420 (40.7)	94 (47.0)	17 (47.2)		713 (38.9)	75 (31.6)	7 (7.0)	
Osteoporosis	158 (15.4)	53 (26.5)	13 (36.1)		520 (28.3)	141 (59.5)	91 (92.0)	
BMI (kg/m²)	24.19 ± 3.31	24.03 ± 3.27	23.77 ± 2.87	0.649	24.28 ± 3.49	24.59 ± 3.93	24.38 ± 3.05	0.441
WHR	0.88 ± 0.07	0.88 ± 0.07	0.88 ± 0.11	0.824	0.83 ± 0.07	0.85 ± 0.07	0.86 ± 0.07	<0.001▲▲▲

y, years; p, p-value; vBMD, QCT volumetric bone mineral density; BMI, body mass index; WHR, waist-to-hip ratio.
Continuous variables were shown as mean ± standard deviance, and were tested by ANOVA; ordinal categorical variables were shown as frequency(n) and percentage (%), and were tested by Kruskal-Wallis H tests.
*, the p-value is always<0.001 before and after being adjusted by age.
▲, male age shows no significant difference between Grade 1 group and other two groups, while age of non-fracture group is significantly different from Grade 2and3 group with p=0.010.
△,the p-value of all comparison among groups <0.001.
▲▲,the p-value among Grade 1 group and Grade 2and3 group =0.065, while p-value of other pairs<0.001.
▲▲▲, the p-value among Grade 1 group and Grade 2and3 group =1.000, while p-value of non-fracture group vs. Grade 1 group<0.001 and p-value of non-fracture group vs. Grade 2and3 group=0.002.

VFs by identifying fractured vertebra from 3340 lateral CT scout views and 117 CT sagittal views and used volumetric BMD derived from QCT to calculate the prevalence of osteoporosis. Volumetric BMD was compared between the Grade 1 VF population and the non-fractured population, as well as between subgroups of the Grade 1 VF population according to the number of fractured vertebrae.

The results show that the prevalence of VFs and osteoporosis increases with age in both men and women. Men before the age of 60 are approximately three times more likely than women to

TABLE 3   Comparison of age and vBMD by gender between non-fracture group and Grade 1 vertebral fracture (VF) group in different age bands. .

Agebands	Characteristics	Male			Female		
		Non-fracture	Grade 1	p_1	Non-fracture	Grade 1	p_1
<50y	Number	110	17	–	241	12	–
	Age (y)	46.00 ± 2.09	46.18 ± 2.40	0.751	46.07 ± 2.30	47.00 ± 1.41	0.050
	vBMD (mg/cm^3), n (%)	141.80 ± 32.6	130.23 ± 23.46	0.162	152.41 ± 32.63	128.52 ± 47.84	0.016
	Normal	88 (80.0)	12 (70.6)	0.341	201 (83.4)	7 (58.3)	0.034
	Osteopenia	18 (16.4)	5 (29.4)		37 (15.4)	4 (33.3)	
	Osteoporosis	4 (3.6)	0 (0)		3 (1.2)	1 (8.4)	
50-64y	Number	468	82	–	950	83	–
	Age (y)	58.34 ± 4.36	57.91 ± 4.51	0.548	57.64 ± 4.31	59.72 ± 3.85	<0.001
	vBMD (mg/cm^3), n (%)	121.46 ± 31.69	104.85 ± 25.57	<0.001	109.45 ± 34.48	90.16 ± 28.66	<0.001*
	Normal	233 (49.7)	24 (29.3)	0.002	334 (35.1)	10 (12.1)	<0.001
	Osteopenia	195 (41.7)	45 (54.9)		432 (45.5)	45 (54.2)	
	Osteoporosis	40 (8.6)	13 (15.8)		184 (19.4)	28 (33.7)	
≥65y	Number	453	101	–	643	142	–
	Age (y)	70.73 ± 4.28	71.08 ± 4.40	0.459	69.77 ± 4.04	71.25 ± 4.27	<0.001
	vBMD (mg/cm^3), n (%)	100.60 ± 32.45	89.48 ± 31.21	0.002	81.54 ± 30.07	61.62 ± 23.78	<0.001*
	Normal	132 (29.1)	17 (16.8)	0.004	66 (10.3)	4 (2.8)	<0.001
	Osteopenia	207 (45.7)	44 (43.6)		244 (37.9)	26 (18.3)	
	Osteoporosis	114 (25.2)	40 (39.6)		333 (51.8)	112 (78.9)	

VF, vertebral fracture; VF, fractured vertebra; vBMD, QCT volumetric bone mineral density; BMI, body mass index; WHR, waist-to-hip ratio; y, years; p, p-value.
Continuous variables were shown as mean ± standard deviance, and were tested by independent-samples t-test; ordinal categorical variables were shown as frequency(n) and percentage (%), and were tested by Kruskal-Wallis H tests.
*, the p -value is always<0.001 before and after being adjusted by age.

TABLE 4   Comparison of age and vBMD in the Grade 1 vertebral fracture (VF) group by number of fractured vertebra (FV) at different age bands♦.

Agebands	Characteristics	Male			Female		
		FV=1	FVs≥2	p	FV=1	FVs≥2	p
50-64y	Number	48	34	–	73	10	–
	Age (y)	58.25 ± 4.20	57.44 ± 5.00	0.427	60.00 ± 3.64	57.7 ± 4.86	0.076
	vBMD (mg/cm^3), n (%)	102.80 ± 21.32	107.74 ± 30.79	0.392	91.30 ± 27.32	81.80 ± 37.32	0.329
	Normal	12 (25)	12 (35.3)	0.604	9 (12.3)	1 (10.0)	0.512
	Osteopenia	28 (48.3)	17 (50.0)		41 (56.2)	4 (40.0)	
	Osteoporosis	8 (17.7)	5 (14.7)		23 (31.5)	5 (50.0)	
≥65y	Number	64	37	–	106	36	–
	Age (y)	70.95 ± 4.47	71.30 ± 4.39	0.707	71.40 ± 4.30	70.81 ± 4.20	0.475
	vBMD (mg/cm^3), n (%)	92.70 ± 30.85	83.90 ± 31.45	0.173	61.96 ± 24.43	60.63 ± 22.08	0.773
	Normal	12 (18.7)	5 (13.5)	0.857	4 (3.7)	0 (0)	0.463
	Osteopenia	30 (46.9)	14 (37.8)		20 (18.9)	6 (16.7)	
	Osteoporosis	22 (34.4)	18 (48.7)		82 (77.4)	30 (83.3)	

VF, vertebral fracture; FV, fractured vertebra; vBMD, QCT volumetric bone mineral density; y, years; p, p-value.
♦, <50y group is excluded due to small sample size.
Continuous variables were shown as mean ± standard deviance, and were tested by independent-samples t-test; ordinal categorical variables were shown as frequency(n) and percentage (%), and were tested by Kruskal-Wallis H tests.

experience VFs, but this is reversed after the age of 70 when the prevalence of VF in females is approximately 1.5 times that of males (33.0% versus 23.2%), with the cross-over occurring in the 60-69 age band. In comparison, the cross-over in the prevalence of osteoporosis occurs earlier at around age 50. Women between the ages of 50 and 59 have similar vBMD to men, but at younger ages vBMD is higher in women than men. This observation is consistent with the cross-sectional study of 69,095 Chinese

adults published by Cheng et al. (30). However, the prevalence of osteoporosis in the present study population aged 50 years and older is higher than that reported by Cheng et al., with the percentages of women and men over 50 with osteoporosis reaching 38.9% and 29.3%, respectively, while in the study of Cheng et al. those numbers were 29.0% and 13.5%, respectively (30). This might be due to a different age distribution between the two populations. In the present study, the percentage of people aged ≥65 years is 38.25%, but there was only 13.26% of people over 65 years in the study of Cheng et al. (30). However, after age-stratification the prevalence of osteoporosis is similar in the two studies.

Cui et al. evaluated the prevalence of VFs in postmenopausal women in Beijing, China, based on conventional radiographs and the GSQ method. The percentages were 13.4%, 22.6%, 31.4%, and 58.1%, respectively, for women aged 50-59 years, 60-69 years, 70-79 years, and ≥80 years (6). The first two numbers are higher than the corresponding results reported in the present paper (6.8% and 15.9% respectively). The discrepancy might be due to the use of different types of radiographic images in the two studies, to genuine differences between the two study populations, or to inter-observer differences. However, our results are similar to those reported by Xu et al. (31), which were based on conventional radiographs and a morphometry method developed by Black et al. (32). A multi-center study in America reported a total prevalence of 3.2% of GSQ VF in middle-aged women of different races, with a prevalence of 3.4% in Chinese American women (33). To our knowledge, the prevalence of VF in Chinese men has not been reported before and is seldom discussed in other countries. A study in a Spanish cohort reported that 21.3% of Spanish men over 50 years old suffered from VFs identified by the GSQ method (34). Our percentage is slightly higher than the present results (19.06%). This study is the first to report the prevalence of VF in people ≥50 years old across different regions of China. Men from the Southwest and women from the East had the highest VF prevalence, and men from the Northeast and women from the Northwest had the lowest VF prevalence. However, the sample size from the Northwest was small (86 women and 62 men aged ≥50 years), which limits the statistical reliability of the results.

Before age-stratification, there was a significant difference in vBMD values in men between the non-fracture and the grade 1 groups. However, this difference was not seen in men aged<50 years old, which implies that those with a vertebral height reduction of<25% were more likely to have deformities caused by degeneration or other disease rather than fractures associated with decreased vBMD. In women aged<50 years old, although mean vBMD of the grade 1 group is significantly lower than the non-fracture group, more than half of women in the grade 1 group had normal bone density. This suggests that in women

too, the grade 1 group might include a significant proportion of individuals with vertebral deformities. Hence, unless there is a decrease in bone density measured by DXA or QCT, or adequate radiographic evidence of a fracture such as distortion of an endplate and/or cortex (11), we prefer to diagnose a vertebral height reduction ratio<25% in those aged<50 years old as a deformity rather than a fracture, especially in men. For individuals aged ≥50 years old, the grade 1 group has lower mean lumbar spine vBMD values compared with the non-fractured group in both men and women. This is consistent with previous studies. Lentle et al. compared DXA derived aBMD in the L1-4, femoral neck, and total hip sites between the VF and non-fractured groups and demonstrated lower aBMD values in the GSQ grade 1 VF group in both men and women aged ≥50 years (22). Johansson et al. found that older Swedish women aged from 75 to 80 years with grade 1 VFs diagnosed by VFA had lower DXA derived aBMD than those without VF in both the lumbar spine and femoral neck (19). Most studies have tended to focus on the relationship between fracture severity and BMD, but less on the relationship between the number of fractured vertebral bodies and BMD. The present study examined this issue and found no correlation between the two variables for grade 1 fractures. In other words, the presence of multiple mild fractured vertebrae does not of itself imply lower BMD.

There are several strengths in the present study. It is a nation-wide multi-center study with participants from 6 geographic regions across China. QCT derived volumetric BMD is superior to DXA derived areal BMD in avoiding the overestimation of values caused by spinal degenerative changes (35, 36). There are also limitations to this study. Due to limitations in the scanned area or overlapping of ribs, not all T4-L6 vertebrae were evaluated, and therefore we might have underestimated the prevalence of VF. Because of limited access, the study did not include hip BMD. Finally, this is a cross-sectional study that was unable to predict future incident fractures.

In conclusion, we examined the prevalence of vertebral fractures in China by age and gender. In women, the prevalence of VF increased rapidly after age 50 along with a rapid decrease in vBMD, while in men it grew more slowly along with a relatively gradual decrease in vBMD. Volumetric BMD of participants with grade 1 vertebral fracture and non-fractured individuals were compared for different age ranges. In general, with the exception of men <50 years old, participants with grade 1 vertebral fracture had lower vBMD than non-fractured individuals. The majority of women younger than 50 years old with a grade 1 vertebral fracture had normal bone mass. We recommend diagnosing a vertebral height reduction ratio of < 25% as a deformity rather than a fracture in people under the age of 50. The presence of multiple mild fractured vertebrae does not of itself imply lower BMD.

Data availability statement

The original contributions presented in the study are included in the article/supplementary material. Further inquiries can be directed to the corresponding author.

Ethics statement

The studies involving human participants were reviewed and approved by the institutional review board of the Beijing Jishuitan Hospital (approval numbers No. 201210-01; No. 201512-02). The patients/participants provided their written informed consent to participate in this study.

Author contributions

YL and XC: Designed the study and conceived the report. YL: Wrote the draft of the manuscript. GB: Edited the manuscript. AY and LW: Funding acquisition and revised the draft critically. KL and JG: Data acquisition and processing. XC: Evaluated vertebral fracture. YL and PH: Statistical analysis, and created the figures and tables. CASH study team: CT scanning. YZ and Y-YD: conducted the cross-calibration CT scans. All authors contributed to the article and approved the submitted version.

Funding

Conflict of interest

The authors declare that the research was conducted in the absence of any commercial or financial relationships that could be construed as a potential conflict of interest.

Publisher's note

All claims expressed in this article are solely those of the authors and do not necessarily represent those of their affiliated organizations, or those of the publisher, the editors and the reviewers. Any product that may be evaluated in this article, or claim that may be made by its manufacturer, is not guaranteed or endorsed by the publisher.

References

1. Cummings SR, Melton LJ. Epidemiology and outcomes of osteoporotic fractures. *Lancet* (2002) 359(9319):1761–7. doi: 10.1016/S0140-6736(02)08657-9

2. Lentle B, Koromani F, Brown JP, Oei L, Ward L, Goltzman D, et al. The radiology of osteoporotic vertebral fractures revisited. *J Bone Miner Res* (2019) 34 (3):409–18. doi: 10.1002/jbmr.3669

3. Cooper C, Atkinson EJ, Jacobsen SJ, O'Fallon WM, Melton LJ3rd. Population-based study of survival after osteoporotic fractures. *Am J Epidemiol* (1993) 137(9):1001–5. doi: 10.1093/oxfordjournals.aje.a116756

4. Ross PD, Davis JW, Epstein RS, Wasnich RD. Pre-existing fractures and bone mass predict vertebral fracture incidence in women. *Ann Intern Med* (1991) 114 (11):919–23. doi: 10.7326/0003-4819-114-11-919

5. Broy SB. The vertebral fracture cascade: Etiology and clinical implications. *J Clin Densitom* (2016) 19(1):29–34. doi: 10.1016/j.jocd.2015.08.007

6. Cui L, Chen L, Xia W, Jiang Y, Cui L, Huang W, et al. Vertebral fracture in postmenopausal Chinese women: A population-based study. *Osteoporos Int* (2017) 28(9):2583–90. doi: 10.1007/s00198-017-4085-1

7. Li K, Zhang Y, Wang L, Duanmu YY, Tian W, Chen H, et al. The protocol for the prospective urban rural epidemiology China action on spine and hip status study. *Quant Imaging Med Surg* (2018) 8(7):667–72. doi: 10.21037/qims.2018.08.07

8. Genant HK, Wu CY, van Kuijk C, Nevitt MC. Vertebral fracture assessment using a semiquantitative technique. *J Bone Miner Res* (1993) 8(9):1137–48. doi: 10.1002/jbmr.5650080915

9. Genant HK, Jergas M. Assessment of prevalent and incident vertebral fractures in osteoporosis research. *Osteoporos Int* (2003) 14 Suppl 3:S43–55. doi: 10.1007/s00198-002-1348-1

10. Schwartz EN, Steinberg D. Detection of vertebral fractures. *Curr Osteoporos Rep* (2005) 3(4):126–35. doi: 10.1007/s11914-996-0015-4

11. Wang YXJ, Diacinti D, Yu W, Cheng XG, Nogueira-Barbosa MH, Che-Nordin N, et al. Semi-quantitative grading and extended semi-quantitative grading for osteoporotic vertebral deformity: A radiographic image database for education and calibration. *Ann Transl Med* (2020) 8(6):398. doi: 10.21037/atm.2020.02.23

12. Fechtenbaum J, Briot K, Paternotte S, Audran M, Breuil V, Cortet B, et al. Difficulties in the diagnosis of vertebral fracture in men: Agreement between doctors. *Joint Bone Spine* (2014) 81(2):169–74. doi: 10.1016/j.jbspin.2013.12.006

13. Lentle B, Cheung AM, Hanley DA, Leslie WD, Lyons D, Papaioannou A, et al. Osteoporosis Canada 2010 guidelines for the assessment of fracture risk. *Can Assoc Radiol J* (2011) 62(4):243–50. doi: 10.1016/j.carj.2011.05.001

14. Schousboe JT, Rosen HR, Vokes TJ, Cauley JA, Cummings SR, Nevitt MC, et al. Prediction models of prevalent radiographic vertebral fractures among older men. *J Clin Densitom* (2014) 17(4):449–57. doi: 10.1016/j.jocd.2013.09.020

15. Delmas PD, Genant HK, Crans GG, Stock JL, Wong M, Siris E, et al. Severity of prevalent vertebral fractures and the risk of subsequent vertebral and nonvertebral fractures: Results from the more trial. *Bone* (2003) 33(4):522–32. doi: 10.1016/s8756-3282(03)00241-2

16. Kanterewicz E, Puigoriol E, Garcia-Barrionuevo J, del Rio L, Casellas M, Peris P, et al. Prevalence of vertebral fractures and minor vertebral deformities evaluated by dxa-assisted vertebral fracture assessment (Vfa) in a population-based study of postmenopausal women: The frodos study. *Osteoporos Int* (2014) 25 (5):1455–64. doi: 10.1007/s00198-014-2628-2

17. Johansson H, Oden A, McCloskey EV, Kanis JA. Mild morphometric vertebral fractures predict vertebral fractures but not non-vertebral fractures. *Osteoporos Int* (2014) 25(1):235–41. doi: 10.1007/s00198-013-2460-0

18. Kanterewicz E, Puigoriol E, Rodriguez Cros JR, Peris P. Prevalent vertebral fractures and minor vertebral deformities analyzed by vertebral fracture assessment (Vfa) increases the risk of incident fractures in postmenopausal women: The frodos study. *Osteoporos Int* (2019) 30(10):2141–9. doi: 10.1007/s00198-019-04962-3

19. Johansson L, Sundh D, Magnusson P, Rukmangatharajan K, Mellstrom D, Nilsson AG, et al. Grade 1 vertebral fractures identified by densitometric lateral spine imaging predict incident major osteoporotic fracture independently of clinical risk factors and bone mineral density in older women. *J Bone Miner Res* (2020) 35(10):1942–51. doi: 10.1002/jbmr.4108

20. Lunt M, O'Neill TW, Felsenberg D, Reeve J, Kanis JA, Cooper C, et al. Characteristics of a prevalent vertebral deformity predict subsequent vertebral fracture: Results from the European prospective osteoporosis study (Epos). *Bone* (2003) 33(4):505–13. doi: 10.1016/s8756-3282(03)00248-5

21. Roux C, Fechtenbaum J, Kolta S, Briot K, Girard M. Mild prevalent and incident vertebral fractures are risk factors for new fractures. *Osteoporos Int* (2007) 18(12):1617–24. doi: 10.1007/s00198-007-0413-1

22. Lentle BC, Berger C, Probyn L, Brown JP, Langsetmo L, Fine B, et al. Comparative analysis of the radiology of osteoporotic vertebral fractures in women and men: Cross-sectional and longitudinal observations from the Canadian multicentre osteoporosis study (Camos). *J Bone Miner Res* (2018) 33(4):569–79. doi: 10.1002/jbmr.3222

23. Liu Y, Wang L, Su Y, Brown K, Yang R, Zhang Y, et al. Ctxa hip: The effect of partial volume correction on volumetric bone mineral density data for cortical and trabecular bone. *Arch Osteoporos* (2020) 15(1):50. doi: 10.1007/s11657-020-00721-8

24. Johannesdottir F, Allaire B, Kopperdahl DL, Keaveny TM, Sigurdsson S, Bredella MA, et al. Bone density and strength from thoracic and lumbar ct scans both predict incident vertebral fractures independently of fracture location. *Osteoporos Int* (2021) 32(2):261–9. doi: 10.1007/s00198-020-05528-4

25. Pickhardt PJ, Graffy PM, Zea R, Lee SJ, Liu J, Sandfort V, et al. Automated abdominal ct imaging biomarkers for opportunistic prediction of future major osteoporotic fractures in asymptomatic adults. *Radiology* (2020) 297(1):64–72. doi: 10.1148/radiol.2020200466

26. Engelke K, Adams JE, Armbrecht G, Augat P, Bogado CE, Bouxsein ML, et al. Clinical use of quantitative computed tomography and peripheral quantitative computed tomography in the management of osteoporosis in adults: The 2007 iscd

official positions. *J Clin Densitom* (2008) 11(1):123–62. doi: 10.1016/j.jocd.2007.12.010

27. Cheng X, Yuan H, Cheng J, Weng X, Xu H, Gao J, et al. Chinese Expert consensus on the diagnosis of osteoporosis by imaging and bone mineral density. *Quant Imaging Med Surg* (2020) 10(10):2066–77. doi: 10.21037/qims-2020-16

28. Samelson EJ, Christiansen BA, Demissie S, Broe KE, Zhou Y, Meng CA, et al. Reliability of vertebral fracture assessment using multidetector ct lateral scout views: The framingham osteoporosis study. *Osteoporos Int* (2011) 22(4):1123–31. doi: 10.1007/s00198-010-1290-6

29. Wu C, van Kuijk C, Li J, Jiang Y, Chan M, Countryman P, et al. Comparison of digitized images with original radiography for semiquantitative assessment of osteoporotic fractures. *Osteoporos Int* (2000) 11(1):25–30. doi: 10.1007/s001980050002

30. Cheng X, Zhao K, Zha X, Du X, Li Y, Chen S, et al. Opportunistic screening using low-dose ct and the prevalence of osteoporosis in China: A nationwide, multicenter study. *J Bone Miner Res* (2021) 36(3):427–35. doi: 10.1002/jbmr.4187

31. Ling X, Cummings SR, Mingwei Q, Xihe Z, Xioashu C, Nevitt M, et al. Vertebral fractures in Beijing, China: The Beijing osteoporosis project. *J Bone Miner Res* (2000) 15(10):2019–25. doi: 10.1359/jbmr.2000.15.10.2019

32. Black DM, Cummings SR, Stone K, Hudes E, Palermo L, Steiger P. A new approach to defining normal vertebral dimensions. *J Bone Miner Res* (1991) 6 (8):883–92. doi: 10.1002/jbmr.5650060814

33. Greendale GA, Wilhalme H, Huang MH, Cauley JA, Karlamangla AS. Prevalent and incident vertebral deformities in midlife women: Results from the study of women's health across the nation (Swan). *PloS One* (2016) 11(9):e0162664. doi: 10.1371/journal.pone.0162664

34. Olmos JM, Hernandez JL, Martinez J, Pariente E, Castillo J, Prieto-Alhambra D, et al. Prevalence of vertebral fracture and densitometric osteoporosis in Spanish adult men: The camargo cohort study. *J Bone Miner Metab* (2018) 36(1):103–10. doi: 10.1007/s00774-017-0812-0

35. Xu XM, Li N, Li K, Li XY, Zhang P, Xuan YJ, et al. Discordance in diagnosis of osteoporosis by quantitative computed tomography and dual-energy X-ray absorptiometry in Chinese elderly men. *J Orthop Translat* (2019) 18:59–64. doi: 10.1016/j.jot.2018.11.003

36. Li N, Li XM, Xu L, Sun WJ, Cheng XG, Tian W. Comparison of qct and dxa: Osteoporosis detection rates in postmenopausal women. *Int J Endocrinol* (2013) 2013:895474. doi: 10.1155/2013/895474

Check for updates

Comparison of four tools to identify painful new osteoporotic vertebral fractures in the postmenopausal population in Beijing

SiJia Guo[†], Ning An[†], JiSheng Lin[†], ZiHan Fan, Hai Meng, Yong Yang and Qi Fei*

Department of Orthopedics, Beijing Friendship Hospital, Capital Medical University, Beijing, China

Objectives: To validate and compare four tools, the Fracture Risk Assessment Tool (FRAX) without bone mineral density (BMD), Beijing Friendship Hospital Osteoporosis Screening Tool (BFH-OST), Osteoporosis Self-Assessment Tool for Asians (OSTA), and BMD, to identify painful new osteoporotic vertebral fractures (PNOVFs).

Methods: A total of 2874 postmenopausal women treated from June 2013 to June 2022 were enrolled and divided into two groups: patients with PNOVFs who underwent percutaneous vertebroplasty (PNOVFs group, n = 644) and community-enrolled females (control group, n = 2230). Magnetic resonance and X-ray imaging were used to confirm the presence of PNOVFs. Dual-energy X-ray absorptiometry was performed to calculate the BMD T-scores. Osteoporosis was diagnosed according to WHO Health Organization criteria. Data on the clinical and demographic risk factors were self-reported using a questionnaire. The ability to identify PNOVFs using FRAX, BFH-OST, OSTA, and BMD scores was evaluated using receiver operating characteristic (ROC) curves. For this evaluation, we calculated the areas under the ROC curves (AUCs), sensitivity, specificity, and optimal cut-off points.

Results: There were significant differences in FRAX (without BMD), BFH-OST, OSTA, and BMD T-scores (total hip, femoral neck, and lumbar spine) between the PNOVFs and control groups. Compared with BFH-OST, OSTA, and BMD, the FRAX score had the best identifying value for PNOVFs; the AUC of the FRAX score (optimal cutoff =3.6%) was 0.825, while the sensitivity and specificity were 82.92% and 67.09%, respectively.

Conclusion: FRAX may be the preferable tool for identifying PNOVFs in postmenopausal women, while BFH-OST and OSTA can be applied as more simple screening tools for PNOVFs.

KEYWORDS

osteoporosis, postmenopausal, vertebral fracture, FRAX, BMD, BFH-OST, OSTA

Introduction

Primary osteoporosis is a systemic metabolic disease characterized by bone mass loss, impaired bone microarchitecture, and increased bone fragility (1). Postmenopausal osteoporosis (type I) is one of the most common primary forms of bone loss encountered in clinical practice[2]. The clinical outcome of osteoporosis is fragility fractures, of which vertebral fractures are the most common. The prevalence of vertebral fractures in women over 50 years old in China is 15%, while it can reach as high as 36.6% among women aged 80 years or older (2). An initial vertebral fracture is generally accepted as a major risk factor for new fractures (3). A previous study reported that the presence of one or more vertebral fractures increased the risk of sustaining a vertebral fracture by 5-fold in the first year, and that 20% of affected women will experience another fracture within the first year of a vertebral fracture (4). The annual cost of vertebral fractures among women in the United States was $663 million in 2005, and this cost is expected to increase by more than 53% by 2025 (5).

Early identification of painful new osteoporotic vertebral fractures (PNOVFs) is still challenging worldwide, especially in communities and primary medical institutions. The clinical onset of PNOVFs is often hidden, as affected patients generally only have a history of mild low-energy injuries, or even no trauma history at all. Furthermore, the degree of pain varies greatly, with some patients developing chronic pain, while physical examination often does not reveal any clear localization signs, and it should be noted that some patients complain that the pain site is not consistent with the actual fracture level (6). These factors may all contribute to mis- and missed diagnosis, especially in communities and primary medical institutions with limited professional experience and equipment. As such, there is an urgent need to identify a reliable, simple, and cost-effective tool for screening PNOVFs in postmenopausal women.

Bone mineral density (BMD) is the gold standard for diagnosing osteoporosis using dual-energy X-ray absorptiometry (DXA). Osteoporosis can be diagnosed when an individual's T value for BMD is 2.5 standard deviations or more below the average of young adult women (7). Previous studies have indicated that bone mineral density (BMD) is the best predictor of fractures in perimenopausal women (8). However, BMD only accounts for 60-70% of the variation in bone strength, and therefore does not provide a complete picture of bone strength (9). It has been reported that approximately 36.21% to 55.91% of patients with fragility fractures in the postmenopausal population have T-scores above the osteoporotic threshold (10). However, the high cost of DXA machines prevents their widespread use in primary hospitals, particularly in developing countries. Moreover, DXA examinations involve exposure to ionizing radiation, making this procedure highly complex, expensive, and inconvenient.

As a result, a convenient and economical tool for PNOVFs screening is urgently needed.

The FRAX (https://www.sheffield.ac.uk/FRAX) is a computer-based tool used to assess the probability of a 10-year hip fracture or major osteoporotic fracture in male and female patients. Several studies have validated the FRAX for identifying PNOVFs in China, but the optimal threshold varies greatly among previous studies (11, 12). Therefore, the use of FRAX in China should be reconsidered. In addition, it has been reported that the use of FRAX without BMD had approximately the same performance as BMD without FRAX (13). As such, it is necessary to validate the FRAX and to determine the optimal threshold for identifying PNOVFs.

The OSTA is a screening tool developed and validated in eight Asian countries to screen for postmenopausal osteoporosis in Asian populations. The OSTA index can be used to identify women at low (index > -1), intermediate (index –1 to -4), and high (index < –4) risk of osteoporosis (14). Our previous study showed that OSTA was a valuable tool for identifying PVNOFs in a population of 1201 postmenopausal women (15). However, it is still unknown whether this is the best tool to identify PNOVFs.

The Beijing Friendship Hospital Osteoporosis Screening Tool (BFH-OST tool) was developed based on community-dwelling postmenopausal Han Chinese women in Beijing, and includes four clinical risk factors: history of fragility fracture, age, height, and weight (16). Previous studies have confirmed that this tool can accurately identify postmenopausal osteoporosis, with a sensitivity of 73.6% and a specificity of 72.7% for identifying osteoporosis at a cutoff of 9.1 according to the WHO criteria, with an area under the receiver operating characteristic curve (AUC) of 0.797 (16). However, it is unclear whether this tool has any value in detecting and identifying PNOVFs.

This study aimed to compare and validate OSTA, BMD, FRAX, and BFH-OST, to identify PNOVFs and determine the optimal threshold.

Patients and methods

This retrospective study was approved by the Ethics Committee of Beijing Friendship Hospital, Capital Medical University. All participants provided written informed consent to participate in the study. A flowchart of the study is shown in Figure 1.

Study design

The study population included postmenopausal Chinese women consecutively recruited from the Osteoporosis Clinic
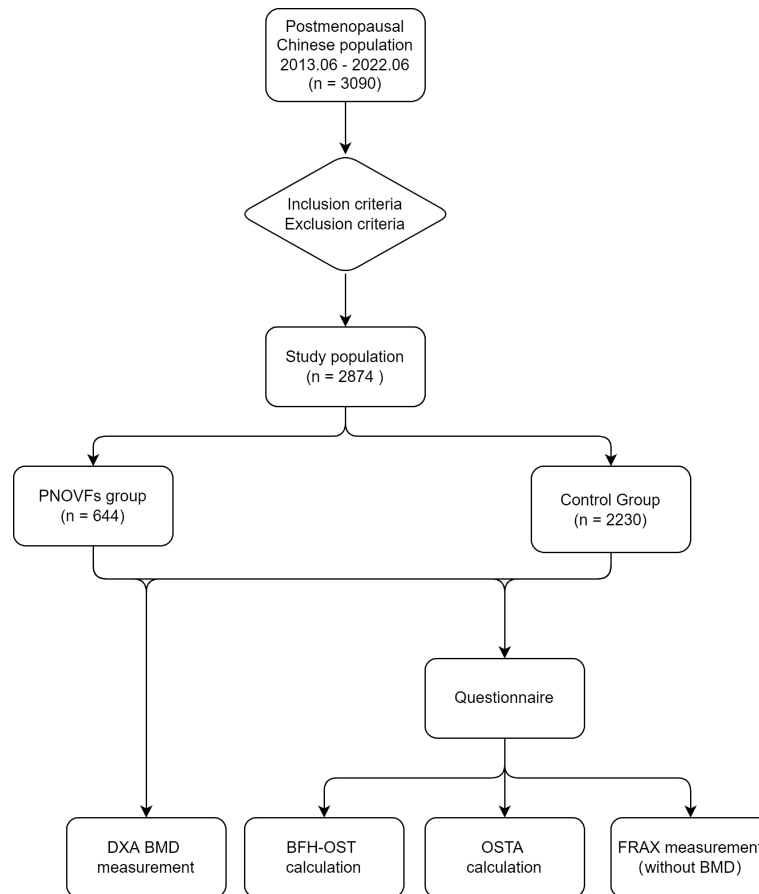
FIGURE 1
Flowchart of the study.

of Beijing Friendship Hospital from June 2013 to June 2022. The cohort comprised clinically symptomatic patients with PNOVFs verified by X-ray and MRI within the past 6 months who presented for further examination and treatment (PNOVFs group), as well as community-enrolled women who presented to our hospital for routine health examinations (control group). The inclusion and exclusion criteria are listed in Table 1.

BMD measurements and identification of PNOVFs

All participants underwent DXA BMD measurement (Hologic Inc., Bedford, MA, USA) of the hip and spine, and were interviewed by a trained interviewer using a standardized questionnaire investigating participants' demographic and clinical risk factors. To standardize measurements, all DXA scans were conducted by the same technician who was well-trained and qualified. The DXA machine was calibrated by the same technician every day by using a lumbar module. There

TABLE 1 Inclusion and exclusion criteria for this study.

Inclusion criteria	Exclusion criteria
Han Chinese nationality	A history or evidence of metabolic bone disease
Postmenopausal women	History of organ transplant;
Residing in Beijing ≥ 20 years	Prior use of anti-resorptive or anabolic agents
	Cancer with metastasis to the bone
	Significant renal impairment
	A condition of prolonged immobility

were less than 50 cases of BMD measurements per day to ensure the accuracy of the results. The following data were collected: age, weight, height, previous fracture, parent-fractured hip, current smoking, glucocorticoid use, history of rheumatoid arthritis, and alcohol consumption per day. The database was developed by two researchers (Sijia Guo and Ning An) in order

to guarantee the accuracy of the data, and on the second day, another senior researcher (Yong Yang) verified it. The corresponding author completed the final data entry in order to confirm that the analysis and confirmation of the data were done objectively. If a mistake was made, it would be corrected by going back to the patient's answers on the questionnaire. According to the WHO criteria, osteoporosis is defined as a T-score (lumbar spine, femoral neck, or total hip) −2.5 standard deviations or lower than that of the average young adult.

Following identification of PNOVFs, data for the following four previously reported clinical criteria were collected: (1) postmenopausal status without trauma history or with a low-energy trauma history (low-energy trauma fracture was defined as a fracture resulting from a fall from a standing position or lower); (2) pain occurring within 6 months prior to BMD measurement; (3) acute or subacute vertebral fractures with correlating clinical signs and signs demonstrated by X-ray (i.e., height loss in the anterior, middle, or posterior dimension of a vertebral body that exceeds 20% of the vertebral body area in a lateral-view image of the thoracic/lumbar spine; or the presence of endplate deformities, a lack of parallelism of the endplates, and a generally altered appearance relative to neighboring vertebrae) and spine MRI imaging (new bone marrow edema apparent in sagittal T1-weighted and fat-suppressed T2-weighted images); and (4) no history or indicative evidence of metabolic bone disease or cancer (15).

FRAX score

The FRAX is a computer-based algorithm used to calculate the 10-year probability of major osteoporotic and hip fractures. FRAX scores were calculated based on clinical risk factors, for which optional BMD could enhance their prediction efficacy. The FRAX models are available in China. To identify PNOVFs in this study, FRAX (without BMD) scores for the 10-year probability of major osteoporotic fractures were obtained.

BFH-OST

The BFH-OST was calculated from the following formula (16):
BFH-OST = [body weight (kg) – age (years)] ×0.5+0.1× height (cm) -[previous fracture (0/1)]
For example, a 70-year-old woman with a body weight of 50 kg, height of 160 cm, and a previous fracture would have a BFH-OST index of 5.

OSTA

The OSTA was calculated based on age and body weight using the following formula (14):

OSTA = [body weight (kg) - age(years)] × 0.2
The decimal points of the calculation results were disregarded. For example, a 71-year-old woman with a body weight of 50 kg would have an OSTA score of -4.

Statistical analysis

Categorical variables are grouped and presented as numerical values, and continuous data are presented as mean ± standard deviation. The Kolmogorov-Smirnov test was used to test the data distribution. Normally distributed data were assessed using the t-test, whereas the Mann-Whitney U test was applied for non-normally distributed data. Categorical data were analyzed using the chi-squared test. The diagnostic value was assessed using the receiver operating characteristic curve (ROC), and the area under the curve (AUC) and 95% confidence interval (CI) were subsequently calculated. The predictive efficacies of the above tools were estimated according to the AUC values as follows: AUC=1, perfectly predictive; 0.9≤AUC <1, highly predictive; 0.7≤AUC<0.9, moderately predictive; 0.5≤AUC<0.7, less predictive; and AUC<0.5, non-predictive (17). Statistical significance was set at P < 0.05. All data analyses were performed using SPSS v25.0 software (IBM Corp., Armonk, NY, USA), and graphics were drawn using OriginPro 2022 (OriginLab, Northampton, MA, USA).

Results

A sample of 3090 women were initially included in this study. In total, 216 subjects were excluded from the study for meeting the exclusion criteria, so 2874 subjects were analyzed. This cohort included 644 women with PNOVFs within 6 months before the BMD measurement (PNOVFs group), as well as 2230 community-enrolled women (control group) without specific osteoporosis-associated symptoms. The demographic characteristics of the study participants are shown in Table 2.

Age, weight, height, and BMI were all lower in the PNOVFs group than in the control group (Table 2, P<0.001). The PNOVFs group had a greater proportion of previous fractures, current smokers, rheumatoid arthritis, and history of glucocorticoid use. Moreover, the PNOVFs group had lower average BMD values and T-scores at the total hip, femoral neck, and lumbar spine than in the control group (Table 3, P<0.001). A higher FRAX value (without BMD) was observed in the PNOVFs group (Table 3, P<0.001).

In the PNOVFs group, 58.6%, 53.2%, and 36.3% of women were found to have osteoporosis at the lumbar spine, femoral neck, and total hip, respectively (defined as BMD T-scores ≤ −2.5; Figure 2). The AUCs of BMD for identifying PNOVFs at the level of the total hip, femoral neck, and lumbar spine were 0.780, 0.753, and 0.799, respectively, with optimal cutoffs of −1.6, −2.4, and

TABLE 2   Summary of descriptive characteristics of PNOVFs Group and Control Group.

Characteristics	PNOVFs group	Control group	p (t/χ2)
Subjects, n	644	2230	
Weight, kg	58.44 ± 10.42	61.58 ± 9.24	<0.001 (4.141)
Age, year	72.76 ± 8.46	61.11 ± 8.57	<0.001 (-30.488)
Height, cm	157.23 ± 5.36	158.94 ± 5.13	<0.001 (4.359)
BMI, kg/m^2	23.61 ± 3.93	24.37 ± 3.45	<0.001 (2.664)
Previous fracture	150 (23.3%)	318 (14.3%)	<0.001 (29.901)
BMD, g/cm^2			
Femoral neck	0.570 ± 0.125	0.700 ± 0.128	<0.001 (9.052)
Total hip	0.678 ± 0.139	0.802 ± 0.136	<0.001 (9.998)
Lumbar spine	0.731 ± 0.146	0.869 ± 0.159	<0.001 (8.118)
Family history, n	70 (10.9%)	270 (12.1%)	0.391 (0.734)
Current smoker, n	39 (6.1%)	55 (2.5%)	<0.001 (20.351)
Alcohol > 30 g/d, n	11 (1.7%)	32 (1.4%)	0.615 (0.253)
Rheumatoid arthritis, n	16 (2.5%)	107 (4.8%)	0.011 (6.350)
Glucocorticoids taking, n	15 (2.3%)	90 (4.0%)	0.042 (4.135)

Data are presented as n (%) or mean ± standard deviation.
BMD, bone mineral density.

TABLE 3   BMD T-score, BFH-OST, and FRAX scores of the PNOVFs group and control group.

Parameter	PNOVFs group	Control group	z/t	P-value
Subjects, n	644	2230		
BMD T-score				
Total hip	-1.996 ± 1.227	-0.678 ± 1.213	24.209	<0.001
Femoral neck	-2.463 ± 1.191	-1.396 ±1.049	22.038	<0.001
L1-L4	-2.669 ± 1.325	-1.085 ± 1.394	25.678	<0.001
BFH-OST	8.331 ± 7.529	15.983 ± 6.534	25.268	<0.001
OSTA	-2.600 ± 2.720	0.060 ± 2.211	22.8	<0.001
FRAX (%)	6.606 ± 3.278	3.460 ± 2.189	-28.416	<0.001

BMD, bone mineral density; BFH-OST, Beijing Friendship Hospital Osteoporosis Screening Tool; OSTA, Osteoporosis Self-Assessment Tool for Asians; FRAX, Fracture Risk Assessment Tool.

−2.2 (P<0.001 for all). The AUC of FRAX (without BMD) was 0.825, with an optimal cutoff of 3.6%. The AUC of the OSTA was 0.774, with an optimal cutoff of -1. The area under the curve of the BFH-OST was 0.775, with an optimal cutoff of 13.3 (Table 4 and Figure 3). The comparison of the four tools is shown in Figure 4.

Discussion

This study retrospectively assessed and compared the performance of BMD, OSTA, FRAX (without BMD), and BFH-OST in identifying PNOVFs in postmenopausal Chinese populations. The mean height, weight, and BMI were lower in the PNOVFs group than in the control group, whereas the mean age, previous fracture, history of rheumatoid arthritis, and history of glucocorticoid use were higher in the PNOVFs group than in the control group. This finding is consistent with the results of previous studies (6, 15, 16). Conversely, no significant difference was found

in parent hip fracture and alcohol consumption between the PNOVF and control groups. The lower height in the PNOVFs group may be attributed to the height loss of the vertebra or kyphotic deformity caused by vertebral compression fracture.

BMD measured using dual-energy DXA is the gold standard for diagnosing osteoporosis. Furthermore, it has been reported that BMD is an important determinant of bone strength, and its value could represent approximately 70% of bone strength. Osteoporosis can be diagnosed when the BMD T-scores are ≤-2.5. In this study, the prevalence of osteoporosis ranged from 36.3% to 72.3%, according to different criteria in PNOVFs population. The prevalence was 72.3% at the any site, 58.6% at the lumbar spine site, 53.2% at the femoral neck site and 36.3% at the total hip sites. The T-scores of the femoral neck, total hip, and lumbar spine in the PNOVFs group were significantly lower than those in the control group (all P < 0.001). When BMD was applied to identify PNOVFs, the AUC of femoral neck BMD, total hip BMD, and lumbar spine BMD were 0.753, 0.780, and
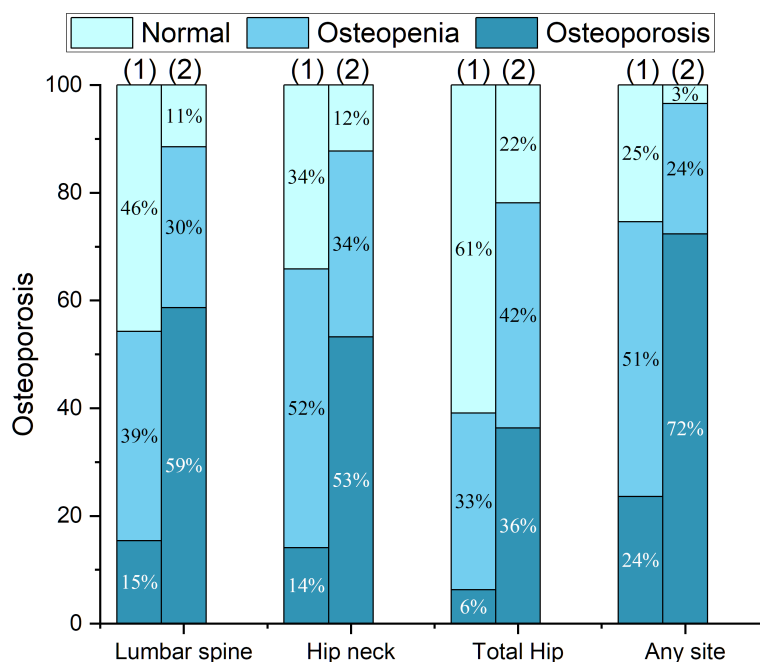
FIGURE 2
Proportions of BMD T-scores at different sites in the fracture and control groups, including: (1) the control group; (2) the PNOVFs group.

TABLE 4 AUC and sensitivity and specificity values of the FRAX, BMD T-score, OSTA, and BFH-OST for identifying PNOVFs.

Parameter	AUC (95% CI)	Z	P-value	Cutoff	Sensitivity, %	Specificity, %	+LR, %	−LR, %
FRAX	0.825 (0.810 - 0.839)	36.054	<0.001	>3.6	82.92	67.09	2.52	0.25
BMD T-score								
Total hip	0.780 (0.765 - 0.795)	26.599	<0.001	≤-1.6	66.77	76.64	2.86	0.43
Femoral neck	0.753 (0.737 - 0.769)	21.767	<0.001	≤-2.4	57.14	82.87	3.34	0.52
Lumbar spine	0.799 (0.784 - 0.814)	29.377	<0.001	≤-2.2	66.77	78.52	3.11	0.42
OSTA	0.774 (0.758 - 0.789)	26.253	<0.001	≤-1	73.91	67.62	2.28	0.39
BFH-OST	0.775 (0.760 - 0.791)	26.196	<0.001	≤13.3	73.91	67.67	2.29	0.39

BMD, bone mineral density; BFH-OST, Beijing Friendship Hospital Osteoporosis Screening Tool; OSTA, Osteoporosis Self-Assessment Tool for Asians;FRAX, Fracture Risk Assessment Tool; AUC, area under the receiver operating characteristic curve; PNOVFs, painful new osteoporotic vertebral fractures; CI, confidence interval; +LR: positive likelihood ratio; -LR: negative likelihood ratio.

0.799, respectively with corresponding optimal cutoff values of −2.4, −1.6, and −2.2, sensitivities of 57.14%, 66.77%, and 66.77%, and specificities of 82.87%, 76.64%, and 78.52%. The specificity of BMD measurement in identifying PNOVFs was high, but its sensitivity was low; thus, it cannot be used as a screening tool for PNOVFs. Furthermore, BMD measurement requires dual-energy X-ray equipment, which is not feasible for community and primary medical institutions.

In this study, FRAX showed the best identification performance. The AUC of FRAX in screening PNOVFs was 0.825, with an optimal cutoff of 3.6%, a sensitivity of 82.92%, and

a specificity of 67.09%. The efficacy and sensitivity of FRAX were preferable at a cut-off value of 3.6%. However, the National Osteoporosis Foundation (NOF) recommends that pharmacologic treatments should be initiated when an individual's 10-year hip fracture probability is ≥3%, or 10-year major osteoporosis-related fracture probability ≥20% (10). As such, the optimal threshold in this study was much lower than the NOF threshold. Liu et al. previously found that the sensitivity and specificity of the FRAX with a threshold of 4.95% were 0.76 and 0.69, respectively, which is similar to the results of our study (11). Crandall et al. found that the performance of FRAX is unsatisfactory based on dichotomous cut-
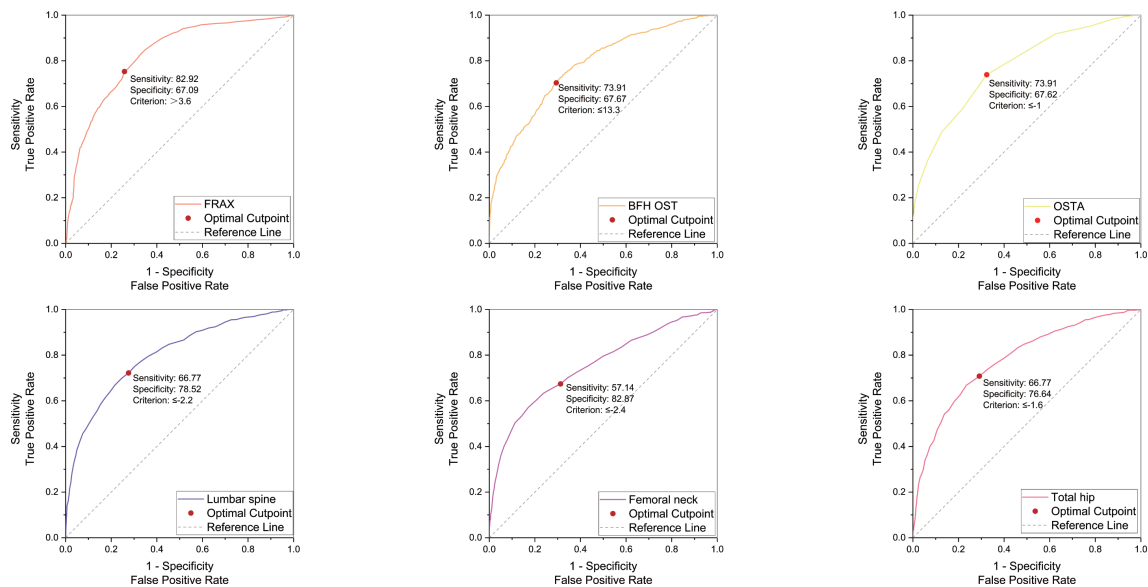
FIGURE 3
ROC curve of the FRAX without BMD, BFH-OST, OSTA, and BMD T-score (femoral neck, total hip, and lumbar spine) for identifying PNOVFs with optimal cutoff value.
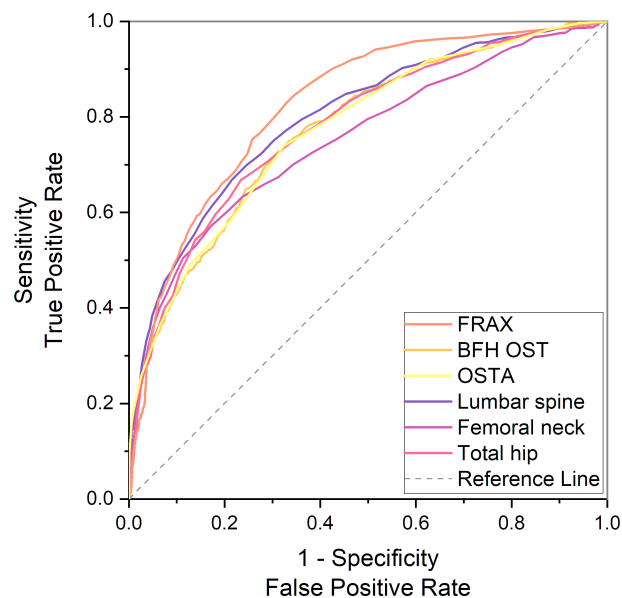
FIGURE 4
Comparison of different AUCs, including FRAX without BMD, BFH-OST, OSTA, and BMD T-score for identifying PNOVFs.

offs, and threshold-based approaches should be reassessed, particularly in younger women (12). Thus, threshold adjustments are required before the application of the FRAX tool in Chinese local practice. In addition, the calculation of FRAX scores requires relevant software and a certain amount of clinical data; thus, it is not convenient for community and primary medical institutions to screen for PNOVFs.

The OSTA was developed by Koh to identify osteoporosis in Asian women based on age and body weight (14). The distribution of OSTA scores between women with PNOVFs

and the control group was significantly different. The discriminating ability of OSTA for identifying PNOVFs was found to be moderately predictive (AUC=0.774) at the optimal cutoff of -1, with an acceptable sensitivity of 73.91% and a specificity of 67.62%. This finding is consistent with the results of a previous study. Although the identifying value of OSTA is not as good as that of FRAX, its calculation includes only two clinical risk factors and this tool is more convenient for application in communities and primary medical institutions.

BFH-OST is an osteoporosis screening tool developed by the Beijing Friendship Hospital. The calculation of the BFH-OST includes the following four clinical risk factors: body height, weight, age, and previous fracture. The efficacy, sensitivity, and specificity of the BFH-OST for identifying osteoporosis have all been validated in previous studies. However, the ability of BFH-OST to screen for PNOVFs remains unclear. In this study, the AUC of BFH-OST in screening for PNOVFs was 0.775, with an optimal cutoff of 13.3, a sensitivity of 73.91, and a specificity of 67.67. The sensitivity of the BFH-OST is higher than that of the BMD of the total hip, femoral neck, and lumbar spine. BFH-OST could not only identify osteoporosis, but also PNOVFs in postmenopausal women. Although the sensitivity of BFH-OST is lower than that of FRAX in identifying PNOVFs, it has the advantage of simple calculations, and is suitable for communities and primary medical institutions to screen PNOVFs.

This study has several advantages. First, this study provides the first comparison of the four tools for identifying PNOVFs in postmenopausal women. Second, strict inclusion and exclusion criteria were introduced to rule out possible selection bias. In addition, we chose a community-enrolled population as the control group, which may be helpful for community screening. Furthermore, the selection of the clinical population was Han Chinese; thus, the calculated thresholds may not be applicable in other populations.

This study has some limitations. First, it had a retrospective design, and therefore future prospective studies are warranted to validate the results. Moreover, this was a single-center study and only included postmenopausal women in Beijing, and thus it cannot represent the overall population characteristics of China. Future multicenter, multi-regional, and multi-ethnic sample studies are therefore essential.

Conclusion

Overall, the results of this study indicate that BMD is not sufficiently effective to identify PNOVFs in clinical practice.

FRAX may be a preferable tool for identifying PNOVFs in postmenopausal women. Furthermore, BFH-OST and OSTA may be simple screening tools for PNOVFs.

Data availability statement

The raw data supporting the conclusions of this article will be made available by the authors, without undue reservation.

Ethics statement

The studies involving human participants were reviewed and approved by Ethics Committee of Beijing Friendship Hospital, Capital Medical University. The patients/participants provided their written informed consent to participate in this study.

Author contributions

Each author made substantial contributions to this work. SJG, NA and QF contributed to the conception and design of the work. SJG and NA contributed to the acquisition of study data. SJG, NA, JSL contributed to the analysis and interpretation of data. ZHF, YY, and HM revised this article. All authors have drafted the work or substantively revised it. All authors contributed to the article and approved the submitted version.

Conflict of interest

The authors declare that the research was conducted in the absence of any commercial or financial relationships that could be construed as a potential conflict of interest.

Publisher's note

All claims expressed in this article are solely those of the authors and do not necessarily represent those of their affiliated organizations, or those of the publisher, the editors and the reviewers. Any product that may be evaluated in this article, or claim that may be made by its manufacturer, is not guaranteed or endorsed by the publisher.

References

1. Lane JM, Russell L, Khan SN. Osteoporosis. *Clin Orthop Relat Res(372) 139-50* (2000) (372):139–50. doi: 10.1097/00003086-200003000-00016

2. Ling X, Cummings SR, Mingwei Q, Xihe Z, Xioashu C, Nevitt M, et al. Vertebral fractures in Beijing, China: the Beijing osteoporosis project. *J Bone Miner Res* (2000) 15(10):2019–25. doi: 10.1359/jbmr.2000.15.10.2019

3. Kanis JA, Johansson H, Oden A, Harvey NC, Gudnason V, Sanders KM, et al. Characteristics of recurrent fractures. *Osteoporos Int* (2018) 29(8):1747–57. doi: 10.1007/s00198-018-4502-0

4. Lindsay R, Silverman SL, Cooper C, Hanley DA, Barton I, Broy SB, et al. Risk of new vertebral fracture in the year following a fracture. *JAMA* (2001) 285(3):320–3. doi: 10.1001/jama.285.3.320

5. Burge R, Dawson-Hughes B, Solomon DH, Wong JB, King A, Tosteson A. Incidence and economic burden of osteoporosis-related fractures in the united states, 2005-2025. *J Bone Miner Res* (2007) 22(3):465–75. doi: 10.1359/jbmr.061113

6. An N, Lin JS, Fei Q. Beijing Friendship hospital osteoporosis self-assessment tool for elderly Male (BFH-OSTM) vs fracture risk assessment tool (FRAX) for identifying painful new osteoporotic vertebral fractures in older Chinese men: a cross-sectional study. *BMC Musculoskelet Disord* (2021) 22(1):596. doi: 10.1186/s12891-021-04476-2

7. Kanis JA, McCloskey EV, Johansson H, Oden A, Melton LJ3rd, Khaltaev N. A reference standard for the description of osteoporosis. *Bone* (2008) 42(3):467–75. doi: 10.1016/j.bone.2007.11.001

8. Lips P. Epidemiology and predictors of fractures associated with osteoporosis. *Am J Med* (1997) 103(2A):3S–8S. doi: 10.1016/s0002-9343(97)90021-8

9. Ammann P, Rizzoli R. Bone strength and its determinants. *Osteoporos Int* (2003) 14 Suppl:3, S13–8. doi: 10.1007/s00198-002-1345-4

10. Schuit SC, van der Klift M, Weel AE, de Laet CE, Burger H, Seeman E, et al. Fracture incidence and association with bone mineral density in elderly men and women: the Rotterdam study. *Bone* (2004) 34(1):195–202. doi: 10.1016/j.bone.2003.10.001

11. Liu S, Chen R, Ding N, Wang Q, Huang M, Liu H, et al. Setting the new FRAX reference threshold without bone mineral density in Chinese postmenopausal women. *J Endocrinol Invest* (2021) 44(2):347–52. doi: 10.1007/s40618-020-01315-4

12. Crandall CJ, Schousboe JT, Morin SN, Lix LM, Leslie W. Performance of FRAX and FRAX-based treatment thresholds in women aged 40 years and older: The Manitoba BMD registry. *J Bone Miner Res* (2019) 34(8):1419–27. doi: 10.1002/jbmr.3717

13. Gregson CL, Armstrong DJ, Bowden J, Cooper C, Edwards J, Gittoes NJL, et al. UK Clinical guideline for the prevention and treatment of osteoporosis. *Arch Osteoporos* (2022) 17(1):58. doi: 10.1007/s11657-022-01061-5

14. Koh LK, Sedrine WB, Torralba TP, Kung A, Fujiwara S, Chan SP, et al. A simple tool to identify asian women at increased risk of osteoporosis. *Osteoporos Int* (2001) 12(8):699–705. doi: 10.1007/s001980170070

15. Yang Y, Wang B, Fei Q, Meng Q, Li D, Tang H, et al. Validation of an osteoporosis self-assessment tool to identify primary osteoporosis and new osteoporotic vertebral fractures in postmenopausal Chinese women in Beijing. *BMC Musculoskelet Disord* (2013) 14:271. doi: 10.1186/1471-2474-14-271

16. Ma Z, Yang Y, Lin J, Zhang X, Meng Q, Wang B, et al. BFH-OST, a new predictive screening tool for identifying osteoporosis in postmenopausal han Chinese women. *Clin Interv Aging* (2016) 11:1051–9. doi: 10.2147/CIA.S107675

17. Greiner M, Pfeiffer D, Smith RD. Principles and practical application of the receiver-operating characteristic analysis for diagnostic tests. *Prev Vet Med* (2000) 45(1-2):23–41. doi: 10.1016/s0167-5877(00)00115-x

Application of metabolomics in osteoporosis research

Zhenyu Zhao[1,2], Zhengwei Cai[2], Aopan Chen[1],
Ming Cai[1]* and Kai Yang[2]*

[1]Department of Orthopaedics, Shanghai Tenth People's Hospital, School of Medicine, Tongji University, Shanghai, China, [2]Shanghai Key Laboratory for Prevention and Treatment of Bone and Joint Diseases, Shanghai Institute of Traumatology and Orthopaedics, Ruijin Hospital, Shanghai Jiao Tong University School of Medicine, Shanghai, China

Osteoporosis (OP) is a systemic disease characterized by bone metabolism imbalance and bone microstructure destruction, which causes serious social and economic burden. At present, the diagnosis and treatment of OP mainly rely on imaging combined with drugs. However, the existing pathogenic mechanisms, diagnosis and treatment strategies for OP are not clear and effective enough, and the disease progression that cannot reflect OP further restricts its effective treatment. The application of metabolomics has facilitated the study of OP, further exploring the mechanism and behavior of bone cells, prevention, and treatment of the disease from various metabolic perspectives, finally realizing the possibility of a holistic approach. In this review, we focus on the application of metabolomics in OP research, especially the newer systematic application of metabolomics and treatment with herbal medicine and their extracts. In addition, the prospects of clinical transformation in related fields are also discussed. The aim of this study is to highlight the use of metabolomics in OP research, especially in exploring the pathogenesis of OP and the therapeutic mechanisms of natural herbal medicine, for the benefit of interdisciplinary researchers including clinicians, biologists, and materials engineers.

KEYWORDS

metabolomics, osteoporosis, pathogenic mechanism, herbal medicine, treatment

1. Introduction

OP is a systemic metabolic bone disease characterized by damage to the microstructure of bone tissue and reduced bone mass, resulting in increased bone fragility and susceptibility to fractures. The main clinical manifestations of OP are height loss and hunchback, which increases the risk of fractures in multiple parts such as the hip and spine, and the probability of fracture varies from country to country (1–3). Fractures are predicted to occur in women over age 50 and in one in five men, resulting in limited quality of life and increased morbidity and mortality (4–6). Therefore, with the increasing aging of the

population, complications such as osteoporotic fractures have become a worldwide problem, and the economic burden is increasing exponentially. Therefore, it is particularly important to comprehensively prevent and treat OP from the aspects of pathogenic mechanism, prevention, and treatment.

At present, OP has received great attention and extensive research, and a routine prevention and treatment system has also been formed in clinical practice (7–11). For instance, for the prevention of OP, patients are mainly encouraged to take calcium and vitamin D supplements early in clinical practice, and increase the time of sunlight exposure. However, this method has poor specificity and effectiveness, and lacks pertinence and targeting, making it difficult to effectively slow down the development of bone loss. At the same time, dual energy X-ray is insufficient in revealing the strength and structure of the bone tissue (12, 13). Although various drugs are developed in clinical OP treatment *via* confirmed mechanisms, including hormone replacement, alendronate sodium, parathyroid hormone, and RANKL inhibitors, etc. (14–16), the osteoporotic symptom still hard to completely reverse. Therefore, more therapeutic clues, especially metabolic ones should be concerned in the field of OP prevention.

The collection of small-molecule chemical entities involved in metabolic forms the metabolome. Metabolomics has been redefined from a simple biomarker identification tool to a technique for discovering active drivers of biological processes (17–19). It detects multiple metabolite changes during environmental exposure in a high-throughput form and are closely related to pathological phenotype, especially for multifunctional disease such as OP (20, 21). Therefore, metabolomics emerges an increasingly important role in the systematic study of OP. It is worth noting that, using metabolomics, the functions of traditional Chinese medicines such as Epimedium, Gushudan on OP treatment have been explored. However, there is a lack of systematic induction and research on the metabolic mechanism of various natural herbs in the treatment of OP.

Thus, metabolomics plays an important role in multi-field research of OP, which can deeply explore many problems closely related to OP and provide a new approach for comprehensive research and evaluation of OP. This review systematized various applications of metabolomics in OP research, including mechanism exploration, prevention, prediction, and drug treatment effect. In particular, we focused on the key metabolite changes in OP and after treatment with natural herbal medicines. Lots of metabolites are summarized to correlated with OP treatment, which could be useful for clinical transformation in related fields.

2. Abnormal metabolism in OP

Bone undergoes a constantly active metabolic cycle which is essential to maintain a healthy bone composition through the deposition and absorption of bone matrix and minerals. Imbalance and/or dysregulation of specific biochemical cascades of enzymes involved in protein, fat, and carbohydrates in bone metabolism can lead to various types of osteocyte dysfunction and related metabolic bone disease (22, 23).

Postmenopausal OP is characterized by loss of estrogen that leads to metabolic disorders in bone tissue. Metabolomics assays are factors associated with biological or metabolic status, and these metabolites are highly correlated pathogenic mechanisms of postmenopausal OP (24–31). On the other hand, abnormal differentiation of bone mesenchymal stem cells is related to the occurrence of senile OP. What's more, under the influence of endogenous and exogenous factors such as hormone abuse, menopause, and aging, BMS over-differentiate into fat cells instead of osteoblasts, which often leads to bone metabolism imbalance and even OP. Therefore, a comprehensive understanding of the cellular metabolism and functional changes of bone marrow mesenchymal stem cells with aging is of great significance for the mechanism exploration and clinical treatment of senile OP.

There is increasing evidence that some of the causative factors are modifiable risk factors for OP, such as abnormal drug intake, high fat, and abnormal hormone levels. Studies have shown that these substances can induce secondary OP by regulating changes in metabolite levels (32–38).

Cholesterol participates in many cellular structures, and hydroxysterols, steroid hormones and bile acids play an important role in the formation of cell membranes. Therefore, dysfunction in cholesterol synthesis associates with various diseases and disorders (39, 40). In the OP model, the precise control of cholesterol synthesis and transport is affected, evidenced by the abnormal level of isoprene and squalene. Fatty acid metabolism involves a series of enzymes that degrade fatty acids into bioactive substrates to synthesize straight chain fatty acids, which are stored in adipose tissue as triglycerides (41, 42). In postmenopausal OP, fatty acyl-coa and pyruvate are converted to acetyl-coa by glycolysis, and subsequent metabolic pathways for synthesis of NADH, guanosine triphosphate and amino acids are disrupted (42, 43). Glycogen is easily mobilized as a long-branched polymer of glucose residues and can be broken down into glucose to provide the body with the required energy. Human osteoblasts and bone marrow mesenchymal stem cells in patients with secondary OP can be manifested as abnormal glucose metabolism of creatine, glucokinase and phosphorylase (44).

Therefore, in recent years, it has been found that there are many metabolic pathways in OP, related with abnormal bone remodeling. However, the changes of these metabolites and pathways and their roles in the pathogenesis of OP remain unclear (44, 45).

3. Metabolomics sample preparation and platform technologies

3.1 Metabolomics sample preparation

OP can be classified as primary or secondary according to its cause. For primary OP, biological samples can be collected from postmenopausal women and the elderly in clinical studies, whereas animal models could be accomplished by surgical ovaries resection (46, 47). For secondary OP, most samples are come from animal models, including glucocorticoids injection, fixation, special diet and retinoic acid lavage (45).

In sample preparation for metabolomics of OP, the following samples are usually included: urine, plasma, serum, osteocytes, bone cells, etc (48, 49). Urine samples are usually centrifuged directly without any dilution treatment, or diluted with pure water. Protein-rich serum and plasma are deproteinized with organic solvents such as acetonitrile and methanol. In metabolomics analysis, plasma and serum samples also require the use of silylation reagents such as trifluoroacetamide and trimethylsilane to improve the stability of metabolites. Proteins in blood samples are ultrafiltered through high molecular weight cut-off filters. The pH of the sample has a significant effect on the chemical shifts observed in NMR spectroscopy, so it is important to control the pH of the biofluid sample. To provide a stable environment for urine samples, a phosphate buffer (pH 6.8) is usually used (50–52).

For osteoblast samples, the cell pellet was resuspended in water, and then the membrane was broken with ultrasound and extracted with cold water mixed with methanol (53). After the above extraction process, samples are diluted or centrifuged in mobile phase, evaporated to dryness, and finally resuspended in a compatible solvent for further injection into metabolomics-related systems (17, 54). To obtain accurate metabolites, cells need to stop their metabolic activity almost immediately, and the classical methods include enzymatic denaturation and freezing (55). After extraction of metabolites from bone tissue samples, the tissue is pressed between metal plates in the presence of liquid nitrogen for rapid collection and rapid freezing of bone tissue. Care must be taken before and during sampling to avoid metabolic changes, which may be caused by anesthesia and other procedures (56).

3.2 Metabolomics platform technologies

After preparing the relevant samples, it is important to choose a suitable protocol and platform technologies in exploring the metabolomics. Currently, LC/MS (liquid chromatography/MS), GC/MS (gas chromatography/MS) and 1H NMR (nuclear magnetic resonance) are the main tools for exploring OP metabolomics (1, 57, 58). 1H NMR is suitable for the preliminary

exploration of metabolomics, where most compounds can be detected. This method does not damage the sample, pre-treatment is relatively simple and can be used for quantitative data analysis. At now, 1H NMR still plays an important role in metabolomics because of its high ability in detecting the metabolites and elucidate structures *in vivo*. Its disadvantage is the narrow detection window and lack of sensitivity (59, 60).

MS has great advantages over 1H NMR in terms of sensitivity and specificity, and MS can detect potential new biomarkers associated with OP and has a good ability to detect metabolites at low concentrations and without parental interference, which, combined with modern high-resolution MS, plays an important role in the study of metabolomics. However, it also has the disadvantage of poor homogeneity and integrity (61, 62). Chromatography can be used for the separation of complex osteoporotic compounds and has promising applications. Another advantage of chromatography is the possibility of separating isomers. The addition of chromatography can improve the detection of low concentrations of metabolites, increase the coverage of metabolomics, and improve the quantitative accuracy of MS, but it also has disadvantages, such as insufficient qualitative capabilities. There are many kinds of chromatographic derivatives, such as reversed-phase liquid chromatography (RPLC), high performance liquid chromatography (HPLC), reversed-phase liquid chromatography (RPLC) hydrophilic liquid chromatography (HILC), and ultra-high energy liquid chromatography (UHPLC) (54). Currently, different chromatographic methods are often combined with MS to complement each other. It is often used in combination with GC/MS and LC/MS and has a wide range of applications in exploring OP with high sensitivity and good selectivity. It also allows the quantitative and qualitative analysis of complex metabolic compounds (57, 63, 64).

4. Metabolomics in OP pathogenesis research

In recent years, using metabolomics, the pathogenesis of OP has been comprehensively studied. OP can lead to profound metabolic changes in bone marrow and bone, involving many different metabolites and metabolic pathways (65, 66), as shown in Figure 1. The related mechanisms mainly involve amino acid metabolism, lipid metabolism, glucose metabolism, energy metabolism, etc. Lipid metabolism plays an important role in the pathogenesis of senile OP. In addition, lipid metabolism in idiopathic OP is also disturbed. Secondary OP has a clear etiology, and its metabolization-related pathogenesis varies from disease to disease, usually involving lipid metabolism, amino acid metabolism, mitochondrial energy metabolism, etc. (24–38, 67, 68), as shown in Table 1.

4.1 Different types of metabolism

4.1.1 Amino acid metabolism

The metabolism of amino acids in the body includes two aspects. On the one hand, it is mainly used to synthesize proteins, polypeptides, and other nitrogen-containing substances unique to the body itself. In addition, amino acids can be decomposed into amines, α-keto acids, and carbon dioxide through a series of combined deamination, deamination, decarboxylation, and transamination effects. These carbon dioxide, alpha-keto acids and amines can be converted into lipids, non-essential amino acids, and sugars, and can also be oxidized to release energy using the tricarboxylic acid cycle, while producing water and carbon dioxide. Therefore, amino acid metabolism plays an important role in the pathogenesis of OP. Some studies have consistently demonstrated that some substances in amino acid metabolism might related with the pathogenesis of OP. Scientist studied in the metabolism of middle-aged Japanese women showed that lysine was correlated with the menopausal status of women, and increased gradually with the change of premenopausal, perimenopausal and postmenopausal (31). In addition, the effects of glucocorticoid-induced short-and long-term OP on lipids and plasma metabolites was investigated in ovariectomized sheep. Lysine was also found to distinguish between normal and low bone mineral density (BMD) groups (38). What's more, a GC-MS analysis in metabolic profiles of postmenopausal OP progression in 364 Chinese women reflected the epochal changes of lysine in the pathogenesis of OP (72).

Novel metabolite changed in middle-aged Japanese women were studied. The study found that carnitine was associated with women's menopausal status and gradually increased with the change of menopause (31). The metabolites and metabolic pathways associated with changes in BMD in postmenopausal and perimenopausal women with OP was systematically investigated. Carnitine significantly affects changes in BMD (25). In addition, patient serum samples are efficiently analyzed by metabolomics using untargeted MS. The study found that compared with the control group, the carnitine content of the OP group was significantly imbalanced (74). These studies would help to establish that the pathogenic mechanism of healthy bones and OP was closely related to metabolite carnitine.

Metabolomics techniques were used to discover differences in metabolites of bone metabolic disorders between healthy volunteers and osteoporotic patients. Abnormal metabolism of valine might serve as a key mechanism of OP (31, 38, 75). The

FIGURE 1
Venn diagram of metabolite changes in different types of OP pathogenesis. Dark blue: Amino acid metabolism product, dark yellow: Lipid metabolism product, dark green: Energy metabolism product, red: sugar metabolite.

relationship between OP and amino acid metabolism was further explored. The results of the study indicate that the change of the metabolite glutamate may play an important role in the pathogenesis of OP (26, 36, 70).

In addition, some recent studies have also suggested that the following amino acids may be closely related to the pathogenesis of OP, including: alanine (30, 36, 75), tryptophan (34, 38, 72), methionine (36, 38, 70), phosphatidylserine (67, 68), urea (28, 30), glycine (69, 73, 75), threonine (69, 70), leucine (69, 75), proline (31, 70, 75), aspartic acid (36, 75), hydroxyproline (31, 72), taurine (31, 71, 73), glutamine (31, 75), as shown in Table 2.

4.1.2 Lipid metabolism

Lipids are an important material basis for maintaining cell function and cell proliferation. Several studies have found that some lipid metabolites have been found many times in various samples of OP, which might play an important role in the pathogenesis of OP.

Senescence-related lipid metabolism might play an important role in the abnormal differentiation of BMSCs. The declining trend of sphingomyelin describes lipid responses that might lead to abnormal differentiation of bone marrow-derived mesenchymal stem cells during aging (67). Mendelian randomization analysis showed that sphingomyelin was inversely associated with BMD (32). In Singaporean Chinese postmenopausal women, the association between blood lipids and femoral neck BMD was explored using metabolomics. There was a significant correlation between sphingomyelin and BMD reduction (69). In addition, other studies have also explored the association between BMD and sphingomyelin, indicating that sphingomyelin plays a key role in the pathogenesis of OP (70, 74).

Metabolomics with OP bone marrow and bone also showed that hydroxybutyric acid biosynthesis was disturbed. Assessment of differential metabolites improves understanding of metabolic relationships between kidney-bone axis and tissues in ovariectomized rats. Using a metabolomic approach, serum samples from early menopausal and perimenopausal women were analyzed. These results suggested that hydroxybutyric acid might play a role in the mechanism of osteoporotic bone remodeling (25, 28, 30).

TABLE 1 The application of metabolomics in exploring the pathogenic mechanism of various types of OP.

Types of OP	Sample type	Study size	Analyticalmethod	Key metabolic mechanism pathways	References
postmenopausal OP	patient serum	571	LC-MS	amino acid metabolism	(29)
	patient serum	1193	CE-TOFMS	energy metabolism, amino acid metabolism	(31)
	patient serum	499	LC-MS	lipid metabolism, phenylpropionic acid metabolism and bile acid metabolism	(28)
	patient stool	108	LC-MS	amino acid metabolism, nucleotide metabolism	(26)
	patient serum	517	LC-MS	fatty acid metabolism	(25)
	patient serum	631	Not mentioned	amino acid metabolism, adrenal androgen metabolism	(24)
	rat bone tissue	18	GC-MS	amino acid metabolism, purine metabolism, fatty acid metabolism	(30)
	rat serum	14	LC-MS	bile acid metabolism	(27)
	patient serum	1552	LC-MS	amino acid metabolism, lipid metabolism	(69)
	patient serum	97	LC-MS	amino acid metabolism, lipid metabolism, glucose metabolism	(70)
	patient serum	109	LC-MS	lipid metabolism, sugar metabolism, amino acid metabolism, nucleic acid metabolism	(48)
	patient urine	322	GC-MS	energy metabolism, amino acid metabolism, glucose metabolism	(71)
	patient serum	364	GC-MS	lipid metabolism, amino acid metabolism	(72)
Senile OP	cell culture	cells at 90% density	UPLC–MS	lipid metabolism, amino acid metabolism	(67)
	cell culture	Not mentioned	MS-MS	lipid metabolism, amino acid metabolism	(68)
	patient serum	729	LC-MS	amino acid metabolism, energy metabolism	(73)
	patient serum	69	LC-MS	amino acid metabolism, lipid metabolism	(74)
Secondary OP	patient serum	18	1H NMR	energy metabolism, amino acid metabolism, glucose metabolism	(75)
	patient serum	1545	UHPLC-MS	fat metabolisim	(32)
	patient serum	119	LC-MS	energy metabolism, amino acid metabolism	(33)
	laying hen serum	88	Not mentioned	lipid metabolism, amino acid metabolism	(34)
	mouse serum	12	UHPLC-MS/MS	purine metabolism, lipid metabolism	(35)
	goat serum	28	LC–MS	amino acid metabolism, lipid metabolism	(38)

TABLE 2 Metabolomics is used to explore mechanisms of OP, with the same metabolites found in different studies.

Type of metabolism	Co-discovered metabolites	Types of OP	Sample type	References
Amino acid metabolism	lysine	postmenopausal OP, secondary OP	patient serum, goat serum	(31, 38, 72)
	carnitine	postmenopausal OP	patient serum	(25, 31, 74)
	valine	postmenopausal OP, secondary OP	patient serum, goat serum	(31, 38, 75)
	glutamate	postmenopausal OP, secondary OP	patient stool	(26, 36)
	alanine	secondary OP, postmenopausal OP	rat bone tissue	(30, 36, 75)
	tryptophan	secondary OP	laying hen serum, goat serum	(34, 38, 72)
	methionine	secondary OP	goat serum	(36, 38, 70)
	phosphatidylserine	senile OP	cell culture	(67, 68)
	urea	postmenopausal OP	rat bone tissue, patient serum	(28, 30)
	glycine	postmenopausal OP, senile OP secondary OP	patient serum	(69, 73, 75)
	threonine	postmenopausal OP	patient serum	(69, 70)
	leucine	postmenopausal OP, secondary OP	patient serum	(69, 75)
	proline	postmenopausal OP, secondary OP	patient serum	(31, 70, 75)
	aspartic acid	secondary OP	patient serum, patient stool	(36, 75)
	hydroxyproline	postmenopausal OP	patient serum	(31, 72)
	taurine	postmenopausal OP, senile OP	patient serum	(31, 71, 73)
	glutamine	postmenopausal OP, secondary OP	patient serum	(31, 75)
Lipid metabolism	dodecanoic acid	postmenopausal OP	patient serum	(25, 28)
	hydroxybutyric acid	postmenopausal OP	rat bone tissue, patient serum	(25, 28, 30)
	sphingomyelin	senile OP, secondary OP	cell culture, patient serum	(32, 67, 69, 70) (74)
	phosphatidylinositol	senile OP	cell culture	(67, 68)
	glycerophospholipids	senile OP, secondary OP	cell culture, patient serum	(32, 68, 70)
	phosphatidylcholine	postmenopausal OP, senile OP	patient serum	(67, 69, 74)
	glycerides	postmenopausal OP, secondary OP	patient serum	(32, 70)
	succinic acid	postmenopausal OP	patient serum	(31, 71)
Energy metabolism	creatine	postmenopausal OP, secondary OP	rat serum, patient serum	(27, 69, 75)
	citric acid	postmenopausal OP, secondary OP	patient serum, patient urine	(48, 71, 75)
Glucose metabolism	glucose	postmenopausal OP, secondary OP	patient serum	(28, 71, 75)

The lipidomic strategy was used to observe the expression of related enzymes and lipids in the membranes of MSCs of different ages and proliferation states. Several studies have found that the changes of glycerophospholipids are closely related to the metabolic function mechanism mediated by bone marrow mesenchymal stem cells (32, 68, 70). Serum samples were analyzed using an untargeted MS-based metabolomic approach. Phosphatidylcholine metabolites were significantly dysregulated in the OP group compared with the control group. This metabolome will contribute to the study of disease mechanisms that promote bone health and OP progression (67, 69, 74).

In addition, other lipid metabolites, such as Glycerides (32, 70), succinic acid (31, 71), dodecanoic acid (37, 40), phosphatidylinositol (67, 68), etc., have been proved by many studies to be closely related to the pathogenesis of OP, as shown in Table 2.

4.1.3 Other metabolism

In recent years, the pathogenesis of OP has been continuously explored by means of metabolomics, and some key metabolites of energy metabolism and glucose metabolism also play an important role in the mechanism of OP.

A postmenopausal OP mouse model was used to compare metabolome changes in the control and OP groups. Metabolites creatine was significantly different (27). The pathogenesis of OP is revealed from the perspective of microbe-gut-metabolic bone axis regulation, which provided a new entry point for the pathogenesis of OP. OP-related metabolomic markers were examined to reveal underlying mechanisms of OP. Creatine has changed significantly (69). In addition, metabolomic techniques were used to discover differences in metabolites of bone metabolic disorders between healthy volunteers and diabetic patients. Changes in creatine levels were also found (75). Therefore, the metabolic abnormalities of creatine might

serve as a key substance in the underlying pathogenic mechanism of OP.

Metabolites with significant differences between estrogen levels and BMD. Metabolite citric acid changes were useful markers of bone loss and/or estrogen deficiency (48). Metabolomics techniques were used to discover differences in metabolites of bone metabolic disorders between healthy volunteers and diabetic patients. Citric acid level was also significantly changed (75). This metabolite abnormality could be used as a key indicator of the pathogenesis of diabetic OP. Pathological features of postmenopausal OP were revealed, and metabolic pathways and biomarkers that might be associated with OP were explored. citric acid was also found to be a potential biomarker of OP (71). Therefore, citric acid was related to the pathogenesis of OP.

Using metabolomic profiling methods, metabolic alterations in postmenopausal women and elderly OP compared with healthy people were analyzed. These studies all found that glucose played a role in the mechanism of osteoporotic bone remodeling (28, 71, 75).

OP is a classic age-related disease that is often considered a "silent disease" because there are no symptoms for many years before a fracture occurs. Therefore, it is of great practical significance to deeply study the pathogenic mechanism of OP from the perspective of metabolism, which can further promote the early prevention, diagnosis, and intervention of OP from the perspective of mechanism (1–3). To sum up, many studies have shown that OP will experience various metabolite changes in various stages of the disease, including amino acid metabolism, lipid metabolism and energy metabolism (40, 69, 71). These different studies all found some of the same metabolites for the above metabolic pathways. Therefore, these same metabolites played important roles in the pathogenesis of OP, and future monitoring of changes in these metabolites by metabolomics is important to achieve further research in OP.

4.2 Factors associated with the metabolomic outcome of OP

OP is a heterogeneous disease. Therefore, vitamin D, diabetes, race, and other factors should be considered when studying OP using metabolomic approaches. Vitamin D inhibits osteoclast recruitment, prevents estrogen deficiency, and enhances osteoblast precursor cell proliferation and osteoblast activity (76). A series of studies found that vitamin D levels can significantly alter amino acids, energy metabolism, levels of sugars and their derivatives, and organic acids in patients with OP, thus affecting the metabolomic outcome of OP (77, 78). In addition, different blood calcium levels affected the metabolism of lipids and amino acids such as taurine, glycerophospholipids and glycine, thus causing changes in the metabolomic outcome of OP, which ultimately affected BMD and bone degeneration

(79, 80). Recent studies have found that temperature increases the total amount of polyamines in the body, and that inhibition of polyamine biosynthesis in the body limited the protective effect on bone (81).

Severe metabolic disturbances in diabetes can lead to OP. Findings suggest that diabetes mellitus combined with OP will further lead to significant changes in amino acid metabolism and energy metabolism, such as tricarboxylic acid cycle products and various branched-chain amino acids (75). OP combined with osteoarthritis will further alter the phospholipid precursors, energy metabolism and amino acid metabolites of OP (82). In addition, lipoprotein and amino acid metabolites are significantly different when OP is associated with atherosclerosis (83).

Ethnic differences are also important factors influencing metabolomic outcomes in OP. The association between lipid and amino acid metabolites and BMD changes was significant in Asian women with OP in China and Singapore. In particular, dodecanoic acid played an important role in metabolites (25, 70). However, TwinsUK-based studies have mainly identified amino acid and hormone metabolites and found a causal relationship between them and BMD. Lipid metabolites and other amino acid metabolites were different from those in Asians (24). In addition, these studies have shown that the severity of OP varies among ethnic groups. Therefore, the changes in the levels of osteoporotic metabolites and the occurrence and development of OP explored by metabolomics are different based on different races (24, 25, 70).

As a secondary OP, OP caused by intestinal flora has attracted more and more attention in recent years. The microorganisms in the gastrointestinal tract are collectively referred to as the gut flora and consist of approximately 10 trillion bacteria (84). Recent studies have provided substantial evidence for the existence of a "gut microbiota-metabolite-bone axis", and OP is closely associated with the development and progression of gut microbiota imbalances (26, 27, 35, 85–87). He et al (26) combined LC-MS metabolomics with 16S rRNA gene sequencing. The results showed that mutations in gut bacteria such as Klebsiella and Clostridium interfered with changes in the metabolic levels of acetylmannosamine, type I collagen C-terminal peptide and collagenogenic peptide, and mediated postmenopausal bone loss. Other studies have found that OP was associated with the functional, taxonomic and β-diversity composition of the gut microbiota. Oscillating bacteria, Brucella, Actinomyces and other intestinal flora acted mainly on the metabolism of tryptophan and tyrosine and the degradation of isoleucine, leucine and valine, thus negatively regulating BMD in OP (86). Wen et al. (27) found that the onset and progression of OP is closely related to the metabolic regulation of the intestinal flora. The gut microbiota is one of the important pathogenic factors of OP and regulates the pathogenesis of OP through the microbial-gut metabolic-bone axis. Liu et al. (85) found that the effect of ethanol intake on the gut microbiota mainly increased

the ratio of firmicutes and Bacteroidetes, which led to an increase in 5-hydroxytryptamine and inhibited the mineralization and proliferation of osteoblast-associated cells, thus affecting BMD. In addition, high lipids led to a significant increase in the relative abundance of bacteria, with a decrease in B. phenotypicus, B. actinomycetemcomitans and the bacteria of lipolysis and purine metabolism, which decrease the BMD (35). In addition, bone loss induced by salivary microbiota through the "oral-gut axis" in patients with periodontitis may be related to tryptophan metabolism and lipid degradation (88). These studies will contribute to a better understanding of the mechanisms and relationships between changes in osteoporotic metabolite levels and the gut microbiota, and how the gut microbiota is involved in and mediates the development and progression of OP, making gut microbiota regulation a new therapeutic strategy to promote healthy bone development.

Therefore, vitamin D, blood calcium, temperature, race, diabetes, osteoarthritis, atherosclerosis, gut microbiota and other factors both influence the metabolomic outcome of OP. In the future, it will be a meaningful research direction to further pay attention to and integrate various factors such as age, BMI, smoking and physical activity to explore the changes of metabolomics in OP.

5. Metabolomics for the development of OP therapeutics

At present, the therapeutic mechanism of mature OP drugs such as alendronate sodium, teriparatide, calcitriol, etc. and the therapeutic effect of biomaterials have been systematically and deeply studied. There are also many studies and reviews summarized these drugs. In this review, we systematically summarized the OP treatment drugs that have been studied more in recent years, especially natural herbal medicine (Figure 2), and related extracts (Table 3), which have been found both protect bone from osteoporosis, but the mechanism need to be further explored. The introduction of metabolomics provides a good platform for the study of these drugs in regulating the biochemical metabolism of bone tissue, and can further explore the side effects, efficacy, and dose effect of their therapeutic methods. We provide a series of novel OP treatments to be developed and even laid a solid foundation for clinical transformation.

5.1 Natural herbal medicine

5.1.1 Natural compound herbal medicine

XianLingGuBaoJiaoNang was used to prevent and treat OP. However, there was no comprehensive metabolic profile of XianLingGuBaoJiaoNang. The results showed that cleavage

and deglycosylation of glycosylated groups were the main metabolic pathways of various glycosides. Notably, amino acid binding was first found in the metabolism of pentene-flavonoid glycosides in the intestinal flora of rats (117).

The mechanism of Zishen Jiangtang Pill maintaining blood glucose and BMD is still unclear. These results indicate that Zishen Jiangtang Pill could effectively improve abnormal bone metabolism and glucose metabolism in diabetic OP, and was expected to be an effective alternative drug for the treatment of diabetic OP (101). Fufang Zhenshu Tiaozhi could treat hyperlipidemia and OP caused by glucocorticoid. Fufang Zhenshu Tiaozhi had a protective effect on senile OP, and its mechanism might be related to the interference of arachidonic acid metabolism, glycerophospholipin and sphingomyelin (104).

Xie et al (107) studied the effect of QingEWan on intestinal microflora in rats with OP. The levels of butyric acid, propionic acid and acetic acid were increased. In addition, QingEWan could regulate intestinal flora and improve OP.

5.1.2 Natural single herbal medicine

Gushudan is a kind of traditional Chinese medicine preparation designed for secondary OP. Yuan et al (93) discussed the anti-OP effect of Gushudan on hormone-induced OP rats and its mechanism, and identified 40 different metabolites, mainly involving energy metabolism, amino acid metabolism, intestinal flora metabolism and fat metabolism. Using UPLC-MS technology of metabolomics, the overall therapeutic effect of Gushudan on secondary OP was effectively explored by detecting urine blood samples (94). By 1H NMR metabolomics method, 27 differential metabolites were found after Gushudan treatment. It was further proved that Gushudan may ultimately treat OP by changing these metabolites (95). Through a non-targeted metabolomic approach, Gushudan was further used to explore the therapeutic effect and related mechanism of secondary OP. The results showed that energy, fat, and amino acid metabolism play a huge role in this pathway (96). These correlation studies have systematically explored the therapeutic effect and metabolic mechanism of Gushudan. Metabolomics was also used to explore the mechanism of OP according to the above section. Several studies simultaneously found that the pathogenesis of OP is closely related to lipid metabolism, amino acid metabolism and energy metabolism. We summarized some key and jointly validated metabolites related with Gushudan in the Table 3. In combination with the regulation of Gushudan on metabolites of OP, we found that Gushudan significantly regulated taurine, creatine, Valine, tryptophan, and Leucine metabolites of OP (Table 3).

Tao et al (97) found that the Dipsacus asper treatment group had abnormal metabolic pathways. Dipsacus asper segment of liquor could treat and prevent OP by intervening energy metabolism, carbohydrate metabolism and amino acid metabolism in the body.

FIGURE 2
Metabolic pathways of different types of natural herbal action and therapeutic effects on different types of OP.

Wang et al (98) discussed the effects of Echinops latifolius Tausch on ovariectomized rats and the metabolic pathways involved in the changes in trabecular microstructure in OP. Echinops latifolius Tausch effected on bone trabecular microstructure of castrated rats may be related to intervention of glycerophospholipids.

Morinda officinalis and its chemical constituents could prevent OP caused by aging and estrogen deficiency. Metabolomics analysis showed that 37 different metabolites were present in the control group compared with the dexamethasone group, and 20 of them were significantly reversed after treatment with Morinda officinalis. Further Western blot analysis and metabolic pathway enrichment showed that Morinda officinalis prevented bone loss mainly through interference with arachidonic acid metabolism (99).

The mechanism of Rhizoma Drynariae anti-OP was still unclear. Using metabolomics, some potential biomarkers

involving nine metabolic pathways were identified. These experimental results showed that Rhizoma Drynariae can prevent and treat OP by regulating the above-mentioned metabolic pathways, and provided a new theoretical basis for natural herbal medicines (100).

Cimicifuga heracleifolia was a traditional American herb that promises to counteract the ills of menopause. Serum metabolite composition was analyzed by serum metabolomics. The results showed that Cimicifuga heracleifolia has the effect of lowering blood lipid and anti-OP on climacteric syndrome. At the same time, its potential in improving metabolic disorders caused by postmenopausal OP was found (102).

Radices rehmanniae or dry Radices rehmanniae could prevent postmenopausal OP and senile OP. In metabolomics studies, 10 cases were significantly reversed after Radices rehmanniae treatment. These metabolites were mainly involved in amino acid metabolism, sex hormone regulation and steroid hormone

TABLE 3   Metabolomics for the development of OP therapeutics.

Type of drug	Therapeutic research subjects	Types of OP	Sample type	Analytical method	Significantly changed metabolites	Metabolic pathways targeted by drugs	References
Icariin	mouse, rat, chicken	postmenopausal OP, secondary OP	serum, bile, and urine	^{1}H-NMR, UHPLCMS/MS, UPLC-QTOF/MS	**up-regulated:** alanine, creatine, taurine, glycine, β-glucose, uridine, palmitic acid, adrenic acid, fexofenadine, LysoPC (18:1) **down-regulated:** lactate, LysoPE (20:3)	glucose metabolism, lipid metabolism, energy metabolism, taurine metabolism	(89–92)
Gushudan	rat	secondary OP	serum, urine	UHPLC-MS, ^{1}H-NMR	**up-regulated:** pyruvate, taurine, glycocholic acid, phenylalanine, creatine, valine, tryptophan, epoxyeicosatrienoic acid, hydroxyvaleric acid, benzoate **down-regulated:** lysoPC, creatinine, hippuric acid, lactic acid, leucine, citrate, hippurate, lndoxyl sulfate	lipid metabolism, amino acid metabolism, energy metabolism, purine metabolism	(93–96)
Dipsacus asper	rat	postmenopausal OP	serum, tissue	GC-MS	phenylalanine, serine, tyrosine, tryptophan biosynthesis, valine, isoleucine, biosynthesis, methane metabolism, glycine, threonine, galactose	amino acid metabolism, glucose metabolism and energy metabolism	(97)
Echinops latifolius Tausch	rat	postmenopausal OP	serum	UPLC-MS	**up-regulated:** proline, lysoPC, creatine, lysoPE, 9-cis-Retinoic acid, 4-Acetamidobutanoic acid, arginine, glycerophosphocholine, hydroxyprogesterone, N-acetylornithine **down-regulated:** 2-phenylethyl beta-D-glucopyranoside, anserine, quinaldic acid, pentahomomethionine,	amino acid metabolism, glycerophospholipid metabolism	(98)
Morinda officinalis	rat	secondary OP	serum	UHPLC-MS	**up-regulated:** 4-Pyridoxic acid, 11-dehydrocorticosterone **down-regulated:** L-valine, glycylproline, 4-Pyridoxic acid, valerylcarnitine, androsterone, N-phenylacetylaspartic acid, galactosylhydroxylysine, cortisol, docosapentaenoic acid, thromboxane A2, cortolone	amino acid metabolism, arachidonic acid metabolism, lipid metabolism	(99)
Rhizoma Drynariae	rat	secondary OP	serum	UPLC-MS	**up-regulated:** acrylic acid-2-acrylamido-2-methyl, cuscohygrine, santalyl phenylacetate, tetraHCA, N-oleoylethanolamine, **down-regulated:** indoxyl sulfate, narirutin, lysoPE, artocarpin, chenodeoxyglycocholic acid, L-palmitoylcarnitine, lysoPC, boviquinone, cholesterol sulfate	linoleic acid metabolism, glycerophospholipid metabolism and arachidonic acid metabolism	(100)
Syringin	mouse	postmenopausal OP	serum	UPLC-MS	**up-regulated:** 2-ketobutyric acid, cytosine, 3-methylhistidine, acetoacetic acid, normetanephrine, arachidonic acid, creatine, L-arginine, 3-methylglutaconic acid, lysoPC **down-regulated:** sarcosine, 3-aminoisobutanoic acid, dimethylglycine, d-ornithine, 2-aminoisobutyric acid, D-limonene	amino acid metabolism, lipid metabolism, Nucleic acid metabolism	(52)
Zishen Jiangtang Pill	rat	secondary OP	serum	^{1}H-NMR	tryptophan, serine, 2-hydroxyisovalerate, anthosine, fumarate, uracil, creatine, acetate, threonine, 3-hydroxybutyrate, glutamate, formate, tyrosine, isoleucine, 2-oxoisocaproate	glucose metabolism, amino acid metabolism, nucleic acid metabolism	(101)
Cimicifuga heracleifolia	rat	postmenopausal OP	serum	GC-MS	**up-regulated:** oxalic acid, hydroxybutyric acid, glycine, L-phenylalanine, L-glutamine, D-glucose, stearic acid, arachidonic acid, myo-Inositol, palmitic acid, alpha-linolenic acid, cholesterol **down-regulated:** L-lactic acid, urea, creatinine, L-proline, L-glutamic acid,	lipid metabolism, amino acid metabolism, energy metabolism	(102)
Lignan-rich fraction	rat	postmenopausal OP	serum	UPLC-MS	**up-regulated:** uric acid, tryptophan, lysoPC (22:6), arachidonic acid, linoleic acid, oleic acid **down-regulated:** p-cresyl sulfate, sulfate	lipid metabolism, amino acid metabolism	(103)

(Continued)

TABLE 3 Continued

Type of drug	Therapeutic research subjects	Types of OP	Sample type	Analytical method	Significantly changed metabolites	Metabolic pathways targeted by drugs	References
					metabolite, taurochenodeoxycholate, deoxycortisol/isomer, lysoPE (18:1)		
Fufang Zhenshu Tiaozhi	mouse	senile OP	serum	UPLC-MS	**up-regulated:** LPA, DG (36:3), PC (40:9), neuroprotectin D1 **down-regulated:** sphingosine 1-phosphate, lysoPE, arachidonic acid, fructose 1,6-bisphosphate, NADH, glycocholic acid, taurodeoxycholic acid	sphingomyelin metabolism, glycerophospholipid metabolism and arachidonic acid metabolism	(104)
Osthole	rat	postmenopausal OP	serum	UPLC-MS	**up-regulated:** 3-hydroxybutyric acid, taurocholic acid, LysoPC (15:0), citric acid, corticosterone, 8-HETE, Cer(d18:0/18:0), glutamine, uric acid **down-regulated:** lysine, linoleic acid, prostaglandin F2a, L-carnitine, glucose, arginine, ornithine, tryptophan, arachidonic acid, estriol	glucose metabolism, amino acid metabolism, energy metabolism, nucleotide metabolism, lipid metabolism	(105)
Eleutheroside E	rat	postmenopausal OP	serum	UPLC-MS	**up-regulated:** creatine, L-carnitine, creatinine, N-acetylhistidine, pyroglutamic acid, dopaquinone, N-a-acetyl-L-arginine, isoleucylproline, N-acetylvanilalanine, 5-acetamidovalerate, N-acetyl-L-tyrosine, estrone glucuronide, N-acetyl-L-phenylalanine **down-regulated:** kynurenic acid, cortolon, cortisol, dihydrocortisol, 18-hydroxycorticosterone, taurocholic acid, cholesterol, corticosterone, sulfate, 11-dehydrocorticosterone, cholic acid, 17-hydroxyprogesterone, tetrahydrocortisol, cholic acid glucuronide, prostaglandin G2	arachidonic acid metabolism, amino acid metabolism, glucose metabolism, lipid metabolism	(106)
Qing'e Pills	rat	postmenopausal OP	serum	UPLC-MS	sphinganine, 17a-Hydroxypregnenolone, arachidonic acid, alpha-Linolenic acid, corticosterone, docosahexaenoic acid, phytosphingosine, octadecadienoic acid,11-cis-Retinol, lysoPC, l-tryptophan, Tetrahydrocorticosterone, sphingosine1-phosphate, cholic acid, 1-lyso-2-arachidonoyl-phosphatidate, glycocholic acid	amino acid metabolism, fatty acid metabolism	(107)
Rehmanniae	rat	Secondary OP	urine	UPLC-MS	**up-regulated:** 4-Pyridoxic acid, 11-dehydrocorticosterone, corticosterone, 18-hydroxycorticosterone, **down-regulated:** benzoic acid, N-acetylproline, N-phenylacetylaspartic acid, androsterone/epiandrosterone, cortolone, lysoPA(i-14:0/0:0)	amino acid metabolism, Vitamin B6 metabolism, Steroid hormone biosynthesis, lipid metabolism	(108)
Achyranthes bidentata, chondroitin sulfate calcium	rat	postmenopausal OP	serum	UPLC-MS, LC-MS	**up-regulated:** glutarylcarnitine, lysoPC (18:1) and 9-cis-retinoic acid **down-regulated:** fatty acids, carbohydrates, dipeptides, carboxylic acids	glucose metabolism, amino acid metabolism, energy metabolism, lipid metabolism, nucleotide metabolism	(50, 109)
Estradiol	rat, osteoclasts	postmenopausal OP	skeletal muscle	UPLC-MS	**up-regulated:** phytosphingosine, palmiticamide, stearamide, alpha-aminobutyric acid, threonine, hydroxyproline, l-cystine **down-regulated:** lysoPC, lysoPE, stearamide, deoxycytidine, phospho-L-serine	purine metabolism, lipid metabolism, amino acid metabolism	(110, 111)
Lactobacillus	mouse, human	Secondary OP, Senile OP	stool, serum	UPLC-MS, LC–MS	**up-regulated:** lysoPC, L-alpha-Amino-1H-pyrrole-1-hexanoic acid, PE-NMe, N-oleoyl	lipid metabolism, fatty acid	(112, 113)

(Continued)

TABLE 3 Continued

Type of drug	Therapeutic research subjects	Types of OP	Sample type	Analytical method	Significantly changed metabolites	Metabolic pathways targeted by drugs	References
					tyrosine, 15-HETE-VA, Lucidenic acid M, dihydropiperlonguminine **down-regulated:** reticulatamol, lsoleucyl-phenylalanine, N-acetyl-leukotriene E4, cysteine s-sulfate, fibrinopeptide A	metabolism, amino acid metabolism	
Tocotrienol	human	postmenopausal OP	serum	LC-MS	**up-regulated:** betaine, 5-methylthioadenosine, methionine, gamma-glutamylleucine, gamma-glutamyltyrosine, N-acetylmethionine, N-acetylmethionine, cysteine sulfinic acid, S-adenosylhomocysteine, cystathionine, **down-regulated:** dimethylglycine, methionine sulfone	fatty acid metabolism, lipid metabolism, amino acid metabolism	(114)
Rubus coreanus Vinegar	rat	postmenopausal OP	serum	GC-MS, UPLC-MS	phenylalanine, tryptophan, butyric acid, lysoPC 22:6	amino acid metabolism, glucose metabolism	(115)
Bone marrow MSC	mouse	postmenopausal OP	femoral tissue	LC-MS	**up-regulated:** Acetylcholine chloride, Lipoxin B4 **down-regulated:** 3-Hydroxyanthranilic acid, l-Dopa, d-Xylitol, 5-l-Glutamyl-taurine, 5-l-Glutamyl-taurine, Melphalan	amino acid metabolism, lipid metabolism	(116)

biosynthesis. The mechanism of Radices rehmanniae action might be related to steroid hormone biosynthesis (108).

Rubus coreanus Vinegar had a good effect on postmenopausal OP. Of note, the Rubus coreanus Vinegar group had slightly increased levels of tryptophan, phenylalanine, lysophosphatidylcholine, glucose, and butyric acid compared with the postmenopausal OP group. Rubus coreanus Vinegar might be an effective natural substitute for prevention of postmenopausal OP (115).

5.1.3 Natural herbal medicinal extracts

Icariin, the main component of icariin flavonoid glycoside, has been widely confirmed to have anti-OP effect. Some studies combined 1H NMR metabolomics and proteomics, and elucidated 8 metabolites in serum and 23 proteins in femur which were significantly changed (89). After a single oral administration of Epimedium, Cheng et al (90) determined the metabolites in rat urine, plasma, feces, and bile. The results also showed that the main metabolic pathways of icariin in rats were glycosylation and glycoaldehyde acidification after glycosylation. Pan et al (91) systematically analyzed the metabolomics characteristics of glucocorticoid-induced OP model rats. Huang et al (92) discussed the therapeutic effect and mechanism of icariin on low bone density in cage laying hens. Icariin mainly interfered with fat metabolism, taurine metabolism and pyrimidine metabolism of laying hens, resulting in increased BMD in old laying hens. Cobined these study of metabolomics applied to OP, we found that alanine, creatine, Taurine, Glycine, and β-glucose metabolites of the pathogenesis of OP were significantly regulated (Table 3).

Syringin had strong anti-OP activity, but the specific mechanism of its anti-OP was still unclear. High resolution mass spectrometry (MS) showed that metabolic pathways were closely related to catecholamine biosynthesis, butyric acid metabolism, glycine, tyrosine, methionine, and serine metabolism (52).

The part of Lignan-rich fraction in lignan was a traditional Chinese medicine used to treat bone diseases in China. Studies were conducted to identify potentially related metabolic pathways and metabolites. Studies have shown that Lignan-rich fraction can effectively restore amino acid-related tryptophan metabolism, lipids, and antioxidant systems (103).

Si et al (105) discussed the efficacy of osthole treatment. In the ovariectomized OP model, 28 metabolites were identified as biomarkers, some of which had significant regulatory effects.

In a study, the interventional effect of Eleutheroside E on postmenopausal OP was evaluated by analyzing the related metabolic network, potential biomarkers, and urinary metabolic profile of postmenopausal osteoporotic rats. This study explained the metabolic effects and pharmacological mechanisms of Eleutheroside E on postmenopausal OP (106).

Some studies have shown that Achyranthes polysaccharides can treat OP through various ways. This study evaluated the effect of Achyranthes bidentata polysaccharides on OP based on metabolomics analysis. Achyranthes bidentata polysaccharides had good potential in the treatment of OP (50). Metabolomics highly integrates the "top-down" integration strategy, and responds to various functional pathways and indicators through changes in metabolic pathways, networks, and end products, to understand the overall trend of system change.

Therefore, using metabolomics methods, natural herbal formulations and extracts have received more extensive research and attention.

5.2 Hormone drugs

Estradiol is the main clinical drug for OP treatment. Wei et al. discussed metabolic changes in myogenic OP and the therapeutic effects of estradiol. The analysis showed that the changes of oxidative phosphorylation, tryptophan metabolism, glycerol phospholipid metabolism, thermogenesis, histidinine metabolism, arginine biosynthesis and purine metabolism were the most common pathogenic factors of myogenic OP (110). Liu et al. studied the response of osteoclast metabolites to estradiol using a metabolomics-based approach (111). Some 27 metabolites such as amino acids and lipid derivatives were significantly altered after estrogen action. The metabolomic pathway enrichment analysis showed that estrogen affects glycerophospholipid metabolism and played a therapeutic role in OP. Estradiol-induced changed in phosphatidylcholine-sterol acyltransferase activity, methyldialdehyde and malondialdehyde further affected glycerophospholipid metabolism. Studies have shown that estradiol is highly conditioned dependent on osteoclast metabolism.

5.3 Gut microbes

So far, fecal microbiota transplantation and probiotic supplementation have gradually attracted the attention of scholars as a new organ transplantation method in the alleviation and even treatment of OP. This approach aims to alter the abundance and composition of gut microbes in the recipient's gut, thus affecting the metabolite levels in the body for the treatment of OP (118). Zhang et al (119) showed that gut microbiota treatment increased the levels of propionic and acetic acids, optimized the abundance and composition of the gut microbiota, inhibited the production of excess osteoclasts, and prevented bone loss in postmenopausal osteoporotic rats. Lactobacillus reassorts intestinal flora and alters metabolite composition, particularly lysophosphatidylcholine levels. Lactobacillus might be an effective and safe treatment strategy in some types of osteoporotic diseases (112). Lactic acid bacteria significantly reduced bone loss in older women with low bone density. Lactobacillus-regulated metabolites are involved in a variety of metabolic pathways, including acylcarnitine, peptide and lipid metabolism, as well as amino acid metabolism (113).

In addition, various drugs and bioactive substances could indirectly treat OP by directly modulating the abundance and composition of the intestinal microbiota. Calcium supplementation could increase the number of propionibacteria and immobile bacilli in the feces, thus

affecting the concentration of short-chain fatty acids. Inulin could significantly increase the number of bifidobacteria and cocci, acting on the production of single-chain fatty acids and ultimately improving the mechanical strength, bone mineral content and BMD of the femur (120). lignan-rich induced high abundance of actinomycetes and restores microbial composition, which reduced abnormal lipid metabolism, prevents glucose tolerance, improves liver function, and reduced the risk of OP in castrated rats (121). Gushudan promoted the production of lactobacilli, which in turn acted on the production of lysine, acetate, and butyrate, ultimately acting as an anti-OP agent (122). Temperature exposure could reduce rumen bacteria and digestive cocci and increase lactic acid bacteria, lactobacilli and Lybacilaceae, thereby leading to changes in spermidine, spermine and polyamine levels and increasing bone strength (81). Qinga pill could change the composition of Firmicutes, Verumobacteria and Bacteroides in intestinal flora, and increase the content of butyric acid, propionic acid, and acetic acid in intestinal flora. The combination of anti-OP drugs and gut microbiota might be a new treatment for OP (107). In addition, Achyranthes achyranthes could regulate the levels of polyunsaturated fatty acids, lipids, glucose, and amino acids by acting on Escherichia coli, Roche, and anaerobic bacteria, thus exerting an anti-OP effect (123).

5.4 Other treatment strategies

Mao et al (80) investigated whether calcium supplementation can reduce bone loss in rats caused by calcium restriction and estrogen deficiency. The results of metabolomics analysis suggested that calcium supplementation was a metabolic pathway closely related to glycerophospholipid metabolism, and that the effect of calcium supplementation on OP might be due to increased estrogen levels, resulting in changes in metabolite levels, and ultimately increased BMD, thereby reducing bone degeneration.

In a population of postmenopausal women with OP, the effect of tocotrienols on metabolites was assessed using patient serum systems. When treated with tocotrienols, oxidative stress and inhibition of inflammation were significantly modulated resulting in a significant reduction in bone loss in patients (114).

Wang et al (116) discussed the efficacy of bone marrow mesenchymal stem cells in the treatment of OP in ovariectomized mice. Stem cell therapy could be intertransformed by glucuronic acid and pentose, metabase and taurine metabolism, and arachidonic acid metabolism. This study laied a foundation for the study of bone marrow mesenchymal stem cells as a treatment strategy for OP.

Chondroitin sulfate calcium complex was considered to have *in vitro* bone health activity. It was found that intervention with calcium chondroitin sulfate could alter fecal metabolite

composition and intestinal microflora of castrated rats. Correlation analysis showed that certain intestinal flora was significantly associated with metabolite-rich and OP phenotypes (109).

As mentioned above, metabolomics has made a lot of progress in developing new treatments for OP. From the perspective of biochemical metabolism mechanism, in-depth research has been conducted on how various drugs such as Chinese herbal medicine, polysaccharides, hormones, and Lactobacillus act on metabolic reprogramming of the body and play a therapeutic role in OP (52, 89, 110, 113). Among a variety of Chinese herbal medicines, studies on the regulation of icariin and Gushudan on various OP metabolism are comprehensive and in-depth, involving fat metabolism, sugar metabolism, amino acid metabolism, pyrimidine metabolism, taurine metabolism and intestinal microflora disorders, etc (89, 93). Notably, we found that metabolites of the pathogenesis of OP, including Taurine, creatine, Valine, Tryptophan, Leucine, Alanine, creatine, Taurine, Glycine, and β-glucose were significantly regulated by icariin (90, 92). Therefore, further research on the therapeutic mechanisms of these two drugs should be more attached for clinical application.

6. Application of metabolomics in other researches of OP

The imbalance of bone resorption and bone formation caused by osteoclasts relatively active, leading to OP and accompanied by various metabolic disorders (124, 125). Therefore, specific changes of markers in various samples such as blood, tissue, and urine of patients with OP will reflect the characteristics of metabolic disorders of bone tissue, which can support the prevention and prediction of the disease (126, 127). Subtle changes in metabolites can be revealed by metabolomics, but these changes have not yet resulted in changes in bone density or structure. Furthermore, substances produced as the end products of metabolic activity are factors related to biological or metabolic states. Therefore, these specific metabolic markers are highly sensitive markers for the prevention and prediction of OP specific pathologic states.

6.1 Prevention

It is extremely important to explore some risk factors that reflect abnormal bone metabolism, and they can be used for early prevention of OP. For example, nutrition is closely related to BMD values in children and adulthood, therefore, rational nutritional intervention and treatment are crucial for the prevention of OP, which can further reduce the risk of osteoporotic fractures. Mangano et al (128) used an untargeted

metabolomics approach to determine the biochemical factors driving the relationship between vegetable and fruit intake and the risk of OP. Vegetables and fruits can inhibit the synthesis pathway of lipid metabolites, and lead to increased concentrations of other metabolites in the body, thereby stimulating estrogen synthesis and slowing the progression of OP. Dietary prevention strategies with adequate intake of dark green leafy vegetables, berries, and melons are associated with significant improvements in OP development and progression in both men and women. Chau et al (129) studied metabolites associated with coffee and assessed their association with OP. The results showed that 12 serum metabolites were positively correlated with coffee intake, among which fenugreek, 3-hydroxypyridine sulfate and quinic acid had the strongest correlation. Of these metabolites, 11 were known to be involved in coffee intake, and six of them were involved in caffeine metabolism. In addition, explosion to some metals and heavy metals may also lead to bone metabolism disorders (130). 1 μM cadmium significantly affected the malate-aspartate and citric acid cycles, and 10 μM cadmium significantly affected the pyrimidine, alanine, glutamate, glucose-alanine, and citric acid cycles.

6.2 Prediction

Predicting OP is critical for people to maintain bone health and improve their overall quality of life. Existing series of risk factors are difficult to predict complicated OP risk. In recent years, through metabolomics technology, some studies have found that several types of metabolites can be used as potential predictive markers of OP. Kong et al (131) conducted a survey with an average follow-up of 9 years. In a community cohort study, high spermidine concentrations were associated with an increased risk of osteoporotic fractures. With further validation studies, spermidine baseline concentration may be a new alternative marker for OP associated brittle fractures. Therefore, spermidine and its related metabolites may be reliable predictors of OP. Untargeted metabolomics analysis was performed on serum samples from 32 normal controls and 32 patients with OP. Hyocholic acids plays an important role in the development of OP and may be a potential marker. Hyocholic acids may be a new target for predicting OP (132). OP is a chronic disease that manifests insidiously and is age-related, often not detected until after a fracture. Therefore, some studies have established a sensitive, accurate, and rapid predictive test method, and the related aminobutyric acid enantiomers and isomers are accurately detected and used to predict the progression of OP (133). Serum (R) -3-aminoiso-butyric acid and γ -aminobutyric acid were positively correlated with physical activity in young, lean women. This study opens new possibilities for aminobutyric acid as a potential predictor of OP.

7. Technological innovations in metabolomics and multi-omics integration to explore OP

With the rapid development of metabolomics in the field of OP, a series of traditional testing and analysis techniques and methods have drawbacks. Therefore, in recent years, technological innovations have been made in many aspects of metabolomics in the process of exploring OP diseases, and certain progress has been made. Furthermore, OP is a multi-factorial disease. Therefore, it is of great practical significance for OP to integrate metabolomics and multi-omics data for a comprehensive and systematic exploration. Wang et al (134) proposed a simple method to correlate the relative retention time of peaks in chromatograms with the intrinsic peaks and to assess their off-target performance using an LC-MS dataset obtained from plasma samples of rats with OP. The relative retention time method have fewer missing values, low peak intensity relative standard deviation, and good pattern recognition performance, which showed great potential in future metabolomics research. To improve the interpretability of the multiregional orthogonal projection model, they integrated targeted analyses of oxygen lipids, metabolomics, fatty acids, sphingolipids, and transcriptome. Clinical closure was also used for analysis. They identified OP genes associated with dysregulation of inhaled glucocorticoid metabolites, providing insights into the mechanism of BMD loss in asthma patients taking glucocorticoids. These results suggested that a combination of multi-block associative variable selection with multi-block orthogonal projection and interactive visualization techniques could generate hypotheses from multi-omics studies and inform biology (135). Yier et al (51) studied the anti-OP effects of oleanolic acid and used metabolomics methods to predict the mechanism of action. Oleanolic acid and methionine, cysteine metabolism, isoleucine, valine, phenylalanine, tryptophan, leucine and tyrosine biosynthesis, linoleic acid metabolism and other metabolic pathways were significantly affected. Using the new analytical platform, they will further understand the relationship between the therapeutic effect of oleanolic acid in improving OP and glucocorticoid-induced lipid metabolism, molecular transport, and metabolic changes in rats with dysglycemia.

The combination of metabolomic and metallomic methods to study OP is also one of the research hotspots in recent years. Tao et al (136) developed metabolomic and metallomic methods to explain the biochemical basis of the anti-OP effects of salt and raw achyranthes. Iron, manganese, zinc, glycine, ammonia cycle, alanine metabolism, arginine, galactose metabolism, copper, selenium, serine metabolism, lactose degradation, proline metabolism and urea cycle were increased. The combination of metabolomics and metallomics with pattern recognition and enrichment analysis of metabolites provided a useful tool for revealing the mechanism of action of traditional Chinese medicine. As a Chinese medicine prescription for clinical treatment of OP, it had the function of improving renal function and strengthening muscles and bones. Metabolic analysis identified 17 potential biomarkers associated with OP, including β -aminobutyric acid, glucose, arachidonic acid, and malic acid. Metallomic analysis showed that there were seven metal elements in rat kidney tissue: arsenic, iron, manganese, barium, molybdenum, selenium, and zinc. Metabolic pathways mainly included amino acid metabolism and glycolysis of the neurotransmitter. The combination of renal metabolomics and metallomics could effectively supplement the study of urine and blood metabolomics, which can not only effectively explore the pathogenesis of OP, but also explore the therapeutic mechanism of Gushudan on the disease (137).

Using bioinformatics methods, it was found that osteoblast differentiation was associated with an increased requirement for proline, and highlighted the strong demand of proline for osteoblast differentiation and bone formation (138). Kodriˇc et al. combined a variety of perspectives, including metabolomics, transcriptomics, proteomics, and genomics. The intersections were then analyzed to identify the common pathways or molecules that played an important role in OP prediction, prevention, diagnosis, or treatment (139). Combined with cell metabolomics and network biology analysis, fatty acid metabolism and galactose metabolism might be the main pathways affected by jujube side treatment (140). The pharmacological effects of naringin on OP remain unclear. Metabolomics analysis showed that 21 species were significantly regulated by naringin, including: pyruvate, amino acids, glycerophospholipids, polyunsaturated fatty acid metabolism, etc. Naringin was associated with changes in expression of 13 important protein targets by network predictive pharmacologic analysis. This revealed that the combination of network pharmacology and high-throughput metabolomics can further explore the metabolic mechanism (141). Heat exposure improves BMD and thus strength in castrated mice, primarily due to improved trabecular bone thickness, bone connection density, and bone volume. Comprehensive metabolomics and metagenomic analysis showed that temperature promoted bacterial polyamines biosynthesis, resulting in increased levels of total polyamines *in vivo*. The results of the study showed that the supplementation of spermidine enhanced bone density, and at the same time, the synthesis of polyamines in the body was inhibited (81). Tween-2 decoction is a Mongolian medicine for postmenopausal OP rats. Researchers combine untargeted metabolomics and network pharmacology and identified three key protein targets - hydroxysteroid dehydrogenase, cytochrome, and vitamin D receptors. Network pharmacology suggested that major changes in vitamin B6 metabolism were related to vitamin D receptor targets. Thus, Tween-2 decoction on postmenopausal OP rats might be related to down-regulation of vitamin D receptor (142).

In conclusion, the organic combination of metabolomics and bioinformatics, genetics, genomics, transcriptome, proteome, network biology, metagenomics, network pharmacology has made a lot of progress, realizing the systematic exploration of OP prevention, detection, and treatment (135, 137, 139, 141).

8. Challenges of clinical translation of metabolomics in OP research

Over the past decade, metabolomics has been increasingly used to identify biomarkers in disease and is currently considered a very powerful tool with great clinical translational potential (143). The development and utilization of metabolomics has enabled in-depth study of the metabolic characteristics of clinical disease, thereby optimizing disease mechanism exploration, prevention, prediction, and treatment monitoring. In theory, metabolomics can target metabolic therapy based on the metabolic dependence of OP to improve the specificity of clinical treatment (48, 49). From disease prediction to treatment, metabolomics opens new opportunities for comprehensive OP research. However, the clinical development and mass application of metabolomics still need to overcome some challenges and difficulties.

So far, non-targeted and targeted metabolomics have been widely used in OP disease mechanism and treatment research, especially natural Chinese herbal medicine. However, they need to overcome many obstacles and challenges before they can achieve clinical translation and widespread application (144). To overcome these drawbacks, a variety of complementary methods should be adopted to conduct metabolome research. At this time, more advanced instruments and platforms are required, which are difficult to achieve in both clinical and general laboratories. After obtaining a large amount of data, professional data processing and analysis software is often required, which requires certain professional skills of analysts, especially for non-targeted metabolomics. During data analysis, when the choice of the peak selection algorithm is changed, the data results will vary slightly. In addition, rational and rigorous experimental design is essential for analyzing large metabolomic datasets, which is also critical for the choice of statistical analysis (1, 57, 58). Therefore, targeting large-scale metabolomics research and clinical practice requires interdisciplinary collaboration and efforts of biologists, statisticians, and chemists. It is worth noting that, because metabolomics requires more high-end instrument platforms and specialized data processing algorithms, how to achieve standardization of clinical-level laboratory execution is crucial. In addition, the uniform standardization of institutional reporting and data analysis for metabolomics is another important challenge. Currently, most metabolomics studies produce relatively quantitative results. Absolute quantification is critical when normalizing across platforms. Previously, the Metabolomics Association had launched a standards initiative for a unified standard for metabolomics data communication. However, many published datasets still fall short of these criteria due to a lack of consensus among laboratories (145).

The results suggest that metabolomics can be used for prevention and diagnostic clinical treatment of OP. According to the results of a series of studies, these metabolites are indeed associated with OP. However, it remains to be determined whether these differential metabolites play a causal role in the pathogenic and pharmacological mechanisms of OP or are merely early manifestations of preclinical disease (57, 64). Therefore, patients with other diseases within 2 years of OP diagnosis should be excluded when exploring whether these differential metabolites play a direct causal role. In addition, the key point is that metabolomics generally uses plasma, urine, etc. of organisms for more overall evaluation and detection. At this time, it is difficult to distinguish between the metabolome changes caused by OP and those caused by other factors (146). Therefore, metabolomic analysis needs to effectively address these biological confounding effects in order to be better utilized in various studies of OP.

9. Conclusions

OP is a systemic metabolic disease. Metabolomics can effectively reveal the specific metabolic mechanisms of OP and the metabolic trajectories related to treatment response. In this review, the metabolomics of OP pathogenesis and metabolomics of natural herbal medicine are elaborated and summarized systematically. Some clinical translational studies have shown that metabolomics is a valuable tool to predict the therapeutic effect of osteoprotective agents and natural herbal medicine on OP recovery or to evaluate their side effects on normal bone function. In addition, metabolomics combined with gut microbiota studies have provided convincing evidence in the study of OP metabolism. In the future, the integration of gut microbiota and host may lead to more research breakthroughs and clinical application in the OP study. Therefore, metabolomics has good exploration value and clinical transformation prospect in many fields with many advantages in the study of OP.

However, the application of metabolomics in OP research still has some limitations. The multiple factors such as food intake, microbiota activity, the liver and muscle work together influence the levels of various metabolites. Therefore, which metabolites in urine, plasma, serum, bone tissue of OP patients can accurately reflect the development of OP in clinical application is still in the urgent exploration stage. In addition, the clinical transformation limitations of metabolomics are further reflected by the cellular heterogeneity. Thus, what metabolomics has in common with other omics approaches is

that each technique alone does not capture a complete view of OP. Therefore, it might be helpful to combine metabolomics with other omics studies to further improve its selectivity and the effectiveness of clinical transformation. Further, the results of OP metabolomics may be affected by age, BMI, smoking, physical activity, gender, and other factors. At present, there is a lack of relevant targeted studies, and the extent and mechanism of the effects need to be clarified, which is a series direction for further investigation in the future. It is worth noting that the application of metabolomics technology in common clinical diseases is becoming more and more popular, but its application in the field of OP started late. At present, most of them stay in the stage of animal experiment, there are huge differences between animal experiment and clinical research, and there is still a long distance in clinical transformation.

Author contributions

MC and KY conceived and revised the manuscript. ZZ and ZC wrote the manuscript. AC participated in the literature search and related data sorting during the revision. In addition, all authors contributed to the article and approved the submitted version.

Conflict of interest

The authors declare that the research was conducted in the absence of any commercial or financial relationships that could be construed as a potential conflict of interest.

Publisher's note

All claims expressed in this article are solely those of the authors and do not necessarily represent those of their affiliated organizations, or those of the publisher, the editors and the reviewers. Any product that may be evaluated in this article, or claim that may be made by its manufacturer, is not guaranteed or endorsed by the publisher.

References

1. Yang TL, Shen H, Liu AQ, Dong SS, Zhang L, Deng FY, et al. A road map for understanding molecular and genetic determinants of osteoporosis. *Nat Rev Endocrinol* (2020) 16:91–103. doi: 10.1038/s41574-019-0282-7

2. Compston JE, McClung MR, Leslie WD. Osteoporosis. *Lancet* (2019) 393:364–76. doi: 10.1016/S0140-6736(18)32112-3

3. Noh JY, Yang Y, Jung H. Molecular mechanisms and emerging therapeutics for osteoporosis. *Int J Mol Sci* (2020) 21:7623. doi: 10.3390/ijms21207623

4. Khosla S, Hopbauer LC. Osteoporosis treatment: recent developments and ongoing challenges. *Lancet Diabetes Endocrinol* (2017) 5:898–907. doi: 10.1016/S2213-8587(17)30188-2

5. Curry SJ, Krist AH, Owens DK, Barry MJ, Caughey AB, Davidson KW, et al. Screening for osteoporosis to prevent fractures US preventive services task force recommendation statement. *Jama-Journal Am Med Assoc* (2018) 319:2521–31. doi: 10.1001/jama.2018.7498

6. Swank KR, Furness JE, Baker EA, Gehrke CK, Biebelhausen SP, Baker KC. Metabolomic profiling in the characterization of degenerative bone and joint diseases. *Metabolites* (2020) 10:223. doi: 10.3390/metabo10060223

7. Black DM, Rosen CJ. Clinical practice. postmenopausal osteoporosis. *New Engl J Med* (2016) 374:254–62. doi: 10.1056/NEJMcp1513724

8. Miller PD. Management of severe osteoporosis. *Expert Opin pharmacotherapy* (2016) 17:473–88. doi: 10.1517/14656566.2016.1124856

9. Kerschan-Schindl K. Prevention and rehabilitation of osteoporosis. *Wiener medizinische Wochenschrift (1946)* (2016) 166:22–7. doi: 10.1007/s10354-015-0417-y

10. Dominguez LJ, Farruggia M, Veronese N, Barbagallo M. Vitamin d sources, metabolism, and deficiency: Available compounds and guidelines for its treatment. *Metabolites* (2021) 11:255. doi: 10.3390/metabo11040255

11. Chandra A, Rajawat J. Skeletal aging and osteoporosis: Mechanisms and therapeutics. *Int J Mol Sci* (2021) 22:3553. doi: 10.3390/ijms22073553

12. Marra M, Sammarco R, De Lorenzo A, Iellamo F, Siervo M, Pietrobelli A, et al. Assessment of body composition in health and disease using bioelectrical impedance analysis (BIA) and dual energy X-ray absorptiometry (DXA): A critical overview. *Contrast media Mol Imaging* (2019) 2019:3548284. doi: 10.1155/2019/3548284

13. Laskey MA. Dual-energy X-ray absorptiometry and body composition. *Nutr (Burbank Los Angeles County Calif.)* (1996) 12:45–51. doi: 10.1016/0899-9007(95)00017-8

14. Anthamatten A, Parish A. Clinical update on osteoporosis. *J midwifery women's Health* (2019) 64:265–75. doi: 10.1111/jmwh.12954

15. Arceo-Mendoza RM, Camacho PM. Postmenopausal osteoporosis: Latest guidelines. *Endocrinol Metab Clinics North America* (2021) 50:167–78. doi: 10.1016/j.ecl.2021.03.009

16. Watts NB. Postmenopausal osteoporosis: A clinical review. *J women's Health (2002)* (2018) 27:1093–6. doi: 10.1089/jwh.2017.6706

17. Rinschen MM, Ivanisevic J, Giera M, Siuzdak G. Identification of bioactive metabolites using activity metabolics. *Nat Rev Mol Cell Biol* (2019) 20:353–67. doi: 10.1038/s41580-019-0108-4

18. Muthubharathi BC, Gowripriya T, Balamurugan K. Metabolomics: small molecules that matter more. *Mol Omics* (2021) 17:210–29. doi: 10.1039/D0MO00176G

19. Wishart DS. NMR metabolomics: A look ahead. *J magnetic resonance (San Diego Calif. 1997)* (2019) 306:155–61. doi: 10.1016/j.jmr.2019.07.013

20. Fan J, Jahed V, Klavins K. Metabolomics in bone research. *Metabolites* (2021) 11:343. doi: 10.3390/metabo11070434

21. Yang YJ, Kim DJ. An overview of the molecular mechanisms contributing to musculoskeletal disorders in chronic liver disease: Osteoporosis, sarcopenia, and osteoporotic sarcopenia. *Int J Mol Sci* (2021) 22:2604. doi: 10.3390/ijms22052604

22. Si J, Wang C, Zhang D, Wang B, Zhou Y. Osteopontin in bone metabolism and bone diseases. *Med Sci monitor Int Med J Exp Clin Res* (2020) 26:e919159. doi: 10.12659/MSM.919159

23. Suzuki A, Minamide M, Iwaya C, Ogata K, Iwata J. Role of metabolism in bone development and homeostasis. *Int J Mol Sci* (2020) 21:8992. doi: 10.3390/ijms21238992

24. Moayyeri A, Cheung CL, Tan KC, Morris JA, Cerani A, Mohney RP, et al. Metabolomic pathways to osteoporosis in middle-aged women: A genome-Metabolome-Wide mendelian randomization study. *J Bone mineral Res Off J Am Soc Bone Mineral Res* (2018) 33:643–50. doi: 10.1002/jbmr.3358

25. Gong R, Xiao HM, Zhang YH, Zhao Q, Su KJ, Lin X, et al. Identification and functional characterization of metabolites for bone mass in peri- and postmenopausal Chinese women. *J Clin Endocrinol Metab* (2021) 106:e3159–77. doi: 10.1210/clinem/dgab146

26. He J, Xu S, Zhang B, Xiao C, Chen Z, Si F, et al. Gut microbiota and metabolite alterations associated with reduced bone mineral density or bone metabolic indexes in postmenopausal osteoporosis. *Aging* (2020) 12:8583–604. doi: 10.18632/aging.103168

27. Wen K, Tao L, Tao Z, Meng Y, Zhou S, Chen J, et al. Fecal and serum metabolomic signatures and microbial community profiling of postmenopausal osteoporosis mice model. *Front Cell infection Microbiol* (2020) 10:535310. doi: 10.3389/fcimb.2020.535310

28. Greenbaum J, Lin X, Su KJ, Gong R, Shen H, Shen J, et al. Integration of the human gut microbiome and serum metabolome reveals novel biological factors involved in the regulation of bone mineral density. *Front Cell infection Microbiol* (2022) 12:853499. doi: 10.3389/fcimb.2022.853499

29. Miyamoto T, Hirayama A, Sato Y, Koboyashi T, Katsuyama E, Kanagawa H, et al. A serum metabolomics-based profile in low bone mineral density postmenopausal women. *Bone* (2017) 95:1–4. doi: 10.1016/j.bone.2016.10.027

30. Li X, Wang Y, Gao M, Bao B, Cao Y, Cheng F, et al. Metabolomics-driven of relationships among kidney, bone marrow and bone of rats with postmenopausal osteoporosis. *Bone* (2022) 156:116306. doi: 10.1016/j.bone.2021.116306

31. Watanabe K, Iida M, Harada S, Kato S, Kuwabara K, Kurihara A, et al. Metabolic profiling of charged metabolites in association with menopausal status in Japanese community-dwelling midlife women: Tsuruoka metabolomic cohort study. *Maturitas* (2022) 155:54–62. doi: 10.1016/j.maturitas.2021.10.004

32. Mishra BH, Mishra PP, Mononen N, Hilvo M, Sievänen H, Juonala M, et al. Uncovering the shared lipidomic markers of subclinical osteoporosis-atherosclerosis comorbidity: The young finns study. *Bone* (2021) 151:116030. doi: 10.1016/j.bone.2021.116030

33. Qiu C, Yu F, Su K, Zhao Q, Zhang L, Xu C, et al. Multi-omics data integration for identifying osteoporosis biomarkers and their biological interaction and causal mechanisms. *iScience* (2020) 23:100847. doi: 10.1016/j.isci.2020.100847

34. Ye J, Chi X, Wang J, Shen Z, Li S, Xu S. High fat induces activation of the tryptophan-ERK-CREB pathway and promotes bone absorption in cage layers. *Poultry Sci* (2021) 100:101149. doi: 10.1016/j.psj.2021.101149

35. Lu L, Tang M, Li J, Xie Y, Li Y, Xie J, et al. Gut microbiota and serum metabolic signatures of high-Fat-Induced bone loss in mice. *Front Cell infection Microbiol* (2021) 11:788576. doi: 10.3389/fcimb.2021.788576

36. Kang H, Guo Q, Dong Y, Peng R, Song K, Wang J, et al. Inhibition of MAT2A suppresses osteoclastogenesis and prevents ovariectomy-induced bone loss. *FASEB J Off Publ Fed Am Societies Exp Biol* (2022) 36:e22167. doi: 10.1096/fj.202101205RR

37. Baba M, Endoh M, Ma W, Toyama H, Hirayama A, Nishikawa K, et al. Folliculin regulates osteoclastogenesis through metabolic regulation. *J Bone mineral Res Off J Am Soc Bone Mineral Res* (2018) 33:1785–98. doi: 10.1002/jbmr.3477

38. Cabrera D, Kruger M, Wolber FM, Roy NC, Fraser K. Effects of short- and long-term glucocorticoid-induced osteoporosis on plasma metabolome and lipidome of ovariectomized sheep. *BMC musculoskeletal Disord* (2020) 21:349. doi: 10.1186/s12891-020-03362-7

39. Porter FD, Herman GE. Malformation syndromes caused by disorders of cholesterol synthesis. *J Lipid Res* (2011) 52:6–34. doi: 10.1194/jlr.R009548

40. Song Y, Liu J, Zhao K, Gao L, Zhao J. Cholesterol-induced toxicity: An integrated view of the role of cholesterol in multiple diseases. *Cell Metab* (2021) 33:1911–25. doi: 10.1016/j.cmet.2021.09.001

41. Christianson MS, Shen W. Osteoporosis prevention and management: nonpharmacologic and lifestyle options. *Clin obstetrics gynecology* (2013) 56:703–10. doi: 10.1097/GRF.0b013e3182a9d15a

42. Lee WC, Guntur AR, Long F, Rosen CJ. Energy metabolism of the osteoblast: Implications for osteoporosis. *Endocrine Rev* (2017) 38:255–66. doi: 10.1210/er.2017-00064

43. Wang Y, Deng P, Liu Y, Wu Y, Chen Y, Guo Y, et al. Alpha-ketoglutarate ameliorates age-related osteoporosis *via* regulating histone methylations. *Nat Commun* (2020) 11:5596. doi: 10.1038/s41467-020-19360-1

44. Burda P, Hochuli M. Hepatic glycogen storage disorders: what have we learned in recent years? *Curr Opin Clin Nutr Metab Care* (2015) 18:415–21. doi: 10.1097/MCO.0000000000000181

45. Turner RT, Maran A, Lotinun S, Hefferan T, Evans GL, Zhang M, et al. Animal models for osteoporosis. *Rev endocrine Metab Disord* (2001) 2:117–27. doi: 10.1023/A:1010067326811

46. Komori T. Animal models for osteoporosis. *Eur J Pharmacol* (2015) 759:287–94. doi: 10.1016/j.ejphar.2015.03.028

47. Zhang Z, Ren H, Shen G, Qiu T, Liang D, Yang Z, et al. Animal models for glucocorticoid-induced postmenopausal osteoporosis: An updated review. *Biomedicine pharmacotherapy = Biomedecine pharmacotherapie* (2016) 84:438–46. doi: 10.1016/j.biopha.2016.09.045

48. Miyamoto T, Hirayama A, Sato Y, Koboyashi T, Katsuyama E, Kanagawa H, et al. Metabolomics-based profiles predictive of low bone mass in menopausal women. *Bone Rep* (2018) 9:11–8. doi: 10.1016/j.bonr.2018.06.004

49. Lv H, Jiang F, Guan D, Lu C, Guo B, Chan C, et al. Metabolomics and its application in the development of discovering biomarkers for osteoporosis research. *Int J Mol Sci* (2016) 17:2018. doi: 10.3390/ijms17122018

50. Zhang M, Wang Y, Zhang Q, Wang C, Zhang D, Wan JB, et al. UPLC/Q-TOF-MS-based metabolomics study of the anti-osteoporosis effects of achyranthes bidentata polysaccharides in ovariectomized rats. *Int J Biol macromolecules* (2018) 112:433–41. doi: 10.1016/j.ijbiomac.2018.01.204

51. Xu Y, Chen S, Yu T, Qiao J, Sun G. High-throughput metabolomics investigates anti-osteoporosis activity of oleanolic acid *via* regulating metabolic networks using ultra-performance liquid chromatography coupled with mass spectrometry. *Phytomedicine Int J phytotherapy phytopharmacology* (2018) 51:68–76. doi: 10.1016/j.phymed.2018.09.235

52. Shi Z, Zou S, Shen Z, Luan F, Yan J. High-throughput metabolomics using UPLC/Q-TOF-MS coupled with multivariate data analysis reveals the effect and mechanism of syringin against ovariectomized osteoporosis. *J chromatography B Analytical Technol Biomed Life Sci* (2021) 1183:122957. doi: 10.1016/j.jchromb.2021.122957

53. Wishart DS. Emerging applications of metabolomics in drug discovery and precision medicine. *Nat Rev Drug Discovery* (2016) 15:473–84. doi: 10.1038/nrd.2016.32

54. Musilova J, Glatz Z. Metabolomics - basic concepts, strategies and methodologies. *Chem Listy* (2011) 105:745–51.

55. Alseekh S, Aharoni A, Brotman Y, Contrepois K, D'Auria J, J. Ewald CEJ, et al. Mass spectrometry-based metabolomics: a guide for annotation, quantification and best reporting practices. *Nat Methods* (2021) 18:747–56. doi: 10.1038/s41592-021-01197-1

56. Johnson CH, Ivanisevic J, Siuzdak G. Metabolomics: beyond biomarkers and towards mechanisms. *Nat Rev Mol Cell Biol* (2016) 17:451–9. doi: 10.1038/nrm.2016.25

57. Podgórska B, Wielgórska-Partyka M, Godzień J, Siemińska J, Ciborowski M, Szelachowska M, et al. Applications of metabolomics in calcium metabolism disorders in humans. *Int J Mol Sci* (2022) 23:10407. doi: 10.3390/ijms231810407

58. Yan M, Xu G. Current and future perspectives of functional metabolomics in disease studies-a review. *Anal Chim Acta* (2018) 1037:41–54. doi: 10.1016/j.aca.2018.04.006

59. You YS, Lin CY, Liang HJ, Lee SH, Tsai KS, Chiou JM, et al. Association between the metabolome and low bone mineral density in Taiwanese women determined by (1)H NMR spectroscopy. *J Bone mineral Res Off J Am Soc Bone Mineral Res* (2014) 29:212–22. doi: 10.1002/jbmr.2018

60. Wishart DS, Cheng LL, Copié V, Edison AS, Eghbalnia HR, Hoch JC, et al. NMR and metabolomics-a roadmap for the future. *Metabolites* (2022) 12:678. doi: 10.3390/metabo12080678

61. Ramautar R, de Jong GJ. Recent developments in liquid-phase separation techniques for metabolomics. *Bioanalysis* (2014) 6:1011–26. doi: 10.4155/bio.14.51

62. Chen CJ, Lee DY, Yu J, Lin YN, Lin TM. Recent advances in LC-MS-based metabolomics for clinical biomarker discovery. *Mass spectrometry Rev* (2022): e21785. doi: 10.1002/mas.21785

63. Chen Y, Li EM, Xu LY. Guide to metabolomics analysis: A bioinformatics workflow. *Metabolites* (2022) 12:357. doi: 10.3390/metabo12040357

64. D'Alessandro A, Giardina B, Gevi F, Timperio AM, Zolla L. Clinical metabolomics: the next stage of clinical biochemistry. *Blood Transfusion* (2012) 10:S19–24. doi: 10.2450/2012.005S

65. Li J, Chen X, Lu L, Yu X. The relationship between bone marrow adipose tissue and bone metabolism in postmenopausal osteoporosis. *Cytokine Growth factor Rev* (2020) 52:88–98. doi: 10.1016/j.cytogfr.2020.02.003

66. Armas LA, Recker RR. Pathophysiology of osteoporosis: new mechanistic insights. *Endocrinol Metab Clinics North America* (2012) 41:475–86. doi: 10.1016/j.ecl.2012.04.006

67. Lu X, Chen Y, Wang H, Bai Y, Zhao J, Zhang X, et al. Integrated lipidomics and transcriptomics characterization upon aging-related changes of lipid species and pathways in human bone marrow mesenchymal stem cells. *J Proteome Res* (2019) 18:2065–77. doi: 10.1021/acs.jproteome.8b00936

68. Kilpinen L, Tigistu-Sahle F, Oja S, Greco D, Parmar A, Saavalainen P, et al. Aging bone marrow mesenchymal stromal cells have altered membrane

glycerophospholipid composition and functionality. *J Lipid Res* (2013) 54:622–35. doi: 10.1194/jlr.M030650

69. Zhang X, Xu H, Li GH, Long MT, Cheung CL, Vasan RS, et al. Metabolomics insights into osteoporosis through association with bone mineral density. *J Bone mineral Res Off J Am Soc Bone Mineral Res* (2021) 36:729–38. doi: 10.1002/jbmr.4240

70. Cabrera D, Kruger M, Wolber FM, Roy NC, Totman JJ, Henry CJ, et al. Association of plasma lipids and polar metabolites with low bone mineral density in Singaporean-Chinese menopausal women: A pilot study. *Int J Environ Res Public Health* (2018) 15:1045. doi: 10.3390/ijerph15051045

71. Yu L, Qi H, An G, Bao J, Ma B, Zhu J, et al. Association between metabolic profiles in urine and bone mineral density of pre- and postmenopausal Chinese women. *Menopause (New York N.Y.)* (2019) 26:94–102. doi: 10.1097/GME.0000000000001158

72. Qi H, Bao J, An G, Ouyang G, Zhang P, Wang C, et al. Association between the metabolome and bone mineral density in pre- and post-menopausal Chinese women using GC-MS. *Mol Biosyst* (2016) 12:2265–75. doi: 10.1039/C6MB00181E

73. Miyamoto K, Hirayama A, Sato Y, Ikeda S, Maruyama M, Soga T, et al. A metabolomic profile predictive of new osteoporosis or sarcopenia development. *Metabolites* (2021) 11:278. doi: 10.3390/metabo11050278

74. Aleidi SM, Alnehmi EA, Alshaker M, Masood A, Benabdelkamel H, Al-Ansari MM, et al. A distinctive human metabolomics alteration associated with osteopenic and osteoporotic patients. *Metabolites* (2021) 11:628. doi: 10.3390/metabo11090628

75. Liang WD, Huang PJ, Xiong LH, Zhou S, Ye RY, Liu JR, et al. Metabolomics and its application in the mechanism analysis on diabetic bone metabolic abnormality. *Eur Rev Med Pharmacol Sci* (2020) 24:9591–600. doi: 10.26355/eurrev_202009_23047

76. Erben RG, Mosekilde L, Thomsen JS, Weber K, Stahr K, Leyshon A, et al. Prevention of bone loss in ovariectomized rats by combined treatment with risedronate and 1alpha,25-dihydroxyvitamin D3. *J Bone mineral Res Off J Am Soc Bone Mineral Res* (2002) 17:1498–511. doi: 10.1359/jbmr.2002.17.8.1498

77. Elsayyad NME, Gomaa I, Salem MA, Amer R, El-Laithy HM. Efficient lung-targeted delivery of risedronate sodium/vitamin D3 conjugated PAMAM-G5 dendrimers for managing osteoporosis: Pharmacodynamics, molecular pathways and metabolomics considerations. *Life Sci* (2022) 309:121001. doi: 10.1016/j.lfs.2022.121001

78. Chen SY, Yu HT, Kao JP, Yang CC, Chiang SS, Mishchuk DO, et al. Consumption of vitamin D2 enhanced mushrooms is associated with improved bone health. *J Nutr Biochem* (2015) 26:696–703. doi: 10.1016/j.jnutbio.2015.01.006

79. Wang M, Yang X, Wang F, Li R, Ning H, Na L, et al. Calcium-deficiency assessment and biomarker identification by an integrated urinary metabonomics analysis. *BMC Med* (2013) 11:86. doi: 10.1186/1741-7015-11-86

80. Mao H, Wang W, Shi L, Chen C, Han C, Zhao J, et al. Metabolomics and physiological analysis of the effect of calcium supplements on reducing bone loss in ovariectomized rats by increasing estradiol levels. *Nutr Metab* (2021) 18:76. doi: 10.1186/s12986-021-00602-y

81. Chevalier C, Kieser S, Çolakoğlu M, Hadadi N, Brun J, Rigo D, et al. Warmth prevents bone loss through the gut microbiota. *Cell Metab* (2020) 32:575–590.e7. doi: 10.1016/j.cmet.2020.08.012

82. Pertusa C, Mifsut D, Morales JM, Tarín JJ, Cano A, Monleón D, et al. Metabolomic analysis of severe osteoarthritis in a Spanish population of women compared to healthy and osteoporotic subjects. *Metabolites 12* (2022) 12:677. doi: 10.3390/metabo12080677

83. Värri M, Niskanen L, Tuomainen TP, Honkanen R, Kröger H, Tuppurainen MT. Metabolite profiling of osteoporosis and atherosclerosis in postmenopausal women: A cross-sectional study. *Vasc Health Risk Manage* (2020) 16:515–24. doi: 10.2147/VHRM.S279028

84. He Y, Chen Y. The potential mechanism of the microbiota-gut-bone axis in osteoporosis: a review. *Osteoporosis Int J established as result cooperation between Eur Foundation Osteoporosis Natl Osteoporosis Foundation USA* (2022). doi: 10.1007/s00198-022-06557-x

85. Liu Z, Xu X, Shen Y, Hao Y, Cui W, Li W, et al. Altered gut microbiota and metabolites profile are associated with reduced bone metabolism in ethanol-induced osteoporosis. *Cell Prolif* (2022) 55:e13245. doi: 10.1111/cpr.13245

86. Ling CW, Miao Z, Xiao ML, Zhou H, Jiang Z, Fu Y, et al. The association of gut microbiota with osteoporosis is mediated by amino acid metabolism: Multiomics in a Large cohort. *J Clin Endocrinol Metab* (2021) 106:e3852–64. doi: 10.1210/clinem/dgab492

87. Gong J, He L, Zou Q, Zhao Y, Zhang B, Xia R, et al. Association of serum 25-hydroxyvitamin d (25(OH)D) levels with the gut microbiota and metabolites in postmenopausal women in China. *Microbial Cell factories* (2022) 21:137. doi: 10.1186/s12934-022-01858-6

88. Wang N, Zheng L, Qian J, Wang M, Li L, Huang Y, et al. Salivary microbiota of periodontitis aggravates bone loss in ovariectomized rats. *Front Cell infection Microbiol* (2022) 12:983608. doi: 10.3389/fcimb.2022.983608

89. Xue L, Jiang Y, Han T, Zhang N, Qin L, Xin H, et al. Comparative proteomic and metabolomic analysis reveal the antiosteoporotic molecular mechanism of icariin from epimedium brevicornu maxim. *J ethnopharmacology* (2016) 192:370–81. doi: 10.1016/j.jep.2016.07.037

90. Cheng T, Sheng T, Yi Y, Zhang T, Han H. Metabolism profiles of icariin in rats using ultra-high performance liquid chromatography coupled with quadrupole time-of-flight tandem mass spectrometry and *in vitro* enzymatic study. *J chromatography B Analytical Technol Biomed Life Sci* (2016) 1033-1034:353–60. doi: 10.1016/j.jchromb.2016.09.010

91. Pan S, Chen A, Han Z, Wang Y, Lu X, Yang Y. (1)H NMR-based metabonomic study on the effects of epimedium on glucocorticoid-induced osteoporosis. *J chromatography B Analytical Technol Biomed Life Sci* (2016) 1038:118–26. doi: 10.1016/j.jchromb.2016.10.015

92. Huang J, Hu Y, Tong X, Zhang L, Yu Z, Zhou Z. Untargeted metabolomics revealed therapeutic mechanisms of icariin on low bone mineral density in older caged laying hens. *Food Funct* (2020) 11:3201–12. doi: 10.1039/C9FO02882J

93. Yuan X, Wen J, Jia H, Tong L, Zhao J, Zhao L, et al. Integrated metabolomic analysis for intervention effects of gushudan on glucocorticoid-induced osteoporostic rat plasma based on RP/HILIC-UHPLC-Q-Orbitrap HRMS. *Analytical Biochem* (2020) 591:113559. doi: 10.1016/j.ab.2019.113559

94. Huang Y, Bo Y, Wu X, Wang Q, Qin F, Zhao L, et al. An intergated serum and urinary metabonomic research based on UPLC-MS and therapeutic effects of gushudan on prednisolone-induced osteoporosis rats. *J chromatography B Analytical Technol Biomed Life Sci* (2016) 1027:119–30. doi: 10.1016/j.jchromb.2016.05.019

95. Liu S, Yuan X, Ma C, Zhao J, Xiong Z. (1)H-NMR-based urinary metabolomic analysis for the preventive effects of gushudan on glucocorticoid-induced osteoporosis rats. *Analytical Biochem* (2020) 610:113992. doi: 10.1016/j.ab.2020.113992

96. Wu X, Huang Y, Sun J, Wen Y, Qin F, Zhao L, et al. A HILIC-UHPLC-MS/MS untargeted urinary metabonomics combined with quantitative analysis of five polar biomarkers on osteoporosis rats after oral administration of gushudan. *J chromatography B Analytical Technol Biomed Life Sci* (2018) 1072:40–9. doi: 10.1016/j.jchromb.2017.10.005

97. Tao Y, Chen X, Li W, Cai B, Di L, Shi L, et al. Global and untargeted metabolomics evidence of the protective effect of different extracts of dipsacus asper wall. ex C.B. Clarke on estrogen deficiency after ovariectomia in rats. *J ethnopharmacology* (2017) 199:20–9. doi: 10.1016/j.jep.2017.01.050

98. Wang J, Dong X, Ma F, Li C, Bu R, Lu J, et al. Metabolomics profiling reveals echinops latifolius tausch improves the trabecular micro-architecture of ovariectomized rats mainly *via* intervening amino acids and glycerophospholipids metabolism. *J ethnopharmacology* (2020) 260:113018. doi: 10.1016/j.jep.2020.113018

99. Xia T, Dong X, Lin L, Jiang Y, Ma X, Xin H, et al. Metabolomics profiling provides valuable insights into the underlying mechanisms of morinda officinalis on protecting glucocorticoid-induced osteoporosis. *J Pharm Biomed Anal* (2019) 166:336–46. doi: 10.1016/j.jpba.2019.01.019

100. Jiang YC, Li YF, Zhou L, Zhang DP. UPLC-MS metabolomics method provides valuable insights into the effect and underlying mechanisms of rhizoma drynariae protecting osteoporosis. *J chromatography B Analytical Technol Biomed Life Sci* (2020) 1152:122262. doi: 10.1016/j.jchromb.2020.122262

101. Li H, Chu S, Zhao H, Liu D, Liu X, Qu X, et al. Effect of zishen jiangtang pill, a Chinese herbal product, on rats with diabetic osteoporosis. *Evidence-Based complementary Altern Med eCAM* (2018) 2018:7201914. doi: 10.1155/2018/7201914

102. Miao LY, Chu TTH, Li P, Jiang Y, Li HJ. Cimicifuga heracleifolia is therapeutically similar to black cohosh in relieving menopausal symptoms: evidence from pharmacological and metabolomics studies. *Chin J Natural Medicines* (2019) 17:435–45. doi: 10.1016/S1875-5364(19)30051-2

103. Xiao HH, Sham TT, Chan CO, Li MH, Chen X, Wu QC, et al. A metabolomics study on the bone protective effects of a lignan-rich fraction from sambucus williamsii ramulus in aged rats. *Front Pharmacol* (2018) 9:932. doi: 10.3389/fphar.2018.00932

104. Luo D, Li J, Chen K, Rong X, Guo J. Untargeted metabolomics reveals the protective effect of fufang zhenshu tiaozhi (FTZ) on aging-induced osteoporosis in mice. *Front Pharmacol* (2018) 9:1483. doi: 10.3389/fphar.2018.01483

105. Si Z, Zhou S, Shen Z, Luan F. High-throughput metabolomics discovers metabolic biomarkers and pathways to evaluating the efficacy and exploring potential mechanisms of osthole against osteoporosis based on UPLC/Q-TOF-MS coupled with multivariate data analysis. *Front Pharmacol* (2020) 11:741. doi: 10.3389/fphar.2020.00741

106. Ma YS, Hou ZJ, Li Y, Zheng BB, Wang JM, Wang WB. Unveiling the pharmacological mechanisms of eleutheroside e against postmenopausal osteoporosis through UPLC-Q/TOF-MS-Based metabolomics. *Front Pharmacol* (2020) 11:1316. doi: 10.3389/fphar.2020.01316

107. Xie H, Hua Z, Guo M, Lin S, Zhou Y, Weng Z, et al. Gut microbiota and metabonomics used to explore the mechanism of qing'e pills in alleviating osteoporosis. *Pharm Biol* (2022) 60:785–800. doi: 10.1080/13880209.2022.2056208

108. Xia T, Dong X, Jiang Y, Lin L, Dong Z, Shen Y, et al. Metabolomics profiling reveals rehmanniae radix preparata extract protects against glucocorticoid-induced osteoporosis mainly *via* intervening steroid hormone biosynthesis. *Molecules (Basel Switzerland)* (2019) 24:253. doi: 10.3390/molecules24020253

109. Shen Q, Zhang C, Qin X, Zhang H, Zhang Z, Richel A. Modulation of gut microbiota by chondroitin sulfate calcium complex during alleviation of osteoporosis in ovariectomized rats. *Carbohydr polymers* (2021) 266:118099. doi: 10.1016/j.carbpol.2021.118099

110. Wei Z, Ge F, Che Y, Wu S, Dong X, Song D. Metabolomics coupled with pathway analysis provides insights into sarco-osteoporosis metabolic alterations and estrogen therapeutic effects in mice. *Biomolecules* (2021) 12:41. doi: 10.3390/biom12010041

111. Liu X, Liu Y, Cheng M, Zhang X, Xiao H. A metabolomics study of the inhibitory effect of 17-beta-estradiol on osteoclast proliferation and differentiation. *Mol Biosyst* (2015) 11:635–46. doi: 10.1039/C4MB00528G

112. Liu H, Gu R, Li W, Zhou W, Cong Z, Xue J, et al. Lactobacillus rhamnosus GG attenuates tenofovir disoproxil fumarate-induced bone loss in male mice *via* gut-microbiota-dependent anti-inflammation. *Ther Adv chronic Dis* (2019) 10:2040622319860653. doi: 10.1177/2040622319860653

113. Li P, Sundh D, Ji B, Lappa D, Ye L, Nielsen J, et al. Metabolic alterations in older women with low bone mineral density supplemented with lactobacillus reuteri. *JBMR plus* (2021) 5:e10478. doi: 10.1002/jbm4.10478

114. Shen CL, Mo H, Dunn DM, Watkins BA. Tocotrienol supplementation led to higher serum levels of lysophospholipids but lower acylcarnitines in postmenopausal women: A randomized double-blinded placebo-controlled clinical trial. *Front Nutr* (2021) 8:766711. doi: 10.3389/fnut.2021.766711

115. Lee MY, Kim HY, Singh D, Yeo SH, Baek SY, Park YK, et al. Metabolite profiling reveals the effect of dietary rubus coreanus vinegar on ovariectomy-induced osteoporosis in a rat model. *Molecules (Basel Switzerland)* (2016) 21:149. doi: 10.3390/molecules21020149

116. Wang W, Wang Y, Hu J, Duan H, Wang Z, Yin L, et al. Untargeted metabolomics reveal the protective effect of bone marrow mesenchymal stem cell transplantation against ovariectomy-induced osteoporosis in mice. *Cell Transplant* (2022) 31:9636897221079745. doi: 10.1177/09636897221079745

117. Gao MX, Tang XY, Zhang FX, Yao ZH, Yao XS, Dai Y. Biotransformation and metabolic profile of xian-Ling-Gu-Bao capsule, a traditional Chinese medicine prescription, with rat intestinal microflora by ultra-performance liquid chromatography coupled with quadrupole time-of-flight tandem mass spectrometry analysis. *Biomed Chromatogr BMC* (2018) 32:e4160. doi: 10.1002/bmc.4160

118. Ooijevaar RE, Terveer EM, Verspaget HW, Kuijper EJ, Keller JJ. Clinical application and potential of fecal microbiota transplantation. *Annu Rev Med* (2019) 70:335–51. doi: 10.1146/annurev-med-111717-122956

119. Zhang YW, Cao MM, Li YJ, Lu PP, Dai GC, Zhang M, et al. Fecal microbiota transplantation ameliorates bone loss in mice with ovariectomy-induced osteoporosis *via* modulating gut microbiota and metabolic function. *J orthopaedic translation* (2022) 37:46–60. doi: 10.1016/j.jot.2022.08.003

120. He W, Xie Z, Thøgersen R, Rasmussen MK, Zachariassen LF, Jørgensen NR, et al. Effects of calcium source, inulin, and lactose on gut-bone associations in an ovariectomized rat model. *Mol Nutr Food Res* (2022) 66:e2100883. doi: 10.1002/mnfr.202100883

121. Xiao HH, Lu L, Poon CC, Chan CO, Wang LJ, Zhu YX, et al. The lignan-rich fraction from sambucus williamsii hance ameliorates dyslipidemia and insulin resistance and modulates gut microbiota composition in ovariectomized rats. *Biomedicine pharmacotherapy = Biomedecine pharmacotherapie* (2021) 137:111372. doi: 10.1016/j.biopha.2021.111372

122. Tong L, Feng Q, Lu Q, Zhang J, Xiong Z. Combined (1)H NMR fecal metabolomics and 16S rRNA gene sequencing to reveal the protective effects of gushudan on kidney-yang-deficiency-syndrome rats *via* gut-kidney axis. *J Pharm Biomed Anal* (2022) 217:114843. doi: 10.1016/j.jpba.2022.114843

123. Yin Y, Zhu F, Pan M, Bao J, Liu Q, Tao Y. A multi-omics analysis reveals anti-osteoporosis mechanism of four components from crude and salt-processed achyranthes bidentata blume in ovariectomized rats. *Molecules (Basel Switzerland)* (2022) 27:5012. doi: 10.3390/molecules27155012

124. Kitaura H, Marahleh A, Ohori F, Noguchi T, Shen WR, Qi J, et al. Osteocyte-related cytokines regulate osteoclast formation and bone resorption. *Int J Mol Sci* (2020) 21:5169. doi: 10.3390/ijms21145169

125. An J, Yang H, Zhang Q, Liu C, Zhao J, Zhang L, et al. Natural products for treatment of osteoporosis: The effects and mechanisms on promoting osteoblast-mediated bone formation. *Life Sci* (2016) 147:46–58. doi: 10.1016/j.lfs.2016.01.024

126. Karlamangla AS, Burnett-Bowie SM, Crandall CJ. Bone health during the menopause transition and beyond. *Obstetrics gynecology Clinics North America* (2018) 45:695–708. doi: 10.1016/j.ogc.2018.07.012

127. Eastell R, Szulc P. Use of bone turnover markers in postmenopausal osteoporosis. *Lancet Diabetes Endocrinol* (2017) 5:908–23. doi: 10.1016/S2213-8587(17)30184-5

128. Mangano KM, Noel SE, Lai CQ, Christensen JJ, Ordovas JM, Dawson-Hughes B, et al. Diet-derived fruit and vegetable metabolites show sex-specific inverse relationships to osteoporosis status. *Bone* (2021) 144:115780. doi: 10.1016/j.bone.2020.115780

129. Chau YP, Au PCM, Li GHY, Sing CW, Cheng VKF, Tan KCB, et al. Serum metabolome of coffee consumption and its association with bone mineral density: The Hong Kong osteoporosis study. *J Clin Endocrinol Metab* (2020) 105:dgz210. doi: 10.1210/clinem/dgz210

130. Tian J, Li Z, Wang L, Qiu D, Zhang X, Xin X, et al. Metabolic signatures for safety assessment of low-level cadmium exposure on human osteoblast-like cells. *Ecotoxicology Environ Saf* (2021) 207:111257. doi: 10.1016/j.ecoenv.2020.111257

131. Kong SH, Kim JH, Shin CS. Serum spermidine as a novel potential predictor for fragility fractures. *J Clin Endocrinol Metab* (2021) 106:e582–91. doi: 10.1210/clinem/dgaa745

132. Deng D, Pan C, Wu Z, Sun Y, Liu C, Xiang H, et al. An integrated metabolomic study of osteoporosis: Discovery and quantification of hyocholic acids as candidate markers. *Front Pharmacol* (2021) 12:725341. doi: 10.3389/fphar.2021.725341

133. Wang Z, Bian L, Mo C, Shen H, Zhao LJ, Su KJ, et al. Quantification of aminobutyric acids and their clinical applications as biomarkers for osteoporosis. *Commun Biol* (2020) 3:39. doi: 10.1038/s42003-020-0766-y

134. Wang Y, Ma L, Zhang M, Chen M, Li P, He C, et al. A simple method for peak alignment using relative retention time related to an inherent peak in liquid chromatography-mass spectrometry-based metabolomics. *J chromatographic Sci* (2019) 57:9–16. doi: 10.1093/chromsci/bmy074

135. Reinke SN, Galindo-Prieto B, Skotare T, Broadhurst DI, Singhania A, Horowitz D, et al. OnPLS-based multi-block data integration: A multivariate approach to interrogating biological interactions in asthma. *Analytical Chem* (2018) 90:13400–8. doi: 10.1021/acs.analchem.8b03205

136. Tao Y, Huang S, Yan J, Li W, Cai B. Integrated metallomic and metabolomic profiling of plasma and tissues provides deep insights into the protective effect of raw and salt-processed achyranthes bidentata blume extract in ovariectomia rats. *J ethnopharmacology* (2019) 234:85–95. doi: 10.1016/j.jep.2019.01.033

137. Jia H, Yuan X, Liu S, Feng Q, Zhao J, Zhao L, et al. Integrated renal metabolomic and metallomic profiling revealed protective effect and metabolic mechanism of gushudan on glucocorticoid-induced osteoporotic rat based on GC-MS and ICP-MS. *J Pharm Biomed Anal* (2021) 193:113705. doi: 10.1016/j.jpba.2020.113705

138. Shen L, Yu Y, Zhou Y, Pruett-Miller SM, Zhang GF, Karner CM. SLC38A2 provides proline to fulfill unique synthetic demands arising during osteoblast differentiation and bone formation. *eLife* (2022) 11:e76963. doi: 10.7554/eLife.76963.sa2

139. Kodrič K, Čamernik K, Černe D, Komadina R, Marc J. P4 medicine and osteoporosis: a systematic review. *Wiener klinische Wochenschrift* (2016) 128:480–91. doi: 10.1007/s00508-016-1125-3

140. Wang YF, Chang YY, Zhang XM, Gao MT, Zhang QL, Li X, et al. Salidroside protects against osteoporosis in ovariectomized rats by inhibiting oxidative stress and promoting osteogenesis *via* Nrf2 activation. *Phytomedicine Int J phytotherapy phytopharmacology* (2022) 99:154020. doi: 10.1016/j.phymed.2022.154020

141. Li Y, Liu J, Zhou H, Liu J, Xue X, Wang L, et al. Liquid chromatography-mass spectrometry method for discovering the metabolic markers to reveal the potential therapeutic effects of naringin on osteoporosis. *J chromatography B Analytical Technol Biomed Life Sci* (2022) 1194:123170. doi: 10.1016/j.jchromb.2022.123170

142. Yang F, Dong X, Ma F, Xu F, Liu J, Lu J, et al. The interventional effects of tubson-2 decoction on ovariectomized rats as determined by a combination of network pharmacology and metabolomics. *Front Pharmacol* (2020) 11:581991. doi: 10.3389/fphar.2020.581991

143. Goodpaster BH, Sparks LM. Metabolic flexibility in health and disease. *Cell Metab* (2017) 25:1027–36. doi: 10.1016/j.cmet.2017.04.015

144. Masoodi M, Gastaldelli A, Hyötyläinen T, Arretxe E, Alonso C, Gaggini M, et al. Metabolomics and lipidomics in NAFLD: biomarkers and non-invasive diagnostic tests. *Nat Rev Gastroenterol Hepatol* (2021) 18:835–56. doi: 10.1038/s41575-021-00502-9

145. Cui L, Lu H, Lee YH. Challenges and emergent solutions for LC-MS/MS based untargeted metabolomics in diseases. *Mass spectrometry Rev* (2018) 37:772–92. doi: 10.1002/mas.21562

146. Krautkramer KA, Fan J, Bäckhed F. Gut microbial metabolites as multi-kingdom intermediates. *Nat Rev Microbiol* (2021) 19:77–94. doi: 10.1038/s41579-020-0438-4

*CORRESPONDENCE
Qiuying Yu
yuqiuying131@163.com
Riken Chen
chenriken@126.com
Jinhua Liang
81446069@qq.com

†These authors have contributed
equally to this work

Relationship between obstructive sleep apnea-hypopnea syndrome and osteoporosis adults: A systematic review and meta-analysis

Chaoyu Wang[1,2†], Zhiping Zhang[3†], Zhenzhen Zheng[1†], Xiaojuan Chen[4†], Yu Zhang[5†], Chunhe Li[6], Huimin Chen[7], Huizhao Liao[5], Jinru Zhu[1], Junyan Lin[5], Hongwei Liang[3], Qiuying Yu[2*], Riken Chen[5*] and Jinhua Liang[8*]

[1]Department of Pulmonary and Critical Care Medicine, The Second Affiliated Hospital of Guangdong Medical University, Zhanjiang, Guangdong, China, [2]Department of Pulmonary and Critical Care Medicine, Taishan Hospital of Traditional Chinese Medicine, Jiangmen, Guangdong, China, [3]Department of Pulmonary and Critical Care Medicine, The People's Hospital of JiangMen (Jiangmen Hospital, Southern Medical University), Jiangmen, China, [4]Medical College, Jiaying University, Meizhou, Guangdong, China, [5] State Key Laboratory of Respiratory Disease, National Clinical Research Center for Respiratory Disease, Guangzhou Institute of Respiratory Health, The First Affiliated Hospital of Guangzhou Medical University, Guangzhou, Guangdong, China, [6]Department of Critical Care Medicine, The First Affiliated Hospital of Guangzhou University of Chinese Medicine, Guangzhou, Guangdong, China, [7]Department of Traditional Chinese Medicine, The Second Affiliated Hospital of Guangdong Medical University, Zhanjiang, Guangdong, China, [8]Department of Endocrinology, The Second Affiliated Hospital of Guangdong Medical University, Zhanjiang, Guangdong, China

Objective: This study is undertaken to explore the relationship between obstructive sleep apnea-hypopnea syndrome (OSAHS) and osteoporosis, including the relationship between OSAHS and osteoporosis incidence, lumbar spine bone mineral density (BMD), and lumbar spine T-score.

Method: Cochrane Library, PubMed, Embase, Web of Science, and other databases are searched from their establishment to April 2022. Literature published in 4 databases on the correlation between OSAHS and osteoporosis,lumbar spine BMD,lumbar spine T-score is collected. Review Manager 5.4 software is used for meta-analysis.

Results: A total of 15 articles are selected, including 113082 subjects. Compared with the control group, the OSAHS group has a higher incidence of osteoporosis (OR = 2.03, 95% CI: 1.26~3.27, Z = 2.90, P = 0.004), the lumbar spine BMD is significantly lower (MD = -0.05, 95% CI: -0.08~-0.02, Z = 3.07, P = 0.002), and the lumbar spine T-score is significantly decreased (MD = -0.47, 95% CI: -0.79~-0.14, Z = 2.83, P = 0. 005).

Conclusion: Compared with the control group, the OSAHS group has a higher incidence of osteoporosis and decreased lumbar spine BMD and T-score. In order to reduce the risk of osteoporosis, attention should be paid to the treatment and management of adult OSAHS, and active sleep intervention should be carried out.

1 Introduction

Obstructive sleep apnea-hypopnea syndrome (OSAHS) is a sleep disorder characterized by recurrent episodes of apnea that lead to hypoxia, hypercapnia, and sleep disruption (1). Osteoporosis is a bone metabolism disorder characterized by decreased bone mass, destruction of bone microstructure, and susceptibility to fractures (2). It is generally believed that OSAHS is associated with a higher incidence of osteoporosis (3–5), and spinal deformity is one of its main clinical manifestations, as well as kyphosis, limited spinal extension, etc., causing great distress to the affected population and warranting further research. Several studies have explored the relationship between OSAHS and lumbar osteoporosis. Studies by Liguori, Chen et al. (4, 6) suggest that OSA may be a risk factor in bone mineral density (BMD), leading to osteopenia and osteoporosis. The reason may be that hypoxia slows down the growth of osteoblasts, it promotes the activation of osteoclasts. Sforza et al. (7) showed that the protective effects of intermittent hypoxia on bone metabolism, after taking into account the age-related decrease in BMD, reduced the risk of osteopenia and osteoporosis in elderly people with OSAHS. The results of these studies are inconsistent, which has not only caused great trouble for clinicians, but also affected the prevention and treatment of lumbar osteoporosis in patients with OSAHS. The purpose of this study is to conduct a meta-analysis of existing clinical studies so as to explore the relationship between OSAHS and the occurrence of lumbar osteoporosis and BMD changes, thereby providing evidence-based prevention and intervention for lumbar osteoporosis in patients with medical evidence of OSAHS.

2 Materials and methods

2.1 Retrieval strategy

According to the Meta-analysis of Observational Studies in Epidemiology (MOOSE) statement (8) and the Systematic Review and Meta-analysis report (Preferred Reporting Items for Systematic) Reviews and Meta-Analyses, PRISMA) standard (9). Cochrane Library, PubMed, Embase, and Web of Science databases were searched from their establishment to April 2022. English search terms included Sleep apnea, obstructive, Obstructive Sleep Apnea, Sleep Apnea Hypopnea syndrome, Sleep-related breathing disorder, Osteoporosis, Bone density, Bone mass, Bone loss and Osteo. The protocol was registered in the Prospective Register of Systematic Reviews(Prospero CRD42022339017).

2.2 Literature inclusion and exclusion criteria

Inclusion criteria (1): the subjects of the study were adults over 18 years of age (2); the article types were cohort studies, case-control studies, and cross-sectional studies, observing BMD and T-score in patients with sleep apnea or obstructive sleep apnea, evaluating the incidence or prevalence of osteoporosis, and comparing them with the control group (3); OSAHS was diagnosed by polysomnography or portable sleep monitor, and the severity was evaluated by the apnea hypopnea index (AHI), which is the sum of the average number of apnea and hypopnea events per hour (10) (4); lumbar spine BMD (measured in g/cm^2) and/or T-score were measured by dual energy X-ray densitometer, and osteoporosis was defined as BMD and T-score < -2.5 SD (11) (5); based on different reports from the same research population, the articles with the largest sample sizes were included.

Exclusion criteria (1): languages other than English (2); studies without a control group (3); studies where the effect size cannot be extracted or calculated (4); studies for which the authors did not respond to contact or could not provide meta-analysis data (5); application of glucocorticoids or other drugs that affect BMD.

2.3 Literature screening, quality assessment, and data extraction

Two researchers independently searched, extracted and screened the literature, checked each other's work, and

provided literature with differences to the third researcher for analysis to decide whether or not it should be included. The methodological quality of the included literature was assessed. The quality of the included studies was assessed using the Newcastle-Ottawa Scale (NOS) (12). Only high-quality articles rated higher than 6 stars were included.The extracted data included the first author, study area, publication time, study type, sample size, age, AHI, OSAHS assessment method, BMD, T-score, outcome measures, and adjustment for confounders. After data extraction, the data was checked, and inconsistent data was extracted again. After checking, the data was analyzed.

2.4 Ending and exposure

The lumbar spine BMD (measured in g/cm^2) and/or T-score of the subjects were obtained by dual-energy X-ray densitometry, and OSAHS was diagnosed by polysomnography or portable sleep monitor. The incidence of osteoporosis, BMD, and lumbar spine T-score in the OSAHS group and control group were used as outcome indicators. The difference in the incidence of osteoporosis between the OSAHS group and control group indicated the correlation between OSAHS and osteoporosis; the difference in BMD between the OSAHS group and control group indicated the effect of OSAHS on BMD; when the OSAHS group was compared with the control group, the level of lumbar spine T-score was different, indicating the influence of OSAHS.

2.5 Statistical methods

Statistical analysis was performed using Review Manager 5.4 software. MD and OR values were used for effect evaluation, and 95% CI was calculated. The heterogeneity of the studies was analyzed using the I^2 statistic test and Q test. I^2 < 50% and P > 0.1 indicated no significant heterogeneity among the studies, while I^2 > 50% and P < 0.1 indicated statistical heterogeneity. If there is obvious heterogeneity, the random effect model is used for analysis. Sensitivity analysis can also be conducted to eliminate articles with obvious heterogeneity, and then fixed effect model meta-analysis can be conducted. The presence of publication bias was estimated by funnel plot and Egger's test. For the analysis results with heterogeneity, the included studies will be stratified according to differences in countries and regions, population age differences, gender, and OSAHS severity for subgroup analysis.

3 Results

3.1 Literature screening results

A total of 887 articles were retrieved, 603 were obtained after deduplication, 248 were excluded by reading the titles and

FIGURE 1
Flow diagram of literature screening.
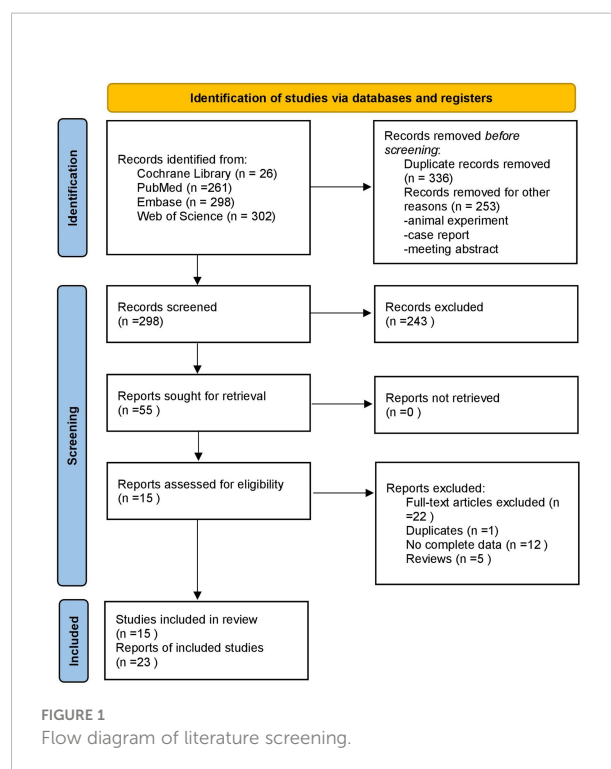
abstracts, and 15 were finally included after reading the full text (Figure 1). The study populations were from China; Taiwan, China; Turkey; Croatia; Italy; and France. The basic characteristics of the literature included in the study are shown in Table 1.

3.2 Quality assessment of included studies

The quality of the included observational studies was assessed using the NOS scale, which is shown in Table 2. The lowest overall rating was 6★ and the highest was 7★, all moderate to high quality, with low to moderate risk of bias, and no studies were excluded for poor quality (< 5★).

3.3 Results

Our results include: ① the relationship between OSAHS and the incidence rate of osteoporosis; ② The relationship between OSAHS and lumbar bone mineral density; ③ The relationship between OSAHS and lumbar T-score. We describe the corresponding statistical results in detail below and we have summarized the effect size value for the mean difference of each study, as shown in Table 3.

3.3.1 Association of OSAHS with osteoporosis incidence

Three studies (4, 13, 14) provided specific numbers of patients with osteoporosis among their study subjects. All

TABLE 1 Basic features of the included studies.

Study	Countryregion	Age	Sample size(/n)	Criteria for OSA	Gender	Research object characteristics
Uzkeser2013 (3)	Turkey	54(37~69)	47	AHI>10events/h	Male	no concomitant disease
Sforza2013 (7)	France	68.6±0.8	832	AHI≥15events/h	M/F	Concomitant DM and HTN
Yen2014 (13)	Taiwan,China	48.9±14.5	90226	ICD-9-CM	M/F	Concomitant DM,HTN,COPD, cancer,etc
Chen2014 (4)	Taiwan,China	>40	21032	ICD-9-CM	M/F	Concomitant DM,HTN, CHD,cancer,etc
ASLAN2015 (14)	Turkey	48.5(40~68)	46	AHI≥6events/h	Male	no concomitant disease
Yuceege2015 (15)	Turkey	35.5±50.7	85	AHI≥15events/h	M/F	no concomitant disease
Terzi2015 (16)	Turkey	52.37±8.58	50	AHI≥5events/h	Male	Concomitant HTN
Wang2015 (17)	Taiwan,China	71.6±8.5	66	AHI≥15events/h	M/F	Concomitant COPD
Liguori2016 (6)	Italy	51.72±11.82	142	AHI>15events/h	Male	no concomitant disease
Chen2017 (18)	China	42.44±11.84	84	AHI≥10events/h	Male	no concomitant disease
Qiao2018 (19)	China	30~65	119	AHI≥5events/h	Male	no concomitant disease
Pazarli2018 (20)	Turkey	48.55±11.8	89	AHI≥5events/h	M/F	no concomitant disease
Ma2018 (21)	China	18~60	68	AHI≥5events/h	Male	no concomitant disease
Vilovic2020 (22)	Croatia	20~65	103	AHI≥15events/h	Male	no concomitant disease
Sadaf2021 (23)	Turkey	48.02±8.435	93	AHI>5events/h	M/F	no concomitant disease

OSA, Obstructive sleep apnea; M/F,Male to Female; BMI, Body Mass Index; CHD,coronary heart disease; DM, Diabetes mellitus; HTN, High Twisted Nematic; COPD, Chronic obstructive pulmonary diseases;
ICD-9-CM, CM International Classification of Diseases, Ninth Revision, Clinical Modification.

three studies were included in the analysis (Figure 2). The results of the heterogeneity test indicated that there was statistical heterogeneity among the studies (P = 0.1, I^2 = 57%), so a random effect model was used. The results showed that compared with the control group, the OSAHS group had a higher incidence of osteoporosis (OR = 2.03, 95% CI: 1.26~3.27, Z = 2.90, P = 0.004).

Two studies (4, 13) provided specific numbers of osteoporosis in men, women, elderly people (> 65 years), and middle-aged people (40~65 years). To reduce the clinical heterogeneity of the study subjects, subgroup analyses were performed by gender (Figure 3) and age (Figure 4). The results showed that, compared with the control group, in the gender subgroup analysis of the OSAHS group, the combined heterogeneity of the two groups was (P = 0.36, I^2 = 7%), and there was no statistically significant heterogeneity among the male group (P = 0.36, I^2 = 7%) = 0.2, I^2 = 38%), female group (P = 0.76, I^2 = 0%), so a fixed effect model was used. After gender subgroup analysis, the heterogeneity of the osteoporosis studies was significantly reduced, male (OR = 1.90, 95% CI: 1.33-2.72, Z = 3.53, P < 0.001), female (OR = 2.56, 95% CI:

TABLE 2 Newcastle−Ottawa Scale of the included studies.

Study	Year	Selection	Comparablity	Exposure	Quality scores
Uzkeser	2013	★★★	★★	★★	7
Sforza	2013	★★★	★★	★	6
Yen	2014	★★★	★	★★	6
Chen	2014	★★★	★	★★	6
ASLAN	2015	★★★	★★	★★	7
Yuceege	2015	★★★	★★	★	6
Terzi	2015	★★★	★★	★	6
Wang	2015	★★★	★★	★★	7
Liguori	2016	★★★	★★	★	6
Chen	2017	★★★	★★	★	6
Qiao	2018	★★★	★★	★	6
Pazarli	2018	★★★	★	★★	6
Ma	2018	★★★	★★	★★	7
Vilovic	2020	★★★★	★★	★	7
Sadaf	2021	★★★	★★	★	6

Each ★ represents a quality score of 1 point, and the sum of all ★ is the final quality score.

**TABLE 3** The effect size value for mean differences of the included studies.

Study	Year	Outcome	Results
Uzkeser	2013	Lumbar Spine BMD	Lumbar Spine BMD:MD=-0.02 (95%CI:-0.09~0.05)
		Lumbar Spine T-score	Lumbar Spine T-score:MD=-0.53 (95%CI:-1.07~-0.01)
Sforza	2013	Lumbar Spine BMD	Lumbar Spine BMD:MD=0.04 (95%CI:-0.14~0.22)
		Lumbar Spine T-score	Lumbar Spine T-score:MD=0.26 (95%CI:0.07~0.4)
Yen	2014	Osteoporosis Incidence	Osteoporosis Incidence:OR=1.60 (95%CI:1.27~2.02)
Chen	2014	Osteoporosis Incidence	Osteoporosis Incidence:OR=2.52 (95%CI:1.58~4.02)
ASLAN	2015	Osteoporosis Incidence	Osteoporosis Incidence:OR=12.69 (95%CI:0.66~244.42)
Yuceege	2015	Lumbar Spine BMD	Lumbar Spine BMD:MD=-0.08 (95%CI:-0.14~-0.02)
		Lumbar Spine T-score	Lumbar Spine T-score:MD=-0.74 (95%CI:-1.26~-0.22)
Terzi	2015	Lumbar Spine BMD	Lumbar Spine BMD:MD=-0.08 (95%CI:-0.16~-0.00)
Wang	2015	Lumbar Spine T-score	Lumbar Spine T-score:MD=-0.72 (95%CI:-1.22~-0.22)
Liguori	2016	Lumbar Spine BMD	Lumbar Spine BMD : MD=-0.13 (95%CI:-0.18~-0.08)
		Lumbar Spine T-score	Lumbar Spine T-score:MD=-1.11 (95%CI:-1.52~-0.70)
Chen	2017	Lumbar Spine BMD	Lumbar Spine BMD : MD=0.01 (95%CI:-0.09~-0.11)
		Lumbar Spine T-score	Lumbar Spine T-score:MD=005 (95%CI:-0.64~0.74)
Qiao	2018	Lumbar Spine BMD	Lumbar Spine BMD : MD=-0.01 (95%CI:-0.09~0.11)
Pazarli	2018	Lumbar Spine BMD	Lumbar Spine BMD : MD=-0.02 (95%CI:-0.04~-0.00)
		Lumbar Spine T-score	Lumbar Spine T-score:MD=-0.15 (95%CI:-0.34~0.04)
Ma	2018	Lumbar Spine BMD	Lumbar Spine BMD : MD=-0.08 (95%CI:-0.13~-0.03)
		Lumbar Spine T-score	Lumbar Spine T-score:MD=-0.59 (95%CI:-1.03~-0.15)
Vilovic	2020	Lumbar Spine BMD	Lumbar Spine BMD : MD=-0.02 (95%CI:-0.11~-0.07)
		Lumbar Spine T-score	Lumbar Spine T-score:MD=-0.23 (95%CI:-0.78~0.32)
Sadaf	2021	Lumbar Spine T-score	Lumbar Spine T-score:MD=-0.99 (95%CI:-1.43~-0.55)

BMD, Bone mineral density.

1.96-3.34, Z = 6.95, P < 0.001), The incidence of osteoporosis in OSAHS group was higher and statistically significant; the combined final effect size of the gender subgroup analysis was (OR = 2.29, 95% CI: 1.86-2.83, Z = 7.68, P < 0.001); The incidence of osteoporosis in OSAHS group is high and statistically significant. In the subgroup analysis of age, the combined heterogeneity of the two groups was (P = 0.19, I^2 = 38%), and there was slight heterogeneity in the statistics. The elderly (> 65 years old) group was (P = 0.69, I^2 = 0%) and the middle-aged (40~65 years old) group was (P = 0.25, I^2 = 24%), so a fixed effect model was used. After age subgroup analysis, the heterogeneity of the osteoporosis studies was significantly

reduced. The elderly (> 65 years old) group was (OR = 2.62, 95% CI: 1.86~3.71, Z = 0.89, P < 0.001) and the middle-aged (40~65 years old) group was (OR = 1.73, 95% CI: 1.31~2.28, Z = 3.31, P < 0.001), so the OSAHS group had a higher incidence of osteoporosis, which was statistically significant. The combined final effect size of the age subgroup analysis was (OR = 2.02, 95% CI: 1.63~2.51, Z = 6.42, P < 0.001); the OSAHS group had a higher incidence of osteoporosis, which was statistically significant.

The forest plot analysis of OSAHS and the incidence of osteoporosis suggest that OSAHS is associated with the prevalence of osteoporosis and is a risk factor for the disease.
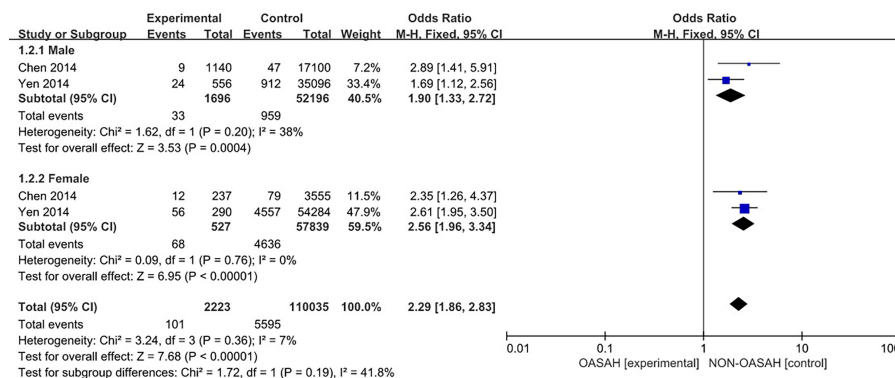

FIGURE 2
Forest plot of the incidence of osteoporosis in OSAHS group and control group.
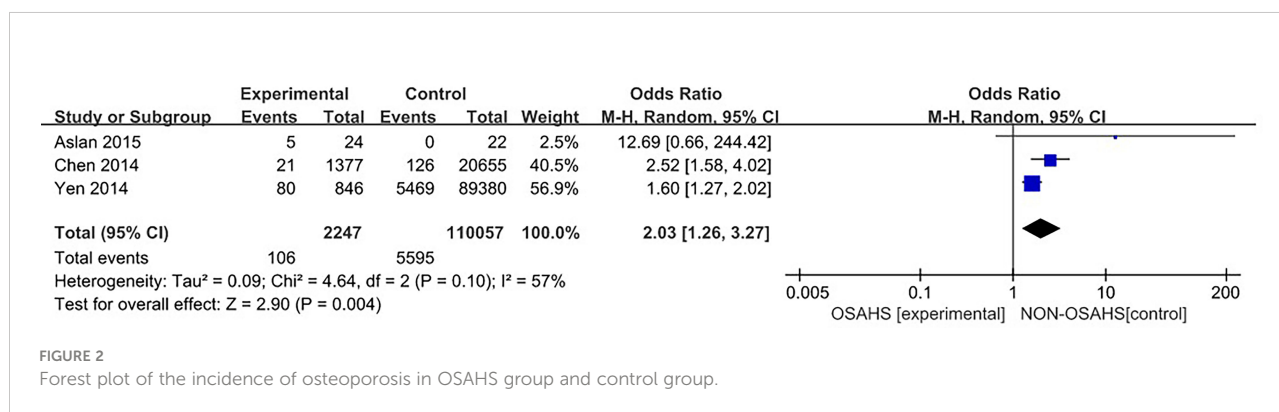
FIGURE 3
Forest plot of incidence of osteoporosis in male and female subgroups.

3.3.2 Association of OSAHS with lumbar spine BMD

Ten studies (3, 6, 7, 15, 16, 18–22) were included in a meta-analysis of lumbar spine BMD (Figure 5). Compared with the control group, lumbar spine BMD was significantly lower in the OSAHS group (MD = -0.05, 95% CI: -0.08~-0.02, Z = 3.07, P = 0.002). There was moderate heterogeneity between studies (I^2 = 66%, P = 0.002), so a random effect model was used. The elderly population is at increased risk for OSAHS (24, 25) due to changes in the anatomy and function of the upper airway (26), and the frequent coexistence of other medical conditions such as diabetes, hypertension, and cardiovascular disease. Meanwhile, BMD gradually decreases with age (27). Risk factors such as old age, diabetes, hypertension, and some diseases that affect osteoporosis may affect the results of osteoporosis research, leading to unstable results for the association between OSAHS and lumbar spine BMD. To further verify the relationship between OSAHS and lumbar spine BMD, and further reduce

the clinical heterogeneity of the study subjects, we conducted a subgroup analysis after excluding osteoporosis-related risk factors, including a subgroup analysis of AHI grouping by OSAHS diagnostic criteria and regional subgroup analysis. The research population of Sforza2013 (7) was older than 65 and accompanied by hypertension, diabetes, and other diseases; in Terzi2015 (16), some of the research subjects had hypertension complications; and all of the above may affect the results of a lumbar spine BMD study.

3.3.2.1 AHI subgroup analysis

In a subgroup analysis of AHI grouping with OSAHS diagnostic criteria (after the exclusion of osteoporosis-related risk factors) (Figure 6), 8 studies were included (3, 6, 15, 18–22), and the groups were combined for heterogeneity (P = 0.001, I^2 = 71%). There was moderate heterogeneity in the statistics. In the subgroup analysis, the OSAHS diagnostic heterogeneity criteria of AHI > 5~10 events/h group was (P = 0.26, I^2 = 24%), and the
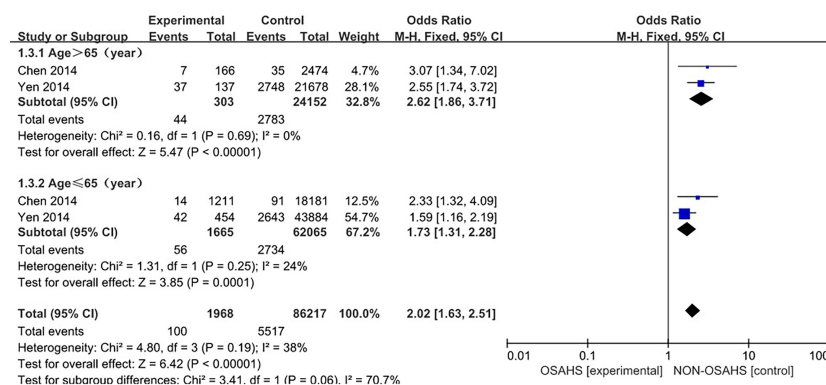

FIGURE 4
Forest plot of the incidence of osteoporosis in elderly (>65 years old) and middle-aged (40-65 years old) subgroups.
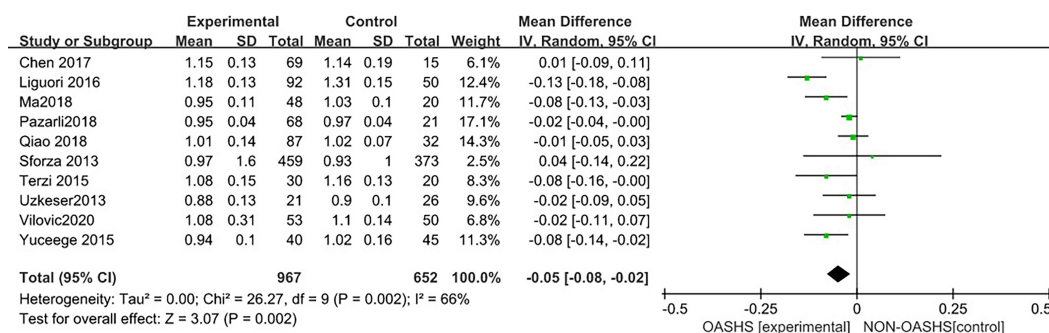
FIGURE 5

Forest plot of lumbar spine bone mineral density between OSAHS group and control group.

grouping heterogeneity of AHI > 15 events/h was (P = 0.09, I^2 = 58%), so a random effect model was used. After the subgroup analysis of OSAHS diagnostic criteria AHI grouping, the correlation between OSAHS and lumbar spine BMD was different. The quality was significantly reduced. The results of subgroup analysis showed that compared with the control group, the lumbar spine BMD of the OSAHS group with AHI > 5~10 events/h was slightly lower (MD = -0.02, 95% CI: -0.05~-0.00, Z = 2.19, P = 0.03), the lumbar spine BMD in the AHI > 15 events/h group was significantly decreased (MD = -0.09, 95% CI: -0.14~-0.03, Z = 3.02, P = 0.003), and the difference was statistically significant. The effect size of lumbar spine BMD in the OSAHS group AHI > 15 events/h was higher than that of the OSAHS diagnostic criteria AHI > 5~10 events/h group, indicating that in patients grouped by OSAHS diagnostic criteria AHI > 15 events/h, compared with AHI > 5~10 events/h, the risk of lumbar BMD decline was higher, so the severity of OSAHS may be related to lumbar BMD. The

combined effect size of the AHI group was (MD = -0.05, 95% CI: -0.08~-0.01, Z = 2.79, P = 0.005). The OSAHS group had lower lumbar spine BMD, the results remained unchanged after excluding risk factors for osteoporosis, and the difference was statistically significant.

3.3.2.2 Regional subgroup analysis

In the regional subgroup analysis (after excluding osteoporosis-related risk factors), (Figure 7), 8 studies were included (3, 6, 15, 18–22), and the combined group heterogeneity was (P = 0.001, I^2 = 71%), indicating moderate statistical heterogeneity. In the subgroup analysis, the grouping heterogeneity in East Asia was (P = 0.08, I^2 = 60%), that in the Middle East was (P = 0.14, I^2 = 49%), and that in Europe was (P = 0.04, I^2 = 77%), so a random effect model was used. The results of the subgroup analysis showed that, compared with the control group, the East Asian group was (MD = -0.03, 95% CI: -0.09~0.02, Z = 1.16, P = 0.25), Middle East group was (MD = -0.04, 95%). CI: -0.07~0.00, Z = 1.89, P = 0.06), and European group was
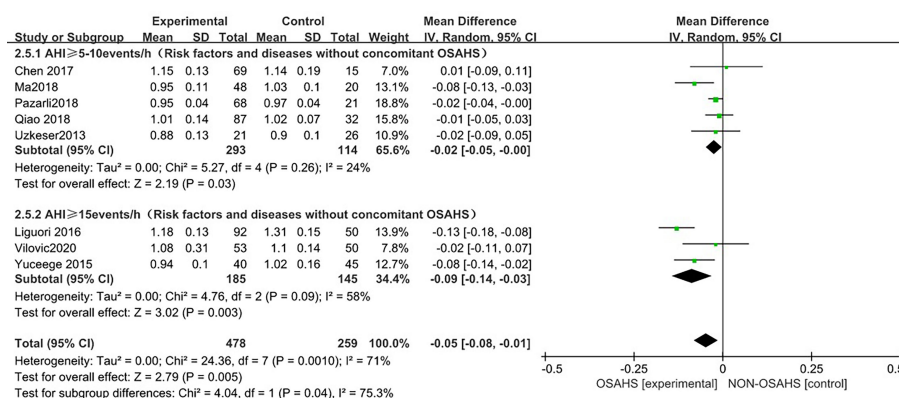

FIGURE 6

Forest plot of subgroup analysis of lumbar spine BMD in OSAHS group and control group by "AHI group" (grouped according to OSAHS diagnostic criteria, after exclusion of osteoporosis-related risk factors).
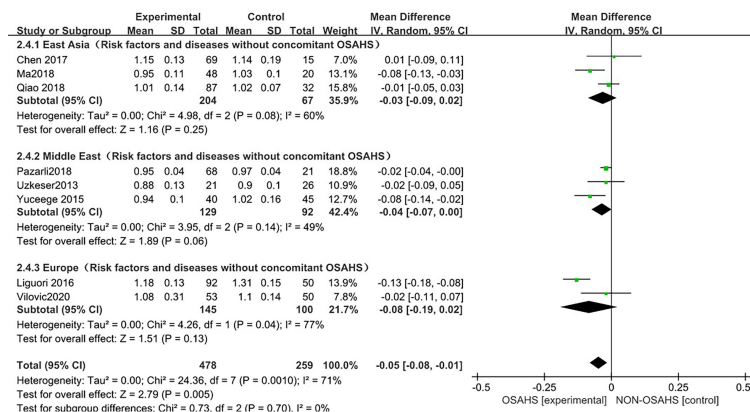
FIGURE 7

Forest plot of subgroup analysis of lumbar spine BMD in OSAHS group and control group (after excluding risk factors related to osteoporosis).

(MD = -0.08, 95% CI: -0.19~0.02, Z = 1.51, P = 0.13), so the lumbar spine BMD was lower in each regional grouping, but the difference was not statistically significant. The combined effect size of the regional grouping was (MD = -0.05, 95% CI: -0.08~-0.01, Z = 2.79, P = 0.005), indicating that the OSAHS group had lower lumbar spine BMD, and the subgroup analysis was performed after excluding osteoporosis risk factors when the results remained stable and the difference was statistically significant.

The forest plot analysis of OSAHS and lumbar spine BMD studies suggested that OSAHS was associated with lumbar spine BMD, OSAHS was a risk factor for the decrease in lumbar spine BMD, and the severity of OSAHS may be related to lumbar spine BMD.

3.3.3 Association of OSAHS with lumbar spine T-score

Ten studies (3, 6, 7, 15, 17, 18, 20–23) were included in the meta-analysis of lumbar spine T-score (Figure 8). Compared

with the control group, the lumbar spine T-score was significantly lower in the OSAHS group (MD = -0.47, 95% CI: -0.79~-0.14, Z = 2.83, P = 0.005). There was high heterogeneity between studies (I^2 = 87%, P < 0.001), so a random effect model was used. Similarly, risk factors such as old age, diabetes, hypertension, and some diseases that affect osteoporosis may affect the results of osteoporosis research, leading unstable results for the association between OSAHS and lumbar spine T-score. In order to further verify the relationship between OSAHS and lumbar spine T-score, and further reduce the clinical heterogeneity of the studies, we conducted a subgroup analysis after excluding risk factors related to osteoporosis, including subgroups grouped by AHI according to the OSAHS diagnostic criteria. The research population of Sforza2013 (7) was older than 65 and accompanied by hypertension, diabetes, and other diseases; the mean age of the research population of Wang2015 (17) was more than 65 and accompanied by chronic obstructive pulmonary disease; as both may affect the results of
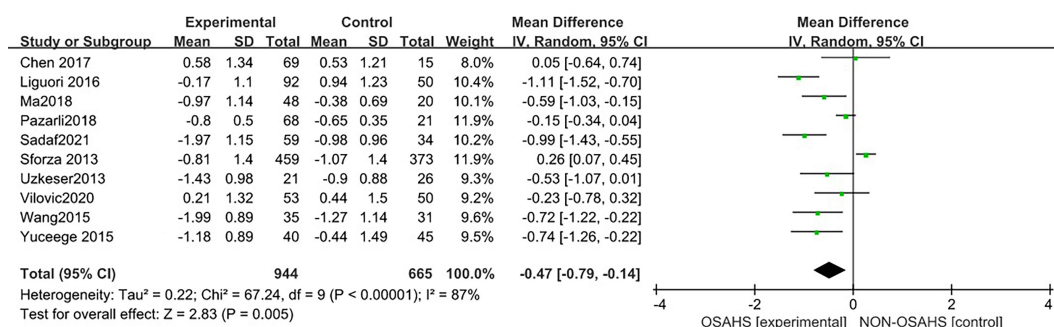

FIGURE 8

Forest plot of lumbar spine T-score between OSAHS group and control group.

lumbar spine BMD studies, they were not included in the subgroup analysis.

3.3.3.1 AHI subgroup analysis

In a subgroup analysis of AHI grouping according to OSAHS diagnostic criteria (after the exclusion of osteoporosis-related risk factors) (Figure 9), 8 studies were included (3, 6, 15, 18, 20–23) with heterogeneous groupings. In the subgroup analysis, the grouping heterogeneity of OSAHS diagnostic criteria AHI > 5~10 events/h was (P = 0.004, I^2 = 74%). %), and the grouping heterogeneity of AHI ≥ 15 events/h was (P = 0.04, I^2 = 69%), so a random effect model was used. After the OSAHS diagnostic criteria AHI grouping subgroup analysis, The heterogeneity in the correlation study between OSAHS and lumbar spine T-score was significantly reduced, and the heterogeneity of AHI ≥ 5~10 events/h group and AHI ≥ 15 events/h group were reduced to moderate heterogeneity. The results of the subgroup analysis showed that compared with the control group, the lumbar spine T-score in the OSAHS AHI ≥ 5~10 events/h group was decreased (MD = -0.45, 95% CI: -0.82~-0.09, Z = 2.42, P < 0.001), the lumbar spine T-score in the AHI > 15 events/h group was significantly decreased (MD = -0.72, 95% CI: -1.22~-0.21, Z = 2.79, P = 0.005), and the difference was statistically significant. The lumbar spine T-score effect size of the OSAHS diagnostic criteria AHI ≥ 15 events/h group was higher than that of the OSAHS diagnostic criteria AHI ≥ 5~10 events/h group, indicating that compared with AHI ≥ 5-10 events/h group, The risk of lumbar T-score decline was higher in the the patients in the OSAHS diagnostic criteria AHI ≥ 15 events/h group, and the severity of OSAHS may be related to lumbar T-score. The combined effect size of the AHI group (MD = -0.55, 95% CI: -0.86~-0.24, Z = 3.46, P < 0.001), the lumbar spine T-score of the OSAHS group was also lower, excluding the risk factors related to osteoporosis. After

group analysis, the results remained stable and the difference was statistically significant.

3.3.3.2 Regional subgroup analysis

In the regional subgroup analysis (after the exclusion of osteoporosis-related risk factors), (Figure 10), 8 studies were included (3, 6, 15, 18, 20–23), and the combined group heterogeneity was (P = 0.0001, I^2 = 76%), indicating a high degree of statistical heterogeneity. In the subgroup analysis, the grouping heterogeneity in East Asia was (P = 0.13, I^2 = 57%), that in the Middle East was (P = 0.13, I^2 = 57%). = 0.002, I^2 = 80%), and that in Europe was (P = 0.01, I^2 = 84%), so a random effect model was used; after the regional subgroup analysis, the heterogeneity of OSAHS and lumbar spine T-score correlation analysis was lower than before, among which the heterogeneity of East Asian grouping was reduced to moderate heterogeneity. The results of the subgroup analysis showed that, compared with the control group, the OSAHS group had a statistically significant difference in the Middle East group (MD = -0.58, 95% CI: -1.02~-0.13, Z = 2.53, P = 0.01); in the East Asian group (MD = -0.33, 95% CI: -0.94~0.29, Z = 1.04, P = 0.30), lumbar spine T-score was lower, but the difference was not statistically significant. In the Europe group (MD = -0.69, 95% CI: -1.55~0.17, Z = 1.57, P = 0.12), the lumbar spine T-score was lower, and the difference was also not statistically significant. The combined effect size of regional grouping (MD = -0.55, 95% CI: -0.86~-0.24, Z = 3.46, P < 0.001), the lumbar spine T-score of the OSAHS group was lower, After excluding the risk factors for osteoporosis, the results remained stable and the difference was statistically significant.

The forest plot analysis of OSAHS and lumbar spine T-score studies indicated that OSAHS is associated with lumbar spine T-score, OSAHS is a risk factor for lumbar spine T-score reduction, and the severity of OSAHS may be related to the lumbar spine T-score.
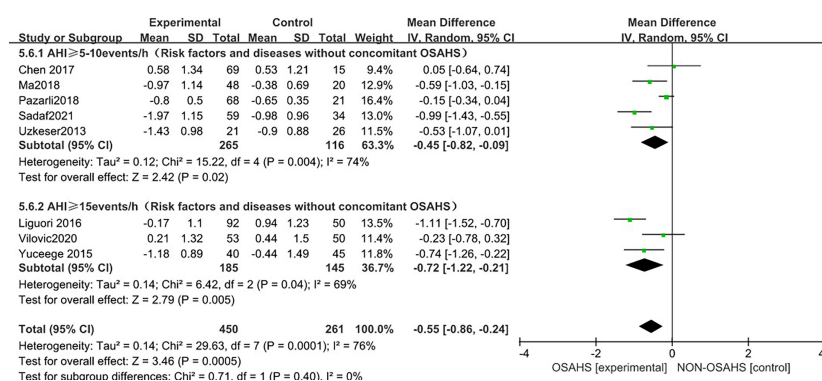

FIGURE 9
Forest plot of lumbar spine T-score "AHI grouping" subgroup analysis between OSAHS group and control group (grouped according to OSAHS diagnostic criteria, after exclusion of osteoporosis-related risk factors).
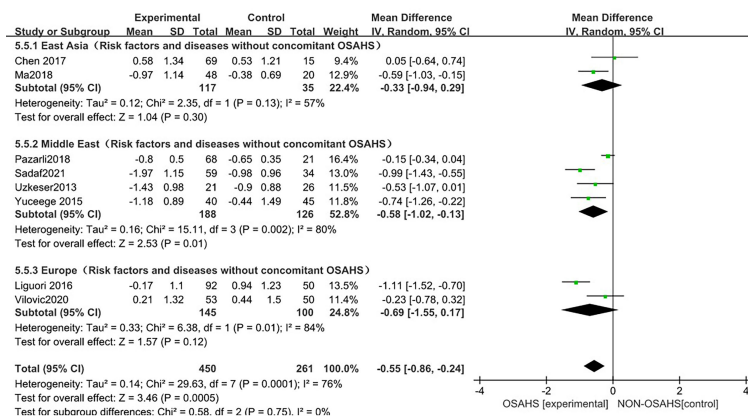
FIGURE 10
Forest plot of lumbar spine T-score "regional grouping" subgroup analysis between OSAHS group and control group (after excluding osteoporosis-related risk factors).

3.4 Sensitivity analysis

In this study, a sensitivity analysis was performed for the results with high heterogeneity. In the sensitivity analysis of the incidence of osteoporosis, lumbar bone mineral density, and lumbar spine T-score between OSAHS and the control group, the results and studies were combined after excluding any literature. There was no significant change in heterogeneity.

3.5 Publication bias

The presence of publication bias was assessed using Egger's method (Figure 11). There were 3 literatures related to OSAHS and the incidence of osteoporosis in the control group, P = 0.291>0.05 (Figure 11A), and the results indicated that there was no publication bias; there were 10 literatures related to OSAHS and the bone mineral density of the lumbar spine in the control group, P = 0.433 >0.05 (Figure 11B), the results suggest that there is no publication bias. There are 10 related literatures about lumbar spine T-score between OSAHS and control group, P=0.042<0. 05 (Figure 11C), the results suggest that there is mild publication bias, there may be reasons:1.The number of literatures included in our meta-analysis is small, which is easy to cause certain bias.2. Some study populations combined with other diseases may also have certain biases, which was further confirmed by our subgroup analysis.

4 Discussion

Osteoporosis is a common human skeletal disease characterized by osteopenia, microarchitectural deterioration, and fragility fractures (28). According to World Health Organization (WHO) standards, it is estimated that 15% of postmenopausal Caucasian women in the United States and 35% of women over the age of 65 have significant osteoporosis. One in two Caucasian women will experience an osteoporotic fracture at some point in their life. As early as 1994, a study showed that fragility fracture patients received more than 400,000 hospitalizations and more than 2.5 million doctor visits each year, causing a serious economic burden (29). Tomiyama et al. (30) first reported the correlation between OSAHS and abnormal bone metabolism in 2008. They studied the abnormal bone metabolism of 50 OSAHS patients and found that compared with the control group, a marker of bone resorption (urinary Type I collagen cross-linked C-terminal peptide) was significantly increased in the OSAHS group, and the elevated bone resorption marker levels decreased somewhat after three months of continuous positive airway pressure therapy. Subsequently, experimental and epidemiological studies have continuously explored the relationship between OSAHS and osteoporosis, BMD, and T-score, and its possible mechanism, but the results have not agreed.

Sikarin,Wang et al. (31, 32) conducted a meta-analysis of the correlation between OSAHS and bone marrow.Too few studies were included in the Sikarin's analysis, and Sensitivity analysis, meta-regression, and publication bias were not performed.Wang's analysis is mainly based on the Chinese population, so the research objects may not be representative of the general population, and there may be selection bias. The two meta-analyses did not conduct a global multi-regional population study, nor did further analysis based on the severity of OASHS, and the analysis indicators were relatively single. Therefore, in response to these problems, we conducted an update of the meta-analysis of the correlation between OSAHS and bone marrow.

This meta-analysis included 15 studies. The included studies were all high-quality studies with 6 stars and above according to
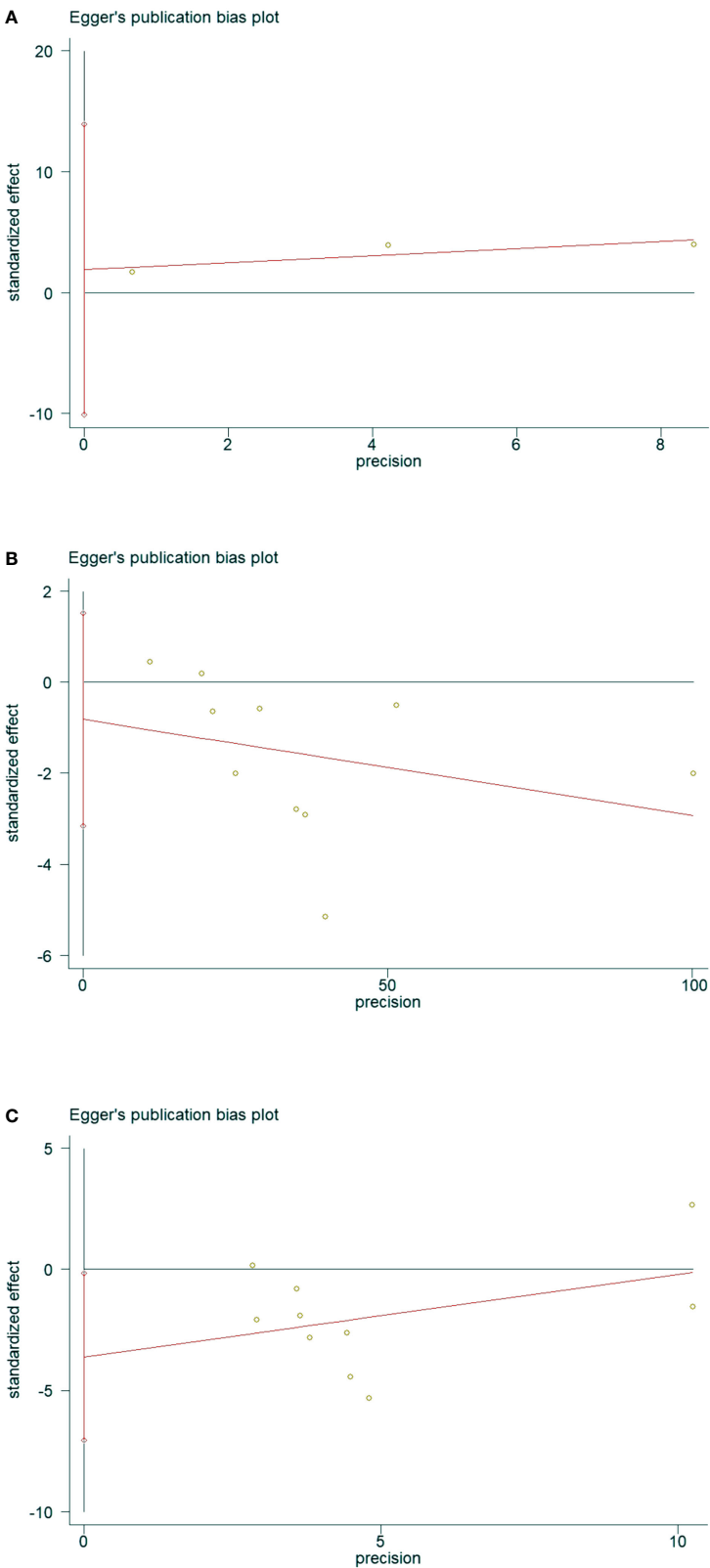
FIGURE 11

Data plot of Egger's test for various studies included in the literature.(Note: **(A)** Data plot of Egger's test for Osteoporosis incidence. **(B)** Data plot of Egger's test for lumbar spine BMD. **(C)** Data plot of Egger's test for lumbar spine T-score.).

the NOS quality evaluation. The results of the meta-analysis on the correlation between OSAHS and osteoporosis showed that in males, females, middle-aged people (40~65 years old) and elderly people (> 65 years old), patients with OSAHS had osteoporosis. Although the incidence of osteoporosis is high, only three articles were included in the literature, so more research is needed to further stabilize the results; in addition, the study population included in the literature may have been combined with old age, hypertension, diabetes, cardiovascular disease, COPD, etc., which may have affected the osteoporosis risk factors, and there is currently no prevalence data to exclude the relevant risk factors; thus, further investigation and analysis cannot be carried out, and the results are not stable.

BMD is an important indicator reflecting bone mineral content per unit area. It is mainly used to detect the osteoporosis degree, predict the risk of fracture, and provide a strong laboratory test basis for fractures caused by osteoporosis. BMD is clinically the gold standard for the diagnosis of osteoporosis (33). In recent years, many studies have focused on the relationship between OSAHS and BMD. Tomiyama, Sforza, and Chen et al. (7, 18, 30) found that compared with the control group, OSAHS patients had significantly higher BMD levels; and more studies, including Liguori, Uzkeser, Yuceege, Terzi, Qiao, Pazarli, Ma, and Vilovic et al. (3, 6, 15, 16, 19–22) found that compared with the control group, the bone marrow of OSAHS patients was significantly higher than that of the control group. In order to further confirm the relationship between OSAHS patients and BMD, we conducted a meta-analysis of the correlation between OSAHS and lumbar spine BMD which showed that compared with the control group, the OSAHS group had lower lumbar spine BMD. After further subgroup analysis, the combined effect size still confirms that the OSAHS group has lower lumbar spine BMD compared with the control group. In the subgroup analysis of AHI grouping with OSAHS diagnostic criteria, compared with the control group, the lumbar spine BMD of the OSAHS AHI > 5~10 events/h group and AHI > 15 events/h group were decreased, and the difference was statistically significant. The effect size of lumbar spine BMD in the OSAHS diagnostic criteria AHI > 15 events/h group was higher than that of the OSAHS diagnostic criteria AHI > 5~10 events/h group. Compared with the AHI > 5~10 events/h group, the risk of lumbar spine BMD decline is higher, so the severity of lumbar spine BMD may be related. In the regional subgroup analysis (after excluding risk factors related to osteoporosis), the results showed that compared with the control group, the OSAHS group had lower lumbar spine BMD in the East Asian group, Middle East group, and Europe group, but the differences were not statistically significant. After subgroup analysis, the heterogeneity of the studies could be further reduced, and the research bias was also reduced, indicating that the conclusions of this study are more reliable.

Regarding the possible mechanism of the association between OSAHS and decreased BMD: 1. OSAHS may lead to a state of vitamin D deficiency and induce secondary hyperparathyroidism,

which may lead to bone demineralization and decreased BMD (34); 2. Hypoxia is closely related to changes in bone turnover, and recent *in vitro* studies have shown that lower nighttime oxygen levels are a feature of OSAHS, while hypoxia promotes osteoclast formation and activity while inhibiting osteoblast function, thus determining bone resorption (35, 36).

The T-score is also an important basis for detecting the degree of osteoporosis. According to the results of BMD and the WHO standard, patients are divided into three groups: normal BMD (T-score > -1.0 SD), osteopenia (T-score -1.0 to -2.5 SD) and osteoporosis (T-score < -2.5 SD) (37). In recent years, many studies have focused on the relationship between OSAHS and lumbar spine T-score. Sforza, Chen et al. (7, 18) showed that compared with the control group, the lumbar spine T-score level of OSAHS patients was significantly higher; and more studies by Liguori, Uzkeser, Yuceege, Wang, Terzi, Qiao, Pazarli, Ma and Vilovic et al. (3, 6, 15–17, 20–23) showed that compared with the control group, the lumbar spine T-score level of OSAHS patients was significantly lower. In order to further confirm the relationship between OSAHS patients and lumbar spine T-score levels, we conducted a meta-analysis of the correlation between OSAHS and lumbar spine T-score levels which showed that compared with the control group, the OSAHS group had lower lumbar spine T-score levels. After excluding the related factors of osteoporosis, further subgroup analysis was performed, and the combined effect size still confirmed that the lumbar spine T-score level was lower in the OSAHS group compared with the control group.

In the subgroup analysis of AHI grouping with OSAHS diagnostic criteria (after excluding osteoporosis-related risk factors), compared with the control group, OSAHS diagnostic criteria AHI > 5~10 events/h group and AHI > 15 events/h group, the lumbar spine T-score of all groups decreased, and the difference was statistically significant. The effect size of the lumbar spine T-score in the OSAHS diagnostic criteria AHI > 15 events/h group was higher than that in the OSAHS diagnostic criteria AHI > 5~10 events/h group, and the risk of lumbar spine T-score decline was higher than that in the AHI > 5~10 events/h group, indicating that the severity of OSAHS may be related to the lumbar spine T-score. In the regional subgroup analysis (after excluding risk factors related to osteoporosis), the results showed that compared with the control group, the OSAHS group had lower lumbar spine BMD in the East Asian group, Middle East group, and Europe group, but only the Middle East subgroup was statistically significant. In conclusion, compared with the control group, the OSAHS group had lower lumbar spine T-score levels in the OSAHS diagnostic criteria AHI > 5~10 events/h group, AHI > 15 events/h group and Middle East group. The heterogeneity and research bias can be further reduced, indicating that the conclusions of this study are more reliable. At present, there is a lack of research that clearly clarifies the relationship between T-score and BMD and osteoporosis. However, because T-score is scored according to BMD, the possible mechanism of the correlation between OSAHS and T-score reduction can also be understood.

This study has certain limitations: first, the number of included studies on the relationship between OSAHS and osteoporosis was small, and combined with the related risk factors of osteoporosis, the results were not stable, so more research is needed to further stabilize the study. Second, the diagnostic methods and grading methods of OSAHS in each study were slightly different, and the study populations were from different ethnic groups, which may have led to greater heterogeneity in the results. Third, osteoporosis is more common in women (38), but there were fewer women OSAHS patients in our meta-analysis, which may have generated a selection bias. Fourth, the study sample size was relatively small compared to a large, multicentric, randomized controlled trial. Fifth, the quality of some included literature was not very high, and there may have been selection bias. Therefore, the conclusions should be interpreted with caution.

In conclusion, the results of this study suggest that OSAHS patients have a higher incidence of osteoporosis, and both lumbar spine BMD and lumbar spine T-score are reduced. The severity of AHI may be related to lumbar spine BMD and lumbar spine T-score. Understanding the incidence of osteoporosis in patients with OSAHS and the effect of OSAHS on lumbar spine BMD and T-score provides medical evidence. However, a homogeneous and large-scale prospective study with further adjustment for factors such as age and related diseases affecting osteoporosis is still needed to clarify whether OSAHS is a risk factor for osteoporosis and whether OSAHS has an effect on lumbar spine BMD and T-score. Many drugs have been developed to treat osteoporosis (39), and patients should receive treatment if they have osteoporosis, and should be treated with preventive measures if they have osteopenia. Obviously, prevention is much better than treatment. Through the meta-analysis of this paper, it can be concluded that the effective management of OSAHS can effectively reduce the risk of osteoporosis.

Data availability statement

The raw data supporting the conclusions of this article will be made available by the authors, without undue reservation.

Author contributions

Funding

Acknowledgments

Conflict of interest

The authors declare that the research was conducted in the absence of any commercial or financial relationships that could be construed as a potential conflict of interest.

Publisher's note

All claims expressed in this article are solely those of the authors and do not necessarily represent those of their affiliated organizations, or those of the publisher, the editors and the reviewers. Any product that may be evaluated in this article, or claim that may be made by its manufacturer, is not guaranteed or endorsed by the publisher.

References

1. Young T, Peppard PE, Gottlieb DJ. Epidemiology of obstructive sleep apnea: a population health perspective. *Am J Respir Crit Care Med* (2002) 165:1217–39. doi: 10.1164/rccm.2109080

2. Guiglia R, Di Fede O, RL Lo, Sprini D, GB R, Campisi G. Osteoporosis, jawbones and periodontal disease. *Med Oral Patol Oral Cir Bucal.* (2013) 18:e93–9. doi: 10.4317/medoral.18298

3. Uzkeser H, Yildirim K, Aktan B, Karatay S, Kaynar H, Araz O, et al. Bone mineral density in patients with obstructive sleep apnea syndrome. *SLEEP BREATH* (2013) 17:339–42. doi: 10.1007/s11325-012-0698-y

4. Chen YL, Weng SF, Shen YC, Chou CW, Yang CY, Wang JJ, et al. Obstructive sleep apnea and risk of osteoporosis: a population-based cohort study in Taiwan. *J Clin Endocrinol Metab* (2014) 99:2441–7. doi: 10.1210/jc.2014-1718

5. Choi SB, Lyu IS, Lee W, Kim DW. Increased fragility fracture risk in Korean women who snore: a 10-year population-based prospective cohort study. *BMC Musculoskelet Disord* (2017) 18:236. doi: 10.1186/s12891-017-1587-0

6. Liguori C, Mercuri NB, Izzi F, Romigi A, Cordella A, Piccirilli E, et al. Obstructive sleep apnoea as a risk factor for osteopenia and osteoporosis in the male population. *Eur Respir J* (2016) 47:987–90. doi: 10.1183/13993003.01830-2015

7. Sforza E, Thomas T, Barthelemy JC, Collet P, Roche F. Obstructive sleep apnea is associated with preserved bone mineral density in healthy elderly subjects. *SLEEP* (2013) 36:1509–15. doi: 10.5665/sleep.3046

8. Stroup DF, Berlin JA, Morton SC, Olkin I, Williamson GD, Rennie D, et al. Meta-analysis of observational studies in epidemiology: A proposal for reporting. meta-analysis of observational studies in epidemiology (MOOSE) group. *JAMA* (2000) 283:2008–12. doi: 10.1001/jama.283.15.2008

9. Zhang X, Tan R, Lam WC, Yao L, Wang X, Cheng CW, et al. PRISMA (Preferred reporting items for systematic reviews and meta-analyses) extension for Chinese herbal medicines 2020 (PRISMA-CHM 2020). *Am J Chin Med* (2020) 48:1279–313. doi: 10.1142/S0192415X20500639

10. Thornton AT, Singh P, Ruehland WR, Rochford PD. AASM criteria for scoring respiratory events: interaction between apnea sensor and hypopnea definition. *SLEEP* (2012) 35:425–32. doi: 10.5665/sleep.1710

11. Kanis JA. Diagnosis of osteoporosis and assessment of fracture risk. *LANCET* (2002) 359:1929–36. doi: 10.1016/S0140-6736(02)08761-5

12. Stang A, Jonas S, Poole C. Case study in major quotation errors: a critical commentary on the Newcastle-Ottawa scale. *Eur J EPIDEMIOL.* (2018) 33:1025–31. doi: 10.1007/s10654-018-0443-3

13. Yen CM, Kuo CL, Lin MC, Lee CF, Lin KY, Lin CL, et al. Sleep disorders increase the risk of osteoporosis: a nationwide population-based cohort study. *SLEEP Med* (2014) 15:1339–44. doi: 10.1016/j.sleep.2014.07.005

14. Aslan SH, Yosunkaya S, Kiyici A, Sari O. Obstructive sleep apnea syndrome may be a risk factor for the development of osteoporosis in men at an early age? *Türkiye Fiziksel Tip ve Rehabilitasyon Dergisi.* (2015) 61:216–22. doi: 10.5152/tftrd.2015.59913

15. Yüceege M, Dülgerolu DE, Firat H, Yalcindag A. Can sleep apnea be a secondary cause of osteoporosis in young people? *SLEEP Biol RHYTHMS* (2015) 13:189–94. doi: 10.1111/sbr.12106

16. Terzi R, Yilmaz Z. Bone mineral density and changes in bone metabolism in patients with obstructive sleep apnea syndrome. *J Bone MINER Metab* (2016) 34:475–81. doi: 10.1007/s00774-015-0691-1

17. Wang TY, Lo YL, Chou PC, Chung FT, Lin SM, Lin TY, et al. Associated bone mineral density and obstructive sleep apnea in chronic obstructive pulmonary disease. *Int J Chron Obstruct Pulmon Dis* (2015) 10:231–7. doi: 10.2147/COPD.S72099

18. Chen DD, Huang JF, Lin QC, Chen GP, Zhao JM. Relationship between serum adiponectin and bone mineral density in male patients with obstructive sleep apnea syndrome. *SLEEP BREATH.* (2017) 21:557–64. doi: 10.1007/s11325-017-1492-7

19. Qiao Y, Wang B, Yang JJ, Fan YF, Guo Q, Dou ZJ, et al. Bone metabolic markers in patients with obstructive sleep apnea syndrome. *Chin Med J (Engl)* (2018) 131:1898–903. doi: 10.4103/0366-6999.238149

20. Pazarli AC, Ekiz T, Inonu KH. Association between 25-hydroxyvitamin d and bone mineral density in people with obstructive sleep apnea syndrome. *J Clin DENSITOM.* (2019) 22:39–46. doi: 10.1016/j.jocd.2018.10.001

21. Ma XR, Wang Y, Sun YC. Imbalance of osteoprotegerin/receptor activator of nuclear factor-kappaB ligand and oxidative stress in patients with obstructive sleep apnea-hypopnea syndrome. *Chin Med J (Engl)* (2019) 132:25–9. doi: 10.1097/CM9.0000000000000046

22. Vilovic M, Dogas Z, Ticinovic KT, Borovac JA, Supe-Domic D, Vilovic T, et al. Bone metabolism parameters and inactive matrix gla protein in patients with obstructive sleep apneadagger. *SLEEP* (2020) 43(3):zsz243. doi: 10.1093/sleep/zsz243

23. Sadaf S, Shameem M, Siddiqi SS, Anwar S, Mohd S. Effect of obstructive sleep apnea on bone mineral density. *Turk Thorac J* (2021) 22:301–10. doi: 10.5152/TurkThoracJ.2021.20051

24. Young T, Shahar E, Nieto FJ, Redline S, Newman AB, Gottlieb DJ, et al. Predictors of sleep-disordered breathing in community-dwelling adults: the sleep heart health study. *Arch Intern Med* (2002) 162:893–900. doi: 10.1001/archinte.162.8.893

25. Neikrug AB, Ancoli-Israel S. Sleep disorders in the older adult - a mini-review. *GERONTOLOGY* (2010) 56:181–9. doi: 10.1159/000236900

26. Eikermann M, Jordan AS, Chamberlin NL, Gautam S, Wellman A, Lo YL, et al. The influence of aging on pharyngeal collapsibility during sleep. *CHEST* (2007) 131:1702–9. doi: 10.1378/chest.06-2653

27. Mora S, Gilsanz V. Establishment of peak bone mass. *Endocrinol Metab Clin North Am* (2003) 32:39–63. doi: 10.1016/s0889-8529(02)00058-0

28. Melton LR. Epidemiology of spinal osteoporosis. *Spine (Phila Pa 1976)* (1997) 22:2S–11S. doi: 10.1097/00007632-199712151-00002

29. Alexeeva L, Burkhardt P, Christiansen C, Cooper C, Delmas P, Johnell O, et al. Assessment of fracture risk and its application to screening for postmenopausal osteoporosis. Report of a WHO study group. *World Health Organ Tech Rep Ser* (1994) 843:1–129.

30. Tomiyama H, Okazaki R, Inoue D, Ochiai H, Shiina K, Takata Y, et al. Link between obstructive sleep apnea and increased bone resorption in men. *Osteoporos Int* (2008) 19:1185–92. doi: 10.1007/s00198-007-0556-0

31. Upala S, Sanguankeo A, Congrete S. Association between obstructive sleep apnea and osteoporosis: A systematic review and meta-analysis. *Int J Endocrinol Metab* (2016) 14:e36317. doi: 10.5812/ijem.36317

32. Wang Y, Shen Q, Cheng Y, Zhang Y. A meta-analysis of association between obstructive sleep apnea-hypopnea syndrome and low bone mass in adults. *Chin J Osteoporos* (2021) 27(02):190–7. doi: 10. 3969/j.issn.1006-7108. 2021. 02. 006

33. Muller D, Pulm J, Gandjour A. Cost-effectiveness of different strategies for selecting and treating individuals at increased risk of osteoporosis or osteopenia: A systematic review. *VALUE Health* (2012) 15:284–98. doi: 10.1016/j.jval.2011.11.030

34. Liguori C, Romigi A, Izzi F, Mercuri NB, Cordella A, Tarquini E, et al. Continuous positive airway pressure treatment increases serum vitamin d levels in Male patients with obstructive sleep apnea. *J Clin SLEEP Med* (2015) 11:603–7. doi: 10.5664/jcsm.4766

35. Arnett TR, Gibbons DC, Utting JC, Orriss IR, Hoebertz A, Rosendaal M, et al. Hypoxia is a major stimulator of osteoclast formation and bone resorption. *J Cell Physiol* (2003) 196:2–8. doi: 10.1002/jcp.10321

36. Utting JC, Robins SP, Brandao-Burch A, Orriss IR, Behar J, Arnett TR. Hypoxia inhibits the growth, differentiation and bone-forming capacity of rat osteoblasts. *Exp Cell Res* (2006) 312:1693–702. doi: 10.1016/j.yexcr.2006.02.007

37. Orimo H, Hayashi Y, Fukunaga M, Sone T, Fujiwara S, Shiraki M, et al. Diagnostic criteria for primary osteoporosis: year 2000 revision. *J Bone MINER Metab* (2001) 19:331–7. doi: 10.1007/s007740170001

38. McClain JJ, Lewin DS, Laposky AD, Kahle L, Berrigan D. Associations between physical activity, sedentary time, sleep duration and daytime sleepiness in US adults. *Prev Med* (2014) 66:68–73. doi: 10.1016/j.ypmed.2014.06.003

39. Lane JM, Russell L, Khan SN. Osteoporosis. *Clin Orthop Relat Res* (2000) 372:139–50. doi: 10.1097/00003086-200003000-00016

Sclerostin as a biomarker of physical exercise in osteoporosis: A narrative review

Anna Oniszczuk[1], Agnieszka Kaczmarek[1*],
Mateusz Kaczmarek[2], Maria Ciałowicz[3], Ersan Arslan[4],
Ana Filipa Silva[5,6,7], Filipe Manuel Clemente[5,6]
and Eugenia Murawska-Ciałowicz[1*]

[1]Department of Physiology and Biochemistry, Wroclaw University of Health and Sport Sciences,
Wroclaw, Poland, [2]Gynecology and Obstetrics Department, St. Hedwig's of Silesia Hospital,
Trzebnica, Poland, [3]Physiotherapy Faculty, Wroclaw University of Health and Sport Sciences,
Wroclaw, Poland, [4]Faculty of Sport Science, Gaziosmanpaşa University, Tokat, Turkey, [5]Escola
Superior Desporto e Lazer, Instituto Politécnico de Viana do Castelo, Rua Escola Industrial e
Comercial de Nun'Álvares, Viana do Castelo, Portugal, [6]Research Center in Sports Performance,
Recreation, Innovation and Technology (SPRINT), Melgaço, Portugal, [7]The Research Centre in
Sports Sciences, Health Sciences and Human Development (CIDESD), Vila Real, Portugal

Osteoporosis, a disease of low bone mass, is characterized by reduced bone mineral density (BMD) through abnormalities in the microarchitecture of bone tissue. It affects both the social and economic areas, therefore it has been considered a lifestyle disease for many years. Bone tissue is a dynamic structure exhibiting sensitivity to various stimuli, including mechanical ones, which are a regulator of tissue sclerostin levels. Sclerostin is a protein involved in bone remodeling, showing an anti-anabolic effect on bone density. Moderate to vigorous physical activity inhibits secretion of this protein and promotes increased bone mineral density. Appropriate exercise has been shown to have an osteogenic effect. The effectiveness of osteogenic training depends on the type, intensity, regularity and frequency of exercise and the number of body parts involved. The greatest osteogenic activity is demonstrated by exercises affecting bone with high ground reaction forces (GRF) and high forces exerted by contracting muscles (JFR). The purpose of this study was to review the literature for the effects of various forms of exercise on sclerostin secretion.

KEYWORDS

sclerostin, osteoporosis, bone mineral density, physical activity, exercise, physical training

Introduction

Osteoporosis, as a disease of low bone mass, has been the subject of numerous studies worldwide for many years. The underlying cause of this disease is a disturbance of metabolic processes in bone tissue leading to excessive bone fragility (1). Recently, increasing scientific attention has focused on the protein called sclerostin, which, while

influencing the balance between bone tissue formation and resorption, simultaneously exhibits sensitivity to mechanical stimuli (2). This fact became the basis for research on the effects of physical exercise on bone tissue metabolism, including the processes that cause osteoporosis (3–5). In the present study, the relationship between the physical activity and exercise level and the preservation or increase in bone mineral density was correlated with the level of sclerostin in bone tissue.

Osteoporosis – low bone mass disease

Osteoporosis is a disease of the skeletal system characterized by increased bone fragility due to decreased bone mass and disruption of the microarchitecture of bone tissue. It is a disease that does not manifest obvious symptoms for a long time, despite its progressive, destructive effects on bone tissue. The first noticeable symptom is an osteoporotic fracture, otherwise known as a low-energy fracture (a spontaneous fracture caused by falling from one's standing position height or minor trauma) (4). Osteoporosis is diagnosed when bone mineral density (BMD) reaches a value of less than 2 standard deviations, compared to the average BMD value in young people (6, 7).

Osteoporosis as a lifestyle disease

Osteoporosis is recognized as a lifestyle disease on a global scale (8, 9). In 2010, 22 million women and 5.5 million men were diagnosed with low bone mass disease in European Union countries, while the number of new fractures was 3.5 million (7), 800,000 more have already been recorded in 2019 (6, 7). The most numerous fractures occurred in the proximal femur. In 2019, 25.5 million women and 6.5 million men were estimated to have osteoporosis in the European Union plus Switzerland and the United Kingdom. The population age 50 years or more is projected to increase by 11.4% in men and women between 2019 and 2034 and the annual number of osteoporotic fractures in those countries will increase by 25% (10). In Poland, 2 million patients over 50 years of age suffered from osteoporosis in a given year, and among them 168,000 suffered a fracture, 60% of them were women (7).

An osteoporotic fracture occurring as a result of decreased bone mass can lead to disability, especially in the case of femoral neck fractures. It devastates stabilization of life and leads to the reduction of its quality (11). Nowadays, 1 of 3 women over 50 years old (over breast cancer) and 1 of 5 men over 50 years old (over prostate cancer) are affected by osteoporosis (11, 12).

Osteoporosis is not only a social problem, but also an economic one. There is an increase in the aging population in developed countries. The economic burden of incident and prior fragility fractures in 2019 was estimated at € 57 billion in European Union countries with Switzerland and United Kingdom (13). The population of elderly people (aged 65 years or more) in European Union countries will increase significantly, rising from 90.5 million at the start of 2019 to reach 129.8 million by 2050. This age structure of population and increased percentage of elderly people will increase the prevalence of osteoporosis. Consequently, this will increase the monetary outlay associated with both the treatment immediately following the fracture and the lengthy rehabilitation and subsequent care. The cost of treatment is estimated to increase from 593 million euros in 2010 to 753 million euros in 2025 (14, 15).

Causes and risk factors

The main cause of osteoporosis is low bone mineral mass, which depends on two types of factors: non-modifiable (impossible to eliminate) and modifiable (possible to change or eliminate).

Non-modifiable factors:

- age (there is a slow decline in bone mass after the age of 30);
- sex (women develop the disease four times more often than men);
- ethnic group (most common in Caucasian and Asian women);
- genetic conditions.

Modifiable factors:

- diet, eating habits (too little in the diet: vit. D, C and K, magnesium, phosphorus, potassium, omega 3 fatty acids, isoflavonoids; excess in diet: protein, vitamin A, sodium, alcohol, caffeine; smoking cigarettes);
- reduced physical activity;
- presence of other diseases (including hyperthyroidism, diseases affecting bone metabolism, diseases associated with impaired absorption, anorexia);
- use of certain medications (e.g., anticonvulsants, heparin, glucocorticoids) (14, 16, 17).

Symptoms of osteoporosis

Osteoporosis is a disease that is asymptomatic, especially in its early stages. Very often, the first symptom of already advanced disease is the so-called osteoporotic fracture (or low-energy fracture) (18). These fractures usually involve the proximal end of the femur, the proximal end of the tibia, the

spine, the pelvis, the proximal forearm, the proximal humerus and the ribs (19). According to Perry et al. (20), an osteoporotic fracture is a fracture that is disproportionate to the forces causing it, and occurs after a fall from one's own standing height level, after ruling out another cause such as a pathological fracture. The risk of fracture doubles with a 10% decrease in BMD from the mean value (5). Low-energy fractures are followed by pain of varying degrees of intensity when performing simple motor activities, such as sitting down, bending the trunk, and even when standing. As the disease progresses, along with successive fractures, there is a limitation of mobility, a decrease in body height by about 2 – 4 cm, skeletal deformation, deepening of spinal kyphosis (the so-called widow's hump), and symptoms of the respiratory, circulatory and digestive systems appear as a result (16).

According to many authors physical exercise ought to be one of the most suitable strategy in prophylaxis of osteoporosis, especially in postmenopausal women but not only, as a crucial element of life style (21–24).

Sclerostin – bone remodeling protein

Sclerostin is a human bone tissue protein encoded by the SOST gene. It is located on chromosome 17 in the 17q12-q21 region (25). Sclerostin belongs to the bone morphogenetic protein (BMP) family of antagonists, and is involved in the anti-anabolic processes of bone formation (26). There are several regulatory elements in the SOST gene responsible for its transcription in bone tissue cells (27). Sclerostin was first detected in adult human osteocytes through the study by Winkler et al. (26). Studies have also shown the presence of

this protein in hypertrophic chondrocytes (28). Sclerostin is a strong inhibitor of osteoblastogenesis (29, 30).

This protein plays a key role in maintaining the balance between the processes of bone formation and resorption (bone remodeling) (Figure 1). It is a specific negative regulator of bone formation. Expression of this protein occurs in bone, cartilage, kidney, liver, pancreas and heart, among others, but it is mainly produced in bone tissue by mature osteocytes and cementocytes, and is detectable in plasma (31). Studies in genetically modified mice have shown that deletion of the SOST gene in the rodent genome resulted in high bone mass, a characteristic of humans with hereditary sclerostin deficiency (27). Sclerostin is released to inhibit bone formation. Its production is mainly regulated by mechanical loads on bone tissue and hormones affecting bone metabolism (calcitonin, parathyroid hormones, glucocorticoids). Calcitonin inhibits osteoclast resorption and up-regulates sclerostin expression by osteocytes. Glucocorticoids increase sclerostin expression *in vivo* and *in vitro* as well but there is a difference between results, probably due to different treatment regimens (32). Moreover studies have shown that serum sclerostin concentration in humans and expression in rodent bone tissue decreased in response to PTH treatment. Although sclerostin acts in a paracrine manner, changes in bone cell activities partly regulated by osteocytes may be reflected by circulation of sclerostin concentrations (33).

Mechanical stimuli damaging the bone tissue are perceived by osteocytes as changes in cytoplasmatic space. This leads to inhibiting the expression of sclerostin and to initiation of the bone tissue repair and formation processes (34). Exogenous sclerostin added to osteogenic cultures inhibits proliferation and differentiation of mouse and human osteoblastic cells. Moreover it decreases their life span by stimulating their apoptosis. Since sclerostin inhibits osteoblasts stimulation and
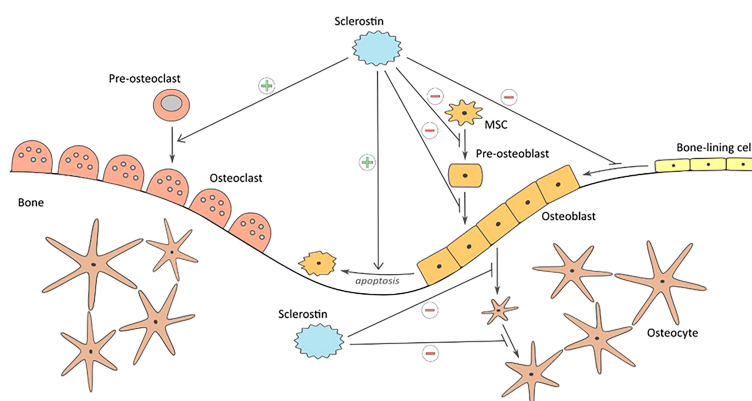

FIGURE 1
Influence of sclerostin on bone formation and resorption: inhibiting proliferation and differentiation of mesenchymal cells to osteoblasts, keeping the bone lining cells in dormant state, inhibition of bone matrix formation, inhibition of ostoblasts differentiation to osteocytes, promoting osteoblast apoptosis, and stimulating bone resorption.

bone formation processes, it leaves cells lining the bone tissue at rest (35). Moreover, studies have shown that another extracellular matrix protein – periostin - impacts on inhibition of sclerostin (36). The activity sclerostin as a regulator in bone tissue metabolism is dependent on the Wnt/β-catenin signaling pathway, whose modulator is periostin (37). The protein reacts directly with sclerostin and inhibits its antagonistic effect on this signaling pathway. As a consequence periostin promotes bone formation process. The study conducted by Bonnet et al. (38) has shown that periostin presence inhibits sclerostin expression and thereby increases level of osteoblasts. Mutual interaction of these two proteins has impact on bone tissue formation process in response to biomechanical loads.

Sclerostin as an inhibitor of the Wnt/β pathway – catenin

The Wnt pathway proteins form a ligand for Frizzled and lipoprotein receptor-related proteins (LPRs) located in the plasma membrane of the target cell. As low-density lipoproteins (LDL), LPR receptors have transport and signaling roles in the pathway (30). Once proteins bind to their receptors, the conduction of signals from the cell membrane to the cell nucleus is triggered, where gene expression occurs. The combination of Dvl (Dishevelled)

protein with Frizzled receptor and axin with LRP receptor further leads to the activation of β-catenin, which then combines with TCF/LEF (T- cell transcription factor/lymphocyte enhancer factor) transcription factors to form an active complex leading to the expression of target genes. Lack of Wnt protein expression or inhibition of their attachment to receptors degrades β-catenin and inactivates the signaling pathway (39). As an inhibitor of the Wnt pathway, sclerostin binds to LRP5/6 receptors and masks them from Wnt proteins (27). This blocks the formation of the Wnt-Frizzled-LRP5/6 system leading to inactivation of signaling pathway transmitters. This ultimately leads to inhibition of anabolic processes of bone tissue by deactivating osteoblast differentiation (40) (Figure 2). Additionally, via the Wnt pathway, the lifespan of osteoblasts is prolonged by inhibiting their apoptosis (39).

The discovery of the effect of sclerostin on Wnt pathway signaling may be crucial in the prevention and treatment of bone remodeling disorders. Studies in mice and rats have shown that increased mechanical loading on bone tissue resulted in decreased sclerostin activity by osteocytes (41). Similar studies in wild-type mice have shown that mechanical stress relief of tissue has the effect of increasing sclerostin production, which in turn reduces the activity of the Wnt pathway (42). According to Sharif et al. (43) downregulation of sclerostin might be effective in the treatment of osteoporosis (44). conducted an experiment in which 7180 postmenopausal women suffering from
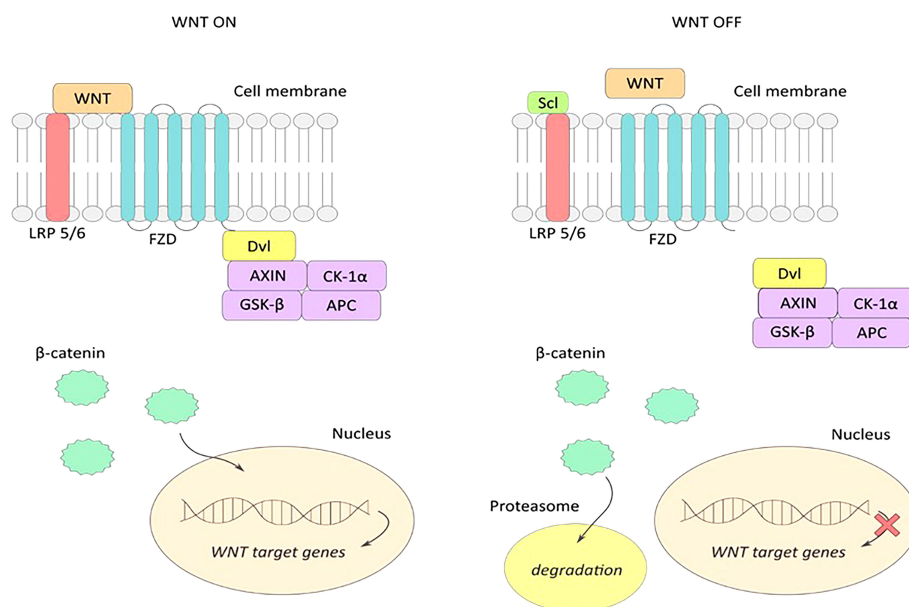
FIGURE 2
WNT ON-active signaling pathway: extracellular Wnt proteins bind to LRP5/6 and frizzled (FZD) receptors, and form an active Wnt-FZD-LRP5/6 receptor system leading to accumulation of the active form of β-catenin and its translocation to the cell nucleus. Attachment of β-catenin to the transcription factor TCF activates transcription of Wnt pathway target genes. WNT OFF – inactive signaling pathway: sclerostin binds to LRP5/6 receptors on the cell surface preventing the formation of an active Wnt-FZD-LRP5/6 complex, resulting in inhibition of the WNT signaling pathway. Accumulated β-catenin is degraded in the proteasome, and transcription of the WNT gene in the nucleus is stopped.

osteoporosis were randomly divided into two groups – one group received romosozumab, a monoclonal antibody binding sclerostin, and the second group received placebo for 12 months. The risk of vertebral fractures in women receiving romosozumab was 73% lower, compared to placebo group. Also according to Brandenburg et al. (45) blocking sclerostin is a quite promising treatment perspective against osteoporosis moreover authors underly the Wnt signaling pathway and sclerostin secretion with evident cardiovascular calcification observed in different diseases.

Effect of physical activity on sclerostin and bone mass

The precise influence of physical training on sclerostin level stays unclear. Many studies show a negative correlation between increased physical activity and sclerostin level. Ardawi et al. (32, 46) conducted two experiments including premenopausal women divided into two groups, one of which consisted of physically active women, and the second one - sedentary women. In both experiments, blood and urine levels of sclerostin were significantly lower in physically active women. Similar results were obtained in women aged 50-75, suffering from osteopenia, by Janik et al. (47). Exposing osteocytes to sera of obese women undergoing physical activity program shows negative correlation between duration of the program (sera were collected 48 hours before training program, and then after 4, 6 and 12 months of training) and sclerostin level (48). Similar results were achieved by Wannenes et al. (49), who also noted lower mRNA levels of some key osteogenic factors, like Runx2, BNP4 and BALP, compared to control group. There was also a significant decrease in expression of cMyc and axin2, specific target genes of canonical Wnt/β-catenin signaling pathway.

Studies including male participants show corresponding results. Hinton et al. (50) conducted a study in apparently healthy men aged 25 to 60 years whose physical activity in the past 24 months was ≥4 hours per week. The study group was divided into those doing resistance training or jump training and underwent their 12 month intervention. After this time, a significant decrease in serum sclerostin levels was examined and observed.

However, there are many experiments showing results contrary to the above. Pickering et al. (51) subjected young, healthy women to a 45-minute treadmill run. They achieved a significant increase in sclerostin level. Similar results were obtained by Gombos et al. (52), who observed an increase in sclerostin level after a single exercise session in both the resistance exercise and walking groups, compared to its baseline level.

Kouvelioti et al. (53) studied young, healthy women and subjected them to two exercise tests: interval running on a treadmill and cycling on a cycle ergometer. They obtained an increase in sclerostin level after training in both trials.

Interestingly, sclerostin levels returned to baseline values one hour after the end of training regardless of the exercise regimen.

During a study conducted by Armamento-Villareal et al. (54) older, obese individuals were randomly assigned to a control group that included diet or exercise, and exercise combined with diet. Attempts were made to see how weight loss would affect serum sclerostin levels. After a 12-month study, there was an increase in sclerostin in the diet group. It remained unchanged in the other groups. Śliwicka et al. (55) conducted a study in healthy men after a marathon. Sclerostin levels were observed to increase 1.3-fold 72 hours after the marathon compared to baseline.

Detailed information of different studies about influence of various form of physical activity/training in healthy/obese/ athletes are presented in Tables 1, 2.

Next to sclerostin there are some other bone formation and resorption biomarkers which can be considered in relation to physical effort. Studies conducted by Kouvelioti et al. have shown that sclerostin level increase after five minutes in response to high intensity exercises but PINP (procollagen type I amino-terminal propeptide) and CTXI (cross linkedtelopeptide of type I collagen) do not correspond to the sclerostin response. Moreover, no correlation between sclerostin and PINP or CTXI values at any time of exercises was noted (56). Gombos et al. conducted experiments on three groups: resistance exercise group, walking group and control group. Increase in sclerostin level in both study groups with significant difference was observed but there was no significant change in BALP values in any of the groups. Next, the changes in CTX concentrations were significant in the resistance exercise group but not in the walking group. Physical effort of appropriate type, intensity and duration may affect bone formation and resorption causing detectable changes in serum concentrations of biochemical markers of bone metabolism such as PINP, CTXI, BALP and sclerostin. Forces generated by muscle contraction play an important role in stimulating bone resorption (58).

Physical activity of professional athletes and sclerostin level in bone tissue

Previous studies on the effects of physical activity levels on bone tissue sclerostin levels have shown that mechanical loading of bone tissue increases bone density, promotes tissue formation processes, and inhibits resorption. Are sclerostin levels at similar levels at very high exercise loads in professional athletes whose bones are subjected to daily high mechanical loads?

Many studies seem to support that thesis. Zagrodna et al. (53) compared sclerostin levels in professional football players and in healthy individuals with low levels of physical activity. A significantly higher mean level of sclerostin was observed in the football players group compared to the control group. Similar

TABLE 1 Studies showing the effect of physical activity on changing sclerostin levels.

Ref:	Group	Group Characteristic	Type of physical activity/ /exercise/ training	Sclerostin	Other biochemical parameters	Additional effects/ Comments
(32)	♀ n=120	Age: 30-42 years Premenopausal;BMI: 30.0 kg/ m² or less; sedentary lifestyle; stable body mass; not being on the special diet; lack of participation in another program during the study; randomly classified to PA training group (PAT) or sedentary (SG);	Duration: 8-week 120 min/ session, 4d/wk; (20 min walking, 25 min running, 10 min cycling, 10 min step ups, 35 min stretching and mobilizing the spine, upper and lower body);	↓ Sclerostin level by 33.9% (26.06 pmol/L pre-test and 19.46 pmol/L post-test) in PAT group; CG: no changes 25.69 pmol/L before, 26,41 pmol/L post-test;	PAT : ↑ IGF-1 pre- 50.26 ng/ ml to 87.54ng/ml;↑ BALP pre 8.16 U/L to 12.01 U/L after test; ↓CTX form 166.5 to 151.5pg/ml;↑ intact parathormone (PTH) from 2.76pmol/L to 3.38 pmol/L;	Exclusion criteria as in ref (46).;No correlation were observed between Sclerostin and bone resorption markers in PAT group;
(32)	♀ n=1235	Age: 33.83 ± 8.41yearsHealthy; Premenopausal; Serum FSH level ≤15mIU/L and a normal cycle; normal blood count, renal and hepatic tests; All inclusion data as above;	All group divided into four groups based on PA level: <30, 30-60, 60-120, >120 (min/week);	↓Sclerostin level by 36% (17.60 pmol/L) in the groupwith PA >120 min/ wk compared to the PA < 30 min/wk. (27.84 pmol/ L). Sclerostin level in group with PA = 30-60 min/wk =27.11 pmol/L, and in group with PA = 60-120 min/wk Sclerostin level =21.64 pmol/L;	IGF was the highest in PA group >120min/wk (101.89ng/ ml) and the lowest in PA group <30 min/ wk (49.27ng/ ml);BALP was the highest in PA group >120min/wk (11.13U/L) and the lowest in PA group < 30min/wk (8.93U/ L);CXT was also the highest in PA group >120min/wk (238.5pg/ml) and the lowest in PA group <30 min/ wk (191.7 pg/ml);	Exclusion criteria the sameas ref (46).;No correlation were observed between Sclerostin and bone resorption markers in PAT group;
(41)	♂ n=8	Age: 25.0 ± 4.0 years Range: 18-30 years; Obese; exercised no more 2-3x /week (150 min); waist circumference > 98cm; no cardiometabolic diseases, no medication, non-smoking; BMI = 35 ± 4 kg/m²;	Duration: 4 weeks of sprint interval training (SIT); 4 session/week /4 weeks on cycle ergometer; Session: 5 min warm-up, 8 x 20s work at 170% work rate at VO$_{2peak}$/ 10s rest, total time =9 min; Post training serum and subcutaneous white adipose tissue (WAT) biopsy have been taken;	↓Sclerostin in serum 15 % pre- to post- SIT, 5/7 showed decrease, n.s.); WAT - ↓sclerostin (37% pre v post);	↑Wnt/ β-catenin signaling in WAT (52%); ↓ TNF-α (−0.36 pg/ml) and IL-6 (−1.44 pg/ ml);	VO$_{2\ peak}$ increased (5%); no anthropometric changes after 4 weeks; Sclerostin in regulating human adipose tissue in response to exercise training;
(46)	Women (♀) n=50	Age: 64.8 ± 5.0years; Range: 50-75 years;With clinically diagnosed osteopenia;	Duration: 12-week observation /12-weeks physical activity; Interval training on a cycle ergometer 4 min exercise/2 min rest, 3 times a week for 40 min);	↓ Sclerostin 12.04% (275.82 ng/mL pre-test and 242.60 ng/mL post-test);	↑ Osteocalcin (OC) level from 21.67 ng/mL to 23.64 ng/mL after the study; ↑ vit.D₃ from 23.7 ng/ml to 32.55 after study; no changes of C-terminal telopeptide type 1 collagen (β-CTX/ β-CrossLaps); no changes of Alkaline Phosphatase (ALP) activity, Phosphorus and Calcium (Ca) level;	Supplementation with vit. D₃ (1800IU) and Ca (500mg) during entire study in all women. No significant correlations between OC and Sclerostin;
(50)	♀ n=28	Age - 53 ± 8.2 years Obese; BMI≥ 30 kg/m²; Body mass; 101.3±3.9 kg; Sedentary lifesyle;	Duration: 12–months; daily aerobic training; individualized prescribe physical activity and hypo caloric diet.Time of training session varied from 30 min/2 months and 60 min to the end of study;	↓ Sclerostin levels after 4, 6 and 12 months compared to baseline;	Decrease of insulin and leptin levels; increased of adiponectin receptor-1 (Adipo R1) after 6 and 12 months; time-dependent total β-catenin increase and others intracellular markers;	Significant reduction of body mass (to 91.0 ± 9.5 kg after 12 months due to fat and fat free mass; Body composition variation achieved after 4 months and maintained for for the end of study;
(52)	Men (♂) n=38	Age: 43.7 ± 10. 1years Range: 25-60 years. Healthy, physically active (≥4 hours of leisure-time physical activity/ week with low lumbar spine	Duration: 12 months; All group randomized into two groups: (RT) resistance training and (JUMP) jump training; 8 cycles of 6 weeks	↓ Sclerostin levels by about 7% from 39.2± 11.6 pmol/L to 36.8± 13.3 pmol/L in both group; Mean % of change was	IGF-I increase of 26% from 203± 71ng/mL to 239± 109ng/ mL in both group;PTH - no changes; Whole body and LS BMD increased after 6 months	All participants were provided supplementation with Ca (1200mg calcium

(Continued)

TABLE 1 Continued

Ref:	Group	Group Characteristic	Type of physical activity/ /exercise/ training	Sclerostin	Other biochemical parameters	Additional effects/ Comments
		or hip BMD (>-2.5 SD T-score ≤ -1.0 SD);	training/1 week rest, progressive intensity; JUMP – 3x/wk; RT 2x/wk;	−4.5 ± 3.6% for JUMP and −9.5 ± 3.5% for RT;	in both groups; Hip BMD significantly increased at 6 and 12 months only in RT;	carbonate/d) and vit. D (10 μg/d);
(53)	♀ n=32	Healthy, Two groups:Practicing PA less than 120min/wk (age: 22.9± 1.5years) n=23; Resting test (age: 26.1±3.1 years) n=9;	Duration: 45 min low-speed, treadmill running test;	↑Sclerostin levels in practicing PA group by 44.3% from 290 ± 19 pg/mL before test to 410± 27pg/mL after Resting test: Stabile level (303 vs 294 pg/ml);	Increase in level by 7.7%from 370.9+/-31.5 to 386.2+/-28.5 pg/mL);	
(54)	♀ n=150	Age: 58.80±7.5 years;With diagnosed osteoporosis/ osteopenia. Randomly assigned to three groups: Resistance (RG), Walking (WG), Control (CG);	Duration: 46 minRG: 8min warm-up, 30 min exercises with elements of core stabilization and muscle strengthening 3 sets/ 2 min rest, 8 min cool-down;WG: 46 min outdoor walking (3–6 MET), rhythm 100 steps/min CG: any intervention;	↑ Sclerostin levels in RG: pre - 6.8 pmol/L to 29.8 pmol/L post intervention; WG: pre- 23.6 pmol/L to 29.9 pmol/L post-; CG: Pre - 24.0 pmol/L v 24.20 pmol/L post intervention;	RG:↑CTX/β-CrossLaps) (303.60 to 276.40 pg/mL post intervention) WG:↑Bone-Specific Alkaline Phosphatase (BALP);	Exclusion criteria:Any condition influencing Ca and bone metabolism (expect dietary Ca and vit. D supplementation), Ongoing hormone replacement therapy, renal and hepatic diseases, cardiovascular disease, physical injury, anabolic steroids, anticoagulants, diuretics within last 6 months;
(55)	♀ n=20	Age: 22.5±2.7 years Range: 18-28 years. Healthy, recreationally active (2 to 5x/ wk , free of injuries or chronic conditions, having no fracture in the last year, nonsmokers, and not taking any medication or dietary supplements (protein, vit. D, and calcium);	Duration: 16 min Two exercise tests:High intensity interval running (HIIR) on a treadmill and HII cycling on a cycle ergometer (HIIC);HIIR and HIIC lasted 8 x 1 min running /cycling at ≥90% of HR$_{max}$ separated by 1 min passive recovery between work; During both trials 5x blood samples were collected: pre and 5 min, 1h, 24h, and 48h post exercise;	↑Sclerostin level in 5 min after exercise in both trials, in HIIR from 100.2 to 131.6 pg/mL and from 102.3 to 135.8 pg/mL in HIIC.Recorded significant effect of time but not exercise mode; at 1h after exercise Sclerostin level returned to pre- test value;	No significant time effect for CTXI in both trials; A significant time effect for procollagen type I amino-terminal propeptide (PINP) was found only in HIIR; No significant differences in CTXI and PINP concentrations between both trials at any time point. No significant correlations were found between the sclerostin, CTXI and PINP levels at any time point;	During both training mean heart rate was >90% of HRmax (93.2 ±4.7% for HIIR and 90.2 ±4.8% for HIIC) Borg rating of perceived exertion (RPE) was recorded in both trials = 19;
(56)	♀♂ n=107	Age: ≥65 years, Obese (BMI ≥30kg/m²); no physicaly active; stable body weight (±2 kg) in past year; on stable medications within last 6 months;	Duration: 12 weeks;All participants divided into four groups: control group, with diet induced weight loss, exercise training group, diet and exercise group. Exercised groups: 90 min (15 min flexibility exercise, 30 min aerobic, 30 min progressive resistant exercises 15 min balance exercise);	↑ Sclerostin levels in the diet group by 6.6± 1.7% and 10.5% ± 1.9% in 6 and 12 month compared to baseline. There was no changes in the other groups;	Body weight decreased in diet and in diet + exercise but not in exercise and control;	All received with Ca (1500 mg/d) and vit. D (1000 IU/day); Exclusion of subjects taking bone-acting drugs, sex-steroid compounds within last year;
(53)	♂ n=14	Age: 22.1 ± 4.05 years; Range: 18-39 years; Volunteers; Healthy, Active Duty Army Solders; not having used glucocorticoids in the past 2 years; BMI: 27.3±3.8 kg/m²	Single bout of exercise; Randomized crossover study; 10 sets /10 repetitions of plyometric jumps at 40% of 1 -RM leg press or a nonexercised control period; Blood was drawn at baseline, 12, 24, 48, 72h following exercise or rest	No significant effect of time or exercise on sclerostin levels;	Markers of bone metabolism: (PTH, Ca); markers od bone formation: bone Alkaline Phosphatase (BAP); osteocalcin (OCN); markers of bone resorption (CXT (lower in 12h in comparison to baseline), Dickkpopf-1 (DKK-1);	Calcium controlled diet (1000mg/day) was implemented;

(Continued)

TABLE 1 Continued

Ref:	Group	Group Characteristic	Type of physical activity/ /exercise/ training	Sclerostin	Other biochemical parameters	Additional effects/ Comments
(57)	Girls and boys ♀ n=12 ♂ n=12	Age: ♀ - 11.00 ± 0.5 years, ♂ - 10.2 ± 0.3 years. All girls premenarcheal; all children recreationally active; no difference between ♀ and ♂ in daily energy intake and Ca intake, but below recommendation for children in this year. BMI <85th percentile for their age; no fracture (within 6 past months); growth no premature or delayed, no pharmaceuticals;	Duration and exercise: High impact of plyometric exercise protocol in form of circuit training stations (3x): 5 min warm-up, different stations, 3 min rest between stations; exercises: jumping jacks, lunge jumps, single-leg hops, hurdle jumps, tuck jumps, drop jumps (entire session about 100-144 jumps);	↑Sclerostin in ♀ in comparison to boys before (♀-187.1 pg/ml v ♂-161.4 pg/ml) and at 24h post exercise (♀-200.3 pg/ml v ♂-162.9 pg/ml); In girls post exercise the level was lower in comparison to the pre exercise at 5 min and 1h, at 24h much higher than in previous stages. No changes in boys post exercise;	DKK-1 – ↓in ♀than in ♂ at the same time; no changes post exercise in both groups.OPG - ↓ in ♀ than in ♂ at the same time, except 24h;RANKL (receptor activator of nuclear factor kappa-β ligand) ↓ in ♀ than in ♂ in each stage of study; In ♀ post exercise lower then pre exercise; no changes in ♂ post exercise;	Plyometric training induces osteokine response favoring osteoblastogenesis than osteoclastogenesis;

♀, women, ♂ men, ↓ reduced level, ↑ decreased level.

TABLE 2 Studies depicting the effects of physical activity on the bone mass of professional athletes.

Ref:	Group	Group Characteristic	Type of physical activity/ training	Sclerostin	Other biochemical parameters	Additional effects/Comments
(58)	♂ n=10	Age: 41±7.7 years Range: 32-51 years Healthy; recreational runners;	Visegrad Marathon (42.195 km);	↑ Sclerostin levels 1.3-fold 72 h after the marathon in comparison to the baseline;	24 h after marathon, an increase in myostatin (1.2-fold), osteoprotegerin (OPG) (1.5-fold) and PTH (1.3-fold), high-sensitive interleukin-6 (hsIL-6) (1.9-fold), myoglobin (4.1-fold), hs C-reactive protein (hsCRP) (5-fold), and tumor necrosis factor α (TNFα) (2.6-fold); After 72h and in myostatin (1.2-fold), irisin (1.1-fold). OPG (1.3-fold) and PTH(1.4-fold), hsIL-6 (1.4-fold), TNFα (1.9-fold);	Sclerostin was correlated with hsIL-6; negative correlation was noted fo sclerostin and myostatin and PTH and OPG;
(59)	♂ n=59	Range: 17-37 years; Healthy;Athletes-footballers (A) n=43; aged 26.5 ± 3.4 years body mass 76.3 ± 7.3 kg, BMI 23.1 ± 1.5kg/m²; Mean career duration 14.7 ± 4.5 years; Non-athletes (NA) n=16; Aged 29.5 ± 4.3 years, non-smokers; low physical activity per week; body mass 81.7 ±8.7 kg; BMI 25.6±3.1 kg/m²; All NA participants worked indoors;	Winter season; Training lasted every day by 3 h/d in uniforms covered 80% of their body;	↑ sclerostin in A group (35.3 ±8.9 pmol/L) than in the NA group (28.0 ± 5.6 pmol/L);	A group had higher concentrations of P1NP (145.6 ±77.5 vs 61.2 ± 22.3 ng/ml; and vit. D₃ (16.9±8.4 vs 10.3 ± 4.3 ng/ ml; lower concentrations of PTH (25.8 ± 8.3 vs 38.2 ± 11.5 pg/ml in comparison to NA. VO₂max = 56.09 ± 4.29 ml/ kg/min in A group;	Vitamin D deficiency was found in 77% of A and 100% of NA;
(60)	♂ n=9	Age 28.8 +/- 3.6 years; Healthy, cyclists;	The 3-week stage cycling race Giro d'Italia 2012Saliva was collected at days:-1, 4, 8, 12, 14,	↑Sclerostin; average level of sclerostin on the 1st day: 254.5 ±134 pg/ mL, in 12th day:	Cortisol remained constant, testosterone decreased at day 4, estradiol and DHEA firstly increased and then	DHEA and estradiol correlated with the physical effort and the bone-muscular markers;

(Continued)

TABLE 2 Continued

Ref:	Group	Group Characteristic	Type of physical activity/ training	Sclerostin	Other biochemical parameters	Additional effects/Comments
			19, 23; Blood and urine were collected at days: -1, 1, 23;	477.5± 137.9 pg/mL, in 23th day: 762.1 ± 143.3 pg/mL;	returned to basal levels. LDH, CK, AST, and urinary Ca and phosphorous increased;	
(61)	♀ n=62	Age - 14-18 years; Eumenorrheic adolescents;Healthy;	Three study groups: rhythmic gymnasts (RG), swimmers (SW), untrained control group (UC);	↑ Sclerostin levels was higher in RG (129.35 ± 51.01 pg/ml; by 74%) and SW; (118.05 ± 40.05 pg/ml; by 59%) v UC: (74.32± 45.41 pg/ml);	No differences between groups in preadipocyte factor-1 (Pref-1), Osteocalcin and CTx;	Adolescent have higher sclerostin compared to UC; Sclerostin correlated with whole-body BMD and lumbar spine (LS) areal bone mineral density (aBMD) in RG, and femoral neck aBMD in UC. No correlation was found between sclerostin and BMD in SW;
(61)	♂ , ♀ n=61 Control n=16 8 ♂ 8♀	Age: 27.2 ± 6.8 years; 15 – Italian national rugby team (29.1 ± 1.7 ys; 13 professional cycling team (31.1. ± 2.7 years); 6 professional tennis players (23.2 ± 6.2 years); 11 professional endure motorcycling team (29.1 ± 11.8 years); 8♀ professional basketball players firs Italian league (27.0 ± 3.0 s); 8♀ figure ice skaters Italian national (19.5 ± 4.9 years);	All athletes classified into three group based on work-load: - (1) weigh bearing, (WB: rugby, endure, basket), (2) non-weight bearing (NWB: cycling), (3) high impact sports (HI: ice skating, tennis); Blood taken after 10 min resting;	Sclerostin level was the same for entire group of athletes and control (0.42 ± 0.09 ng/ml, n.s.); Significant differences between genders in whole cohort: ♂-0.45 ± 0.07 ng/ml, ♀-0.40 ± 0.09 ng/ml) and sedentary group: ♂-0.36 ± 0.05 ng/ml, ♀-0.46 ± 0.09 ng/ml; Differences between men in athletes – rugby players (0.44 ± 0.11ng/ml) and endure (0.42 ± 0.04 ng/ml) had much higher Sclerostin level than cyclists (0.34 ± 0.08 ng/ml);	ALP – 22.4 ± 7.6U/L in athletes and 24.3 ± 8.5U/L in sedentary; Differences of ALP between whole cohort of men and women (21.3 ± 6.8 U/L v 26.1 ± 8.8 U/L) and in athletes: men (20.4 ± 5.5U/l v women (28.4 ± 9.8U/L); No differences in sedentary group. No differences in athletes men and women between sport categories;	Significant correlation were noted for sclerostin level and age; no differences within gender in entire athletes group. No correlation between sclerostin level and category of sport in females. No gender differences in athletes group (♂-0.41 ± 0.09 ng/ml v ♀-045. ± 0.07 ng/ml); No differences in ♀ group of athletes within sport category and to sedentary; In WB athletes sclerostin much higher (0.43 ± 0.0ng/ml) than in NWB athletes (0.34 ± 0.08 ng/ml);
(62)	♀ n=64	Age: 9-10 years Healthy; Gymnasts (RG), n=32; Untrained control (UC), n=32;	Comparison between two groups;	RG: Sclerostin 19.8 ± 6.3 pmol/l was higher in comparison to UC;	RG: Pref-1 (1.6±1.0 ng/ml) was higher than in control (untrained);	Sclerostin and Pref-1 levels are higher in RG compared to UC girls. Sclerostin was related to adiponectin in UC;
(63)	♂ n=9	Age: median 45 years; No specific inclusion and exclusion criteria; Healthy; amount of training about 100km during winter time and more than 200km during summer, up to 7000km/ year;	Spartathlon race 246 km (ultramarathon food race). Runners start in Athens and have to reach Sparta with 36h; It took them 34h 3 min (32h 29 min; 35h 3 min) to reach Sparta;	↓Sclerostin after the race (pre-29.15 pmol/L v 27.75 pmol/L, post- race (n.s.);	Significant ↑myostatin (23.73 ng/ml v 26.73 ng/ml); ↑↑Follistatin (300.8 pg/ml v 1211 pg/ml); ↓ Dkk-1 (38,68 pmol/L v 38.14 pmol/L); ↓ P1NP (54.37 ng/ml v 41.14 ng/ml); ↑ CTX (0.299 ng/ml v 0.542 ng/ml); The increase of myostatin can reflect muscle catabolism processes induced by overstrenuous exercise;	

♀, women, ♂ men, ↓ reduced level, ↑ decreased level.

conclusions may be drawn from comparing sclerostin levels in athletes from many other sports with different workloads to people who do not practice any sports (60, 64).

Sclerostin levels, already high in professional athletes before physical effort, seem to grow even higher during long-term exercise. The study conducted by Grasso et al. (59) involved 9 professional cyclists who raced a total distance of 3503.8 km during the 3-week stage cycling race Giro d'Italia 2012. One of the many parameters measured was the mean sclerostin level in the blood samples of the competitors taken in the morning during the intervals between successive stages. The authors showed that the blood sclerostin level in the cyclists increases during the race in successive stages. The implication is that prolonged high-intensity exercise, as during a 3-week cycling race, may lead to increased bone resorption by steadily increasing serum sclerostin levels during exercise and maintaining high levels between activity stages. This wouldn't be surprising, since there's already data showing that consistent

high loads due to continuous training stimulus increase the sclerostin level through increased bone metabolism (60), which is especially evident in strength sports (61).

Physical training in the prevention of osteoporosis

Physical training to prevent bone mass loss and to maintain or increase BMD levels is based on different principles than training to improve cardiovascular or muscular capacity. When properly selected, composed and conducted, the training has an osteogenic effect, while improper training can lead to the so-called saturation of the osteogenic response to a mechanical stimulus. The bone tissue then becomes resistant to the training stimulus (5).

Exercise as a mechanical stimulus to the skeletal system increases bone mineral density through a mechanotransduction mechanism in bone, involving the sclerostin protein as described previously (62, 65). Based on that, the effectiveness of physical training in the prevention of skeletal disorders can be assessed by BMD, depending on factors such as:

- type of training (66);
- exercise intensity (63, 67);
- frequency of exercises, breaks between exercises and series (63, 67)
- the number of body parts involved (68)
- systematic approach (69)

Exercise to prevent osteoporosis must be of such intensity that bone tissue shows a threshold sensitivity to mechanical stimulus, because bones show an osteogenic effect only when this threshold is exceeded (70). Studies among menopausal women have confirmed the effect of high-intensity walking on increasing BDM, particularly in the lower body. The threshold for osteogenic activity in the study group occurred at a speed of just over 6.14 km/h and a load of 872.3 N, which translated to 80% of age-specific maximum heart rate (HRmax), 74% of VO_2max, and 115% of ventilation threshold (71). If the stimulus intensity is increased during training or a training cycle, the potentiation of the osteogenic effect will occur until the so-called saturation of the osteogenic response (72).

As per Bailey et al. (69) daily exercises results in greater osteogenic activity. Moreover, Ardawi et al. (32) showed that physical activity levels above 120 min per week result in significantly higher serum sclerostin levels, leading to increased bone mineral density. Exercise should involve as many body parts as possible because of the fact that osteogenic activity occurs in the part of skeleton directly loaded by the mechanical stimulus (68). Breaks between repetitions of a given exercise in a cycle allow the mechanical stimulus to activates more bone-forming cells or osteoblasts and achieve an osteogenic effect with fewer repetitions, but also to shift the threshold at which saturation of the osteogenic response occurs later (73, 74). Moreover exercise should be repeated several to a dozen times, and the intervals between exercise cycles should be more than 4 - 8 hours in order to avoid saturation of the osteogenic response (72, 73).

Research to date confirms that exercise has a beneficial effect on bone health (75). However, the size of osteogenic effect obtained depends not only on the factors mentioned above, but also on the type of physical training performed (5). Exercise exerts two types of mechanical load on the bone in the form of JFR e.g. running, walking, climbing stairs and GRF e.g. rowing, weightlifting. A study of 39 postmenopausal women found that both types of exercise resulted in a significant increase in BDM, but GRF-based training resulted in a greater increase in both the entire body, and the individual skeletal parts tested (76). Table 3 lists the types of exercise along with the degree of osteogenic effects (77).

High- and moderate-intensity exercise involving both JFR and GRF causes a strong osteogenic effect. The greatest osteogenic activity is found in running, tennis, and weight training using equipment, among others. In addition, a slightly higher mean BDM (across skeletal parts) was observed among women performing GFR-based exercise training (76). Power training based on dynamic exercises will be more effective in preventing osteoporosis than training based on strength exercises (72).

There is also an interesting question of the influence of the level of physical activity during childhood and adolescence on bone mass in elderly people. There's data showing that peripubertal exercise causes at least two types of skeletal adaptations: periosteal expansion and better trabecular microarchitecture (78). Especially high sensitivity of the

TABLE 3 Types and examples of exercises with their corresponding osteogenic effect coefficient.

Type of physical exercise	Example	Osteogenic effect coefficient
Exercises without or with smallGRF and JRF	cycling, swimming	0
Exercises or games with small GRF and JRF	bowling, walking	1
Exercises or games with moderate GRF and JRF	dancing, aerobic exercises with light loads rhythmics	2
Exercises or games with GRF > 1000μE	Running, aerobic exercise with heavy loads,tennis, squash	3
Exercises with large JRF	strength training using equipment	3

skeleton to exercise at this time of life may be due to high growth hormone level. The extent to which the forementioned skeletal changes may last to the old age remains unclear. Nevertheless, it is worth mentioning that structural changes may persist despite the loss of bone mass (79, 80)

Studies have shown that exercise programs which includes at least two kinds of activities such as weight-bearing activities, progressive resistance training (PRT) and/or power training and balance/mobility training have positive effect on skeletal system and fall-related risk factors (81). Detailed training program recommended in osteoporosis and osteoporotic fractures prevention with physical activities, frequency, intensity and sets/repetitions descriptions is presented in Table 4.

Exercising regularly has a beneficial effect on health but not every type of activity shows equal osteogenic effect. Previous studies about aerobic training such as swimming, cycling or walking and its positive impact on all body systems are contrary to those suggesting that these activities do not provide notable stimulus to bone and next to that do not cause an osteogenic effect. However there are types of activities which have positive influence on bone health. A lot of bone adaptive responses depends on magnitude, rate and frequency of loading. They must be dynamic, cyclic and induce relatively high bone strains. In order to elicit a bone system adaptive response relatively few loading cycles with adequate load intensity are required. Moreover breaks between repetition are equally or even more important than number of repetitions in cycle. Finally, loading diversification is required to stimulate an adaptive skeletal response (83).

Summary

Based on the foregoing considerations, sclerostin is a marker to determine the effect of exercise on bone tissue processes. By inhibiting tissue formation processes, this protein mediates bone remodeling. In recent years, numerous studies have shown that properly selected physical training has a preventive effect on skeletal diseases, especially osteoporosis, by increasing bone mineral density (82, 84). This disease, which is considered to be a civilization disease, is a huge problem both socially and economically, so the

TABLE 4 Training program recommended in osteoporosis and osteoporotic fractures prevention (82).

Type	Progressive resistance training	Weight-bearing impact exercise	Challenging balance, steppingand mobility
Exercises	Exercises: squats, lunges, hip abduction/adduction, leg press, thoracic/lumbar extension, plantar/dorsi-flexion, abdominal/postural exercises, bent over row, wall/counter/floor pushup, triceps dips and lateral shoulder raises.	Multidirectional and novel loading activities: jumping, bounding, skipping, hopping, bench stepping and drop jumps or participation in weight-bearing sports (e.g., tennis, dancing, netball, recreational gymnastics and football).	Include static and dynamic movements: reduce base of support, shift weight to limits of stability (e.g., leaning/ reaching), perturb center of mass, stepping over obstacles, alter surface (foam mats) and multi-sensory activities (e.g. reduce vision) and dual tasking. Consider Tai Chi and rapid stepping movements in different directions.
Frequency	≥2 days per week	4- 7 times per week	Accumulate at least 2- 3 h per week. This could be achieved within other exercise bouts during the course of a week.
Intensity	Start with slow and controlled movements and emphasize correct lifting technique.Progress to 75-85% of 1-RM(5-7/8 on Borg 0-10 point RPE scale or hard-very hard).Consider progressing to high velocity (power) resistance and functional training for lower extremities to increase rate of loading and improve movement speed and power.Light-to-moderate loads (30-70% 1-RM) can be used.	Moderate to high impact activities (>2-4 BW), as tolerated.Increase height of jump, step heigh, weights or a weighted vest and incorporate change of direction movement.For sedentary individual and those with poor muscle strength or function, start with PRT for 6-12 weeks to strengthen lower limb muscles and/or introduce low impact exercises and core muscle training.	Must be progressively challenging (close to limit of balance) and preferably specific to everyday functional tasks.Progress to dynamic/mobility and rapid stepping exercises and introduce secondary motor or cognitive tasks to improve dual task performance.
Sets/ Repetitions	≥8 exercises targeting muscles attached too or crossing the hip and spine At least 2 sets 8- 12 repetitions1- 3 min rest between sets	50-100 jumps per session divided into 3-5 sets of 10-20 repetitions. 1-2 min rest between sets.	Incorporate into daily activities or combine with resistance or impact exercise (e.g., balance for 10-30 s while waiting for kettle to boil, cooking or watching TV).
Precautions	Emphasize exercises performed in a standing (weight-bearing) position.Use caution with lifting weights higher than shoulder height to limit rotator cuff injury.For individuals with low spine BMD avoid spine flexion or twisting and encourage spine-sparing strategies.Include core stability and postural strengthening/endurance exercises as well as pelvic floor activities.	Teach correct landing technique.Progress slowly.Intersperse between strength and balance exercises.For those with incontinence issues first strengthen pelvic floor muscles and avoid jumping exercises with feet wide apart. For those with (osteo)arthritis, prescribe within limits of pain.	For individuals with impaired balance or high fracture risk, start with static and progress to dynamic balance exercises.

BW, body weight; RPE, Rating of Perceived Exertion; 1-RM, one-repetition maximum.
In accordance with most national physical activity guidelines, women should accumulate ≥150 min per week of moderate to vigorous intensity physical activity. To realistically accomplish all of the above therapeutic goals, one could combine activities e.g., lunges as a leg strengthening exercise that also challenges balance, step class that includes impact exercise and moderate/ vigorous aerobic challenge and simultaneously challenges balance (91).

fact of the beneficial effect of physical exercise as the cheapest and most beneficial cure is all the more convincing. This study demonstrates the relationship between the physical activity level and serum sclerostin level and bone mineral density, as osteogenic factors. This raises the question: why do near-maximal mechanical stress and high bone mineral density in athletes not correlate with reduced blood sclerostin levels, as in people with low or moderate activity levels? Are there other mechanisms involved in the osteogenic response with very high mechanical loading? Furthermore, it has been noted that not every type of physical activity results in a significant increase in BMD. According to selected studies osteogenic activity is affected by the load of exercise, type of physical training, and its effectiveness depends on the intensity and frequency of exercise, and the intervals between repetitions, among other factors. Moreover the very essential factors are gender and season, because in bone turnover markers secretion the seasonal variations was observed (85). The question remains, will osteoporosis be preventable and treatable in the near future with well-timed physical training as an alternative to medication?

There is still a need for further research to answer this question and to clearly establish the dynamics of sclerostin changes in relation to the factors influencing its secretion.

Author contributions

Conceptualization: EM-C, AO, and AK. Writing—original draft preparation: AO, AK, MK, MC, EA, AS, FC and EM-C. Supervision: EM-C and FC. Project administration: EM-C. Funding acquisition: EM-C and AK. All authors have contributed to the article and approved the submitted version.

Conflict of interest

The authors declare that the research was conducted in the absence of any commercial or financial relationships that could be construed as a potential conflict of interest.

Publisher's note

All claims expressed in this article are solely those of the authors and do not necessarily represent those of their affiliated organizations, or those of the publisher, the editors and the reviewers. Any product that may be evaluated in this article, or claim that may be made by its manufacturer, is not guaranteed or endorsed by the publisher.

References

1. Sewerynek E, Bajon K, Stuss M. Secondary osteoporosis during long-term steroid treatment. *Menopasal Rev* (2007) 6:336–43.

2. Khosala S, Westendor JJ, Oursler MJ. Building bone to reverse osteoporosis and repair fractures. *J Clin Invest.* (2008) 118(2):421–8. doi: 10.1172/JCI33612

3. Tong X, Chen X, Zhang S, Huang M, Shen X, Xu J, et al. The effect of exercise on the prevention of osteoporosis and bone angiogenesis. *BioMed Res Int* (2019) 2019:8171897. doi: 10.1155/2019/8171897

4. Föger-Samwald U, Dovjak P, Azizi-Semrad U, Kerschan-Schindl K, Pietschmann P. Osteoporosis: Pathophysiology and therapeutic options. *EXCLI J* (2020) 19:1017–37. doi: 10.17179/excli2020-2591

5. Czarkowska – Paczek B, Wesołowska K, Przybylski J. Exercise in prophylaxis of osteoporosis przy. *Lek* (2011) 68(2):103–6.

6. Cosman F, de Beur SJ, LeBoff MS, Lewiecki EM, Tanner B, Randall S, et al. Clinician's guide to prevention and treatment of osteoporosis. *Osteoporos Int* (2014) 25(10):2359–81. doi: 10.1007/s00198-014-2794-2

7. Hernlund E, Svedbom A, Ivergard M, Compston J, Cooper C, Stenmark J, et al. Osteoporosis in the European union: medical management, epidemiology and economic burden. a report prepared in collaboration with the international osteoporosis foundation (IOF) and the European federation of pharmaceutical industry associations (EFPIA). *Arch Osteoporos* (2013) 8(1):1–115. doi: 10.1007/s11657-013-0136-1

8. Compston J. Osteoporosis: social and economic impact. *Radiol Clin North Am* (2010) 48(3):477–82. doi: 10.1016/j.rcl.2010.02.010

9. Kucharska E. Osteoporosis: a social problem in the elderly population. *Horizons of Education* (2017) 16(40):37–57. doi: 10.17399/HW.2017.164003

10. Horizons Educ. (2017) 16(40):37 57. doi: 10.17399/HW.2017.164003

11. Kanis JA, Norton N, Harvey NC, Jacobson T, Johansson H, Lorentzon M, et al. SCOPE 2021: a new scorecard for osteoporosis in Europe. *Arch Osteoporos* (2021) 16(1):82. doi: 10.1007/s11657-020-00871-9

12. Abdolalipour S, Mirghafourvand M, Ghassab-Abdollahi N, Farshbaf-Khalili A. Health-promoting lifestyle and quality of life in affected and unaffected menopausal women by primary osteoporosis. *J Educ Health Promot* (2021) 10:45. doi: 10.4103/jehp.jehp_450_20

13. Choi MH, Yang JH, Seo JS, Y-j K, Kang S-W. Prevalence and diagnosis experience of osteoporosis in postmenopausal women over 50: Focusing on socioeconomic factors. *PloS One* (2021) 16(3):e0248020. doi: 10.1371/journal.pone.0248020

14. Willers C, Norton N, Harvey NC, Jacobson T, Johansson H, Lorentzon M, et al. Osteoporosis in Europe: a compendium of country-specific reports. *Arch Osteoporos* (2022) 17:23. doi: 10.1007/s11657-021-00969-8

15. Dardzińska J, Chabaj-Kędroń H, Małgorzewicz S. Osteoporosis as a social disease : prevention methods. *Hygeia Public Health* (2016) 51(1):23–30.

16. *Ageing Europe - statistics on population developments*. Luxembourg: Publications Office of the European Union, (2020). Available at: https://ec.europa.eu/eurostat/statistics-explained/index.php?title=Ageing_Europe_-_statistics_on_population_developments

17. Janiszewska M, Kulik T, Dziedzic M, Żołnierczuk-Kieliszek D, Barańska A. Osteoporosis as a social problem – pathogenesis, symptoms and risk factors of postmenopausal osteoporosis. *Probl Hig Epidemiol* (2015) 96(1):106–14.

18. Todd JA, Robinson RJ. Osteoporosis and exercise. *Postgrad Med J* (2003) 79 (932):320–3. doi: 10.1136/pmj.79.932.320

19. Malhan D, Muelke M, Rosch S, Schaefer AB, Merboth F, Weisweiler D, et al. An optimized approach to perform bone histomorphometry. *Front Endocrinol* (2018) 9:666. doi: 10.3389/fendo.2018.00666

20. Wilson N, Hurkmans E, Adams J, Bakkers M, Balážová P, Baxter M, et al. Prevention and management of osteoporotic fractures by non-physician health professionals: a systematic literature review to inform EULAR points to consider. *RMD Open* (2020) 6:e001143. doi: 10.1136/rmdopen-2019-001143

21. Perry SP, Downey PA. Fracture risk and prevention: A multidimensional approach. *Physic Ther* (2012) 92(1):164–78. doi: 10.2522/ptj.20100383

22. Cariati I, Bonanni R, Onorato F, Mastrogregori A, Rossi D, Iundusi R, et al. Role of physical activity in bone–muscle crosstalk: Biological aspects and clinical implications. *J Funct Morphol Kinesiol.* (2021) 6(2):55. doi: 10.3390/jfmk6020055

23. Moreira LD, Oliveira ML, Lirani-Galvão AP, Marin-Mio RV, Santos RN, Lazaretti-Castro M. Physical exercise and osteoporosis: effects of different types of exercises on bone and physical function of postmenopausal women. *Arq Bras Endocrinol Metabol.* (2014) 58(5):514–22. doi: 10.1590/0004-2730000003374

24. Troy KL, Mancuso ME, Butler TA, Johnson JE. Exercise early and often: Effects of physical cctivity and exercise on women's bone health. *Int J Environ Res Public Health* (2018) 15(5):878. doi: 10.3390/ijerph15050878

25. Morris HA. Osteoporosis prevention–a worthy and achievable strategy. *Nutrients.* (2010) 2(10):1073–4. doi: 10.3390/nu2101073

26. Balemans W, Ebeling M, Patel N, Van Hul E, Olson P, Dioszegi M, et al. Increased bone density in sclerosteosis is due to the deficiency of a novel secreted protein (SOST). *Hum Mol Genet* (2001) 10:537–43. doi: 10.1093/hmg/10.5.537

27. Winkler DG, Yu C, Geoghegan JC, Ojala EW, Skonier JE, Shpektor D, et al. Noggin and sclerostin bone morphogenetic protein antagonists form a mutually inhibitory complex. *J Biol Chem* (2004) 279:36293–8. doi: 10.1074/jbc.M400521200

28. Delgado-Calle J, Sato AY, Bellido T. Role and mechanism of action of sclerostin in bone. *J Bone* (2017) 96:29–37. doi: 10.1016/j.bone.2016.10.007

29. Weivoda MM, Youssef SJ, Jo Oursler M. Sclerostin expression and functions beyond the osteocyte. *J Bone* (2017) 96:45–50. doi: 10.1016/j.bone.2016.11.024

30. Silverman SL. Sclerostin. *J Osteoporos* (2010) 2010:941419. doi: 10.4061/2010/941419

31. Pietrzyk B, Smertka M, Chudek J. Sclerostin: Intracellular mechanisms of action and its role in the pathogenesis of skeletal and vascular disorders. *Adv Clin Exp Med* (2017) 26(8):1283–91. doi: 10.17219/acem/68739

32. Catalano A, Bellone F, Morabito N, Corica F. Sclerostin and vascular pathophysiology. *IJMS* (2020) 21:4779. doi: 10.3390/ijms21134779

33. Yavropoulou MP, Xygonakis C, Lolou M, Karadimou F, Yovos JG. The sclerostin story: From human genetics to the development of novel anabolic treatment for osteoporosis. *Hormones* (2014) 13(4):476–87. doi: 10.14310/horm.2002.1552

34. Sharma-Ghimire P, Chen Z, Sherk V, Bemben D. Sclerostin and parathyroid hormone responses to acute whole-body vibration and resistance exercise in young women. *J Bone Miner Metab* (2019) 37:358–67. doi: 10.1007/s00774-018-0933-0

35. Ardawi MS, Rouzi AA, Qari HM. Physical activity in relation to serum sclerostin, insulin-like growth factor-1 and bone turnover markers in healthy premenopausal women: a cross-sectional and a longitudinal study. *J Clin Endocrinol Metab* (2012) 97(10):3691–9. doi: 10.1210/jc.2011-3361

36. Moester MJC, Papapoulos SE, Lowik CWGM, van Bezooijen RL. Sclerostin: current knowledge and future perspectives. *Calcif Tissue Int* (2010) 87:99–107. doi: 10.1007/s00223-010-9372-1

37. Bonnet N, Garnero P, Ferrari S. Periostin action in bone. *Mol Cell Endocrinol* (2016) 432:75–82. doi: 10.1016/j.mce.2015.12.014

38. Kramer I, Halleux C, Keller H, Pegurri M, Gooi JH, Brander Weber P, et al. Osteocyte wnt/beta-catenin signaling is required for normal bone homeostasis. *Mol Cell Biol* (2010) 30(12):3071–85. doi: 10.1128/MCB.01428-09

39. Bonnet N, Standley KN, Bianchi EN, Stadelmann V, Foti M, Conway SJ, et al. The matricellular protein periostin is required for sost inhibition and the anabolic response to mechanical loading and physical activity. *J Biol Chem* (2009) 284(51):35939–50. doi: 10.1074/jbc.M109.060335

40. Wolski H, Drwęska – Matelska N, Seremak – Mrozikiewicz A, Łowicki Z, Czerny B. The role of wnt/β-catenin pathway and LRP5 protein in metabolism of bone tissue and osteoporosis etiology. *Ginekol Pol* (2015) 86:311–4. doi: 10.17772/gp/2079

41. Holdsworth G, Roberts SJ, Ke HZ. Novel actions of sclerostin on bone. *J Mol Endocrinol* (2019) 62(2):R167–85. doi: 10.1530/JME-18-0176

42. Robling AG, Niziolek PJ, Baldridge LA, Condon KW, Allen MR, Alam I, et al. Mechanical stimulation of bone *in vivo* reduces osteocyte expression of sost/sclerostin. *J Biol Chem* (2008) 283:5866–75. doi: 10.1074/jbc.M705092200

43. Lin C, Jiang X, Dai Z, Guo X, Weng T, Wang J, et al. Sclerostin mediates bone response to mechanical unloading through antagonizing wnt/β-catenin signaling. *J Bone Miner Res* (2009) 24:1651–61. doi: 10.1359/jbmr.090411

44. Sharifi M, Ereifej L, Lewiecki EM. Sclerostin and skeletal health. *Rev Endocr Metab Disord* (2015) 16:149–56. doi: 10.1007/s11154-015-9311-6

45. Cosman F, Crittenden DB, Adachi JD, Binkley N, Czerwinski E, Ferrari S, et al. Romosozumab treatment in postmenopausal women with osteoporosis. *N Engl J Med* (2016) 375(16):1532–43. doi: 10.1056/NEJMoa1607948

46. Brandenburg VM, D'Haese P, Deck A, Mekahli D, Meijers B, Neven E, et al. From skeletal to cardiovascular disease in 12 steps–the evolution of sclerostin as a major player in CKD-MBD. *Pediatr Nephrol* (2016) 31:195–206. doi: 10.1007/s00467-015-3069-7

47. Frings-Meuthen P, Boehme G, Liphardt AM, Baecker N, Hee M, Rittweger J. Sclerostin and DKK1 levels during 14 and 21 days of bed rest in healthy young men. *J Musculoskelet Neuronal Interact* (2013) 13(1):45–52.

48. Janik M, Stuss M, Michalska-Kasiczak M, Jegier A, Sewerynek E. Effects of physical activity on sclerostin concentrations. *Endokrynol Pol* (2018) 69(2):142–9. doi: 10.5603/EP.a2018.0008

49. Bimonte VM, Fittipaldi S, Marocco C, Emerenziani GP, Fornari R, Guidetti L, et al. Physical activity and hypocaloric diet recovers osteoblasts homeostasis in women affected by abdominal obesity. *Endocrine* (2017) 58(2):340–8. doi: 10.1007/s12020-016-1193-1

50. Wannenes F, Papa V, Greco EA, Fornari R, Marocco C, Baldari C, et al. Abdominal fat and sarcopenia in women significantly alter osteoblasts homeostasis *in vitro* by a WNT/β-catenin dependent mechanism. *Int J Endocrinol* (2014) 2014:278316. doi: 10.1155/2014/278316

51. Hinton PS, Nigh P. Thyfault JSerum sclerostin decreases following 12 months of resistance- or jump-training in men with low bone mass. *Bone* (2017) 96:85–90. doi: 10.1016/j.bone.2016.10.011

52. Pickering ME, Simon M, Sornay-Rendu E, Chikh K, Carlier MC, Raby AL, et al. Serum sclerostin increases after acute physical activity. *Calcif Tissue Int* (2017) 101(2):170–3. doi: 10.1007/s00223-017-0272-5

53. Gombos CG, Bajsz V, Pek E, Schmidt B, Sió E, Molics B, et al. Direct effects of physical training on markers of bone metabolism and serum sclerostin concentrations in older adults with low bone mass. *BMC Musculoskelet Dis* (2016) 17:254. doi: 10.1186/s12891-016-1109-5

54. Kouvelioti R, Kurgan N, Falk B, Ward WE, Josse AR, Klentrou P. Response of sclerostin and bone turnover markers to high intensity interval exercise in young woman: does impact matter? *BioMed Res Int* (2018) 2018:4864952. doi: 10.1155/2018/4864952

55. Armamento-Villareal R, Sadler C, Napoli N, Shah K, Chode S, Sinacore DR. Weight loss in obese older adults increases serum sclerostin and impairs hip geometry but both are prevented by exercise traning. *J Bone Miner Res* (2012) 27 (5):1215–21. doi: 10.1002/jbmr.1560

56. Śliwicka E, Cisoń T, Pilczyńska-Szcześniak Ł, Ziemba A, Straburzyńska-Lupa A. Effects of marathon race on selected myokines and sclerostin in middle-aged male amateur runners. *Sci Rep* (2021) 11:2813. doi: 10.1038/s41598-021-82288-z

57. Zagrodna A, Jóźków P, Mędraś M, Słowińska – Lisowska M. Sclerostin as a novel marker of bone turnover in athletes. *Biol Sport* (2016) 33:83–7. doi: 10.5604/20831862.1194125

58. Kouvelioti R, Kurgan N, Falk B, WE W, Josse AR, Klentrou P. Response of sclerostin and bone turnover markers to high intensity interval exercise in young women: Does impact matter? *BioMed Res Int* (2018) 2018:1–8. doi: 10.1155/2018/4864952

59. Jürimäe J, Tillmann V, Cicchella A, Stefanelli C, Võsoberg K, Tamm AL, et al. Increased sclerostin and preadipocyte factor-1 levels in prepubertal rhythmic gymnasts: associations with bone mineral density, body composition, and adipocytokine values. *Osteoporos Int* (2016) 27(3):1239–43. doi: 10.1007/s00198-015-3301-0

60. Grasso D, Corsetti R, Lanteri P, Di Bernardo C, Colombini A, Graziani R, et al. Bone-muscle unit activity, salivary steroid hormones profile, and physical effort over a 3-week stage race. *Scand J Med Sci Sports* (2015) 25:70–80. doi: 10.1111/sms.12147

61. Lombardi G, Lanteri P, Colombini A, Mariotti M, Banfi G. Sclerostin concentrations in athletes: role of load and gender. *J Biol Regul Homeost Agents* (2012) 26(1):157–63.

62. Garnero P, Sornay-Rendu E, Munoz F, Borel O, Chapurlat RD. Association of serum sclerostin with bone mineral density, bone turnover, steroid and parathyroid hormones, and fracture risk in postmenopausal women: the OFELY study. *Osteoporos Int* (2013) 24:489–94. doi: 10.1007/s00198-012-1978-x

63. Benedetti MG, Furlini G, Zati A, Letizia Mauro G. The effectiveness of physical exercise on bone density in osteoporotic patients. *BioMed Res Int* (2018) 2018:4840531. doi: 10.1155/2018/4840531

64. Jürimäe J, Karvelyte V, Remmel L, Al T, Purge P, Gruodyte-Raciene R, et al. Sclerostin, preadipocyte factor 1 and bone mineral values in eumenorrheic adolescent athletes with different training patterns. *J Bone Miner Metab* (2020) 39(2):245–52. doi: 10.1007/s00774-020-01141-x

65. Bonewald LF, Johnson ML. Osteocytes, mechanosensing and wnt signaling. *Bone* (2008) 42:606. doi: 10.1016/j.bone.2007.12.224

66. Isaksson H, Gröngröft I, Wilson W, van Donkelaar C, van Rietbergen B, Tami A, et al. Remodeling of fracture callus in mice is consistent with mechanical loading and bone remodeling theory. *J Orthop Res* (2009) 27:664. doi: 10.1002/jor.20725

67. Hong AR, Kim SW. Effects of resistance exercise on bone health. *Endocrinol Metab (Seoul)* (2018) 33(4):435–44. doi: 10.3803/EnM.2018.33.4.435

68. Kemmler W, Shojaa M, Kohl M, von Stengel S. Effects of different types of exercise on bone mineral density in postmenopausal women: A systematic review and meta-analysis. *Calcif Tissue Int* (2020) 107:409–39. doi: 10.1007/s00223-020-00744-w

69. Stengel SV, Kemmler W, Pintag R, Beeskow C, Weineck J, Lauber D, et al. Power training is more effective than strength training for maintaining bone mineral density in postmenopausal women. *J Appl Physiol* (2005) 99:181. doi: 10.1152/japplphysiol.01260.2004

70. Bailey CA, Brooke-Wavell K. Optimum frequency of exercise for bone health: randomised controlled trial of a high-impact unilateral intervention. *Bone* (2010) 46:1043. doi: 10.1016/j.bone.2009.12.001

71. Siller-Jackson AJ, Burra S, Gu S, Xia X, Bonewald LF, Sprague E, et al. Adaptation of connexin 43-hemichannel prostaglandin release to mechanical loading. *J Biol Chem* (2008) 283:26374. doi: 10.1074/jbc.M803136200

72. Borer KT, Fogleman K, Gross K, La New JM, Dengel D. Walking intensity for postmenopausal bone mineral preservation and accrual. *Bone* (2007) 41:713. doi: 10.1016/j.bone.2007.06.009

73. Robling AG, Hinant FM, Burr DB, Turner CH. Improved bone structure and strength after long-term mechanical loading is greatest if loading is separated into short bouts. *J Bone Miner Res* (2002) 17:1545. doi: 10.1359/jbmr.2002.17.8.1545

74. Srinivasan S, Ausk BJ, Poliachik SL, Warner SE, Richardson TS. Gross TS rest- inserted loading rapidly amplifies the response of bone to small increases in strain and load cycle. *J Appl Physiol* (2007) 102:1945. doi: 10.1152/japplphysiol.00507.2006

75. Gross TS, Poliachik SL, Ausk BJ, Sanford DA, Becker BA, Srinivasan S. Why rest stimulates bone formation: a hypothesis based on complex adaptive phenomenon. *Exerc Sport Sci Rev* (2004) 32:9. doi: 10.1097/00003677-200401000-00003

76. Hejazi K, Askari R, Hofmeister M. Effects of physical exercise on bone mineral density in older postmenopausal women: a systematic review and meta-analysis of randomized controlled trials. *Arch Osteoporos.* (2022) 17(1):102. doi: 10.1007/s11657-022-01140-7

77. Kohrt WM, Ehsani AA, Birge SJJr. Effect of exercise involving predominantly either joint-reaction or ground-reaction forces on bone mineral density in older women. *J Bone Miner Res* (1997) 12:1253. doi: 10.1359/jbmr.1997.12.8.1253

78. Kemmler W, Weineck J, Kalender WA, Engelke K. The effect of habitual physical activity, non-athletic exercise, muscle strength, and VO2max on bone mineral density is rather low in early postmenopausal women. *J Musculosceletal Neuron Interact* (2004) 4:325.

79. Kirmani S, Christen D, van Lenthe GH, Fischer PR, Bouxsein ML, McCready LK, et al. Bone structure at the distal radius during adolescent growth. *J Bone Miner Res* (2009) 24(6):1033–42. doi: 10.1359/jbmr.081255

80. Warden SJ, Fuchs RK, Castillo AB, Nelson IR, Turner CH. Exercise when young provides lifelong benefits to bone structure and strength. *J Bone Miner Res* (2007) 22(2):251–9. doi: 10.1359/jbmr.061107

81. Warden SJ, Mantila Roosa SM, Kersh ME, Hurd AL, Fleisig GS, Pandy MG, et al. Physical activity when young provides lifelong benefits to cortical bone size and strength in men. *Proc Natl Acad Sci U.S.A.* (2014) 111(14):5337–42. doi: 10.1073/pnas.1321605111

82. Amato A, Baldassano S, Cortis C, Cooper J, Proia P. Physical activity, nutrition, and bone health. *Hum Mov* (2018) 19(4):1–10. doi: 10.5114/hm.2018.77318

83. Daly RM, Dalla Via J, Rachel L. Duckham RL, Fraser SF, Wulff Helge E. Exercise for the prevention of osteoporosis in postmenopausal women: an evidence-based guide to the optimal prescription. *Braz J Phys Ther* (2019) 23 (2):170–80. doi: 10.1016/j.bjpt.2018.11.011

84. Beck BR, Daly RM, Fiatarone Singh MA, Taaffe DR. Exercise and sports science Australia (ESSA) position statement onexercise prescription for the prevention and management ofosteoporosis. *J Sci Med Sport* (2017) 20(5):438–445. doi: 10.1016/j.jsams.2016.10.001

85. Mero A, Häkkinen K, Kyröläinen H, Mero A. Effects of training on bone metabolism in young athletes. *Hum Mov* (2021) 22(4):105–12. doi: 10.5114/hm.2021.104181

Causal associations of hand grip strength with bone mineral density and fracture risk: A mendelian randomization study

Jidong Song, Tun Liu, Jiaxin Zhao, Siyuan Wang, Xiaoqian Dang* and Wei Wang*

The Second Affiliated Hospital, Xi'an Jiaotong University, Xi'an, Shaanxi, China

Background: Muscle strength has been shown to exert positive effects on bone health. The causal relationship between hand grip strength and osteoporosis is an important public health issue but is not fully revealed. The goal of this study was to investigate whether and to what extent hand grip strength affects bone mineral density (BMD) and fracture risk.

Methods: We conducted a state-of-the-art two-sample Mendelian randomization analysis. Genomewide significant ($P<5\times10^{-8}$) single nucleotide polymorphisms associated with hand grip strength were obtained. Summary level data of BMD and fractures at different body sites (lumbar spine, heel, forearm and femoral neck) was obtained from a large-scale osteoporosis database. The inverse variance weighted method was the primary method used for analysis, and the weighted-median, MR-Egger were utilized for sensitivity analyses.

Results: The results provided strong evidence that hand grip strength trait was causally and positively associated with lumbar spine BMD (β: 0.288, 95% CI: 0.079 to 0.497; $P=0.007$), while no causal relationship was found between hand grip strength and BMD at heel (β: -0.081, 95% CI: -0.232 to 0.070; $P=0.295$), forearm (β: 0.-0.101, 95% CI: -0.451 to 0.248; $P=0.571$) or femoral neck (β: 0.054, 95% CI: -0.171 to 0.278; $P=0.639$). In addition, no statistically significant effects were observed for hand grip strength on fracture risks (β: -0.004, 95% CI: -0.019 to 0.012; $P=0.662$).

Conclusions: This study showed a positive causal relationship between hand grip strength and lumbar BMD, which is the most common site of osteoporotic fracture, but did not find a causal relationship between hand grip strength and BMD of heel, forearm, or femoral neck. No statistically significant effect of hand grip strength on fracture risk was observed. This study indicates variations in the abilities of hand grip strength trait to causally influence BMD at different

skeleton sites. These results should be considered in further studies and public health measures on osteoporosis prevention strategies.

1 Introduction

Osteoporosis is a common musculoskeletal disorder characterized by low bone mass and deterioration of bone microstructure, resulting in decreased bone density and increased risk of fracture. The incidence of osteoporosis increases significantly with age. The prevalence of osteoporosis is 16.0% among men aged 50 years or older and 29.9% among postmenopausal women, and the annual cost of osteoporotic fractures is estimated to reach \$25 billion by 2025 in the USA (1–3). Low bone mineral density (BMD) and fracture risk are two major characteristics of osteoporosis. Although several genetic loci influencing this disease have been detected, the genetic mechanism is still not fully understood.

Sarcopenia is also an age-related condition characterized by progressive and generalized accelerated loss of muscle mass and function, associated with an increased likelihood of adverse outcomes including falls, functional decline, frailty, and mortality (4, 5). The stepwise diagnostic protocol starts with the measurement of muscle strength, including grip strength and chair stand tests (5, 6). Prevalence estimations for sarcopenia vary widely across clinical settings, with reported prevalence rates of 1-29% in community-dwelling residents and 14-33% in residents requiring long-term care (7, 8), resulting in an estimated \$18.5 billion in direct medical costs in the USA in 2000 (9). Osteoporosis and sarcopenia may coexist in the elderly.Identifying the relationship between the two may have implications for clinicians to intervene and improve osteoporosis (10). The grip strength test is a simple and effective way of measuring muscle strength (11). However, the epidemiological conclusions on the relationship between grip strength and BMD or fracture risk remain inconsistent (12–14). Moreover, it is not clear whether these relationships are causal because of the inherent limitations of conventional observational studies, including small sample sizes and confounding and reverse causality. Although randomized controlled trials (RCTs) are the gold standard for inferring causality, they are expensive, time-consuming and sometimes impractical.

The popularity of genome-wide association analysis (GWAS) has revolutionized the study of human genetics and the genetic mechanisms of complex diseases (15). Mendelian randomization (MR) uses GWAS data to analyze the causal relationship between different exposures and outcomes. Alleles follow the law of independent assortment and are constant during their whole lifetime, which imitates the design of an RCT (16). MR analyses effectively overcome the limitations of traditional observational studies. Therefore, MR is a feasible way to analyze the causal association between grip strength and BMD or fracture risk.

Here, we performed two-sample MR analysis using large-scale GWAS summary statistics to explore the causal associations of BMD at different skeletal sites and the risk of bone fracture with grip strength.
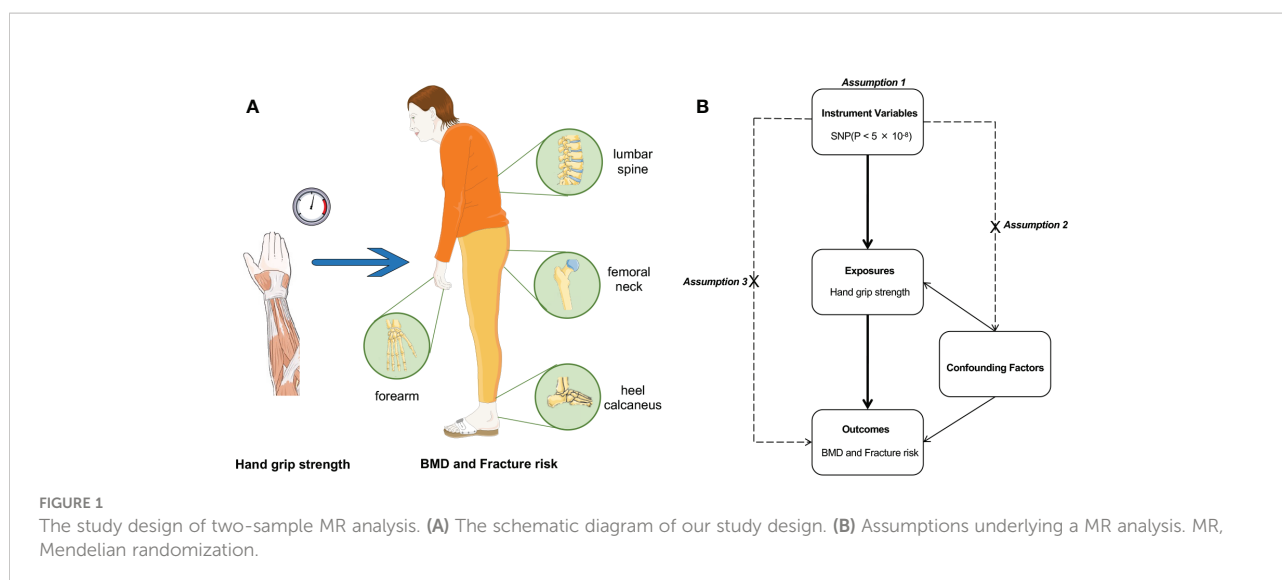
2 Methods

2.1 Study design

Our study utilized a two-sample Mendelian randomization analysis of grip strength with different bone locations. Hand grip strength was categorized as the exposure, and BMD at four skeletal sites (heel, forearm, lumbar spine and femoral neck) and fracture risk were considered outcomes. MR is based on three main assumptions (15): the instrumental variables should be correlated with the exposure; the instrumental variables should not be associated with confounders; and the instrumental variables should influence the outcome only through the exposure (no horizontal pleiotropy) (Figure 1). The significant genome-wide single-nucleotide polymorphisms (SNPs) ($P<5\times10^{-8}$) were selected as instrumental variables. Further sensitivity and pleiotropy analyses were performed to ensure the robustness of the results.

2.2 Data sources

The participants of the GWAS are of European descent. For the exposure, the summary statistics data on hand grip strength (right) were retrieved from the United Kingdom Biobank (UKB), including 499,260 white British individuals.

For the outcomes, the summary statistics data on BMD of the femoral neck, lumbar spine and forearm were retrieved from the Genetic Factors for Osteoporosis Consortium (GeFOS),

FIGURE 1

The study design of two-sample MR analysis. **(A)** The schematic diagram of our study design. **(B)** Assumptions underlying a MR analysis. MR, Mendelian randomization.

including 53,236 individuals (17). The datasets for the eBMD of the heel calcaneus and fracture risk were obtained from the UKB, including 142,487 participants (18).

2.3 Instrumental variable selection

To select instrumental variables that satisfy the three assumptions of the MR analysis, we performed the following five steps. Genome-wide single-nucleotide polymorphisms (SNPs) that are closely associated with hand grip strength were identified from the exposed GWAS ($P<5\times10^{-8}$). To estimate linkage disequilibrium (LD) between SNPs, a clumping process ($r^2>0.6$, window size=250 kb or 1000 SNPs) was performed on 1000 Genomes Project data (19). For specific requested SNPs not present in the BMD GWAS, their LD proxies were estimated using 1000 Genomes Project data (19, 20). SNPs with minor allele frequencies <0.05 were further excluded. Ambiguous SNPs with nonconcordant alleles (e.g., G/A vs. G/T) were excluded, and coordinates with ambiguous palindromic SNPs were harmonized (e.g., A/T vs. C/G).

2.4 Statistical analyses

In this study, we performed an inverse variance weighted (IVW) meta-analysis to analyze each Wald ratio to initially estimate the causal relationship between exposure and outcome. However, if any evidence of horizontal pleiotropy exists in the IV, this method is considered biased in estimating causality, and the robustness of the IVW method depends on the pleiotropy of IV. Even when nearly 50% of SNPs are invalid instrumental variables, the weighted median method yields an estimate that is compatible with the final effect; this approach can be used to

achieve unbiased estimates of causal effects in the presence of unbalanced level pleiotropy. Under the InSIDE assumption that instrumental variables are independent of direct effects, MR–Egger regression can provide consistent estimations even if all SNPs are not valid instrumental variables. Nevertheless, MR–Egger estimates are less accurate than weighted median methods and may be affected by outlying genetic variants. We also used MR–Egger regression intercepts to assess directional pleiotropy and 'leave-one-out' sensitivity analysis to evaluate whether causal effects were driven by a single potentially influential SNP. The association between exposure and outcome phenotype was considered statistically significant at $P<0.05$. All MR analyses were performed using the 'TwoSampleMR' package in R software.

3 Results

3.1 Casual relationships between hand grip strength and BMD

The MR results between hand grip strength and BMD are shown in Figure 2. We selected 97, 92, 93 and 92 SNPs as instrumental variables for the causal analyses between hand grip strength and heel, lumbar spine, forearm and femoral neck BMD, respectively. According to the IVW method, only lumbar spine BMD was casually influenced by hand grip strength (β=0.288, 95% confidence interval [CI]=0.079-0.497, P=0.007), suggesting that a one-standard deviation (SD, 11.2 kg) increase in hand grip strength was associated with a 0.288-SD increase in lumbar BMD. This result was supported by weighted median sensitivity analyses (β=0.347, 95% CI=0.100-0.595, P=0.006). There was no evidence of directional pleiotropy among the SNPs associated with hand grip strength in the

FIGURE 2

Casual associations between hand grip strength and BMD. IVW, inverse variance weighted; MR Egger, mendelian randomization egger; CI, confidence interval; BMD, bone mineral density; SNP, single nucleotide polymorphism.

MR–Egger regression (intercept=-0.002, P=0.74). In the leave-one-out analyses, no single SNP strongly drove the overall effect of hand grip strength on lumbar spine BMD. The symmetry in the funnel plots also suggested that there were no violations of the MR assumptions (Figure 3). However, no statistically significant relationships between hand grip strength and BMD in the other three skeleton sites (heel, forearm and femoral neck) were observed from the IVW method. The intercepts of the MR–
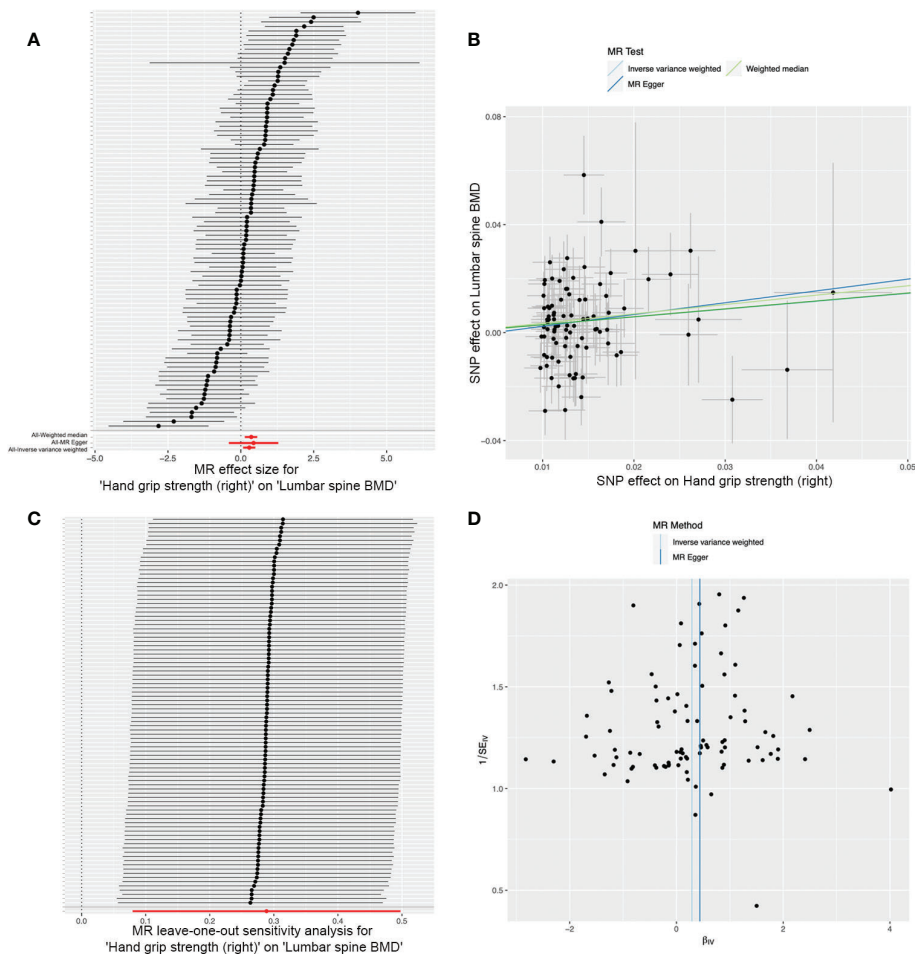

FIGURE 3

Effects of hand grip strength on lumbar spine BMD. **(A)** Forrest plot. **(B)** Scatter plot. The slopes of each line represent the causal association for each method. **(C)** Leave-one-out analysis. **(D)** Funnel plot.

Egger method were 0.001, 0.004 and 0.005, and *P* values for pleiotropy were 0.81, 0.64 and 0.41, respectively, suggesting that there was no directional pleiotropy among the SNPs we used.

3.2 Casual relationships between hand grip strength and fracture risk

The MR results between hand grip strength and fracture risk are shown in Figure 4. We selected 97 and 49 SNPs as instrumental variables for the causal analyses between hand grip strength and overall fracture risk and lumbar spine fracture risk, respectively. However, the IVW methods yielded no evidence to support a causal association between hand grip strength and overall fracture risk (β=-0.004, 95% CI=-0.0190-0.012, *P*=0.662) or lumbar spine fracture risk (β=-0.002, 95% CI=-0.004-0.001, *P*=0.187). No evidence of causal relationship was apparent using the weighted median and MR–Egger methods.

The intercepts of the MR–Egger test were 0.0001 and 8.65×10^{-6}, respectively, and the *P* values for pleiotropy were 0.77 and 0.24, respectively, suggesting that there was no directional pleiotropy among the SNPs we used.

4 Discussion

The present study aimed to explore whether and to what extent hand grip strength affects BMD and fracture risk. We used GWAS data and performed a state-of-the-art two-sample Mendelian randomization analysis to investigate the causal relationship between hand grip strength and BMD at different skeleton sites and fracture risks. Our results suggested that there was a positive causal relationship between hand grip strength and lumbar spine BMD, which is the most common site of osteoporotic fracture (21), but no causal relationship was found between hand grip strength and BMD at the heel, forearm or femoral neck. However, we found no evidence to support a causal relationship between hand grip strength and fracture risks.

Hand grip strength is a well-established indicator of muscle strength and is the most commonly used measurement in large epidemiological studies to assess muscle condition (22–24). It is a sensitive index for metabolic health, including metabolic

syndrome and sarcopenic obesity in the elderly (25, 26). Our previous MR study assessed the causal relationships of overall and central obesity with BMD. In terms of overall obesity, we found that BMI, a measurement of overall obesity, was causally and positively associated with BMD, and the genetic determination of BMI is different but similar across different skeletons (27). In terms of central obesity, our study suggested variations in the ability of different central obesity traits to influence BMD and found that hip circumference adjusted by BMI (negatively) and waist-to-hip ratio (positively) may be important factors causally influencing BMD (28). Recent studies have demonstrated that sarcopenic obesity is associated with an increased risk of physical disability, osteoporosis and nonvertebral fractures in older adults when compared to those with obesity (29, 30). The analysis of body components also revealed that lean mass actually contributes more to BMD than fat mass (31), and whether large BMI is a stronger contributor to lean or fat mass remains unclear (31, 32). Therefore, understanding the hand grip strength-osteoporosis relationship is an important part of obesity-osteoporosis studies, and the present study is an extension of our previous studies. The similarity between this study and our previous MR studies is that they both sought to elucidate the relationship between obesity and osteoporosis using a novel causal arguing method, and examine differences in genetic determinants of BMD measurements between various traits. The novelty of this study is that the use of grip strength as a proxy for sarcopenia provides a more specific analysis of the effect of sarcopenic obesity on BMD from the perspective of genetic variation, which is a transition from the traditional concept of obesity to the new one. Our findings may shed light on the level of grip strength metrics to predict the risk of osteoporosis.

The relationship between hand grip strength and osteoporosis is a crucial public health issue, and risk exposure can slowly progress toward disease. However, there have been controversial results about the role of hand grip strength in osteoporosis. Our results were consistent with previous observational studies showing a positive relationship of hand grip strength with BMD at nonadjacent bones. A cross-sectional study of 1850 American participants found that hand grip strength is associated with increased BMD of nonadjacent bones (femoral neck and total lumbar spine) across gender

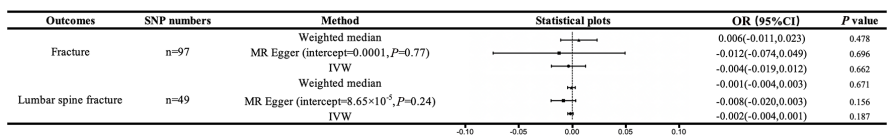| Outcomes	SNP numbers	Method	Statistical plots	OR (95%CI)	*P* value
		Weighted median		0.006(-0.011,0.023)	0.478
Fracture	n=97	MR Egger (intercept=0.0001,*P*=0.77)		-0.012(-0.074,0.049)	0.696
		IVW		-0.004(-0.019,0.012)	0.662
		Weighted median		-0.001(-0.004,0.003)	0.671
Lumbar spine fracture	n=49	MR Egger (intercept=8.65×10^{-5},*P*=0.24)		-0.008(-0.020,0.003)	0.156
		IVW		-0.002(-0.004,0.001)	0.187

FIGURE 4

Casual associations between hand grip strength and fracture. IVW, inverse variance weighted; MR Egger, mendelian randomization egger; CI, confidence interval; BMD, bone mineral density; SNP, single nucleotide polymorphism.

and menopausal statuses (12). A similar protective effect of hand grip strength on nonadjacent bones was also found in a Chile study including 1427 adolescent students (14) and a small Chinese study including 120 postmenopausal women (33). In terms of adjacent bone, Mclean et al. analyzed the Framingham osteoporosis cohort including 1159 participants and found that higher hand grip strength was associated with higher radius bone size and strength but not volumetric BMD (34). The authors speculate that the unaffected BMD may be because larger bone has similar bone mineral content. Similar positive results were also found in the relationship between the cross-sectional area of the hip flexors and quadriceps for hip BMD (35). However, our study did not find a causal relationship between hand grip strength and forearm BMD. In terms of fracture risk, a population-based study of community-dwelling older adults found that sarcopenic obese older men have over 3-fold increased rate of self-reported fractures over 10 years compared to both non-sarcopenic non-obese and obese alone counterparts (30). However, we did not find a causal association between hand grip strength and fracture risk. The observational nature of these studies did not permit the establishment of causality. Their observation was also limited to a relatively small sample size. Additionally, conventional observational studies cannot distinguish unmeasured confounders or quantify the magnitude of this association.

The relationship between muscle strength and BMD is complex and complicated by many factors. The mechanostat theory posits that mechanical strain applied to bone is a determinant of bone remodeling and that bones adapt not only to static forces but also to the dynamic forces created by muscular contractions (36). Lifting weights increases the load on the lumbar spine and thus increases BMD, which will automatically increase grip strength due to holding on to the weights. In addition, MR analysis lies between traditional observational studies and interventional trials and it is important to triangulate evidence from different studies. We would not expect an IV estimate to reflect the effect of current treatment on prognosis. Therefore, our findings cannot simply be interpreted as increasing lumbar spine BMD by increasing grip strength alone. Endocrine factors also interact with bone modeling. Skeletal muscle can act as an endocrine organ to regulate bone anabolism in a nonmechanical manner (37). Skeletal muscle secretes various myokines (e.g., myostatin, IL6, IGF-1, irisin) in an autocrine, paracrine, or endocrine manner to regulate the metabolic activities of bone cells in various ways and ultimately contribute to the pathogenesis of osteoporosis mechanisms (38). Several studies have indicated that sarcopenia and osteoporosis are co-occurring in the elderly (39, 40), the results of these studies or common sense knowledge may be somewhat misleading to the conclusions of this study. The conclusion of this study, that there was a positive causal relationship between HGS and lumbar spine BMD, was not specific to a particular age, such as the elderly, but was based on a large sample of people after the methodological exclusion of the confounding factor of age. The underlying mechanisms of the effect of muscle strength on BMD, including mechanical and metabolic aspects, still need to be further studied in the future.

This study has several strengths. First, MR may minimize confounding factors and reverse causal effects existing in the observational studies. Second, MR lies between observational studies and interventional trials and provides information about public health interventions in cases when randomized controlled trials may not be feasible. Third, the large sample size and robustly associated SNPs give sufficient power to detect causal effects.

There are still some limitations in the present study. First, all individuals in the study are of European descent. MR is dependent on ethnicity, so it may be inaccurate when extending our conclusions to other populations. Second, although we found no evidence of horizontal pleiotropy in several analyses, we have to admit that MR-Egger regression loosens the constraints and reduces the accuracy of the estimates (41), it is impossible to prove the validity of all three MR assumptions. Nevertheless, considering the unique advantages of MR-Egger regression for detecting and adapting to bias arising from unbalanced pleiotropy, we finally employed this method in the standard MR analysis. Third, we used heel eBMD instead of the standard BMD in this study. However, the potential biological characteristics are similar, and the heel eBMD traits were also successfully utilized in previous MR studies (42–44).

In conclusion, our Mendelian randomization study suggested that there was a positive causal relationship between hand grip strength and lumbar spine BMD, which is the most common site of osteoporotic fracture, but no causal relationship was found between hand grip strength and BMD at the heel, forearm or femoral neck. In addition, no statistically significant effects of hand grip strength on fracture risks were observed. These results should be considered in future research and in the development of public health measures and osteoporosis prevention strategies.

Data availability statement

Publicly available datasets were analyzed in this study. This data can be found here: MR-Base platform.

Ethics statement

Ethical review and approval was not required for the study on human participants in accordance with the local legislation and institutional requirements. Written informed consent for participation was not required for this study in accordance with the national legislation and the institutional requirements.

Author contributions

All authors contributed to the article and approved the submitted version. JS and WW Designed and performed the

study. TL, SW and JZ collected and analyzed the data. XD interpreted the results. JS and TL wrote the paper.

Funding

Acknowledgments

Conflict of interest

The authors declare that the research was conducted in the absence of any commercial or financial relationships that could be construed as a potential conflict of interest.

Publisher's note

All claims expressed in this article are solely those of the authors and do not necessarily represent those of their affiliated organizations, or those of the publisher, the editors and the reviewers. Any product that may be evaluated in this article, or claim that may be made by its manufacturer, is not guaranteed or endorsed by the publisher.

References

1. Wright NC, Saag KG, Dawson-Hughes B, Khosla S, Siris ES. The impact of the new national bone health alliance (NBHA) diagnostic criteria on the prevalence of osteoporosis in the USA. *Osteoporos Int* (2017) 28(4):1225–32. doi: 10.1007/s00198-016-3865-3

2. Clynes MA, Westbury LD, Dennison EM, Kanis JA, Javaid MK, Harvey NC, et al. Bone densitometry worldwide: A global survey by the ISCD and IOF. *Osteoporosis Int* (2020) 31(9):1779–86. doi: 10.1007/s00198-020-05435-8

3. Wright NC, Looker AC, Saag KG, Curtis JR, Delzell ES, Randall S, et al. The recent prevalence of osteoporosis and low bone mass in the united states based on bone mineral density at the femoral neck or lumbar spine. *J Bone Miner Res* (2014) 29(11):2520–6. doi: 10.1002/jbmr.2269

4. Anker SD, Morley JE, von Haehling S. Welcome to the ICD-10 code for sarcopenia. *J Cachexia Sarcopenia Muscle* (2016) 7(5):512–4. doi: 10.1002/jcsm.12147

5. Cruz-Jentoft AJ, Bahat G, Bauer J, Boirie Y, Bruyère O, Cederholm T, et al. Sarcopenia: Revised European consensus on definition and diagnosis. *Age Ageing* (2019) 48(1):16–31. doi: 10.1093/ageing/afy169

6. Cruz-Jentoft AJ, Sayer AA. Sarcopenia. *Lancet* (2019) 393(10191):2636–46. doi: 10.1016/S0140-6736(19)31138-9

7. Janssen I, Shepard DS, Katzmarzyk PT, Roubenoff R. The healthcare costs of sarcopenia in the united states. *J Am Geriatrics Soc* (2004) 52(1):80–5. doi: 10.1111/j.1532-5415.2004.52014.x

8. Dennison EM, Sayer AA, Cooper C. Epidemiology of sarcopenia and insight into possible therapeutic targets. *Nat Rev Rheumatol* (2017) 13(6):340–7. doi: 10.1038/nrrheum.2017.60

9. Cruz-Jentoft AJ, Landi F, Schneider SM, Zúñiga C, Arai H, Boirie Y, et al. Prevalence of and interventions for sarcopenia in ageing adults: A systematic review. report of the international sarcopenia initiative (EWGSOP and IWGS). *Age Ageing* (2014) 43(6):748–59. doi: 10.1093/ageing/afu115

10. Clynes MA, Gregson CL, Bruyère O, Cooper C, Dennison EM. Osteosarcopenia: Where osteoporosis and sarcopenia collide. *Rheumatology* (2021) 60(2):529–37. doi: 10.1093/rheumatology/keaa755

11. Bao W, Sun Y, Zhang T, Zou L, Wu X, Wang D, et al. Exercise programs for muscle mass, muscle strength and physical performance in older adults with sarcopenia: A systematic review and meta-analysis. *Aging Dis* (2020) 11(4):863–73. doi: 10.14336/AD.2019.1012

12. Luo Y, Jiang K, He M. Association between grip strength and bone mineral density in general US population of NHANES 2013-2014. *Arch Osteoporos* (2020) 15(1):47. doi: 10.1007/s11657-020-00719-2

13. Aydin G, Atalar E, Keles I, Tosun A, Zog G, Keles H, et al. Predictive value of grip strength for bone mineral density in males: Site specific or systemic? *Rheumatol Int* (2006) 27(2):125–9. doi: 10.1007/s00296-006-0178-4

14. Cossio-Bolanos M, Lee-Andruske C, de Arruda M, Luarte-Rocha C, Almonacid-Fierro A, Gomez-Campos R. Hand grip strength and maximum peak expiratory flow: Determinants of bone mineral density of adolescent students. *BMC Pediatr* (2018) 18(1):96. doi: 10.1186/s12887-018-1015-0

15. Davies NM, Holmes MV, Smith GD. Reading mendelian randomisation studies: A guide, glossary, and checklist for clinicians. *BMJ* (2018) 362:k601. doi: 10.1136/bmj.k601

16. Evans DM, Davey Smith G. Mendelian randomization: New applications in the coming age of hypothesis-free causality. *Annu Rev Genomics Hum Genet* (2015) 16:327–50. doi: 10.1146/annurev-genom-090314-050016

17. Zheng H-F, Forgetta V, Hsu Y-H. Whole-genome sequencing identifies EN1 as a determinant of bone density and fracture. *J Nat* (2015) 112:112–7. doi: 10.1038/nature14878

18. Kemp JP, Morris JA, Medina-Gomez C, Forgetta V, Warrington NM, Youlten SE, et al. Identification of 153 new loci associated with heel bone mineral density and functional involvement of GPC6 in osteoporosis. *Nat Genet* (2017) 49:1468. doi: 10.1038/ng.3949

19. Hemani G, Zheng J, Elsworth B, Wade KH, Haberland V, Baird D, et al. The MR-base platform supports systematic causal inference across the human phenome. *eLife* (2018) 7:e34408. doi: 10.7554/eLife.34408

20. Genomes Project C, Auton A, Brooks LD, Durbin RM, Garrison EP, Kang HM, et al. A global reference for human genetic variation. *Nature* (2015) 526 (7571):68–74. doi: 10.1038/nature15393

21. Clynes MA, Harvey NC, Curtis EM, Fuggle NR, Dennison EM, Cooper C. The epidemiology of osteoporosis. *Br Med Bull* (2020) 133(1):105–17. doi: 10.1093/bmb/ldaa005

22. Ortega FB, Ruiz JR, Castillo MJ, Moreno LA, González-Gross M, Wärnberg J, et al. Low level of physical fitness in Spanish adolescents. relevance for future cardiovascular health (AVENA study). *Rev Esp Cardiol* (2005) 58(8):898–909. doi: 10.1157/13078126

23. Ortega FB, Artero EG, Ruiz JR, Vicente-Rodriguez G, Bergman P, Hagströmer M, et al. Reliability of health-related physical fitness tests in European adolescents. the HELENA study. *Int J Obes (Lond)* (2008) 32(Suppl 5): S49–57. doi: 10.1038/ijo.2008.183

24. Ruiz JR, Castro-Piñero J, España-Romero V, Artero EG, Ortega FB, Cuenca MM, et al. Field-based fitness assessment in young people: the ALPHA health-related fitness test battery for children and adolescents. *Br J Sports Med* (2011) 45 (6):518–24. doi: 10.1136/bjsm.2010.075341

25. Wu H, Liu M, Chi VTQ, Wang J, Zhang Q, Liu L, et al. Handgrip strength is inversely associated with metabolic syndrome and its separate components in middle aged and older adults: A large-scale population-based study. *Metabolism* (2019) 93:61–7. doi: 10.1016/j.metabol.2019.01.011

26. McLean RR, Shardell MD, Alley DE, Cawthon PM, Fragala MS, Harris TB, et al. Criteria for clinically relevant weakness and low lean mass and their longitudinal association with incident mobility impairment and mortality: The foundation for the national institutes of health (FNIH) sarcopenia project. *J Gerontol A Biol Sci Med Sci* (2014) 69(5):576–83. doi: 10.1093/gerona/glu012

27. Song J, Zhang R, Lv L, Liang J, Wang W, Liu R, et al. The relationship between body mass index and bone mineral density: A mendelian randomization study. *Calcif Tissue Int* (2020) 107(5):440–5. doi: 10.1007/s00223-020-00736-w

28. Du D, Jing Z, Zhang G, Dang X, Liu R, Song J. The relationship between central obesity and bone mineral density: A mendelian randomization study. *Diabetol Metab Syndr* (2022) 14(1):63. doi: 10.1186/s13098-022-00840-x

29. Batsis JA, Villareal DT. Sarcopenic obesity in older adults: aetiology, epidemiology and treatment strategies. *Nat Rev Endocrinol* (2018) 14(9):513–37. doi: 10.1038/s41574-018-0062-9

30. Scott D, Chandrasekara SD, Laslett LL, Cicuttini F, Ebeling PR, Jones G. Associations of sarcopenic obesity and dynapenic obesity with bone mineral density and incident fractures over 5-10 years in community-dwelling older adults. *Calcif Tissue Int* (2016) 99(1):30–42. doi: 10.1007/s00223-016-0123-9

31. Hars M, Trombetti A. Body composition assessment in the prediction of osteoporotic fractures. *Curr Opin Rheumatol* (2017) 29(4):394–401. doi: 10.1097/BOR.0000000000000406

32. Ornstrup MJ, Harsløf T, Kjær TN, Langdahl BL, Pedersen SB. Resveratrol increases bone mineral density and bone alkaline phosphatase in obese men: a randomized placebo-controlled trial. *J Clin Endocrinol Metab.* (2014) 99(12):4720–9. doi:10.1210/jc.2014-2799

33. Li YZ, Zhuang HF, Cai SQ, Lin CK, Wang PW, Yan LS, et al. Low grip strength is a strong risk factor of osteoporosis in postmenopausal women. *Orthop Surg* (2018) 10(1):17–22. doi: 10.1111/os.12360

34. McLean RR, Samelson EJ, Lorbergs AL, Broe KE, Hannan MT, Boyd SK, et al. Higher hand grip strength is associated with greater radius bone size and strength in older men and women: The framingham osteoporosis study. *JBMR Plus* (2021) 5(5):e10485. doi: 10.1002/jbm4.10485

35. Ahedi H, Aitken D, Scott D, Blizzard L, Cicuttini F, Jones G. The association between hip muscle cross-sectional area, muscle strength, and bone mineral density. *Calcif Tissue Int* (2014) 95(1):64–72. doi: 10.1007/s00223-014-9863-6

36. Lerebours C, Buenzli PR. Towards a cell-based mechanostat theory of bone: The need to account for osteocyte desensitisation and osteocyte replacement. *J Biomech* (2016) 49(13):2600–6. doi: 10.1016/j.jbiomech.2016.05.012

37. Gomarasca M, Banfi G, Lombardi G. Chapter four - myokines: The endocrine coupling of skeletal muscle and bone. In: Makowski GS, editor. *Advances in clinical chemistry*. Elsevier (2020) 94:155-218. doi: 10.1016/bs.acc.2019.07.010

38. Kaji H. Effects of myokines on bone. *Bonekey Rep* (2016) 5:826. doi: 10.1038/bonekey.2016.48

39. Huo YR, Suriyaarachchi P, Gomez F, Curcio CL, Boersma D, Muir SW, et al. Phenotype of osteosarcopenia in older individuals with a history of falling. *J Am Med Directors Assoc* (2015) 16(4):290–5. doi: 10.1016/j.jamda.2014.10.018

40. Morley JE. Frailty and sarcopenia: The new geriatric giants. *Rev Invest Clin* (2016) 68(2):59–67.

41. Bowden J, Davey Smith G, Burgess S. Mendelian randomization with invalid instruments: Effect estimation and bias detection through egger regression. *Int J Epidemiol* (2015) 44(2):512–25. doi: 10.1093/ije/dyv080

42. Morris JA, Kemp JP, Youlten SE, Laurent L, Logan JG, Chai RC, et al. An atlas of genetic influences on osteoporosis in humans and mice. *Nat Genet* (2019) 51(2):258–66. doi: 10.1038/s41588-018-0302-x

43. Ma B, Li C, Pan J, Zhang S, Dong H, Wu Y, et al. Causal associations of anthropometric measurements with fracture risk and bone mineral density: A mendelian randomization study. *J Bone Miner Res* (2021) 36(7):1281–7. doi: 10.1002/jbmr.4296

44. Yuan S, Michaëlsson K, Wan Z, Larsson SC. Associations of smoking and alcohol and coffee intake with fracture and bone mineral density: A mendelian randomization study. *Calcif Tissue Int* (2019) 105(6):582–8. doi: 10.1007/s00223-019-00606-0

The role of advanced glycation end products in fracture risk assessment in postmenopausal type 2 diabetic patients

Liu Gao[1,2†], Chang Liu[1,2†], Pan Hu[3,4†], Na Wang[1,2], Xiaoxue Bao[1,2], Bin Wang[1,2], Ke Wang[1,2], Yukun Li[1,2*] and Peng Xue[1,2*]

[1]Department of Endocrinology, The Third Hospital of Hebei Medical University, Shijiazhuang, China, [2]Key Laboratory of Orthopedic Biomechanics of Hebei Province, The Third Hospital of Hebei Medical University, Shijiazhuang, China, [3]Trauma Medicine Center, Peking University People's Hospital, Beijing, China, [4]National Center for Trauma Medicine, Peking University People's Hospital, Beijing, China

Objective: The objective of this study was to analyze the quantitative association between advanced glycation end products (AGEs) and adjusted FRAX by rheumatoid arthritis (FRAX-RA) in postmenopausal type 2 diabetic (T2D) patients. The optimal cutoff value of AGEs was also explored, which was aimed at demonstrating the potential value of AGEs on evaluating osteoporotic fracture risk in postmenopausal T2D patients.

Methods: We conducted a cross-sectional study including 366 postmenopausal participants (180 T2D patients [DM group] and 186 non-T2D individuals [NDM group]). All the subjects in each group were divided into three subgroups according to BMD. Physical examination, dual-energy x-ray absorptiometry (DXA), and serum indicators (including serum AGEs, glycemic parameters, bone turnover markers and inflammation factors) were examined. The relationship between FRAX-RA, serum laboratory variables, and AGEs were explored. The optimal cutoff value of AGEs to predict the risk of osteoporotic fracture was also investigated.

Results: Adjusting the FRAX values with rheumatoid arthritis (RA) of T2D patients reached a significantly increased MOF-RA and an increasing trend of HF-RA. AGEs level was higher in the DM group compared to the NDMs, and was positively correlated with MOF-RA (r=0.682, *P<0.001*) and HF-RA (r=0.677, *P*<0.001). The receiver operating characteristic curve analysis revealed that the area under the curve was 0.804 (*P*<0.001), and the optimal AGEs cut-off value was 4.156mmol/L. Subgroup analysis for T2D patients revealed an increase in TGF-β, IL-6 and SCTX in the osteoporosis group, while a decreased PINP in the osteoporosis group compared to the other two subgroups. AGEs were positively associated with FBG, HbA1c, HOMA-IR, S-CTX, IL-6 and TGF-β in T2D patients, and negatively associated with PINP.

Conclusions: RA-adjusted FRAX is a relevant clinical tool in evaluating fracture risk of postmenopausal T2D patients. Our study analyzed the relationship between AGEs and FRAX-RA, and explored the threshold value of AGEs for predicting fracture risk in postmenopausal T2D patients. AGEs were also associated with serum bone turnover markers and inflammation factors, indicating that the increasing level of AGEs in postmenopausal T2D patients accelerated the expression of inflammatory factors, which led to bone metabolism disorders and a higher risk of osteoporotic fractures.

Introduction

Osteoporosis is prevalent in type 2 diabetes mellitus (T2D) postmenopausal patients, which affects human health, life quality and increases the socioeconomic burden (1). T2D patients have bone mineral density (BMD) that is either unchanged or slightly higher than normal, but they exhibit skeletal fragility independent of BMD (2, 3), even after accounting for some factors (such as body mass index [BMI] and falls) (4, 5), which indicates patients with T2D have a higher fracture risk due to bone fragility independent of BMD. Besides, Diabetes status was associated with low muscle mass and low muscle strength, and the association depended on BMI (6). The concomitance of sarcopenia and osteoporosis which was so-called "osteosarcopenia", may lead to an increase in fracture risk of T2D than the non-diabetic ones (7). Older adults with osteosarcopenia have to be regarded as the most at-risk population for fractures (8). Thus, the unadjusted fracture risk assessment tool (FRAX) mostly depends on dual-energy x-ray absorptiometry (DXA) detection could also underestimate the fracture risk in T2D patients (9, 10).

Approximately 70% of bone strength is determined by BMD, while collagen fiber composition depends on bone tissue's tensile strength and ductility. Collagen molecular crosslinking can be divided into beneficial enzyme-catalyzed immature bivalent cross-linking and mature trivalent crosslinking, and unfavorable non-enzyme-catalyzed crosslinking, such as advanced glycation end products (AGEs). AGEs are the spontaneous reaction products between extracellular sugars and amino acid residues on collagen fibers (11). The accumulation of AGEs in the bone can reduce skeletal hardness biomechanical properties (12). Previous studies showed a significantly increased AGEs level in T2D patients (13, 14), which was related to low bone quality and high fracture risk in postmenopausal women (15). Meanwhile, the accumulation of

AGEs is associated with impaired bone microarchitecture. It has been reported that AGEs bone content correlated with worse bone microarchitecture in trabecular, including lower volumetric BMD, bone volume fraction, and increased separation/spacing (16). Bone microarchitecture could be regarded as an independent predictor of fracture risk (17). Although the FRAX includes some diseases related to osteoporosis, other risk factors were not accounted for, such as falls, the duration and dosage of glucocorticoids, the etiology and type of diabetes, or other secondary osteoporosis. FRAX base on BMD may not always accurately predict the fracture risk of T2D patients. Therefore, we speculate that abnormal cross-linking of collagen molecules may be an important factor contributing to impaired bone quality and increased skeletal fragility, which increased the fracture risk in postmenopausal T2D patients.

In this study, we adopted a method previously reported by both Hu et al. and Leslie et al. (18, 19), rheumatoid arthritis (RA) was selected as an analogous variable of T2D to obtain the FRAX predictive value for fracture risk. Thus, the objective of this study was to analyze the quantitative association between AGEs and adjusted FRAX by RA (FRAX-RA) in postmenopausal T2D patients. The optimal cutoff value of AGEs was also explored, which was aimed at demonstrating the potential influence of AGEs on osteoporotic fracture risk in postmenopausal T2D patients. Moreover, we tried to use HR-pQCT to verify the status of bone microstructure of T2DM patients in "High-AGEs" or "Low-AGEs" group defined by its cut off value in a small-size sample.

Materials and methods

Subject recruitment

We collected 180 postmenopausal T2D patients (DM group) and 186 healthy individuals (NDM group) who were recruited

from the Endocrinology Department of the Third Hospital of Hebei Medical University from October 2019 to May 2020. Each cohort was divided into three subgroups (non-diabetic subjects with normal BMD [Control], non-diabetic subjects with osteopenia [OPN], non-diabetic subjects with osteoporosis [OP], diabetic patients with normal BMD[DMN], diabetic patients with osteopenia [DMOPN], diabetic patients with osteoporosis [DMOP]) according to BMD. All subjects submitted written informed consent prior to participating in this study, which was authorized by the Third Hospital of Hebei Medical University's ethical committee.

Inclusion and exclusion criteria

The subjects were chosen based on the following criteria: 1) All subjects were aged between 45 and 80, natural menopause for more than 3 years or menopause caused by surgery (operating time after 40 years old); 2) the WHO's (1999) diabetes criteria: diabetic symptoms (polydipsia, polyuria, polyphagia, weight loss) + blood glucose level at any time $\geq$ 11.1mmol/L or fasting glucose $\geq$ 7.0mmol/L or 2hours postprandial glucose$\geq$11.1mmol/L. Type 1 diabetes mellitus were excluded from this study; 3) the WHO's osteoporosis criteria: the diagnosis of osteoporosis in postmenopausal women is based on the T value. T value $\geq$ -1SD was normal bone mineral density, -1SD < T value < -2.5SD was osteopenia; T value $\leq$ -2.5SD was osteoporosis.

Subjects with these conditions were excluded: severe heart, liver, and kidney disease, thyroid and parathyroid disease, autoimmune disease, rheumatism, long-term use of hormones and thiazide diuretics, use of antidiabetic drugs that may affect bone metabolism for more than three months (metformin, thiazolidinediones, glucagon-like peptide-1 receptor agonist, sodium-glucose cotransporter 2 inhibitor), long-term stay in bed or chronic smoking (smoking for more than 15 years, averaging more than 15 cigarettes a day), BMI is less than 20kg/m^2.

Laboratory assessment

We collected data from all subjects (including age, menopausal age, weight, and height), measured serum concentrations of fasting plasma glucose (FPG), glycosylated hemoglobin (HbA1c) and fasting insulin (FIns) by using standard laboratory techniques, measured serum AGEs, insulin, 25-hydroxyvitamin D3 (25-OHD3), procollagen type I N-peptide (PINP), serum C-terminal telopeptide of type I collagen (S-CTX) by the enzyme-linked immunosorbent assay (ELISA) kit (Cusabio, Wuhan, China), measured serum concentrations of insulin, Interleukin-1β (IL-1β), IL-6, tumor necrosis factor-α (TNF-α) and transforming growth factor-β

(TGF-β) by the ELISA kit (Excellbio, shanghai, China). BMI was determined using the following equation: BMI=Weight/Height^2 (kg/m^2). The following formula was used to calculate the insulin resistance index (HOMA-IR): HOMA-IR = FPG * FIns/22.5.

BMD assessment

We evaluated the level of areal BMDs at the lumbar spine (LS, L2-L4), proximal femur (femoral neck and total hip) for each individual using a DXA device (Hologic, USA). The measurements were all taken by the same technician to ensure consistent and reliable results, and the CVs were 1.73% across the board.

Fracture risk assessment tool

The predicted 10-year risk of major and hip osteoporotic fractures was determined using the Asian-China Assessment System (https://www.sheffield.ac.uk/FRAX/tool.aspx?country=2). The FRAX algorithm includes risk factors of age, gender, height, weight, previous fracture history, parents' history of fragility fractures, smoking status, long-term corticosteroid use, RA history, daily alcohol consumption, secondary OP, and femoral neck bone density. The history of RA was replaced in the algorithm for the current study to calculate FRAX-RA.

Bone microarchitectural measurements

HR-pQCT was used to verify the status of bone microstructure of T2DM patients in both "High-AGEs" (AGEs>4.156mmol/L) or "Low-AGEs" (AGEs<4.156mmol/L) group defined by its cut off value. We chose 14 subjects aged 50-60yr without fracture history (8 in High-AGEs group and 6 in Low-AGEs group) underwent HR-pQCT of the nondominant distal radius and tibia (Xtreme CT II; Scanco Medical AG, Bassersdorf, Switzerland) according to the manufacturer's standard *in vivo* acquisition protocol (68 kVp, 1470 μA, matrix size of 2304×2304) [20]. The reference line was placed at the endplates of the distal radius and tibia in all tested participants. The scan region was 10.2mm in length, and was fixed starting at 9.0 mm and 22.0 mm proximal to the reference lines of the radius and tibia respectively. The measured parameters were as follows: cortical thickness (Ct.Th, mm); cortical porosity (Ct.Po, %); trabecular bone volume fraction (Tb.BV/TV, %), number (Tb.N, 1/mm), thickness (Tb.Th, mm) and separation (Tb.Sp, mm). The measurements were all taken by the same technician to ensure consistent and reliable results.

Statistical analyses

All statistical analysis was performed using SPSS version 21.0. We used the Kolmogorov-Smirnov test to confirm the normal distribution of variables for each group. The median (interquartile range) was used to express data for non-continuous variables, whereas the mean ± SD was used to express data for continuous variables. The Student's T-Test is utilized to compare 2 groups that adhere to the normal distribution and uniform variance, and the Wilcoxon test is used to compare 2 groups that do not obey the normal distribution. We used the ANOVA or Friedman test to compare the quantitative variables among groups. Pearson or Spearman correlation tests were used to determine relationships between variables. In order to determine or assess the best AGE cutoff value for predicting or evaluating the risk of osteoporotic fracture, receiver operating characteristic (ROC) curves were used. Maximum sensitivity and specificity for fracture risk are achieved by the cut-off value. Estimating the area under the curve was served to evaluate the test's discriminatory ability. A difference with a P value of 0.05 or lower is considered statistically significant for all statistical tests.

Results

Baseline features of the subjects

The general characteristics of the subjects are displayed in Table 1. T2D patients had higher BMI compared to non-diabetics (P=0.034), while the two groups were comparable in age and menopause duration. Analysis of subgroups indicates that BMI in DMOP group was considerably lower than in DMN and DMOPN groups (P<0.05), and OP group had significantly lower BMI than the Control and OPN groups (P<0.05).

BMD, FRAX, and RA-FRAX comparation among DM and NDM groups

DM group had substantially higher BMD than the non-diabetics (P<0.05), as shown in Figure 1A. The probabilities of major osteoporotic fractures (MOF) and hip osteoporotic fractures (HF) in T2D patients were lower than the non-diabetics (P<0.05, Figure 1B). Then, in order to obtain MOF-RA and HF-RA, we altered the FRAX values of T2D patients by choosing RA as an analogous variable. A significant increase of MOF-RA in DM group was found than the NDM group (P<0.05), while DM group tends to have higher HF-RA than NDM group (Figure 1C).

AGEs level comparison between DM and NDM groups

In comparison to non-diabetics, we found that DM patients had considerably higher AGEs levels (P<0.05, Figure 1D). According to Pearson correlation analysis, AGEs level was positively correlated with MOF-RA (r=0.682, P<0.001) (Figure 2A) and HF-RA (r=0.677, P<0.001) (Figure 2B).

TABLE 1 Baseline characteristics of the study population.

	NDM					DM				
	Total (n=186)	Control (n=58)	OPN (n=63)	OP (n=65)	*P Value*	Total (n=180)	DMN (n=52)	DMOPN (n=60)	DMOP (n=68)	*P Value*
Age (years)	63.978 ± 9.234	63.621 ± 8.626	63.444 ± 9.193	64.815 ± 9.861	0.662	65.000 ± 8.574	64.423 ± 8.696	64.383 ± 8.015	65.985 ± 8.983	0.488
Menopausal duration (years)	14.000 (13.000)	13.000 (11.000)	13.000 (11.000)	16.000 (17.000)	0.529	15.000 (10.750)	15.000 (15.500)	14.000 (9.000)	15.000 (12.000)	0.780
T2D duration (years)	–	–	–	–	–	10.000 (9.750)	10.000 (8.750)	11.000 (12.000)	8.000 (13.000)	0.169
Fracture history, n (%)	17/186 (9.140%)	2/58 (3.448%)	2/63 (3.175%)	13/65 (20.000%)△※	<0.001	17/180 (9.444%)	2/52 (3.846%)	3/60 (5.000%)	16/68 (23.529%)△※	<0.001
BMI (kg/m^2)	24.361 ± 3.264	25.437 ± 3.218	24.587 ± 3.252	23.181 ± 2.967△※	<0.001	25.422 ± 4.353	25.421 ± 3.358	26.943 ± 4.968	24.082 ± 4.050*#	<0.001
MOF	3.750(2.700)	3.050(1.300)	3.500 (2.300)	6.100 (5.100)△※	<0.001	3.500(2.300)	2.700(1.750)	3.100(1.100)	4.950(3.450)*#	<0.001
HF	0.900(1.825)	0.450(0.600)	0.800 (1.100)	2.500 (4.000)△※	<0.001	0.900(1.200)	0.400(0.775)	0.600(0.900)	1.700(2.000)*#	<0.001
MOF-RA	–	–	–	–	–	4.650(3.700)	3.500(2.250)	4.050(2.750)	6.700(3.950)*#	<0.001
HF-RA	–	–	–	–	–	1.450(2.100)	0.800(1.275)	0.900(1.600)	2.750(3.100)*#	<0.001

△P < 0.05 compared to Control group, ※P < 0.05 compared to OPN group, *P < 0.05 compared to DMN group, #P < 0.05 compared to DMOPN group.
Control, non-diabetic subjects with normal BMD; OPN, non-diabetic subjects with osteopenia; OP, non-diabetic subjects with osteoporosis; DMN, diabetic patients with normal BMD; DMOPN, diabetic patients with osteopenia; DMOP, diabetic patients with osteoporosis; MOF, major osteoporotic fractures; HF, hip osteoporotic fractures; MOF-RA, MOF adjusted by rheumatoid arthritis; HF-RA, HF adjusted by rheumatoid arthritis.
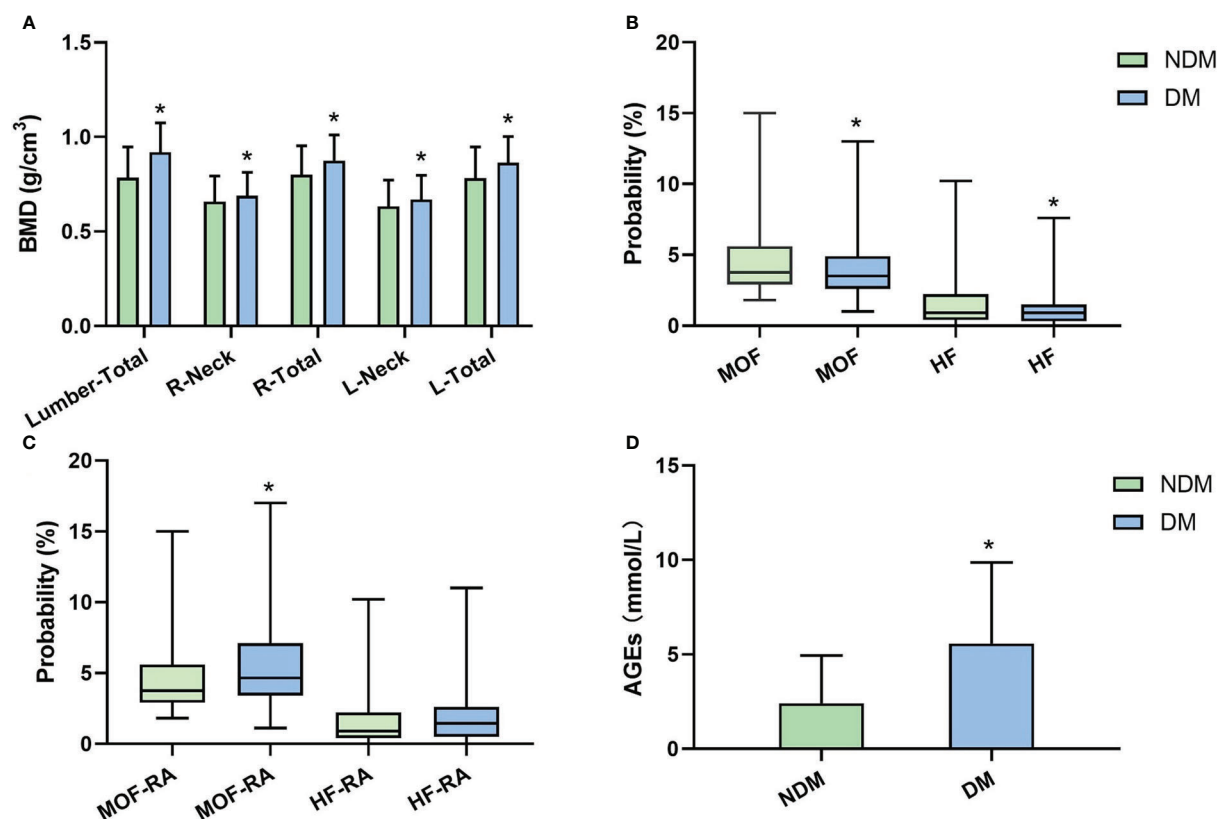
FIGURE 1
BMD, FRAX values (without correction), FRAX values (corrected by rheumatoid arthritis [RA]), and AGEs level between NDM and DM groups. **(A)** BMD comparison in each area; **(B)** major osteoporotic fractures (MOF) and hip osteoporotic fractures (HF) comparison; **(C)** Adjusted MOF by RA (MOF-RA) and adjusted MOF by RA (HF-RA) comparison; **(D)** AGEs comparison. (*$P<0.05$ compared to the NDM group).

Evaluation of the AGEs optimal cutoff value to predict osteoporotic fracture risk

To determine the ideal AGE cut-off value for evaluating fracture risk in postmenopausal T2D patients, the ROC curve was used. As shown in Figure 3, the area under ROC curve (AUC) was recorded as 0.804 (95% confidence interval [CI]:0.749-0.858, $P<0.001$), and the optimal AGEs cut-off value leading to a high fracture risk was 4.156mmol/L. This suggests postmenopausal T2D patients have an increased risk of fracture when AGEs level is higher than 4.156mmol/L. We then tried to verify our AGEs cut-off value by measuring bone microstructure in T2D postmenopausal women. A total of 14 subjects aged 50-60yr without fracture history underwent HR-pQCT examination in nondominant distal radius and tibia, 8 in High-AGEs group and 6 in Low-AGEs group. The Ct.Po was increased in the High-AGEs group than the Low-AGEs group at tibia. And the results of radius were consistent with tibia ($P<0.05$, Supplementary Figures 1D, 2D). No difference was found in Ct.Th and trabecular parameters (Tb.BV/TV, Tb.N, Tb.Th, and Tb.Sp)

between these two groups in both tibia and radius (Supplementary Figures 1A–C, E–H, 2A–C, E–H).

Glucose parameters, bone turnover markers, and inflammation factors comparison among DMN, DMOPN and DMOP groups

First, no differences were found when comparing FBG, HbA1c, insulin, and HOMA-IR among the three groups ($P>0.05$, Table 2). Then we compared bone turnover markers among the three groups. Results revealed that the DMOP group had lower levels of PINP and 25-OHD3 than the DMN and DMOPN groups ($P<0.05$, Table 2), while an increase of S-CTX in DMOP group than the other two groups. Next, the comparison of inflammation factors showed that DMOP patients had higher IL-6 and TGF-β levels compared to both DMN and DMOPN groups ($P<0.05$, Table 2). However, in terms of IL-1β and TNF-α, there were no noticeable differences among the three groups ($P>0.05$, Table 2).
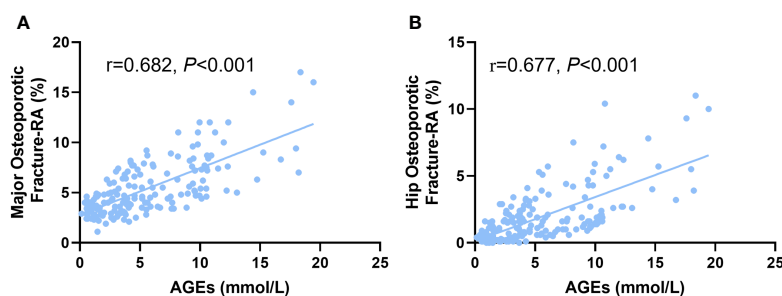
FIGURE 2
The correlation of AGEs with **(A)** major osteoporotic fractures and **(B)** hip osteoporotic fractures adjusted by rheumatoid arthritis (RA) in postmenopausal T2D patients.

Correlations of glycemic parameters, bone turnover markers, and inflammatory factors with AGEs among T2D patients

We used Spearman or Pearson correlation to analyze the relationship among glycemic parameters, bone turnover markers, inflammatory factors, and AGEs in postmenopausal T2D patients. As shown in Table 3, AGEs were positively correlated with FBG, HbA1c, and HOMA-IR levels (r=0.323, r=0.191, r=0.190 respectively, $P<0.05$). No linear correlations were found between AGEs and insulin. Besides, AGEs were negatively correlated with PINP (r=-0.161, $P<0.05$) and positively correlated with S-CTX (r=0.167, $P<0.05$), while no correlation was found between AGEs and 25-OHD3. Serum levels of AGEs were found to be significantly positively correlated with IL-6 and TGF-β (r=0.417, r=0.580 respectively, $P<0.05$), but no linear correlation was found between IL-1β, TNF-α and AGEs.

Discussion

Osteoporosis is a frequent metabolic bone disease. Moreover, diabetic patients with osteoporosis would have a greater overall disease burden. Even after adjusting for BMD, BMI, visual impairment and falls, T2D individuals have a higher risk of fragility fractures (21). However, previous studies showed that individuals with T2D show unaltered (22, 23) or paradoxically increased (24, 25) BMD. Our results also showed that BMDs in DM group was significantly higher than the non-diabetics in postmenopausal women, which may partly be due to higher BMI. Therefore, diabetes-related changes in bone metabolism or biochemistry may be independent of other changes in bone microstructure and tissue properties other than BMD (26). Despite the fact that BMD understates the

risk of fracture in diabetic patients, it remains to be the gold standard for evaluating bones in this population due to its high accessibility and low cost (27–29).

The most popular tool for assessing fracture risk is FRAX, and it can be used to calculate an individual's 10-year risk of hip and severe osteoporotic fracture (30). Recent research indicates that T2D considerably raises fracture risk independent of other risk factors (31, 32). However, T2D is not one of the clinical risk variables in the FRAX algorithm. To increase the performance of FRAX in patients with T2D, it is advised to input RA to represent the condition of diabetes (18, 33). In the present study, we used a conventional BMD-based FRAX score to analyze the incidence of MOF and HF in all subjects and found both MOF and HF were significantly lower in DM patients. We subsequently selected RA as the equivalent variable of T2D based on the prior work to increase the precision of FRAX in the fracture risk evaluation of T2D patients (18), and found DM group had a significant increase in MOF-RA and a trend of higher HF-RA than NDM group. This result indicates that adjusting for RA when calculating FRAX may reflect the fracture risk of T2D patients more realistically.

After adjusting by RA, the FRAX score was numerically closer to the realistically fracture risk in T2D patients, but it could not explain the pathogenesis of the increased fracture risk in T2D individuals. Fractures are influenced by a complicated pathophysiological interplay between T2D parameters including a prolonged illness duration (34), diabetic complications, poor glycemic control (35), insulin resistance (36), and the use of insulin or oral antidiabetic medication (37, 38). It is yet unknown how deteriorating glycemic control might alter the characteristics of bone tissue. Hypothesized mechanisms include impaired bone remodeling, bone microvascular insufficiency, alterations in endocrine function, and accumulation of AGEs (21). It's worth noting that in a prolonged hyperglycemia state, glucose reacts with proteins to form AGEs, which may degrade
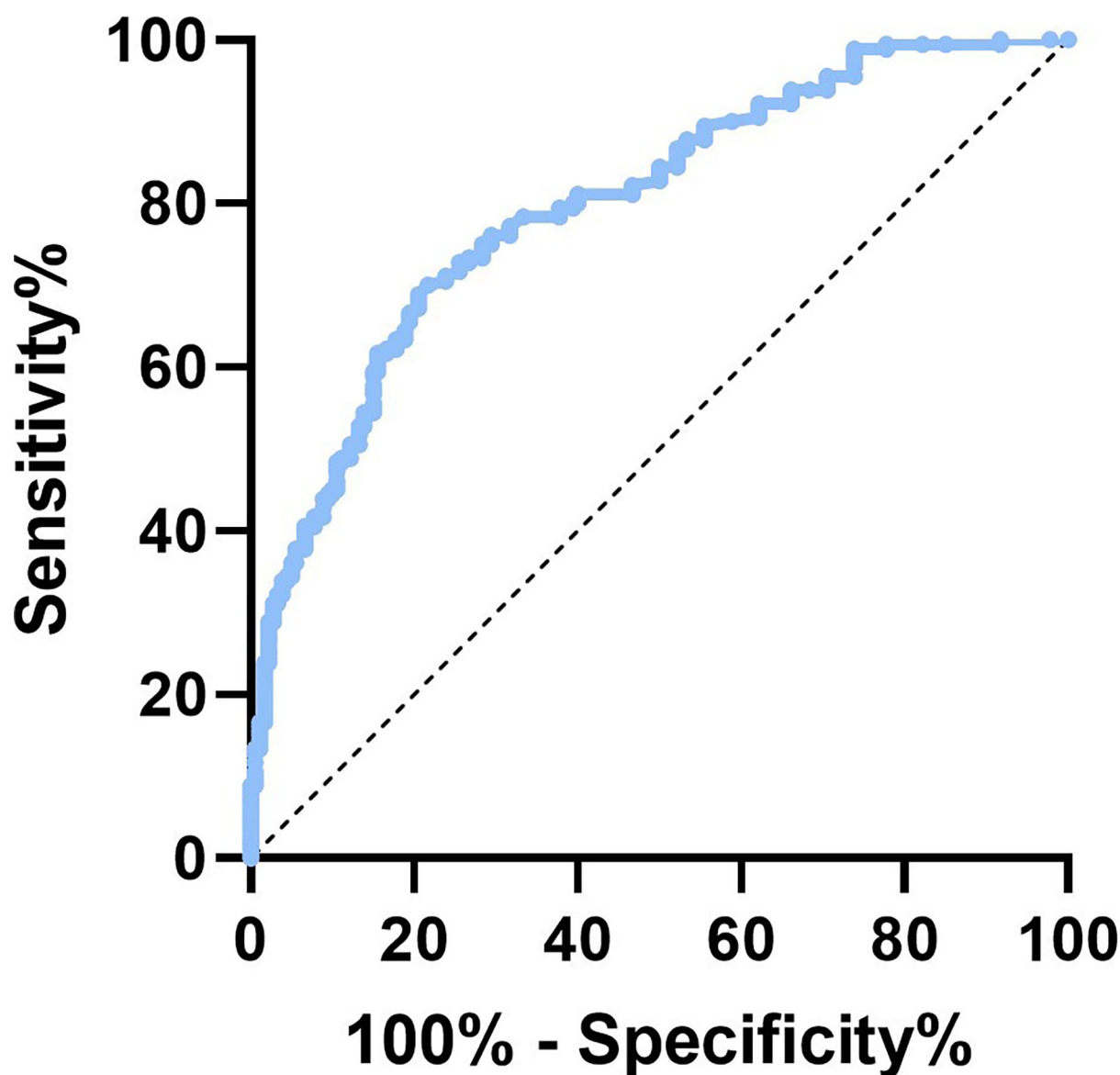
FIGURE 3
The ROC curve of AGEs in predicting fracture risk of postmenopausal T2D patients.

bone tissue properties (39–42). The interaction of AGEs with the receptor (RAGE) on osteoblastic lineage cells results in decreased enzymatic collagen maturity, altered collagen fibrils profile, and further disrupts the mineralization process (43, 44). Additionally, the accumulation of AGEs leads to a promotion of inflammation and oxidative stress, which increases the differentiation and activation of osteoclasts (45) and induces osteoblast apoptosis (46, 47). This process also contributes to a low bone turnover state (48, 49). Our result showed that the elevated AGEs level was positively correlated with MOF-RA and HF-RA in postmenopausal women with T2D, indicating AGEs

levels are strongly associated with fracture risk in T2D patients. The optimal AGEs cut-off value leading to a high fracture risk was 4.156mmol/L, which suggests postmenopausal T2D patients have an increased fracture risk when the AGEs level is higher than 4.156mmol/L. Previous studies indicated that the impaired bone microarchitecture has a considerable influence on bone strength and is essential in fracture initiation and propagation (50, 51). A meta-analysis reported the increase of cortical porosity is relevant to bone quality decline and increased fracture risk. It was also proved that cancellous bone preferentially accumulates AGEs relative to cortical bone (52).

TABLE 2   Glucose parameters, bone turnover markers, and inflammation factors comparison among DMN, DMOPN and DMOP groups.

	Glucose parameters				Bone turnover markers			Inflammation factors			
	FBG (mmol/L)	HbA1c (%)	Insulin (mU/L)	HOMA-IR	25-OHD$_3$ (µg/L)	PINP (pg/ml)	S-CTX (ng/ml)	IL-1β (pg/ml)	IL-6 (pg/ml)	TNF-α (pg/ml)	TGF-β (pg/ml)
DMN (n=52)	8.450 (3.250)	8.792 ± 2.462	16.070 (11.455)	5.889 (5.220)	3723.175 ± 940.977	3822.100 (3654.725)	5.028 (4.518)	4.409 (4.070)	3.185 (7.021)	34.493 (42.574)	24470.560 ± 7809.782
DMOPN (n=60)	8.300 (4.725)	8.875 ± 2.255	15.056 (11.017)	5.249 (4.229)	2830.517 ± 794.228	3744.500 (1314.45)	5.883 (3.985)	6.394 (5.058)	3.152 (5.750)	37.802 (34.771)	27949.802 ± 8559.8723
DMOP (n=68)	8.150 (3.600)	8.893 ± 2.041	15.557 (12.046)	5.125 (5.084)	2819.125 ± 883.256	3068.900 (1298.325)*#	7.527 (7.209)*#	6.233 (1.935)	4.535 (6.575) *#	40.729 (57.955)	33206.162 ± 7112.012*#
P Value	0.873	0.968	0.991	0.930	0.449	<0.001	<0.001	0.165	<0.001	0.418	<0.001

*$P < 0.05$ compared to DMN group, #$P < 0.05$ compared to DMOPN group.
DMN, diabetic patients with normal BMD; DMOPN, diabetic patients with osteopenia; DMOP, diabetic patients with osteoporosis.

TABLE 3   Correlations of glycemic parameters, bone turnover markers, and inflammatory factors with AGEs among postmenopausal type 2 diabetic patients.

		Glucose parameters				Bone turnover markers			Inflammation factors			
		FBG (mmol/L)	HbA1c (%)	Insulin (mU/L)	HOMA-IR	25-OHD$_3$ (µg/L)	PINP (pg/ml)	S-CTX (ng/ml)	IL-1β (pg/ml)	IL-6 (pg/ml)	TNF-α (pg/ml)	TGF-β (pg/ml)
AGEs	r	0.323	0.191	-0.025	0.190	0.044	-0.161	0.167	0.259	0.417	0.046	0.580
	P	<0.001	0.010	0.736	0.011	0.559	0.031	0.025	0.073	<0.001	0.097	<0.001

We thus verify the status of bone microstructure of T2DM patients in both High-AGEs or Low-AGEs group defined by its cut off value. The result showed the cortical porosity was increased in the High-AGEs group than the Low-AGEs group at tibia. No difference was found in cortical thickness and trabecular parameters between these two groups in both tibia and radius. These results were consistent with previous studies that AGEs bone content correlated with worse bone microarchitecture (16). However, Hunt et al. observed the trend of higher BV/TV values and greater mineral content in the T2D specimens which increased the bone strength (11). We speculated that the difference was because of Hunt et al. only analyzed cancellous bone structure, and their subjects was male T2D patients, which was quite different from us. Therefore, we suggest that the AGEs level as a correction factor that could improve the capacity of FRAX algorithm to predict fracture risk in T2D postmenopausal women.

Serum bone turnover markers can be used to assess bone loss or formation more sensitive than BMD (53–55). Previous studies demonstrated reduced bone resorption and formation in T2D individuals (56–58), suggesting that hyperglycemia and AGEs crosslinking may impair the function of osteoblasts and osteoclasts, thereby inhibiting bone formation and promoting bone resorption. Correlation analysis in our study also

confirmed the AGEs level was positively correlated with glycemic parameters including FBG, HbA1c, HOMA-IR, bone resorption marker S-CTX, and negatively correlated with bone formation marker PINP in postmenopausal T2D patients. These findings imply that deteriorating glycemic control may contribute to the accumulation of AGEs, which interfere with normal osteoblast function and impair osteoblast development. AGEs may also reduce bone resorption by suppressing osteoclastic differentiation as well as changing the structural integrity of matrix proteins.

Patients with T2D have higher levels of AGEs due to hyperglycemia, which can also increase the production of inflammatory cytokines and reactive oxygen species, setting off a vicious cycle of chronic inflammation and bone resorption (59). Activating of RAGE in both osteoclasts (60, 61) and osteoblasts (46, 62) could induce up-regulation of pro-inflammatory cytokines such as IL-1β, IL-6, and TNF-α, which could directly affect bone homeostasis (63, 64). Accumulating evidence indicates that the TGF-β also plays an important role in the osteogenic progress affected by AGEs, especially biologically potent AGE2 and AGE3 (65, 66). Yamaguchi et al. conducted a series of studies and found that AGE2 and AGE3 suppressed stomal ST2 cell growth, differentiation, and mineralization, as well as increased

apoptosis of osteoblastic cells by up-regulating TGF-β (67–69). As was shown in a clinical study, T2D patients have increased serum levels of IL-6, TGF-β, and TNF-α (70). We also found elevated levels of IL-6 and TGF-β in postmenopausal T2D patients, both of which positively correlated with AGEs levels. Thus, we hypothesized that the bone fragility and increased fracture risk of T2D patients may be due to AGE-induced IL-6 and TGF-β related inflammatory response. At present, the related mechanism of IL-6 and TGF-β on bone collagen abnormal cross-linking is still incomplete, and further research is needed.

In conclusion, both DXA and FRAX scores underestimated the accurate fracture risk in T2D patients. RA-adjusted FRAX is an efficient clinical tool for determining the risk of fracture in postmenopausal T2D patients. AGEs were also associated with serum bone turnover markers and inflammation factors, indicating that the increasing level of AGEs in postmenopausal T2D patients accelerated the expression of inflammatory factors, which led to bone metabolism disorders and a higher risk of osteoporotic fractures.

Data availability statement

The original contributions presented in the study are included in the article/Supplementary Material. Further inquiries can be directed to the corresponding authors.

Ethics statement

The studies involving human participants were reviewed and approved by Ethics Committee of the Third Hospital of Hebei Medical University. The patients/participants provided their written informed consent to participate in this study.

Author contributions

PX, LG, CL and PH designed the research. LG, CL, PH, NW and XB organized the database. BW and KW performed the statistical analysis. PX, LG, CL and PH wrote the first draft of the manuscript. PX, YL and LG thoroughly revised the manuscript.

All authors contributed to manuscript revision and approved the submitted version.

Conflict of interest

The authors declare that the research was conducted in the absence of any commercial or financial relationships that could be construed as a potential conflict of interest.

Publisher's note

All claims expressed in this article are solely those of the authors and do not necessarily represent those of their affiliated organizations, or those of the publisher, the editors and the reviewers. Any product that may be evaluated in this article, or claim that may be made by its manufacturer, is not guaranteed or endorsed by the publisher.

Supplementary material

The Supplementary Material for this article can be found online at: https://www.frontiersin.org/articles/10.3389/fendo.2022.1013397/full#supplementary-material

References

1. Bommer C, Heesemann E, Sagalova V, Manne-Goehler J, Atun R, Barnighausen T, et al. The global economic burden of diabetes in adults aged 20-79 years: A cost-of-Illness study. *Lancet Diabetes Endocrinol* (2017) 5(6):423–30. doi: 10.1016/S2213-8587(17)30097-9

2. Karim L, Rezaee T, Vaidya R. The effect of type 2 diabetes on bone biomechanics. *Curr Osteoporos Rep* (2019) 17(5):291–300. doi: 10.1007/s11914-019-00526-w

3. Hofbauer LC, Busse B, Eastell R, Ferrari S, Frost M, Muller R, et al. Bone fragility in diabetes: Novel concepts and clinical implications. *Lancet Diabetes Endocrinol* (2022) 10(3):207–20. doi: 10.1016/S2213-8587(21)00347-8

4. Martineau P, Leslie WD. The utility and limitations of using trabecular bone score with frax. *Curr Opin Rheumatol* (2018) 30(4):412–9. doi: 10.1097/BOR.0000000000000504

5. Rasmussen NH, Dal J. Falls and fractures in diabetes-more than bone fragility. *Curr Osteoporos Rep* (2019) 17(3):147–56. doi: 10.1007/s11914-019-00513-1

6. Nishimoto K, Doi T, Tsutsumimoto K, Nakakubo S, Kurita S, Kiuchi Y, et al. Relationship between diabetes status and sarcopenia in community-dwelling older adults. *J Am Med Dir Assoc* (2022) 23(10):1718 e7– e12. doi: 10.1016/j.jamda.2022.07.020

7. Moretti A, Palomba A, Gimigliano F, Paoletta M, Liguori S, Zanfardino F, et al. Osteosarcopenia and type 2 diabetes mellitus in post-menopausal women: A case-control study. *Orthop Rev (Pavia)* (2022) 14(6):38570. doi: 10.52965/001c.38570

8. Drey M, Sieber CC, Bertsch T, Bauer JM, Schmidmaier RFiAT intervention Group. Osteosarcopenia is more than sarcopenia and osteopenia alone. *Aging Clin Exp Res* (2016) 28(5):895–9. doi: 10.1007/s40520-015-0494-1

9. Giangregorio LM, Leslie WD, Lix LM, Johansson H, Oden A, McCloskey E, et al. Frax underestimates fracture risk in patients with diabetes. *J Bone Miner Res* (2012) 27(2):301–8. doi: 10.1002/jbmr.556

10. Schacter GI, Leslie WD. Dxa-based measurements in diabetes: Can they predict fracture risk? *Calcif Tissue Int* (2017) 100(2):150–64. doi: 10.1007/s00223-016-0191-x

11. Hunt HB, Torres AM, Palomino PM, Marty E, Saiyed R, Cohn M, et al. Altered tissue composition, microarchitecture, and mechanical performance in cancellous bone from men with type 2 diabetes mellitus. *J Bone Miner Res* (2019) 34 (7):1191–206. doi: 10.1002/jbmr.3711

12. Karim L, Moulton J, Van Vliet M, Velie K, Robbins A, Malekipour F, et al. Bone microarchitecture, biomechanical properties, and advanced glycation end-products in the proximal femur of adults with type 2 diabetes. *Bone* (2018) 114:32–9. doi: 10.1016/j.bone.2018.05.030

13. Osawa S, Katakami N, Sato I, Ninomiya H, Omori K, Yamamoto Y, et al. Skin autofluorescence is associated with vascular complications in patients with type 2 diabetes. *J Diabetes Complications* (2018) 32(9):839–44. doi: 10.1016/j.jdiacomp.2018.06.009

14. Hunt HB, Pearl JC, Diaz DR, King KB, Donnelly E. Bone tissue collagen maturity and mineral content increase with sustained hyperglycemia in the kk-ay murine model of type 2 diabetes. *J Bone Miner Res* (2018) 33(5):921–9. doi: 10.1002/jbmr.3365

15. Yang DH, Chiang TI, Chang IC, Lin FH, Wei CC, Cheng YW. Increased levels of circulating advanced glycation end-products in menopausal women with osteoporosis. *Int J Med Sci* (2014) 11(5):453–60. doi: 10.7150/ijms.8172

16. Piccoli A, Cannata F, Strollo R, Pedone C, Leanza G, Russo F, et al. Sclerostin regulation, microarchitecture, and advanced glycation end-products in the bone of elderly women with type 2 diabetes. *J Bone Miner Res* (2020) 35 (12):2415–22. doi: 10.1002/jbmr.4153

17. Sornay-Rendu E, Boutroy S, Duboeuf F, Chapurlat RD. Bone microarchitecture assessed by hr-pqct as predictor of fracture risk in postmenopausal women: The ofely study. *J Bone Miner Res* (2017) 32(6):1243–51. doi: 10.1002/jbmr.3105

18. Hu L, Li T, Zou Y, Yin XL, Gan H. The clinical value of the Ra-adjusted fracture risk assessment tool in the fracture risk prediction of patients with type 2 diabetes mellitus in China. *Int J Gen Med* (2021) 14:327–33. doi: 10.2147/IJGM.S296399

19. Leslie WD, Johansson H, McCloskey EV, Harvey NC, Kanis JA, Hans D. Comparison of methods for improving fracture risk assessment in diabetes: The Manitoba bmd registry. *J Bone Miner Res* (2018) 33(11):1923–30. doi: 10.1002/jbmr.3538

20. Boutroy S, Bouxsein ML, Munoz F, Delmas PD. *In vivo* assessment of trabecular bone microarchitecture by high-resolution peripheral quantitative computed tomography. *J Clin Endocrinol Metab* (2005) 90(12):6508–15. doi: 10.1210/jc.2005-1258

21. Hunt HB, Miller NA, Hemmerling KJ, Koga M, Lopez KA, Taylor EA, et al. Bone tissue composition in postmenopausal women varies with glycemic control from normal glucose tolerance to type 2 diabetes mellitus. *J Bone Miner Res* (2021) 36(2):334–46. doi: 10.1002/jbmr.4186

22. Asokan AG, Jaganathan J, Philip R, Soman RR, Sebastian ST, Pullishery F. Evaluation of bone mineral density among type 2 diabetes mellitus patients in south karnataka. *J Nat Sci Biol Med* (2017) 8(1):94–8. doi: 10.4103/0976-9668.198363

23. Agius R, Galea R, Fava S. Bone mineral density and intervertebral disc height in type 2 diabetes. *J Diabetes Complications* (2016) 30(4):644–50. doi: 10.1016/j.jdiacomp.2016.01.021

24. Wen Y, Li H, Zhang X, Liu P, Ma J, Zhang L, et al. Correlation of osteoporosis in patients with newly diagnosed type 2 diabetes: A retrospective study in Chinese population. *Front Endocrinol (Lausanne)* (2021) 12:531904. doi: 10.3389/fendo.2021.531904

25. Vestergaard P. Discrepancies in bone mineral density and fracture risk in patients with type 1 and type 2 diabetes–a meta-analysis. *Osteoporos Int* (2007) 18 (4):427–44. doi: 10.1007/s00198-006-0253-4

26. Eller-Vainicher C, Cairoli E, Grassi G, Grassi F, Catalano A, Merlotti D, et al. Pathophysiology and management of type 2 diabetes mellitus bone fragility. *J Diabetes Res* (2020) 2020:7608964. doi: 10.1155/2020/7608964

27. Reistetter TA, Graham JE, Deutsch A, Markello SJ, Granger CV, Ottenbacher KJ. Diabetes comorbidity and age influence rehabilitation outcomes after hip fracture. *Diabetes Care* (2011) 34(6):1375–7. doi: 10.2337/dc10-2220

28. Wang C, Liu J, Xiao L, Liu D, Yan W, Hu T, et al. Comparison of frax in postmenopausal Asian women with and without type 2 diabetes mellitus: A retrospective observational study. *J Int Med Res* (2020) 48(2): 1–14. doi: 10.1177/0300060519879591

29. Leighton PM, Little JA. Identification of coagulase-negative staphylococci isolated from urinary tract infections. *Am J Clin Pathol* (1986) 85(1):92–5. doi: 10.1093/ajcp/85.1.92

30. Kanis JA, Harvey NC, Johansson H, Liu E, Vandenput L, Lorentzon M, et al. A decade of frax: How has it changed the management of osteoporosis? *Aging Clin Exp Res* (2020) 32(2):187–96. doi: 10.1007/s40520-019-01432-y

31. Schousboe JT, Morin SN, Kline GA, Lix LM, Leslie WD. Differential risk of fracture attributable to type 2 diabetes mellitus according to skeletal site. *Bone* (2022) 154:116220. doi: 10.1016/j.bone.2021.116220

32. Guo Y, Wang Y, Chen F, Wang J, Wang D. Assessment of risk factors for fractures in patients with type 2 diabetes over 60 years old: A cross-sectional study from northeast China. *J Diabetes Res* (2020) 2020:1508258. doi: 10.1155/2020/1508258

33. Schwartz AV, Vittinghoff E, Bauer DC, Hillier TA, Strotmeyer ES, Ensrud KE, et al. Association of bmd and frax score with risk of fracture in older adults with type 2 diabetes. *JAMA* (2011) 305(21):2184–92. doi: 10.1001/jama.2011.715

34. Poiana C, Capatina C. Osteoporosis and fracture risk in patients with type 2 diabetes mellitus. *Acta Endocrinol (Buchar)* (2019) 15(2):231–6. doi: 10.4183/aeb.2019.231

35. Rianon NJ, Smith SM, Lee M, Pervin H, Musgrave P, Watt GP, et al. Glycemic control and bone turnover in older Mexican americans with type 2 diabetes. *J Osteoporos* (2018) 2018:7153021. doi: 10.1155/2018/7153021

36. Napoli N, Conte C, Pedone C, Strotmeyer ES, Barbour KE, Black DM, et al. Effect of insulin resistance on bmd and fracture risk in older adults. *J Clin Endocrinol Metab* (2019) 104(8):3303–10. doi: 10.1210/jc.2018-02539

37. Khosla S, Samakkarnthai P, Monroe DG, Farr JN. Update on the pathogenesis and treatment of skeletal fragility in type 2 diabetes mellitus. *Nat Rev Endocrinol* (2021) 17(11):685–97. doi: 10.1038/s41574-021-00555-5

38. Losada-Grande E, Hawley S, Soldevila B, Martinez-Laguna D, Nogues X, Diez-Perez A, et al. Insulin use and excess fracture risk in patients with type 2 diabetes: A propensity-matched cohort analysis. *Sci Rep* (2017) 7(1):3781. doi: 10.1038/s41598-017-03748-z

39. Lekkala S, Taylor EA, Hunt HB, Donnelly E. Effects of diabetes on bone material properties. *Curr Osteoporos Rep* (2019) 17(6):455–64. doi: 10.1007/s11914-019-00538-6

40. Sihota P, Yadav RN, Dhaliwal R, Bose JC, Dhiman V, Neradi D, et al. Investigation of mechanical, material, and compositional determinants of human trabecular bone quality in type 2 diabetes. *J Clin Endocrinol Metab* (2021) 106(5): e2271–e89. doi: 10.1210/clinem/dgab027

41. Tang SY, Zeenath U, Vashishth D. Effects of non-enzymatic glycation on cancellous bone fragility. *Bone* (2007) 40(4):1144–51. doi: 10.1016/j.bone.2006.12.056

42. Karim L, Bouxsein ML. Effect of type 2 diabetes-related non-enzymatic glycation on bone biomechanical properties. *Bone* (2016) 82:21–7. doi: 10.1016/j.bone.2015.07.028

43. de Paula FJ, Horowitz MC, Rosen CJ. Novel insights into the relationship between diabetes and osteoporosis. *Diabetes Metab Res Rev* (2010) 26(8):622–30. doi: 10.1002/dmrr.1135

44. Hamann C, Kirschner S, Gunther KP, Hofbauer LC. Bone, sweet bone–osteoporotic fractures in diabetes mellitus. *Nat Rev Endocrinol* (2012) 8(5):297–305. doi: 10.1038/nrendo.2011.233

45. Park SY, Choi KH, Jun JE, Chung HY. Effects of advanced glycation end products on differentiation and function of osteoblasts and osteoclasts. *J Korean Med Sci* (2021) 36(37):e239. doi: 10.3346/jkms.2021.36.e239

46. Suzuki R, Fujiwara Y, Saito M, Arakawa S, Shirakawa JI, Yamanaka M, et al. Intracellular accumulation of advanced glycation end products induces osteoblast apoptosis *Via* endoplasmic reticulum stress. *J Bone Miner Res* (2020) 35(10):1992–2003. doi: 10.1002/jbmr.4053

47. Alikhani M, Alikhani Z, Boyd C, MacLellan CM, Raptis M, Liu R, et al. Advanced glycation end products stimulate osteoblast apoptosis *Via* the map

kinase and cytosolic apoptotic pathways. *Bone* (2007) 40(2):345–53. doi: 10.1016/j.bone.2006.09.011

48. Shanbhogue VV, Mitchell DM, Rosen CJ, Bouxsein ML. Type 2 diabetes and the skeleton: New insights into sweet bones. *Lancet Diabetes Endocrinol* (2016) 4(2):159–73. doi: 10.1016/S2213-8587(15)00283-1

49. Starup-Linde J, Hygum K, Harslof T, Langdahl B. Type 1 diabetes and bone fragility: Links and risks. *Diabetes Metab Syndr Obes* (2019) 12:2539–47. doi: 10.2147/DMSO.S191091

50. Burghardt AJ, Issever AS, Schwartz AV, Davis KA, Masharani U, Majumdar S, et al. High-resolution peripheral quantitative computed tomographic imaging of cortical and trabecular bone microarchitecture in patients with type 2 diabetes mellitus. *J Clin Endocrinol Metab* (2010) 95(11):5045–55. doi: 10.1210/jc.2010-0226

51. Heilmeier U, Joseph GB, Pasco C, Dinh N, Torabi S, Darakananda K, et al. Longitudinal evolution of bone microarchitecture and bone strength in type 2 diabetic postmenopausal women with and without history of fragility fractures-a 5-year follow-up study using high resolution peripheral quantitative computed tomography. *Front Endocrinol (Lausanne)* (2021) 12:599316. doi: 10.3389/fendo.2021.599316

52. Karim L, Tang SY, Sroga GE, Vashishth D. Differences in non-enzymatic glycation and collagen cross-links between human cortical and cancellous bone. *Osteoporos Int* (2013) 24(9):2441–7. doi: 10.1007/s00198-013-2319-4

53. Xia N, Cai Y, Wang W, Bao C, Li Y, Xie Q, et al. Association of bone-related biomarkers with femoral neck bone strength. *BMC Musculoskelet Disord* (2022) 23(1):482. doi: 10.1186/s12891-022-05427-1

54. Jain S, Camacho P. Use of bone turnover markers in the management of osteoporosis. *Curr Opin Endocrinol Diabetes Obes* (2018) 25(6):366–72. doi: 10.1097/MED.0000000000000446

55. Szulc P. Bone turnover: Biology and assessment tools. *Best Pract Res Clin Endocrinol Metab* (2018) 32(5):725–38. doi: 10.1016/j.beem.2018.05.003

56. An Y, Liu S, Wang W, Dong H, Zhao W, Ke J, et al. Low serum levels of bone turnover markers are associated with the presence and severity of diabetic retinopathy in patients with type 2 diabetes mellitus. *J Diabetes* (2021) 13(2):111–23. doi: 10.1111/1753-0407.13089

57. Wang L, Li T, Liu J, Wu X, Wang H, Li X, et al. Association between glycosylated hemoglobin A1c and bone biochemical markers in type 2 diabetic postmenopausal women: A cross-sectional study. *BMC Endocr Disord* (2019) 19(1):31. doi: 10.1186/s12902-019-0357-4

58. Xu L, Niu M, Yu W, Xia W, Gong F, Wang O. Associations between Fgf21, osteonectin and bone turnover markers in type 2 diabetic patients with albuminuria. *J Diabetes Complications* (2017) 31(3):583–8. doi: 10.1016/j.jdiacomp.2016.11.012

59. Napoli N, Chandran M, Pierroz DD, Abrahamsen B, Schwartz AV, Ferrari SL, et al. Mechanisms of diabetes mellitus-induced bone fragility. *Nat Rev Endocrinol* (2017) 13(4):208–19. doi: 10.1038/nrendo.2016.153

60. Yang X, Gandhi C, Rahman MM, Appleford M, Sun LW, Wang X. Age-related effects of advanced glycation end products (Ages) in bone matrix on osteoclastic resorption. *Calcif Tissue Int* (2015) 97(6):592–601. doi: 10.1007/s00223-015-0042-1

61. Dong XN, Qin A, Xu J, Wang X. *In situ* accumulation of advanced glycation endproducts (Ages) in bone matrix and its correlation with osteoclastic bone resorption. *Bone* (2011) 49(2):174–83. doi: 10.1016/j.bone.2011.04.009

62. Gossiel F, Paggiosi MA, Naylor KE, McCloskey EV, Walsh J, Peel N, et al. The effect of bisphosphonates on bone turnover and bone balance in postmenopausal women with osteoporosis: The T-score bone marker approach in the trio study. *Bone* (2020) 131:115158. doi: 10.1016/j.bone.2019.115158

63. Chen H, Liu W, Wu X, Gou M, Shen J, Wang H. Advanced glycation end products induced il-6 and vegf-a production and apoptosis in osteocyte-like mlo-Y4 cells by activating rage and Erk1/2, P38 and Stat3 signalling pathways. *Int Immunopharmacol* (2017) 52:143–9. doi: 10.1016/j.intimp.2017.09.004

64. Sakamoto E, Mihara C, Ikuta T, Inagaki Y, Kido J, Nagata T. Inhibitory effects of advanced glycation end-products and porphyromonas gingivalis lipopolysaccharide on the expression of osteoblastic markers of rat bone marrow cells in culture. *J Periodontal Res* (2016) 51(3):313–20. doi: 10.1111/jre.12310

65. Brownlee M. Biochemistry and molecular cell biology of diabetic complications. *Nature* (2001) 414(6865):813–20. doi: 10.1038/414813a

66. Brownlee M. The pathobiology of diabetic complications: A unifying mechanism. *Diabetes* (2005) 54(6):1615–25. doi: 10.2337/diabetes.54.6.1615

67. Otsuka E, Yamaguchi A, Hirose S, Hagiwara H. Characterization of osteoblastic differentiation of stromal cell line St2 that is induced by ascorbic acid. *Am J Physiol* (1999) 277(1):C132–8. doi: 10.1152/ajpcell.1999.277.1.C132

68. Yamaguchi A, Ishizuya T, Kintou N, Wada Y, Katagiri T, Wozney JM, et al. Effects of bmp-2, bmp-4, and bmp-6 on osteoblastic differentiation of bone marrow-derived stromal cell lines, St2 and Mc3t3-G2/Pa6. *Biochem Biophys Res Commun* (1996) 220(2):366–71. doi: 10.1006/bbrc.1996.0411

69. Okazaki K, Yamaguchi T, Tanaka K, Notsu M, Ogawa N, Yano S, et al. Advanced glycation end products (Ages), but not high glucose, inhibit the osteoblastic differentiation of mouse stromal St2 cells through the suppression of osterix expression, and inhibit cell growth and increasing cell apoptosis. *Calcif Tissue Int* (2012) 91(4):286–96. doi: 10.1007/s00223-012-9641-2

70. Qiao YC, Shen J, He L, Hong XZ, Tian F, Pan YH, et al. Changes of regulatory T cells and of proinflammatory and immunosuppressive cytokines in patients with type 2 diabetes mellitus: A systematic review and meta-analysis. *J Diabetes Res* (2016) 2016:3694957. doi: 10.1155/2016/3694957

Check for updates

Association of metformin use with fracture risk in type 2 diabetes: A systematic review and meta-analysis of observational studies

Yining Wang[1,2†], Liming Yu[3†], Zhiqiang Ye[2], Rui Lin[1,2], Antonia RuJia Sun[4,5], Lingna Liu[2,6], Jinsong Wei[7], Feifu Deng[7], Xiangxin Zhong[7], Liao Cui[2*], Li Li[2*] and Yanzhi Liu[1,2,6*]

[1]Zhanjiang Key Laboratory of Orthopaedic Technology and Trauma Treatment, Zhanjiang Central Hospital, Guangdong Medical University, Zhanjiang, China, [2]Guangdong Provincial Key Laboratory for Research and Development of Natural Drug, School of Pharmacy, Guangdong Medical University, Zhanjiang, China, [3]Department of Stomatology, Affiliated Hospital of Guangdong Medical University, Zhanjiang, China, [4]Centre for Biomedical Technologies, Queensland University of Technology, Brisbane, Queensland, Australia, [5]Center for Translational Medicine Research and Development, Shenzhen Institute of Advanced Technology, Chinese Academy of Science, Shenzhen, Guangdong, China, [6]Marine Medical Research Institute of Zhanjiang, Zhanjiang, China, [7]Department of Orthopedics, Affiliated Hospital of Guangdong Medical University, Zhanjiang, China

Aims: Increasing evidence suggests that metformin can affect bone metabolism beyond its hypoglycemic effects in diabetic patients. However, the effects of metformin on fracture risk in type 2 diabetes mellitus (T2DM) patients remain unclear. A systematic review and meta-analysis were performed in this study to evaluate the association between metformin application and fracture risk in T2DM patients based on previous studies published until June 2021.

Methods: A systematic search was performed to collect publications on metformin application in T2DM patients based on PubMed, Embase, Cochran, and Web of Science databases. Meta-analysis was performed by using a random-effects model to estimate the summary relative risks (RRs) with 95% confidence intervals (CIs). Subgroup analyses based on cohort/case-control and ethnicity and sensitivity analyses were also performed.

Results: Eleven studies were included in the meta-analysis. Results demonstrated metformin use was not significantly associated with a decreased risk of fracture (RR, 0.91; 95% CI, 0.81–1.02; I^2 = 96.8%). Moreover, metformin use also demonstrated similar results in subgroup analyses of seven cohort studies and four case-control studies, respectively (RR, 0.90; 95% CI, 0.76–1.07; I^2 = 98.0%; RR, 0.96; 96% CI, 0.89–1.03; I^2 = 53.7%). Sensitivity analysis revealed that there was no publication bias.

Conclusion: There was no significant correlation between fracture risk and metformin application in T2DM patients. Due to a limited number of existing studies, further research is needed to make a definite conclusion for clinical consensus.

1 Introduction

Diabetes mellitus (DM) is one of the leading causes of mortality and reduced life expectancy (1, 2). The estimated global number of individuals diagnosed with DM has increased from 422 million in 2014 (3) to over 536.6 million currently, and it is projected to reach 783.2 million by 2045, accounting for 12.2% of 20-79 year-olds (4). Type 2 DM (T2DM) represents approximately 90%–95% of all DM cases (5, 6). Diabetes-related complication costs are substantial and have significantly increased the healthcare burden of diabetes patients (7, 8). The estimated global direct health cost of diabetes is projected to rise to $845 billion by 2045 (9). Previous studies have demonstrated an increased risk for fragility fractures as an important complication of T2DM (10–12).

In contrast to patients with type 1 diabetes, T2DM patients exhibited increased or normal bone mineral density in the clinic but with increased bone fragility and fracture risk (13–15). The pivotal causes of higher bone fragility in T2DM are strongly associated with the phenotype of abnormal osseous architecture (especially the increased cortical porosity), collagen disorganization, bone vasculopathy, increased bone marrow adiposity, and low bone turnover, which together contribute to impairments in bone material properties (16–18). Patients with T2DM who have suffered fractures are prone to frequent wound infections, resulting in delayed fracture healing and an increased risk of nonunion or pseudoarthropathy (19–21). Fractures in T2DM patients result in prolonged immobility and hospitalizations and lead to substantial morbidity and mortality. In addition to the direct effects of diabetes on bone fragility, current medical management of T2DM also substantially impacts bone health and fracture risk (22, 23). For instance, thiazolidinediones have been associated with an increased fracture risk (24, 25), whereas metformin administration has been shown to have a protective effect on the bone health of diabetic patients (24–26).

Metformin, a biguanide antidiabetic drug, is considered the standard initial treatment for T2DM patients. It affects several aging-related processes, including bone deterioration, by suppressing cellular senescence and chronic inflammation and promoting autophagy (27, 28). Previous studies demonstrated that metformin directly promoted osteoblastic differentiation of different kinds of stem cells (including umbilical cord mesenchymal stem cells (29), adipose-derived stem cells (30), dental pulp stem cells (31), and bone marrow derived mesenchymal stem cells (32), enhanced the anabolic action of the bone (including beneficial effects on bone microarchitecture, bone mineral density, and bone turnover markers), and improved bone quality in patients with T2DM (33–36). Furthermore, a previous report suggested a potential benefit of metformin in contributing to decreased bone cancer risk in T2DM patients (37).

Nonetheless, whether metformin can reduce the risk of fractures remains unconfirmed and controversial. Previous studies have reported no significant correlation between fracture risk and metformin application (38) and no significant effects of metformin on bone marrow density (BMD) (39, 40). However, another investigation showed that 10 µg/mL of metformin might partially suppress the mineralization of osteoblasts (41). Borges et al. found that the effects of metformin monotherapy showed only small but not significant increases in lumbar spine BMD at all time points from baseline to week 80 in T2DM patients (42). Therefore, the effect of metformin on bone metabolism and whether metformin medication reduces the risk of fracture in patients with T2DM needs further evaluation.

In this study, to determine whether metformin treatment could reduce fracture risk in T2DM, a comprehensive meta-analysis was performed on the fracture risk of T2DM patients receiving metformin administration; it included all previous reports up to June 2021.

2 Methods

2.1 Search strategy

This meta-analysis was performed according to the Preferred Reporting Items for Systematic reviews and Meta-Analyses (PRISMA) statement guideline for systematic reviews

and meta-analyses (43, 44), and it was registered with PROSPERO (No. CRD42022344967). We searched for studies on the fracture risk of diabetic patients with metformin administration published until June 2021 by using PubMed, Embase, Cochran library, and Web of Science databases. The following keywords were used for publication collection: ("Metformin" OR "dimethylbiguanide" OR "metformin HCI") AND ("bone" OR "bone fracture" OR "fracture" OR "osteoporotic fracture" OR "broken bone" OR "bone mineral density" OR "BMD" OR "bone mass density" OR "osteoporosis" OR "bone health" OR "bone quality").

2.2 Inclusion criteria

Each title and abstract were reviewed to identify relevant papers. Full texts of the articles were reviewed if the abstract was deemed potentially relevant. Studies that met the following criteria were eligible for inclusion:

(1) observational studies where metformin was the exposure variable and fractures were the main outcome variable or one of the outcome variables.

(2) T2DM participants aged ≥18 years.

(3) The odds ratio (OR), risk ratio (RR), and hazard ratio (HR) were reported as the effect size (ES).

2.3 Exclusion criteria

The exclusion criteria excluded studies that:

(1) Related to other drugs in combination treatment with metformin.

(2) Excluded placebo diabetic control.

(3) Included Type 1 diabetes patients.

(4) Included single gender.

A total of 1,031 publications were identified with the search strategy. Then, these studies were independently screened according to the inclusion and exclusion criteria. A total of 11 studies were eligible and included in the meta-analysis. (Figure 1)

2.4 Data extraction

Two authors (WYN and YLM) independently conducted study screening and data extraction from the eligible literature. When disputes were encountered, they were resolved through discussion or assisted by the main investigator (LYZ). The following data were collected from all included studies: first author's surname, publication year, study design, country, follow-up duration, mean age or age range of participants,

FIGURE 1
Flowchart of the study selection process.
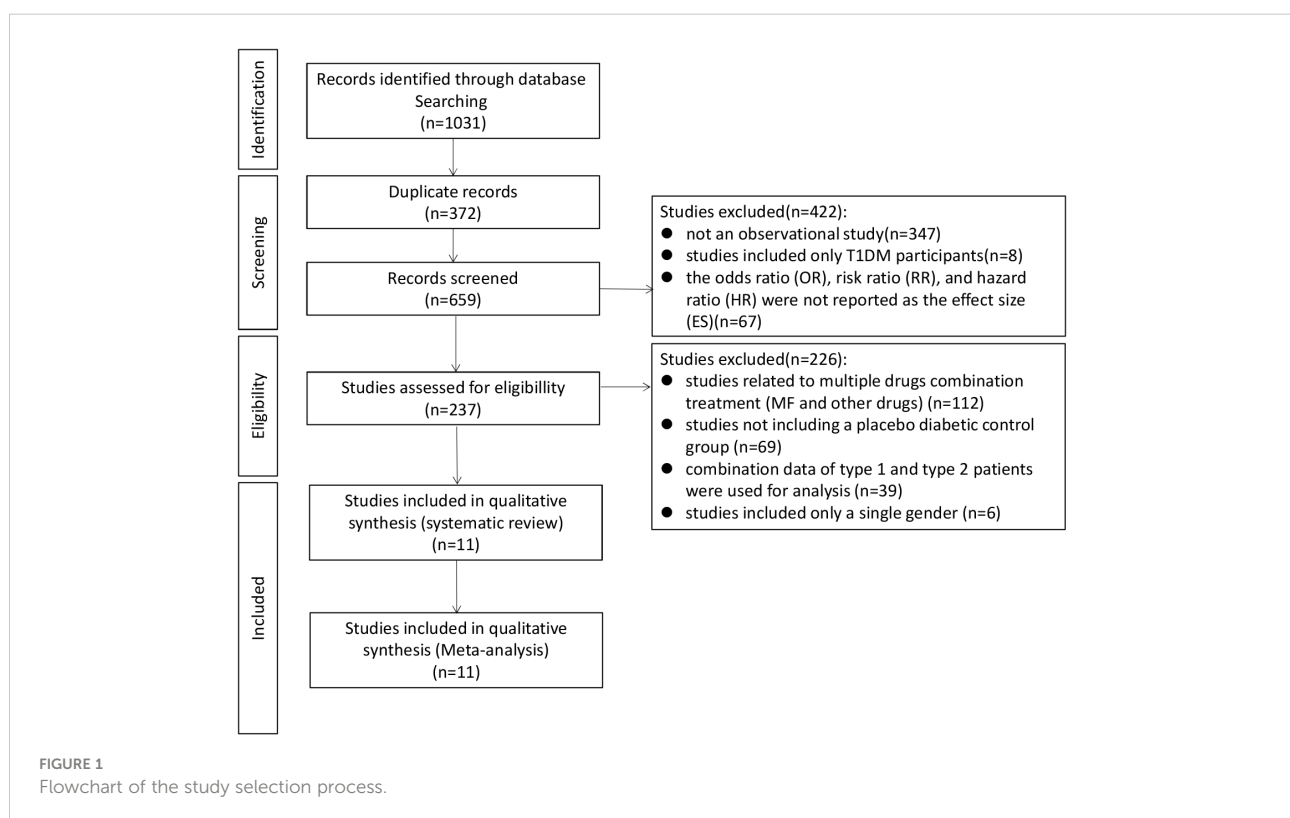
gender, sample size, number of cases, outcome variables and fracture assessment method, the adjusted ORs, RRs, or HRs, and the corresponding 95% confidence intervals (CIs) (Table 1). The Newcastle-Ottawa Scale (NOS) quality assessment was used to evaluate the studies.

2.5 Statistical analysis

Stata software was used for meta-analysis (Stata, version 16, College Station, TX, USA). All reported ORs, RRs, HRs, and the 95% CIs for fracture risk were used to calculate the logarithmic RR and its standard error (SE). A random effects model was used to estimate the summary relative risks with 95% CIs. Q and I^2 tests were performed to analyze the homogeneity of the included studies. For the Q test, statistical significance was set at $p \leq 0.05$; for I^2 statistics, the following critical points were specified to define the degree of heterogeneity: <25% (low heterogeneity),

25%–50% (moderate heterogeneity), 50%–75% (high heterogeneity), and >75% (severe heterogeneity).

The subgroup analyses of cohort, case-control, and ethnicity were respectively performed on the included studies. In addition, sensitivity analysis was used to investigate the extent to which inferences might depend on a particular study or research group. Visual inspection of the funnel chart was used to assess publication bias. A formal statistical assessment of funnel plot asymmetry was performed using Egger's regression asymmetry test. *P* values of < 0.05 were considered statistically significant.

3 Results

3.1 Study characteristics

Among the 1,031 retrieved papers, 11 related to the application of metformin and the risk of fracture in T2DM

TABLE 1   Characteristic table of studies on the relationship between MF use and fracture risk in diabetic patients.

First author (year)	Country	Duration of follow-up (years)	Design	Mean age	Samples sizes	Cases	Adjusted OR, RR, or HR (95% CI)	Nos	Fracture types
Tseng CH (2021) (37)	Taiwan	5.3	Cohort	62	29,222	977	0.62 (0.55,0.71)	9	vertebral fracture
Tak Kyu Oh (2020) (38)	South Korea	5	Cohort	60	37378	972	1.00 (0.86,1.16)	7	Hip fracture
Starup-Linde J (45)	Denmark	5.5	Cohort	Cases: 58 Controls:73	180,073	20,557	0.73 (0.71,0.76)	9	Any fracture, vertebral fracture, forearm fracture, and osteoporotic fracture
Wallander M (46)	Sweden	1.3	Cohort	Cases: 79 Controls:81	79,159	2394	1.05 (0.96,1.14)	9	Hip fracture
Hung YC (47)	Taiwan	3.9	Cohort	70	7,761	367	1.02 (0.83,1.26)	9	Hip fracture
Majumdar (48)	USA	2.2	Cohort	52	72,738	741	1.00 (0.80,1.20)	9	Osteoporotic fracture
Colhoun (49)	Scotland	9	Cohort	65	173,113	2,433	1.02 (1.00,1.05)	9	Hip fracture
Charlier (50)	UK	23	Case-control	71	28617	5692	1.00 (0.95,1.05)	8	Low-trauma fracture (non-vertebral fractures of the proximal and distal upper and lower extremities, ribs and thorax, hip and foot)
Vavanikunnel J (51)	UK	21	Case-control	72	27124	5366	0.96 (0.91,1.01)	8	Low-trauma fracture (non-vertebral fractures of the proximal and distal upper and lower extremities, ribs and thorax, hip, and foot)
Puar TH (52)	Singapore	5	Case-control	Cases: 77 Controls:76	1,116	558	0.73 (0.57,0.94)	8	Hip fracture
Monami M (53)	Italy	4.1	Nested Case-control	Cases: 69 Controls:68	332	83	0.94 (0.54,1.65)	8	Total fracture

Mean age only displayed integers, ignoring numbers after the decimal point. OR, odds ratio; RR, risk ratio; HR, hazard ratio; CI, confidence interval; Nos, Newcastle-Ottawa scale.

Wang et al.

patients and were included in this meta-analysis according to the inclusion/exclusion criteria (Table 1). Among the 11 studies, there were seven cohort studies (38, 45–49, 54), and four case-control studies (50–53). All studies included both genders (Figure 1).

These studies collectively included 635,945 participants and were published between 2008 and 2021; they were conducted in various regions, including one study each in the United States (48), Denmark (45), South Korea (38), Singapore (52), Italy (53), and Sweden (46), two in Taiwan (47, 54), and three in the United Kingdom (49–51).

Regarding the types of fractures, five studies included fractures at multiple sites, such as fractures of the proximal and distal upper and lower extremities, ribs and thorax, hip, and foot (45, 48, 50, 51, 53), two studies included vertebral fracture (45, 54), six studies included hip fractures (38, 45–47, 49, 52), and three studies included osteoporotic fracture (45, 46, 48).

3.2 Results of the meta-analysis

There were seven cohort studies and four case-control studies involved in the meta-analysis. Four studies revealed that metformin treatment reduced fracture risk, seven studies demonstrated that metformin had no significant effect associated with fracture risk, and no studies showed that metformin increased fracture risk.

In this meta-analysis, we had 11 effect sizes obtained from 11 studies. The meta-analysis results are shown as forest plots (Figure 2). Results demonstrated that metformin administration was not significantly associated with a decrease

in the fracture rate of diabetic patients (RR, 0.91; 95% CI, 0.81–1.02). Significantly high between-study heterogeneity was found ($I^2 = 96.8\%$, $p < 0.001$).

In the sensitivity analysis, no single study significantly influenced the findings. No evidence of publication bias was found in this meta-analysis with Egger's test evaluation ($p = 0.99$).

4 Discussion

The occurrence of fractures is closely related to low BMD and osteoporosis development (55, 56). Previous studies have demonstrated that BMD significantly decreased in patients with T1DM, leading to an increased risk of fractures (57). Although T2DM patients showed bone formation suppression, microarchitecture deterioration, and microvascular complications in the bone (58), unlike T1DM patients, T2DM patients might not demonstrate significant BMD decline (59). Since T2DM accounts for more than 90%–95% of all diabetes cases, the factors associated with type 2 diabetic fractures attract a lot of concerns. The effects of T2DM on bone are multifactorial, including hyperglycemia (60), insulin imbalance (61), obesity (62), and medications (63). Among several factors that might influence the risk of fracture, much attention has been given to glucose-lowering medications, for example, metformin.

In this study, we performed a meta-analysis and a series of sub-group meta-analyses to examine the association between metformin use and the risk of fracture in T2DM patients. We found no significant association between metformin use and fracture risk. Due to only a small number of studies (n=11) being

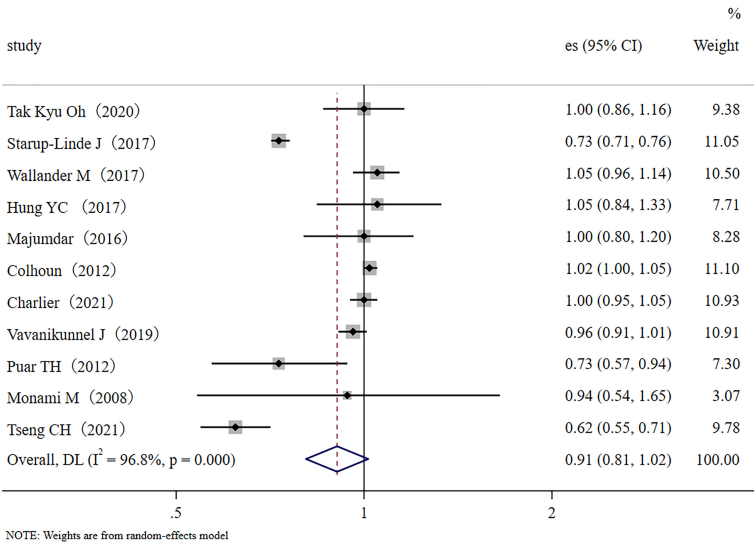
FIGURE 2
Forest plot of the 11 studies that examined the association between metformin application and fracture risk in T2DM patients; (Study: author and year of publication; es, effect size; 95% CI, 95% confidence interval).

included in this study, investigation of fractures in specific sites was not possible; therefore, our study used the same strategy as that of a previous report (64) that focused on the association of metformin use and fracture risk from any sites with no focus on a specific site.

We conducted a subgroup meta-analysis that only included the seven cohort studies to demonstrate multiple validations of our conclusion. The results showed that metformin administration was not closely related to a decreased fracture risk in diabetic patients (RR, 0.90; 95% CI, 0.76–1.07). Inter-study heterogeneity was significant; $I^2 = 98.0\%$, $p < 0.001$ (Figure 3A). We also conducted a subgroup meta-analysis that only included the four case-control studies. Like the cohort studies, the case-control studies also demonstrated that metformin administration was not closely related to a decreased fracture risk in diabetic patients (RR, 0.96; 95% CI, 0.89–1.03), but heterogeneity was not significant, $I^2 = 53.7\%$, $p=0.090$ (Figure 3B). In addition, ethnicity was used as a categorical variable for subgroup analysis. Based on the eleven collected studies, four studies were performed in Asian countries (traditional major population mainly of Far-Eastern origins), and seven were performed in Europe/the United States of

America (traditional major population mainly of European origins). Therefore, we used the Far-Eastern origins/the European origins as the ethnic category for sub-group analysis. Results demonstrated that metformin administration was not closely related to a decreased fracture risk in diabetic people of Far-Eastern origins (RR 0.83, 95% CI, 0.63–1.09) (Figure 4A). The subgroup analysis in the diabetic people of European origins similarly demonstrated that metformin administration was not closely related to a decreased fracture risk (RR 0.95, 95% CI, 0.83–1.09) (Figure 4B). Overall, the subgroup meta-analyses demonstrated that different subgroup analyses support the same conclusion.

After subgroup analyses, we conducted a bias analysis on the quality of the included studies, and STATA was used to prepare a funnel chart for the 11 included studies. Funnel plot analysis showed that five studies might significantly affect the overall heterogeneity of the analysis (Figure S1). We excluded four of the five studies that may have affected the overall heterogeneity of this analysis (Starup-Linde et al., 2017 (45), Colhoun et al., 2012 (49), Puar et al., 2012 (52), and Tseng et al., 2021 (54)) and the remaining seven studies were used for further meta-analysis (Figure S2). The results further demonstrated that metformin
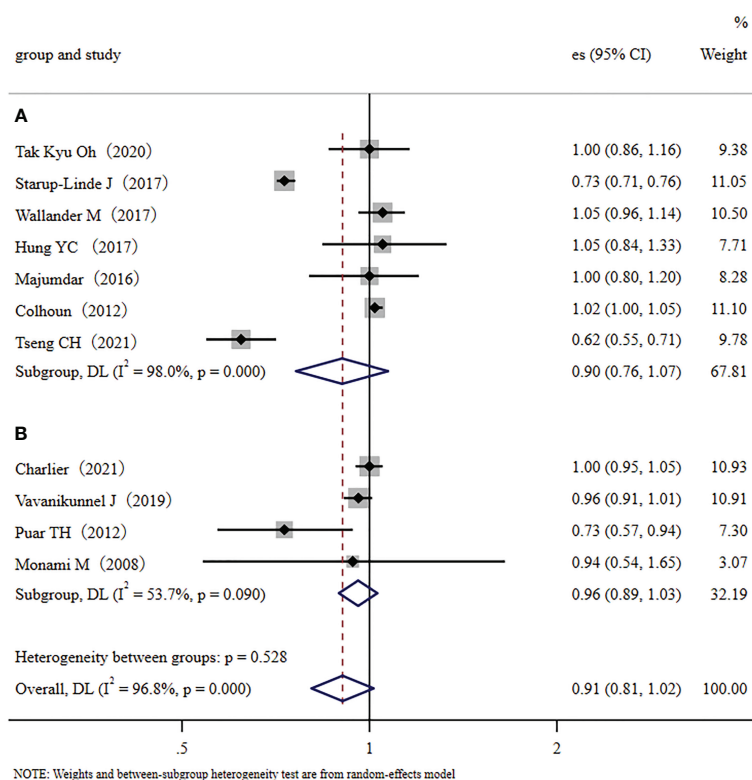

FIGURE 3
The cohort/case-control subgroup analysis: **(A)**: Forest plot of the included Cohort studies that examined the association between metformin application and fracture risk in type 2 diabetic patients; **(B)**: Forest plot of the included Case-control studies that examined the association between metformin application and fracture risk in type 2 diabetic patients. (Study: author and year of publication; es, effect size; 95% CI, 95% confidence interval; Weight, weight).
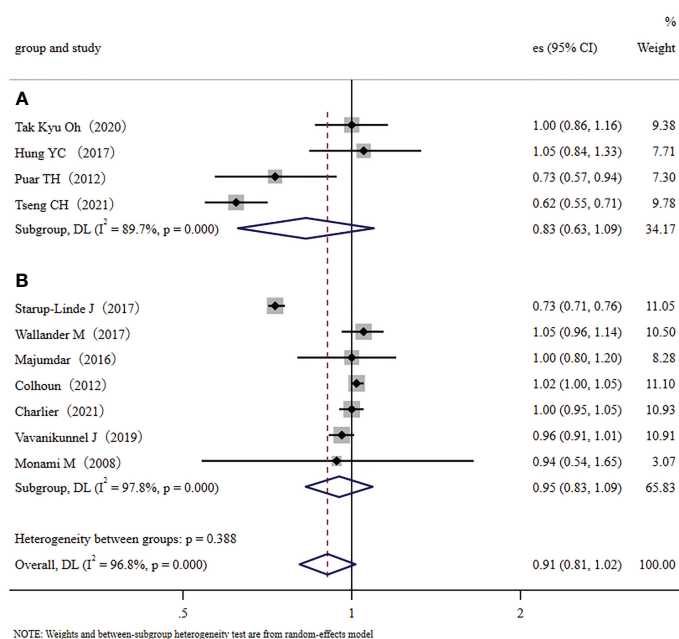
FIGURE 4

The ethnic subgroup analysis: **(A)**: Forest plot of the four studies that were performed in Asia (major population: Far-Eastern origins); **(B)**: Forest plot of the seven studies that were performed in Europe/the United States (major population: European origins); Study: author and year of publication; es, effect size; 95% CI, 95% confidence interval; Weight, weight).

administration and the fracture risk of diabetic patients were not significantly inversely related (RR, 0.99; 95% CI, 0.96–1.02). The heterogeneity between studies was $I^2 = 0.0\%$, which demonstrated that the high heterogeneity across all 11 studies did not significantly affect the results in this meta-analysis. Therefore, the conclusion of this meta-analysis was robust and credible. The Egger's test result was $p=0.9301$ and $p>0.05$, which indicated that the meta-analysis has no publication bias. A sensitivity analysis was used to test the stability of the effect size (ES) estimates (Figure S3). Overall, the data of these analyses all suggested that metformin use is not significantly associated with a decreased risk of fractures in T2DM patients.

Several studies demonstrated that metformin treatment was associated with significant low bone fracture risks in patients with diabetes (65, 66). The treatment of T2DM patients and osteoporosis with metformin and dietary intervention could decrease blood glucose levels, increase bone density, and alleviate osteoporosis (67–70). A recent study also reported that metformin use was associated with a lower risk of osteoporosis/vertebral fracture in T2DM patients (37). A prior systematic review and meta-analysis suggested that metformin use was inversely associated with the risk of fracture in diabetes (RR, 0.82; 95% CI, 0.72–0.93; n=7; $I^2 = 22.4\%$; $p=0.259$) (64). Another meta-analysis demonstrated that the use of metformin appears to decrease the fracture risk (RR, 0.86; 95% CI, 0.75–0.99; $I^2 = 95.2\%$; $p <0.001$). The reduced fracture risk with metformin could be related to metformin prescriptions that

typically start in the early stages of type 2 diabetes mellitus (63). Furthermore, metformin has several relevant contraindications, including renal insufficiency, severe liver disease, and heart failure. A lower comorbidity may contribute to the influence of metformin on the lower incidence of bone fractures (53).

This study found that metformin use is not significantly associated with a decreased risk of fractures in T2DM patients. Our results are inconsistent with previous studies including type 1 and type 2 patients and single-gender data. Our study focused on T2DM patients and only included studies that examined both genders. A previous study by Wallander et al. (46), demonstrated that women with T2DM-oral medication had an increased risk of hip fracture compared to men. Therefore, we excluded studies that reported on single-gender involvement. According to the data we collected in the 11 studies, four studies revealed that metformin treatment could reduce fracture risk (45, 50, 52, 54), and another seven demonstrated that metformin had no significant effect associated with fracture risk (38, 46–48, 52). None of the studies in this review showed that metformin increased fracture risk. The differing results between studies may be due to variations in metformin dose and duration. However, we noted that all the included observational studies did not reveal the specific metformin dose, which makes it difficult to interpret and analyze the underlying reason. To model the univariate effects of metformin, the 11 included studies selected individuals who could be stratified based on

cumulative exposure to metformin. For example, current metformin users were defined by Charlier et al. as participants with their last prescription ≤ 60 days prior to the index date (50), whereas Colhoun et al. included metformin users with a cumulative exposure of 1 year (49). Therefore, in this meta-analysis, we focused on T2DM patients with current metformin duration (at least>30 days) as the outcome and ignored the dose. We summarized the relevant information on metformin administration reported in the 11 included studies (Table S1). The data on ever-exposure to metformin was not used in this study, as we assumed that there were no legacy or carry-over effects from remote exposure to any antidiabetic drugs. Colhoun et al. considered that cumulative metformin exposure does not depend on the events in the unexposed and, therefore, cannot be affected by allocation bias (49). We used cumulative metformin exposure in this study was consistent with them. Therefore, the data from current cumulative exposure to metformin was considered more accurate than data from ever exposure to metformin. In addition, though several studies have various sub-group settings, they may not provide comprehensive information for analysis. Therefore, we preferred to use the total integrated data for the present analysis. For example, in a study by Charlier et al. (50), current metformin exposure was divided into three categories: ①HbA1c ≤ 7.0%, ②HbA1c>7.0% and ≤ 8.0%, and ③HbA1c>8.0%. Our study only collected the general comprehensive data for analysis, independently based on patients' HbA1c levels. The results demonstrated that metformin treatment was not significantly associated with fracture risk. However, we noticed that HbA1 level is an important parameter in metformin use that may significantly affect fracture risk. Patients with current metformin use that controlled the HbA1 levels at the range of ≤7.0% and >7.0% but ≤8.0% demonstrated a significantly reduced risk of fractures (aOR, 0.89; 95% CI, 0.83–0.96, and 0.81; 95% CI, 0.73–0.90, respectively). The results suggested that proper blood sugar management by metformin may help to decrease fracture risk. However, Hung et al. demonstrated that severe hypoglycemia in T2DM patients significantly increases the risk of falls and the cumulative incidence of hip fracture (47). The study by Puar et al. also suggested a greater risk of falls in older adults with tight glycemic control (HbA1c<7%) (52). If metformin administration significantly contributes to severe hypoglycemia, then the fall risk may increase and decrease the beneficial effects of metformin on bone. Wallander et al. suggested that metformin administration was independently associated with an increased risk of non-skeletal fall injury (46).

In summary, our data demonstrated that metformin treatment was not significantly associated with the risk of fracture, and our results are independent of patients' HbA1c levels/glycemic control levels. When the data with HbA1c control is considered for analysis, for example, If the data of HbA1c ≤ 7.0% (OR, 0.89; 95% CI, 0.83–0.96) (Charlier, 2021) (50) was used for our meta-analysis, it shifted the overall

estimate (OR, 0.87; 95% CI, 0.77–0.97) and the results demonstrated that metformin treatment was related to a decreased fracture risk in T2DM patients (Figure S4).

Metformin is often prescribed in combination with other antidiabetic medications. The possible effect of interaction between metformin with other antidiabetic medications may also affect bone fracture risk. A previous study investigated the effect of metformin relative to placebo in combination with insulin analogs (Metformin + Insulin vs. Placebo + Insulin) on bone markers P1NP Procollagen type 1 N-terminal propeptide (P1NP) and C-terminal telopeptide of type I collagen (CTX) in patients with T2DM (71). The levels of bone formation marker P1NP and bone resorption marker CTX increased significantly in both groups. However, the Metformin+Insulin combination increased P1NP less than the Placebo+Insulin combination. There was no statistical difference in CTX between groups. There were no adverse effects on bone or muscle when metformin was used in combination with sitagliptin (72). The current use of metformin plus SGLT-2 inhibitor compared to the current use of metformin plus DPP-4 inhibitor was not associated with fractures in patients with type 2 diabetes (73). SGLT2 inhibitors + metformin combination treatment do not affect fracture risk compared to GLP-1 receptor agonists + metformin combination (74). SGLT2 and metformin combination therapy did not influence fracture risk compared with metformin monotherapy or other medications in patients with T2DM (75). Low-dose combination therapy with rosiglitazone and metformin was highly effective in preventing type 2 diabetes in patients with impaired glucose tolerance, with little effect on the clinically relevant adverse events of these two drugs (76). Another previous study demonstrated that metformin combined with sulfonylurea, meglitinide, acarbose, pioglitazone, immunosuppressants, or estrogen (women only) for diabetes management, all revealed a significant association with lower fracture risk. However, metformin combined with insulin or rosiglitazone for diabetes management did not show a decreased fracture risk. Significant interactions between metformin, insulin, sulfonylurea, and pioglitazone were found (p-values for interaction<0.05). The protective effect of metformin was not significant in insulin-treated patients, while metformin revealed greater beneficial effects in sulfonylurea or pioglitazone-treated patients (28). The possible effect of the interaction of metformin with other antidiabetic medications on bone fracture protection still needs more direct evidence to show specific indications clearly.

This meta-analysis has some limitations. There was significant heterogeneity between the 11 included studies. The reason may be due to differences in the sample sizes of the included studies. For instance, the study of Starup-Linde et al., 2017 (45) included the most fracture cases (20,557), while Monami et al., 2008 (53) included only 83 cases. The significant case differences in the sample size may have contributed to the high heterogeneity (77). Additionally, study

differences in the quality, design, and country and continent of origin may have also contributed to the high heterogeneity. The high heterogeneity may have been caused by the difference in the strength of the correlation between the studies rather than the difference in the direction of the correlation (78). Further, the number of studies (n=11) included in this meta-analysis was limited, and it is expected that more sufficient samples and high-quality clinical data will be available in the future. Studies with a larger sample size will provide more accurate evidence to support metformin administration and its role in fracture risk in diabetic patients. In this study, we only focus on the association of metformin therapy and fracture risk. However, T2DM patients commonly use multiple medications for hyperglycemia management. The potential interaction effects between metformin and other antidiabetic medication on bone fracture protection also need more direct evidence to clearly show specific indication.

5 Conclusion

In this systematic review and meta-analysis, we found that metformin administration was not significantly correlated with a decreased fracture risk in T2DM patients. These results were independent of patients' HbA1c levels and glycemic control levels. Due to the limited number of studies included in this meta-analysis, further investigations are needed to make stronger conclusions for clinical consensus.

Data availability statement

The original contributions presented in the study are included in the article/Supplementary Material. Further inquiries can be directed to the corresponding authors.

Author contributions

Study design/manuscript preparation: YL, LL, and LC. Original draft preparation/Meta analysis: YW and LY. Sub-Group Meta analysis and validation: ZY and RL. Review and editing: AS, LL, and JW. Conduct data/Publication collection/ Analysis: FD, and XZ. Funding acquisition: YL, LL, and LC. All authors have read and agreed to the published version of the

manuscript. All authors contributed to the article and approved the submitted version.

Conflict of interest

The authors declare that the research was conducted in the absence of any commercial or financial relationships that could be construed as a potential conflict of interest.

Publisher's note

All claims expressed in this article are solely those of the authors and do not necessarily represent those of their affiliated organizations, or those of the publisher, the editors and the reviewers. Any product that may be evaluated in this article, or claim that may be made by its manufacturer, is not guaranteed or endorsed by the publisher.

Supplementary material

The Supplementary Material for this article can be found online at: https://www.frontiersin.org/articles/10.3389/fendo.2022.1038603/full#supplementary-material

References

1. Wang F, Wang W, Yin P, Liu Y, Liu J, Wang L, et al. Mortality and years of life lost in diabetes mellitus and its subcategories in China and its provinces, 2005-2020. *J Diabetes Res* (2022) 2022:1609267. doi: 10.1155/2022/1609267

2. Kotwas A, Karakiewicz B, Zabielska P, Wieder-Huszla S, Jurczak A. Epidemiological factors for type 2 diabetes mellitus: evidence from the global burden of disease. *Arch Public Health* (2021) 79(1):110. doi: 10.1186/s13690-021-00632-1

3. Knudsen JS, Knudsen SS, Hulman A, Witte DR, Gregg EW, Lauritzen T, et al. Changes in type 2 diabetes incidence and mortality associated with introduction of HbA1c as diagnostic option: A Danish 24-year population-based study. *Lancet Reg Health Eur* (2022) 14:100291. doi: 10.1016/j.lanepe.2021.100291

4. Saeedi P, Karuranga S, Pinkepank M, Ogurtsova K, Duncan BB, et al. IDF diabetes atlas: Global, regional and country-level diabetes prevalence estimates for 2021 and projections for 2045. *Diabetes Res Clin Pract* (2022) 183:109119. doi: 10.1016/j.diabres.2021.109119

5. Petersmann A, Muller-Wieland D, Muller UA, Landgraf R, Nauck M, Freckmann G, et al. Definition, classification and diagnosis of diabetes mellitus. *Exp Clin Endocrinol Diab* (2019) 127(S 01):S1–7. doi: 10.1055/a-1018-9078

6. Ortiz-Martinez M, Gonzalez-Gonzalez M, Martagon AJ, Hlavinka V, Willson RC, Rito-Palomares M. Recent developments in biomarkers for diagnosis and screening of type 2 diabetes mellitus. *Curr Diabetes Rep* (2022) 22(3):95–115. doi: 10.1007/s11892-022-01453-4

7. Wang Y, Zhang P, Shao H, Andes LJ, Imperatore G. Medical costs associated with diabetes complications in Medicare beneficiaries aged 65 years or older with type 2 diabetes. *Diabetes Care* (2022) 45(11):2570–6. doi: 10.2337/figshare.20611344

8. Morton JI, Lazzarini PA, Shaw JE, Magliano DJ. Trends in the incidence of hospitalization for major diabetes-related complications in people with type 1 and type 2 diabetes in Australia, 2010-2019. *Diabetes Care* (2022) 45(4):789–97. doi: 10.2337/dc21-2268

9. Williams R, Karuranga S, Malanda B, Saeedi P, Basit A, Besancon S, et al. Global and regional estimates and projections of diabetes-related health expenditure: Results from the international diabetes federation diabetes atlas, 9th edition. *Diabetes Res Clin Pract* (2020) 162:108072. doi: 10.1016/j.diabres.2020.108072

10. Napoli N, Chandran M, Pierroz DD, Abrahamsen B, Schwartz AV, Ferrari S, et al. Mechanisms of diabetes mellitus-induced bone fragility. *Nat Rev Endocrinol* (2017) 13(4):208–19. doi: 10.1038/nrendo.2016.153

11. Hofbauer LC, Busse B, Eastell R, Ferrari S, Frost M, Muller R, et al. Bone fragility in diabetes: novel concepts and clinical implications. *Lancet Diabetes endocrinol* (2022) 10(3):207–20. doi: 10.1016/S2213-8587(21)00347-8

12. Khosla S, Samakkarnthai P, Monroe DG, Farr JN. Update on the pathogenesis and treatment of skeletal fragility in type 2 diabetes mellitus. *Nat Rev Endocrinol* (2021) 17(11):685–97. doi: 10.1038/s41574-021-00555-5

13. Sihota P, Yadav RN, Dhaliwal R, Bose JC, Dhiman V, Neradi D, et al. Investigation of mechanical, material, and compositional determinants of human trabecular bone quality in type 2 diabetes. *J Clin Endocrinol Metab* (2021) 106(5):e2271–89. doi: 10.1210/clinem/dgab027

14. Sheu A, Greenfield JR, White CP, Center JR. Assessment and treatment of osteoporosis and fractures in type 2 diabetes. *Trends Endocrinol metabolism: TEM* (2022) 33(5):333–44. doi: 10.1016/j.tem.2022.02.006

15. Napoli N, Schwartz AV, Schafer AL, Vittinghoff E, Cawthon PM, Parimi N, et al. Vertebral fracture risk in diabetic elderly men: The MrOS study. *J Bone mineral Res Off J Am Soc Bone Mineral Res* (2018) 33(1):63–9. doi: 10.1002/jbmr.3287

16. Ferrari SL, Abrahamsen B, Napoli N, Akesson K, Chandran M, Eastell R, et al. Diagnosis and management of bone fragility in diabetes: an emerging challenge. *Osteoporosis Int J established as result cooperation between Eur Foundation Osteoporosis Natl Osteoporosis Foundation USA* (2018) 29(12):2585–96. doi: 10.1007/s00198-018-4650-2

17. Wolfel EM, Fiedler IAK, Dragoun Kolibova S, Krug J, Lin MC, Yazigi B, et al. Human tibial cortical bone with high porosity in type 2 diabetes mellitus is accompanied by distinctive bone material properties. *Bone*. (2022) 165:116546. doi: 10.1016/j.bone.2022.116546

18. Hunt HB, Torres AM, Palomino PM, Marty E, Saiyed R, Cohn M, et al. Altered tissue composition, microarchitecture, and mechanical performance in cancellous bone from men with type 2 diabetes mellitus. *J Bone mineral Res Off J Am Soc Bone Mineral Res* (2019) 34(7):1191–206. doi: 10.1002/jbmr.3711

19. Tanios M, Brickman B, Cage E, Abbas K, Smith C, Atallah M, et al. Diabetes and impaired fracture healing: A narrative review of recent literature. *Curr osteoporosis Rep* (2022) 20(5):229–39. doi: 10.1007/s11914-022-00740-z

20. Figeac F, Tencerova M, Ali D, Andersen TL, Appadoo DRC, Kerckhofs G, et al. Impaired bone fracture healing in type 2 diabetes is caused by defective functions of skeletal progenitor cells. *Stem Cells* (2022) 40(2):149–64. doi: 10.1093/stmcls/sxab011

21. Marin C, Luyten FP, van der Schueren B, Kerckhofs G, Vandamme K. The impact of type 2 diabetes on bone fracture healing. *Front endocrinol* (2018) 9:6. doi: 10.3389/fendo.2018.00006

22. Chandran M. Diabetes drug effects on the skeleton. *Calcified Tissue Int* (2017) 100(2):133–49. doi: 10.1007/s00223-016-0203-x

23. Stage TB, Christensen MH, Jorgensen NR, Beck-Nielsen H, Brosen K, Gram J, et al. Effects of metformin, rosiglitazone and insulin on bone metabolism in patients with type 2 diabetes. *Bone*. (2018) 112:35–41. doi: 10.1016/j.bone.2018.04.004

24. Yang BR, Cha SH, Lee KE, Kim JW, Lee J, Shin KH. Effect of dipeptidyl peptidase IV inhibitors, thiazolidinedione, and sulfonylurea on osteoporosis in patients with type 2 diabetes: population-based cohort study. *Osteoporosis Int J established as result cooperation between Eur Foundation Osteoporosis Natl Osteoporosis Foundation USA* (2021) 32(9):1705–12. doi: 10.1007/s00198-020-05801-6

25. Tsai WH, Kong SK, Lin CL, Cheng KH, Cheng YT, Chien MN, et al. Risk of fracture caused by anti-diabetic drugs in individuals with type 2 diabetes: A network meta-analysis. *Diabetes Res Clin Pract* (2022) 192:110082. doi: 10.1016/j.diabres.2022.110082

26. Bahrambeigi S, Yousefi B, Rahimi M, Shafiei-Irannejad V. Metformin; an old antidiabetic drug with new potentials in bone disorders. *Biomed pharmacother = Biomed pharmacother* (2019) 109:1593–601. doi: 10.1016/j.biopha.2018.11.032

27. Barzilai N, Crandall JP, Kritchevsky SB, Espeland MA. Metformin as a tool to target aging. *Cell Metab* (2016) 23(6):1060–5. doi: 10.1016/j.cmet.2016.05.011

28. Blumel JE, Arteaga E, Aedo S, Arriola-Montenegro J, Lopez M, Martino M, et al. Metformin use is associated with a lower risk of osteoporosis in adult women independent of type 2 diabetes mellitus and obesity. *REDLINC IX study Gynecol Endocrinol* (2020) 36(5):421–5. doi: 10.1080/09513590.2020.1718092

29. Shen M, Yu H, Jin Y, Mo J, Sui J, Qian X, et al. Metformin facilitates osteoblastic differentiation and M2 macrophage polarization by PI3K/AKT/mTOR pathway in human umbilical cord mesenchymal stem cells. *Stem Cells Int* (2022) 2022:9498876. doi: 10.1155/2022/9498876

30. Zhang M, Yang B, Peng S, Xiao J. Metformin rescues the impaired osteogenesis differentiation ability of rat adipose-derived stem cells in high glucose by activating autophagy. *Stem Cells Dev* (2021) 30(20):1017–27. doi: 10.1089/scd.2021.0181

31. Zhang S, Zhang R, Qiao P, et al. Metformin-induced MicroRNA-34a-3p downregulation alleviates senescence in human dental pulp stem cells by targeting CAB39 through the AMPK/mTOR signaling pathway. *Stem Cells Int* (2021) 2021:6616240. doi: 10.1155/2021/6616240

32. Ma J, Zhang ZL, Hu XT, Wang XT, Chen AM. Metformin promotes differentiation of human bone marrow derived mesenchymal stem cells into osteoblast *via* GSK3β inhibition. *Eur Rev Med Pharmacol Sci* (2018) 22(22):7962–8. doi: 10.26355/eurrev_201811_16424

33. Shaik AR, Singh P, Shaik C, Kohli S, Vohora D, Ferrari SL. Metformin: Is it the well wisher of bone beyond glycemic control in diabetes mellitus? *Calcified Tissue Int* (2021) 108(6):693–707. doi: 10.1007/s00223-021-00805-8

34. Loh DKW, Kadirvelu A, Pamidi N. Effects of metformin on bone mineral density and adiposity-associated pathways in animal models with type 2 diabetes mellitus: A systematic review. *J Clin Med* (2022) 11(14):4193. doi: 10.3390/jcm11144193

35. Sun J, Liu Q, He H, Jiang L, Lee KO, Li D, et al. Metformin treatment is associated with an increase in bone mineral density in type 2 diabetes mellitus patients in China: A retrospective single center study. *Diabetes Metab* (2022) 48(5):101350. doi: 10.1016/j.diabet.2022.101350

36. Mu W, Liang G, Feng Y, Jiang Y, Qu F. The potential therapeutic role of metformin in diabetic and non-diabetic bone impairment. *Pharmaceuticals*. (2022) 15(10):1274. doi: 10.3390/ph15101274

37. Tseng CH. Metformin and primary bone cancer risk in Taiwanese patients with type 2 diabetes mellitus. *Bone*. (2021) 151:116037. doi: 10.1016/j.bone.2021.116037

38. Oh TK, Song IA. Metformin therapy and hip fracture risk among patients with type II diabetes mellitus: A population-based cohort study. *Bone*. (2020) 135:6. doi: 10.1016/j.bone.2020.115325

39. Nordklint AK, Almdal TP, Vestergaard P, Lundby-Christensen L, Boesgaard TW, Breum L, et al. The effect of metformin versus placebo in combination with insulin analogues on bone mineral density and trabecular bone score in patients with type 2 diabetes mellitus: a randomized placebo-controlled trial. *Osteoporosis Int J established as result cooperation between Eur Foundation Osteoporosis Natl Osteoporosis Foundation USA* (2018) 29(11):2517–26. doi: 10.1007/s00198-018-4637-z

40. Schwartz AV, Pan Q, Aroda VR, Crandall JP, Kriska A, Piromalli C, et al. Long-term effects of lifestyle and metformin interventions in DPP on bone density. *Osteoporosis Int J established as result cooperation between Eur Foundation Osteoporosis Natl Osteoporosis Foundation USA* (2021) 32(11):2279–87. doi: 10.1007/s00198-021-05989-1

41. Salai M, Somjen D, Gigi R, Yakobson O, Katzburg S, Dolkart O. Effects of commonly used medications on bone tissue mineralisation in SaOS-2 human bone cell line: an in vitro study. *Bone Joint J* (2013) 95-B(11):1575–80. doi: 10.1302/0301-620X.95B11.31158

42. Borges JL, Bilezikian JP, Jones-Leone AR, Acusta AP, Ambery PD, Nino AJ, et al. A randomized, parallel group, double-blind, multicentre study comparing the

efficacy and safety of avandamet (rosiglitazone/metformin) and metformin on long-term glycaemic control and bone mineral density after 80 weeks of treatment in drug-naive type 2 diabetes mellitus patients. *Diabetes Obes Metab* (2011) 13 (11):1036–46. doi: 10.1111/j.1463-1326.2011.01461.x

43. Page MJ, McKenzie JE, Bossuyt PM, Boutron I, Hoffmann TC, Mulrow CD, et al. The PRISMA 2020 statement: an updated guideline for reporting systematic reviews. *BMJ* (2021) 372:n71. doi: 10.1136/bmj.n71

44. Page MJ, Moher D, Bossuyt PM, Boutron I, Hoffmann TC, Mulrow CD, et al. PRISMA 2020 explanation and elaboration: updated guidance and exemplars for reporting systematic reviews. *BMJ.* (2021) 372:n160. doi: 10.1136/bmj.n160

45. Starup-Linde J, Gregersen S, Frost M, Vestergaard P. Use of glucose-lowering drugs and risk of fracture in patients with type 2 diabetes. *Bone.* (2017) 95:136–42. doi: 10.1016/j.bone.2016.11.026

46. Wallander M, Axelsson KF, Nilsson AG, Lundh D, Lorentzon M. Type 2 diabetes and risk of hip fractures and non-skeletal fall injuries in the elderly: A study from the fractures and fall injuries in the elderly cohort (FRAILCO). *J Bone Miner Res* (2017) 32(3):449–60. doi: 10.1002/jbmr.3002

47. Hung YC, Lin CC, Chen HJ, Chang MP, Huang KC, Chen YH, et al. Severe hypoglycemia and hip fracture in patients with type 2 diabetes: a nationwide population-based cohort study. *Osteoporosis Int* (2017) 28(7):2053–60. doi: 10.1007/s00198-017-4021-4

48. Majumdar SR, Josse RG, Lin M, Eurich DT. Does sitagliptin affect the rate of osteoporotic fractures in type 2 diabetes? population-based cohort study. *J Clin Endocrinol Metab* (2016) 101(5):1963–9. doi: 10.1210/jc.2015-4180

49. Colhoun HM, Livingstone SJ, Looker HC, Morris AD, Wild SH, Lindsay RS, et al. Hospitalised hip fracture risk with rosiglitazone and pioglitazone use compared with other glucose-lowering drugs. *Diabetologia.* (2012) 55(11):2929–37. doi: 10.1007/s00125-012-2668-0

50. Charlier S, Vavanikunnel J, Becker C, Jick SS, Meier C, Meier CR. Antidiabetic treatment, level of glycemic control, and risk of fracture in type 2 diabetes: a nested, case-control study. *J Clin Endocrinol Metab* (2021) 106(2):554–66. doi: 10.1210/clinem/dgaa796

51. Vavanikunnel J, Charlier S, Becker C, Schneider C, Jick SS, Meier CR, et al. Association between glycemic control and risk of fracture in diabetic patients: A nested case-control study. *J Clin Endocrinol Metab* (2019) 104(5):1645–54. doi: 10.1210/jc.2018-01879

52. Puar TH, Khoo JJ, Cho LW, Xu Y, Chen YT, Chuo AM, et al. Association between glycemic control and hip fracture. *J Am Geriatr Soc* (2012) 60(8):1493–7. doi: 10.1111/j.1532-5415.2012.04052.x

53. Monami M, Cresci B, Colombini A, Pala L, Balzi D, Gori F, et al. Bone fractures and hypoglycemic treatment in type 2 diabetic patients: A case-control study. *Diabetes Care* (2008) 31(2):199–203. doi: 10.2337/dc07-1736

54. Tseng CH. Metformin use is associated with a lower risk of osteoporosis/ vertebral fracture in Taiwanese patients with type 2 diabetes mellitus. *Eur J Endocrinol* (2021) 184(2):299–310. doi: 10.1530/EJE-20-0507

55. Fuggle NR, Curtis EM, Ward KA, Harvey NC, Dennison EM, Cooper C. Fracture prediction, imaging and screening in osteoporosis. *Nat Rev Endocrinol* (2019) 15(9):535–47. doi: 10.1038/s41574-019-0220-8

56. Wang L, Yu W, Yin X, Cui L, Tang S, Jiang N, et al. Prevalence of osteoporosis and fracture in China: The China osteoporosis prevalence study. *JAMA Netw Open* (2021) 4(8):e2121106. doi: 10.1001/jamanetworkopen.2021.21106

57. Pan H, Wu N, Yang T, He W. Association between bone mineral density and type 1 diabetes mellitus: A meta-analysis of cross-sectional studies.*Diabetes Metab Res Rev* (2015) 30(7):531–42. doi: 10.1002/dmrr.2508

58. Rubin MR. Skeletal fragility in diabetes. *Ann New York Acad Sci* (2017) 1402 (1):18–30. doi: 10.1111/nyas.13463

59. Valderrábano, Linares MICD. Diabetes mellitus and bone health: epidemiology, etiology and implications for fracture risk stratification. *Endocrinology* (2018) 4(1):9. doi: 10.1186/s40842-018-0060-9

60. Tanaka KI, Yamaguchi T, Kanazawa I, Sugimoto T. Effects of high glucose and advanced glycation end products on the expressions of sclerostin and RANKL as well as apoptosis in osteocyte-like MLO-Y4-A2 cells. *Biochem Biophys Res Commun* (2015) 461(2):193–9. doi: 10.1016/j.bbrc.2015.02.091

61. Patsch JM, Kiefer FW, Varga P, Pail P, Rauner M, Stupphann D, et al. Increased bone resorption and impaired bone microarchitecture in short-term and extended high-fat diet-induced obesity. *Metab-Clin Exp* (2011) 60(2):243–9. doi: 10.1016/j.metabol.2009.11.023

62. Ellegaard M, Jorgensen NR, Schwarz P. Parathyroid hormone and bone healing. *Calcified tissue international* (2010) 87(1):1–13. doi: 10.1007/s00223-010-9360-5

63. Hidayat K, Du X, Wu M-J, Shi B-M. The use of metformin, insulin, sulphonylureas, and thiazolidinediones and the risk of fracture: Systematic review and meta-analysis of observational studies. *Obes Rev* (2019) 20(10):1494–503. doi: 10.1111/obr.12885

64. Salari-Moghaddam A, Sadeghi O, Keshteli AH, Larijani B, Esmaillzadeh A. Metformin use and risk of fracture: a systematic review and meta-analysis of observational studies. *Osteoporosis Int* (2019) 30(6):1167–73. doi: 10.1007/s00198-019-04948-1

65. Josse RG, Majumdar SR, Zheng YG, Adler A, Bethel MA, Buse JB, et al. Sitagliptin and risk of fractures in type 2 diabetes: Results from the TECOS trial. *Diabetes Obes Metab* (2017) 19(1):78–86. doi: 10.1111/dom.12786

66. Vestergaard P, Rejnmark L, Mosekilde L. Relative fracture risk in patients with diabetes mellitus, and the impact of insulin and oral antidiabetic medication on relative fracture risk. *Diabetologia.* (2005) 48(7):1292–9. doi: 10.1007/s00125-005-1786-3

67. Huang X, Li S, Lu W, Xiong L. Metformin activates wnt/beta-catenin for the treatment of diabetic osteoporosis. *BMC Endocr Disord* (2022) 22(1):189. doi: 10.1186/s12902-022-01103-6

68. Lu CH, Chung CH, Kuo FC, Chen KC, Chang CH, Kuo CC, et al. Metformin attenuates osteoporosis in diabetic patients with carcinoma in situ: A nationwide, retrospective, matched-cohort study in Taiwan. *J Clin Med* (2020) 9 (9):2839. doi: 10.3390/jcm9092839

69. Chen B, He Q, Yang J, Pan Z, Xiao J, Chen W, et al. Metformin suppresses oxidative stress induced by high glucose via activation of the Nrf2/HO-1 signaling pathway in type 2 diabetic osteoporosis. *Life Sci* (2022) 312:121092. doi: 10.1016/j.lfs.2022.121092

70. Wang LX, Wang GY, Su N, Ma J, Li YK. Effects of different doses of metformin on bone mineral density and bone metabolism in elderly male patients with type 2 diabetes mellitus. *World J Clin Cases* (2020) 8(18):4010–6. doi: 10.12998/wjcc.v8.i18.4010

71. Nordklint AK, Almdal TP, Vestergaard P, Lundby-Christensen L, Jorgensen NR, Boesgaard TW, et al. Effect of metformin vs. placebo in combination with insulin analogues on bone markers P1NP and CTX in patients with type 2 diabetes mellitus. *Calcified Tissue Int* (2020) 107(2):160–9. doi: 10.1007/s00223-020-00711-5

72. Koshizaka M, Ishikawa K, Ishibashi R, Maezawa Y, Sakamoto K, Uchida D, et al. Effects of ipragliflozin versus metformin in combination with sitagliptin on bone and muscle in Japanese patients with type 2 diabetes mellitus: Subanalysis of a prospective, randomized, controlled study (PRIME-V study). *J Diabetes Investig* (2021) 12(2):200–6. doi: 10.1111/jdi.13340

73. Schmedt N, Andersohn F, Walker J, Garbe E. Sodium-glucose co-transporter-2 inhibitors and the risk of fractures of the upper or lower limbs in patients with type 2 diabetes: A nested case-control study. *Diabetes Obes Metab* (2019) 21(1):52–60. doi: 10.1111/dom.13480

74. Al-Mashhadi ZK, Viggers R, Starup-Linde J, Vestergaard P, Gregersen S. SGLT2 inhibitor treatment is not associated with an increased risk of osteoporotic fractures when compared to GLP-1 receptor agonists: A nationwide cohort study. *Front endocrinol* (2022) 13:861422. doi: 10.3389/fendo.2022.861422

75. Qian BB, Chen Q, Li L, Yan CF. Association between combined treatment with SGLT2 inhibitors and metformin for type 2 diabetes mellitus on fracture risk: a meta-analysis of randomized controlled trials. *Osteoporosis Int J established as result cooperation between Eur Foundation Osteoporosis Natl Osteoporosis Foundation USA* (2020) 31(12):2313–20. doi: 10.1007/s00198-020-05590-y

76. Zinman B, Harris SB, Neuman J, Gerstein HC, Retnakaran RR, Raboud J, et al. Low-dose combination therapy with rosiglitazone and metformin to prevent type 2 diabetes mellitus (CANOE trial): a double-blind randomised controlled study. *Lancet.* (2010) 376(9735):103–11. doi: 10.1016/S0140-6736(10)60746-5

77. Sedgwick P. Meta-analyses: what is heterogeneity? *BMJ Br Med J* (2015) 350: h1435. doi: 10.1136/bmj.h1435

78. Imrey PB. Limitations of meta-analyses of studies with high heterogeneity. *JAMA Network Open* (2020) 3(1):e1919325–e1919325. doi: 10.1001/jamanetworkopen.2019.19325

Influence of image reconstruction kernel on computed tomography-based finite element analysis in the clinical opportunistic screening of osteoporosis— A preliminary result

Chenyu Jiang, Dan Jin, Ming Ni, Yan Zhang and Huishu Yuan*

Department of Radiology, Peking University Third Hospital, Beijing, China

Purpose: This study aimed to evaluate the difference in vertebral mechanical properties estimated by finite element analysis (FEA) with different computed tomography (CT) reconstruction kernels and evaluate their accuracy in the screening and classification of osteoporosis.

Methods: There were 31 patients enrolled retrospectively from the quantitative CT database of our hospital, uniformly covering the range from osteoporosis to normal. All subjects' CT raw data were reconstructed both with a smooth standard convolution kernel (B40f) and a sharpening bone convolution kernel (B70f), and FEA was performed on L1 of each subject based on two reconstructed images to obtain vertebral estimated strength and stiffness. The trabecular volumetric bone mineral density (vBMD) of the same vertebral body was also measured. FEA measurements between two kernels and their accuracy for osteoporosis screening were compared.

Results: The vertebral stiffness and strength measured in FEA-B40f were significantly lower compared with those of FEA-B70f (12.0%, $p = 0.000$ and 10.7%, $p = 0.000$, respectively). The correlation coefficient between FEA-B70F and vBMD was slightly higher than that of FEA-B40F in both vertebral strength and stiffness (strength: r^2-B40f = 0.21, $p = 0.009$ vs. r^2-B70f = 0.27, $p = 0.003$; stiffness: r^2-B40f = 0.37, $p = 0.002$ vs. r^2-B70f = 0.45, $p=0.000$). The receiver operator characteristic curve showed little difference in the classification of osteoporosis between FEA-B40f and FEA-B70f.

Conclusion: Two kernels both seemed to be applicable to the opportunistic screening of osteoporosis by CT-FEA despite variance in FE-estimated bone strength and bone stiffness. A protocol for CT acquisition and FEA is still required to guarantee the reproducibility of clinical use.

KEYWORDS

osteoporosis, finite element, vertebral fracture, opportunistic screening, computed tomography

1 Introduction

Osteoporosis is a skeletal disorder characterized by compromised bone strength and an increased risk of fracture (1). Although areal bone mineral density (aBMD) assessed by dual-energy X-ray absorptiometry (DXA) is a standard clinical protocol for estimating fracture risk, it has been criticized for low accuracy and underutilization. Nearly half of the fragility fractures occur in individuals with normal aBMD, and 21% to 50% of patients with fragility fractures had a femoral neck BMD in the range of osteoporosis (2–4). On the other hand, although DXA was the most meaningful examination for osteoporosis, more than 60% of patients had never undergone DXA before or after fragility fractures (5). Conversely, accessibility to computed tomography (CT) scans are markedly better (6), and approximately 54.5% of those CT scans are performed at relevant osteoporotic fracture sites (7). In 2015, the International Society of Clinical Densitometry identified the priority of quantitative computed tomography (QCT) for its use in fracture prediction (8), as it simultaneously allows DXA-equivalent femoral aBMD, volumetric BMD (vBMD), and finite element analysis (FEA).

The FE method has been used to simulate the mechanical behavior of bone with increasing fidelity for decades, which has shown great reliability to assess bone strength and fracture risk (8–10). Previous studies confirmed the superiority of FEA to DXA-aBMD (11) and even QCT-vBMD (12) in both prevalent and incident vertebral fracture prediction (13–16). Aside from fracture prediction, FEA has a unique value in the opportunistic screening of osteoporosis (7), drug efficacy (17), and postoperative evaluation of internal fixation (18).

However, material property mapping for the finite elements entails conversion from CT attenuation Hounsfield units (HU) to Young's modulus through empirical equations, which thus introduces variability in fracture risk prediction from CT acquisition protocols. It is well established that CT acquisition, including tube current (mAs), voltage (kVp), reconstruction algorithms, and scanner type, will affect the grayscale value measured in HU (19, 20). Starting with this angle, several studies investigated the estimation of bone strength and stiffness *in vitro* by FEA based on different voltage and reconstruction kernels (21, 22). Later, Michalski further compared the *in vivo* femur strength estimated by FEA with different imaging reconstruction kernels (23). However, the accuracy of FEA with different reconstruction kernels on osteoporosis stratified risk assessment *in vivo* had not been fully investigated yet, which is crucial to the application of FEA in opportunistic osteoporosis screening.

Therefore, the purpose of this study was to compare the difference in vertebral mechanical properties obtained by FEA with different reconstruction kernels and evaluate the accuracy of the different reconstructed kernels in the screening and classification of osteoporosis with FEA.

2 Materials and methods

This retrospective study was reviewed and approved by the local institutional review board. Due to its retrospective nature, the ethics committee waived the requirement of written informed consent for participation.

2.1 Participants

Three sex–age-matched groups were retrospectively screened from the QCT database of our hospital, which were normal bone mass, osteopenia, and osteoporosis. All subjects underwent thoracolumbar or lumbar imaging and were identified with available raw data in the scanner's local storage at our institution. Exclusion criteria were spinal infectious lesions, metastases, and hematological or metabolic bone disorders aside from osteoporosis.
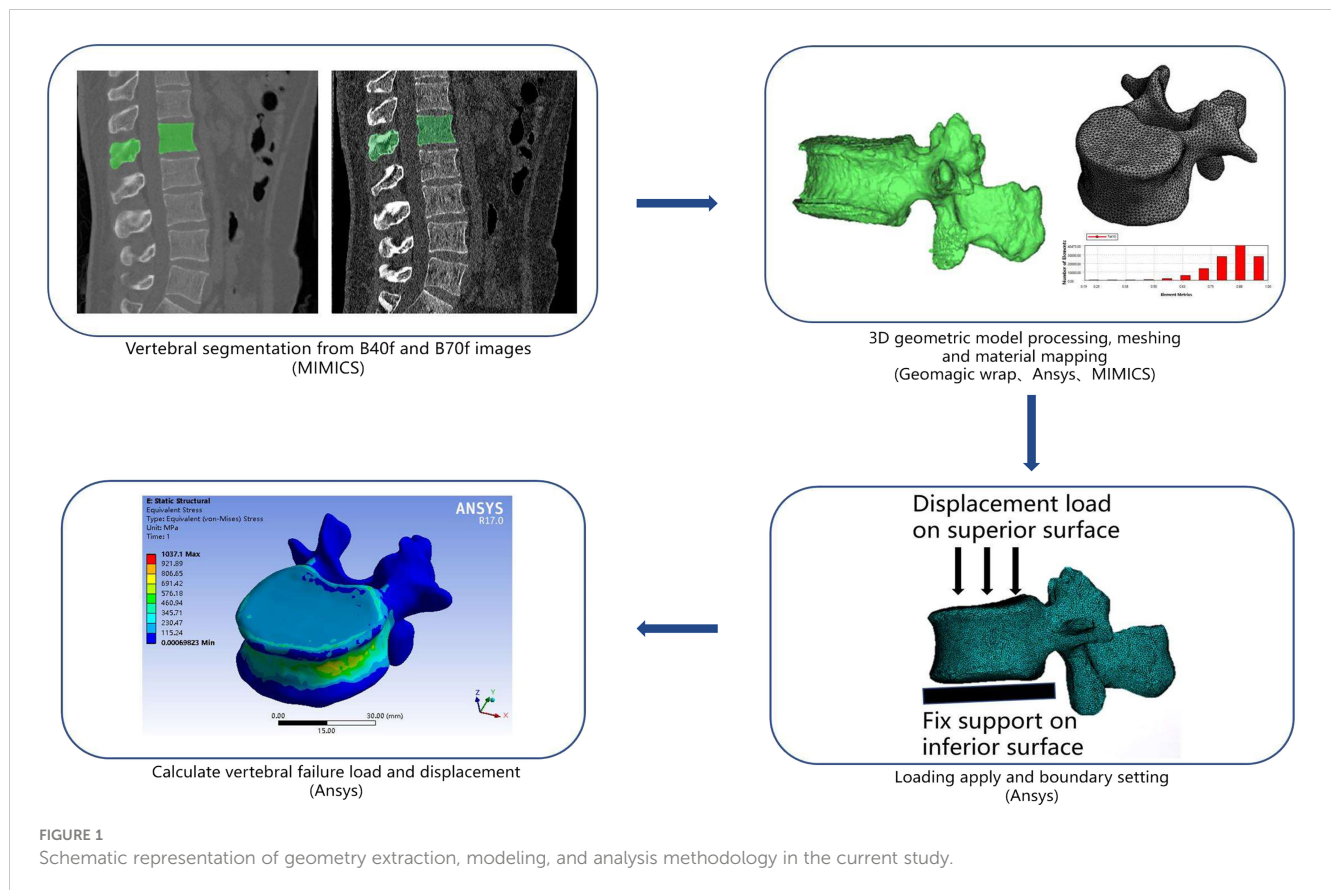
2.2 Imaging

All images were acquired using the same CT scanner (128-row Somatom Definition Flash, Siemens Healthineers, Ellingen, Germany). The scanning protocol was tailored to low back pain and acquired with parameters of 120 kVp of tube voltage, 250 mAs of tube current, 128×0.6 mm of collimation, a pitch of 0.6, a field of view (FOV) of 199 mm, and a reconstruction thickness of 1 mm. All image raw data were reconstructed with two different statistical iterative reconstruction kernels, a smooth standard reconstruction kernel (B40f) and a sharpening bone reconstruction kernel (B70f), respectively, which are commonly used in clinical settings. A density-calibrated phantom (Mindways Inc., Austin, TX, USA) was placed in the field of view to convert HU to equivalent K_2HPO_4 density ($\rho_{K_2HPO_4}$), assumed to be equal to bone ash density (ρ_{ash}). Due to the influence of the imaging reconstruction kernel, two linear calibrating regression equations for B40f (Eq. 1) and B70f (Eq. 2) images were fit (24).

$$\rho_{ash} = \rho_{K_2HPO_4} = -4.2 \times 10^{-3} + 7.0 \times 10^{-4} \cdot HU \qquad (1)$$

$$\rho_{ash} = \rho_{K_2HPO_4} = -3.7 \times 10^{-3} + 7.3 \times 10^{-4} \cdot HU \qquad (2)$$

2.3 Finite element analysis

Finite element analysis was performed on segmented L1 vertebra based on the MDCT datasets of B40f and B70f, respectively. If L1 was not suitable for analysis, then L2 or T12 were alternative choices in practice. The CT scan data were imported into the commercial three-dimensional (3D) medical image processing software Mimics (Materialise NV, Harrislee, Germany) for segmenting and generating 3D vertebral model. These 3D models were then imported to Geomagic software (Raindrop Company, Marble Hill, USA) for smooth geometry meshing with smooth geometry meshing with quadratic tetrahedral elements of 2-mm element edge length for downstream analysis (Figure 1). In consideration of bone's nonhomogeneity, each element was assigned elastic material properties based on empirical material-mapping relations proposed by Morgan et al. (Eq. 3) (25), assuming ρ_{ash} is

FIGURE 1
Schematic representation of geometry extraction, modeling, and analysis methodology in the current study.

measured in grams per cubic centimeter and a ratio between ρ_{ash} and an apparent density (ρ_{app}) = 0.6. Poisson's ratio was set to 0.3 for all elements. The meshed and material-mapped 3D vertebra models were then imported into the commercial analysis software ANSYS (ANSYS Company, Canonsburg, PA, USA) for downstream FEA (25).

$$E = 4,730 \times \rho_{app}^{1.56} \quad (3)$$

Referring to load and boundary settings in previous studies, the inferior surface of the vertebral body was fully constrained in all directions, and a displacement load was applied on the superior surface. Vertebral strength (N) was estimated using effective stress at 2% deformation, and vertebral stiffness was defined as the slope of the force-displacement curve (8).

2.4 Quantification of vBMD

For opportunistic screening purposes, Mindways QCT Pro Version 5.0 (Mindways Software Inc., Austin, TX, USA) with an asynchronous calibration module allowing BMD measurement from CT images without a calibration phantom had been installed in our institution (26). A new Model 4 asynchronous calibration phantom (Mindways Sofware Inc., Austin, TX, USA) was scanned for quality assurance and calibration with the same subjects' imaging protocol weekly to maintain scanner stability. Images of subjects were sent to Mindways QCT Pro Version 5.0 to

measure trabecular vBMD (mg/cm^3) of the same vertebra that FEA was performed on.

2.5 Statistical analysis

All statistical analyses were performed on the software SPSS version 26.0 (IBM, Armonk, New York). Differences between FEA-B40f and FEA-B70f were compared using paired t-tests, and mean differences with 95% confidence intervals were computed. Linear regression analyses were used to determine the coefficient of association (r^2) between FEA results and the trabecula vBMD of the same vertebra. Spearman's correlation test was used to analyze the correlation between FEA based on two different reconstruction kernels and the clinical classification of osteoporosis fracture risk. A ROC curve was used to compare the diagnostic efficacy of FEA based on prevalent vertebral fractures to illustrate the validity of two reconstruction kernels in fracture risk assessment.

3 Results

3.1 General characteristics of participants

Finally, 11 patients of the osteoporosis group (age: 71.1 ± 9.3, M/F patients: 3/8), every 10 patients of the osteopenia group (63.8 ± 8.2; M/F patients: 4/6) and the normal bone mass group (64.2 ± 7.8;

M/F patients: 3/7), for a total of 31 subjects, were included in this study. There was no difference in gender and age among the three groups ($p = 0.204$). Of 31 subjects, 15 patients underwent lumbar CT for lumber disc herniation, seven for low back pain, four for lumbar spondylolisthesis, three for vertebral fracture, and two for spinal stenosis. For two participants in the osteoporosis group, T12 vertebral body was analyzed due to compression changes in the lumber vertebra; for one in osteoporosis and two in the osteopenia group, L2 was analyzed due to obvious osteophytosis in L1.

3.2 The variance of FEA measurements between two kernels

Patient-specific FEA results illustrated significant differences in the vertebral estimated strength and stiffness between B40f and B70f images (strength-B40f vs. strength-B70f: 6,457.5 ± 1,579.3 N vs. 7,482.8 ± 1,612.3 N; stiffness-B40f vs. stiffness-B70f: 8,834.3 ± 3,747.4 N/mm vs. 1,0047.4 ± 4,063.3 N/mm). Both vertebral estimated strength and stiffness were higher in FEA-based B70f (Figures 2A, B). We further compared the differences in FEA

measurements between the two kernels in three different subgroups, and the bias was similar within subgroups (Table 1).

3.3 Applicability of two kernels in osteoporosis opportunistic screening

Subsequently, we analyzed the correlation between FEA-B40f and FEA-B70F with trabecular vBMD. The results showed that both FEA-B40f and FEA-B70f had a certain correlation with vBMD, and the correlation coefficient between FEA-B70F and vBMD was slightly higher than that of FEA-B40F in both vertebral strength and stiffness (Figures 3A, B). Compared with vertebral strength, vertebral stiffness had a significantly higher correlation coefficient. Likewise, the ROC curve showed that stiffness-B70f was the most accurate in distinguishing osteoporosis, osteopenia, and the normal group (Figure 4), but FEA-B40f and FEA-B70f reveal little difference in the classification of osteoporosis. Moreover, we obtained variable cutoff values for clinical interventional thresholds of osteoporosis and osteopenia with different FEA measurements (Table 2).

TABLE 1 Estimated vertebral strength and stiffness by FEA based on standard and bone reconstruction kernels.

Kernel	Osteoporosis		Osteopenia		Normal bone mass		All subjects	
	B40f	B70f	B40f	B70f	B40f	B70f	B40f	B70f
Strength (N)	5,602.0	6,120.8	6,531.6	7,308.6	7,324.3	8,155.4	6,457.5	7,482.8
Mean absolute difference	−518.7		−777.0		−831.0		−702.8	
Mean percent difference	−9.7		−11.7		−11.1		−10.7	
p-value	0.003		0.000		0.000		0.000	
Stiffness (N\mm)	5,561.0	6,356.6	9,720.2	10,715.2	11,549.1	12,839.7	8,834.3	9,853.9
Mean absolute difference	−704.6		−994.9		−1,290.5		−1,213	
Mean percent difference	−14.0		−9.7		−11.2		−12.0	
p-value	0.000		0.001		0.024		0.000	

Absolute values are presented as average, absolute, and percent mean differences, and p-values were calculated from paired t-tests.
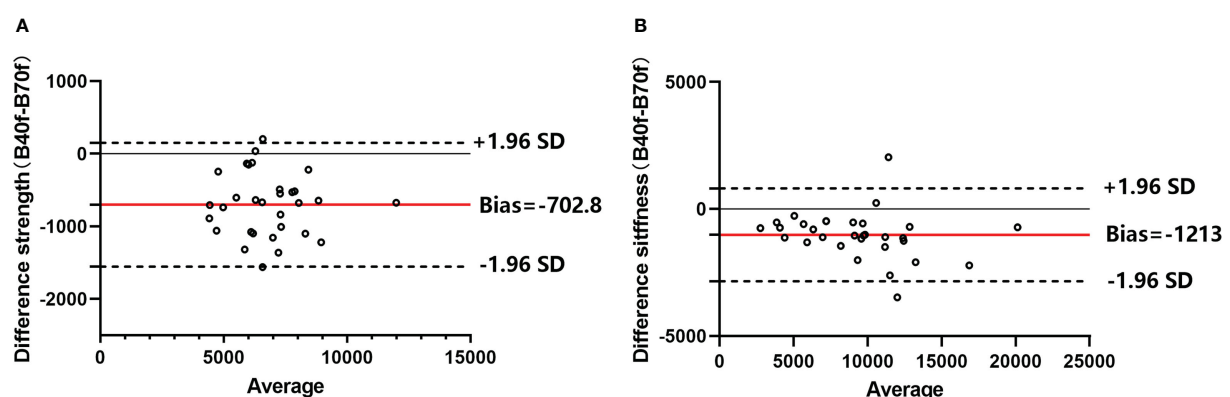

FIGURE 2
Bland−Altman plots of FE-estimated strength (A) and stiffness (B) between smooth standard kernel (B40f) and sharp bone kernel (B70f). Horizontal red lines represent the average difference between the two kernels (B40f−B70f), and the dashed line means a 95% confidence interval.
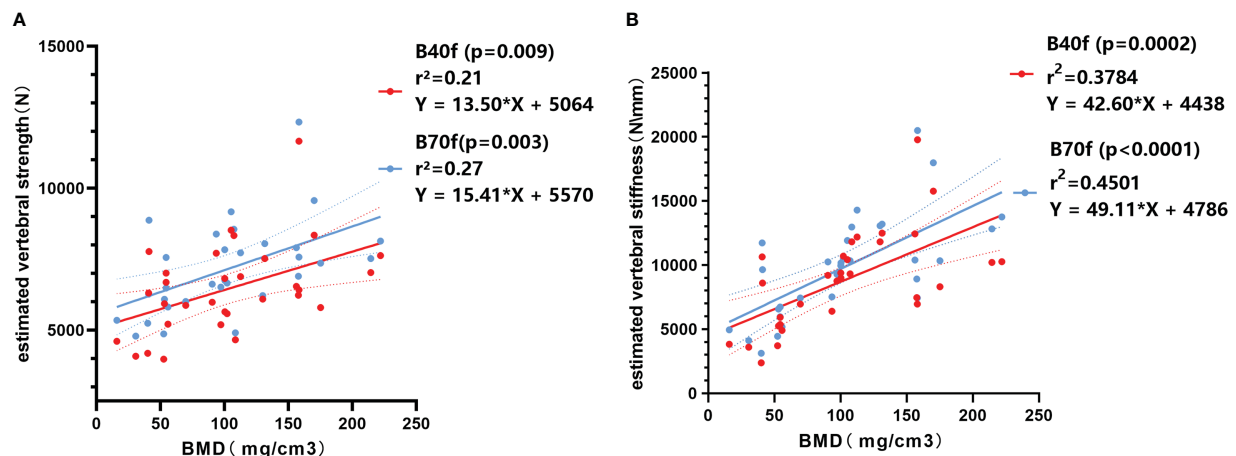
FIGURE 3
Linear regression correlation plot between BMD and FE-estimated strength **(A)** and stiffness **(B)** based on smooth standard kernel (B40f) and sharp bone kernel (B70f).

4 Discussion

This study explored the impact of two reconstruction kernels commonly used in clinical musculoskeletal CT imaging—the bone-sharpening kernel and the standard kernel on vertebral estimated strength and stiffness by FEA. The reconstruction kernel is the type of filtering applied to the CT raw data to reconstruct clinical visual images (19, 20), which can significantly alter the underlying grayscale data. The sharp reconstruction kernel has the advantage of better identification of bone structures and distinction of cortical and trabecular bone at expense of high image noise. While the smooth kernel improves image density resolution and reduces image noise, it makes harder to segment bone geometry and map bone inhomogeneity (21). Our results of vertebral FEA *in vivo* agreed with those of previous studies (21–23). The estimated vertebral strength and stiffness obtained by FEA-B70f was higher than that obtained by FEA-B40f, and the consistency bias between two kernels was noted within three subgroups, indicating that it is crucial to determine the appropriate image reconstruction kernel for clinical use of CT-FEA.

We adopted diagnostic categories based on spine QCT-trabecular vBMD measurements as the gold standard since previous FEA studies verified the equivalence of FEA and vBMD osteoporotic fracture predictivity, which is superior to DXA (8, 9). Compared to QCT, the FE method takes bone geometry and the

contribution of cortical bone to bone strength into consideration and requires no additional imaging hardware and radiation exposure (7). It has a promising future in opportunistic screening for osteoporosis and postoperative implant evaluation (18). With the improvement of the simulation technique, we believe the FE method will become the most valuable indicator in the screening of osteoporosis. Most of the previous studies were *in vitro* and contained a too-narrow range of bone mineral densities to reflect the impact of the reconstruction kernel on osteoporosis screening and fracture risk estimation. Therefore, the subjects we enrolled uniformly covered the range from osteoporosis to normal in order to evaluate the accuracy of FEA classification and screening for osteoporosis. Our results showed that both FEA-B40f and FEA-B70f had certain correlation with vBMD and clinical classification, but the R^2 with vBMD and accuracy of classification screening for osteoporosis by FEA-B70f was slightly higher than that by FEA-B40f, which indicated that FEA of the standard kernel can achieve similar performance in osteoporosis screening with the FEA of the bone kernel. Given that the standard kernel is widely used in clinical imaging, we recommend using FEA based on standard kernel images for the purpose of opportunistic screening.

Another strength of this study is that we established interventional thresholds for vertebral strength and stiffness based on vBMD-defined osteoporosis, which allows FEA to identify individuals at high risk of fracture. The ROC curve was used to obtain the cutoff values of estimated vertebral strength and stiffness under the two reconstruction kernels. Although we did not adjust for gender, the strength-B40f results were closer to the intervention threshold published by Kopperdahl et al. (15), who used soft B30 kernel for FEA, while distinct from strength-B70, indicating reconstruction algorithm kernel with different frequency filter may cause different degrees of variation in estimated strength. The big variance of the cutoff values for classification of osteoporosis brought by the reconstruction kernel in our results (Table 2) indicated a great challenge for cross-sectional analysis of fracture risk in osteoporosis presents, where interventional

TABLE 2 Cutoff value for osteoporosis and osteopenia by FEA based on smooth standard kernel (B40f) and sharp bone kernel (B70f) images.

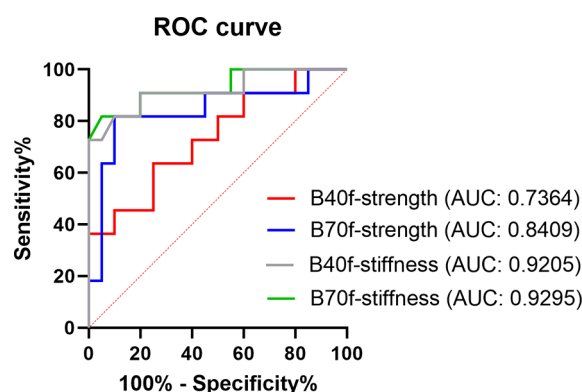|	Osteoporosis	Osteopenia
Strength-B40f (N)	4,633	6,038
Strength-B70f (N)	6,498	7,129
Stiffness-B40f (N\mm)	8,676	12,314
Stiffness-B70f (N\mm)	7,478	13,016

FIGURE 4
ROC curve showing the efficacy in distinguishing osteoporosis from the normal bone mass of FE-estimated strength and stiffness based on smooth standard kernel (B40f) and sharp bone kernel (B70f) images.

thresholds of FEA estimated bone strength is an important practice guideline for clinical interpretation of fragility fractures. In order to increase acceptability and standardize the continuous methodology of FEA, further improvements are needed to increase the robustness of consolidating the proposed interventional thresholds in the setting of different imaging protocols.

Regardless of B40f or B70f images, our FE measurements showed that estimated stiffness is more suitable for the opportunistic screening of osteoporosis than estimated strength because the linear finite element model in this study makes it impossible to obtain the peak value of the stress displacement curve, which was considered a reasonable definition of FE-estimated strength. Therefore, the equivalent stress at 2% deformation is selected as the bone failure strength in this study, which has been verified in previous studies and makes the estimated stiffness more relevant with vBMD and classification of bone mass than the estimated strength because bone stiffness obtained by a linear FEA model often correlates rather well with experiment strength, while nonlinear FE analyses deliver better results for estimated strength (8).

A consensus has not been reached on which material properties are best for the prediction of osteoporotic fracture, and several "optimal" FE modeling process exist in the literature (27). Previous studies have found that different reconstruction kernels only moderately affect the pixel intensity of a water-filled phantom (22), which is also illustrated by the almost identical parameters of the calibration equations (Eqs. 1 and 2) for two kernels in this study. The power-law relationship (Eq. 3) we choose for density elasticity allows a drastic change of elasticity moduli with a small change in the image gray value. Regardless of the chosen material property, our results showed that different reconstruction kernels generated different FEA outcomes as expected, but to what extent may depend on elastic-density relationships and other modeling methods used. Apart from this, other FE modeling approaches (e.g., nonlinear FE, various loading settings, and failure criteria) will also affect osteoporosis screening or fracture prediction. Further evaluation of the impact of imaging protocols on these various FE modeling remains to be done.

This study has several limitations. Firstly, the sample size of this study is relatively small, and we did not perform a power analysis.

However, the participants cover the range from osteoporotic to normal, and we believe that our results also illustrate the influence of reconstruction kernel on the use of the FEA classification to screen for osteoporosis. Nonetheless, this study was only a preliminary step; future studies with larger sample populations will help better understand any differences caused by image acquisition and FE modeling. Secondly, nonlinear FEA normally delivers better results for strength; however, the reconstruction kernel caused the nonlinear yielding behavior of the element to change and influence the relationship between models and validation outcome. Hence, we built linear FEA models. Thirdly, our study compared only two kernels in clinical scenarios; however, a smoother kernel for soft tissue imaging like B30f or B25f might be used in the most clinical practice setting, and thus future studies with a wider range of reconstruction kernels will help to better understand their influence on FEA in the clinical setting. Finally, only one scanner was used in this study, but there will be a wide variety of scanner manufacturers, and image reconstruction algorithm kernels as well as scanning protocols will vary within and between institutions, potentially leading to widely different estimates.

5 Conclusion

Our results revealed that the FE-estimated bone strength and bone stiffness obtained by the two reconstruction kernels reveal a significant discrepancy. FEA based on two kernels both seemed to apply to the opportunistic screening of osteoporosis, but different fragility fracture strength thresholds were noted, which has implications for the clinical management of fragility fracture. We recommend the standard reconstruction kernel for FEA because it is the most used imaging kernel and suitable for opportunistic screening of osteoporosis with considerable accuracy to differentiate osteoporosis from normal individuals. However, whether strength or stiffness is more suitable for opportunistic screening of osteoporosis by FEA may depend on the chosen modeling approach.

Data availability statement

The raw data supporting the conclusions of this article will be made available by the authors, without undue reservation.

Ethics statement

The studies involving human participants were reviewed and approved by Ethics Committee of Peking University Third Hospital, Beijing, China. Written informed consent for participation was not required for this study in accordance with the national legislation and the institutional requirements.

Author contributions

HY led and coordinated this study. DJ, MN, and YZ performed the material preparation and data collection. CJ performed data interpretation and statistical analyses under the supervision of HSY. CJ wrote the majority of the manuscript. All authors read and approved the final manuscript.

Funding

Conflict of interest

The authors declare that the research was conducted in the absence of any commercial or financial relationships that could be construed as a potential conflict of interest.

Publisher's note

All claims expressed in this article are solely those of the authors and do not necessarily represent those of their affiliated organizations, or those of the publisher, the editors and the reviewers. Any product that may be evaluated in this article, or claim that may be made by its manufacturer, is not guaranteed or endorsed by the publisher.

References

1. NIH Consensus development panel on osteoporosis prevention, diagnosis, and therapy. *JAMA*. (2001) 285:785–95. doi: 10.1001/jama.285.6.785

2. Reid IR. A broader strategy for osteoporosis interventions. *Nat Rev Endocrinol* (2020) 16:333–9. doi: 10.1038/s41574-020-0339-7

3. Tei RMH, Ramlau-Hansen CH, Plana-Ripoll O, Brink O, Langdahl BL. OFELIA: prevalence of osteoporosis in fragility fracture patients. *Calcif. Tissue Int* (2019) 104:102–14. doi: 10.1007/s00223-018-0476-3

4. Mai HT, Tran TS, Ho-Le TP, Center JR, Eisman JA, Nguyen TV. Two-thirds of all fractures are not attributable to osteoporosis and advancing age: Implications for fracture prevention. *J Clin Endocrinol Metab* (2019) 104:3514–20. doi: 10.1210/jc.2018-02614

5. Barton DW, Behrend CJ, Carmouche JJ. Rates of osteoporosis screening and treatment following vertebral fracture. *Spine J* (2019) 19:411–7. doi: 10.1016/j.spinee.2018.08.004

6. Cheng X, Zhao K, Zha X, Du X, Li Y, Chen S, et al. China Health big data (China biobank) project investigators. opportunistic screening using low-dose CT and the prevalence of osteoporosis in China: A nationwide, multicenter study. *J Bone Miner Res* (2021) 36(3):427–35. doi: 10.1002/jbmr.4187

7. Michalski AS, Besler BA, Burt LA, Boyd SK. Opportunistic CT screening predicts individuals at risk of major osteoporotic fracture. *Osteoporos Int* (2021) 32(8):1639–49. doi: 10.1007/s00198-021-05863-0

8. Zysset P, Qin L, Lang T, Khosla S, Leslie WD, Shepherd JA, et al. Clinical use of quantitative computed tomography-based finite element analysis of the hip and spine in the management of osteoporosis in adults: the 2015 ISCD official positions-part II. *J Clin Densitom*. (2015) 18:359–92. doi: 10.1016/j.jocd.2015.06.011

9. Schileo E, Taddei F. Finite element assessment of bone fragility from clinical images. *Curr Osteoporos Rep* (2021) 19:688–98. doi: 10.1007/s11914-021-00714-7

10. Löffler MT, Sollmann N, Mei K, Valentinitsch A, Noël PB, Kirschke JS, et al. X-Ray-based quantitative osteoporosis imaging at the spine. *Osteoporos Int* (2020) 31:233–50. doi: 10.1007/s00198-019-05212-2

11. Dall'Ara E, Pahr D, Varga P, Kainberger F, Zysset P. QCT-based finite element models predict human vertebral strength *in vitro* significantly better than simulated DEXA. *Osteoporos Int* (2012) 23:563–72. doi: 10.1007/s00198-011-1568-3

12. Crawford RP, Cann CE, Keaveny TM. Finite element models predict *in vitro* vertebral body compressive strength better than quantitative computed tomography. *Bone*. (2003) 33:744–50. doi: 10.1016/s8756-3282(03)00210-2

13. Allaire BT, Lu D, Johannesdottir F, Kopperdahl D, Keaveny TM, Jarraya M, et al. Prediction of incident vertebral fracture using CT-based finite element analysis. *Osteoporos Int* (2019) 30:323–31. doi: 10.1007/s00198-018-4716-1

14. Johannesdottir F, Allaire B, Kopperdahl DL, Keaveny TM, Sigurdsson S, Bredella MA, et al. Bone density and strength from thoracic and lumbar CT scans both predict incident vertebral fractures independently of fracture location. *Osteoporos Int* (2021) 32:261–9. doi: 10.1007/s00198-020-05528-4

15. Kopperdahl DL, Aspelund T, Hoffmann PF, Sigurdsson S, Siggeirsdottir K, Harris TB, et al. Assessment of incident spine and hip fractures in women and men using finite element analysis of CT scans. *J Bone Miner Res* (2014) 29(3):570–80. doi: 10.1002/jbmr.2069

16. Greve T, Rayudu NM, Dieckmeyer M, Boehm C, Ruschke S, Burian E, et al. Finite element analysis of osteoporotic and osteoblastic vertebrae and its association with the proton density fat fraction from chemical shift encoding-based water-fat MRI - a preliminary study. *Front Endocrinol (Lausanne)* (2022) 13:900356. doi: 10.3389/fendo.2022.900356

17. Brown JP, Engelke K, Keaveny TM, Chines A, Chapurlat R, Foldes AJ, et al. Romosozumab improves lumbar spine bone mass and bone strength parameters relative to alendronate in postmenopausal women: results from the active-controlled fracture study in postmenopausal women with osteoporosis at high risk (ARCH) trial. *J Bone Miner Res* (2021) 36(11):2139–52. doi: 10.1002/jbmr.4409

18. Yan J, Liao Z, Yu Y. Finite element analysis of dynamic changes in spinal mechanics of osteoporotic lumbar fracture. *Eur J Med Res* (2022) 27(1):142. doi: 10.1186/s40001-022-00769-x

19. Paul J, Krauss B, Banckwitz R, Maentele W, Bauer RW, Vogl TJ. Relationships of clinical protocols and reconstruction kernels with image quality and radiation dose in a 128-slice CT scanner: study with an anthropomorphic and water phantom. *Eur J Radiol* (2012) 81:e699–703. doi: 10.1016/j.ejrad.2011.01.078

20. Cann CE. Quantitative CT applications: comparison of current scanners. *Radiology*. (1987) 162:257–61. doi: 10.1148/radiology.162.1.3786773

21. Giambini H, Dragomir-Daescu D, Nassr A, Yaszemski MJ, Zhao C. Quantitative computed tomography protocols affect material mapping and quantitative computed tomography-based finite-element analysis predicted stiffness. *J Biomech Eng*. (2016) 138:0910031–7. doi: 10.1115/1.4034172

22. Dragomir-Daescu D, Salas C, Uthamaraj S, Rossman T. Quantitative computed tomography-based finite element analysis predictions of femoral strength and stiffness depend on computed tomography settings. *J Biomech*. (2015) 48:153–61. doi: 10.1016/j.jbiomech.2014.09.016

23. Michalski AS, Edwards WB, Boyd SK. The influence of reconstruction kernel on bone mineral and strength estimates using quantitative computed tomography and finite element analysis. *J Clin Densitom*. (2019) 22:219–28. doi: 10.1016/j.jocd.2017.09.001

24. Cong A, Buijs JO, Dragomir-Daescu D. *In situ* parameter identification of optimal density-elastic modulus relationships in subject-specific finite element models of the proximal femur. *Med Eng Phys* (2011) 33:164–73. doi: 10.1016/j.medengphy.2010.09.018

25. Morgan EF, Bayraktar HH, Keaveny TM. Trabecular bone modulus-density relationships depend on anatomic site. *J Biomech.* (2003) 36:897–904. doi: 10.1016/s0021-9290(03)00071-x

26. Brown JK, Timm W, Bodeen G, Chason A, Perry M, Vernacchia F, et al. Asynchronously calibrated quantitative bone densitometry. *J Clin Densitom.* (2017) 20:216–25. doi: 10.1016/j.jocd.2015.11.001

27. Groenen KHJ, Bitter T, van Veluwen TCG, van der Linden YM, Verdonschot N, Tanck E, et al. Case-specific non-linear finite element models to predict failure behavior in two functional spinal units. *J Orthop Res* (2018) 36(12):3208–18. doi: 10.1002/jor.24117

Bioinformatics identification and experimental validation of m6A-related diagnostic biomarkers in the subtype classification of blood monocytes from postmenopausal osteoporosis patients

Peng Zhang[1,2†], Honglin Chen[1,2,3†], Bin Xie[1†], Wenhua Zhao[1,2], Qi Shang[1,2], Jiahui He[1,2], Gengyang Shen[3], Xiang Yu[3], Zhida Zhang[3], Guangye Zhu[1], Guifeng Chen[1,2], Fuyong Yu[1,2], De Liang[3], Jingjing Tang[3], Jianchao Cui[3], Zhixiang Liu[4*], Hui Ren[2,3*] and Xiaobing Jiang[2,3*]

[1]Guangzhou University of Chinese Medicine, Guangzhou, China, [2]Lingnan Medical Research Center of Guangzhou University of Chinese Medicine, Guangzhou, China, [3]The First Affiliated Hospital of Guangzhou University of Chinese Medicine, Guangzhou, China, [4]Affiliated Huadu Hospital, Southern Medical University, Guangzhou, China

Background: Postmenopausal osteoporosis (PMOP) is a common bone disorder. Existing study has confirmed the role of exosome in regulating RNA N6-methyladenosine (m6A) methylation as therapies in osteoporosis. However, it still stays unclear on the roles of m6A modulators derived from serum exosome in PMOP. A comprehensive evaluation on the roles of m6A modulators in the diagnostic biomarkers and subtype identification of PMOP on the basis of GSE56815 and GSE2208 datasets was carried out to investigate the molecular mechanisms of m6A modulators in PMOP.

Methods: We carried out a series of bioinformatics analyses including difference analysis to identify significant m6A modulators, m6A model construction of random forest, support vector machine and nomogram, m6A subtype consensus clustering, GO and KEGG enrichment analysis of differentially expressed genes (DEGs) between different m6A patterns, principal component analysis, and single sample gene set enrichment analysis (ssGSEA) for evaluation of immune cell infiltration, experimental validation of significant m6A modulators by real-time quantitative polymerase chain reaction (RT-qPCR), etc.

Results: In the current study, we authenticated 7 significant m6A modulators *via* difference analysis between normal and PMOP patients from GSE56815 and GSE2208 datasets. In order to predict the risk of PMOP, we adopted random forest model to identify 7 diagnostic m6A modulators, including FTO, FMR1,

YTHDC2, HNRNPC, RBM15, RBM15B and WTAP. Then we selected the 7 diagnostic m6A modulators to construct a nomogram model, which could provide benefit with patients according to our subsequent decision curve analysis. We classified PMOP patients into 2 m6A subtypes (clusterA and clusterB) on the basis of the significant m6A modulators *via* a consensus clustering approach. In addition, principal component analysis was utilized to evaluate the m6A score of each sample for quantification of the m6A subgroups. The m6A scores of patients in clusterB were higher than those of patients in clusterA. Moreover, we observed that the patients in clusterA had close correlation with immature B cell and gamma delta T cell immunity while clusterB was linked to monocyte, neutrophil, CD56dim natural killer cell, and regulatory T cell immunity, which has close connection with osteoclast differentiation. Notably, m6A modulators detected by RT-qPCR showed generally consistent expression levels with the bioinformatics results.

Conclusion: In general, m6A modulators exert integral function in the pathological process of PMOP. Our study of m6A patterns may provide diagnostic biomarkers and immunotherapeutic strategies for future PMOP treatment.

Introduction

Postmenopausal osteoporosis (PMOP) is a common bone disorder associated with ageing occurring in postmenopausal women, which is resulted from bone mass decrease and structural changes in bone tissue due to estrogen deficiency, resulting in increased bone fragility and susceptibility to fracture, as well as pain, bone deformation, comorbidities and even death caused by fracture (1–3). It is reported that approximately 50% of women experience at least one PMOP-related fracture (4). Existing drugs including vitamin D, calcium, denosumab, teriparatide, and bisphosphonates serve as recommended therapies for the treatment of PMOP (5), but long-term use of them trigger some side effects causing rapid bone loss and increasing the risks of the jaw osteonecrosis, atypical femoral fractures, and multiple rebound-related vertebral fractures (6). Therefore, PMOP still remains clinically not well managed (7). PMOP seriously impacts the health and life quality of the elderly and even shortens their life expectancy, increasing the financial and social burden on the countries and the families (8). Therefore, it is indispensable and critical to early identify patients at high risk of developing PMOP. Mounting evidence on the extensive developments in PMOP research shows that PMOP is a complicated disease of great heterogeneity that involves genetic changes (9). Hence, early identification and effective prevention of high-risk patients from a genetic perspective will exert a profound influence on the epidemiological control of PMOP.

Notably, recent studies have reported the promise of exosomes as potential therapies in osteoporosis (10, 11). Exosomes are small single-membrane organelles between 40 and 160 nm in diameter (12), which can carry a variety of cargos, such as lipids, proteins, glycoconjugates, and nucleic acids (13). Exosomes can transmit signals or molecules between cells and reshape the extracellular matrix by releasing these substances (14). Moreover, exosome can carry circular RNAs (circRNAs) to regulate bone metabolism in PMOP *via* sponging microRNAs (miRNAs), which can control mRNA expression by regulate the interaction with m6A methylation (15). N6-methyladenosine (m6A) is a widespread epigenetic modification that affects the variable splicing, translocation, translation and degradation of mRNA, as well as the epigenetic effects of certain non-coding RNAs (16). As an essential epigenetic modification, m6A modification needs numerous regulatory proteins encoded by writers, erasers, and readers to coorperate together (17). Abnormalities in m6A methylation can lead to a variety of diseases such as obesity, glioblastoma, acute myeloid leukaemia, type 2 diabetes, infertility, neuronal diseases, premature ovarian failure and various malignancies (18, 19). With the further study on m6A, researchers also found that bone marrow mesenchymal stem cells (BMSCs), chondrocytes, osteoblasts, osteoclasts, osteosarcoma, and adipocytes cells are all subject to m6A modification to regulate the methylation of RNA in cells, affecting the transduction of mRNA and/or non-coding RNA associated genes, thus activating cellular signaling pathways and affecting cell cycle and DNA damage repair, which in turn determines the occurrence and development process of musculoskeletal disorders (20–24). Recently, existing researches have verified that m6A modifications exert vital functions on the pathology of PMOP *via* modulating the expression level of m6A-associated genes (25, 26). However, it still stays unclear on the roles of m6A modulators derived from serum exosome in PMOP.

In this study, we performed a comprehensive evaluation on the roles of m6A modulators in the diagnostic biomarkers and subtype identification of PMOP on the basis of GSE56815 and GSE2208 datasets with monocyte samples. We developed a PMOP susceptibility prediction gene model based on seven candidate m6A modulators including FMR1, FTO, WTAP, YTHDC2, HNRNPC, RBM15 and RBM15B, and found that the model provided good clinical benefits for patients. Our RT-qPCR experiments further validated these m6A modulators, exhibiting consistent expression levels with the bioinformatics results. Additionally, we excavated two different m6A patterns that were closely correlated with immature B cell, gamma delta T cell, CD56dim natural killer cell, monocyte, neutrophil and regulatory T cell immunity, indicating that m6A patterns may be used to identify PMOP and provide subsequent treatment strategies. Figure 1 displayed the flowchart of study design and process.

Materials and methods

Sample retrieval

We collected monocyte samples separated from whole blood of elderly women by retrieving the GEO database (http://www.ncbi.nlm.nih.gov/geo/). The search terms were "BMD", "Postmenopausal Osteoporosis", "Gene expression", "Microarray", and the datasets were based on the following criteria: (1) each dataset includes at least 10 samples; (2) each dataset includes at least 5 cases in the groups of control and PMOP respectively; and (3) Both raw data and series matrix file can be obtained from the GEO datasets. Two datasets, GSE56815 (27) and GSE2208 (28) were eventually screened, which fully met our criteria. We chose 5 cases of control group and 5 cases of PMOP group from the dataset of GSE2208 as well as 20 cases of

PMOP and 20 controls in GSE56815 dataset for subsequent analysis. Table 1 showed specific information of the corresponding datasets.

Data acquisition

We downloaded the annotated R package *via* Bioconductor (http://bioconductor.org/) to convert microarray probes to symbols in R (v4.1.2) software (Statistics Department of the University of Auckland, New Zealand). After data preparation, we carried out consolidation of the two datasets *via* SVA batch difference processing of combat and obtained the final dataset which contained 25 controls and 25 PMOP cases. Differential m6A madulators were identified from the dataset by difference analysis of control and PMOP cases using the R package of Limma. The screening thresholds to determine the significant m6A madulators were P-Value <0.05 and $|\log_2$ fold change (FC)| >0 (29).

Model construction

We established random forest (RF) and support vector machine (SVM) models as training models to evaluate the PMOP occurrence, which were detected by "Reverse cumulative distribution of residual", receiver operating characteristic (ROC) curve, and "Boxplots of residual". In RF model, we used the R package of "RandomForest" to build an RF model to screen candidate m6A modulators with importance score (Mean Decrease Gini)>2. In SVM model, n stands for the number of m6A modulators and every data dot is presented as a dot in an n-dimensional space. We then selected an optimal hyperplane that distinguishes these two groups of control and PMOP very well (30). We then used the R package of "rms" to establish a nomogram model to
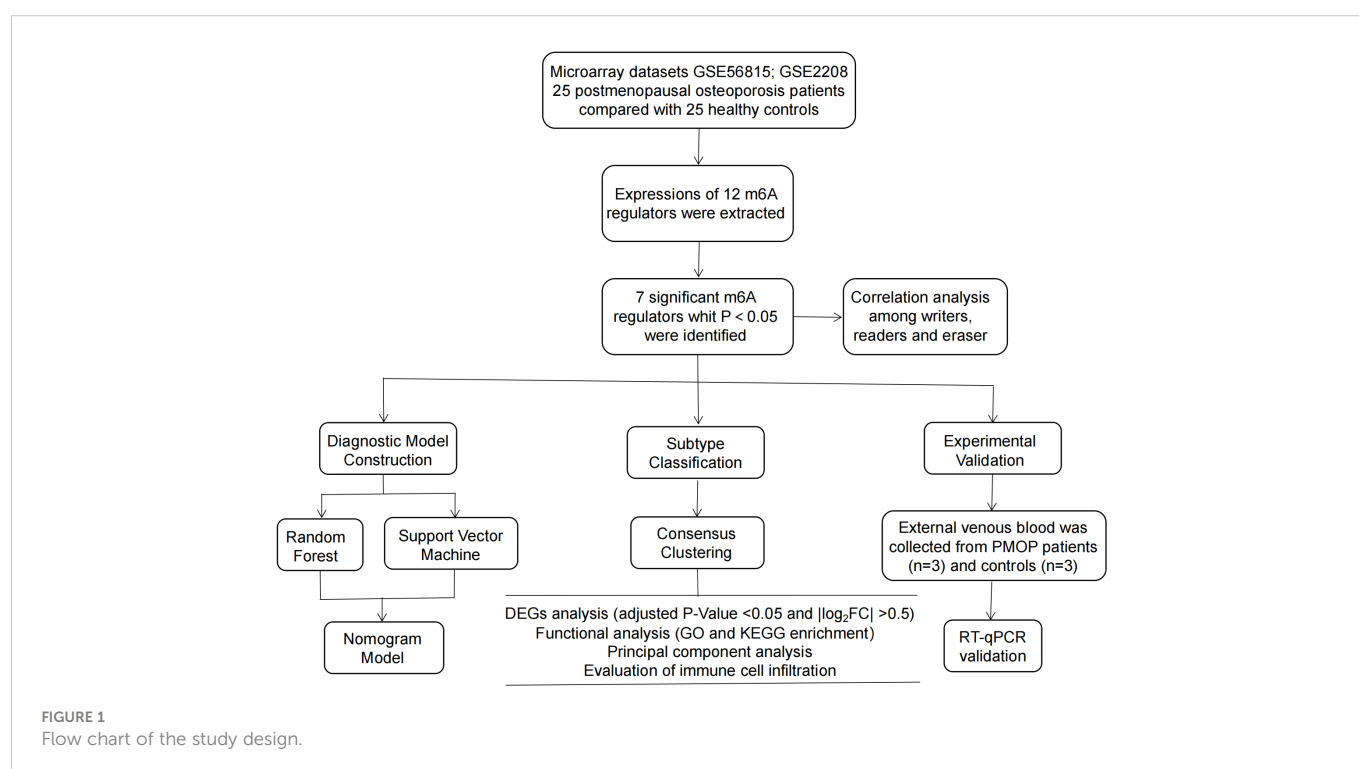

FIGURE 1
Flow chart of the study design.

TABLE 1 Information for the selected microarray datasets.

GEO Accession Total samples	Selected samples Platform	Source tissue
19 samples	10 samples	blood monocytes
GSE2208 Sample types:	GPL96 Sample types:	
10 high BMD	5 PreH BMD (Control)	
9 low BMD	5 postL BMD (PMOP)	
80 samples	40 samples	blood monocytes
GSE56815 Sample types:	GPL96 Sample types:	
40 high BMD	20 PreH BMD (Control)	
40 low BMD	20 postL BMD (PMOP)	

BMD, bone mineral density; PreH BMD: Premenopausal High BMD; postL BMD: Postmenopausal Low BMD.

predict the prevalence of PMOP patients according to screened candidate m6A modulators. We utilized the calibration curve to assess how well our predicted values align with reality. We also carried out decision curve analysis (DCA) to draw a clinical impact curve and assess whether decisions based on the model produced benefit to patients (31).

Subtype classification

Consensus clustering is a resampling-based algorithm that identifies each member and its subcluster number, and verifies the rationality of the clusters (31). Using the R package of "ConsensusClusterPlus", a consensus clustering method was conducted to identify different m6A patterns on the basis of significant m6A moderators (32).

Classification of differentially expressed genes between different m6a patterns and GO and KEGG enrichment analysis

We utilized Limma package to identify differentially expressed genes (DEGs) between different m6A patterns with the threshold of adjusted P-Value <0.05 and $|\log_2 FC| > 0.5$. Next, we used the R package of "clusterProfiler" to perform GO and KEGG analyses so as to investigate the possible mechanism of the DEGs involved in PMOP (33).

Calculation of the m6A score

We utilized principal component analysis to calculate the m6A score for each sample for quantification of the m6A patterns, with the m6A score evaluated based on the following formula: m6A score = $PC1_i$, where PC1 denotes principal component 1, and i denotes significant m6A gene expression (34).

Evaluation of immune cell infiltration

We utilized single sample gene set enrichment analysis (ssGSEA) to evaluate the level of immune cell infiltration in the samples from PMOP groups. First, the gene expression levels in the samples were sequenced using ssGSEA to obtain a ranking of gene expression levels. Next, we searched for the significant m6A madulators in the input dataset and then summed their expression levels. According to these evaluations, we obtained the abundance of immune cells in each sample (35).

Experimental validation by RNA extraction and real-time quantitative polymerase chain reaction

The clinical experiments involved in this paper were authorized by the Ethics Committee of the 1st Affiliated Hospital of GZUCM (No. K [2019]129). In the current research, all patients who participated in this trial provided informed consent at the beginning. Then, external venous blood was drawn from PMOP patients (n=3) and healthy controls (n=3) respectively. The two groups were age-matched. The manipulation of human peripheral blood monocytes (HPBMs) was performed as described previously (36). First, whole blood from patients was put into a 50-mL centrifuge tube, then diluted with 10-mL PBS and gently mixed. Afterwards, we continuously centrifuged the initial blood specimen at 2000 rpm for 20 minutes. When centrifugation was finished, the blood sample was stratified and the leukocyte layer in the center of the sample containing HPBMs was aspirated by pipette and transferred to a single fresh 15 mL centrifuge tube in liquid with 10-15 mL of PBS. Next the solution was centrifuged at 1500 rpm in 10 min and the supernatant was lifted to precipitate and be the wanted HPBMs. HPBMs were inoculated in 6-well plates, and then 1mL of TRIzol reagent was applied to each well for total RNA extraction from the cells. Subsequently, retrotranscription of 1μg of total RNA was done using a cDNA synthesis kit (Takara Inc.Shiga, Japan). 20μL SYBR Green qPCR SuperMix (Takara Inc.) was used for detection of m6A cDNAs and RT-qPCR machine (Bio-Rad, Hercules, CA, USA). The thermal cycling conditions for the final gene amplification were: 95°C for 30s, 40 cycles of 95°C for 5s, and a final step of 60°C for 30s. Quantitative analysis was performed using the $2^{-\Delta\Delta CT}$ method to calculation of the relative expression of each gene. The gene-related detection primers of m6A modulators were compounded by Shanghai Sangon Biotechnology Co.Ltd (China), as shown in Table 2.

Statistical analysis

The correlations among writer, reader and eraser were evaluated *via* linear regression analyses. The differences between groups were calculated through Kruskal-Wallis tests in bioinformatics analysis, while unpaired t-tests with Welch's correction were utilized in RT-qPCR data analysis. Two-tailed tests were conducted to estimate all parametric analyses with $P < 0.05$ considered as statistical significance. All results were expressed as mean ± standard deviation.

Results

Identification of the 12 m6A modulators in PMOP

Totally 12 m6A modulators were identified based on difference analysis between controls and PMOP cases. These modulators
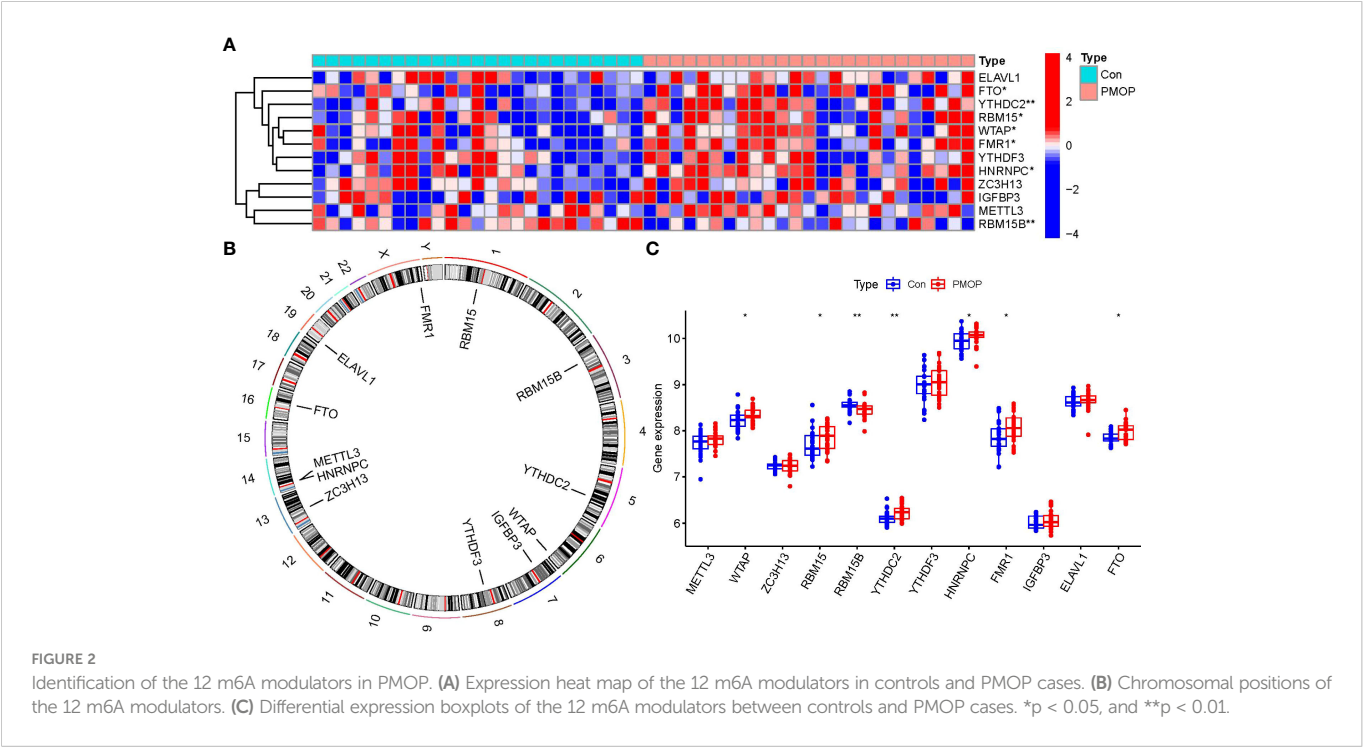
included one eraser (FTO), five writers (METTL3, ZC3H13, RBM15B, WTAP, and RBM15), and six readers (YTHDC2, ELAVL1, FMR1, YTHDF3, HNRNPC, and IGFBP3). We finally filtrated 7 vital m6A modulators (HNRNPC, YTHDC2, FMR1, FTO, WTAP, RBM15B, and RBM15), which were visualized by a heat map and histogram. We observed that RBM15B expression was decreased in PMOP cases compared to controls, while the other significant m6A regulators displayed the opposite results (Figures 2A, C). And we visualized the chromosomal positions of the 12 m6A modulators *via* the "RCircos" package (Figure 2B).

Correlation among writers, readers and eraser in PMOP

We utilized linear regression analyses to investigate whether gene expression levels of writers or readers in PMOP exhibit correlation with the gene expression level of eraser. We observed that the gene

TABLE 2 Sequences of m6A gene-specific primers used for RT-qPCR.

m6A genes	Sequence (5'->3')	
	Forward primer	Reverse primer
FTO	ATTCTATCAGCAGTGGCAGC	GGATGCGAGATACCGGAGTG
FMR1	CCTGAACTCAAGGCTTGGCA	TCTCTTCCTCTGTTGGAGCTTTA
YTHDC2	ACGGGGACCAGAGAGAAATG	TTGTTGAGTCGCCCACTTGT
RBM15	ATGCCTTCCCACCTTGTGAG	CAACCAGTTTTGCACGGACA
WTAP	GCTTCTGCCTGGAGAGGATT	GTGTACTTGCCCTCCAAAGC

FIGURE 2

Identification of the 12 m6A modulators in PMOP. **(A)** Expression heat map of the 12 m6A modulators in controls and PMOP cases. **(B)** Chromosomal positions of the 12 m6A modulators. **(C)** Differential expression boxplots of the 12 m6A modulators between controls and PMOP cases. *p < 0.05, and **p < 0.01.

expression levels of writers RBM15, WTAP, ZC3H13, and readers FMR1, YTHDC2, and HNRNPC in PMOP cases were positively correlated with eraser gene FTO. The other readers or writers were not significantly linked to eraser gene FTO (Figure 3). Thus, we demonstrated different correlations between different writers, readers and eraser.

Establishment of the RF and SVM models

Figure 4A showed "Reverse cumulative distribution of residual" and Figure 4B presented "Boxplots of residual", which confirmed that the RF model has the smallest residuals. The residuals for most of the samples in the model are relatively small, suggesting that the RF model is better than the SVM model. Therefore, we determined the RF model to be the most suitable model for the prediction of PMOP occurrence. Then, we plotted ROC curve to estimate the models, and found that the RF model is more accurate than the SVM model according to their AUC values of the ROC curves (Figure 4C). Finally, we visualized these 7 significant m6A regulators after ranking them in order of importance and selected m6A regulators with importance score>2 as the candidate genes (Figure 4D).

Establishment of the nomogram model

We utilized the "rms" package in R to establish a nomogram model of the seven candidate m6A modulators for the prediction of the

prevalence of PMOP patients (Figure 5A). We observed that the nomogram model exhibits high accuracy of prediction according to calibration curves (Figure 5B). The red line in the DCA curve stayed above the gray and black lines from 0 to 1, suggesting that decisions based on the nomogram model may be beneficial to PMOP patients (Figure 5C). Moreover, we noticed that the predictive power of the nomogram model was remarkable according to the clinical impact curve (Figure 5D).

Identification of two distinct m6A patterns

We identified two m6A patterns (clusterA and clusterB) based on the 7 significant m6A regulators *via* the R package of "ConsensusClusterPlus" (Figures 6A–D). There were 16 cases in clusterA, and 9 cases in clusterB. Then, we plotted the heat map and histogram, which clearly displayed the differential expression levels of the 7 significant m6A modulators between the two clusters. We observed that the expression levels of RBM15, WTAP, FMR1, FTO, YTHDC2, and HNRNPC in clusterA were higher than those in clusterB, while the expression level of RBM15B exhibited no significant differences between the two cluster (Figures 6E, F). The PCA results revealed that the two m6A patterns could be distinguished by 7 significant m6A modulators (Figure 6G). We screened totally 90 m6A-associated DEGs between the two m6A patterns, and we carried out GO and KEGG enrichment analyses to excavate the role of these DEGs in PMOP (Figures 6H, I). The detailed information of GO and KEGG enrichment analysis was
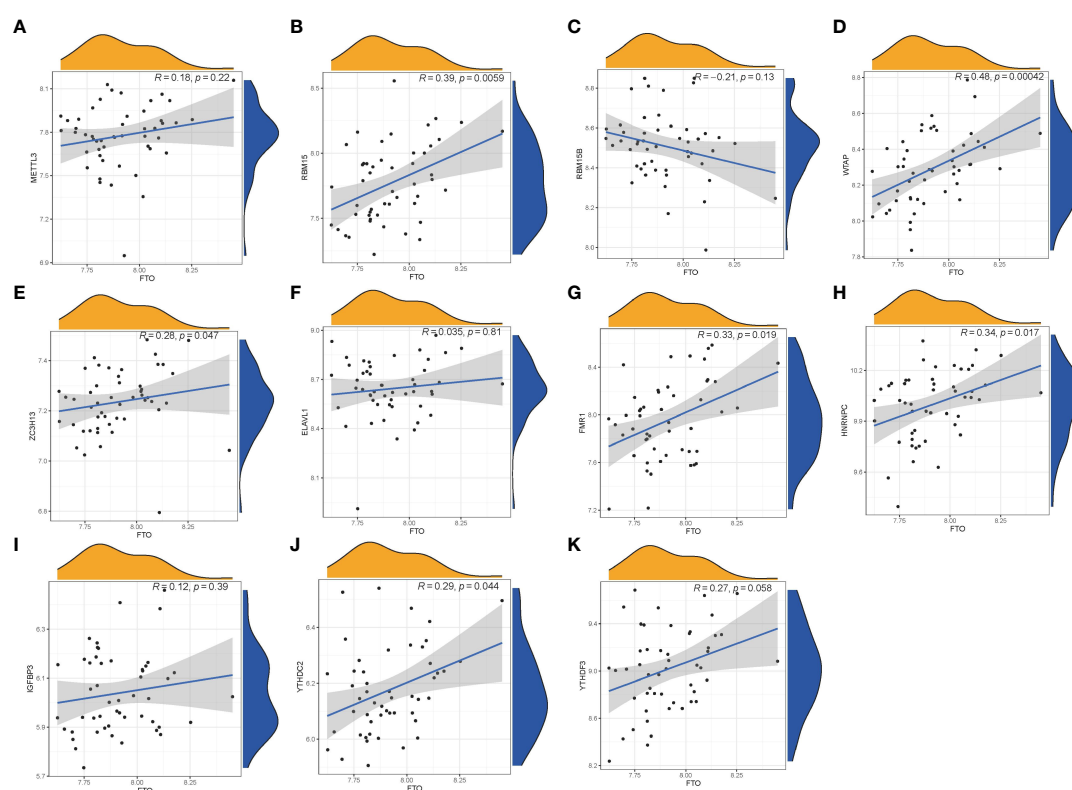

FIGURE 3
Correlation among Writers, Readers and Eraser in PMOP **(A−K)**. Writer genes: RBM15, RBM15B, METTL3, WTAP, and ZC3H13; reader genes: ELAVL1, FMR1, HNRNPC, IGFBP3, YTHDC2, and YTHDF3; eraser gene: FTO.
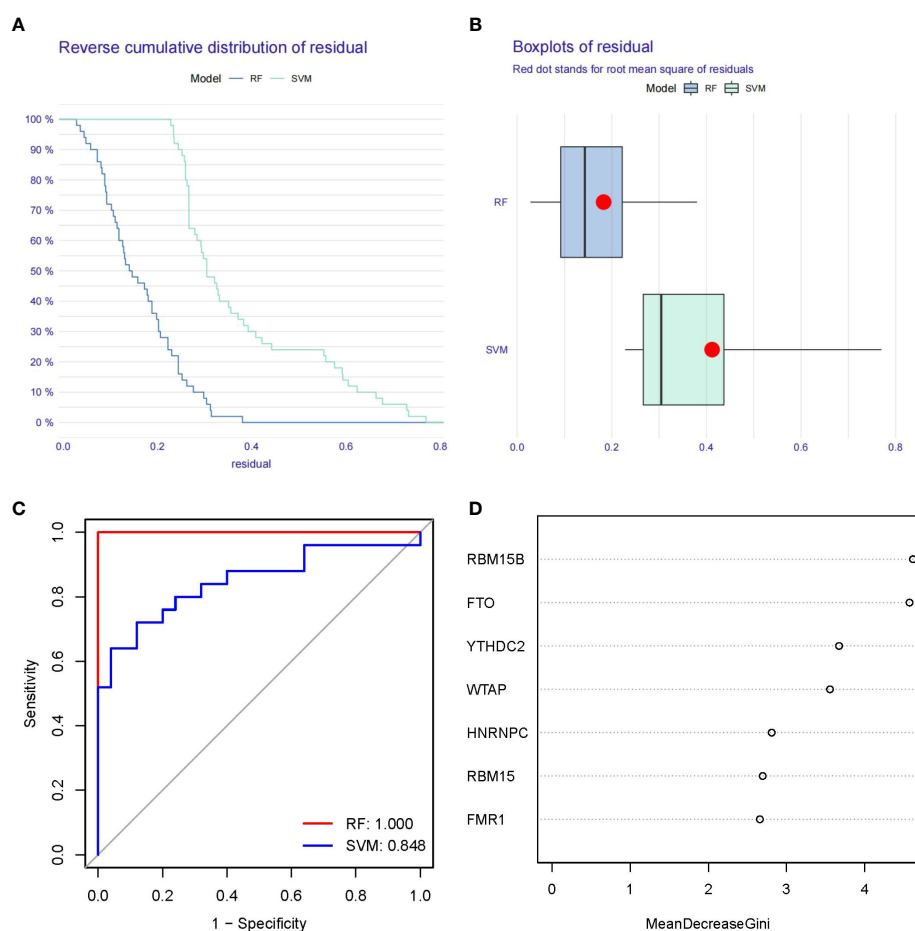
FIGURE 4
Establishment of the RF and SVM Models. **(A)** Reverse cumulative distribution of residual was constructed to display the residual distribution of RF and SVM models. **(B)** Boxplots of residual was construct to display the residual distribution of RF and SVM models. **(C)** ROC curves indicated the accuracy of the RF and SVM models. **(D)** The importance score of the 7 m6A modulators on the basis of the RF model.

shown in Supplementary Tables 1, 2. We observed that GO: 0031331 (positive regulation of cellular catabolic process), GO:0030055(cell-substrate junction), GO:0005925(focal adhesion), and GO:0045296 (cadherin binding) were the mainly enriched entries. We finally got totally 12 pathways as shown in Figure 6I. These signaling pathways like C-type lectin receptor signaling pathway, and Relaxin signaling pathway may exert regulatory functions on the pathological process of PMOP. Notably, KEGG enrichment analysis showed that osteoclast differentiation was one of the mainly enriched pathways. Specially, several key targets were involved in the pathway of osteoclast differentiation (e.g., RELB, SPI1, LILRA6, TGFB1).

Then, ssGSEA was performed to evaluate the immune cell abundance in PMOP samples, and we also assessed the correlation between immune cells and seven important m6A modulators. We observed that FMR1 was positively correlated with many immune cells (Figure 7A). We evaluated the differences in immune cell infiltration between patients with high and low FMR1 expressions. The results showed that patients with low FMR1 expression were more likely to exhibit increased immune cell infiltration than those

with high FMR1 expression (Figure 7B). We found that clusterA was correlated with the immunity of immature B cell and gamma delta T cell while clusterB was related to CD56dim natural killer cell, monocyte, neutrophil and regulatory T cell immunity, indicating that clusterB may be more correlated with PMOP (Figure 7C).

Classification of two distinct m6A gene patterns and construction of the m6A gene signature

To lucubrate the m6A patterns, we used a consensus clustering approach to classify the PMOP cases into different genomic subtypes on the basis of the 90 m6A-related DEGs. We identified two distinct m6A gene patterns (gene clusterA and gene clusterB), which aligned with the sectionalization of m6A patterns (Figures 8A–D). Figure 8E displayed the expression levels of the 90 m6A-associated DEGs in gene clusterA and gene clusterB. The
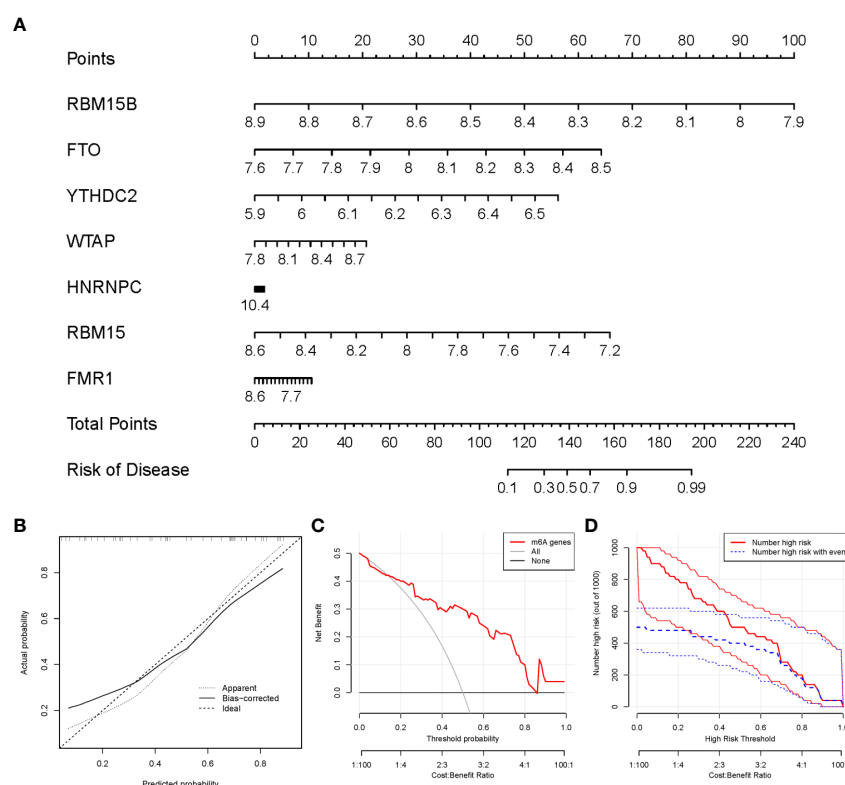
FIGURE 5
Establishment of the nomogram model. **(A)** The nomogram model was established on the basis of the 7 candidate m6A modulators. **(B)** The calibration curve was utilized to evaluate the predictive accuracy of the nomogram model. **(C)** Decisions on the basis of this nomogram model may be beneficial to PMOP patients. **(D)** The clinical impact curve was used to assess clinical impact of the nomogram model.

differential expression levels of immune cell infiltration and the 7 significant m6A modulators between gene clusterA and gene clusterB were also analogous to those in the m6A patterns (Figures 8F, G). These results again verified the veracity of our sectionalization *via* the consensus clustering approach. The m6A scores for each sample between the two distinct m6A patterns or m6A gene patterns were calculated through PCA algorithms for the quantification of the m6A patterns. We found that the clusterB or gene clusterB exhibited higher m6A score than clusterA or gene clusterA (Figures 8H, I).

Role of m6A patterns in distinguishing PMOP

We utilized a Sankey diagram to display the correlation among m6A scores, m6A patterns, and m6A gene patterns (Figure 9A). To lucubrate the link between m6A patterns and PMOP, we explored the relationship between m6A patterns and RELB, SPI1, LILRA6, and TGFB1, which were enriched in osteoclast differentiation according to KEGG enrichment analysis. We observed that clusterB or gene clusterB displayed higher expression levels of RELB, SPI1, LILRA6, and TGFB1 than clusterA or gene clusterA, indicating that clusterB or gene clusterB were closely correlated with PMOP characterized by osteoclast differentiation (Figures 9B, C).

RT-qRCR validation of significant m6A modulators

It was verified that m6A genes FTO, FMR1, YTHDC2, RBM15, WTAP exhibited significantly higher expression levels in PMOP cases than controls (Figure 10), which was consistent with the bioinformatics results.

Discussion

PMOP is a widespread musculoskeletal disorder accompanied by bone system symptoms in postmenopausal women (37). Existing researches have confirmed that m6A modulators play an indispensable role in numerous biological processes (38). However, the role of m6A rmodulators in PMOP stays unclear. This present study aimed at investigating the role of m6A modulators in PMOP.

Firstly, a total of 7 significant m6A modulators were screened from 12 m6A modulators *via* differential expression analysis between controls and PMOP cases, which were selected as diagnostic m6A modulators (FMR1, WTAP, YTHDC2, HNRNPC, FTO, RBM15, and RBM15B) based on an established RF model to predict the occurrence of PMOP. Then, we established a nomogram model on the basis of the seven candidate m6A modulators, which has been evaluated *via* the DCA curve to produce benefit to PMOP patients in virtue of decisions based on the nomogram model.
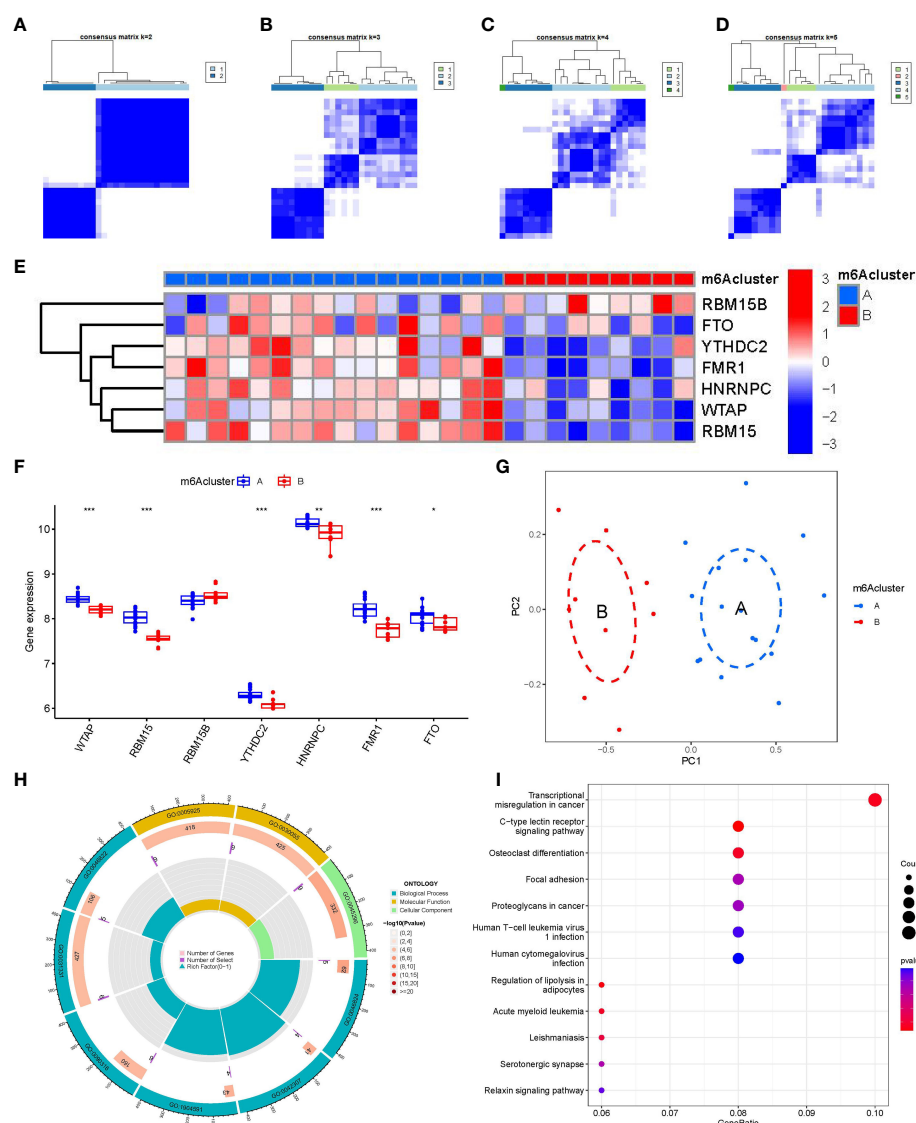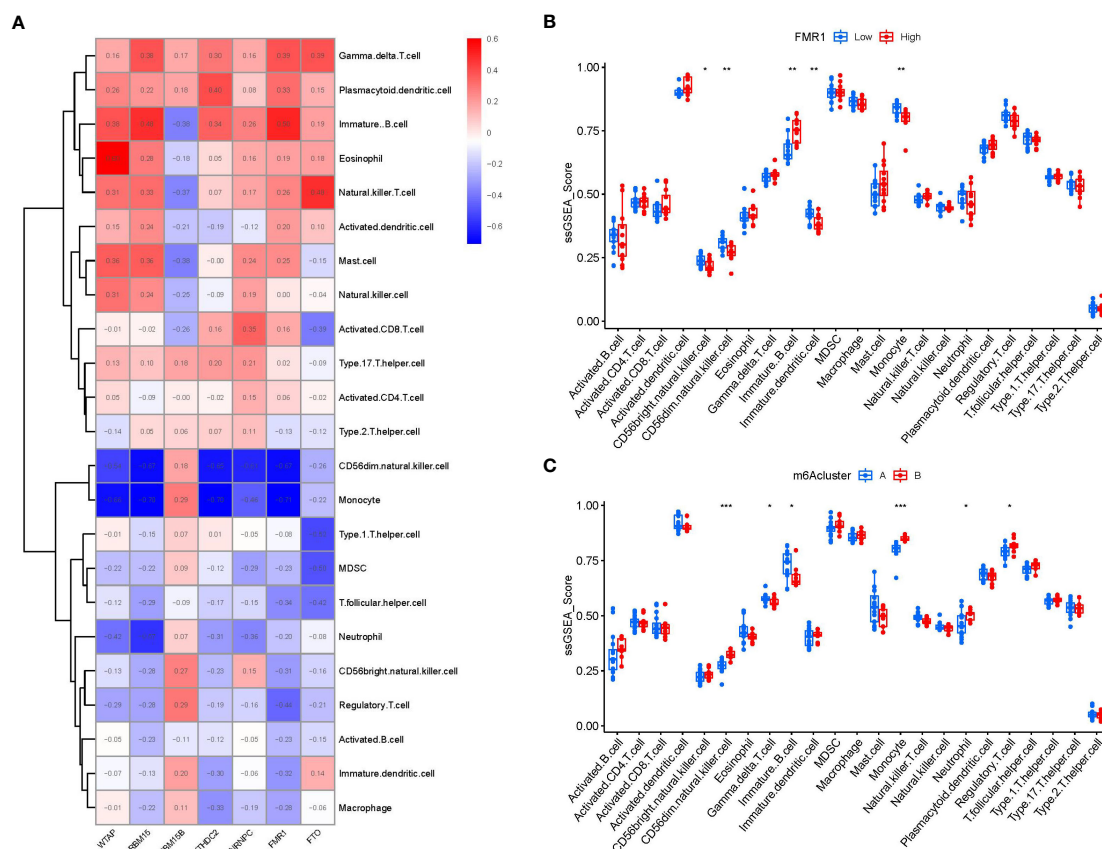
FIGURE 6

Consensus clustering of the 7 significant m6A modulators in PMOP. **(A−D)** Consensus matrices of the 7 significant m6A modulators for k = 2−5. **(E)** Expression heat map of the 7 significant m6A modulators in clusterA and clusterB. **(F)** Differential expression boxplots of the 7 significant m6A modulators in clusterA and clusterB. **(G)** Principal component analysis for the expression profiles of the 7 significant m6Amodulators that shows a remarkable difference in transcriptomes between the two m6A patterns. **(H, I)** GO and KEGG analysis that explores the potential mechanism underlying the effect of the 90 m6A-related DEGs on the occurrence and development of PMOP. *p < 0.05, **p < 0.01, and ***p < 0.001.

FMR1 encodes an RNA-binding protein FMRP, which maintains mRNA stability by binding to the m6A site of mRNA (39). Existing study has confirmed that FMR1-deficiency affects skeleton and bone microstructure, demonstrating that knock-out (KO) of FMR1 in mice showed increased femoral cortical thickness, reduced cortical eccentricity, decreased femoral trabecular pore volumes, and a higher range of trabecular thickness distribution compared to controls (40). WTAP (Wilm's tumor 1 protein) is a ubiquitous nuclear protein that has been reported to facilitate the formation of m6A (41). In addition, existing evidence has confirmed that the WTAP expression level was remarkably upregulated 7 days after fracture (42). Moreover, the increased expression of WTAP has

been reported to promote cellular senescence in aging-related diseases (43). YTHDC2 belongs to the DExD/H box RNA helicase family, which exerts important functions in regulating the transcription of mRNA and maintaining the stability of mRNA (44). YTHDC2 knockdown can exert a stimulative effect on the osteogenic differentiation of human BMSCs and suppress the adipogenic differentiation (45). As a DNA binding protein, HNRNPC (Heterogeneous nuclear ribonucleoprotein C) plays an essential part in RNA processing, exerting a remarkably suppressive effect on the transcription of the vitamin D hormone,1,25-dihydroxyvitamin D (1,25(OH)2D) (46). And HNRNPC has properties of species-specific heterodimerization that functions as

FIGURE 7

Single sample gene set enrichment analysis. **(A)** Correlation between immune cell infiltration and the 7 significant m6A modulators. **(B)** Difference in the abundance of infiltrating immune cells between high and low FMR1 protein expression groups. **(C)** Differential immune cell infiltration between clusterA and clusterB. *p < 0.05, **p < 0.01, and ***p < 0.001.

an indispensable prerequisite for DNA binding and down-regulation of 1,25(OH)2D-related gene transactivation in osteoblasts (47). FTO is a primary m6A demethylase that suppresses osteogenic differentiation by demethylating runx2 mRNA, thus accelerating the process of osteoporosis (48). It has also been found that FTO is a regulator that determines the differentiation of BMSCs by affecting the activation of the GDF11 signaling axis in the bone marrow, promoting Smad2/3 phosphorylation to stimulate osteoclastogenesis and inhibit osteoblast differentiation, thus leading to the development of osteoporosis (49–51). The RNA binding motif protein 15 (RBM15/OTT1) and its paralogue RBM15B (OTT3) belong to SPEN family members (52). Existing studies have confirmed that RBM15 in stress hematopoiesis have a variety of aging-related physiologic changes, including increased DNA damage and NF-κB activation (53), which may serve as important pathological factors in the development of osteoporosis. In addition, study has reported that knockdown of RBM15 and RBM15B impairs XIST-mediated gene silencing (52), which influences osteoblast differentiation in osteoporosis (54). Therefore, to our knowledge, the seven candidate m6A modulators may play an important part in

the occurrence and development of osteoporosis according to previous studies.

Existing researches reveal that the dysfunction of T and B lymphocytes may play an essential role in the pathogenesis of PMOP (55). We found that clusterA was correlated with the immunity of immature B cell and gamma delta T cell while clusterB was related to CD56dim natural killer cell, monocyte, neutrophil and regulatory T cell immunity, indicating that clusterB may be more correlated with PMOP (Figure 7C). Regulatory T cell (Treg) exerts an essential regulatory function in maintaining immune homeostasis and inhibiting the evolution of PMOP (56). Treg cells negatively regulate osteoclasts in bone metabolism, inhibiting osteoclast formation and differentiation and reducing osteoclast activity (57). The immune and skeletal systems share many regulatory factors, such as transforming growth factor-β (TGFB1), which inhibits osteoclast function of bone resorption and regulates new bone formation in bone resorption region (58). Bozec et al (59) found that Treg cells can regulate osteoclastogenesis by secreting cytokines such as TGFB1, IL-10 and IL-4. In this study, we identified two distinct m6A patterns (clusterA and clusterB) on the basis of the 7 significant m6A modulators as well as two distinct m6A gene patterns

FIGURE 8

Consensus clustering of the 90 m6A-associated DEGs in PMOP. **(A–D)** Consensus matrices of the 90 m6A-associated DEGs for k = 2–5. **(E)** Expression heat map of the 90 m6A-associated DEGs in gene clusterA and gene clusterB. **(F)** Differential expression boxplots of the 7 significant m6A modulators in gene clusterA and gene clusterB. **(G)** Differential immune cell infiltration between gene clusterA and gene clusterB. **(H)** Differences in m6A score between clusterA and clusterB. **(I)** Differences in m6A score between gene clusterA and gene clusterB. *p < 0.05, **p < 0.01, and ***p < 0.001.

(gene clusterA and gene clusterB) based on the 90 m6A-associated DEGs. RELB, SPI1, LILRA6, and TGFB1 were enriched in the pathway of osteoclast differentiation according to KEGG enrichment analysis of the 90 m6A-associated DEGs. ClusterB was closely correlated with the regulatory T cell (Treg) immunity and displayed higher expression levels of RELB, SPI1, LILRA6, and TGFB1, suggesting that clusterB may be linked to osteoclast differentiation. Moreover, the m6A scores for each sample between the two distinct m6A patterns or m6A gene patterns were calculated through PCA algorithms for the quantification of the m6A patterns. We found that the clusterB or gene clusterB exhibited higher m6A score than clusterA or gene clusterA.

Our RT-qPCR experiments verified that m6A genes FTO, FMR1, YTHDC2, RBM15, WTAP exhibited significantly higher expression levels in PMOP cases than controls (Figure 10), which was consistent with the bioinformatics results and previous studies. Our results confirm the involvement of these m6A regulators in PMOP and provide new clues to their role in the pathogenesis of PMOP, which

further verified the possibility that m6A modulators may play an important role in the development of PMOP. To the best of our knowledge, this study is the first time to report m6A-related diagnostic biomarkers of PMOP in the subtype classification of blood monocytes.

However, there remain some limitations in our study. This study analyzed the relationship between m6A regulators and immune cell infiltration and briefly validated the expression of key m6A regulators in the samples from PMOP patients, but the underlying regulatory mechanisms in the progression of PMOP have not yet been fully elucidated. In the future, more *in vivo*, *in vitro* and clinical experiments are needed to verify the bioinformatics results.

Conclusion

In general, our present study screened seven diagnostic m6A modulators and constructed a nomogram model providing accurate
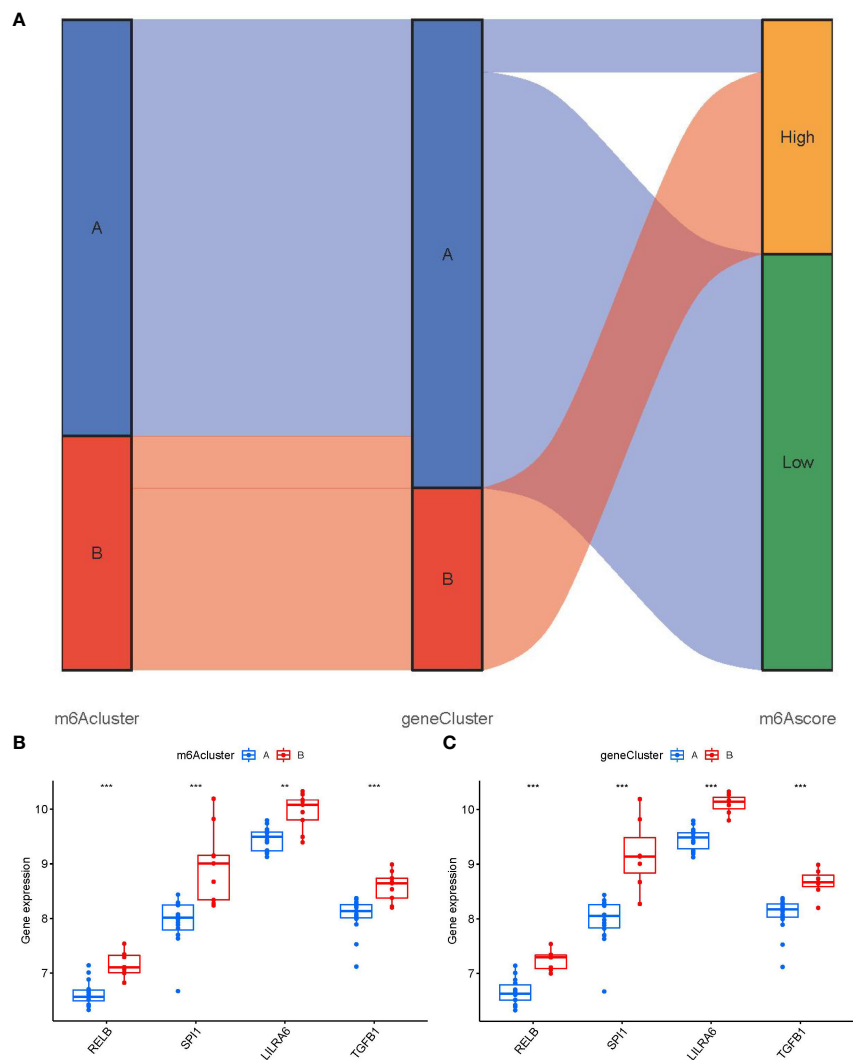
FIGURE 9

Role of m6A patterns in distinguishing PMOP. **(A)** Sankey diagram showing the relationship between m6A patterns, m6A gene patterns, and m6A scores. **(B)** Differential expression levels of osteoclast differentiation-related genes between clusterA and clusterB. **(C)** Differential expression levels of osteoclast differentiation-related genes between gene clusterA and gene clusterB. **p < 0.01, and ***p < 0.001.
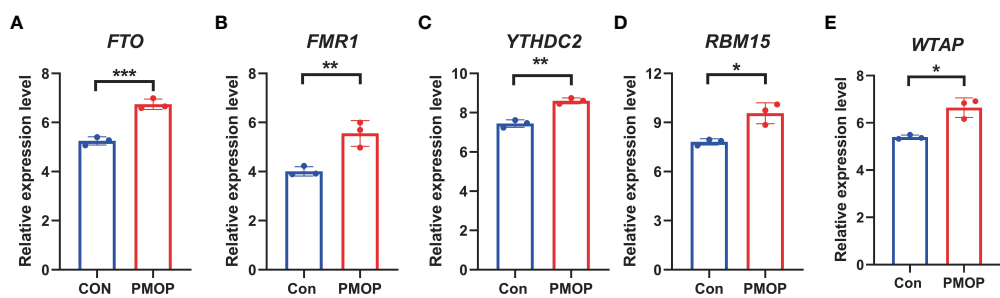

FIGURE 10

RT-qPCR experimental validation of significant m6A modulators. **(A–E)** Relative mRNA expressions of 5 key m6A modulators including FTO, FMR1, YTHDC2, RBM15 and WTAP between the two groups. All results were expressed as mean ± standard deviation. *p < 0.05, **p < 0.01, and ***p < 0.001.

prediction for the prevalence of PMOP. Then, we authenticatd two m6A patterns based on the 7 m6A modulator, and found that clusterB may be more correlated with PMOP. To our knowledge, this study is the first to report m6A-related diagnostic biomarkers of PMOP in the subtype classification of blood monocytes.

Data availability statement

The datasets presented in this study can be found in online repositories. The names of the repository/repositories and accession number(s) can be found in the article/Supplementary Material.

Ethics statement

The clinical experiments involved in this paper were authorized by the Ethics Committee of the First Affiliated Hospital of Guangzhou University of Chinese Medicine (No. K[2019]129). The patients/participants provided their written informed consent to participate in this study.

Author contributions

PZ, HC, DL, JT, JC, ZL, HR, and XJ contributed to the study conception and design. PZ, HC, BX, WZ, and QS contributed to the bioinformatics analysis and experimental validation. JH, GS, XY, ZZ, GZ, GC, and FY contributed to data analysis, and drafting the manuscript. All authors contributed to the article and approved the submitted version.

Funding

Acknowledgments

Conflict of interest

The authors declare that the research was conducted in the absence of any commercial or financial relationships that could be construed as a potential conflict of interest.

Publisher's note

Supplementary material

The Supplementary Material for this article can be found online at: https://www.frontiersin.org/articles/10.3389/fendo.2023.990078/full#supplementary-material

References

1. Arceo-Mendoza RM, Camacho PM. Postmenopausal osteoporosis: Latest guidelines. *Endocrinol Metab Clin North Am* (2021) 50(2):167–78. doi: 10.1016/j.ecl.2021.03.009

2. Slupski W, Jawien P, Nowak B. Botanicals in postmenopausal osteoporosis. *Nutrients* (2021) 13(5). doi: 10.3390/nu13051609

3. Huidrom S, Beg MA, Masood T. Post-menopausal osteoporosis and probiotics. *Curr Drug Targets* (2021) 22(7):816–22. doi: 10.2174/1389450121666201027124947

4. Reid IR. A broader strategy for osteoporosis interventions. *Nat Rev Endocrinol* (2020) 16(6):333–9. doi: 10.1038/s41574-020-0339-7

5. Tian A, Jia H, Zhu S, Lu B, Li Y, Ma J, et al. Romosozumab versus teriparatide for the treatment of postmenopausal osteoporosis: A systematic review and meta-analysis through a grade analysis of evidence. *Orthop Surg* (2021) 13(7):1941–50. doi: 10.1111/os.13136

6. Han J, Li L, Zhang C, Huang Q, Wang S, Li W, et al. Eucommia, cuscuta, and drynaria extracts ameliorate glucocorticoid-induced osteoporosis by inhibiting osteoclastogenesis through PI3K/Akt pathway. *Front Pharmacol* (2021) 12:772944. doi: 10.3389/fphar.2021.772944

7. McNeil MA, Merriam SB. Menopause. *Ann Intern Med* (2021) 174(7):ITC97–ITC112. doi: 10.7326/AITC202107200

8. Si L, Winzenberg TM, Jiang Q, Chen M, Palmer AJ. Projection of osteoporosis-related fractures and costs in China: 2010-2050. *Osteoporos Int* (2015) 26(7):1929–37. doi: 10.1007/s00198-015-3093-2

9. Yin L, Zhu X, Novak P, Zhou L, Gao L, Yang M, et al. The epitranscriptome of long noncoding RNAs in metabolic diseases. *Clin Chim Acta* (2021) 515:80–9. doi: 10.1016/j.cca.2021.01.001

10. Dong Q, Han Z, Tian L. Identification of serum exosome-derived circRNA-miRNA-TF-mRNA regulatory network in postmenopausal osteoporosis using bioinformatics analysis and validation in peripheral blood-derived mononuclear cells. *Front Endocrinol (Lausanne)* (2022) 13:899503. doi: 10.3389/fendo.2022.899503

11. Cui Y, Guo Y, Kong L, Shi J, Liu P, Li R, et al. A bone-targeted engineered exosome platform delivering siRNA to treat osteoporosis. *Bioact Mater* (2022) 10:207–21. doi: 10.1016/j.bioactmat.2021.09.015

12. Kalluri R, LeBleu VS. The biology, function, and biomedical applications of exosomes. *Science* (2020) 367(6478). doi: 10.1126/science.aau6977

13. Jeppesen DK, Fenix AM, Franklin JL, Higginbotham JN, Zhang Q, Zimmerman LJ, et al. Reassessment of exosome composition. *Cell* (2019) 177(2):428–445 e418. doi: 10.1016/j.cell.2019.02.029

14. Pegtel DM, Gould SJ. Exosomes. *Annu Rev Biochem* (2019) 88:487–514. doi: 10.1146/annurev-biochem-013118-111902

15. Liu Z, Li C, Huang P, Hu F, Jiang M, Xu X, et al. CircHmbox1 targeting miRNA-1247-5p is involved in the regulation of bone metabolism by TNF-alpha in postmenopausal osteoporosis. *Front Cell Dev Biol* (2020) 8:594785. doi: 10.3389/fcell.2020.594785

16. Xu T, He B, Sun H, Xiong M, Nie J, Wang S, et al. Novel insights into the interaction between N6-methyladenosine modification and circular RNA. *Mol Ther Nucleic Acids* (2022) 27:824–37. doi: 10.1016/j.omtn.2022.01.007

17. Yang Y, Hsu PJ, Chen YS, Yang YG. Dynamic transcriptomic m(6)A decoration: writers, erasers, readers and functions in RNA metabolism. *Cell Res* (2018) 28(6):616–24. doi: 10.1038/s41422-018-0040-8

18. Zhang N, Ding C, Zuo Y, Peng Y, Zuo L. N6-methyladenosine and neurological diseases. *Mol Neurobiol* (2022) 59(3):1925–37. doi: 10.1007/s12035-022-02739-0

19. Meng L, Lin H, Huang X, Weng J, Peng F, Wu S. METTL14 suppresses pyroptosis and diabetic cardiomyopathy by downregulating TINCR lncRNA. *Cell Death Dis* (2022) 13(1):38. doi: 10.1038/s41419-021-04484-z

20. Liu T, Zheng X, Wang C, Wang C, Jiang S, Li B, et al. The m(6)A "reader" YTHDF1 promotes osteogenesis of bone marrow mesenchymal stem cells through translational control of ZNF839. *Cell Death Dis* (2021) 12(11):1078. doi: 10.1038/s41419-021-04312-4

21. Huang M, Xu S, Liu L, Zhang M, Guo J, Yuan Y, et al. m6A methylation regulates osteoblastic differentiation and bone remodeling. *Front Cell Dev Biol* (2021) 9:783322. doi: 10.3389/fcell.2021.783322

22. Chen S, Li Y, Zhi S, Ding Z, Wang W, Peng Y, et al. WTAP promotes osteosarcoma tumorigenesis by repressing HMBOX1 expression in an m(6)A-dependent manner. *Cell Death Dis* (2020) 11(8):659. doi: 10.1038/s41419-020-02847-6

23. Zhang Y, Liang C, Wu X, Pei J, Guo X, Chu M, et al. Integrated study of transcriptome-wide m(6)A methylome reveals novel insights into the character and function of m(6)A methylation during yak adipocyte differentiation. *Front Cell Dev Biol* (2021) 9:689067. doi: 10.3389/fcell.2021.689067

24. Chen X, Gong W, Shao X, Shi T, Zhang L, Dong J, et al. METTL3-mediated m(6)A modification of ATG7 regulates autophagy-GATA4 axis to promote cellular senescence and osteoarthritis progression. *Ann Rheum Dis* (2022) 81(1):87–99. doi: 10.1136/annrheumdis-2021-221091

25. Wu Y, Xie L, Wang M, Xiong Q, Guo Y, Liang Y, et al. Mettl3-mediated m(6)A RNA methylation regulates the fate of bone marrow mesenchymal stem cells and osteoporosis. *Nat Commun* (2018) 9(1):4772. doi: 10.1038/s41467-018-06898-4

26. Sun Z, Wang H, Wang Y, Yuan G, Yu X, Jiang H, et al. MiR-103-3p targets the m (6) a methyltransferase METTL14 to inhibit osteoblastic bone formation. *Aging Cell* (2021) 20(2):e13298. doi: 10.1111/acel.13298

27. Zhou Y, Gao Y, Xu C, Shen H, Tian Q, Deng HW. A novel approach for correction of crosstalk effects in pathway analysis and its application in osteoporosis research. *Sci Rep* (2018) 8(1):668. doi: 10.1038/s41598-018-19196-2

28. Liu YZ, Dvornyk V, Lu Y, Shen H, Lappe JM, Recker RR, et al. A novel pathophysiological mechanism for osteoporosis suggested by an *in vivo* gene expression study of circulating monocytes. *J Biol Chem* (2005) 280(32):29011–6. doi: 10.1074/jbc.M501164200

29. Ritchie ME, Phipson B, Wu D, Hu Y, Law CW, Shi W, et al. Limma powers differential expression analyses for RNA-sequencing and microarray studies. *Nucleic Acids Res* (2015) 43(7):e47. doi: 10.1093/nar/gkv007

30. Bao X, Shi R, Zhao T, Wang Y. Mast cell-based molecular subtypes and signature associated with clinical outcome in early-stage lung adenocarcinoma. *Mol Oncol* (2020) 14 (5):917–32. doi: 10.1002/1878-0261.12670

31. Dai B, Sun F, Cai X, Li C, Liu H, Shang Y. Significance of RNA N6-methyladenosine regulators in the diagnosis and subtype classification of childhood asthma using the gene expression omnibus database. *Front Genet* (2021) 12:634162. doi: 10.3389/fgene.2021.634162

32. Wilkerson MD, Hayes DN. ConsensusClusterPlus: A class discovery tool with confidence assessments and item tracking. *Bioinformatics* (2010) 26(12):1572–3. doi: 10.1093/bioinformatics/btq170

33. Denny P, Feuermann M, Hill DP, Lovering RC, Plun-Favreau H, Roncaglia P. Exploring autophagy with gene ontology. *Autophagy* (2018) 14(3):419–36. doi: 10.1080/15548627.2017.1415189

34. Zhang B, Wu Q, Li B, Wang D, Wang L, Zhou YL. m(6)A regulator-mediated methylation modification patterns and tumor microenvironment infiltration characterization in gastric cancer. *Mol Cancer* (2020) 19(1):53. doi: 10.1186/s12943-020-01170-0

35. Zhang N, Zhao YD, Wang XM. CXCL10 an important chemokine associated with cytokine storm in COVID-19 infected patients. *Eur Rev Med Pharmacol Sci* (2020) 24 (13):7497–505. doi: 10.26355/eurrev_202007_21922

36. Chen H, Shen G, Shang Q, Zhang P, Yu D, Yu X, et al. Plastrum testudinis extract suppresses osteoclast differentiation *via* the NF-kappaB signaling pathway and ameliorates senile osteoporosis. *J Ethnopharmacol* (2021) 276:114195. doi: 10.1016/j.jep.2021.114195

37. Eastell R, Szulc P. Use of bone turnover markers in postmenopausal osteoporosis. *Lancet Diabetes Endocrinol* (2017) 5(11):908–23. doi: 10.1016/S2213-8587(17)30184-5

38. Oerum S, Meynier V, Catala M, Tisne C. A comprehensive review of m6A/m6Am RNA methyltransferase structures. *Nucleic Acids Res* (2021) 49(13):7239–55. doi: 10.1093/nar/gkab378

39. Zhang F, Kang Y, Wang M, Li Y, Xu T, Yang W, et al. Fragile X mental retardation protein modulates the stability of its m6A-marked messenger RNA targets. *Hum Mol Genet* (2018) 27(22):3936–50. doi: 10.1093/hmg/ddy292

40. Leboucher A, Bermudez-Martin P, Mouska X, Amri EZ, Pisani DF, Davidovic L. Fmr1-deficiency impacts body composition, skeleton, and bone microstructure in a mouse model of fragile X syndrome. *Front Endocrinol (Lausanne)* (2019) 10:678. doi: 10.3389/fendo.2019.00678

41. Zhang SY, Zhang SW, Liu L, Meng J, Huang Y. m6A-driver: Identifying context-specific mRNA m6A methylation-driven gene interaction networks. *PloS Comput Biol* (2016) 12(12):e1005287. doi: 10.1371/journal.pcbi.1005287

42. Mi B, Xiong Y, Yan C, Chen L, Xue H, Panayi AC, et al. Methyltransferase-like 3-mediated N6-methyladenosine modification of miR-7212-5p drives osteoblast differentiation and fracture healing. *J Cell Mol Med* (2020) 24(11):6385–96. doi: 10.1111/jcmm.15284

43. Li G, Ma L, He S, Luo R, Wang B, Zhang W, et al. WTAP-mediated m(6)A modification of lncRNA NORAD promotes intervertebral disc degeneration. *Nat Commun* (2022) 13(1):1469. doi: 10.1038/s41467-022-28990-6

44. He JJ, Li Z, Rong ZX, Gao J, Mu Y, Guan YD, et al. m(6)A reader YTHDC2 promotes radiotherapy resistance of nasopharyngeal carcinoma *via* activating IGF1R/AKT/S6 signaling axis. *Front Oncol* (2020) 10:1166. doi: 10.3389/fonc.2020.01166

45. Wen JR, Tan Z, Lin WM, Li QW, Yuan Q. [Role of m (6)A reader YTHDC2 in differentiation of human bone marrow mesenchymal stem cells]. *Sichuan Da Xue Xue Bao Yi Xue Ban* (2021) 52(3):402–8. doi: 10.12182/20210560204

46. Zhou R, Park JW, Chun RF, Lisse TS, Garcia AJ, Zavala K, et al. Concerted effects of heterogeneous nuclear ribonucleoprotein C1/C2 to control vitamin d-directed gene transcription and RNA splicing in human bone cells. *Nucleic Acids Res* (2017) 45(2):606–18. doi: 10.1093/nar/gkw851

47. Lisse TS, Vadivel K, Bajaj SP, Chun RF, Hewison M, Adams JS. The heterodimeric structure of heterogeneous nuclear ribonucleoprotein C1/C2 dictates 1,25-dihydroxyvitamin d-directed transcriptional events in osteoblasts. *Bone Res* (2014) 2. doi: 10.1038/boneres.2014.11

48. Wang J, Fu Q, Yang J, Liu JL, Hou SM, Huang X, et al. RNA N6-methyladenosine demethylase FTO promotes osteoporosis through demethylating Runx2 mRNA and inhibiting osteogenic differentiation. *Aging (Albany NY)* (2021) 13(17):21134–41. doi: 10.18632/aging.203377

49. Jin M, Song S, Guo L, Jiang T, Lin ZY. Increased serum GDF11 concentration is associated with a high prevalence of osteoporosis in elderly native Chinese women. *Clin Exp Pharmacol Physiol* (2016) 43(11):1145–7. doi: 10.1111/1440-1681.12651

50. Lu Q, Tu ML, Li CJ, Zhang L, Jiang TJ, Liu T, et al. GDF11 inhibits bone formation by activating Smad2/3 in bone marrow mesenchymal stem cells. *Calcif Tissue Int* (2016) 99(5):500–9. doi: 10.1007/s00223-016-0173-z

51. Liu W, Zhou L, Zhou C, Zhang S, Jing J, Xie L, et al. GDF11 decreases bone mass by stimulating osteoclastogenesis and inhibiting osteoblast differentiation. *Nat Commun* (2016) 7:12794. doi: 10.1038/ncomms12794

52. Patil DP, Chen CK, Pickering BF, Chow A, Jackson C, Guttman M, et al. m(6)A RNA methylation promotes XIST-mediated transcriptional repression. *Nature* (2016) 537 (7620):369–73. doi: 10.1038/nature19342

53. Xiao N, Jani K, Morgan K, Okabe R, Cullen DE, Jesneck JL, et al. Hematopoietic stem cells lacking Ott1 display aspects associated with aging and are unable to maintain quiescence during proliferative stress. *Blood* (2012) 119(21):4898–907. doi: 10.1182/blood-2012-01-403089

54. Chen X, Ma F, Zhai N, Gao F, Cao G. Long noncoding RNA XIST inhibits osteoblast differentiation and promotes osteoporosis *via* Nrf2 hyperactivation by targeting CUL3. *Int J Mol Med* (2021) 48(1). doi: 10.3892/ijmm.2021.4970

55. Brunetti G, Storlino G, Oranger A, Colaianni G, Faienza MF, Ingravallo G, et al. LIGHT/TNFSF14 regulates estrogen deficiency-induced bone loss. *J Pathol* (2020) 250 (4):440–51. doi: 10.1002/path.5385

56. Bhadricha H, Patel V, Singh AK, Savardekar L, Patil A, Surve S, et al. Increased frequency of Th17 cells and IL-17 levels are associated with low bone mineral density in postmenopausal women. *Sci Rep* (2021) 11(1):16155. doi: 10.1038/s41598-021-95640-0

57. Zhu L, Hua F, Ding W, Ding K, Zhang Y, Xu C. The correlation between the Th17/Treg cell balance and bone health. *Immun Ageing* (2020) 17:30. doi: 10.1186/s12979-020-00202-z

58. Lee B, Oh Y, Jo S, Kim TH, Ji JD. A dual role of TGF-beta in human osteoclast differentiation mediated by Smad1 versus Smad3 signaling. *Immunol Lett* (2019) 206:33–40. doi: 10.1016/j.imlet.2018.12.003

59. Bozec A, Zaiss MM. T Regulatory cells in bone remodelling. *Curr Osteoporos Rep* (2017) 15(3):121–5. doi: 10.1007/s11914-017-0356-1

Frontiers in Endocrinology

Chronic airway disease as a major risk factor for fractures in osteopenic women: Nationwide cohort study

Sung Hye Kong[1,2†], Ae Jeong Jo[3†], Chan Mi Park[4], Kyun Ik Park[4], Ji Eun Yun[4*] and Jung Hee Kim[2,5*]

[1]Department of Internal Medicine, Seoul National University Bundang Hospital, Seongnam, Republic of Korea, [2]Department of Internal Medicine, Seoul National University College of Medicine, Seoul, Republic of Korea, [3]Department of Information Statistics, Andong National University, Kyongbuk, Republic of Korea, [4]Department of Health Technology Assessment, National Evidence-Based Healthcare Collaborating Agency (NECA), Seoul, Republic of Korea, [5]Department of Internal Medicine, Seoul National University Hospital, Seoul, Republic of Korea

Introduction: The study aimed to demonstrate the risk factors for fractures and to develop prediction models for major osteoporotic and hip fractures in osteopenic patients using the nationwide cohort study in South Korea.

Methods: The study was a retrospective nationwide study using the national screening program for transitional ages from the National Health Insurance Services database in Korea from 2008 to 2019. Primary outcomes were incident fracture events of major osteoporotic and hip fractures. Major osteoporotic and hip fracture events were defined as diagnostic and procedural codes. Patients were followed until the fragility fractures, death, or 2019, whichever came first.

Results: All participants were 66-year-old females, with a mean body mass index was $25.0 \pm 3.1 \, kg/m^2$. During a median follow-up of 10.5 years, 26.9% and 6.7% of participants experienced major osteoporotic and hip fractures. In multivariate analysis, a history of fracture, chronic airway disease, falls, diabetes mellitus and cerebrovascular diseases were significant risk factors for major osteoporotic (hazard ratio [HR] 2.35 for a history of fracture; 1.17 for chronic airway disease; 1.10 for falls; 1.12 for diabetes mellitus; 1.11 for cerebrovascular disease) and hip fractures (HR 1.75 for a history of fracture; 1.54 for diabetes mellitus; 1.27 for cerebrovascular disease; 1.17 for fall; 1.15 for chronic airway disease). The performances of the prediction models were area under the receiver operating curve of 0.73 and 0.75 for major osteoporotic and hip fractures.

Conclusion: The study presented prediction models of major osteoporotic and hip fractures for osteopenia patients using simple clinical features.

Introduction

The treatment is cost-effective for patients with osteoporosis, defined according to the World Health Organization criterion, with low bone mineral density (BMD T-score of -2.5 or less), or a history of a fragility fracture, as previously reported (1). However, there is little consensus on when to start treatment in patients with osteopenia. Osteopenia, a subclinical condition of low bone mass with a T-score between -1.0 and -2.5, is significantly more common than osteoporosis in South Korea and the US and accounts for more than half of patients with fragility fractures (2–4). Considering these factors, some patients with osteopenia may warrant treatment, and it is also essential to determine the high-risk patients among them.

Thus, there is a practical need for an individualized assessment of fracture risk in patients with osteopenia. Although the fracture risk assessment tool (FRAX) and Garvan fracture risk models help to predict fracture risk (5), they tend to underestimate the risk in low-risk patients in some studies (5–8). Furthermore, while various diseases such as secondary osteoporosis are included as risk factors in FRAX, chronic diseases such as cardiovascular and cerebrovascular diseases, type 2 diabetes mellitus, and a history of falls, which are critical risk factors for fractures, were not included. In addition, bone density alone offers limited predictive power in osteopenic patients (9). Hence, to identify patients with osteopenia with a high risk of fracture before the bone density worsens, it is necessary to assess known risk factors such as chronic diseases (4, 10). Therefore, it is essential to design a new fracture prediction model and associated risk factors according to fracture types for patients with osteopenia. Herein, the study aimed to identify additional risk factors for fractures and to develop prediction models for major osteoporotic and hip fractures in patients with osteopenia using the nationwide cohort study in South Korea.

Methods

Data source

This retrospective nationwide study was conducted using the information retrieved from National Health Insurance Services (NHIS) database of South Korea from 2008 to 2019. This insurance system by the Korean government covers approximately 97.2% of Korean residents and contains data on healthcare services reimbursed including demographics, diagnoses, prescriptions, diagnostic or surgical procedures, and medical costs. The national screening program for transitional ages (NSPTA) launched in 2007, by the Korean government, conducts BMD testing for 66-year-old women (11). BMD was primarily measured using dual-energy X-ray absorptiometry (DXA) at the spine or at the femoral neck, if it was not possible to measure at the spine due to vertebral fracture or surgery (12). Every individual was anonymized using a personal identification number, which enabled the longitudinal follow-up. The Institutional Review Board of the National Evidence-based healthcare Collaborating Agency (NECA) (No.NECAIRB20-004) approved the study protocol, and the requirement for informed consent was waived-off as the patient

information was anonymized. The study was funded by the National Research Foundation of Korea (NRF) and NECA.

Study population

A total of 236,582 individuals received NSPTA health examinations at the age of 66 between January 1, 2008, and December 31, 2009. They were followed up until December 31, 2019, to ensure a maximum of 10 years of follow-up. Among them, 91,268 individuals diagnosed with osteopenia were initially selected. From the selected individuals, 26,780 who received treatment for osteoporosis during follow-up (bisphosphonate, denosumab, teriparatide, or romosozumab), 541 who received treatment for osteoporosis before the screening, and 1,133 without test results due to system error were excluded from the study. A total of 62,814 individuals were included in the final analysis set (Figure 1). The study participants were randomly split into 7:3 training and test sets. The cohort entry date was defined as the date of BMD screening. A year prior to the entry date of the cohort was used to determine study eligibility and baseline clinical characteristics.

Operational definition of primary outcomes and comorbidities

The major osteoporotic and hip fractures events, defined by the diagnostic codes of the 10th version of the International Classification of Diseases (ICD-10), occurred during the follow-up period were considered the primary outcomes. The major osteoporotic fracture events were defined as hospital visits of ≥2 times due to the diagnostic codes (S22.0, S22.1, S32.0, M48.4, M48.5, S42.2, S42.3, S52.5, and S52.6) from admission or outpatient department after the index date or hip fracture. Hip fracture events were defined as more than one hospital visits due to the diagnostic codes (S72.0, S72.1) from admission or outpatient department with more than one treatment codes (N0601, N0611, N0305, N0981, N0641, N0652, N0654, N0711, N0715) after the index date. The follow up period was from the date of cohort entry to the occurrence of fragility fractures, death, or end of the study period (December 31, 2019), whichever came first.

Body mass index (BMI) was measured at their entry date. The history of falls, social history (smoking and drinking), and physical activity information was collected using the standardized self-administered questionnaires. Ever smoker was defined as the participants who were ex-smokers and current smokers and drinker as participants who drank alcohol more than once per week.

Physical activity at baseline examination was analyzed using the International Physical Activity Questionnaire (IPAQ), which assessed three domains: the mode, frequency, and intensity of the activity. The survey questionnaire included the number of days of physical activity in a week during the past six months. Physical activity of at least 30 min/day was categorized based on the frequency of the activity (times/week) as 0 times/week: Q1, 1-2 times/week: Q2, 3-5 times/week: Q3, 6-7 times/week: Q4.

Additionally, it was classified based on the intensity of the activity (walking, moderate, or vigorous). Moderate physical activity was defined as a slight increase in breathing or heart rate or fairly-hard perceived exertion, such as carrying light loads, slow cycling, and fast walking. Vigorous physical activity was defined as a substantial increase in breathing or heart rate or in moderately-hard perceived exertion, such as carrying heavy loads, fast cycling, running, mountain climbing, playing soccer, or any other activity. Moderate-to-vigorous physical activity was defined in this study as moderate or vigorous physical activity more than once/week during the past 6 months.

History of fractures, diabetes mellitus, cardiovascular diseases, cerebrovascular diseases, chronic renal failure, and chronic airway diseases (asthma/chronic obstructive pulmonary diseases (COPD)) were determined by diagnostic codes. To ensure an accurate diagnosis, diabetes mellitus (E10-E14), cardiovascular diseases (I20-I22), cerebrovascular diseases (I63, I64, I693, I694, G45, I60-62, I690-692), chronic renal failure (N183, N184, N185, N258, Z491, Z492, Z940), and chronic airway disease including asthma/COPD (J45) were regarded as present if a participant was treated ≥2 times. Steroid users were defined as participants who had chronic exposure to glucocorticoids (≥5 mg of prednisolone-equivalent steroid/day for ≥3 months). Secondary causes for osteopenia were defined as type 1 diabetes, osteogenesis imperfecta in adults, hyperthyroidism, hypogonadism, premature menopause (<45 years), chronic malnutrition, malabsorption, and chronic liver disease (5).

Additionally, laboratory findings such as hemoglobin and liver enzymes levels were considered risk factors for osteoporotic fractures. Quality control procedures of laboratory data complied with the Korean Association of Laboratory Quality Control guidelines. Hemoglobin levels were categorized as desirable (≥15.5 g/dL), borderline-low (12–15.49 g/dL), and low (<12 g/dL). Gamma glutamate transferase (GGT) values were classified as normal (<35 U/L), and abnormal (≥35 U/L). Total cholesterol values were classified as normal (≤200 mg/dL), and abnormal (>200 mg/dL).

Statistical analyses

The cohort data was randomly stratified into two groups: 70% random sampling for the model development and 30% for validation. Continuous data were presented as mean ± standard deviation, and categorical data were reported as actual numbers (%). Participant characteristics in both groups were compared using Student's t-test for continuous variables and the χ^2 test for categorical variables. The risk factors considered in the initial model were body mass index, history of falls, smoking status, alcohol drinking, physical activity, comorbidity, history of fractures, concomitant drugs used, and laboratory data, including hemoglobin, cholesterol, and GGT levels. Univariate analyses were used to regress the sub-distribution hazard of osteoporotic fracture incidence on all candidate variables.

Cox proportional hazard regression models were used to estimate β coefficient, hazard ratios (HRs), and 95% confidence intervals (CIs) of major osteoporotic and hip fractures, considering death as a competing risk using the Fine and Gray model (13). Variable selection was performed using a multivariate model to build a risk prediction model. The Cox models assigned risk scores based on HR for each risk factor. Considering significant covariates from univariate analysis and variables with clinical importance, three models confirmed to fit through the Hosmer-Lemeshow test, a statistical test for the fit of the model (Supplementary Tables 1, 2). Among them, the model with the highest discriminatory power, assessed by the area under the receiver operating curve (AUROC) was selected. The predictive models were estimated by applying the risk function calculated through the cumulative incidence curve. Survival time was calculated from cohort entry until the occurrence of primary outcomes or until December 31, 2019, whichever came first. The performance of the developed model was tested through the validation dataset. All analyses were conducted using SAS, version 9.4 (SAS Institute Inc., Cary, NC) and R, version 3.4.3 (R Foundation for Statistical Computing, Vienna, Austria).
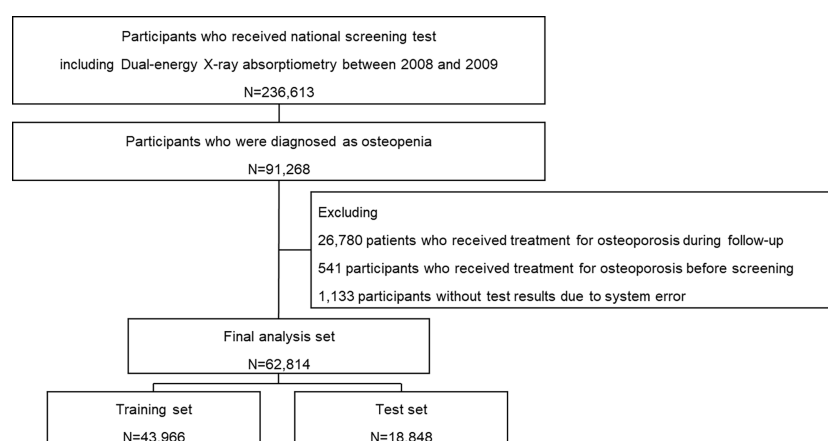

FIGURE 1
Selection of study participants.

Results

Clinical characteristics

The clinical characteristics of 62,814 participants (training set: 43,966 and test set: 18,848) are presented in Table 1. All the participants were 66-year-old females with a mean body mass index of 25.0 ± 3.1 kg/m^2. Among them, 6,613 (10.5%) experienced falls and 1,332 (2.1%) had a history of osteoporotic fractures and 27,637 (24.4%) did moderate-to-vigorous physical activity. The frequency of the participants with co-morbidities at the baseline were: diabetes mellitus (24.4%), cardiovascular diseases (9.1%), cerebrovascular diseases (5.7%), cancer (2.3%), chronic renal failure (0.3%), and chronic airway disease (8.9%). Among the participants, 786 (1.2%) were long-term steroids users. The baseline characteristics were similar between training and test sets. During a median follow-up of 10.5 years (range 1.0–12.0), major osteoporotic and hip fracture events occurred in 17,265 (26.9%) and 4,284 (6.7%) cases, respectively (Supplementary Figure 1).

Factors associated with major osteoporotic and hip fractures

The participants with a history of falls had 1.23 and 1.38-times increased risk and with a history of a previous fracture had 2.33 and 2.25-times higher risk, for major osteoporotic and hip fractures (Table 2). A high level of GGT increased risk of both major osteoporotic and hip fractures. Diabetes mellitus, cardiovascular and cerebrovascular diseases, chronic airway disease, secondary causes for osteopenia, and use of steroids, were other common risk factors.

The participants with a history of drinking had increased risk of major osteoporotic fractures. In addition, participants who had low physical activity in their daily routine had an increased risk of major osteoporotic fracture than those with low physical activity, but were not associated with hip fractures. Participants with chronic kidney disease also had an increased risk of hip fractures. However, history of drinking, moderate-to-vigorous physical activity, and history of chronic kidney diseases were found to be insignificant in multivariate analysis.

TABLE 1   Clinical characteristics of patients with osteopenia.

	Total		Training set		Test set		p
	(n=62,814)		(n=43,996)		(n=18,848)		
Body mass index	25.0	± 3.1	25.0	± 3.1	25.0	± 3.1	0.406
Ever smoker	1,271	(2.0)	893	(2.0)	378	(2.0)	0.834
Current drinker	6,853	(10.9)	4,797	(10.9)	2,056	(10.9)	0.993
Low physical activity	35,177	(56.0)	24,651	(56.0)	10,556	(56.0)	0.989
History of fall	6,613	(10.5)	4,612	(10.5)	2,001	(10.6)	0.635
Diabetes mellitus	15,329	(24.4)	10,668	(24.3)	4,661	(24.7)	0.213
Cardiovascular disease	5,736	(9.1)	4,045	(9.2)	1,691	(9.0)	0.362
Cerebrovascular disease	3,608	(5.7)	2,527	(5.7)	1,081	(5.7)	0.951
Chronic kidney disease	212	(0.3)	142	(0.3)	70	(0.4)	0.337
Epilepsy	439	(0.7)	309	(0.7)	130	(0.7)	0.856
Dementia	659	(1.0)	458	(1.0)	201	(1.1)	0.780
Chronic airway diseases	5,631	(9.0)	3,951	(9.0)	1,680	(8.9)	0.768
Idiopathic hypercalciuria	213	(0.3)	137	(0.3)	76	(0.4)	0.070
Secondary causes for osteopenia	2,164	(3.4)	1,499	(3.4)	665	(3.5)	0.454
History of fracture	1,332	(2.1)	935	(2.1)	397	(2.1)	0.871
Use of steroid	786	(1.3)	555	(1.3)	231	(1.2)	0.704
Hemoglobin, mg	12.9	± 1.1	12.9	± 1.1	12.9	± 1.1	0.273
Total cholesterol, mg/dL	206.1	± 42.9	206.1	± 40.3	206.2	± 48.4	0.785
γ-GGT, mg/dL	26.3	± 30.3	26.3	± 30.9	26.1	± 28.6	0.465

GGT, Glutamyl transpeptidase. Every patient was 66-year-old woman due to the date characteristics. Low physical activity was defined as patients who do not have moderate or vigorous physical activity during the past 6 months. Chronic airway diseases include asthma or chronic obstructive pulmonary disease. Use of steroids was defined as patients who have been exposed to oral glucocorticoids for more than 3 months at a dose of prednisolone of 5mg daily or more during the past year. Continuous variables are expressed as mean ± standard deviation and categorical variables as numbers (percentages). Comparisons between groups were analyzed by Student t-test for continuous variables and χ^2 test for categorical variables.

Prediction models for major osteoporotic and hip fractures in osteopenia

The variables that showed statistical significance in univariate analysis were introduced into multivariate analysis to develop the prediction models (Supplemental Tables 1, 2). In the multivariate analysis, a history of fracture (HR=2.35, 95% CI=2.14–2.58), chronic airway disease (HR=1.17, 95% CI=1.12–1.24), fall (HR=1.10, 95% CI=1.04–1.16), diabetes mellitus (HR=1.12, 95% CI=1.08 – 1.16), and cerebrovascular disease (HR=1.11, 95% CI 1.03–1.19) showed significance. After the selection process to derive the model with the best performance, a history of fracture, chronic airway disease, fall, diabetes mellitus, and cerebrovascular diseases remained major contributing factors (Table 3). The model showed AUROCs of 0.732 and 0.726 in training and test sets, respectively.

$$h(t) = h_0(t)e \quad (0.130 \times history \ of \ fall + 0.125$$
$$\times \ diabetes \ mellitus + 0.099$$
$$\times \ cerebrovascular \ disease + 0.180$$
$$\times \ chronic \ airway \ disease + 0.850$$
$$\times \ history \ of \ fracture),$$

where $h_0(10)=0.279$.

The multivariate analysis for hip fracture showed significance for a history of fracture (HR=1.75, 95% CI=1.46–2.10), diabetes mellitus (HR=1.54, 95% CI=1.43–1.65), smoking (HR=1.25, 95% CI=1.01–1.53), cerebrovascular disease (HR=1.27, 95% CI=1.12–1.43), fall (HR=1.17, 95% CI=1.06–1.30), and chronic airway disease (HR=1.15, 95% CI=1.04–1.28). After the selection process to derive the model with the best performance, a history of fracture, diabetes mellitus, cerebrovascular disease, chronic airway disease, and falls remained major contributing factors for hip fractures (Table 4). The model showed AUROCs of 0.743 and 0.745 in training and test sets, respectively.

$$h(t) = h_0(t)e \quad (0.175 \times history \ of \ fall + 0.407$$
$$\times \ diabetes \ mellitus + 0.228 \times cerebrovascular \ disease$$
$$+ 0.193 \times chronic \ airway \ disease + 0.656$$
$$\times \ history \ of \ fracture),$$

where $h_0(10)=0.064$.

Discussion

The data from the Korean nationwide cohort of 66-year-old women with osteopenia, showed that 26.9% and 6.7% of the

TABLE 2 Risk factors for major osteoporotic and hip fractures in osteopenia patients.

Variables	Major osteoporotic fracture				Hip fracture			
	HR	95% CI		p	HR	95% CI		p
		Lower	Higher			Lower	Higher	
BMI < 18.5 kg/m^2	Ref				Ref			
≥ 18.5, <25 kg/m^2	0.89	0.75	1.06	.206	1.13	0.78	1.64	.499
≥ 25 kg/m^2	0.91	0.76	1.08	.299	1.27	0.88	1.84	.197
Ever smoker	1.12	0.99	1.25	.051	1.36	1.12	1.66	.001
Current drinker	1.08	1.03	1.14	.001	1.15	1.04	1.27	.003
Moderate-to-vigorous physical activity	Ref				Ref			
Low physical activity	1.04	1.01	1.08	.006	0.94	0.88	1.00	.091
History of fall	1.22	1.16	1.29	<.001	1.27	1.16	1.40	<.001
Diabetes mellitus	1.15	1.11	1.19	<.001	1.55	1.45	1.66	<.001
Cardiovascular disease	1.08	1.03	1.15	.002	1.25	1.13	1.39	<.001
Cerebrovascular disease	1.13	1.06	1.21	<.001	1.36	1.20	1.53	<.001
Chronic kidney disease	0.99	0.73	1.34	.969	1.77	1.13	2.75	.011
Epilepsy	1.19	0.99	1.43	.063	1.39	0.99	1.94	.051
Dementia	1.20	1.03	1.40	.018	1.28	0.96	1.70	.090
Chronic airway diseases	1.20	1.14	1.27	<.001	1.25	1.13	1.39	<.001
Idiopathic hypercalciuria	1.17	0.87	1.55	.281	1.52	0.94	2.44	.082

(Continued)

TABLE 2 Continued

Variables	Major osteoporotic fracture				Hip fracture			
	HR	95% CI		p	HR	95% CI		p
		Lower	Higher			Lower	Higher	
Secondary causes for osteopenia	1.18	1.08	1.29	<.001	1.23	1.05	1.45	.010
History of fracture	2.45	2.24	2.69	<.001	2.09	1.77	2.47	<.001
Use of steroid	1.61	1.41	1.84	<.001	1.54	1.21	1.96	<.001
Hemoglobin < 12 g/dL	Ref				Ref			
≥ 12, < 15.5 g/dL	1.02	0.83	1.24	.837	0.93	0.64	1.36	.722
≥ 15.5 g/dL	1.08	0.88	1.33	.419	1.00	0.68	1.47	.974
Total cholesterol > 200 mg/dL	Ref				Ref			
≤ 200 mg/dL	0.94	0.91	0.97	<.001	0.95	0.89	1.01	.151
γGTP ≤ 35 mg/dL	Ref				Ref			
> 35 mg/dL	1.05	1.01	1.10	.013	1.16	1.07	1.27	<.001

HR, hazard ratio; CI, confidence interval; GTP, Glutamyl transpeptidase. Low physical activity was defined as patients who do not have moderate or vigorous physical activity during the past 6 months. Chronic airway diseases include asthma or chronic obstructive pulmonary disease. Use of steroids was defined as patients who have been exposed to oral glucocorticoids for more than 6 months at a dose of prednisolone of 5mg daily or more during the past year. Univariate Cox regression analyses were done.

TABLE 3 Prediction model for major osteoporotic fracture in osteopenia patients.

Variables	Beta-coefficient	HR	95% CI	p
History of fracture	0.848	2.34	2.12 – 2.57	<.001
Chronic airway diseases	0.178	1.19	1.13 – 1.26	<.001
History of fall	0.130	1.14	1.08 – 1.20	<.001
Diabetes mellitus	0.127	1.14	1.09 – 1.18	<.001
Cerebrovascular disease	0.101	1.11	1.03 – 1.18	0.004
P for Wald's test	<0.001			
AUC of the training set	0.732			
AUC of the test set	0.726			

HR, hazard ratio; CI, confidence interval; AUC, area under the curve. Cox regression analyses were done. Multivariate analyses were adjusted for history of fracture, asthma/COPD, falls, diabetes mellitus, and cerebrovascular disease.

TABLE 4 Prediction model for hip fracture in osteopenia patients.

Variables	Beta-coefficient	HR	95% CI	p
History of fracture	0.650	1.92	1.62 – 2.27	<0.001
Diabetes mellitus	0.416	1.52	1.41 – 1.63	<0.001
Cerebrovascular disease	0.230	1.26	1.11 – 1.42	<0.001
Chronic airway diseases	0.197	1.22	1.09 – 1.35	<0.001
History of fall	0.171	1.19	1.08 – 1.31	<0.001
P for Wald's test	<0.001			
AUC of the training set	0.743			
AUC of the test set	0.745			

HR, hazard ratio; CI, confidence interval; AUC, area under the curve. Cox regression analyses were done. Multivariate analyses were adjusted for history of fracture, diabetes mellitus, cerebrovascular disease, asthma/COPD, and history of falls.

participants experienced major osteoporotic and hip fracture events during a median follow-up duration of 10.5 years. This study found that a history of fracture, chronic airway disease, falls, diabetes mellitus and cerebrovascular diseases were significant risk factors for major osteoporotic and hip fractures in older women with osteopenia. The prediction models were developed, using the risk factors, for major osteoporotic and hip fractures, and the performances were AUROCs of 0.73 and 0.75 for major osteoporotic and hip fractures without BMD results.

The representative existing fracture prediction models used in patients with osteopenia are FRAX and Garvan (5). Although both FRAX and Garvan models were good prediction models in patients, they tend to underestimate the risk especially for hip fractures in low-risk patients, as reported in previous studies and was also observed in the Korean version of FRAX (5–8, 14). Furthermore, although secondary osteoporosis was included as a risk factor in FRAX, other critical risk factors such as chronic diseases, cardiovascular and cerebrovascular diseases, type 2 diabetes mellitus, and a history of falls are not included. Even though the risk factors for osteopenia and osteoporosis may be similar (4, 10), but how much they contribute to the risk of fracture in patients with osteopenia might differ. In addition, risk factors might show different effect based on the fracture type. For instance, fall is a key risk factor for hip fracture but not for other fractures (15). Therefore, it is clinically advantageous to demonstrate the risk factors in patients with osteopenia for different fracture types, especially the risk factors such as cerebrovascular diseases or chronic airway disease that are relevant but not included in the existing prediction models.

Cerebrovascular disease is one of the major contributing factors to both major osteoporotic and hip fracture prediction models in this study. The risk of hip fracture in stroke patients was reported to be 4-7 times higher than other major osteoporotic fractures (16). Impairments, such as weakness in the lower extremities, imbalance, loss of autonomic and peripheral sensations, visual impairment, and urinary incontinence after a stroke can significantly contribute to the risk of falls (17). Moreover, the elevation of sclerostin, osteoprotegerin, and FGF23 levels may explain the increased risk of both osteoporotic fractures and cerebrovascular events (18–20). Therefore, this study emphasizes the importance of proactive monitoring and treatment of osteoporosis in post-stroke patients and since cerebrovascular diseases greatly impact the increased fracture risk, managing risk factors of cerebrovascular events is vital in patients with osteopenia.

The history of chronic airway disease (asthma/COPD) was incorporated in the final prediction models. chronic airway disease is associated with low BMD at the spine and hip with an increased risk of vertebral and nonvertebral fractures (21), which might be due to inhalation of corticosteroids, commonly used in patients with asthma/COPD. Corticosteroids are known to decrease bone formation and increase bone resorption, and thus increase the risks of fractures (22, 23). In addition, chronic airway disease itself affect bone health owing to chronic and systemic inflammation (24). Previous studies reported that patients with chronic airflow limitation have significantly elevated inflammatory markers, such as tumor necrosis factor-alpha or c-reactive protein, which have a

negative effect on bone (25). Hypercapnia in chronic obstructive lung diseases was associated with increased bone resorption (26). Therefore, this study infers that a history of chronic airway disease could be a valuable risk factor for fracture in patients with osteopenia.

As a major contributing factor, diabetes mellitus, mostly type 2, was included in the final model of both major osteoporotic and hip fractures, with a stronger contribution to hip fractures, which is consistent with other reports (27). This strong contribution might be related to the increased risk of fall caused by autonomic and distal neuropathy, which impairs sensory perception and balance (28). In addition, evidence suggests that impaired insulin metabolism influences bone turnover, leading to decreased bone density and strength (29, 30). Hyperglycemia could lead to increased production of advanced glycosylation end products, which play a vital role in the deterioration of bone quality by inhibiting osteoblastic differentiation (31, 32). Sclerostin levels were substantially increased in patients with diabetes mellitus, associated with inhibition of the Wnt/β-catenin pathway and increased bone fragility (33). Increased cortical porosity, decreased cortical bone strength, obesity, and the effect of antidiabetic medications may be attributed to a higher risk of hip and major osteoporotic fractures (34).

The study did not find obesity or low BMI as a significant risk factor for fractures in women with osteopenia. The association between BMI and fractures is complex and depends on the interaction between BMI and BMD (35). Usually, increased body weight is associated with increased BMD due to the mechanical effect of weight bearing and the metabolic effect of estrogen from adipose tissue (36). However, the effect of obesity on the risk of fractures is controversial (37). In a recent UK Biobank study, an inverted U-shaped association was observed between visceral adipose tissue and risk of fractures in men but not in women (38) which could be attenuated in women due to the differences in the visceral fat distribution and estrogen levels. This partly explains the neutral results observed in this study. On the other hand, low BMI partially correlates with low lean mass, which affects fracture risk (39). However, as this study analyzed only patients with osteopenia, the number of patients with extreme BMI was small. Therefore, BMI might not be a significant factor for fractures in the selected population of older women with osteopenia.

This study has several strengths. This is the largest Asian study on osteopenia confirmed by bone density data. Also, as the data was collected from the nationwide routine health check-up program, it was possible to collect patient information, such as the history of falls, BMI, physical activity, smoking, and drinking, which could not be obtained from the insurance claim database alone. In addition, all participants' reimbursed healthcare use could be obtained. Therefore, follow-up loss due to transfer or referral to different healthcare providers was unlikely to occur. The models developed in the study were developed based on data with a long-term follow-up in a large nationwide population, which made a 10-year fracture prediction model for osteopenia possible.

The study also had several limitations. Only 66-year-old women were included due to the indication for the national health check-up program. Therefore, the model was created without age and gender

information, which may lower the performance. Also, applying the results to high-risk or non-high-risk osteopenia patients, in general, could not be valid since age, sex, and BMD are essential components in the stratification of fracture risks in osteopenia patients. Korean Health Insurance Review and Assessment Service (HIRA) dataset lacks T-score values but only provides in categorical form - normal, osteopenia, or osteoporosis, as the inherent limitation of this dataset, while a more accurate model would be predicted with exact values of bone density. Due to the inherent limitations of the database, we could only present total cholesterol, GTP, and hemoglobin as important laboratory data, while 25-hydroxy vitamin D levels could not be obtained. Although asthma and COPD are different diseases with different etiology, the study analyzed them in combination as chronic airway diseases. Due to the national insurance policy of South Korea, a pulmonary function test (PFT) is necessary to diagnose COPD. However, since PFT may not be readily available in local hospitals, it leads to an excessive diagnosis of asthma even in adult patients because diagnosing asthma does not require PFT according to the policy. Therefore, in a study conducted with the national healthcare database of South Korea, asthma and COPD are often reported as a composite term - asthma/COPD (40–42) because they are hard to distinguish from each other in this unique setting of clinical practice. As the diagnosis of the diseases was operationally defined using diagnostic codes, it could be inaccurate and possibly overestimated. In addition, the information on manufacturer of the DXA machine was not obtain, which could be a major limitation. Since all participants were Korean women, the generalization of the study to other populations should be exercised with caution.

In conclusion, this nationwide cohort study on osteopenia, developed two prediction models of major osteoporotic and hip fractures. The models were developed based on risk factors such as a history of fracture, chronic airway disease, fall, diabetes mellitus, and cerebrovascular disease, with performances of 0.73 and 0.75 in AUROC, respectively. The models have significant clinical importance in the fracture prediction for patients with osteopenia whose fracture burden is rapidly increasing in South Korea and worldwide. However, the prediction models need further validation in external cohorts with various age and gender information.

Data availability statement

Publicly available datasets were analyzed in this study. This data can be found here: National Health Insurance Services (NHIS) database of South Korea.

Ethics statement

The studies involving human participants were reviewed and approved by National Evidence-based healthcare Collaborating Agency. Written informed consent for participation was not required for this study in accordance with the national legislation and the institutional requirements.

Author contributions

SK and AJ equally contributed to this work. SK, All authors read and approved the final version of the manuscript. SK, JY, and JK conceived and designed the study. AJ performed formal analysis. SK wrote the initial draft of the manuscript with assistance from JK. The following drafts were reviewed and edited by SK, AJ, CP, KP, JY, and JK. All authors contributed to the article and approved the submitted version.

Funding

Acknowledgments

The data in the study was open-sourced and was provided by the National Health Insurance Service.

Conflict of interest

The authors declare that the research was conducted in the absence of any commercial or financial relationships that could be construed as a potential conflict of interest.

Publisher's note

All claims expressed in this article are solely those of the authors and do not necessarily represent those of their affiliated organizations, or those of the publisher, the editors and the reviewers. Any product that may be evaluated in this article, or claim that may be made by its manufacturer, is not guaranteed or endorsed by the publisher.

Supplementary material

The Supplementary Material for this article can be found online at: https://www.frontiersin.org/articles/10.3389/fendo.2023.1085252/full#supplementary-material

References

1. Dawson-Hughes B, Tosteson AN, Melton LJ3rd, Baim S, Favus MJ, Khosla S, et al. Implications of absolute fracture risk assessment for osteoporosis practice guidelines in the USA. *Osteoporos Int* (2008) 19(4):449–58. doi: 10.1007/s00198-008-0559-5

2. Ahn SH, Park S-M, Park SY, Yoo J-I, Jung H-S, Nho J-H, et al. Osteoporosis and osteoporotic fracture fact sheet in Korea. *J Bone Metab* (2020) 27(4):281–90. doi: 10.11005/jbm.2020.27.4.281

3. Wright NC, Looker AC, Saag KG, Curtis JR, Delzell ES, Randall S, et al. The recent prevalence of osteoporosis and low bone mass in the united states based on bone mineral density at the femoral neck or lumbar spine. *J Bone Miner Res* (2014) 29(11):2520–6. doi: 10.1002/jbmr.2269

4. Baek YH, Cho SW, Jeong HE, Kim JH, Hwang Y, Lange JL, et al. 10-year fracture risk in postmenopausal women with osteopenia and osteoporosis in south Korea. *Endocrinol Metab (Seoul)* (2021) 36(6):1178–88. doi: 10.3803/EnM.2021.1215

5. Kanis JA, Johnell O, Oden A, Johansson H, McCloskey E. FRAX and the assessment of fracture probability in men and women from the UK. *Osteoporos Int* (2008) 19(4):385–97. doi: 10.1007/s00198-007-0543-5

6. Nguyen TV. Individualized fracture risk assessment: State-of-the-art and room for improvement. *Osteoporos Sarcopenia* (2018) 4(1):2–10. doi: 10.1016/j.afos.2018.03.001

7. Bolland MJ, Siu AT, Mason BH, Horne AM, Ames RW, Grey AB, et al. Evaluation of the FRAX and garvan fracture risk calculators in older women. *J Bone Miner Res* (2011) 26(2):420–7. doi: 10.1002/jbmr.215

8. Dagan N, Cohen-Stavi C, Leventer-Roberts M, Balicer RD. External validation and comparison of three prediction tools for risk of osteoporotic fractures using data from population based electronic health records: retrospective cohort study. *Bmj* (2017) 356:i6755. doi: 10.1136/bmj.i6755

9. Unnanuntana A, Gladnick BP, Donnelly E, Lane JM. The assessment of fracture risk. *J Bone Joint Surg Am* (2010) 92(3):743–53. doi: 10.2106/JBJS.I.00919

10. Cummings SR, Nevitt MC, Browner WS, Stone K, Fox KM, Ensrud KE, et al. Risk factors for hip fracture in white women. study of osteoporotic fractures research group. *N Engl J Med* (1995) 332(12):767–73. doi: 10.1056/NEJM199503233321202

11. Kim HS, Shin DW, Lee WC, Kim YT, Cho B. National screening program for transitional ages in Korea: a new screening for strengthening primary prevention and follow-up care. *J Korean Med Sci* (2012) 27 Suppl(Suppl):S70–5. doi: 10.3346/jkms.2012.27.S.S70

12. Ministry of Health and Welfare of Korea. Enforcement decree of the framework act on health examinations. Available at: https://www.law.go.kr/LSW/eng/engLsSc.do?menuId=2&section=lawNm&query=health+examination&x=0&y=0#liBgcolor02019.

13. Wolbers M, Blanche P, Koller MT, Witteman JC, Gerds TA. Concordance for prognostic models with competing risks. *Biostatistics* (2014) 15(3):526–39. doi: 10.1093/biostatistics/kxt059

14. Kim H, Kim JH, Kim MJ, Hong AR, Choi H, Ku E, et al. Low predictive value of FRAX adjusted by trabecular bone score for osteoporotic fractures in Korean women: A community-based cohort study. *Endocrinol Metab (Seoul)* (2020) 35(2):359–66. doi: 10.3803/EnM.2020.35.2.359

15. Dargent-Molina P, Favier F, Grandjean H, Baudoin C, Schott AM, Hausherr E, et al. Fall-related factors and risk of hip fracture: the EPIDOS prospective study. *Lancet* (1996) 348(9021):145–9. doi: 10.1016/S0140-6736(96)01440-7

16. Batchelor F, Hill K, Mackintosh S, Said C. What works in falls prevention after stroke?: a systematic review and meta-analysis. *Stroke* (2010) 41(8):1715–22. doi: 10.1161/STROKEAHA.109.570390

17. Moylan KC, Binder EF. Falls in older adults: risk assessment, management and prevention. *Am J Med* (2007) 120(6):493. e1–. e6. doi: 10.1016/j.amjmed.2006.07.022

18. Register TC, Hruska KA, Divers J, Bowden DW, Palmer ND, Carr JJ, et al. Sclerostin is positively associated with bone mineral density in men and women and negatively associated with carotid calcified atherosclerotic plaque in men from the African American-diabetes heart study. *J Clin Endocrinol Metab* (2014) 99(1):315–21. doi: 10.1210/jc.2013-3168

19. Arko B, Prezelj J, Kocijancic A, Komel R, Marc J. Association of the osteoprotegerin gene polymorphisms with bone mineral density in postmenopausal women. *Maturitas* (2005) 51(3):270–9. doi: 10.1016/j.maturitas.2004.08.006

20. Ärnlöv J, Carlsson AC, Sundström J, Ingelsson E, Larsson A, Lind L, et al. Serum FGF23 and risk of cardiovascular events in relation to mineral metabolism and cardiovascular pathology. *Clin J Am Soc Nephrol* (2013) 8(5):781–6. doi: 10.2215/CJN.09570912

21. Dam TT, Harrison S, Fink HA, Ramsdell J, Barrett-Connor E. Bone mineral density and fractures in older men with chronic obstructive pulmonary disease or asthma. *Osteoporos Int* (2010) 21(8):1341–9. doi: 10.1007/s00198-009-1076-x

22. Gado M, Baschant U, Hofbauer LC, Henneicke H. Bad to the bone: The effects of therapeutic glucocorticoids on osteoblasts and osteocytes. *Front Endocrinol (Lausanne)* (2022) 13:835720. doi: 10.3389/fendo.2022.835720

23. Koh JW, Kim J, Cho H, Ha YC, Kim TY, Lee YK, et al. Effects of systemic glucocorticoid use on fracture risk: A population-based study. *Endocrinol Metab (Seoul)* (2020) 35(3):562–70. doi: 10.3803/EnM.2020.659

24. Zhang L, Sun Y. Muscle-bone crosstalk in chronic obstructive pulmonary disease. *Front Endocrinol (Lausanne)* (2021) 12:724911. doi: 10.3389/fendo.2021.724911

25. Sin DD, Man SF. Skeletal muscle weakness, reduced exercise tolerance, and COPD: is systemic inflammation the missing link? *Thorax* (2006) 61(1):1–3. doi: 10.1136/thx.2005.044941

26. Dimai HP, Domej W, Leb G, Lau KH. Bone loss in patients with untreated chronic obstructive pulmonary disease is mediated by an increase in bone resorption associated with hypercapnia. *J Bone Miner Res* (2001) 16(11):2132–41. doi: 10.1359/jbmr.2001.16.11.2132

27. Bai J, Gao Q, Wang C, Dai J. Diabetes mellitus and risk of low-energy fracture: a meta-analysis. *Aging Clin Exp Res* (2020) 32(11):2173–86. doi: 10.1007/s40520-019-01417-x

28. Vinik AI, Camacho P, Reddy S, Valencia WM, Trence D, Matsumoto AM, et al. Aging, diabetes, and falls. *Endocr Pract* (2017) 23(9):1117–39. doi: 10.4158/EP171794.RA

29. Thrailkill KM, Lumpkin CKJr., Bunn RC, Kemp SF, Fowlkes JL. Is insulin an anabolic agent in bone? dissecting the diabetic bone for clues. *Am J Physiol Endocrinol Metab* (2005) 289(5):E735–45. doi: 10.1152/ajpendo.00159.2005

30. Starup-Linde J. Diabetes, biochemical markers of bone turnover, diabetes control, and bone. *Front Endocrinol (Lausanne)* (2013) 4:21. doi: 10.3389/fendo.2013.00021

31. Poiana C, Capatina C. Fracture risk assessment in patients with diabetes mellitus. *J Clin Densitom* (2017) 20(3):432–43. doi: 10.1016/j.jocd.2017.06.011

32. Ganeko K, Masaki C, Shibata Y, Mukaibo T, Kondo Y, Nakamoto T, et al. Bone aging by advanced glycation end products: A multiscale mechanical analysis. *J Dent Res* (2015) 94(12):1684–90. doi: 10.1177/0022034515602214

33. Gaudio A, Privitera F, Battaglia K, Torrisi V, Sidoti MH, Pulvirenti I, et al. Sclerostin levels associated with inhibition of the wnt/β-catenin signaling and reduced bone turnover in type 2 diabetes mellitus. *J Clin Endocrinol Metab* (2012) 97(10):3744–50. doi: 10.1210/jc.2012-1901

34. Compston J. Type 2 diabetes mellitus and bone. *J Intern Med* (2018) 283(2):140–53. doi: 10.1111/joim.12725

35. Johansson H, Kanis JA, Odén A, McCloskey E, Chapurlat RD, Christiansen C, et al. A meta-analysis of the association of fracture risk and body mass index in women. *J Bone Miner Res* (2014) 29(1):223–33. doi: 10.1002/jbmr.2017

36. Rinonapoli G, Pace V, Ruggiero C, Ceccarini P, Bisaccia M, Meccariello L, et al. Obesity and bone: A complex relationship. *Int J Mol Sci* (2021) 22(24). doi: 10.3390/ijms222413662

37. Yang S, Shen X. Association and relative importance of multiple obesity measures with bone mineral density: the national health and nutrition examination survey 2005-2006. *Arch Osteoporos* (2015) 10:14. doi: 10.1007/s11657-015-0219-2

38. Hu J, Zhao M, Lin C, Sun Z, Chen GC, Mei Z, et al. Associations of visceral adipose tissue with bone mineral density and fracture: observational and mendelian randomization studies. *Nutr Metab (Lond)* (2022) 19(1):45. doi: 10.1186/s12986-022-00680-6

39. Romero-Corral A, Somers VK, Sierra-Johnson J, Thomas RJ, Collazo-Clavell ML, Korinek J, et al. Accuracy of body mass index in diagnosing obesity in the adult general population. *Int J Obes (Lond)* (2008) 32(6):959–66. doi: 10.1038/ijo.2008.11

40. Kim H, Shin JY, Chen J, Kim JH, Noh Y, Cheong HJ, et al. Risk factors of pertussis among older adults in south Korea: A nationwide health data-based case-control study. *Infect Dis Ther* (2023) 12(2):545–61. doi: 10.1007/s40121-022-00747-0

41. Kim SK, Hong SJ, Yoo DM, Min C, Choi HG. Association between asthma or chronic obstructive pulmonary disease and chronic otitis media. *Sci Rep* (2022) 12(1):4228. doi: 10.1038/s41598-022-08287-w

42. Jung Y, Wee JH, Kim JH, Choi HG. The effects of previous asthma and COPD on the susceptibility to and severity of COVID-19: A nationwide cohort study in south Korea. *J Clin Med* (2021) 10(20). doi: 10.3390/jcm10204626

Check for updates

Deep learning-based artificial intelligence model for classification of vertebral compression fractures: A multicenter diagnostic study

Fan Xu[1†], Yuchao Xiong[1†], Guoxi Ye[1], Yingying Liang[2], Wei Guo[3],
Qiuping Deng[4], Li Wu[1], Wuyi Jia[1], Dilang Wu[1], Song Chen[1],
Zhiping Liang[1] and Xuwen Zeng[1*]

[1]Department of Radiology, Guangzhou Red Cross Hospital (Guangzhou Red Cross Hospital of Jinan
University), Guangzhou, China, [2]Department of Radiology, Guangzhou First People's Hospital,
Guangzhou, Guangdong, China, [3]Department of Radiology, Wuhan Third Hospital, Tongren Hospital
of Wuhan University, Wuhan, Hubei, China, [4]Department of Radiology, Hubei 672 Integrated
Traditional Chinese and Western Medicine Orthopedic Hospital, Wuhan, Hebei, China

Objective: To develop and validate an artificial intelligence diagnostic system based on X-ray imaging data for diagnosing vertebral compression fractures (VCFs)

Methods: In total, 1904 patients who underwent X-ray at four independent hospitals were retrospectively (n=1847) and prospectively (n=57) enrolled. The participants were separated into a development cohort, a prospective test cohort and three external test cohorts. The proposed model used a transfer learning method based on the ResNet-18 architecture. The diagnostic performance of the model was evaluated using receiver operating characteristic curve (ROC) analysis and validated using a prospective validation set and three external sets. The performance of the model was compared with three degrees of musculoskeletal expertise: expert, competent, and trainee.

Results: The diagnostic accuracy for identifying compression fractures was 0.850 in the testing set, 0.829 in the prospective set, and ranged from 0.757 to 0.832 in the three external validation sets. In the human and deep learning (DL) collaboration dataset, the area under the ROC curves(AUCs) in acute, chronic, and pathological compression fractures were as follows: 0.780, 0.809, 0.734 for the DL model; 0.573, 0.618, 0.541 for the trainee radiologist; 0.701, 0.782, 0.665 for the competent radiologist; 0.707,0.732, 0.667 for the expert radiologist; 0.722, 0.744, 0.610 for the DL and trainee; 0.767, 0.779, 0.729 for the DL and competent; 0.801, 0.825, 0.751 for the DL and expert radiologist.

Conclusions: Our study offers a high-accuracy multi-class deep learning model which could assist community-based hospitals in improving the diagnostic accuracy of VCFs.

KEYWORDS

vertebral compression fractures, DL: deep learning, DR: digital radiography, x-ray, CNN

Introduction

Vertebral compression fractures (VCFs) are common diseases that seriously affect human life and pose a very large challenge to the health care system (1). With the rising prevalence of population aging, the occurrence of VCFs due to trauma and osteoporosis is increasing year by year, which increases societal and familial economic burdens. Moreover, pathologic fractures resulting from neoplasms are another leading cause of VCFs worldwide. All types of VCFs foreshadow a high risk of poor outcomes, so early, personalized and effective medical intervention is strongly advised. Therefore, it is desirable to find an accurate and effective method to detect and identify acute, chronic and pathological VCFs.

In recent years, the incidence of back pain due to compression fractures has increased in patients. Many imaging methods are available for early screening and differentiation of compression fractures, such as X-ray (XR) images, Computed tomography (CT) and magnetic resonance imaging (MRI). Among these procedures, CT is the modality of choice for the evaluation of bone structure and fragments. MRI may be the most useful imaging technique based on its excellent soft tissue contrast that shows the change in the signal intensity and morphological characteristics of the collapsed vertebrae. Acute compression fractures show hyperintensity with bone marrow edema, while chronic compression fractures show no bone marrow edema and are isointense on T2WI fat-suppression sequences. The pathologic VCFs shows low signal intensity on T1WI, isointensity or high signal intensity on T2WI, and homogeneous or inhomogeneous enhancement (Figure 1). However, the availability of CT and MRI is limited for overall population diagnosis due to their complexity, high time consuming and high-cost factor (2). In contrast, X-ray images with effective cost and time may be an attractive and widespread method in diagnosis of VCFs, although it could only provide limited detail about 3D anatomy structure or pathology of VCFs.

Deep learning (DL), a branch of machine learning, has already shown potential for assisting humans in various medical fields (3–6). A convolutional neural network(CNN) is a deep learning algorithm that is mainly designed to process image data and has grown to be a fundamental aspect of the medical field (7). In recent years, more and more radiomics model algorithms based on plain X-ray films have been developed in the wrist, humerus, hip, femur, shoulder, hand and foot (8–13). However, very few works are carried out using X-ray -based radiomics to predict VCFs. Recently, Chen et al have developed a DL–based model that distinguish fresh VCFs from digital radiography (DR) with sensitivity, specificity and AUC of 80%, 68% and 0.80

respectively. However, the clinical feasibility and benefit of DL–based model remain to be confirmed because no external and multicenter validation was performed in their study (14).

Thus, the aims of this study were to develop an X-ray-based deep learning model using a four-center dataset and determine whether the model could distinguish the type of VCFs and validate these findings in an independent external cohort.

Materials and methods

Datasets

This multicohort diagnostic study was performed with data from four hospitals in China. This study was approved by the institutional review board and ethics committee of the hospital (IRB 2022-108-01). Our retrospective study was approved by the institutional review board of the hospitals with a waiver for written informed consent. Patients in the prospective validation set of compression fractures provided written informed consent prior to participation.

For the development dataset, we evaluated the medical radiology reports of lumbar spine MRI in *Site 1* from 1 January 2014 to 31 October 2021 to determine acute, chronic, and pathological compression fractures. The inclusion criteria were as follows: (1) less than 2 weeks between Digital radiography (DR) and MRI examinations; and (2) the height of the vertebral body was reduced by at least 20% or 4 mm from the baseline height on the lateral radiography of the lumbar spine (15). The exclusion criteria were as follows: (1) surgical treatment for compression vertebral bodies such as internal fixation or bone cement filling; (2) lumbar spine presenting serious scoliosis or deformity; and (3) images with a low signal-to-noise ratio or foreign matter present.

To verify the applicability of the classified diagnosis deep learning model in clinical practice, from October 1, 2019, to September 31, 2021, lumbar spine lateral X-ray images were also obtained from three hospitals across China: *Site 2*; *Site 3* and *Site 4*. In total, 2609 vertebrae from 1904 participants who underwent X-ray were enrolled at four independent hospitals (Figure 2).

From Nov 1, 2021, an independent dataset of consecutive participants undergoing lumbar spine X-ray in *Site 1* was prospectively enrolled. These participants were defined as the prospective validation set. In total, 74 vertebrae from 57 participants were enrolled at *Site 1* (Figure 2).

Image reading and annotation

Delineated images of acute and chronic compression fractures are based on MRI diagnosis, and pathological compression fractures are diagnosed using MRI, positron emission tomography (PET) or histopathological results. When only MR images are available for a patient, at least two senior diagnosing physicians complete the diagnosis.

Lesion regions of interest (ROIs) were manually represented with bounding boxes on lateral radiographs of the lumbar spine by

---

Abbreviations: VCFs, Vertebral compression fractures; XR, X-ray; CT, Computed tomography; MRI, magnetic resonance imaging; DL, Deep learning; CNN, convolutional neural network; DR, digital radiography; GZFPH, Guangzhou First People's Hospital, School of Medicine, South China University of Technology, Guangzhou; WHTH, Wuhan Third Hospital, Tongren Hospital of Wuhan University, Wuhan; HB672H, Hubei 672 Integrated Traditional Chinese and Western Medicine Orthopedic Hospital, Wuhan; PET, positron emission tomography; ROIs, Lesion regions of interest; ROC, receiver operating characteristic; AUC, area under the ROC curve; PACS, picture archiving and communication systems; CI, confidence interval.
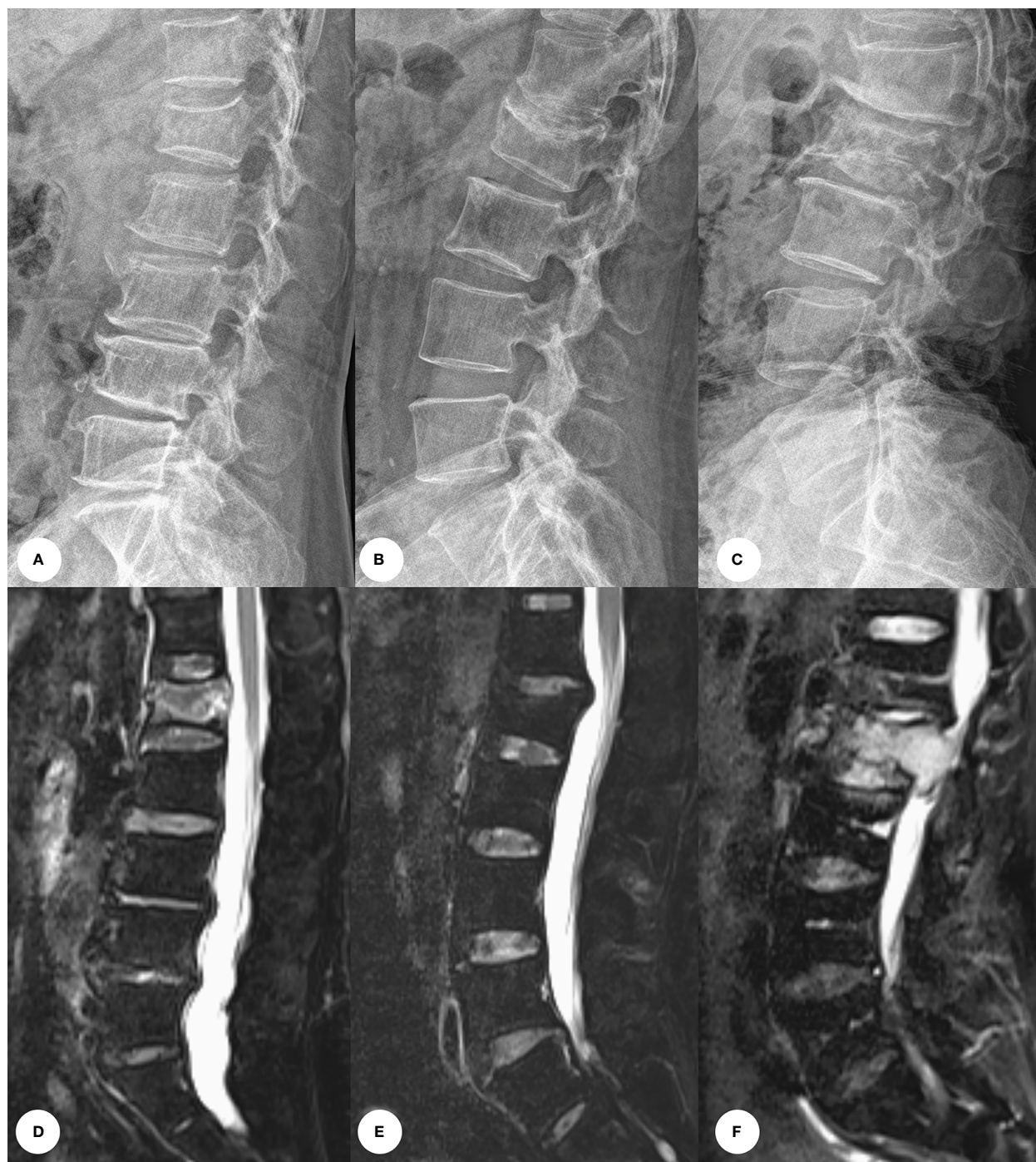
Images of vertebral compression fractures types. **(A, D)** Acute compression fracture of the L1 vertebral; **(B, E)** Chronic compression fracture of the L1 vertebral; **(C, F)** Pathologic compression fracture of the L2 vertebral.

an experienced radiologist using the LabelImg software (https://pypi.org/project/labelImg/) and annotated (224×224) (Figure 3).

Model training

The images from the development dataset were randomly assigned with a ratio of 8:2 for the training datasets (the deep learning model for compression fracture classification) and the testing datasets (for evaluating the performance of the deep learning model). The image of the training set was enhanced, using horizontal flips, vertical flips, and rotations at random angles.

ResNet is a type of CNN where the input from the previous layer is added to the output of the current layer. This skip connection makes it easier for the network to learn and brings better performance. The ResNet architecture has been successful in
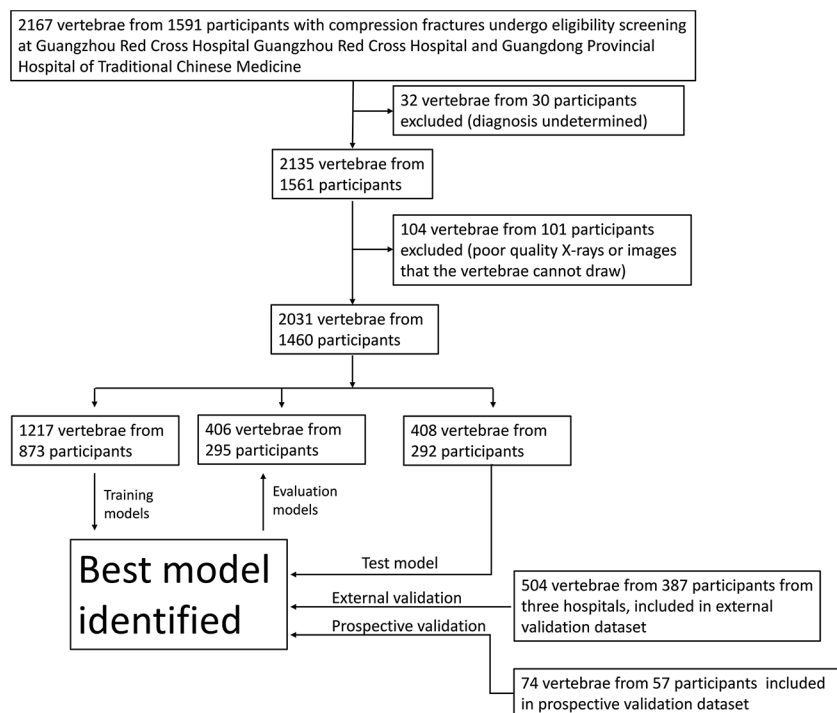
FIGURE 2
Workflow diagram for the development and evaluation of the deep learning model for compression fracture classification.

many tasks, including image classification, objection detection, and semantic segmentation. In addition, because ResNet is composed of layers, these networks can obtain any level of spatial representation at any depth. Each ResNet block has 2 convolutional layers (excluding the 1×1 onvolutional layer), and we connect these two residual blocks as a module. We use 4 such modules, so there are a total of 16 convolutional layers (Figure 4). Together with the first

7×7 onvolutional layer and the final fully connected layer, there are 18 convolutional layers in total, which is ResNet-18 (16).

In this study, we used the ResNet-18 architecture model, and the input image was resized to 224 × 224 pixels and was normalized with mean= [0.485,0.456,0.406] and std= [0.229,0.224,0.225]. We then fine-tuned the model using a dataset of lateral lumbar spine radiographs of acute, chronic, and
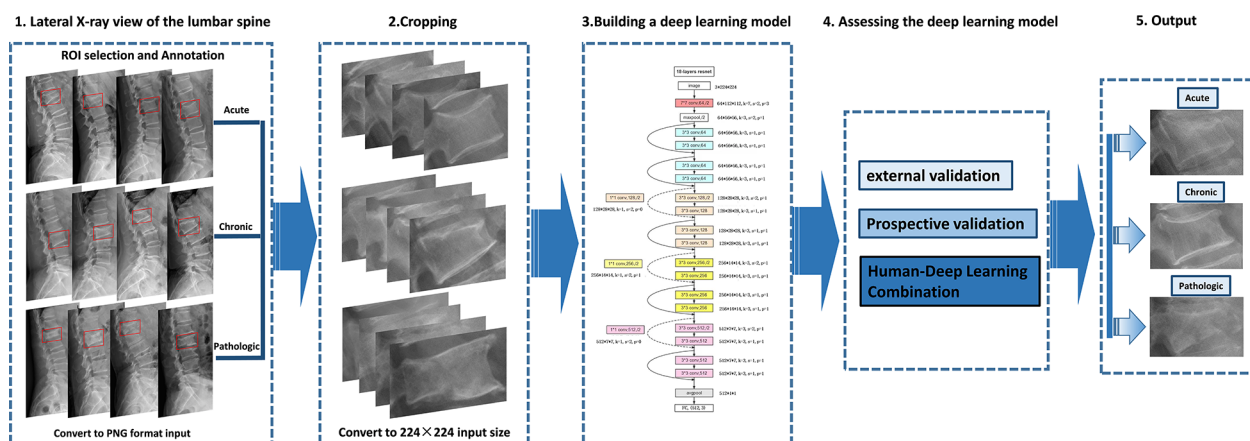

FIGURE 3
Deep learning architecture overview. First (step 1), compression fractures were reliably delineated and annotated on radiographs using labelImg software. For the step, the radiograph was converted to PNG format. Then (step 2), the cropped lateral X-ray of the lumbar spine was resized to 224×224 pixels and used as the input for a deep learning model. The third step (step 3) is to build a compression fracture classification model based on the Resnet-18 algorithm. Model performance was evaluated using external and prospective data and further validated using a radiologist-deep learning combination (step 4). As a result, we can provide adjunctive evaluation of lumbar compression fractures (acute, chronic, and pathological) (step 5).
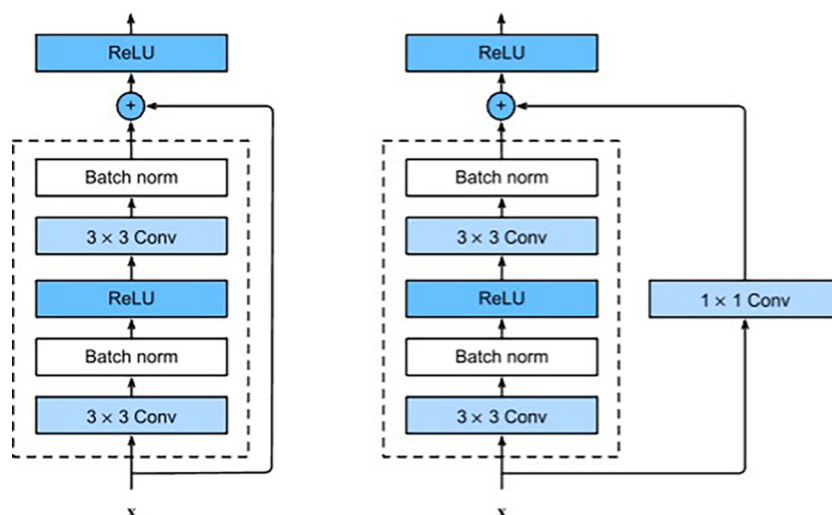
FIGURE 4
ResNet block with and without 1×1 onvolution, which transforms the input into the desired shape for the addition operation.

pathological compression fractures. Codes are available at https://github.com/Xiongyuchao/VCFNet.

Validation of the model

We first validated the performance of the model in classifying VCFs using the testing dataset. We then evaluated the robustness of this model using an external validation dataset from three participating hospitals. Finally, the model was evaluated using prospective data including 74 vertebrae of 57 patients from *Site 1*.

Validation of the radiologists' visual diagnoses combined with DL-model based on collaboration dataset

In addition to the classification research of independent observers, the collaborative research of human and deep learning was also carried out to simulate a real clinical setting. We randomly selected 30% of the images from all external validation sets as the "collaboration dataset". Three radiologists with different levels of expertise (trainee, competent, and expert) were asked to independently complete the same test images and compare their results with those of the model. Then the three radiologists reevaluated all the same test images independently after knowing the DL-model diagnosis. These radiologists were not involved in the selection and labeling of images, and the images were obfuscated and unidentified prior to evaluation. The expert radiologist was a professor with more than 20 years of experience in musculoskeletal diagnosis. The competent radiologist was a radiologist with 7 years of experience and completed standardized training for practicing physicians. The trainee is a radiologist with 2 years of experience and obtained the qualification certificate of a licensed doctor.

Statistical analysis

All computer codes used for data analysis are stored in GitHub (https://github.com/Xiongyuchao/VCFNet). We used receiver operating characteristic (ROC) curves to demonstrate the ability of deep learning algorithms to classify VCFs. An ROC curve is generated by plotting the ratio of true positive cases (sensitivity) to false positive cases (1-specificity) by varying the predicted probability threshold. A larger area under the ROC curve (AUC) indicates better diagnostic performance.

Results

VCF and clinical datasets

Table 1 provides an overview of the participant characteristics and the VCF classification data. 1003 vertebrae of acute compression fractures, 861 vertebrae of chronic compression fractures, and 167 vertebrae of pathologic vertebrae were included in the development dataset. In addition, 504 vertebrae from 387 participants were used to test the deep learning classification model at three external participating hospitals, and 74 vertebrae from 57 participants were prospectively collected at *Site 1* for the prospective validation dataset (Figure 2).

Establishment of deep learning model

After 25 epochs, the training procedure was ended, with no further improvement in accuracy and cross-entropy loss on training, and testing. An accuracy of up to 95.9% was observed in the training set and 77.7% in the testing set (Appendix).

TABLE 1   Patient characteristics.

	Development Dataset		External validation			Prospective dataset	P value
	Training dataset	Testing dataset	GZFPH dataset	WHTH dataset	HB672H dataset		
No. of vertebral readings	1623	408	111	217	176	74	
No. of Patients	1168	292	97	147	143	57	
Age (years)	72.93±13.56	74.10±12.82	71.86±12.29	71.41±15.31	71.98±13.87	73.84±15.87	P<0.05
Sex							P<0.05
Male	365	92	32	65	61	13	
Female	803	200	65	82	83	44	
Compression fracture classification							
Acute	802	201	62	113	94	38	
Chronic	688	173	40	95	57	31	
Pathologic	133	34	9	9	25	5	

GZFPH, Guangzhou First People's Hospital; WHTH, Wuhan Third Hospital; HB672H, Hubei 672 Integrated Traditional Chinese and Western Medicine Orthopaedic Hospital.

Deep learning model performance on the VCF test set

Table 2 shows the performance of the deep learning model in the classification of compression fractures in all five testing sets (Figure 5). Classification accuracies were 0.850 for the testing dataset and 0.829 for the prospective validation dataset. Classification accuracies for the external validation were 0.832 for *Site 2*, 0.757 for *Site 3*, and 0.792 for *Site 4*. Using the proposed model to assess the ability of each compression classification, the AUCs in acute, chronic, and pathological compression fractures were as follows: 0.874 (95% CI: 0.873, 0.875), 0.899 (95% CI: 0.898, 0.900) and 0.935 (95% CI: 0.935, 0.937) in the testing dataset, respectively; 0.803 (95% CI: 0.801, 0.806), 0.906 (95% CI: 0.905, 0.909) and 0.769 (95% CI: 0.771, 0.780) in the GZFPH dataset, respectively; 0.779 (95% CI: 0.777, 0.781), 0.798 (95% CI: 0.796, 0.800) and 0.903 (95% CI: 0.900, 0.907) in the WHTH dataset; 0.807 (95% CI: 0.805, 0.809), 0.836 (95% CI: 0.834, 0.838) and 0.796 (95% CI: 0.793, 0.800) in the HB672H dataset, respectively.

Human and deep learning collaboration

In the human and deep learning collaboration dataset, 80 vertebrae with acute compression fractures, 57 vertebrae with chronic compression fractures, and 13 vertebrae with pathologic compression fractures were included. The classification results of images from human and deep learning collaboration dataset by the deep learning and radiologists are shown in Table 3. The AUCs in acute, chronic, and pathological compression fractures were as follows: 0.780, 0.809, 0.734 for the deep learning model; 0.573, 0.618, 0.541 for the trainee radiologist; 0.701, 0.782, 0.665 for the competent radiologist; 0.707, 0.732, 0.667 for the expert radiologist; 0.722, 0.744, 0.610 for the DL and trainee; 0.767, 0.779, 0.729 for the

DL and competent; 0.801, 0.825, 0.751 for the DL and expert radiologist. The overall accuracy of the deep learning model was 0.764, which was significantly higher than that of the trainee radiologist (0.707), similar to the competent radiologist (0.769), and slightly lower than the expert radiologist (0.782). When combined with the deep learning model, the expert, competent, and trainee radiologists' accuracy all increased significantly (0.853, 0.816, and 0.778, respectively). For sensitivity, combined with the deep learning model, the trainee, competent, and expert radiologists also significantly improved (0.560 *vs.* 0.667, 0.653 *vs.* 0.727, and 0.673 *vs.* 0.776, respectively). For the classification of pathological compression fractures, the sensitivity of expert radiologists was up to 0.385 and the deep learning model was only 0.308. However, when combined with the deep learning model, the expert radiologist, competent radiologist, and trainee radiologist all had increased sensitivity to pathological compression fracture (0.385 *vs.* 0.538, 0.462 *vs.* 0.538, and 0.154 *vs.* 0.308, respectively) (Figure 6). In addition, for pathological compression fractures, 6 out of 13 vertebrae were misjudged by all radiologists and the deep learning model.

Discussion

In this multicenter study, we successfully developed a classification model for acute, chronic and pathological compression fractures by using deep learning neural networks. The model demonstrated high accuracy and specificity in classifying compression fractures in retrospectively stored images as well as in a prospective observational setting. Furthermore, the diagnostic efficiency of deep learning model is higher than that of the trainee radiologists, similar to the competent radiologist, and slightly lower than the expert radiologist. The deep learning model combined with all three expertise levels of radiologists

TABLE 2 Performance of the deep learning in different validation sets.

Dataset	AUC	Accuracy (%)	Sensitivity (%)	Specificity (%)	Precision (%)	F1 Score (%)	PPV (%)	NPV (%)
Testing dataset		85.0	77.5	88.7	77.4	77.4	77.5	88.7
Acute	0.874	79.9	78.1	81.6	80.5	79.3	80.5	79.3
Chronic	0.899	82.4	81.5	83.0	77.9	79.7	77.9	86.0
Pathologic	0.935	92.6	52.9	96.3	56.3	54.5	56.3	95.7
GZFPH dataset		83.2	74.8	87.4	75.7	75.2	74.8	87.4
Acute	0.803	75.7	75.8	75.5	79.7	77.7	79.7	71.2
Chronic	0.906	86.5	82.5	88.7	80.5	81.5	80.5	90.0
Pathologic	0.769	87.4	33.3	92.2	27.3	30.0	27.3	94.0
WHTH dataset		75.7	63.6	81.8	66.8	65.2	63.6	81.8
Acute	0.779	64.5	47.8	82.7	75.0	58.4	75.0	59.3
Chronic	0.798	67.7	83.2	55.7	59.4	69.3	59.4	81.0
Pathologic	0.903	94.9	55.6	96.6	41.7	47.6	41.7	98.0
HB672H dataset		79.2	68.8	84.4	68.6	68.7	68.9	84.4
Acute	0.807	73.9	75.5	72.0	75.5	75.5	75.5	72.0
Chronic	0.836	76.1	70.2	79.0	61.5	65.6	61.5	84.7
Pathologic	0.796	87.5	40.0	95.4	58.8	47.6	58.8	90.6
Prospective dataset		82.9	74.3	87.2	76.9	75.6	74.3	87.2
Acute	0.833	77.0	65.8	88.9	86.2	74.6	86.2	71.1
Chronic	0.857	79.7	87.1	74.4	71.1	78.3	71.1	88.9
Pathologic	0.757	91.9	60.0	94.2	42.9	50.0	42.9	97.0

GZFPH, Guangzhou First People's Hospital; WHTH, Wuhan Third Hospital; HB672H, Hubei 672 Integrated Traditional Chinese and Western Medicine Orthopaedic Hospital.

significantly improved the accuracy, specificity, and sensitivity of evaluating compression fractures. To the best of our knowledge, this is the first multicenter study to apply deep learning with CNNs to the classification of acute, chronic, and pathological compression fractures.

Previous studies have used information from radiographs to classify compression fractures. Usually, plain radiographs are initially performed to diagnose acute compression fractures by observing small changes such as endplate rupture and anterior wall protrusion (17) and diagnosis of pathological compression by cortical penetration, trabecular bone destruction, vertebral bone density, and special compression morphology. Although studies of these conventional features have provided guidance for the classification of compression fractures, the information provided by lumbar spine X-rays is limited, and compression fractures can only be simply assessed from morphological and partial imaging signs. The diagnosis of compression fractures, which is subjective and largely depends on the skills and experience of the diagnosing physician, needs to be based on professional knowledge and the accumulation of diagnostic experience to improve the accuracy of diagnosis. CT (18, 19), MRI (19–22), and PET (23) have shown great advantages in the classification of compression fractures, but their clinical applicability has been limited because of patient noncooperation, high costs, and the need for specialized training

in tomographic image interpretation. The proposed deep learning CNN has instead been found to provide auxiliary diagnosis to non-professional radiologists to improve performance (competent from 0.756 to 0.816 and trainee from 0.707 to 0.796) on compression fracture classification, both exceeded the expert level (0.764). The deep learning model demonstrated high accuracy and specificity in classifying compression fractures in retrospectively stored images as well as in a prospective observational setting. Furthermore, the diagnostic efficiency of deep learning model is higher than that of the trainee radiologists, similar to the competent radiologist, and slightly lower than the expert radiologist (Figure 6). The deep learning model combined with all three expertise levels of radiologists significantly improved the accuracy, specificity, and sensitivity of evaluating compression fractures. Thus, for developing countries such as China or countries with scarce medical resources, where there is an unequal distribution of urban and rural medical resources, this deep learning CNN can help bridge the classification of compression fractures between national and primary hospitals. In addition, with deep learning model assistance, the classification accuracy of three radiologists with different levels of experience was also improved significantly.

The classification sensitivity of pathological compression fractures was found to be low for all three radiologists and the deep learning model. Even the combination of all three radiologists
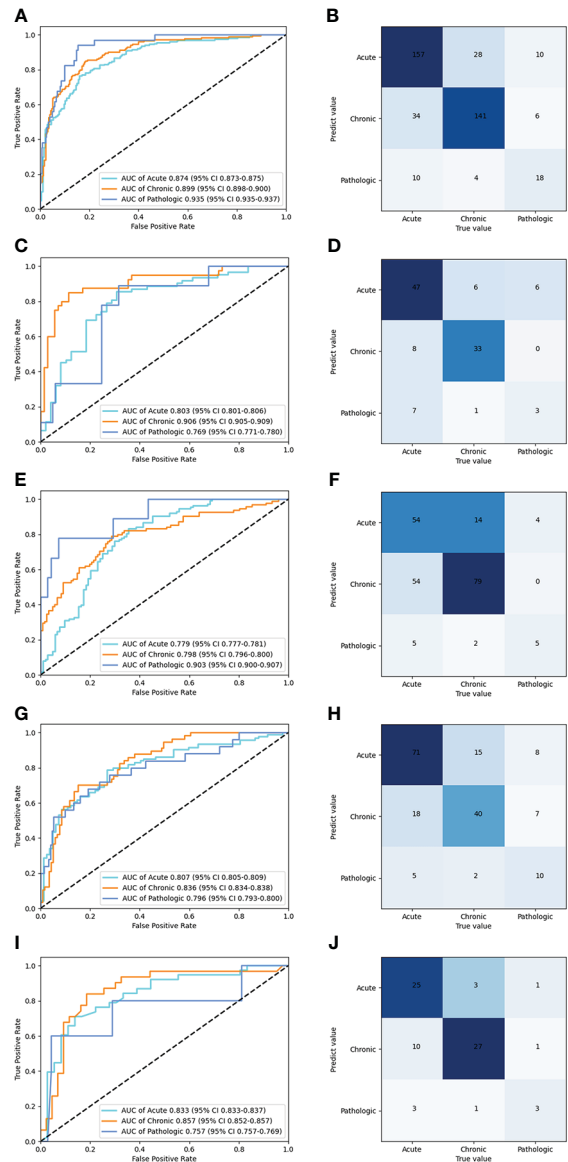
FIGURE 5
Performance of the deep learning model in the classification of acute, chronic, and pathologic compression fracture in X-ray images, in the internal and external validation datasets. ROC **(A)** and normalized confusion matrices **(B)** of the classification mode in the testing dataset. ROC **(C)** and normalized confusion matrices **(D)** of the classification mode in the GZFPH dataset. ROC **(E)** and normalized confusion matrices **(F)** of the classification mode in WHTH dataset. ROC **(G)** and normalized confusion matrices **(H)** of the classification mode in HB672H dataset. ROC **(I)** and normalized confusion matrices **(J)** of the prospective dateset.

TABLE 3 Performance of the deep learning versus radiologists in classifying compression fractures in the human and deep learning collaboration dataset.

Dataset	AUC	Accuracy (%)	Sensitivity (%)	Specificity (%)	Precision (%)	F1 Score (%)	PPV (%)	NPV (%)
Deep learning model		76.4	64.7	82.3	65.0	64.8	64.7	82.3
Acute	0.780	69.3	67.5	71.4	73.0	70.1	73.0	65.8
Chronic	0.809	71.3	68.4	73.1	60.9	64.5	60.9	79.1
Pathologic	0.734	88.7	30.8	94.2	33.3	32.0	33.3	93.5

(Continued)

TABLE 3 Continued

Dataset	AUC	Accuracy (%)	Sensitivity (%)	Specificity (%)	Precision (%)	F1 Score (%)	PPV (%)	NPV (%)
Trainee radiologist		70.7	56.0	78.0	55.7	55.8	56.0	78.0
Acute	0.573	62.0	65.0	58.6	64.2	64.6	64.2	59.4
Chronic	0.618	64.0	52.6	71.0	52.6	52.6	52.6	71.0
Pathologic	0.541	86.0	15.4	92.7	16.7	16.0	16.7	92.0
Competent radiologist		76.9	65.3	82.7	69.9	67.5	65.3	82.7
Acute	0.701	69.3	58.8	81.4	78.3	67.1	78.3	63.3
Chronic	0.782	78.0	78.9	77.4	68.2	73.2	68.2	85.7
Pathologic	0.665	83.3	46.2	86.9	25.0	32.4	25.0	94.4
Expert radiologist		78.2	67.3	83.7	67.4	67.4	67.3	83.7
Acute	0.707	70.7	70.0	71.4	73.7	71.8	73.7	67.6
Chronic	0.732	74.0	70.2	76.3	64.5	67.2	64.5	80.7
Pathologic	0.667	90.0	38.5	94.9	41.7	40.0	41.7	94.2
Deep learning and trainee		77.8	66.7	83.3	67.9	67.3	66.7	83.3
Acute	0.722	72.0	70.0	74.3	75.7	72.7	75.7	68.4
Chronic	0.744	75.3	70.2	78.5	66.7	68.4	66.7	81.1
Pathologic	0.610	86.0	30.8	91.2	25.0	27.6	25.0	93.3
Deep learning and competent radiologist		81.6	72.7	86.0	73.4	73.1	72.2	86.3
Acute	0.767	76.7	76.3	77.1	79.2	77.7	79.2	74.0
Chronic	0.779	79.3	71.9	83.9	73.2	72.6	73.2	83.0
Pathologic	0.729	88.7	53.8	92.0	38.9	45.2	38.9	95.5
Deep learning and expert radiologist		85.3	77.6	89.1	77.4	77.5	77.6	89.1
Acute	0.801	80.0	80.5	79.5	80.5	80.5	80.5	79.5
Chronic	0.825	83.3	78.9	86.0	77.6	78.3	77.6	87.0
Pathologic	0.751	92.7	53.8	96.4	58.3	56.0	58.3	95.7

and the deep learning model was still low. In addition, 6 vertebrae with pathological compression fractures were misdiagnosed by all three radiologists and the deep learning model. We speculate that the main reasons for these false negatives are the low contrast of X-ray images, the fact that there were no obvious signs of bone damage on the vertebral body, intestinal gas interference and bilateral shadows of the vertebral body, which may be an insurmountable limitation caused by the principle of X-ray imaging. However, deep learning model-assisted diagnosis can improve the sensitivity of pathological compression fracture classification, albeit still at a low level. Furthermore, given the high accuracy of classification of acute and chronic compression fractures, deep learning could be considered cost-effective.

There are few studies on compression fractures using deep learning methods, especially based on conventional X-ray images. Only one study used deep learning to evaluate acute and chronic compression fractures on radiographs, which included 1099 patients and used image data from anteroposterior and lateral lumbar spine radiographs as input to a neural network. This study achieved a sensitivity, specificity and AUC of 0.80, 0.68, and 0.80, respectively (14). The clinical applicability of CNN models may be limited as a result of dichotomous disease surveys and retrospective and single-institution studies in homogeneous hospitals. By comparison, the deep learning model of this study demonstrated an overall high accuracy in classifying compression fractures in three retrospective validation sets, suggesting that the model may be generalizable across a variety of scenarios.

Despite these remarkable results, our study has some limitations. First, the subjects who received internal fixation or cementation or who presented with severe scoliosis/deformity were excluded in the development dataset, which may lead to bias. Second, from the nature of CNNs, since a neural network only provides a classification of an image and associated compression fractures, there is no explicit feature definition. Third, the ROIs of
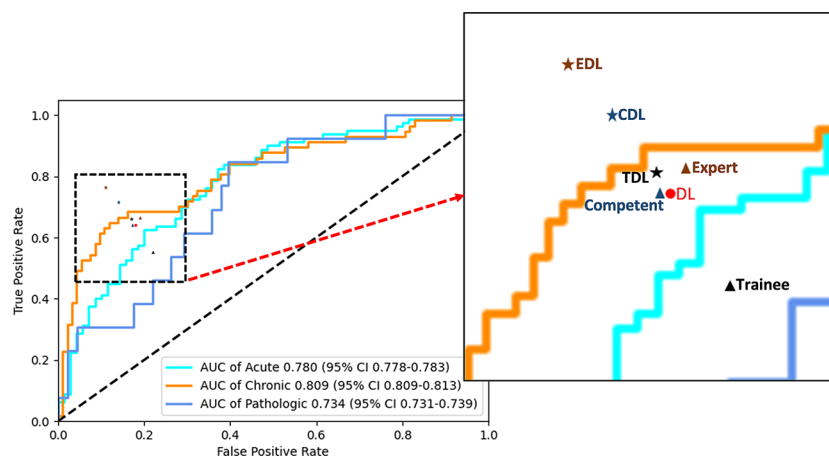
FIGURE 6
Performance of the deep learning and radiologists in classifying VCFs from X-ray images in the human and deep learning collaboration dataset. ROC of the classification mode in the human and deep learning collaboration dataset. The red dot, black triangle, black star, orange triangle, orange star, blue triangle, and blue star indicate the performance of deep learning (DL), trainee, trainee-deep learning collaboration (TDL), competent, competent-deep learning collaboration (CDL), expert, and expert-deep learning collaboration (EDL), respectively.

the compression fracture were delineated by a manual rectangle. The training of the model relies on the accurate identification of compressed vertebral bodies by radiologists, which requires manual delineation by radiologists. Although there are some differences in the ROIs drawn by different doctors, they will be uniformly processed and then classified after the images are imported into the model. Currently ROI delineation could be finished using automatic, semi-automatic and hand-crafted methods. However, automatic and semi-automatic methods may have a certain deviation which need to be further adjusted manually. Fourth, due to the small numbers of pathological compression fractures in this study with low sensitivity, it is likely the features of pathological fracture might be different from the osteoporotic/traumatic compression fracture and will require a large and specific pathological database to clarify the utilization of deep learning model assistance. Therefore, more studies with larger numbers of patients are required to provide stronger evidence for the accuracy of deep learning models in the prediction of pathological compression fractures. Finally, deep learning model alone was not adequate to detect pathological compression fracture due to the absence of clinical information. Thus, the general applicability of our results in clinical practice could be affected. Clinical information is required in future study to validate the performance of deep learning models.

In conclusion, a multiclass deep learning model for compression fractures on radiographs was developed and validated. The classification performance of the model surpassed that of trainee radiologists and was comparable to that of experienced radiologists. When the skills of the radiologists were combined with a deep learning model, better diagnostic performance was observed, which could improve the accuracy of diagnostic classification, thereby improving the diagnostic workflow for patients with compression fractures. We expect to establish an artificial intelligence-assisted diagnosis platform for compression fracture based on X-ray images to provide patients and clinicians

with free access to telemedicine assistance, aiming to eliminate the diagnosis and treatment gap between national hospitals and grassroots hospitals.

Data availability statement

The excel files containing raw data included in the main figures and tables can be found in supplementary material. The lumbar spine X-ray imaging data and clinical information are not publicly available for patient privacy reasons but are available from the corresponding authors upon reasonable request (FX, YCX and XWZ). The models and the code used to test and evaluate the model is available on GitHub (https://github.com/Xiongyuchao/VCFNet). The remaining data are included in the article/Supplementary Material, further inquiries can be directed to the corresponding author/s.

Ethics statement

The studies involving human participants were reviewed and approved by the institutional review board and ethics committee of the Guangzhou Red Cross Hospital (IRB 2022-108-01). The patients/participants provided their written informed consent to participate in this study.

Author contributions

Conception and design: FX, YCX; acquisition of additional data: FX, YCX, GXY, YYL, QPD, WYJ, DLW, SC; analysis and interpretation of data: FX, YCX, GXY, ZPL, XWZ; statistical analysis: FX, YYL, GXY; drafting of the manuscript: FX, YCX; critical revision of the manuscript: FX, XWZ; study supervision: XWZ. All authors listed have contributed substantially to the design, data collection and analysis, and editing of the manuscript.

Funding

Conflict of interest

The authors declare that the research was conducted in the absence of any commercial or financial relationships that could be construed as a potential conflict of interest.

Publisher's note

All claims expressed in this article are solely those of the authors and do not necessarily represent those of their affiliated organizations, or those of the publisher, the editors and the reviewers. Any product that may be evaluated in this article, or claim that may be made by its manufacturer, is not guaranteed or endorsed by the publisher.

Supplementary material

The Supplementary Material for this article can be found online at: https://www.frontiersin.org/articles/10.3389/fendo.2023.1025749/full#supplementary-material

The models and the code used to test and evaluate the model is available on GitHub (https://github.com/Xiongyuchao/VCFNet).

References

1. Parreira PCS, Maher CG, Megale RZ, March L, Ferreira ML. An overview of clinical guidelines for the management of vertebral compression fracture: A systematic review. *Spine J* (2017) 17:1932–8. doi: 10.1016/j.spinee.2017.07.174

2. Musbahi O, Ali AM, Hassany H, Mobasheri R. Vertebral compression fractures. *Br J Hosp Med (Lond)* (2018) 79:36–40. doi: 10.12968/hmed.2018.79.1.36

3. Esteva A, Robicquet A, Ramsundar B, Kuleshov V, DePristo M, Chou K, et al. A guide to deep learning in healthcare. *Nat Med* (2019) 25:24–9. doi: 10.1038/s41591-018-0316-z

4. Li X, Zhang S, Zhang Q, Wei X, Pan Y, Zhao J, et al. Diagnosis of thyroid cancer using deep convolutional neural network models applied to sonographic images: a retrospective, multicohort, diagnostic study. *Lancet Oncol* (2019) 20:193–201. doi: 10.1016/S1470-2045(18)30762-9

5. Luo H, Xu G, Li C, He L, Luo L, Wang Z, et al. Real-time artificial intelligence for detection of upper gastrointestinal cancer by endoscopy: a multicentre, case-control, diagnostic study. *Lancet Oncol* (2019) 20:1645–54. doi: 10.1016/S1470-2045(19)30637-0

6. Razzak I, Naz S. Unit-vise: Deep shallow unit-vise residual neural networks with transition layer for expert level skin cancer classification. *IEEE/ACM Trans Comput Biol Bioinform PP* (2022) 19(2):1225–34. doi: 10.1109/TCBB.2020.3039358

7. LeCun Y, Bengio Y, Hinton G. Deep learning. *Nature* (2015) 521:436–44. doi: 10.1038/nature14539

8. Chung SW, Han SS, Lee JW, Oh K-S, Kim NR, Yoon JP, et al. Automated detection and classification of the proximal humerus fracture by using deep learning algorithm. *Acta Orthop* (2018) 89:468–73. doi: 10.1080/17453674.2018.1453714

9. Gan K, Xu D, Lin Y, Shen Y, Zhang T, Hu K, et al. Artificial intelligence detection of distal radius fractures: a comparison between the convolutional neural network and professional assessments. *Acta Orthop* (2019) 90:394–400. doi: 10.1080/17453674.2019.1600125

10. Olczak J, Fahlberg N, Maki A, Razavian A, Jilert A, Stark A, et al. Artificial intelligence for analyzing orthopedic trauma radiographs. *Acta Orthop* (2017) 88:581–6. doi: 10.1080/17453674.2017.1344459

11. Kim DH, MacKinnon T. Artificial intelligence in fracture detection: transfer learning from deep convolutional neural networks. *Clin Radiol* (2018) 73:439–45. doi: 10.1016/j.crad.2017.11.015

12. Ozkaya E, Topal FE, Bulut T, Gursoy M, Ozuysal M, Karakaya Z. Evaluation of an artificial intelligence system for diagnosing scaphoid fracture on direct radiography. *Eur J Trauma Emerg Surg* (2022) 48(1):585–92. doi: 10.1007/s00068-020-01468-0

13. Mutasa S, Varada S, Goel A, Wong TT, Rasiej MJ. Advanced deep learning techniques applied to automated femoral neck fracture detection and classification. *J Digit Imaging* (2020) 33:1209–17. doi: 10.1007/s10278-020-00364-8

14. Chen W, Liu X, Li K, Luo Y, Bai S, Wu J, et al. A deep-learning model for identifying fresh vertebral compression fractures on digital radiography. *Eur Radiol* (2022) 32(3):1496–505. doi: 10.1007/s00330-021-08247-4

15. McCarthy J, Davis A. Diagnosis and management of vertebral compression fractures. *Am Fam Physician* (2016) 94:44–50.

16. He K, Zhang X, Ren S, Sun J. Deep residual learning for image recognition. *Proc IEEE Conf Comput Vision Pattern Recognition* (2016) 2016:770–8. doi: 10.1109/CVPR.2016.90

17. Yabu A, Hoshino M, Tabuchi H, Takahashi S, Masumoto H, Akada M, et al. Using artificial intelligence to diagnose fresh osteoporotic vertebral fractures on magnetic resonance images. *Spine J* (2021) 21:1652–8. doi: 10.1016/j.spinee.2021.03.006

18. Laredo JD, Lakhdari K, Bellaiche L, Hamze B, Janklewicz P, Tubiana JM. Acute vertebral collapse: CT findings in benign and malignant nontraumatic cases. *Radiology* (1995) 194:41–8. doi: 10.1148/radiology.194.1.7997579

19. Schwaiger BJ, Gersing AS, Baum T, Krestan CR, Kirschke JS. Distinguishing benign and malignant vertebral fractures using CT and MRI. *Semin Musculoskelet Radiol* (2016) 20:345–52. doi: 10.1055/s-0036-1592433

20. Zampa V, Cosottini M, Michelassi C, Ortori S, Bruschini L, Bartolozzi C. Value of opposed-phase gradient-echo technique in distinguishing between benign and malignant vertebral lesions. *Eur Radiol* (2002) 12:1811–8. doi: 10.1007/s00330-001-1229-6

21. Wang KC, Jeanmenne A, Weber GM, Thawait SK, Carrino JA. An online evidence-based decision support system for distinguishing benign from malignant vertebral compression fractures by magnetic resonance imaging feature analysis. *J Digit Imaging* (2011) 24:507–15. doi: 10.1007/s10278-010-9316-3

22. Suh CH, Yun SJ, Jin W, Lee SH, Park SY, Ryu CW. ADC As a useful diagnostic tool for differentiating benign and malignant vertebral bone marrow lesions and compression fractures: a systematic review and meta-analysis. *Eur Radiol* (2018) 28:2890–902. doi: 10.1007/s00330-018-5330-5

23. Kim SJ, Lee JS. Diagnostic performance of f-18 fluorodeoxyglucose positron emission tomography or positron emission Tomography/Computed tomography for differentiation of benign and malignant vertebral compression fractures: A meta-analysis. *World Neurosurg* (2020) 137:e626–33. doi: 10.1016/j.wneu.2020.02.085

Check for updates

Correlation analysis of larger side bone cement volume/vertebral body volume ratio with adjacent vertebral compression fractures during vertebroplasty

Chengqiang Zhou[1,2], Shaolong Huang[1,2], Yifeng Liao[1,2], Han Chen[2], Yazhong Zhang[1], Hua Li[1], Ziqiang Zhu[1] and Yunqing Wang[1*]

[1]Department of Orthopedics, The Second Affiliated Hospital of Xuzhou Medical University, Xuzhou, Jiangsu, China, [2]Graduate School of Xuzhou Medical University, Xuzhou, Jiangsu, China

Objective: To investigate the correlation analysis of larger side bone cement volume/vertebral body volume ratio (LSBCV/VBV%) with adjacent vertebral compression fracture (AVCF) in percutaneous vertebroplasty (PVP) for osteoporotic vertebral compression fracture (OVCF).

Methods: A retrospective analysis of 245 OVCF patients who underwent PVP treatment from February 2017 to February 2021, including 85 males and 160 females. The age ranged from 60 to 92 years, with a mean of (70.72 ± 7.03) years. According to whether AVCF occurred after surgery, they were divided into 38 cases in the AVCF group (fracture group) and 207 cases in the no AVCF group (non-fracture group). The correlation between gender, age, bone mineral density (BMD), body mass index (BMI), thoracolumbar segment fracture, bone cement disc leakage, LSBCV, bone cement volume (BCV), VBV, LSBCV/VBV ratio (LSBCV/VBV%), and BCV/VBV% and AVCF were analyzed in both groups. Risk factors for AVCF after PVP were analyzed by multifactorial logistic regression, and then the receiver operating characteristic curves (ROC curves) were plotted to identify the critical value of LSBCV/VBV%.

Results: 38 patients (15.5%) developed AVCF postoperatively. Univariate analysis showed that BMD, bone cement disc leakage, LSBCV, and LSBCV/VBV% were risk factors for AVCF after PVP ($P<0.05$), while gender, age, BMI, thoracolumbar segment fracture, BCV, VBV, and BCV/VBV% were not significantly different in both groups ($P>0.05$). Multifactorial logistic regression analysis revealed that BMD, bone cement disc leakage, and LSBCV/VBV% were independent risk factors for AVCF after PVP ($P<0.05$). According to the ROC curve, the LSBCV/VBV% had an area under the curve of 71.6%, a sensitivity and specificity of 89.5% and 51.7%, respectively, and a critical value of 13.82%.

Conclusion: BMD, bone cement disc leakage and LSBCV/VBV% are independent risk factors for AVCF after PVP. With LSBCV/VBV at 13.82%, the incidence of AVCF significantly increased.

1 Introduction

As populations age, the incidence of osteoporotic vertebral compression fractures (OVCFs) increases, accompanied by acute and chronic pain and progressive spinal deformities that decrease the quality of life and increase mortality (1). Therefore, attention must be drawn to developing better treatments for OVCF. Percutaneous vertebroplasty (PVP) or percutaneous kyphoplasty (PKP) is one of the effective and widely accepted methods for treating OVCF and is done by inserting cement into the fractured vertebrae for fixation to relieve pain and prevent further collapse of the vertebral body. However, some patients develop adjacent vertebral compression fractures (AVCF) within some time after PVP, which affects treatment outcomes and the quality of patient survival. Studies suggest that there are many reasons for developing AVCF after PVP (2–4). However, the amount of bone cement and its distribution pattern that alters the surgical vertebral stiffness is considered to be one of the main causes (5, 6).

Current studies on AVCF development after PVP mainly focuses on the puncture approach, bone cement volume (BCV), and BCV/vertebral body volume ratio (BCV/VBV%). In PVP, the vertebral body is unevenly filled with bone cement, often with excess on one side over the other, which leads to the uneven elastic modulus of the neighboring vertebrae, and ultimately into AVCF. Fewer systematic reports correlate larger side bone cement volume (LSBCV), LSBCV/VBV% ratio, and AVCF. Therefore, our present study focuses on the factors that influence AVCF and its correlation with LSBCV/VBV%.

2 Materials and methods

2.1 General information

Between February 2017 and February 2021, 245 patients (male: 85; female: 160) underwent PVP for OVCF in our hospital. The average age was 70.72 ± 7.03, with a range of 60-92 years. The patients reported fracture segments: T5, two cases; T6, six cases; T7, four cases; T8, eight cases; T9, 11 cases; T10, 19 cases; T11, 40 cases; T12, 61 cases; L1, 44 cases; L2, 25 cases; L3, 14 cases; L4, eight cases; and L5, three cases (Figure 1). Inclusion criteria: (1) single-segment OVCF patients with obvious low back pain; (2) bone mineral density

(BMD) with T-value ≤ -2.5; (3) PVP operation; (4) bilateral puncture; (5) the compression ratio of the injured spine was ≤ 1/3, T2W1 of the injured spine was a high signal on MRI, and edema signal was present on fat-suppressed sequence imaging; (6) posterior wall of damaged vertebrae was integrated, and the spinal canal was not compressed with no signs and symptoms of nerve compression upon physical examination; and (7) have complete clinical, imaging and follow-up data. Exclusion criteria: (1) infection- or tumor-related pathological fractures; (2) severe cardiac, pulmonary, hepatic, or renal insufficiency; (3) cannot tolerate surgery in the prone position; (4) coagulation disorders; (5) less than 1 year of follow-up. The average follow-up time of all patients was (17.09 ± 3.43) months. Two groups were divided according to whether AVCF occurred after surgery: 38 cases in the group with AVCF (fracture group) and 207 cases in the group without AVCF (no fracture group).

2.2 Surgical method

Intravenous access was established before surgery and necessary vital signs were monitored. The patient was placed prone on the operating bed, with both hands lifted and cushions to support their shoulders and pelvis so the spine is extended backward to restore the injured vertebrae. After the G-arm X-ray machine was positioned, the projection of the injured vertebra on the body surface was marked, routine disinfection after towel laying was done, and the operation was performed under local anesthesia. According to the puncture site of the thoracic and lumbar vertebrae, a puncture with a diameter matching that of surgical instruments was selected. The lower thoracic and lumbar spine can be punctured using a needle with a diameter of 3.0 mm. A bilateral pedicle approach is used for puncture under the monitoring of G-arm fluoroscopy. The 4.2 mm operating sleeve was changed after a successful puncture. The anterior middle 1/3 of the vertebra was drilled with a vertebral body drill, and a cement pusher was inserted to slowly push the cement under X-ray fluoroscopy, no more than 0.3 mL each time and the doctors observed any bone cement leakage, and recorded the total amount of bone cement, and the average amount of bone cement in the thoracic spine was 2.5-4 ml and 3.5-5 ml in the lumbar spine. All patients used the same puncture point, puncture angle and injection speed during the operation. Patients were allowed to wear waist circumference for
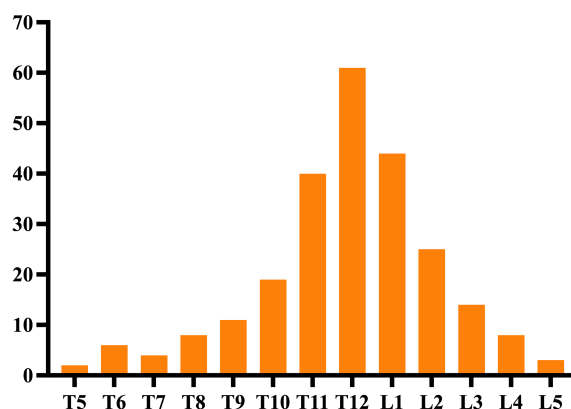
FIGURE 1
Distribution of primary vertebral fractures.

bedside activities 1 day after surgery and were discharged from the hospital with standardized anti-osteoporosis treatment.

2.3 Image evaluation

A 3D *computerized tomography* (CT) reconstruction was performed on the patient 3 days after surgery, and the CT image data were exported as DICOM format files, which were then imported into Mimics 21.0 (Materiallisesoftwar, Belgium) software. All VBV, BCV, and LSBCV were measured, respectively, and LSBCV/VBV% and BCV/VBV% were calculated.

VBV: Use the threshold segmentation tool to quickly separate the bone threshold (226-3071Hu), extract bone tissue, and perform image segmentation. After positioning the surgical vertebral body, the bilateral transverse processes, pedicles, and laminae were erased

using the edit mask function, and the gap was repaired using the gap repair function. Finally, the vertebral was reconstructed by the 3D reconstruction function, and the VBV was calculated (Figure 2).

BCV: Since the density of bone and bone cement are different, the threshold is adjusted to the bone cement threshold (1000-3071Hu) and bone cement is extracted. After the software automatically outlines the bone cement boundary, the edit mask function is used to erase the part of bone cement that leaks outside the vertebral body. Finally, bone cement reconstruction was performed by the 3D reconstruction function and BCV was calculated (Figure 3).

LSBCV: The LSBCV is obtained by dividing the vertebral body coronally into two equal parts on the left and right and the edit mask function was used to erase the side with a smaller volume of bone cement. The LSBCV was then calculated by the reconstruction function (Figure 4).
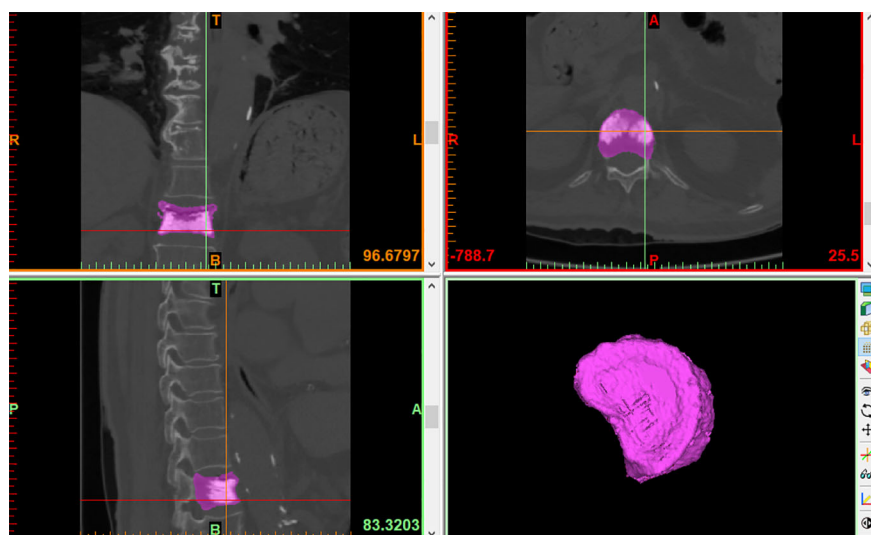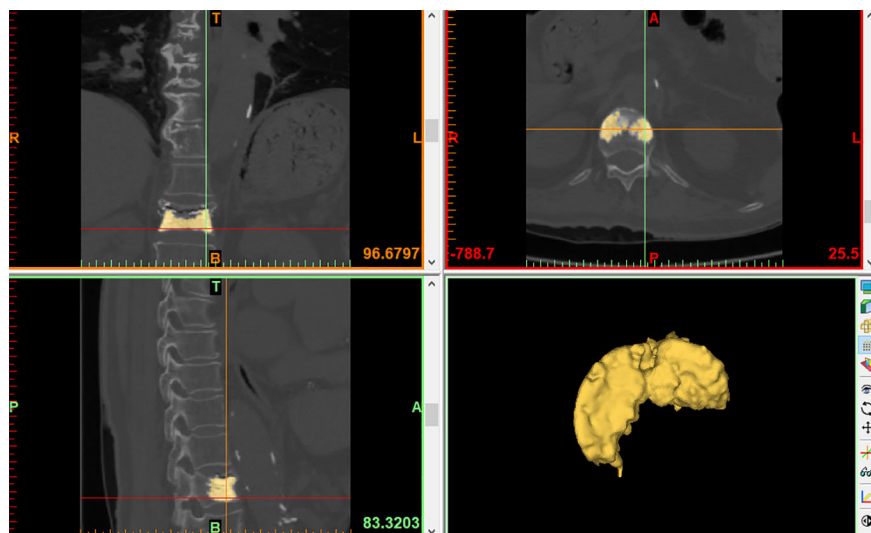

FIGURE 2
VBV.

FIGURE 3
BCV.

2.4 Observation indicators

The gender, age, body mass index (BMI), BMD, thoracolumbar fracture segments, bone cement disc leakage, and LSBCV, BCV, VBV, LSBCV/VBV%, BCV/VBV% indicators that were observed in the fracture and non-fracture group.

2.5 Statistical analysis

We used the SPSS 26.0 software (IBM, Armonk, NY, USA) to analyze the data. The measurement data were expressed as mean ± standard deviation, and independent sample t-tests were used for comparison between groups. The count data were analyzed by the chi-square test. Indicators were screened by univariate analysis first, and those indicators with statistically significant differences were then subjected to multifactorial logistic regression analyses. We also constructed the ROC curve to calculate the area under the curve as well as the critical value of LSBCV/VBV%.

3 Results

All patients completed the surgery successfully. The length of the operation was between 33-62 minutes (average: 42.49 ± 5.06). A total of 245 patients received final follow-up, of which 38 (15.51%) patients developed AVCF and in 20 (8.16%) patients, it occurred within 6 months after the first operation and 12
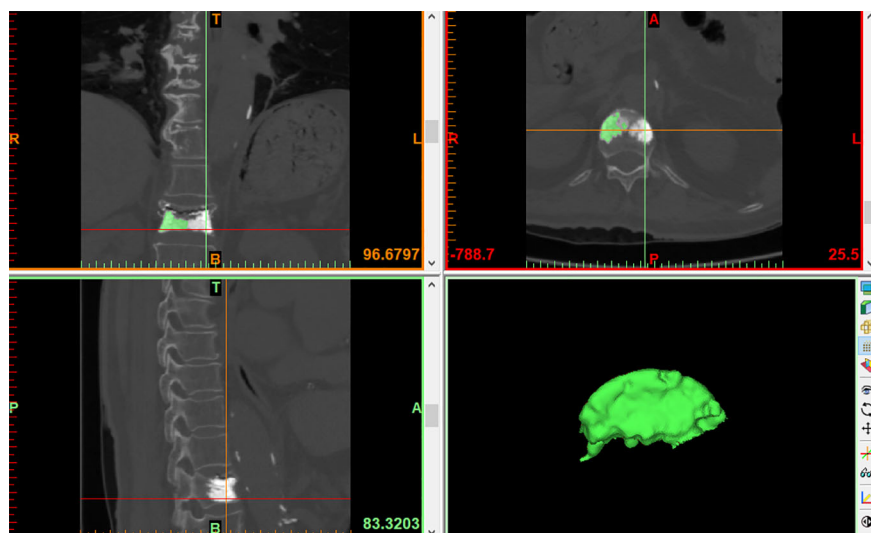

FIGURE 4
LSBCV.

(4.90%) patients reported AVCF within 1 year after their first operation.

Univariate analysis shows that gender, age, BMI, thoracolumbar fracture, BCV, VBV, and BCV/VBV% did not affect AVCF after PVP surgery (P > 0.05). The BMD T-value, bone cement disc leakage, LSBCV, and LSBCV/VBV% significantly affected the AVCF after PVP (P < 0.05) (Table 1).

Multifactorial logistic regression analysis showed that low BMD, bone cement disc leakage, and LSBCV/VBV% were risk factors for AVCF development after PVP surgery (P < 0.05) (Table 2).

ROC curves of BMD, bone cement disc leakage and LSBCV/VBV% were constructed (Figure 5). The area under the curve was 63.1% for BMD, 55.2% for bone cement disc leakage, and 71.6% for LSBCV/VBV% (Table 3).

The sensitivity and specificity of LSBCV/VBV% corresponded to 89.5% and 51.7%, respectively, and the cut-off value at this time was 13.82% (Table 4). Typical cases are shown in Figure 6.

4 Discussion

At present, PVP is a common, minimally invasive technique for treating OVCF that can effectively relieve low back pain and promote early functional activity (7). However, patients are usually subjected to the reoccurrence of surgical/non-surgical vertebral fractures after surgery. A meta-analysis showed (8) that the incidence of refracture after PVP varied from 3.21% to 63%. YI et al. (9) showed that the incidence of AVCF in patients with OVCF and PVP and PKP was 19.59% at 1-year post-surgery. In addition, MAZZANTINI et al. (10) showed a 27.8% incidence of AVCF in patients with vertebral body strengthening at 39 months postoperative follow-up. The incidence of AVCF during patient follow-up was 15.5% in this study and was consistent with the above literature. Moreover, there is no unified view of the risk factors of AVCF after vertebroplasty. Several factors can influence its occurrence, as shown in previous studies (11, 12). In this study, our univariate analysis found that low BMD, bone cement disc leakage, LSBCV, and LSBCV/VBV% were risk factors for AVCF development after PVP. A through multivariate analysis showed that BMD, bone cement disc leakage and LSBCV/VBV% were independent risk factors for AVCF after vertebral augmentation.

Several studies have shown that BMD can reflect the degree of osteoporosis (13–15). The lower the BMD, the more serious the degree of osteoporosis, and vertebral body fracture can be caused by a slight external force. Rho et al. (16) found that a decrease in BMD and leakage of bone cement into the intervertebral disc also were influential factors in AVCF. Lu et al. (17) conducted a retrospective study of 204 patients after vertebroplasty, and found that lower BMD T values were a risk factor for AVCF after vertebroplasty.

TABLE 1 Univariate analysis that affects AVCF.

Relevant factors	Fracture group (n=38)	Non-fracture group (n=207)	t/x^2	P
Gender (M/F)	13/25	72/135	0.005	0.946
Age	70.18 ± 8.27	69.96 ± 7.78	0.164	0.870
BMI	23.17 ± 2.74	23.02 ± 3.32	0.267	0.790
BMD (T)	-3.40 ± 0.56	-3.14 ± 0.59	-2.494	0.013
Thoracolumbar fracture (T_{10}~L_2)	32/38	157/207	1.274	0.259
Bone cement disc leakage	6/32	11/196	3.954	0.047
LSBCV	4.27 ± 0.90	3.72 ± 1.00	3.134	0.002
BCV	6.37 ± 1.37	6.27 ± 1.31	0.429	0.668
VBV	25.63 ± 5.18	26.61 ± 5.80	-0.978	0.329
LSBCV/VBV%	16.90 ± 3.00	14.14 ± 3.18	5.158	<0.001
BCV/VBV%	25.45 ± 5.92	24.08 ± 5.48	1.400	0.163

BMI, body mass index; BMD, bone mineral density; LSBCV, larger side bone cement volume; BCV, bone cement volume; VBV, vertebral body volume; LSBCV/VBV%, larger side bone cement volume/vertebral body volume ratio; BCV/VBV%, bone cement volume/vertebral body volume ratio.

TABLE 2 Multifactorial logistic regression analysis that affects AVCF.

Influencing factors	B	S.E	Wald	P	OR	95% CI
BMD	-0.780	0.318	6.042	0.014	0.458	0.246~0.854
Bone cement disc leakage	1.353	0.604	5.020	0.025	3.869	1.185~12.637
LSBCV	0.085	0.236	0.130	0.719	1.089	0.686~1.728
LSBCV/VBV%	0.254	0.076	11.289	0.001	1.289	1.112~1.496

BMD, bone mineral density; LSBCV, larger side bone cement volume; LSBCV/VBV%, larger side bone cement volume/vertebral body volume ratio.
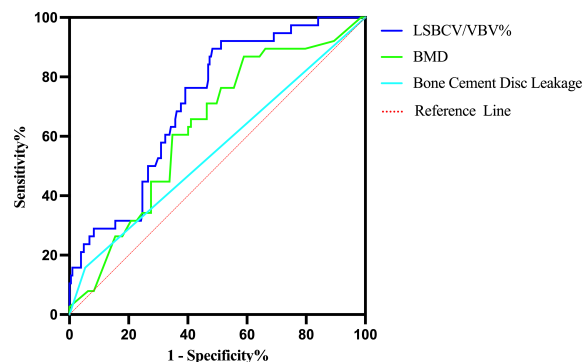
FIGURE 5
ROC curve for the diagnosis of AVCF.

TABLE 3 Area under the ROC curve for the diagnosis of AVCF.

Factors	AUC	P	95% CI	
			Lower	Upper
BMD	0.631	0.010	0.540	0.722
Bone cement disc leakage	0.552	0.305	0.447	0.657
LSBCV/VBV%	0.716	<0.001	0.637	0.794

BMD, bone mineral density; LSBCV/VBV%, larger side bone cement volume/vertebral body volume ratio.

Similarly, in this study, low BMD was also found to be a risk factor for AVCF after vertebroplasty by univariate analysis and binary logistic regression analysis, and the lower the BMD T value, the greater the risk for AVCF. PVP can be treated by fixing the fractured vertebral body through bone cement, and this has no therapeutic effect on osteoporosis. However, there still lies a risk of fracture in other vertebral bodies after PVP, especially the adjacent vertebral bodies due to interference of vertebral bodies with high elastic modulus after enhancement. Thus, for patients with low BMD, anti-osteoporosis therapy should be actively performed after PVP, and regular imaging examinations should also be carried out to prevent the occurrence of postoperative AVCF.

This study shows that the leakage of bone cement can also be a risk factor in AVCF development. Bone cement leakage is a common complication after PVP and PKP, with its incidence ranging from 11% to 73% (18). After the occurrence of a vertebral compression fracture, the internal bone trabeculae become dense due to compression and a hematoma is often present near the fracture line, which requires an increase in pushing pressure of the bone cement to diffuse the cement in the fracture gap, thus predisposing to a cement leakage (19). The bone cement leaks into the intervertebral disc, causing a transient fever, changing the physicochemical properties of the discs and destroying

its structure, accelerating disc degeneration, and making it lose its buffering effect, thus leading to abnormal load conduction. At the same time, this leak can also increase the stress of adjacent vertebral bodies due to the "pillar effect" that increases the risk of AVCF. A meta-analysis showed that cement leakage was a risk factor for AVCF after PVP in patients with OVCF, while cement volume was not a risk factor for AVCF (2), and the results are consistent with the results of our study.

In vertebroplasty, the cement is usually unevenly distributed on both sides of the vertebrae. We believe that this may be related to the angle of bilateral puncture and the different pressure and speed of bilateral push injection during bilateral puncture, often resulting in more bone cement on one side than on the other. This causes the vertical compression force of the entire vertebral body to shift to the other side, which increases the vertical stress in the neighboring vertebrae. However, after the vertebral body is hardened by bone cement, the stiffness is too large, and the stress distribution is uneven that then transfers to the neighboring vertebrae and discs (20), resulting in AVCF. In this study, we maintained the same injection point, angle of puncture, speed of pushing, and amount of bone cement on both sides during bilateral punctures in all patients to ensure that the proportion of bone cement on both sides was as equal as possible. An OVCF model was developed to compare the

TABLE 4 Sensitivity and specificity corresponding to LSBCV/VBV%.

Factor	Sensitivity	Specificity
LSBCV/VBV% (13.82)	0.895	0.517

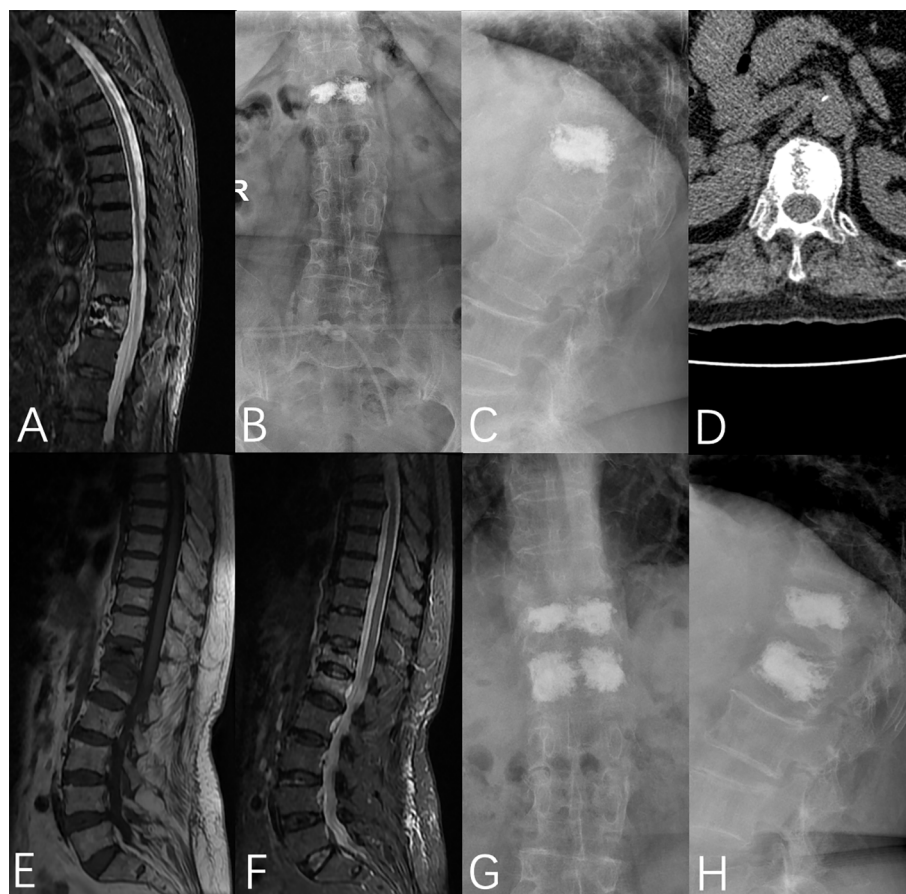LSBCV/VBV%, larger side bone cement volume/vertebral body volume ratio.

FIGURE 6
A 76-year-old female was admitted to the hospital with no obvious cause of low back pain for 1 week, was diagnosed with OVCF (T12), and underwent PVP under local anesthesia on the third day after admission. **(A)** Preoperative fat-suppressed image showed T12 vertebral fracture, **(B, C)** T12 vertebral bone cement filling could be seen in the anterior and lateral X-rays after the operation, **(D)** Postoperative CT showed that the bone cement was unevenly distributed on the bilateral sides of the vertebrae, **(E, F)** MRI showed L1 vertebral fracture 5 months after the operation, **(G, H)** T12 and L1 vertebral bodies were filled with bone cement in the anterior and lateral X-rays after the operation.

stiffness of the entire vertebral body and both sides of the vertebral body after unilateral and bilateral percutaneous vertebroplasty. It was found that when the bone cement was confined only to the punctured side, the unreinforced side was less safe than the reinforced side, and when bone cement distribution extended to the midline and filled the non-punctured side, a balance in stress was obtained on both sides of the vertebral body (21). At the same time, in vertebroplasty, the likelihood of cement leakage increases when it is overly concentrated on one side of the vertebral body compared to an even distribution on both sides. However, there lacks relevant literature which systematically studies the correlation of LSBCV and LSBCV/VBV% with AVCF. Previous studies have mostly concentrated on the impact of BCV and BCV/VBV% on vertebroplasty. Jin et al. (22) concluded that to ensure surgical efficacy and reduce complications, BCV/VBV% should be at least 11.64%. However, in these studies, BCV and BCV/VBV% were mostly described by the amount of cement injected and by a CT scan. The BCV refers to the distribution of bone cement in the vertebral body along the trabecular bone or the gap between the fracture line that forms a 3D spatial structure composed of bone cement, trabecular bone, and its gap. However, during the puncture,

there will be some bone cement remaining in the puncture cannula as well as leakage of bone cement outside the vertebral body, which results in an inconsistency between injected cement volume and the actual BCV within the vertebra. Also, the VBV calculated by CT can differ from the true VBV, so it is not possible to calculate BCV/VBV % accurately in this manner. Therefore, we imported the patient's CT data into the Mimics software and used its 3D reconstruction function to accurately calculate BCV, VBV, and LSBCV to derive LSBCV/VBV% and BCV/VBV%, and included them in the univariate analysis and binary logistic regression analysis. We found that BCV/VBV% was not a risk factor for AVCF, whereas LSBCV/VBV% was the risk factor for AVCF. Thus, by establishing the ROC curve, we found that the optimal cut-off value for LSBCV/VBV% to diagnose AVCF was 13.82%, with a sensitivity of 89.5% and specificity of 51.7%. Therefore, when LSBCV/VBV% exceeded 13.82%, the incidence of AVCF increased significantly.

However, there are some limitations to our study. First, this study was a retrospective single-center study with a short follow-up period and a small sample size. We hope to further analyze other factors that affect AVCF by carrying out a large-sample, multicenter, prospective study in the future. Second, we only

included PVP, not PKP, because PKP and PVP had different effects on the results (23). Lastly, we only studied the effects of cemented disc leakage on AVCF and did not examine if a leakage in bone cement to other sites could also affect AVCF.

In conclusion, BMD, bone cement disc leakage, and LSBCV/VBV% were independent risk factors for AVCF development after PVP. When LSBCV/VBV% reached 13.82%, the incidence of AVCF significantly increased. Therefore, to prevent the occurrence of AVCF after PVP, clinicians should keep the injection point, angle, pressure, and speed of pushing the puncture as consistent as possible during bilateral punctures. When bone cement disc leakage is found during operation, more vigilance is required, and at the same time, attention should also be paid to standardized anti-osteoporosis treatment to reduce the incidence of AVCF after PVP.

Data availability statement

The raw data supporting the conclusions of this article will be made available by the authors without undue reservation.

Ethics statement

The studies involving human participants were reviewed and approved by Ethics Committee of the Second Affiliated Hospital of Xuzhou Medical University. The patients/participants provided their written informed consent to participate in this study. Written informed consent was obtained from the individual(s) for the publication of any potentially identifiable images or data included in this article.

Author contributions

The first draft of the manuscript was written by CZ. Data collection and analysis were performed by CZ, SH, YL.

Interpretation of data was performed by HC, YZ, HL, ZZ and YW had substantively revised it. All authors contributed to the article and approved the submitted version.

Conflict of interest

The authors declare that the research was conducted in the absence of any commercial or financial relationships that could be construed as a potential conflict of interest.

Publisher's note

All claims expressed in this article are solely those of the authors and do not necessarily represent those of their affiliated organizations, or those of the publisher, the editors and the reviewers. Any product that may be evaluated in this article, or claim that may be made by its manufacturer, is not guaranteed or endorsed by the publisher.

References

1. Liang L, Chen X, Jiang W, Li X, Chen J, Wu L, et al. Balloon kyphoplasty or percutaneous vertebroplasty for osteoporotic vertebral compression fracture? An updated systematic review and meta-analysis. *Ann Saudi Med* (2016) 36(3):165–74. doi: 10.5144/0256-4947.2016.165

2. Zhang Z, Fan J, Ding Q, Wu M, Yin G. Risk factors for new osteoporotic vertebral compression fractures after vertebroplasty: A systematic review and meta-analysis. *J Spinal Disord Tech* (2013) 26(4):E150–7. doi: 10.1097/BSD.0b013e31827412a5

3. Ryu KS, Park CK, Kim MC, Kang JK. Dose-dependent epidural leakage of polymethylmethacrylate after percutaneous vertebroplasty in patients with osteoporotic vertebral compression fractures. *J Neurosurg* (2002) 96(1 Suppl):56–61. doi: 10.3171/spi.2002.96.1.0056

4. Hsiao PC, Chen TJ, Li CY, Chu CM, Su TP, Wang SH, et al. Risk factors and incidence of repeat osteoporotic fractures among the elderly in Taiwan: A population-based cohort study. *Med (Baltimore)* (2015) 94(7):e532. doi: 10.1097/MD.0000000000000532

5. Zhang L, Wang Q, Wang L, Shen J, Zhang Q, Sun C. Bone cement distribution in the vertebral body affects chances of recompression after percutaneous vertebroplasty treatment in elderly patients with osteoporotic vertebral compression fractures. *Clin Interv Aging* (2017) 12:431–6. doi: 10.2147/CIA.S113240

6. Nagaraja S, Awada HK, Dreher ML, Bouck JT, Gupta S. Effects of vertebroplasty on endplate subsidence in elderly female spines. *J Neurosurg Spine* (2015) 22(3):273–82. doi: 10.3171/2014.10.SPINE14195

7. Zhou C, Liao Y, Huang S, Li H, Zhu Z, Zheng L, et al. Effect of cement distribution type on clinical outcome after percutaneous vertebroplasty for osteoporotic vertebral compression fractures in the aging population. *Front Surg* (2022) 9:975832. doi: 10.3389/fsurg.2022.975832

8. Yu W, Xu W, Jiang X, Liang D, Jian W. Risk factors for recollapse of the augmented vertebrae after percutaneous vertebral augmentation: A systematic review and meta-analysis. *World Neurosurg* (2018) 111:119–29. doi: 10.1016/j.wneu.2017.12.019

9. Yi X, Lu H, Tian F, Wang Y, Li C, Liu H, et al. Recompression in new levels after percutaneous vertebroplasty and kyphoplasty compared with conservative treatment. *Arch Orthop Trauma Surg* (2014) 134(1):21–30. doi: 10.1007/s00402-013-1886-3

10. Mazzantini M, Carpeggiani P, d'Ascanio A, Bombardieri S, Di Munno O. Long-term prospective study of osteoporotic patients treated with percutaneous vertebroplasty after fragility fractures. *Osteoporos Int* (2011) 22(5):1599–607. doi: 10.1007/s00198-010-1341-z

11. Fang SY, Dai JL, Min JK, Zhang WL. Analysis of risk factors related to the re-fracture of adjacent vertebral body after pkp. *Eur J Med Res* (2021) 26(1):127. doi: 10.1186/s40001-021-00592-w

12. Li YA, Lin CL, Chang MC, Liu CL, Chen TH, Lai SC. Subsequent vertebral fracture after vertebroplasty: Incidence and analysis of risk factors. *Spine (Phila Pa 1976)* (2012) 37(3):179–83. doi: 10.1097/BRS.0b013e3181f72b05

13. Mukherjee S, Yeh J, Ellamushi H. Pain and functional outcomes following vertebroplasty for vertebral compression fractures - a tertiary centre experience. *Br J Neurosurg* (2016) 30(1):57–63. doi: 10.3109/02688697.2015.1096901

14. Wang YT, Wu XT, Chen H, Wang C, Mao ZB. Adjacent-level symptomatic fracture after percutaneous vertebral augmentation of osteoporotic vertebral compression fracture: A retrospective analysis. *J Orthop Sci* (2014) 19(6):868–76. doi: 10.1007/s00776-014-0610-7

15. Ning L, Wan S, Liu C, Huang Z, Cai H, Fan S. New levels of vertebral compression fractures after percutaneous kyphoplasty: Retrospective analysis of styles and risk factors. *Pain Physician* (2015) 18(6):565–72.

16. Rho YJ, Choe WJ, Chun YI. Risk factors predicting the new symptomatic vertebral compression fractures after percutaneous vertebroplasty or kyphoplasty. *Eur Spine J* (2012) 21(5):905–11. doi: 10.1007/s00586-011-2099-5

17. Lu K, Liang CL, Hsieh CH, Tsai YD, Chen HJ, Liliang PC. Risk factors of subsequent vertebral compression fractures after vertebroplasty. *Pain Med* (2012) 13 (3):376–82. doi: 10.1111/j.1526-4637.2011.01297.x

18. Zhang TY, Zhang PX, Xue F, Zhang DY, Jiang BG. Risk factors for cement leakage and nomogram for predicting the intradiscal cement leakage after the vertebra augmented surgery. *BMC Musculoskelet Disord* (2020) 21(1):792. doi: 10.1186/s12891-020-03810-4

19. Zhong BY, He SC, Zhu HD, Pan T, Fang W, Chen L, et al. Nomogram for predicting intradiscal cement leakage following percutaneous vertebroplasty in patients with osteoporotic related vertebral compression fractures. *Pain Physician* (2017) 20(4): E513–E20.

20. Belkoff SM, Mathis JM, Jasper LE, Deramond H. The biomechanics of vertebroplasty. the effect of cement volume on mechanical behavior. *Spine (Phila Pa 1976)* (2001) 26(14):1537–41. doi: 10.1097/00007632-200107150-00007

21. Chen B, Li Y, Xie D, Yang X, Zheng Z. Comparison of unipedicular and bipedicular kyphoplasty on the stiffness and biomechanical balance of compression fractured vertebrae. *Eur Spine J* (2011) 20(8):1272–80. doi: 10.1007/s00586-011-1744-3

22. Jin YJ, Yoon SH, Park KW, Chung SK, Kim KJ, Yeom JS, et al. The volumetric analysis of cement in vertebroplasty: Relationship with clinical outcome and complications. *Spine (Phila Pa 1976)* (2011) 36(12):E761–72. doi: 10.1097/BRS.0b013e3181fc914e

23. Daher M, Kreichati G, Kharrat K, Sebaaly A. Vertebroplasty versus kyphoplasty in the treatment of osteoporotic vertebral compression fractures: A meta-analysis. *World Neurosurg* (2022) 171:65–71. doi: 10.1016/j.wneu.2022.11.123

Changes in bone quality after switching from a TDF to a TAF based ART: A pilot randomized study

Jade Soldado-Folgado[1,2], Oriol Rins-Lozano[2,3], Itziar Arrieta-Aldea[4], Alicia Gonzále-Mena[4], Esperanza Cañas-Ruano[4], Hernando Knobel[4], Natalia Garcia-Giralt[4,5] and Robert Güerri-Fernández[3,4,6]*

[1]Departament de Medicina, Universitat Autònoma de Barcelona, Barcelona, Spain, [2]Department of Internal Medicine, Hospital del Mar Institute of Medical Research (IMIM), Barcelona, Spain, [3]Department of Medicine and Life Sciences (MELIS), University Pompeu Fabra, Barcelona, Spain, [4]Department of Infectious Diseases, Hospital del Mar Institute of Medical Research (IMIM), Barcelona, Spain, [5]Instituto de Salud Carlos III, Centro de Investigación Biomédica en Red Fragilidad y Envejecimiento Saludable (CIBERFES), Madrid, Spain, [6]Instituto de Salud Carlos III, Centro de Investigación Biomédica en Red Enfermedades infecciosas (CIBERINFEC), Madrid, Spain

Background: The impact of tenofovir disoproxil fumarate (TDF) antiretroviral (ART) regimens on bone health has been characterized mostly by bone mineral density (BMD), but recently also by bone quality (BQ). The aim of this pilot study is to assess the changes in BMD and BQ after switch from TDF to tenofovir alafenamide (TAF) ART.

Methods: HIV individuals receiving TDF-based ART were randomized to switch to Bictegravir-TAF-Emtricitabine or to remain in the same regimen. At baseline and 24-weeks after randomization, participants underwent bone mineral density (BMD) by DXA and BQ assessment using bone microindentation, a validated technique that measures bone tissue quality expressed as bone material strength index (BMSi). A panel of plasma bone turnover biomarkers were measured by ELISA at the same time-points. Values are expressed as median [interquartile range] and non-parametric tests were used where appropriate.

Results: A total of 24 HIV individuals were included in the study, 19 of which were men (80%). Median age at baseline was 43 years (IQR 38-54). Half of individuals were allocated in the TDF group while the other half changed to TAF treatment. No differences at baseline between both groups were detected in any parameter. Non-significant changes nor in lumbar or femoral BMD at week 24 was found in any regimen. In contrast, there was an increase in BMSi in the TAF arm at 24 weeks, and thus an improvement in BQ[81.6 (79-83) to 86 (80-88) (+5.1%); p=0.041], whereas the TDF arm remained stable from 82 (76-85) at baseline to 82 (73-83);p=0.812. Hence, at week 24 there were significant differences in BQ between arms (p=0.049). A reduction in bone formation markers was found at week 24 in both regimens: N-terminal propeptide of type-1 collagen decreased a 20% (-35 - -0.6); p=0.031 with TAF and -16% (-25 - -5); p=0.032 with TDF. Also a decrease in bone resorption marker C-telopeptide with TAF was detected [-10%

(-19 - -5);p=0.028] but not with TDF (p=0.232), suggesting a less metabolically active bone after switching to TAF.

Conclusion: A bone quality improvement was found after switching from a TDF to a TAF based ART independently of BMD, suggesting that the bone health benefits of TAF may extend beyond BMD. Future research should be directed to confirm these findings and to identify the underlying mechanisms of ART related bone toxicity.

1 Introduction

People living with HIV (PLWHIV) experience up to 4-fold higher annual rates of fragility fractures than the general population (1–3). As PLWH live longer through effective antiretroviral therapy (ART), fracture rates are expected to further increase in the future.

In clinical trials in PLWHIV, tenofovir disoproxil fumarate (TDF) was associated with a greater decrease in bone mineral density (BMD) and an increase in biochemical markers of bone metabolism, suggesting increased bone turnover relative to comparators. Whether these changes in BMD were associated with an increased risk of fractures has been controversial. However, some cohort studies (2, 4, p.) suggest that having lower BMD is associated with a higher risk of fractures,. Tenofovir alafenamide Fumarate-TAF- has shown a better profile of bone safety when compared with TDF. A prior study showed that people with low bone mineral density who switched from TDF to TAF experienced improvements in bone health such as a reduced risk of osteoporosis.

While several studies have emphasized an increased fracture incidence in PLWHIV (2, 3), this increased fracture incidence is not fully explained by differences in bone mineral density (BMD) between PLWHIV individuals and healthy controls. An emerging explanation for this paradox is that HIV infection and treatment are associated with changes in bone quality. Changes affecting the microarchitecture as well as the composition of the bone matrix and non-collagenous proteins (5) can affect bone quality and, consequently, on a higher risk of fracture. Microindentation is a technique cleared by the FDA that allows direct evaluation of the quality of bone material, encompassing these material-dependent elements not captured by BMD.

Microindentation allows detecting changes in bone quality much earlier than BMD (6). For all these reasons, the present study aims to assess the changes in bone quality in a group of people living with HIV who change from a TDF-based therapy to a TAF-based therapy.

2 Methods

2.1 Population and study design

This is a pilot open-label, randomized, unicenter, 24-week clinical trial conducted that was carried out in a university hospital in Barcelona, Spain between July 2019 to June 2020. This study enrolled HIV-1- positive adults who were virologically suppressed on any TDF (tenofovir disoproxil fumarate plus emtricitabine plus a third drug) based approved 3-drug regimen for at least 48 weeks and were randomly assigned (1:1) to receive bictegravir 50mg plus tenofovir alafenamide 25 mg and emtricitabine 200mg (TAF) for 24 weeks or continue their baseline disoproxil fumarate based regimens.

Inclusion criteria were age ≥18 years, ≥2 HIV-1 RNA measurements <50 copies/mL within 48 weeks of study entry, and a screening HIV-1 RNA <20 copies/mL. We considered as ineligible a history of virologic failure (VF) after 1 year of treatment, pretreatment reverse transcriptase (RT) resistance mutation, or known integrase resistance mutations, and those individuals who had previously received treatments that might have affected the bone quality, such as systemic glucocorticoids or anti-osteoporotic medications. We also excluded individuals who had previously been diagnosed with chronic kidney disease, chronic endocrine conditions, malabsorption syndrome, advanced liver disease, neoplasia, and bone diseases.

2.2 Procedures

After screening of inclusion/exclusion criteria, study visits occurred at day 1 and week 24. At day 1 participants underwent a baseline-randomization visit where clinical history was recorded, and a general physical examination was performed. Lateral spinal X-rays were taken and assessed by two independent observers to detect any vertebral fractures, defined as deformities of grade I or above (a loss of >20% of vertebral height).

2.2.1 Bone mineral density

BMD was measured at the lumbar spine and hip using dual energy x-ray absorptiometry (DXA) (Hologic QDR 4500 SR, Hologic, Inc., Bedford, MA, USA). Values were expressed as g/cm^2 of mineral content. The coefficient of variation for the DXA measurements was 1.8%

2.2.2 Bone microindentation measurements

Bone microindentation was measured using an Osteoprobe instrument (Active Life Scientific, Santa Barbara, CA, USA) according to a protocol previously described (7). In brief the testing takes place on the anterior face of the mid-tibia under local anesthesia. A needle applied through the skin is pushed into the bone surface with a force of 30 N during less than a millisecond creating an indentation, or microfracture, on the bone surface. The software registers the distance from the needle tip right before impact and right after, a distance called the total indentation. Repeated measurements in the same area are taken and right after, five measurements are performed on a piece of Poly-methyl-methacrylate (PMMA). Bone microindentation yields a dimensionless quantifiable parameter called bone material strength index (BMSi), which is positively correlated with bone tissue quality. The BMSi is calculated as 100 times the ratio of the mean total indentation in the PMMA and the tibia.

To minimize interobserver variation, all measurements for this study were taken by the same investigator (RGF) that was blinded for arm of treatment. As previously described, the microindentation procedure is minimally invasive, safe, painless, and takes less than 5 minutes and the software provides results immediately. Contraindications for this technique included local skin infection, significant local oedema, and/or thick subcutaneous adipose tissue at the site of indentation.

2.2.3 Laboratory assays

Chemiluminescent immunoassays (CLIA) was used to determine bone turnover markers and other bone specific parameters (based on fasting blood samples). Each immunoassay had an inter-assay coefficient of variation, iCV, of 10%. Specifically, we measured levels of intact parathyroid hormone (iPTH) (Siemens), bone alkaline phosphatase (Roche Diagnostics), amino propeptide of type I collagen (P1NP, Roche Diagnostics), collagen type I C-telopeptide (CTX, Roche Diagnostics), serum 25-hydroxyvitamin D_3 (Roche Diagnostics).

2.3 Study outcomes

The main outcome was the mean percentage change in bone tissue quality measuring the Bone Material Strenght index (BMSi) by microindentation at 24-weeks post randomization. Secondary endpoints included the change in spine and hip bone mineral density (BMD), the change in CD4 cell count, and the mean percentage change in bone turnover markers from baseline to week 24

2.3.1 Statistical methods

Sample size was calculated according to previous publications (8–10). Accepting an alpha risk of 0.05 and a beta risk of 0.2 in a two-sided test, 12 participants in each arm were needed to recognize a difference greater than or equal to 5 BMSi units as statistically significant. The standard deviation is assumed to be 4. A drop-out rate of 10% was anticipated.

Categorical variables were summarized using frequencies and percentage. Continuous variables were summarized using the median and interquartile range (IQR). Change in bone health parameters post switch to TAF-containing ART was assessed using Wilcoxon rank sum testing. And the Mann-Whithney U test was used to compared both arms.

Correlation between changes in bone quality, weight or body mass index were studied using Spearman's correlation test.

All analyses were conducted using Stata 13.1 (StataCorp, College Station, Texas, USA).

The trial is registered with EUDRAT (num 2018-004499-36).

The institutional review board approved this study, and each participant provided informed consent.

3 Results

3.1 Patient characteristics

Twenty-four HIV individuals were included (Table 1). The median age was 45 years (IQR 38-54) and 19 (80%) were male. Regarding the immune status, the median CD4 T-cell nadir count was 388 cells per ml (IQR 225-423), the median current CD4 T-cell count was 603 cells per ml (IQR 507-789) and the median CD4/CD8 ratio was 1.01 (IQR 0.74-1.23). All individuals reported a good adherence to ART with viral load below 19 copies per ml (Table 1).

Patients were randomly separated in 1:1 proportion in two arms according to ART regimen and all of them completed the 24-week follow-up visit. No differences were detected in any baseline characteristic between arms.

3.2 The switch of TDF to TAF elicited changes regarding bone quality

From baseline to 24-week after randomization we observed a significant increase in bone tissue quality measured by microindentation only in the TAF arm [81.6 (79-83) to 86 (80-88)] (mean percentage change +5.1%); p=0.041, whereas BMSi values remained stable in the TDF group 82.35 (76-85) to 82 (73.5-83) (mean percentage change -0.05%); p=0.812 (Table 1). This result was indicative of improved bone tissue quality after switching to TAF (p=0.041). Moreover, there were significant differences in BQ between arms at week 24 (p=0.049). (Figures 1A, B). In contrast, no significative change was detected in BMD values at any arm (Table 1) (Figures 1C, D).

TABLE 1 Patient characteristics and bone health parameters before and after switch.

	TDF arm		p-value[1]	TAF arm		p-value[2]
	Baseline	24-weeks		Baseline	TAF arm 24-weeks	
Cohort	N=12	N=12		N=12	N=12	
Age, median years (IQR)	46 (40-53)			44 (36-48)		
Male, n(%)	10 (83%)			9 (75%)		
Smoker, n(%)	2 (14%)			3 (25%)		
Weight (Kg)	76.9 (71-85)	77 (67-88)	0.594	75.3 (70-84)	77 (73 – 89)	0.031
Body Mass Index (BMI)	25.3 (24-27)	26.1 (22-27)	0.594	24.6 (23-29)	27.1 (23.9-29.9)	0.026
Regimen at baseline						
Rilpivirine	4 (34%)			6 (50%)		
Elvitegravir/cobicistat	4 (34%)			5 (41%)		
Efavirenz	1 (9%)			1 (9%)		
Boosted Darunavir	2 (14%)			0		
Raltegravir	1 (9%)			0		
Bone Parameters						
BMSi	82.35 (76-85)	82 (73.5-83)	0.812	81.6 (79-83)	86 (80-88)	0.041
Lumbar spine BMD (g/cm^2)	0.985 (0.804-1.042)	0.991(0.811-1.042)	0.552	0.981(0.851-1.036)	0.979 (0.863-1.041)	0.504
Femoral neck BMD (g/cm^2)	0.739 (0.673-0.892)	0.794 (0.689-0.893)	0.109	0.792(0.723-0.830)	0.791 (0.668-0.824)	0.929
T-score spine	-0.9 (-2.2 - -0.4)	-0.9 (-2.1 - -0.3)	0.978	-1 (-2 - -0.4)	-1 (-1.9 – 0)	0.367
T-score femoral neck	-1.3 (-1.7 - -0.2)	-1(-1.6 – 0.1)	0.067	-0.75(-1.35 - -0.6)	-0.8(-1.9 - -0.5)	0.836
Bone Metabolism Markers						
P1NP (ng/ml)	54.9 (46-100)	46 (37-69)	0.031	59.3 (46-73)	47 (39-59)	0.032
CTX (ng/ml)	0.351 (0.317-0.427)	0.441 (0.314-0.712)	0.916	0.362 (0.264-0.556)	0.355 (0.230-0.459)	0.028
Bone Alkaline Phosphatase (µg/ml)	17 (14-21)	15.8 (14.6-17.9)	0.109	14.5 (12.4-17.4)	10.5 (8.9-14.2)	0.202
iPTH(pg/ml)	33 (25-47)	34 (24-48)	0.735	35(26-43)	38(26-44)	0.342
25OH Vitamin D (ng/ml)	26.3 (26-31)	20 (17-24)	0.009	25 (11-34)	16 (6-28)	0.003
HIV specific parameters						
CD4+ T-cell/ml median (IQR)	584 (574-892)	631 (602-738)	0.327	609 (390-751)	740 (412-1093)	0.012
CD4/CD8 ratio median (IQR)	1.06 (0.986-1.224)	0.928 (0.798-1.235)	0.674	0.851 (0.595-1.230)	0.761 (0.593-1.104)	0.139
Viral load median (IQR)	19 (9.5-19)	19 (0-19)	0.373	19 (19-19)	19 (0-19)	0.973

Results are shown as median values (IQR), unless indicated otherwise. [1] corresponds to the p-value when comparing TDF arm 24-week to baseline. [2] corresponds to the p-value when comparing TAF arm 24 week to baseline. Bold font represents significant differences after 24 weeks.

3.3 Bone turnover markers

The bone formation marker N-terminal propeptide of type-1 collagen (P1NP) was significantly decreased in both arms at week 24 (Table 1) with a mean percentage change of -16%; p=0.031 in the TDF arm, and a mean percentage change of -20%; p=0.032 in the TAF arm. Moreover, a significant decrease in bone resorption marker C-telopeptide was detected in the TAF arm with a mean percentage change of -10% (-19 - -5);p=0.028 but not with TDF;

p=0.232, suggesting a less metabolically active bone after switching to TAF. No differences were found in Bone Alkaline Phosphatase neither in the TDF or TAF groups.

In individuals allocated in the TAF arm we detected a positive correlation between changes in weight and changes in bone quality BMSi (Spearman Rho's 0.510;p=0.021) after 24 weeks of follow up.

Significant changes in 25-OH vitamin D_3 levels were also detected in both arms, reflecting the seasonal variation of this hormone (Table 1).
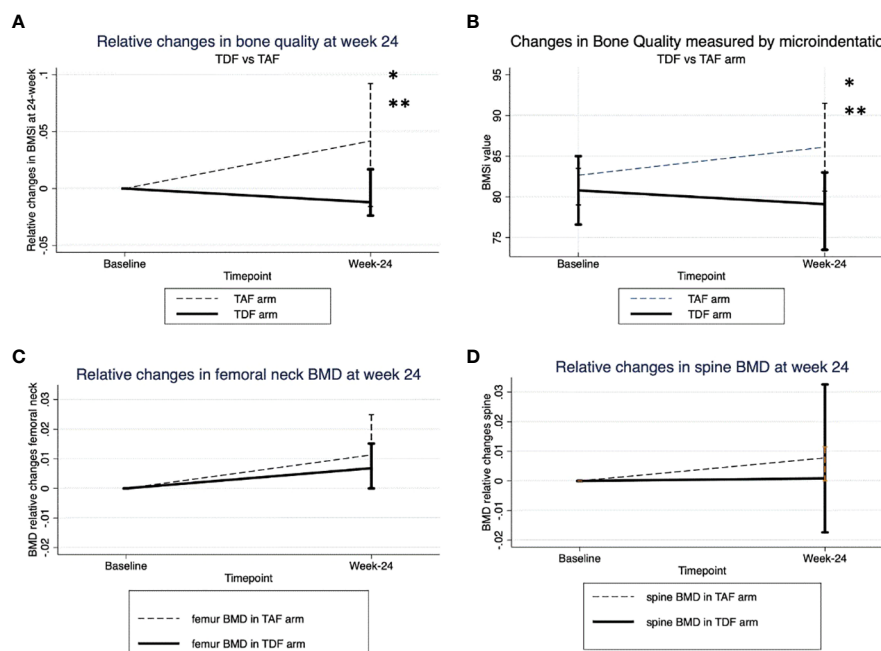
FIGURE 1
(A) Absolute changes in BMSi between two arms. *p-value at week -24 respect to baseline in TAF arm. **p-value at week-24 between TDF and TAF arms. **(B)** Relative changes in bone quality. **(C)** Relative changes in Bone mineral density at femoral neck. **(D)** Relative changes in Bone mineral density at spine neck.

4 Discussion

We report a comprehensive assessment of bone health in treated PLWHIV after a randomized pilot study with switching from a TDF-based regimen to a TAF-based regimen. In this study individuals who switched to a TAF-based regimen experienced a significant improvement in bone tissue quality measured by bone microindentation at week 24, whereas no changes in bone mineral density were found.

Until now, the only way to measure the mechanical resistance of bone was through *ex vivo* techniques, which made it difficult to apply in the clinical setting. Microindentation allows direct study *in vivo* of the resistance of bone tissue to an impact of known and controlled force. Compared with other techniques, microindentation has shown earlier detection of changes in bone quality. For instance, Mellibovsky et al. detected changes in bone quality just 7 weeks after starting treatment with glucocorticoids, while no changes in bone mineral density had yet been detected (6). Our group has reported altered bone quality in PLWHIV compared to HIV negative individuals, while there were no differences in BMD (7).

TDF has been repeatedly associated with its toxic effect on bone. TDF directly interferes with bone homeostasis through the reduction of extracellular adenosine levels, mediated by inhibition of ATP release from cells (11, p.; 12). As a result, there is a stimulation of osteoclast differentiation and osteoblast inhibition, with increased bone resorption. In addition, TDF interferes with the binding of calcidiol with its carrier protein (DBP, vitamin D binding protein) reducing its availability for the production of 1,25-dihydroxyvitamin

D (calcitriol, the active form of vitamin D) in the kidney (13). Reduced calcitriol will also result in less calcium and phosphorus being absorbed in the intestine, which will promote the emergence of secondary hyperparathyroidism and increased bone resorption. However, although we found changes in vitamin D levels, no cases of secondary hyperparathyroidism were found among participants.

Interestingly, we found in a previous study that starting antiretroviral treatment improved bone quality despite the fact that bone mineral density decreased in the first weeks of treatment (9, 10) likely as a consequence of the control of the viral replication along with the immune reconstitution. In this study PLWHIV under chronic treatment with a TDF-based therapy experienced a median increase of 5% in BMSi values, showing an improvement in bone quality. Likely showing a better profile of TAF in bone quality compared to TDF.

In the present study, individuals under TDF regimen at the timepoint of 24 weeks after randomization remained stable regarding bone strength parameters.

Tenofovir alafenamide is the tenofovir prodrug. TAF is mostly metabolized intracellularly by cathepsin A to tenofovir, whereas TDF is hydrolyzed by intestine and plasma esterases to tenofovir (14). As a result, when compared to TDF, the pharmacokinetics of TAF enabled a reduction of nearly 91% in plasma concentrations of the active metabolite of tenofovir, lowering the exposure of the kidney and bone to the medication. This explains the different behavior of bone properties when exposed to both drugs.

TAF-containing regimens showed significantly lower decrease in glomerular filtration rate, less proteinuria and less reduction in

BMD in comparison with those receiving TDF-containing regimens. In addition, patients on TDF who switched to TAF had increased BMD (15). A recent meta-analyisis of switching clinical trials reinforced this beneficial effect of TAF over TDF (16). In this line, Maggiolo et al. (17, 18) reported an increase in bone mineral density at lumbar or hip sites 48 weeks after switching from TDF to TAF in a population older than 60 years. However, we did not find significant changes in BMD values in our study, probably because they constitute a younger population, with a small sample size and with a shorter period of follow up. Nevertheless, bone mineral density usually takes at least 48 weeks to detect some significant changes. Despite of this, we found significant improvement of bone quality in individuals switching to TAF at 24 weeks of follow up. The increases in bone quality observed in the TAF arm after switching from tenofovir disoproxil fumarate have potentially important clinical consequences in terms of reducing the risk of fragility fractures and its associated morbidity and mortality.

Even though BMD is the gold standard predictor of fragility fractures, incident fractures among HIV individuals are not directly correlated with reduced BMD (4). Therefore, bone quality provides additional information about bone health to BMD and needs to be added to the equation of bone resistance to fracture. Interestingly, we found that the switch to a TAF regimen was associated with a significant improvement of bone quality of 5%. This increase is similar to those observed in naïve HIV individuals that start ABC-3TC-based regimen (10) or TDF-based regimen (9).

All of data suggests that TDF has a larger impact in bone than the PI, INSTI, or NNRTI.

In both ART-experienced and ART-naive PLWHIV, INSTI demonstrated better bone safety profile. In a randomized clinical trial, raltegravir was found to be linked with reduced bone loss when taken with TDF/FTC compared to either darunavir/ritonavir (r) or atazanavir/r (19). Similarly, after switching from a triple therapy including TDF in virologically suppressed PLWH with low BMD -1.0 T-score at weeks 24 and 48, raltegravir in combination with a boosted PI has also been linked to a significant rise in BMD at both the spine and hip (20). Similar results have been reported with BIC (18) or DTG (10). Consequently, TDF is the most likely responsible of the changes in bone quality reported in this study.

Finally, in this study we found a significant association between switch to TAF and weight gain as previously reported due to the lowering weight effect of TDF. However, this increase was associated with an improvement in bone quality (21–23). It is well-Known that body weight is a significant predictor of bone mineral status (24–26),thereby we cannot rule out that BMI might have a role in the bone quality improvement.

This study has some limitations that must be stated. This is a pilot trial with a reduced sample size in a single center. The reported results must be confirmed in larger studies. However, changes found in this study are physiologically plausible and deserve further studies. Other limitation could be the differences in vitamin D levels between the two timepoints. This could be due to the inclusion took after summer, and the follow up after Winter

(24 weeks later) likely reflecting the changes of vitamin D over the year. Despite of that, since this is a randomized study and both arms are balanced in the main variables.

One strength of the study is that microindentation is a now plenty available technique that has been recently approved for clinical use and we, as a group, have wide experience with it. The variability between observations is low and the same investigator performed all the measurements.

In conclusion, we present a longitudinal randomized switch study where individuals under TDF-based regimen change to TAF and bone tissue quality is assessed. We found that TAF-based group experienced an improvement in bone quality 24 weeks after switching from TDF independently of BMD. Therefore, microindentation is a sensitive tool for detecting early bone changes. Consequently, measuring other keystone elements of bone strength such as bone tissue quality also provides additional information and may more accurately assess bone health status.

Data availability statement

The raw data supporting the conclusions of this article will be made available by the authors, without undue reservation.

Ethics statement

The studies involving human participants were reviewed and approved by Comité de Etica i del Medicament Parc de Salut Mar. The patients/participants provided their written informed consent to participate in this study.

Author contributions

RG-F, NG-G and JS-F conceptualized and conducted the study. RG-F, OR-L and NG-G revised methodology and did data analysis. RG-F, OR-L, JS-F, HK, IA-A, EC-R, AG-M contributed with recruitment and data curation. All authors have revised and edited the final manuscript. All authos contributed to the article and approved the submitted version.

Funding

Conflict of interest

Publisher's note

References

1. Brown TT, Qaqish RB. Antiretroviral therapy and the prevalence of osteopenia and osteoporosis: a meta-analytic review. *AIDS Lond Engl* (2006) 20:2165–74. doi: 10.1097/QAD.0b013e32801022eb

2. Güerri-Fernandez R, Vestergaard P, Carbonell C, Knobel H, Avilés FF, Castro AS, et al. HIV Infection is strongly associated with hip fracture risk, independently of age, gender, and comorbidities: a population-based cohort study. *J Bone Miner Res Off J Am Soc Bone Miner Res* (2013) 28:1259–63. doi: 10.1002/jbmr.1874

3. Prieto-Alhambra D, Güerri-Fernández R, De Vries F, Lalmohamed A, Bazelier M, Starup-Linde J, et al. HIV Infection and its association with an excess risk of clinical fractures: a nationwide case-control study. *J Acquir Immune Defic Syndr* (2014) 66:90–5. doi: 10.1097/QAI.0000000000000112

4. Borges Á.H., Hoy J, Florence E, Sedlacek D, Stellbrink H-J, Uzdaviniene V, et al. Antiretrovirals, fractures, and osteonecrosis in a Large international HIV cohort. *Clin Infect Dis Off Publ Infect Dis Soc Am* (2017) 64:1413–21. doi: 10.1093/cid/cix167

5. Diez-Perez A, Güerri R, Nogues X, Cáceres E, Peña MJ, Mellibovsky L, et al. Microindentation for *in vivo* measurement of bone tissue mechanical properties in humans. *J Bone Miner Res Off J Am Soc Bone Miner Res* (2010) 25:1877–85. doi: 10.1002/jbmr.73

6. Mellibovsky L, Prieto-Alhambra D, Mellibovsky F, Güerri-Fernández R, Nogués X, Randall C, et al. Bone tissue properties measurement by reference point indentation in glucocorticoid-induced osteoporosis. *J Bone Miner Res Off J Am Soc Bone Miner Res* (2015) 30:1651–6. doi: 10.1002/jbmr.2497

7. Güerri-Fernández R, Molina D, Villar-García J, Prieto-Alhambra D, Mellibovsky L, Nogués X, et al. Brief report: HIV infection is associated with worse bone material properties, independently of bone mineral density. *J Acquir Immune Defic Syndr* (2016) 72:314–8. doi: 10.1097/QAI.0000000000000965. 1999.

8. Güerri-Fernández R, Molina-Morant D, Villar-García J, Herrera S, González-Mena A, Guelar A, et al. Bone density, microarchitecture, and tissue quality after long-term treatment with Tenofovir/Emtricitabine or Abacavir/Lamivudine. *J Acquir Immune Defic Syndr* (2017) 75:322–7. doi: 10.1097/QAI.0000000000001396

9. Güerri-Fernández R, Lerma-Chippirraz E, Fernandez Marron A, García-Giralt N, Villar-García J, Soldado-Folgado J, et al. Bone density, microarchitecture, and tissue quality after 1 year of treatment with tenofovir disoproxil fumarate. *AIDS Lond Engl* (2018) 32:913–20. doi: 10.1097/QAD.0000000000001780

10. Soldado-Folgado J, Lerma-Chippirraz E, Arrieta-Aldea I, Bujosa D, García-Giralt N, Pineda-Moncusi M, et al. Bone density, microarchitecture and tissue quality after 1 year of treatment with dolutegravir/abacavir/lamivudine. *J Antimicrob Chemother* (2020) 75:2998–3003. doi: 10.1093/jac/dkaa254

11. Conesa-Buendía FM, Llamas-Granda P, Atencio P, Cabello A, Górgolas M, Largo R, et al. Adenosine deaminase as a biomarker of tenofovir mediated inflammation in naïve HIV patients. *Int J Mol Sci* (2020) 21:3590. doi: 10.3390/ijms21103590

12. Conesa-Buendía FM, Llamas-Granda P, Larrañaga-Vera A, Wilder T, Largo R, Herrero-Beaumont G, et al. Tenofovir causes bone loss *via* decreased bone formation and increased bone resorption, which can be counteracted by dipyridamole in mice. *J Bone Miner Res* (2019) 34:923–38. doi: 10.1002/jbmr.3665

13. Havens P, Kiser J, Stephensen C, Hazra R, Flynn P, Wilson C, et al. Association of higher plasma vitamin d binding protein and lower free calcitriol levels with tenofovir disoproxil fumarate use and plasma and intracellular tenofovir pharmacokinetics: cause of a functional vitamin d deficiency? Antimicrob *Agents Chemother* (2013) 57:5619–28. doi: 10.1128/AAC.01096-13

14. Gibson AK, Shah BM, Nambiar PH, Schafer JJ. Tenofovir alafenamide. *Ann Pharmacother* (2016) 50:942–52. doi: 10.1177/1060028016660812

15. Wassner C, Bradley N, Lee Y. A review and clinical understanding of tenofovir: Tenofovir disoproxil fumarate versus tenofovir alafenamide. *J Int Assoc Provid AIDS Care* (2020) 19:2325958220919231. doi: 10.1177/2325958220919231

16. Tao X, Lub Y, Zhoub Y, Zhangb L, Chen Y. Efficacy and safety of the regimens containing tenofovir alafenamide versus tenofovir disoproxil fumarate in fixed-dose single-tablet regimens for initial treatment of HIV-1 infection: A meta-analysis of randomized controlled trials - PubMed. *Int J Infect Dis* (2020) 93:108–17. doi: 10.1016/j.ijid.2020.01.035

17. Maggiolo F, Rizzardini G, Molina J-M, Pulido F, De Wit S, Vandekerckhove L, et al. Bictegravir/Emtricitabine/Tenofovir alafenamide in virologically suppressed people with HIV Aged ≥ 65 years: Week 48 results of a phase 3b, open-label trial. *Infect Dis Ther* (2021) 10:775–88. doi: 10.1007/s40121-021-00419-5

18. Maggiolo F, Rizzardini G, Molina J-M, Pulido F, De Wit S, Vandekerckhove L, et al. Bictegravir/emtricitabine/tenofovir alafenamide in older individuals with HIV: Results of a 96-week, phase 3b, open-label, switch trial in virologically suppressed people ≥65 years of age. *HIV Med* (2022). 2021(10):775–88 doi: 10.1111/hiv.13319

19. Tebas P, Kumar P, Hicks C, Granier C, Wynne B, Min S, et al. Greater change in bone turnover markers for efavirenz/emtricitabine/tenofovir disoproxil fumarate versus dolutegravir r abacavir/lamivudine in antiretroviral therapy-naive adults over 144 weeks. *AIDS* (2015) 29(18):2459–64. doi: 10.1097/QAD.0000000000000863

20. Bernardino JI, Mocroft A, Mallon PW, Wallet C, Gerstoft J, Russell C, et al. Bone mineral density and inflammatory and bone biomarkers after darunavir-ritonavir combined with either raltegravir or tenofovir-emtricitabine in antiretroviral-naive adults with HIV-1: a substudy of the NEAT001/ANRS143 randomised trial. *Lancet HIV* (2015) 2(11):464–73. doi: 10.1016/S2352-3018(15)00181-2

21. Mallon PW, Brunet L, Hsu RK, Fusco JS, Mounzer KC, Prajapati G, et al. Weight gain before and after switch from TDF to TAF in a U.S. cohort study. *J Int AIDS Soc* (2021) 24:e25702. doi: 10.1002/jia2.25702

22. Sax PE, Rockstroh JK, Luetkemeyer AF, Yazdanpanah Y, Ward D, Trottier B, et al. Switching to bictegravir, emtricitabine, and tenofovir alafenamide in virologically suppressed adults with human immunodeficiency virus. *Clin Infect Dis Off Publ Infect Dis Soc Am* (2021) 73:e485–93. doi: 10.1093/cid/ciaa988

23. Wood BR, Huhn GD. Excess weight gain with integrase inhibitors and tenofovir alafenamide: What is the mechanism and does it matter? *Open Forum Infect Dis* (2021) 8:ofab542. doi: 10.1093/ofid/ofab542

24. Bedogni G, Simonini G, Viaggi S. Anthropometry fails in classifying bonemineral status in postmenopausal women. *Ann Hum Biol* (1999) 26:561–8. doi: 10.1080/030144699282471

25. Gnudi S, Sitta E, Fiumi N. Relationship between body composition and bone mineral density in women with and without osteoporosis: relative contribution of lean and fat mass. *J Bone Miner Metab* (2007) 25:326–32. doi: 10.1007/s00774-007-0758-8

26. Ravn P, Hetland ML, Overgaard K, Christiansen C. Premenopausal and postmenopausal changes in bone mineral density of the proximal femur measured by dual-energy x-ray absorptiometry. *J Bone Miner Res* (2009) 9:1975–80. doi: 10.1002/jbmr.5650091218

Frontiers in
Endocrinology

Explores the endocrine system to find new therapies for key health issues

The second most-cited endocrinology and metabolism journal, which advances our understanding of the endocrine system. It uncovers new therapies for prevalent health issues such as obesity, diabetes, reproduction, and aging.

Discover the latest Research Topics

See more →

frontiers | Research Topics